3D Tooth Surface Texture Analysis: Methodological Variability and Marine Mammals

Thesis submitted for the degree of

Doctor of Philosophy

At the University of Leicester

by

Robert Harry Goodall

Department of Geology

University of Leicester

2016

Abstract

Tooth microwear occurs when an animal processes food, producing microscopic pits and scratches on tooth surfaces, providing evidence of tooth movements and food properties. 3D microwear analysis is a growing field of study, where sub-micron scale tooth surface textures are used to compare populations with dietary differences. It has been primarily employed to study terrestrial vertebrates, however, the technique has rarely been applied to aquatic vertebrates, and never to aquatic mammals. Furthermore, the technique suffers from methodological variability. To address these points this thesis presents the results of five studies using 3D microwear analysis, three of which investigate different aspects of methodological variability, and two investigate the utility of 3D microwear analysis to differentiate diet in marine mammals, both across multiple species, and within a single species. An investigation of seven commonly used moulding compounds of varying viscosity demonstrated that mid-viscosity President Jet Regular Body produced the most accurate and precise moulds of tooth surface texture. An investigation was also carried out to test the effect of scale limiting 3D surfaces using 40 different combinations of operator (N^{th} order of polynomial) and filter to produce roughness surfaces. It was shown that high variability exists between resulting surfaces depending on the operator and the filter used. A combination of 6^{th} order of polynomial, robust Gaussian filter and 0.025mm nesting index produced the greatest separation of known dietary groups while also being comparable to surfaces generated using many other combinations. An investigation into the effect of using four different microscopes to collect 3D tooth surface texture data showed high variability between resulting roughness parameter values and sensitivity to dietary differences depending on the microscope used. When testing the ability of 3D microwear analysis to separate ten marine mammal species into four known dietary groups, it was shown that this technique is highly sensitive to dietary differences, and provides information about the dietary evolution of extinct cetaceans. Finally, when using dentin tooth surfaces to test the ability of 3D microwear to detect differences between *Orcinus orca* dietary populations, it was found that their surface texture appears highly variable, and that little separation was possible between dietary groups.

Acknowledgements

Studying for a PhD is a long and demanding endeavour with many high points and low points, which would not be possible without the help and support of many people.

I would first like to thank my supervisor, Prof Mark Purnell, for all the support he has provided throughout my studies. His advice and guidance has greatly improved my abilities as a scientist, and has pushed me to achieve things I would not have thought possible. Before I started this PhD I had close to given up on ever being able to carry on in scientific research, so I owe Mark a great deal of thanks for giving me this opportunity.

I would also like to thank my collaborators on this PhD for their advice and assistance throughout, Dr Gildas Merceron (Université de Poitiers), Dr Laurent Darras, Dr Julia Fahlke (Museum für Naturkunde, Berlin), Dr Katharina Bastl (Medizinische Universität, Vienna), Prof Richard Leach (University of Nottingham), Dr Andrew Foote (Universität Bern, Switzerland), Sarah Livengood (University of Arkansas), Dr Wahyudin Syam and Dr Xiaobing Feng (University of Nottingham) and Prof Peter Ungar (University of Arkansas) who is still the only scientist I have even met who fixes an incredibly expensive microscope with gaffer tape and plastic tubing, while shouting the word “Science!”.

For assistance in data collection I would like to thank Lewis Newton and Shah Karim (University of Nottingham). And for assistance with specimen access and advice on specimens I would like to thank Prof Philip Gingerich (University of Michigan), Dr Jerry Herman and Zena Timmons (National Museums Scotland), Roberto Portela Miguez (Natural History Museum London), Daniel Klingberg Johansson (Zoological Museum Copehagen), and Hélène Verheyden Tixier (Institut National de la Recherche Agronomique (INRA), Toulouse, France).

My parents Alison and Harry, grandmother Elsie, brother James, and Becky Wicks, also deserves a great deal of thanks for supporting me throughout my studies, always believing in me and providing advice and kind words at all times. Especially my parents, who have supported me in every possible way, and without whom I would not have coped with some of the most stressful moments. And also to my Grandfather, Ernest Harry Goodall, who passed away on 29th October 2015 and will never see me complete my studies, but who always supported every choice I ever made, and to whom I am eternally grateful for so many things.

Many people both in the Department of Geology and outside have also helped me a great deal, in terms of moral support, and the PhD work its self. As such I would like to thank, in no particular order, Dr Duncan Murdock for many discussions and his useful insight into various issues and complicated problems, Dr Stewart Fishwick for his advice on statistical analyses, and Charlotte Watts for lunches at Jones' Café. I would also like to thank Tom K, Leah, Howard, Laura, Thomas C, Annika, Nicola, Oliver, Gill, Amy, Jonny, Tom Hearing, Sherri, Emily, and Sven, for generally being amazing people who have kept me sane, and who have helped me tremendously throughout the last four years. I would also like to thank several people from the University of Arkansas for making me feel so welcome during my short visit, including Diana Durand for providing a place for me to stay for three weeks and being a great host, plus Jenny Burgman, LeeChaln Hua, and Chris Fletcher.

I would finally like to thank the Natural Environment Research Council (NERC) for providing the funds for me to complete this PhD, without which none of this would have been possible.

Contents

Abstract i

Acknowledgements ii

Contents iv

Table Captions v

Figure Captions xiv

Introduction 1

Chapter 1: Accuracy and precision of silicon based impression media for quantitative areal texture analysis 10

Chapter 2: Investigating dietary behaviours in pinnipeds and odontocetes using 3D microtextural analysis of tooth wear, and its further application to evolutionary hypotheses in stem cetaceans 41

Chapter 3: Investigating Dietary Variability between Two North Atlantic Killer Whale (*Orcinus orca*) Populations; Quantitative 3D Microtextural Analysis of Tooth Surfaces 81

Chapter 4: Investigating how different methods used to scale limit 3D datafiles affect areal texture parameters and the separation of known dietary groups 123

Chapter 5: Testing the Effect of Different Instruments Used to Collect 3D Microtextural Data from Tooth Surfaces 189

Conclusions 260

Appendix 1: Supplementary Figures and Tables 269

Appendix 2: Supplementary Chapter - Investigating the Effect of Gold Coating Surfaces on Resulting 3D Roughness Parameters 274

Appendix 3: List of Planned Publications 279

Appendix 4: Chapter 1 - Publication 280

References 299

Table Captions

Table 1.1 Details of all seven silicon based impression media used in this study. Speedex, President Jet Light and Regular Body, and Accutrans are polyvinylsiloxane compounds. MM913 and MM240TV are room temperature vulcanising (RTV) rubber compounds, and Microset 101RF is a heat accelerated RTV rubber compound. 15

Table 1.2 ISO 25178-2 parameters used, including brief descriptions. Parameter Sal was excluded from analyses, as it only produced normally distributed data in one of the three data treatments, even when using log_{10} values. For detailed parameter descriptions see Purnell et al (2013). 20

Table 1.3 Scale Sensitive Fractal Analysis (SSFA) parameters used, including brief descriptions (after Ungar et al (2003), and Scott et al (2006)). Smc was excluded from statistical analyses as it was rarely normally distributed and almost always returned the same value for each surface. For parameter details and information on methods of calculation see Scott et al 2006...... 21

Table 1.4 Summary of overall Accuracy and Precision for each impression medium, separated across rough and smooth tooth surfaces. For convenience all treatments of the data are summarised as a single result. Impression media showing high Accuracy (one or fewer significant matched pair T-test results across all treatments of the data) or high Precision (a small range of absolute differences between the original surface and each impression medium) are marked with a (✓). Impression media showing low Accuracy (more than one significant matched pair T-test results across all treatments of the data) or low Precision (a medium to high range of absolute differences between the original surface and each impression medium are marked with an (x). Results are highlighted green for instances where both Accuracy and Precision are shown to be high in a given impression medium. 38

Table 2.1 List of all specimens used in this project including Species and Family, plus the institutional specimen number, reported diet, tooth position, and locality for each specimen. For the column "Moulded by", RHG = Robert H Goodall (University of Leicester), JMF = Julia M Fahlke (Museum für Naturkunde, Berlin), KMB = Katharina M Bastl (Medizinische Universität, Vienna 52

Table 2.2 Relative proportion of each food type in the diet of all species included in this study (excluding Orcinus orca, as only isotope data was available for this species, which cannot be converted into proportions). 53

Table 2.3 Full list of ISO 25178-2 parameters, including brief descriptions. Parameters Std, Sal, and Ssk were excluded from analyses. For detailed parameter descriptions see Purnell et al (2013) & Gill et al (2014). 57

Table 2.4 Full list of Scale Sensitive Fractal Analysis (SSFA) parameters, including brief descriptions (after refs 16,17). Parameters Tfv and Smc were excluded from analyses. For parameter details and information on methods of calculation see Scott et al (2006). 58

Table 2.5 ANOVA (A.), and Tukey HSD tests with connecting letter reports (B.) for ranked Proportions of Food tested between the four dietary groups. Significant test results highlighted in bold. 60

*Table 2.6 Results of ANOVA carried out between the four dietary classes based on ISO and SSFA parameter values. Bold values indicate significant test results, and * indicate Welch test results. Degrees of freedom presented in column d.f.* 61

Table 2.7 Tukey Connecting Letters report for comparisons between dietary classes based on ISO and SSFA parameter values. Connections between dietary classes are displayed as shared letters. Colours indicate parameters displaying exactly the same pattern of differences between dietary classes. Text is pale grey where all classes are connected by the same letter (no difference between classes). 64

*Table 2.8 ANOVA results for comparisons between dietary sub-classes; odontocete Fish Eater (oFE), odontocete Cephalopod Eater (oCE), pinniped Fish Eater (pFE), and pinniped Cephalopod Eater (pCE), based on ISO and SSFA parameter values. Bold results indicate significant results and * indicate Welch test results (used when variances are unequal). Tukey HSD test results are also shown for all possible combinations of dietary sub groups, broken down into those between sub groups with taxonomic differences (but the same expected diet), and those with dietary differences. * indicate non-parametric Steel Dwass All Pairs results (used when variances are unequal).* 68

Table 2.9 Tukey connecting letters report for comparisons between dietary sub-classes; odontocete Fish Eater (oFE), odontocete Cephalopod Eater (oCE), pinniped Fish Eater (pFE), and pinniped Cephalopod Eater (pCE) based on ISO and SSFA parameter values. Parameter have not been included where no difference between any sub-classes were recorded. Differences/connections between dietary sub-classes are displayed as different/shared letters. 69

Table 3.1 List of all Orcinus orca specimens used in this paper, with data on specimen number, tooth position, expected diet, and which tests each specimen was used for, included. Museum

collection abbreviations; ZMC = Zoological Museum Copenhagen, NHM = Natural History Museum, London, and NMS = National Museums Scotland, Edinburgh. 86

Table 3.2 Full list of ISO 25178-2 parameters, including brief descriptions. Parameters Std, Sal, and Ssk were excluded from analyses. For detailed parameter descriptions see Purnell et al (2013) & Gill et al (2014). 92

Table 3.3 Full list of Scale Sensitive Fractal Analysis (SSFA) parameters, including brief descriptions (after refs 16,17). Parameter Smc was excluded from analyses. For parameter details and information on methods of calculation see Scott et al (2006). 93

Table 3.4 Blocked ANOVA and Tukey HSD test results and Connecting Letter Reports for all comparisons between locations within and tooth, presented separately for A. NMS Z.2015.172.48, and B). NMS.1956.36.56. Variable tooth position blocked for all ANOVA tests. Results are only presented for parameters where significant ANOVA results were recorded. Significant results highlighted bold. 98

Table 3.5 Blocked ANOVA and Tukey HSD test results and Connecting Letter Reports for all comparisons between tooth positions, presented separately for A. NMS Z.2015.172.48, and B). NMS.1956.36.56. Variable location within a tooth blocked for all ANOVA tests. Results are only presented for parameters where significant ANOVA results were recorded. Significant results highlighted bold. 99

Table 3.6 ANOVA and Tukey HSD test results and Connecting Letter Reports for all comparisons between dentary and maxilla (specimen NMS.1956.36.56), presented separately for A). front teeth, and B). middle teeth. Results are only presented for parameters where significant ANOVA results were recorded. Significant results highlighted bold. 102

Table 3.7 PCA eigenvectors for PC1 and PC2 for comparisons of data from different locations within a tooth, presented separately for A). NMS Z.2015.172.148, and B). NMS 1956.36.56. All parameters used in each PCA are included, based on the results of Blocked ANOVA tests (Table 3.4). Values between 0 and 0.2 are light grey text, values between 0.2 and 0.3 are black text, and values above 0.3 are bold black text. Bold parameters represent those contributing the most to the separation on each principal component. Data are separated into front, middle, and rear teeth for each specimen. 108

Table 3.8 PCA eigenvectors for PC1 and PC2 for comparisons of data from different tooth positions, presented separately for A). NMS Z.2015.172.148, and B). NMS 1956.36.56. All parameters used in each PCA are included, based on the results of Blocked ANOVA tests (Table 3.5). Values between 0 and 0.2 are light grey text, values between 0.2 and 0.3 are black text,

and values above 0.3 are bold black text. Bold parameters represent those contributing the most to the separation on each principal component. Data are separated into labial, mesial, and lingual areas of the tooth for each specimen. 109

Table 3.9 Predicted dietary groups for specimens where isotope data was not available, based on the results of LDA carried out on ISO 25178 and SSFA parameters for all specimens with isotope data present, presented separately for A. front teeth dataset, and B). middle teeth dataset. Expected diet is that predicted from isotope data, and predicted diet is that predicted from the LDA. Probability gives the likelihood of each specimen being assigned to its predicted group. 112

*Table 3.10 Results of LDA carried out to test how well each dataset (front teeth and middle teeth datasets) could assign data from the other. Those specimens predicted (i.e. data from the opposing dataset) are marked with an *. All misclassifications are highlighted in bold. In each case the Assignment gives the group to which the analysis has assigned each specimen, and the probability is the likelihood of that specimen belonging to the assigned group.* 116

Table 4.1 Full specimen list, including all four dietary groups, taxonomic information, sample numbers, host institutions, dietary categories, tooth position used, and collection locality. ... 132

Table 4.2 Details of surfaces produced by scale limiting 3D datafiles. Codes are presented for each resulting surface, providing information about the dietary group from which the surface is taken and the operator, filter, and nesting index applied to the surface. 141

Table 4.3 Descriptions for all ISO 25178-2 areal texture parameters used in this paper. Parameters Std, and Sal were excluded from analyses as they almost always produced the same value for each surface. Ssk was also excluded as it displayed low normality and regularly returned negative values which could not be log transformed. For detailed parameter descriptions see Purnell et al (2013). 142

*Table 4.4 ANOVA comparing data from surfaces scale limited using different operators (2nd to 11th polynomial orders). Tests were carried out for each parameter, separately for each of the four dietary groups and within these groups separately for surfaces scale limited using each filter type. Tests results have only been reported where significant results were recorded. Values with a * indicate where variance was unequal (Bartlett, Levene, O'Brien, and Brown-Forsythe tests), therefore a Welch test result is reported instead.* 146

Table 4.5 ANOVA comparing data from surfaces scale limited using different filter types (robust Gaussian, robust wavelet, and spline). Tests were carried out for each parameter, separately for each of the four dietary groups and within these tests were carried out separately for each

*operator (order of polynomial) used to scale limit the surfaces. Significant results are highlighted in bold. Values with a * indicate where variance was unequal (Bartlett, Levene, O'Brien, and Brown-Forsythe tests), therefore a Welch test result is reported instead.* 149

Table 4.6 T-test results, comparing data from surfaces scale limited using different nesting indices (0.025mm, and 0.08mm). Tests were carried out for each parameter, separately for each of the four dietary groups and within these groups separately for each order of polynomial used to scale limit the surfaces. Only data generated from surfaces scale limited using a robust Gaussian filter have been used. Significant results are highlighted in bold. 155

Table 4.7 T-test results comparing data from two populations of C.capreolus with known dietary differences (Males - acorn eaters, and Females - bramble leaf eaters) across 21 areal texture parameters. Tests were carried out separately for each combination of operator and filter used to scale limited the 3D surfaces. Significant results are highlighted in bold..... 158

Table 4.8 T-test results comparing data from two populations of phocids with known dietary differences (Males - acorn eaters, and Females - bramble leaf eaters) across 21 areal texture parameters. Tests were carried out separately for each combination of operator and filter used to scale limited the 3D surfaces. Significant test results have been highlighted bold 160

Table 4.9 Loadings (eigenvectors) for each parameter on PC1 and PC2 when comparing C.capreolus dietary populations. PCA carried out using 8 areal texture parameters (Sq, Sv, Sz, Sdq, Sdr, Vvv, Svk, and S5z, for parameter descriptions see Table 4.3), across 40 PCA analyses, each using data from surfaces scale limited using different combinations of operator and filter. Values in bold show the greatest loadings...... 168

Table 4.10 Loadings (eigenvectors) for each parameter on PC1 and PC2 when comparing phocid dietary populations. PCA carried out using 16 areal texture parameters (Sq, Sp, Sv, Sz, Str, Sdq, Sdr, Vmp, Vmc, Vvc, Vvv, Spk, Sk, Svk, S5z, and Sa, for parameter descriptions see Table 4.3), across 40 PCA analyses, each using data from surfaces scale limited using different combinations of operator and filter. Values in bold show the greatest loadings. 169

Table 4.11 ANOVA results, Tukey tests, connecting letter reports, and group means for all four dietary groups, when comparing data generated for surfaces scale limited using different orders of polynomial against their position along PC1 and PC2. Principal component axis values are taken from PCA performed separately for each comparison of dietary groups (C.capreolus and phocids; Figure 4.15 and Figure 4.16). For the comparison of C.capreolus dietary groups 8 areal texture parameters were included (Sq, Sv, Sz, Sdq, Sdr, Vvv, Svk, and S5z), and for the comparison of phocid groups 16 were used (Sq, Sp, Sv, Sz, Str, Sdq, Sdr, Vmp, Vmc, Vvc, Vvv,

*Spk, Sk, Svk, S5z, and Sa, for parameter descriptions see Table 4.3). Significant ANOVA results are highlighted bold, and Welch test results from comparisons where variances were unequal are denoted with an *.* 175

Table 4.12 Spearman's rank correlation test results comparing parameter values from surfaces scale limited using different operators, against the position of points along PC1 and PC2. Principal component axis values are taken from PCA performed separately for each comparison of dietary groups (C.capreolus and phocids; Figure 4.15 and Figure 4.16). For the comparison of C.capreolus dietary groups 8 areal texture parameters were included (Sq, Sv, Sz, Sdq, Sdr, Vvv, Svk, and S5z), and for the comparison of phocid groups 16 were used (Sq, Sp, Sv, Sz, Str, Sdq, Sdr, Vmp, Vmc, Vvc, Vvv, Spk, Sk, Svk, S5z, and Sa, for parameter descriptions see Table 4.3). Significant results are highlighted in bold. 176

*Table 4.13 ANOVA results, Tukey test connecting letter reports, and group means for all four dietary groups, when comparing data from surfaces scale limited using different filter types based, against their position along PC1 and PC2. Principal component axis values are taken from PCA performed separately for each comparison of dietary groups (C.capreolus and phocids; Figure 4.15 and Figure 4.16). For the comparison of C.capreolus dietary groups 8 areal texture parameters were included (Sq, Sv, Sz, Sdq, Sdr, Vvv, Svk, and S5z), and for the comparison of phocid groups 16 were used (Sq, Sp, Sv, Sz, Str, Sdq, Sdr, Vmp, Vmc, Vvc, Vvv, Spk, Sk, Svk, S5z, and Sa, for parameter descriptions see Table 4.3). Significant ANOVA results are highlighted bold, and Welch test results from comparisons where variances were unequal are denoted with an *.* 178

Table 4.14 T-test results and group means for all four dietary groups, when comparing data from surfaces scale limited using different nesting indices against their position along PC1 and PC2. Principal component axis values are taken from PCA performed separately for each comparison of dietary groups (C.capreolus and phocids; Figure 4.15 and Figure 4.16). For the comparison of C.capreolus dietary groups 8 areal texture parameters were included (Sq, Sv, Sz, Sdq, Sdr, Vvv, Svk, and S5z), and for the comparison of phocid groups 16 were used (Sq, Sp, Sv, Sz, Str, Sdq, Sdr, Vmp, Vmc, Vvc, Vvv, Spk, Sk, Svk, S5z, and Sa, for parameter descriptions see Table 4.3). Significant results are highlighted in bold. 179

Table 4.15 T-test results comparing C.capreolus data from surfaces scale limited using only a filter and nesting index. Tests were carried out separately, across 21 areal texture parameters, for each combination of filter type, and nesting index applied to surfaces. Tests results have only been reported where significant results were recorded. 181

Table 5.1 Full specimen list, including all specimen numbers, taxonomic information, teeth used, collection locations, gender (where known), dietary categories, host institutions, and date of death (where known). 197

Table 5.2 Descriptions for all ISO 25178-2 areal texture parameters used in this paper. Parameters Sal and Std were excluded from analyses as they rarely produced normally distributed data even when log transformed. Ssk was also excluded as it displayed low normality and regularly returned negative values which could not be log transformed. For detailed parameter descriptions see Purnell et al (2013). 202

Table 5.3 Full list of Scale Sensitive Fractal Analysis (SSFA) parameters, including brief descriptions (after Ungar et al (2003) and Scott et al (2006)). Parameter Smc was excluded from analyses. For parameter details and information on methods of calculation see Scott et al (2006). 203

Table 5.4 Codes for Non-Resampled and Resampled datasets and sub-datasets used in this paper. 204

Table 5.5 Descriptions of all seven interpolation methods tested for resampling the µm/pixel values of datafiles (further information can be found at http://gwyddion.net/documentation/user-guide-en/interpolation.html). 205

Table 5.6 ANOVA carried out separately on each Non-Resampled sub-dataset for all SSFA and ISO 25178 parameters. F Ratio and p values are given for each test, and results are only reported where significant (α=0.05). All significant results were tested using the Benjimini-Hochberg method. 208

Table 5.7 Tukey HSD tests carried out separately on each Non-Resampled sub-dataset for all SSFA and ISO 25178 parameters. p values and connecting letters reports are given for each test, parameters are only reported where significant ANOVA results were recorded (Table 5.6). All significant results were tested using the Benjimini-Hochberg method. 213

Table 5.8 ANOVA carried out separately on each Resampled sub-dataset for all SSFA and ISO 25178 parameters. F Ratio and p values are given for each test, and results are only reported where significant (α=0.05). All significant results were tested using the Benjimini-Hochberg method. 214

Table 5.9 Tukey HSD tests carried out separately on each Resampled sub-dataset for all SSFA and ISO 25178 parameters. p values and connecting letters reports are given for each test, parameters are only reported where significant ANOVA results were recorded (Table 5.8). All significant results were tested using the Benjimini-Hochberg method. 217

Table 5.10 Linear Regression tests comparing all possible pairs of microscopes for all Non-Resampled data. Data for each parameter is tested separately and t-ratio and p values are given for the intercept and regression line of each comparison within each parameter. R^2 values are also reported for each comparisons within each parameter. Significant p values (α=0.05) are highlighted in red, and all significant results were tested using the Benjimini-Hochberg method. 228

Table 5.11 Linear Regression tests comparing all possible pairs of microscopes for all Resampled data. Data for each parameter is tested separately and t-ratio and p values are given for the intercept and regression line of each comparison within each parameter. R^2 values are also reported for each comparions within each parameter. Significant p values (α=0.05) are highlighted in red, and all significant results were tested using the Benjimini-Hochberg method. 232

Table 5.12 Intraclass Correlation tests comparing all possible pairs of microscopes for Non-Resampled (A.) and Resampled (B.) data. Data for each parameter is tested separately and probable error, intraclass correlation and interpretation are given in each case. The interpretation provides a measure of how well the classes are correlated (Cicchetti 1994), with classes based on the correlation result (Poor = 0 to 0.4, Fair = 0.4 to 0.59, Good = 0.6 to 0.74, and Excellent = 0.75 to 1). 233

Table 5.13 T-tests comparing Capreolus capreolus dietary groups, using only Non-Resampled data. Tests were carried out separately for each SSFA and ISO 25178 parameter, significant results are highlighted in bold 241

Table 5.14 T-tests comparing Archosargus probatocephalus dietary groups, using only Non-Resampled data. Tests were carried out separately for each SSFA and ISO 25178 parameter, significant results are highlighted in bold 242

Table 5.15 T-tests comparing Capreolus capreolus dietary groups, using only Resampled data. Tests were carried out separately for each SSFA and ISO 25178 parameter, significant results are highlighted in bold 243

Table 5.16 T-tests comparing Archosargus probatocephalus dietary groups, using only Resampled data. Tests were carried out separately for each SSFA and ISO 25178 parameter, significant results are highlighted in bold 244

Table 5.17 Eigenvectors for PC1 and PC2 from the Principal Component Analyses comparing dietary groups within each microscope, using only Non-Resampled data. Results are given separately for A. Capreolus capreolus data, and B. Archosargus probatocephalus data.

Eigenvecors are coloured light grey where below 0.3, black between 0.3 and 0.4 and highlighted bold when above 0.4. 246

Table 5.18 Eigenvectors for PC1 and PC2 from the Principal Component Analyses comparing dietary groups within each microscope, using only Resampled data. Results are given separately for A. Capreolus capreolus data, and B. Archosargus probatocephalus data. Eigenvecors are coloured light grey where below 0.3, black between 0.3 and 0.4 and highlighted bold when above 0.4. 249

Figure Captions

Figure 1.1 Sample locations of four quadrants from the rough (a) and smooth (b) tooth surfaces (optical images). (c) - (h), digital elevation models of levelled surface data from original surface and examples of replicas made using different impression media for SE quadrant, for rough (c, e, g) and smooth (d, f, h) surfaces. (c) and (d) original surfaces; (e) and (f) replicas, President Jet medium body impression medium; (g) and (h) replicas, Microset impression medium. Scale bars in (a) and (b), 100µm. Digital elevation models all 110 x 145 µm. Vertical scales in µm. 17

Figure. 1.2: Numbers of significant differences (matched pair t-tests) between impression media and original tooth surfaces. With (a) data generated using ISO 25178-2 method and (b) data generated using SSFA method. Bars show the number of parameters that differ, (*) represents treatments where no significant results were recorded. For (a) data treatments (polynomial/spline/Gaussian filter) reflect different approaches to generation of scale-limited surfaces from which texture parameters are generated. R and S indicate whether data were generated from rough or smooth surfaces, respectively. (a) The dotted line on the Y axis (labelled 5%) represents the expected number of false positive results per impression medium based on an average of 20.57 tests per impression medium, and α = 0.05. (a) and (b),The dotted line on the Y axis (labelled 25%) is used to compare numbers of significant results produced using the two different roughness parameterisation methods (ISO & SSFA). 23

Figure.1.3: Numbers of significant differences (matched pair t-tests, ISO 25178-2 parameters) between two moulds of the same compound and the original tooth surface. Bars show the number of parameters that differ, (*) represents treatments where no significant results were recorded. Moulds were created using either different operators (Speedex) or application methods (President Jet Light and Regular Body); four quadrants per tooth, broken down by data treatment. R and S indicate whether data were generated from rough or smooth surfaces, respectively. The dotted line on the Y axis (labelled 5%) represents the expected number of false positive results per impression medium based on an average of 20.57 tests per impression medium, and α = 0.05. 25

Figure.1.4 Absolute differences between original surface and each impression medium for the rough surface (a), and the smooth surface (b), generated using the ISO 25178-2 parameterisation method. Points show the actual differences from the original surface, with zero indicating the same value for replica and original surface. Each quadrant has been given a specific colour (NE=Blue, SE=Green, SW=Red, NW=Orange). Lines connecting points horizontally show mean difference. Whiskers represent the range of the data. For convenience, plot shows

only data collected using a 5th order of polynomial and a robust Gaussian filter, and only parameters returning significant differences for at least one impression medium on the rough surface. Other data are included in Figure1.5 (below)...... 28

Figure 1.5 Absolute differences between original surface and each impression medium for the rough surface (a), and the smooth surface (b), generated using the ISO 25178-2 parameterisation method. Points show the actual differences from the original surface, with zero indicating the same value for replica and original surface. Each quadrant has been given a specific colour (NE=Blue, SE=Green, SW=Red, NW=Orange). Lines connecting points horizontally show mean difference. Whiskers represent the range of the data. For convenience, plot shows only data collected using a 5th order of polynomial and a robust Gaussian filter, and only parameters not returning significant differences for at least one impression medium on the rough surface. 29

Figure 1.6 Absolute differences between original surface and each impression medium for the rough surface (a), and the smooth surface (b), generated using the SSFA parameterisation method. Points show the actual differences from the original surface, with zero indicating the same value for replica and original surface. Each quadrant has been given a specific colour (NE=Blue, SE=Green, SW=Red, NW=Orange). Lines connecting points horizontally show mean difference, with all original tooth values set to zero. Whiskers represent the range of the data. 30

Figure.1.7 Magnitude of differences in texture parameters between impression media compared to the magnitude of differences between dietary ecotypes of Archosargus probatocephalus. Only seven ISO 25178-2 parameters (Sdq, Sdr, Vmc, Vvv, Sk, Smr1, and Sa) were used, as these were the only ones to differ significantly between the two Archosargus probatocephalus dietary populations (Darras 2012). The boxes show those parameters where differences between replica surfaces and the original tooth surfaces exceed those reflecting dietary differences; all possible pairwise comparisons between impression media and the original tooth surfaces were assessed. Whether a parameter value exceeds the dietary difference is calculated by comparing the median value of differences between surfaces (e.g. between the original specimen and Speedex) with the difference between the median value of each the dietary ecotypes. Information towards the lower left shows results for the rough surface, information toward the upper right for the smooth surface. The parameter Sdq is not shown because it exceeds the value for the dietary difference in 27 of 28 comparisons on both surfaces and thus tells us nothing about the relative potential of different impression media to introduce bias into the results of dietary analysis. Highlighted cells represent comparisons

where no difference equalled or exceeded that expected from two dietary populations (not including Sdq). 35

Figure 1.8 Magnitude of differences in texture parameters between impression media compared to the magnitude of differences between individuals in two populations (dietary ecotypes) of Archosargus probatocephalus (compared to smooth tooth surface). The boxes show those parameters where differences between replica surfaces and original tooth surfaces exceed those between individuals in a population; all possible pairwise comparisons between impression media and original tooth surfaces were assessed. Both fish populations are from Florida, USA: Indian River lagoon population is more herbivorous, while Port Canaveral lagoon population consumes and crushes more hard-shelled prey. Only seven ISO 25178-2 parameters (Sdq, Sdr, Vmc, Vvv, Sk, Smr1, and Sa) were compared (the only ones to differ significantly between the two A.probatocephalus populations (Purnell and Darras 2015)). Whether a parameter value exceeds the dietary difference is calculated by comparing the median value of differences between surfaces (e.g. between original specimen and Speedex) with the median value of differences between individuals in each population. Lower left shows results for the comparisons with the Indian River population, upper right for the Port Canaveral population. The parameter Sdq is not shown because it exceeds the value for the dietary difference in almost all comparisons, telling us nothing about the relative potential of different impression media to introduce bias. Highlighted cells represent comparisons where no difference equalled or exceeded that expected from within a wild population (not including Sdq). 36

Figure 2.1 Phylogeny of stem cetacean species included in this paper. Phylogeny on the left reproduced based on Gol'din et al (2014). The phylogeny on the right is a consensus tree based on a number of published phylogenies (Uhen and Gingerich 2001, Geisler et al 2005, Uhen et al 2008, Bianucci and Gingerich 2011, Uhen et al 2011, Gatesy et al 2013, Gol'din et al 2014). Red lines separate stem cetacean "Families". 47

Figure 2.2 Matrix displaying all parameters where pairwise Tukey HSD tests retuned significant results between each combination of dietary classes. Stars represent tests where variances were not equal, and so the results of Steel Dwass All Pairs tests are reported instead. For parameter abbreviations see Table 2.3 and Table 2.4. 63

Figure 2.3 Linear Discriminant Analysis (LDA) for all extant Odontocete and Pinniped specimens. LDA carried out using forward stepwise variable selection, 12 parameters were selected at which point all canonical axes returned significant results for Wilks Lambda tests (CA1 - p=<0.0001, CA2 - p=0.0001, CA3 – p=0.0054). Blue crosses = Fish Eaters, red triangles =

Cephalopod Eaters, grey circles = Invertebrate Eaters, and green squares = Amniote Eaters. Convex hull colours correspond to the symbol colour for each dietary class. 65

Figure 2.4 Linear Discriminant Analysis (LDA) comparing 4 dietary sub-groups (Fish Eating pinnipeds, Fish Eating odontocetes, Cephalopod Eating pinnipeds, and Cephalopod Eating odontocetes). CA1 Wilks' Lambda p = 0.0023, CA2 p = 0.0121, CA3 p = 0.0416. Points and convex hulls coloured based on dietary groupings (Red – Cephalopod Eaters, Blue – Fish Eaters). Labels indicate dietary and taxonomic affinities. Parameters with the greatest scoring coefficients for CA1 are Sq -88.8, and Sa 93.6, for CA2 – Sdr -53.2, and Asfc 68.8, and for CA3 – Sq -299.5, Sdr -313.6, Sa 373.8, and Asfc 280.5. 70

Figure 3.1 Plot of Nitrogen ($\delta^{15}N$) and Carbon ($\delta^{13}C$) Isotope values for 13 Orcinus orca specimens. $\delta^{13}C$ (non-seuss corrected) is on the X-axis, and $\delta^{15}N$ is on the Y-axis. Both are given in parts per thousand (‰). All specimens are denoted by black triangles, while bars represent the isotope ranges of prey items. Figure modified from Foote et al (2013b). 87

Figure 3.2 Diagram of Orcinus orca right dentary, and an individual tooth. The jaw, from specimen NMS 1990.86, is shown in both lateral and dorsal views, the individual tooth is shown only in apical view. Tooth positions are numbered along the jaw and teeth up to position 10 are separated into front, middle and rear teeth. Data for comparisons between location within a tooth, tooth position, and jaw type were collected in 3x2 grids as shown on the individual tooth. 89

Figure 3.3 Tukey HSD test results comparing all possible combinations of data by location within a tooth and tooth position, for two Orcinus orca specimens. All data for NMS Z.2015.172.148 can be found on the bottom left of the figure, and all data for NMS 1956.36.56 can be found on the top right. ISO 25178 Parameter abbreviations are given where a significant Tukey HSD result was recorded for the given comparison (α = 0.05). Green boxes denote comparisons where one or fewer significant results across all parameters were recorded. 100

Figure 3.4 Plots of PCA results (PC1 and PC2) for comparisons between locations within a tooth. Separate PCA are presented for each tooth position and each specimen. Data for NMS Z.2015.172.148 can be seen on the left, and data for NMS 1956.36.56 on the right. Labial area data points are presented as red diamonds, mesial data points as blue triangles, and lingual data points as green squares. Convex hulls are coloured to match that of the data points they represent. PCA for both specimens generated using all parameters returning significant results from Blocked ANOVA tests (Table 3.4). 104

Figure 3.5 Plots of PCA results (PC1 and PC2) for comparisons between tooth positions. Separate PCA are presented for each location within a tooth and each specimen. Data for NMS Z.2015.172.148 can be seen on the left, and data for NMS 1956.36.56 on the right. Front tooth data points are presented as red diamonds, middle tooth data points as blue triangles, and rear tooth data points as green squares. Convex hulls are coloured to match that of the data points they represent. PCA for both specimens generated using all parameters returning significant results from Blocked ANOVA tests (Table 3.5). 105

Figure 3.6 PCA plot for the comparison of jaw types (left, and right, dentary, and maxilla) based on data from front teeth only. Left dentary data points are presented as red diamonds, left maxillary data points as blue triangles, right dentary data points as Green squares, and right maxillary data points as orange circles. Convex hulls are coloured to match that of the data points they represent. PCA based on all parameters returning significant results from ANOVA (Table 3.6.a). 106

Figure 3.7 PCA plot for the comparison of jaw types (left, and right, dentary, and maxilla) based on data from middle teeth only. Left dentary data points are presented as red diamonds, left maxillary data points as blue triangles, right dentary data points as Green squares, and right maxillary data points as orange circles. Convex hulls are coloured to match that of the data points they represent. PCA based on all parameters returning significant results from ANOVA (Table 3.6.b). 107

Figure 3.8 LDA plots of comparisons between Orcinus orca dietary groups for A). front teeth, and B). middle teeth. LDA carried out using stepwise variable selection. Parameters used were A). Str, Ssc, Smr1, Smr2, HAsfc 9x9, and HAsfc 10x10, and B). Sq, Str, Ssc, and HAsfc 2x2 (for all parameter descriptions see Table 3.2 and Table 3.3). For both analyses misclassification was 0%, and Wilks' Lambda test results were p=0.0305 for front teeth, and p=0.0017 for middle teeth. Marine Mammal Eater data points are represented by red triangles, and Herring Eater data points are represented by blue crosses. Two circles are presented for each dietary group, coloured the same as the data points for each. The outer circle represents the normal ellipse region estimated to contain 50% of the population for that group, and the inner circle represents the 95% confidence region to contain the mean of the group. Black arrows point towards those specimens where diet was predicted (i.e. those without associated isotope data). 114

Figure 3.9 PCA plot comparing Orcinus orca dietary groups, using only data from middle teeth. This figure includes data from specimens where dietary class was predicted using LDA. The PCA is based on parameters Str, Sdq, Sdr, and Asfc (those parameters returning significant results

from T-tests between the two dietary groups, using middle teeth data). Marine Mammal Eater data points are represented by red triangles, Herring Eater data points by blue crosses, convex hulls coloured to match the data points their range represents...... 117

Figure 4.1 Representation of the elements making up 3D surface texture. The original surface is presented, followed by surface form, then surface waviness, and finally surface roughness. All images are digital elevation models (DEM) of the same surface exported from Surfstand (software version 5.0.0), and imaged in Gwyddion (software version 2.42). The operator used was a 2nd order polynomial, and the filter was a spline filter, with a 0.8mm nesting index for surface waviness, and a 0.025mm nesting index for surface roughness. DEM colours are not at the same scale...... 126

Figure 4.2 Schematic representation of scale limiting procedures. A. is the original surface with no operators or filters applied. B. Is the primary surface, where extremely small scale features have been removed using an S – Filter. C. is the surface containing both roughness and waviness, where an S –Filter, and a form removing operator have been applied. And D. is the roughness surface produced by applying a filter with set nesting index to the roughness and waviness surface. Surface feature wavelength increases from left to right on the schematic. 127

Figure 4.3 Representations of data collection locations on both phocid and Capreolus capreolus teeth. With orientation information included and sample area highlighted green...... 134

Figure 4.4 Digital Elevation Models (DEMs) showing the form removed by different operators (orders of polynomial) applied to an original surface. All DEMs were produced in Surfstand (software version 5.0.0), and imaged in Gwyddion (software version 2.42). All images are of the same surface treated in different ways. DEM colours are not all to the same scale...... 136

Figure 4.5 Schematic results of Tukey HSD tests comparing data from C.capreolus surfaces scale limited using different operators (2^{nd}-11^{th} polynomial orders). Parameter abbreviations are given for comparisons where a significant test results was recorded. Parameter abbreviations are coloured based on the settings for which those parameters are significant (see key). Comparisons within bramble leaf eaters – top right, and comparisons within acorn eaters – bottom left. 147

Figure 4.6 Schematic results of Tukey HSD tests comparing data from phocid surfaces scale limited using different operators (2^{nd}-11^{th} polynomial orders). Parameter abbreviations are given for comparisons where a significant test results was recorded. Parameter abbreviations are coloured based on the settings for which those parameters are significant (see key).

Comparisons within bramble leaf eaters – top right, and comparisons within acorn eaters – bottom left. 148

Figure 4.7 Schematic results of Tukey HSD tests comparing data from surfaces scale limited using different filter types (robust Gaussian, robust wavelet, and spline). Parameter abbreviations are given for comparisons where a significant test results was recorded. Individual schemes are presented separately for data from surfaces scale limited using each operator. Results are presented in two sets of schemes, A.) Capreolus capreolus: comparisons within bramble leaf eaters – top right of each scheme, and comparisons within acorn eaters – bottom left, and B.) Phocids: comparisons within invertebrate eaters – top right of each scheme, and comparisons within fish eaters – bottom left. 152

Figure 4.8 Schematic results of Tukey HSD tests for parameters returning significant results from 2-way ANOVA tests between data generated using different nesting indices and data generated using different orders of polynomial. For each possible comparison parameter abbreviations are given when a significant Tukey HSD test results was recorded. All surfaces scale limited using a robust Gaussian filter. Only Phocidae data has been tested, and comparisons within invertebrate eater data are on the top right, and comparisons within fish eater data are on the bottom left. 156

Figure 4.9 Total numbers of significant T-test results recorded when comparing dietary groups A.) Phocid fish eaters compared to invertebrate eaters, B.) Capreolus capreolus acorn eaters compared to bramble leaf eaters. Data for each filter type was tested separately and represented by different colours (see key). Data for each order of polynomial was tested separately, represented by the X-axis. 159

Figure 4.10 Magnitudes of difference between C.capreolus dietary groups for all eight parameters where significant differences between dietary groups were recorded (T-tests). Data are presented separately for surfaces scale limited using different operators, filters and nesting indices. Surfaces returning the largest rank magnitude of difference across all parameters are highlighted red, and surfaces producing the greatest number parameters showing difference between dietary groups are highlighted yellow. Those surfaces producing both the largest rank magnitude of difference across all parameters, and the greatest number parameters showing difference between dietary groups are highlighted green. 163

Figure 4.11 Magnitudes of difference between Phocid dietary groups for all sixteen parameters where significant differences between dietary groups were recorded (T-tests). Parameters are only included where at least one third of surfaces showed a significant difference between

dietary groups. Data are presented separately for surfaces scale limited using different operators, filters and nesting indices. Surfaces returning the largest rank magnitude of difference across all parameters are highlighted red, and surfaces producing the greatest number parameters showing difference between dietary groups are highlighted yellow. 164

Figure 4.12 PCA analyses comparing two Capreolus capreolus dietary populations (Acorn Eaters and Bramble Leaf Eaters) using the same parameters for each analysis (Sq, Sv, Sz, Sdq, Sdr, Vvv, Svk, and S5z, for parameter descriptions see Table 4.3). Tests were carried out separately for each surface scale limited using a different combination of operator, filter and nesting index. Points are coloured consistently by dietary group (Acorn eaters – Orange, Bramble Leaf Eaters – Green). Each specimen number is represented by a different symbol, consistent across all tests. Only data from 5 different orders of polynomial across all filter types and nesting indices are shown. Percentage of variance explained by each axes presented for all analyses. 166

Figure 4.13 PCA analyses comparing two Phocid dietary populations (Fish Eaters and Invertebrate Eaters) using the same parameters for each analysis (Sq, Sp, Sv, Sz, Str, Sdq, Sdr, Vmp, Vmc, Vvc, Vvv, Spk, Sk, Svk, S5z, and Sa, for parameter descriptions see Table 4.3). Tests were carried out separately for each surface scale limited using a different combination of operator, filter and nesting index. Points are coloured consistently by dietary group (Fish eaters – Blue, Invertebrate Eaters – Red). Each specimen number is represented by a different symbol, consistent across all tests. Only data from 5 different orders of polynomial across all filter types and nesting indices are shown. Percentage of variance explained by each axes presented for all analyses. 167

Figure 4.14 PCA comparing dietary groups, separately for C.capreolus and Phocid populations. For each comparison PCA analyses are split into those containing the maximum number of parameters where significant differences between the dietary populations were recorded, and those using the actual number recorded for each individual surface, so that number of parameters vary between analyses. Tests were carried out separately for each surface scale limited using a different combination of operator, filter and nesting index. Points are coloured consistently by dietary group (C.capreolus: Acorn Eaters – Orange, Bramble Leaf Eaters – Green; Phocid: Fish Eaters – Blue, Invertebrate Eaters – Red). Each specimen number is represented by a different symbol, consistent across all tests within each pair of dietary groups. Only analyses of data from surfaces scale limited using a robust Gaussian filter and 0.025mm nesting index are shown. Percentage of variance explained by each axes presented for each analyses. 171

Figure 4.15 PCA analysis comparing roughness parameter values between C.capreolus dietary groups. PCA is based on eight parameters (Sq, Sv, Sz, Sdq, Sdr, Vvv, Svk, and S5z, for parameter descriptions see Table 4.3). Parameter Data generated from each surface is included for all specimens. Points are coloured consistently by dietary group (Acorn eaters – Orange, Bramble Leaf Eaters – Green). Each specimen number is represented by a different symbol, consistent across all tests. 173

Figure 4.16 PCA analysis comparing roughness parameter values between phocid dietary groups. PCA is based on sixteen parameters (Sq, Sp, Sv, Sz, Str, Sdq, Sdr, Vmp, Vmc, Vvc, Vvv, Spk, Sk, Svk, S5z, and Sa, for parameter descriptions see Table 4.3). Parameter Data generated from each surface is included for all specimens. Points are coloured consistently by dietary group (Acorn eaters – Orange, Bramble Leaf Eaters – Green). Each specimen number is represented by a different symbol, consistent across all tests. 174

Figure 4.17 PCA analyses comparing dietary groups, separately for Phocids and C.capreolus. Surfaces were only scale limited using a filter and nesting index, without a polynomial. Tests carried out separately for each surface. C.capreolus PCA is based on eight parameters (Sq, Sv, Sz, Sdq, Sdr, Vvv, Svk, and S5z), and Phocid PCA is based on sixteen (Sq, Sp, Sv, Sz, Str, Sdq, Sdr, Vmp, Vmc, Vvc, Vvv, Spk, Sk, Svk, S5z, and Sa, for parameter descriptions see Table 4.3). Points are coloured by dietary group (C.capreolus: Acorn Eaters – Orange, Bramble Leaf Eaters – Green; Phocids: Fish Eaters – Blue, Invertebrate Eaters – Red). Within each dietary group specimen numbers are represented by different symbols, consistently across all tests. Axes are consistent across PCA analyses within each dietary pair. Percentage of variance explained by each axes presented for all analyses. 182

Figure 5.1 Linear Discriminant Analysis for all Non-Resampled data, produced using eighteen 3D roughness parameters (Tfv, epLsar, HAsfc3x3, HAsfc 5x5, HAsfc6x6, HAsfc11x11, Sp, Sv, Sds, Str, Sdq, Ssc, Sdr, Vvv, Svk, Smr1, Smr2, S5z). Canonical Axis 1 (CA1, explains 87.96% of variance) and Canonical Axis 2 (CA2, explains 9.82% of variance) are shown. Points represent each specimen replicated for each of the four microscopes. For each microscope points, convex hulls and labels are consistently coloured. Sensofar Plμ = Blue Triangles, Sensofar Plμ neox = Orange Crosses, Alicona IFM = Pink Diamonds, and Mitaka PAFM = Green Circles. Misclassification is 4/88 samples (4.55%), Wilks Lambda test results for CA1 and CA2 = <.0001 in both cases. 219

Figure 5.2 Linear Discriminant Analysis for all Resampled data, produced using eighteen 3D roughness parameters (Tfv, epLsar, HAsfc3x3, HAsfc 5x5, HAsfc6x6, HAsfc11x11, Sp, Sv, Sds, Str, Sdq, Ssc, Sdr, Vvv, Svk, Smr1, Smr2, S5z), stepwise parameter selection was not used.

Canonical Axis 1 (CA1, explains 91.71% of variance) and Canonical Axis 2 (CA2, explains 7.42% of variance) are shown. Points represent each specimen replicated for each of the four microscopes. For each microscope points, convex hulls and labels are consistently coloured. Sensofar Plμ = Blue Triangles, Sensofar Plμ neox = Orange Crosses, Alicona IFM = Pink Diamonds, and Mitaka PAFM = Green Circles. Misclassification is 5/88 samples (5.68%), Wilks Lambda test results for CA1 and CA2 = <.0001 and 0.0005 respectively. 221

Figure 5.3 Bland-Altman plots of 3D roughness parameter data, comparing pairs of microscopes. All Non-Resampled data for parameters HAsfc2x2 to HAsfc 11x11 are included. X-axis shows the mean of each datafile collected on the two microscopes. Y-axis shows the difference between each datafile. Microscope names at the top are compared to microscope names on the right hand side, with figures representing their comparison where the two cross. The R^2, intercept and Regression test results are given for each plot, black dashed line = zero line, solid red line = mean of Y-axis, dashed red line = 95% confidence intervals of mean, green line = regression line. 234

Figure 5.4 Bland-Altman plots of 3D roughness parameter data, comparing pairs of microscopes. All Non-Resampled data for parameters Sq, Sp, Sv, Sa, Spk, Sk, Svk, S5z are included. X-axis shows the mean of each datafile collected on the two microscopes. Y-axis shows the difference between each datafile. Microscope names at the top are compared to microscope names on the right hand side, with figures representing their comparison where the two cross. The R^2, intercept and Regression test results are given for each plot, black dashed line = zero line, solid red line = mean of Y-axis, dashed red line = 95% confidence intervals of mean, green line = regression line. 235

Figure 5.5 Bland-Altman plots of 3D roughness parameter data, comparing pairs of microscopes. All Non-Resampled data for parameters Vmp, Vmc, Vvc, Vvv are included. X-axis shows the mean of each datafile collected on the two microscopes. Y-axis shows the difference between each datafile. Microscope names at the top are compared to microscope names on the right hand side, with figures representing their comparison where the two cross. The R^2, intercept and Regression test results are given for each plot, black dashed line = zero line, solid red line = mean of Y-axis, dashed red line = 95% confidence intervals of mean, green line = regression line. 236

Figure 5.6 Bland-Altman plots of 3D roughness parameter data, comparing pairs of microscopes. All Resampled data for parameters HAsfc2x2 to HAsfc 11x11 are included. X-axis shows the mean of each datafile collected on the two microscopes. Y-axis shows the difference between each datafile. Microscope names at the top are compared to microscope names on

the right hand side, with figures representing their comparison where the two cross. The R^2, intercept and Regression test results are given for each plot, black dashed line = zero line, solid red line = mean of Y-axis, dashed red line = 95% confidence intervals of mean, green line = regression line. 237

Figure 5.7 Bland-Altman plots of 3D roughness parameter data, comparing pairs of microscopes. All Resampled data for parameters Sq, Sp, Sv, Sa, Spk, Sk, Svk, S5z are included. X-axis shows the mean of each datafile collected on the two microscopes. Y-axis shows the difference between each datafile. Microscope names at the top are compared to microscope names on the right hand side, with figures representing their comparison where the two cross. The R^2, intercept and Regression test results are given for each plot, black dashed line = zero line, solid red line = mean of Y-axis, dashed red line = 95% confidence intervals of mean, green line = regression line. 238

Figure 5.8 Bland-Altman plots of 3D roughness parameter data, comparing pairs of microscopes. All Resampled data for parameters Vmp, Vmc, Vvc, Vvv are included. X-axis shows the mean of each datafile collected on the two microscopes. Y-axis shows the difference between each datafile. Microscope names at the top are compared to microscope names on the right hand side, with figures representing their comparison where the two cross. The R^2, intercept and Regression test results are given for each plot, black dashed line = zero line, solid red line = mean of Y-axis, dashed red line = 95% confidence intervals of mean, green line = regression line. 239

Figure 5.9 Principal Component Analysis (PCA) carried out on Non-Resampled data. Top four PCA carried out on Capreolus capreolus Non-Resampled data, separately for data from each microscope, using parameters Asfc, Sq, Sp, Sv, Sz, Sdq, Sdr, Vvv, Svk, and S5z (parameters showing significant difference between dietary groups). Bottom four PCA carried out on Archosargus probatocephalus Non-Resampled data, separately for data from each microscope, using parameters epLsar, HAsfc2x2 to HAsfc11x11, Sku, Sv, and Str. For all PCA analyses the proportion of variance explained by each axis is presented within the graph, and dietary groups have points, convex hulls and labels with consistent colour coding. 245

Figure 5.10 Principal Component Analysis (PCA) carried out on Resampled data. Top four PCA carried out on Capreolus capreolus Resampled data, separately for data from each microscope, using parameters Asfc, Sq, Sv, Sz, Sdq, Sdr, Vvv, Svk, S5z, and Sa (parameters showing significant difference between dietary groups). Bottom four PCA carried out on Archosargus probatocephalus Resampled data, separately for data from each microscope, using parameters epLsar, Hasfc2x2 to HAsfc11x11, Sp, and Sv. For all PCA analyses the proportion of variance

explained by each axis is presented within the graph, and dietary groups have points, convex hulls and labels with consistent colour coding. 248

Figure 5.11 Comparisons of the magnitude of difference between microscopes with the known magnitude of difference between Capreolus capreolus dietary groups. For each comparison of microscopes, where the difference for a specific parameter exceeds the difference between dietary groups that parameter is listed. Results on the bottom left are for Non-Resampled data, results on the top right are for Resampled data. Only parameters where significant differences between dietary groups were recorded for both Non-Resampled and Resampled data have been tested (Table 5.15 and Table 5.17). 251

Figure 5.12 Comparisons of the magnitude of difference between microscopes with the known magnitude of difference between Archosargus probatocephalus dietary groups. For each comparison of microscopes, where the difference for a specific parameter exceeds the difference between dietary groups that parameter is listed. Results on the bottom left are for Non-Resampled data, results on the top right are for Resampled data. Only parameters where significant differences between dietary groups were recorded for both Non-Resampled and Resampled data have been tested (Table 5.16 and Table 5.18). 252

Introduction

The act of chewing and processing food leads to microscopic scratches and pits forming on tooth surfaces. We refer to this type of damage as microwear (as opposed to macrowear or mesowear which pertain to larger scale tooth wear) and it can provide direct evidence of tooth movements and the mechanical properties of food consumed. The first instance of scratches on tooth surfaces being described as a result of tooth interaction came from a 1926 study into multituberculates (Mammalia: Multituberculata) where scratch direction on tooth surfaces was used to infer chewing movements (Simpson 1926). Dahlberg and Kinzey (1962) were the first to apply this idea to a dietary study, where scratches on prehistoric human teeth were inspected under a binocular light microscope and distinct patterns were inferred to reflect dietary differences. This technique was adapted in the mid-1970s for use in archaeology (Keeley 1974, Odell 1975), investigating chipped stone tools. However, the most famous example of early microwear analysis was published in 1978, when it was used to separate the diet of two Hyrax species based on the microtextural structure of their tooth surfaces derived from two dimensional (2D) SEM images (Walker et al. 1978). Since then studies of 2D tooth microwear have become a common and useful tool for investigating diet in a range of vertebrate taxa. These have all used SEM or stereoscopic light microscope images of tooth surfaces to look at and score pits and scratches on tooth surfaces. Groups of animals studied include anthropoids (Ungar 1996), fish (Purnell et al. 2006), armadillos and tree sloths (Green 2009b, a), and dinosaurs (Williams et al. 2009, Whitlock 2011) among many others. However, it has been suggested that these methods are open to operator error, with variable results when different operators collect data, and when the same operator collects data more than once over an extended period of time (Grine et al. 2002, Galbany et al. 2005, Purnell et al. 2006, Mihlbachler et al. 2012, DeSantis et al. 2013). This is of some concern as it produces lack of comparability between studies. It was suggested that a fully automated approach would remove many of these problems completely (Galbany et al. 2005).

In 2003 a new fully automated method for studying dietary variation was developed using parameters generated from 3D tooth surface roughness (Ungar et al. 2003). This technique was termed Dental Microwear Texture Analysis (DMTA) but is also known as Quantitative Analysis of 3D Tooth Surface Textures, and uses a method called Scale Sensitive Fractal Analysis (SSFA) to parameterise tooth surface roughness (small scale features of surface texture). This method was based on the principles of scratches and pits from 2D microwear analysis. SSFA applies a fractal net to the 3D surface at various scales to determine roughness, scoring surface anisotropy, complexity and heterogeneity. This is operator independent and yields objective and repeatable quantification of surface characteristics. More recently other studies have used an ISO standard (ISO 25178-2) method (International Organization for Standardization 2012) for the same purpose (Purnell et al. 2012, Purnell et al. 2013, Schulz et al. 2013a, Gill et al. 2014, Purnell and Darras 2015), which was originally designed as a methodology in engineering (Jiang et al. 2007). Quantitative analysis of tooth surface textures was first put into use studying intraspecific dietary variation in fossil hominins (Scott et al. 2005), and since its first uses this technique has diversified into several distinct methods of data collection and surface roughness calculation. A number of studies have now used 3D surface roughness data from tooth surfaces to investigate dietary hypotheses for extinct and extant taxa, including primates (Merceron et al. 2006, Ungar et al. 2008, Merceron et al. 2009, Ungar and Sponheimer 2011, Calandra et al. 2012, Krueger and Ungar 2012, Scott et al. 2012, Daegling et al. 2013, Delezene et al. 2013, Gogarten and Grine 2013, Williams 2013, Shearer et al. 2015), modern humans (El Zaatari and Hublin 2014), carnivores (Schubert et al. 2010, DeSantis et al. 2012, DeSantis and Haupt 2014), hoofed mammals (Ungar et al. 2007, Merceron et al. 2010, Schulz et al. 2010, Schulz et al. 2013a, Winkler et al. 2013, Merceron et al. 2014, Gailer et al. 2016), lagomorphs (Schulz et al. 2013b), fish (Purnell et al. 2012, Purnell and Darras 2015), bears (Donohue et al. 2013), rodents (Caporale and Ungar 2016), xenarthrans (Haupt et al. 2013), early stem mammals (Gill et al. 2014), and bats (Purnell et al. 2013). A full review of this technique was published by Calandra and Merceron (2016) in which the authors show the utility of DMTA for dietary analyses in both fossil and modern animals.

A recent study (Lucas et al. 2013) and a review that followed it (Wood 2013) have argued against the use of microwear to investigate diet. Using hominin tooth surfaces, they suggest the marks on their teeth cannot be caused by damage from food items, because they show insufficient hardness to directly abrade enamel. Instead they suggest food items would only be able to displace surface material, which they do not consider as tooth "wear". However, this study is based on simple methodologies. They have used a contact pressure of 2 Newtons, several orders of magnitude lower than those found in human and human ancestor jaws (Wroe et al. 2010). While for a single contact point this makes sense in principle, the pressures they have used are so low as to be negligible. They have also only tested a single contact moment, which hides the effect of a lifetime of chewing food on an enamel surface. This suggests the results are only applicable to very simple principles of microwear and require an acceptance of the author's ideas surrounding what actually constitutes surface "wear". This has now been experimentally refuted by Xia et al. (2015), where phytoliths were shown to abrade enamel under conditions closely mimicking the action of chewing. This is due to the way in which enamel is formed, by "glued together" (protein "glue") hydroxyapatite crystals, where less force is needed to break the bonds and cause wear than for standard metal surfaces.

Three independent studies have shown that 3D surface roughness data provides at least the same level of information as 2D data, if not more, without the issue of operator bias (Scott et al. 2006, Purnell et al. 2012, DeSantis et al. 2013). These studies compared results from data obtained using 2D analytical techniques with data from 3D techniques, each using different methodologies for collecting and recording 3D surface roughness data. As such, dental microwear texture analysis at the sub-micron scale offers a robust and repeatable way of investigating differences in tooth surface microwear caused by diet. However, because methods for collecting tooth replicas, generating 3D data files, and treating 3D data vary, we do not yet know what effect these differences in surface replication, data acquisition, and data processing have on results. For example, some studies have used different moulding compounds to replicate surfaces prior to data collection (Ungar et al. 2010, Purnell and Darras 2015). Different microscopes have also been employed by different research groups

when carrying out quantitative analysis of 3D tooth surface textures, including focus variation microscopy (Purnell et al. 2013, Gill et al. 2014), confocal microscopy (Scott et al. 2009, DeSantis et al. 2012), and a small number have also using Interferometry (Estebaranz et al. 2007, Merceron et al. 2014). There is also variability within just the ISO 25178-2 method, where surfaces must be scale limited (large wavelength information removed) before parameters can be calculated from a surface. Different studies have scale limited surfaces, each applying a different operator and filter to the surface prior to parameter calculation (Calandra et al. 2012, Purnell et al. 2013). Because methodological differences have not yet been properly investigated it is currently not possible to fully compare results from different studies of 3D microwear.

Another issue present in analyses of 3D tooth surface texture is the bias in groups of animals studied. The majority of dietary analyses carried out using tooth surface textures have focussed on terrestrial mammals, either primates (modern and fossil, including close human ancestors) (Scott et al. 2005), or ungulates (Merceron et al. 2014), with a growing number of studies focussed on terrestrial carnivores (mostly big cats) (DeSantis and Haupt 2014). This is due to the research interests of the small number of groups using quantitative analysis of tooth surface textures. This focus means that the applicability of this method to a wider range of animals is currently unknown, especially those animals with teeth that differ significantly from heterodont, occlusal dentition (teeth which have different morphology depending on their position, i.e. incisors, canines, pre-molars and molars, and come together during chewing to form occlusal facets where food can be ground between teeth). This bias also means that aquatic vertebrates, especially mammals, have been poorly studied. Aquatic mammals also display non-occlusal and sometimes homodont dentition (all teeth have the same morphology). Currently no studies of dietary hypotheses using quantitative analysis of tooth surface textures for marine mammals exist. Most analyses using DMTA thus far have focussed on tooth enamel, with only one using dentine (Haupt et al. 2013). Marine mammals often have very thin enamel layers on their tooth surfaces, so that often all that is left on worn teeth is the dentine beneath (Loch et al. 2013b). As such they also offer a perfect case study into the use of this

material to determine dietary differences between animals with non-occlusal tooth facets.

Overview of Project

To address the question of variability between different experimental methods, I will be testing several hypotheses relating to methodological protocols. The aim is to make the results of these studies applicable to all current work on dietary analysis using quantified 3D areal surface texture data. Alternative methods of tooth surface replication, data collection, and data processing will be compared to determine their effects on results, and to compare their relative power for dietary discrimination.

I will also test the utility of 3D tooth surface texture analysis on marine mammals in two case studies. The first will cover a range of marine mammal species and determine the ability of our technique to differentiate diet between species, collecting data from tooth enamel, and further apply our results to extinct members of the cetacean clade to test the utility of 3D tooth surface texture analysis to determine diet in extinct species. The second case study will focus on North Atlantic Killer Whale (*Orcinus orca*) populations, where dietary differences have been indicated from isotope analysis (Foote et al. 2013b). Here tooth dentine will be used to test the consistency of tooth textures in *Orcinus orca* within, and between teeth in an individual, and the sensitivity of DMTA to dietary groups within this species.

The objectives of this PhD are to:

1. Determine any variation in accuracy or precision between different silicon based compounds used to mould teeth for use in 3D microtextural analysis
2. Test the sensitivity of 3D microtextural analysis of tooth textures to dietary differences in modern marine mammal species and their potential utility for detecting dietary habits in fossil cetacean species.

3. Test the variability of 3D tooth surface textures on tooth dentine of non-occlusal teeth in *Orcinus orca*, and the sensitivity of this technique to differentiate diet between North Atlantic *Orcinus orca* populations.
4. Investigate the effect of data processing (different operators and filters), used to produce scale limited surfaces from which roughness values are generated.
5. Compare the comparability of parameter values and sensitivity to known dietary differences when collecting 3D tooth surface texture data using different microscope technologies.

Thesis Structure

The results of testing methodological variability in Quantitative 3D tooth surface texture analysis and the applicability of this technique to marine mammals, both modern and fossil, using enamel and dentine tooth surfaces, are presented in the following chapters. Chapters are presented in the order they are intended to be published (see appendices for planned publications). As most analyses were carried out simultaneously the results of methodological chapters have not always been applied to those testing dietary hypotheses. As chapters are all intended to be published the studies have been referred to as "papers" throughout this PhD.

Chapter One investigates the effects of different moulding compounds on resulting 3D tooth surface textures and tests the null hypothesis that areal texture parameters obtained from replicas do not differ from those obtained from the original surface.

Chapter Two tests the sensitivity of 3D tooth surface texture analysis to differentiate diets in modern and fossil marine mammals, testing the hypotheses that microwear textures of tooth surfaces from extant marine mammals reflect their dietary habits; that phylogenetically distinct taxa (species of odontocete and species of pinniped) have microwear textures that reflect similarities in diet more than phylogenetic relationships, that analysis of microwear texture in stem cetaceans is

comparable to extant marine mammals; and that the hypotheses of diet derived from analysis of microwear texture support hypotheses of a unidirectional dietary transition through the stem cetacean lineage.

Chapter Three continues this theme, using dentine tooth surfaces to compare the variability of tooth surface textures within and between teeth in *Orcinus orca* individuals and test the sensitivity of 3D tooth surface textures to discriminate between different diets in this species. This chapter tests the null hypotheses that the 3D surface texture of *Orcinus orca* teeth does not vary significantly within a single tooth, between teeth from an individual, or between Jaw Types within an individual (i.e. upper left, lower right), and that 3D tooth surface textures cannot differentiate known dietary ecotypes of *Orcinus orca*.

Chapter Four returns to methodological variability, here the effect of different settings used to scale limit 3D surfaces prior to ISO 25178 parameter generation is tested. This chapter tests the hypotheses that application of different polynomials (operators) to remove long wavelength elements of surface form has no effect on the texture of resulting surfaces (as measured by ISO 25178-2 texture parameters); that application of different filter types (robust Gaussian, robust wavelet, and spline) has no effect on the texture of the resulting surface; that application of filters with different nesting indices (cut-off wavelengths) has no effect on the texture of the resulting surface; that when applying different operators, filters, and filters with different nesting indices to a surface, there is no interaction in their effect on resulting texture parameters, and that application of different filters and operators has no effect on the power of areal microwear texture analyses to detect dietary differences between samples.

Chapter Five continues the theme of testing methodological variability, comparing the absolute difference between parameter values generated from 3D tooth surface textures, and the difference in sensitivity to known dietary differences when 3D surface data are collected using different microscopes, covering multiple technological approaches. This will test the hypotheses that using different

microscopes will result in statistically significant differences in 3D microtextural parameter values (ISO 25178, and SSFA); that differences between microscopes are caused in large part by the effect of each microscope collecting data using different sampling resolutions and different field size, thus resampling datafiles collected from each microscope down to the lowest μm/pixel value across all microscopes and then reducing the field of view to the lowest across all microscopes will reduce or remove this difference; that when comparing dietary groups with known variation in the texture of their tooth surfaces, the sensitivity of data collected using different microscopes varies in its ability to detect this variation, so that certain microscopes are more sensitive than others to significant textural differences; and that this difference is mitigated by resampling the data down to the lowest μm/pixel resolution and field size, increasing the comparative sensitivity between microscopes.

“He longs to come back on land and sleep in the sun, with his root in the earth. But instead of that, he must roll and blow, out on the wild sea. And until he is allowed to come back on land, the creatures call him just Whale.”

- Ted Hughes, How the Whale Became; and Other Stories (1963)

Chapter 1: Accuracy and precision of silicon based impression media for quantitative areal texture analysis

This chapter modified from:

Goodall, R. H., Darras, L. P., & Purnell, M. A. (2015). Accuracy and precision of silicon based impression media for quantitative areal texture analysis. *Scientific reports, 5*.

Abstract

Areal surface texture analysis is becoming widespread across a diverse range of applications, from engineering to ecology. In many studies silicon based impression media are used to replicate surfaces, and the fidelity of replication defines the quality of data collected. However, while different investigators have used different impression media, the fidelity of surface replication has not been subjected to quantitative analysis based on areal texture data. Here we present the results of an analysis of the accuracy and precision with which different silicon based impression media of varying composition and viscosity replicate rough and smooth surfaces. Both accuracy and precision vary greatly between different media. High viscosity media tested show very low accuracy and precision, and most other compounds showed either the same pattern, or low accuracy and high precision, or low precision and high accuracy. Of the media tested, mid viscosity President Jet Regular Body and low viscosity President Jet Light Body (Coltène Whaledent) are the only compounds to show high levels of accuracy and precision on both surface types. Our results show that data acquired from different impression media are not comparable, supporting calls for greater standardisation of methods in areal texture analysis.

Introduction

Analysis and quantification of natural and manufactured surfaces at micrometric and sub-micrometric scales is becoming widespread. Applications range from engineering (Jiang et al. 2007) and superconductor technologies in particle accelerators (Jiang et al. 2007, Ge et al. 2011, Leach 2013, Xu et al. 2013), to archaeology (Bello et al. 2009, Bello et al. 2011, Evans et al. 2014), human skin surface

topography (Nardin et al. 2002, Rosén et al. 2005), and biomimetics (e.g. antifouling properties of bivalve shells (Bai et al. 2013)). In particular, quantitative areal surface texture analysis is increasingly applied to analysis of tooth wear as a tool for dietary niche separation (e.g. refs (Ungar et al. 2003, Scott et al. 2005, Scott et al. 2006, Ungar et al. 2008, Merceron et al. 2010, Ungar et al. 2010, Calandra et al. 2012, Purnell et al. 2012, Purnell et al. 2013, Schulz et al. 2013b, Gill et al. 2014)).

In many cases, rather than direct analysis of a surface, replicas are used. Often this is for practical and methodological reasons: some samples cannot be transported to the analytical facility, and some are too large to be accommodated by the measuring instruments; some types of surface are prone to movement during measurement (e.g. in vivo skin measurements); the properties of some surfaces (e.g. highly transparent or highly reflective) are unsuited for data collection using certain instruments. It is also possible for surface replication to be the solution to certain problems in dentistry caused by the inability of intra-oral dental scanners to collect data at high enough resolution (Austin et al. 2015). When replicas are used, data is acquired either from the replica or from a cast made using the replica. Obviously, the quality of data acquired in this way is entirely dependent on the fidelity of surface replication, with significant implications for the accuracy and precision of resulting measurements. Furthermore, if impression media differ in fidelity, this will preclude comparisons between studies based on data acquired using different media.

Clearly, investigations into the precision and accuracy of impression media used are important, but only a few such studies have been conducted (Chee and Donovan 1992, Xia et al. 1996, DeLong et al. 2001, Nilsson and Ohlsson 2001, Chung et al. 2003, Galbany et al. 2004, Rosén et al. 2005, Galbany et al. 2006, Williams et al. 2006, Fiorenza et al. 2009, Rodriguez et al. 2009, Bello et al. 2011, Bai et al. 2013), and none have undertaken systematic, statistical comparisons of areal textural parameters acquired from sub-micrometre resolution replicas, produced using a range of impression media with different properties.

Four studies have undertaken qualitative evaluations of impression media used to replicate tooth surfaces for microwear analysis. Two of these (Galbany et al. 2006, Williams et al. 2006) concluded from visual inspection of SEM images that low viscosity polyvinylsiloxane impression media produced the highest fidelity of replication. Another used similar methods to investigate the fidelity of three moulding compounds of varying viscosity from the President Jet product line (Coltène Whaledent) (Galbany et al. 2004), concluding that both the low and mid viscosity compounds showed high levels of accuracy. A fourth study, investigating accuracy in replicating skin surface textures (Rosén et al. 2005), used a small number of different impression media, and included no information about the media used. However, none of these studies quantified the variation in resulting surfaces.

Of the remaining studies, very few have directly compared the fidelity with which multiple different compounds replicate the same surface. Most have focussed on a small number of compounds, either to examine the most basic questions of whether a surface can be replicated accurately in the first place (Xia et al. 1996, Chung et al. 2003, Bai et al. 2013), or to make recommendations for standard laboratory procedures (Fiorenza et al. 2009). Others examined replication at far too coarse a scale (e.g. refs (Chee and Donovan 1992, DeLong et al. 2001)) to be of use in quantitative areal texture analysis. Analysis of the accuracy of different impression media at replicating sub-micrometre scale surface structure of cuts to bones and tooth surfaces created by tool use in early humans (Bello et al 2011) did not investigate compounds of different viscosity, used only two different impression media, and compared only four parameters (angles within cut marks, derived from 2D profile data). Rodriguez et al. (2009) also collected 2D profile data to investigate the influence of colour and transparency in a number of impression materials on the accuracy of surface reproduction.

Nilsson and Ohlsson (2001) investigated a range of impression media at the sub-micrometre scale using three dimensional surface texture data, comparing original surfaces to replicas. This study was limited to only three media types, and fidelity was

tested only using percentage deviations in surface texture, with no statistical testing of the significance of the differences.

Here we present the results of a quantitative analysis, based on 3D areal texture analysis (see Methods), of the variation in accuracy and precision between seven different silicon based impression media of varying composition and viscosity, investigating their ability to replicate rough and smooth surfaces. For each medium, we present statistical tests of the null hypothesis that areal texture parameters obtained from replicas do not differ from those obtained from the original surface.

Accuracy refers to the degree to which replica surfaces made using different impression media differ from the original surface. We test this through analysis of the number of areal texture parameters that differ significantly when replica and original surfaces are compared. Precision refers to the magnitude of differences for textural parameter values between replicas and original surfaces, and between replicas made using different impression media. As part of this we also test the degree to which differences between original and replica surfaces are systematic rather than random (i.e. do particular impression media consistently increase or decrease parameter values). A moulding compound that produces surfaces with a large number of differences from the original, but all of small magnitude, is inaccurate but relatively precise. An ideal moulding compound would produce surfaces with few significant differences, all of which would be small in magnitude - it would be both accurate and precise. Importantly, we also assess the degree to which imprecision and inaccuracy in replication arising from different moulding compounds are likely to bias the results of analysis. If inaccuracies and imprecision are large in relation to the number and magnitude of differences arising because of variation between different types of original surface under investigation, then their impact on analysis is likely to be significant.

Methods

Materials.

The lower right jaw (dentary) of an adult specimen of *Archosargus probatocephalus* (Perciformes: Sparidae) was dissected and mounted on a temporary base to facilitate manipulation. Two worn teeth with obvious variation in surface texture were selected from among the molariform teeth of the jaw: one exhibiting little wear, with a relatively smooth, enameloid surface; the other, more worn, with a relatively rough surface of exposed dentine (the enameloid having been worn away). A needle was used to scratch two intersecting perpendicular lines across the centre of each tooth surface, dividing it into quadrants. Within each quadrant a relocatable 100 x 145 µm area was identified, based on recognisable surface features, so that data could be collected from the same location on the replicated surfaces (Figure 1.1; areas designated NE, SE, SW, NW). Before the moulds used in this study were collected, tooth surfaces were cleaned by applying a random light body impression medium to the surfaces, which was then discarded.

Seven impression media were selected, representing different viscosity levels (Table 1.1). Four are polyvinylsiloxane compounds, two room temperature vulcanising (RTV) rubber compounds, and one heat accelerated RTV compound. Moulds were taken using each of the different media in a random order. Some media allow use of an applicator gun, which standardizes the mixing of two-components by extruding them through a helical nozzle; others required the body and actuator components to be mixed and applied manually.

For each medium we tested accuracy and precision of replication, and for three media we also tested the effect of how they were applied (manual versus applicator gun, and application by different operators). The latter test was based on moulds taken using three different impression media, representing the compounds currently used in dietary microwear analysis: two moulds of manually mixed Speedex, each made by a different operator, to test for effects of variability between operators; two

moulds of President Jet Light Body, one applied to the surface using the applicator gun, the other applied manually; two moulds of President Jet Regular Body, one applied to the surface using the applicator gun, the other applied manually. Manual versus applicator comparison was not possible with Speedex, because an applicator version is not available.

Impression Media	Application	Viscosity Level	Manufacturer	Colour
Speedex Light Body	Manual	Low	Coltène-Whaledent	Blue
President Jet Light Body	Applicator Gun	Low	Coltène-Whaledent	Green
MM913	Manual	Low	ACC Silicones	Transparent
Accutrans	Applicator Gun	Low	Coltène-Whaledent	Brown
President Jet Regular Body	Applicator Gun	Medium	Coltène-Whaledent	Blue
Microset 101RF	Applicator Gun	High	Microset Products Ltd	Black
MM240TV	Manual	High	ACC Silicones	Light Blue

Table 1.1 *Details of all seven silicon based impression media used in this study. Speedex, President Jet Light and Regular Body, and Accutrans are polyvinylsiloxane compounds. MM913 and MM240TV are room temperature vulcanising (RTV) rubber compounds, and Microset 101RF is a heat accelerated RTV rubber compound.*

Epoxy casts were produced from each mould using EpoTek 320LV. In many studies, particularly of tooth microwear, transparent/translucent epoxy casting material is used, but in order to optimise data acquisition (using focus variation microscopy; see below) we used the black pigmented EpoTek 320LV, which in other respects has similar properties to the commonly used transparent EpoTek 301. After all moulds were taken, data were acquired from the original tooth surfaces (gold coated, using an Emitech K500X sputter coater, for three minutes to optimise data acquisition). This has been shown to produce no difference from original surfaces (Appendix 2: Supplementary Chapter). From this point on each cast will be referred to by the name of the impression media from which it was created.

Data Acquisition.

3D surface texture data were collected using focus variation microscopy (Alicona Infinite Focus Microscope, model IFM G4c, software version: 2.1.2). Data capture

followed the methods of previous studies (Purnell et al. 2012, Purnell et al. 2013, Gill et al. 2014) (x100 objective, field of view of 145 x 110 µm, vertical resolution set to 0.02 µm, lateral optical resolution equivalent to 0.35 - 0.4 µm). Data were captured from exactly the same fields of view across all replicas, and from the original tooth surfaces, so that for each quadrant (NE, SE, SW, and NW), there is an identical sample area for the original surface and each replica (see Figure 1.1 for examples of 3D surface data). The resulting data files were investigated using two different approaches to surface texture analysis: one based on ISO 25178-2 (Jiang et al. 2007, International Organization for Standardization 2012), the other using Scale Sensitive Fractal Analysis. In the first, data files were levelled using all points levelling (fit to a least squares plane via rotation around all three axes) to remove any variation in the 3D surface arising from manual horizontal positioning of the sample. Files were then transferred to SurfStand software (Version: 5.0.0) for further processing. Errors in data collection (e.g. data spikes) were manually deleted and replaced with a mean surface value point. Surface roughness was quantified using ISO 25178-2 texture parameters (Table 1.2) which requires generation of scale-limited surfaces (International Organization for Standardization 2012) (for detailed parameter descriptions see refs (Scott et al. 2006, Purnell et al. 2013)). Scale limited surfaces were generated through application of a robust polynomial (which finds and removes the Least Squares polynomial surface for the levelled data) combined with either a spline or a robust Gaussian wavelength filter (to remove long wavelength features of the tooth surface; gross tooth form). Three different settings were used, producing three complete datasets of eight samples: a 2^{nd} order polynomial with a spline filter, a 5^{th} order polynomial with a spline filter, and a 5^{th} order polynomial with a robust Gaussian filter, all with the wavelength cut-off for the filter set to 0.025mm. This allowed us to account for differences in the process of generating scale-limited surfaces causing variation in assessments of accuracy and precision. Two of the three settings also correspond to previous work carried out on dietary analysis based on ISO texture parameters (Darras 2012, Purnell et al. 2013).

Scale Sensitive Fractal Analysis (SSFA) (Ungar et al. 2003, Scott et al. 2006) was carried out using the programs ToothFrax and SFrax (Surfract, www.surfract.com).

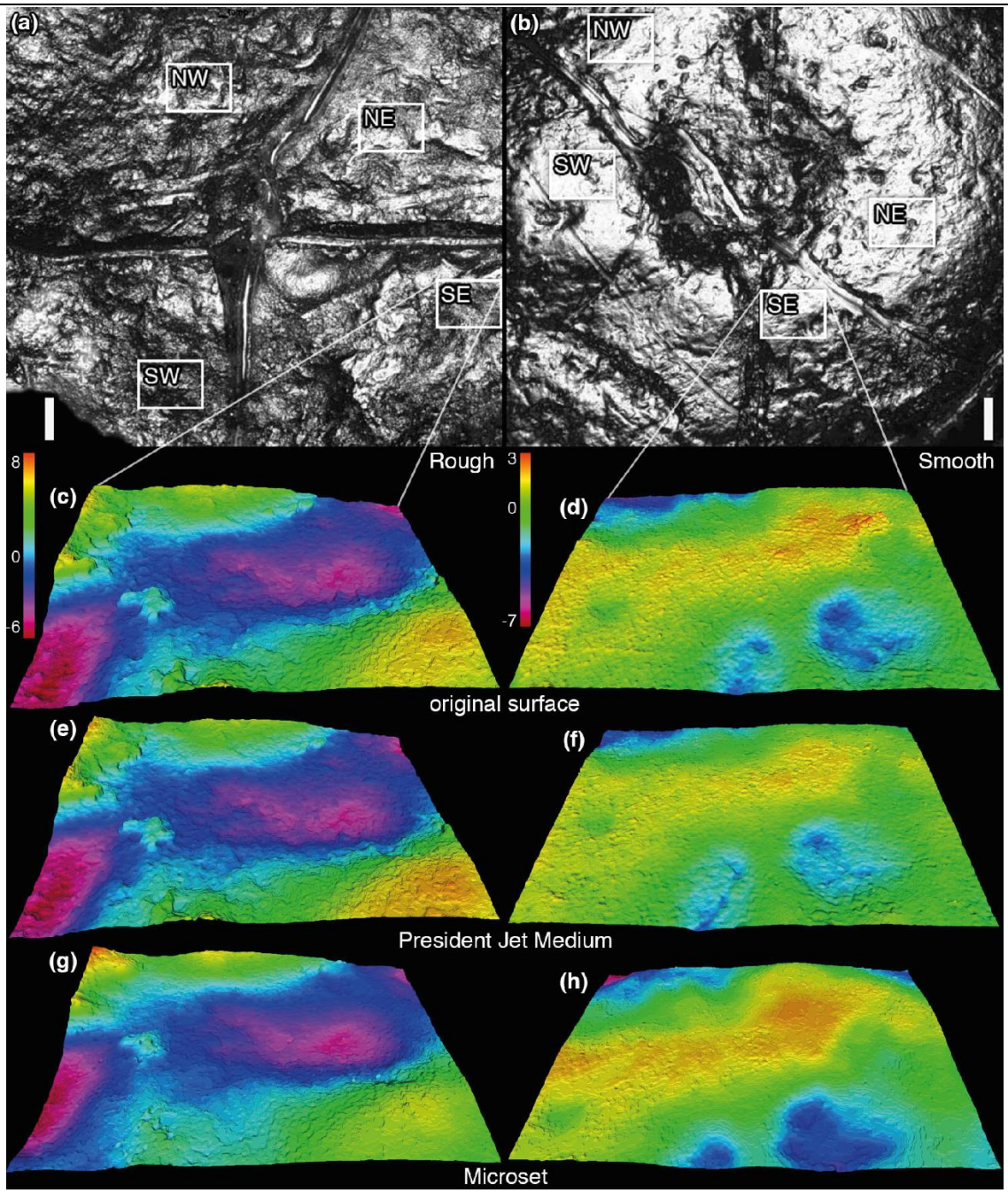

Figure 1.1 *Sample locations of four quadrants from the rough (a) and smooth (b) tooth surfaces (optical images). (c) - (h), digital elevation models of levelled surface data from original surface and examples of replicas made using different impression media for SE quadrant, for rough (c, e, g) and smooth (d, f, h) surfaces. (c) and (d) original surfaces; (e) and (f) replicas, President Jet medium body impression medium; (g) and (h) replicas, Microset impression medium. Scale bars in (a) and (b), 100µm. Digital elevation models all 110 x 145 µm. Vertical scales in µm.*

SSFA does not require surfaces to be scale limited, and quantifies five aspects of surface roughness (Table 1.3). Settings for all parameters followed those used in previous work (Scott et al. 2006), including the use of scale-sensitive "auto splits" to record Surface Heterogeneity (HAsfc), separating individual scanned sections into increasingly reduced sub-regions (we calculated HAsfc across ten different subdivisions). As a small deviation from the published method we used a single data file location for each sampled surface, rather than four adjoining locations normally used. This was necessary in order for us to directly compare the same locations from which ISO parameter data were calculated. Rather than a setting of 1.8µm (Scott et al. 2006), we also used a 3.5µm scale of observation to calculate the parameter epLsar (Merceron et al. 2014) (this value being based on the lateral resolution of the microscope being used).

Statistical Analysis.

Statistical hypothesis testing was carried out using JMP (Version 10.0.0). Data acquired from rough and smooth surfaces were analysed separately. Data sets were tested for normality (Shapiro Wilks W test; by parameter and impression medium); the majority of data were normally distributed so parametric statistical tests were appropriate. Log_{10} data were used for parameters where this produced a greater number of normally distributed media. For each parameter either original data or log_{10} data were used across all media, never a combination of the two. The ISO 25178-2 parameter Sal (Auto-Correlation Length), and the SSFA parameter Smc (Scale of Maximum Complexity) were found rarely to be normally distributed in any impression medium and were excluded from further analysis.

Because data were collected from exactly the same eight locations on the two teeth and each set of replicas, our replica datasets can be considered as 'treatments' of the original surfaces. Consequently, we tested for differences using matched pair t-tests, so that rather than treating the data from a replica as a general sample population, the same quadrants are compared (e.g. comparing the Microset replica

with the original surface, Microset data for the NE quadrant are compared with original data for the NE quadrant, Microset SE compared with original SE etc.)

Although we conducted multiple comparisons, a sequential Bonferroni correction (Holm 1979) was not applied, because knowing when to use this method is difficult and in most cases subjective (Cabin and Mitchell 2000); when used on test numbers as large as ours, the correction has been shown to produce more type II error (false negatives) than the type I error (false positives) it removes (Moran 2003, Nakagawa 2004). Choosing not to use a Bonferroni correction will bias our results towards incorrectly rejecting the null hypothesis of no difference between moulding compounds (i.e. it will increase the likelihood of type I errors), and this is taken into account when drawing our conclusions (e.g. given that an average of 20.57 tests were performed for each impression medium using the ISO 25178-2 data, we might expect, at $\alpha = 0.05$, one false positive for each medium).

Results

Accuracy of Impression Media - ISO 24178-2.

For each impression medium, the null hypothesis of no difference from the original surface was rejected for at least one parameter, but the number of parameters that differed ranged widely: between media, between rough (dentine) and smooth (enameloid) surfaces, and between modes of application (Figure 1.2 (a)). To simplify discussion, we report here the average number of significant differences across all three scale limiting settings for each replicating medium, but Figure 1.2 (a) shows all differences. For low and mid viscosity media, smooth surfaces exhibited a greater number of significant differences than rough. However, the opposite is true for high viscosity media (Microset 101RF and MM240TV).

Parameter Family	Parameter Name	Definition	Units
Height	Sq	Root Mean Square Height of Surface	µm
	Ssk	Skewness of Height Distribution of Surface	n/a
	Sku	Kurtosis of Height Distribution of Surface	n/a
	Sp	Maximum Peak Height of Surface	µm
	Sv	Maximum Valley Depth of Surface	µm
	Sz	Maximum Height of the Surface (Sp – Sv)	µm
	Sa	Average Height of Surface	µm
Spatial	Str	Surface Texture Aspect Ratio (values range 0-1). Ratio from the distance with the fastest to the distance with the slowest decay of the ACF to the value. 0.2-0.3: surface has a strong directional structure. > 0.5: surface has rather uniform texture.	mm/mm
	Sal	Surface Auto-Correlation Length Horizontal distance of the auto correlation function (ACF) which has the fastest decay to the value 0.2. Large value: surface dominated by low frequencies. Small value: surface dominated by high frequencies.	mm
Hybrid	Ssc	Mean Summit Curvature for Peak Structures	1/µm
	Sds	Density of Summits. Number of summits per unit area making up the surface	$1/mm^2$
	Sdq	Root Mean Square Gradient of the Surface	Degrees
	Sdr	Developed Interfacial Area Ratio of the Surface	%
Volume	Vmp	Surface Peak Material Volume	$\mu m^3/mm^2$
	Vmc	Surface Core Material Volume	$\mu m^3/mm^2$
	Vvc	Surface Core Void Volume	$\mu m^3/mm^2$
	Vvv	Surface Dale Void Volume	$\mu m^3/mm^2$
Material Ratio	Spk	Mean height of the peaks above the core material	µm
	Sk	Core roughness depth, Height of the core material	µm
	Svk	Mean depth of the valleys below the core material	µm
	Smr1	Surface bearing area ratio (the proportion of the surface which consists of peaks above the core material)	%
	Smr2	Surface bearing area ratio (the proportion of the surface which would carry the load)	%
Feature	S5z	Ten Point Height of Surface	µm
Miscellaneous	Std	Texture Direction	Degrees

Table 1.2 *ISO 25178-2 parameters used, including brief descriptions. Parameter Sal was excluded from analyses, as it only produced normally distributed data in one of the three data treatments, even when using log_{10} values. For detailed parameter descriptions see Purnell et al (2013).*

Parameter Name	Acronym	Description
Area Scale Fractal Complexity	Asfc	A measure of the complexity of a surface. Area-scale fractal complexity is a measure of change in roughness with scale. The faster a measured surface area increases with resolution, the more complex the surface.
Exact Proportion Length Scale Anisotropy of Relief	epLsar	A measure of the anisotropy of a surface. Anisotropy is characterized as variation in lengths of transect lines measured at a given scale (we use 3.5 μm) with orientations sampled at 5° intervals across a surface. An anisotropic surface will have shorter transects in the direction of the surface pattern than perpendicular to it (e.g. a transect that cross-cuts parallel scratches must trace the peaks and valleys of each individual feature).
Scale of Maximum Complexity	Smc	The parameter represents the full scale range over which Asfc is calculated. High Smc values should correspond to more complex coarse features.
Textural Fill Volume	Tfv	The total volume filled (Tfv) is a function of two components: 1) the shape of the surface, and 2) the texture of the surface. A more concave or convex surface will have a larger total fill volume than a planar surface even if both surfaces have an identical texture.
Heterogeneity of Area Scale Fractal Complexity	HAsfc	variation of Asfc across a surface (across multiple, equal subdivisions of a surface). High HAsfc values are observed for surfaces that vary in complexity across a facet.

Table 1.3 *Scale Sensitive Fractal Analysis (SSFA) parameters used, including brief descriptions (after Ungar et al (2003), and Scott et al (2006)). Smc was excluded from statistical analyses as it was rarely normally distributed and almost always returned the same value for each surface. For parameter details and information on methods of calculation see Scott et al 2006.*

On the rough surface high viscosity Microset 101RF, and MM240TV produce the greatest number of significant differences, with an average of eight for Microset 101RF, and 10.66 for MM240TV. In MM240TV we also see the largest variation in significant differences between the two surfaces, with an average of 10.66 significant differences on the rough surface, but an average of only 2.33 on the smooth surface. Microset 101RF also displays the highest variability on the smooth surface between results recorded using each of the methods for scale limiting surfaces, varying between two significant differences when using a 2nd order of polynomial and a spline filter, and

seven significant differences when using a 5th order of polynomial and a robust Gaussian filter.

The two low viscosity media, MM913 and Speedex, both show high numbers of significant differences across both surface types. They produce smaller numbers of significant differences than high viscosity media in almost all cases (except MM240TV on the smooth surface), but much higher numbers of significant differences than the remaining three low and mid viscosity compounds. The greatest number of significant differences across all impression media on the smooth surface is found in MM913, with an average of nine. The two remaining low viscosity impression media (President Jet Light Body, and Accutrans), along with the mid viscosity President Jet Regular Body, produce the smallest number of significant differences across both surface types with an average of 0.33 significant differences for each of the three compounds on the rough surface, and averages of one significant difference for President Jet Regular Body, 2.33 for President jet Light Body, and 1.66 for Accutrans on the smooth surface.

Looking at the effect of operator and mode of application (Fig.1.3), Speedex shows a great deal of variation in the number of significant differences recorded on both the rough and smooth surfaces, depending on the operator, with moulds produced by operator 1 exhibiting more differences. Comparing applicator gun and manual application, both modes of application of President Jet Light Body to rough surfaces produce few differences. For the smooth surfaces, use of the applicator gun produces a greater number of significant differences than manual application. The converse is true of President Jet regular Body, with manual application to smooth surfaces producing more than twice the number of significant differences compared to using the applicator gun across all scale limiting setting. Manual application to the rough surface also proved less accurate than using the applicator gun, however the difference was only a single significant result in one of the scale limiting settings (2nd order of polynomial with a spline filter).

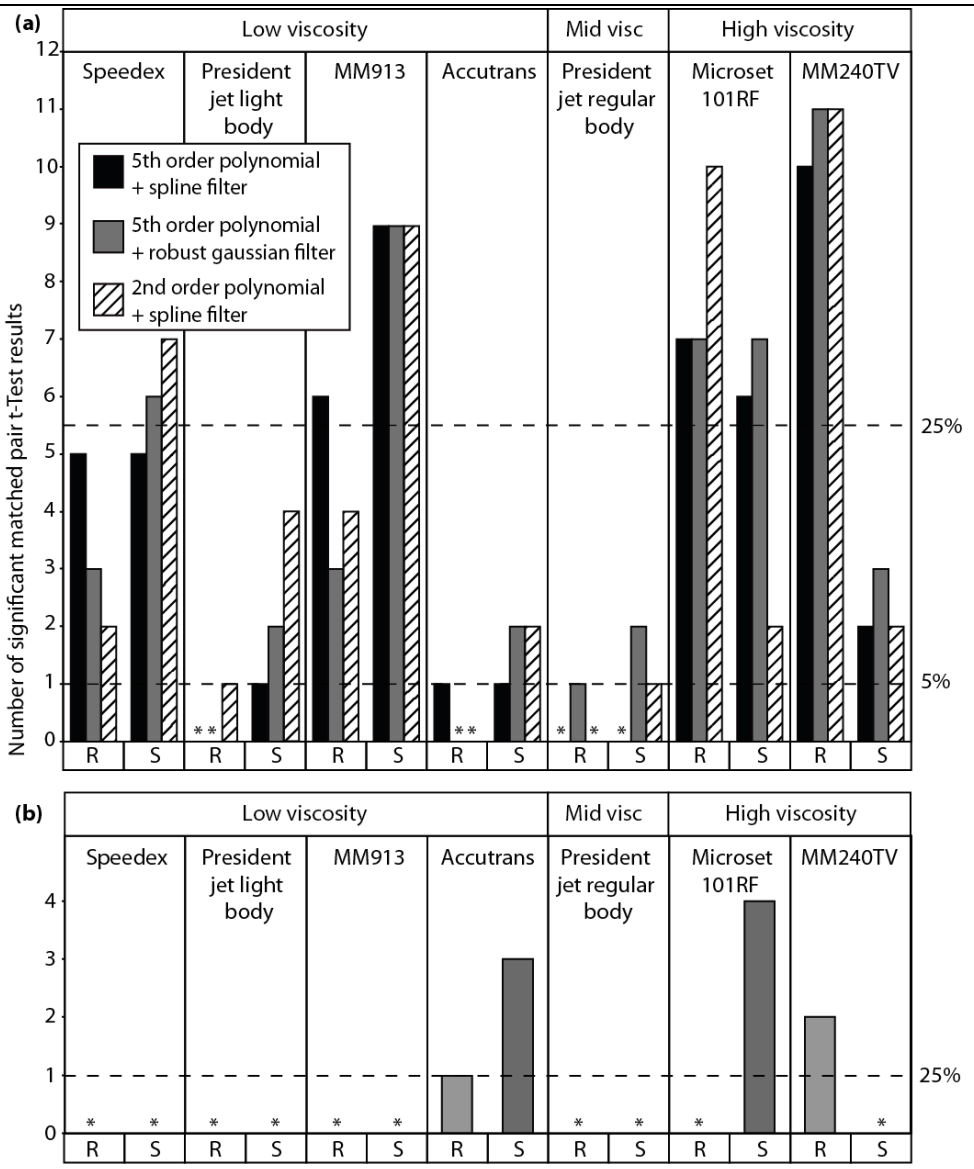

Figure. 1.2: *Numbers of significant differences (matched pair t-tests) between impression media and original tooth surfaces. With (a) data generated using ISO 25178-2 method and (b) data generated using SSFA method. Bars show the number of parameters that differ, (*) represents treatments where no significant results were recorded. For (a) data treatments (polynomial/spline/Gaussian filter) reflect different approaches to generation of scale-limited surfaces from which texture parameters are generated. R and S indicate whether data were generated from rough or smooth surfaces, respectively. (a) The dotted line on the Y axis (labelled 5%) represents the expected number of false positive results per impression medium based on an average of 20.57 tests per impression medium, and α = 0.05. (a) and (b),The dotted line on the Y axis (labelled 25%) is used to compare numbers of significant results produced using the two different roughness parameterisation methods (ISO & SSFA).*

Accuracy of Impression Media - Scale Sensitive Fractal Analysis.

Comparing impression media to the original surfaces using SSFA parameters yields fewer significant differences (matched pair T-tests) than comparisons using the ISO 25178 method (Fig.1.2 (b)). This is partly because SSFA generates fewer parameters. HAsfc is recorded here as a fraction, due to this parameter being calculated across ten different subdivisions (splits) of the sample area.

On the rough surface significant differences were recorded only in the two high viscosity impression media (Microset 101RF & MM240TV), and only in the parameter HAsfc (Surface Heterogeneity; significant differences were recorded in eight of the ten "splits" used to calculate this parameter for each of these impression media).
On the smooth surface there were even fewer significant differences, but they were found in more than one media viscosity level. Again high viscosity Microset 101RF showed significant differences for the parameter HAsfc in four of the ten "splits" used, however MM240TV recorded no significant differences in any parameter. Significant differences were also found when using low viscosity Accutrans, in the parameters HAsfc (2/10 "splits"), and Asfc (Surface Complexity).

However, if we consider the percentage of significant differences, as opposed to the overall number, it may give us a better comparison between the SSFA and ISO 25178 results. In this situation one significant result using SSFA parameters is 25% of the total possible significant differences. If we apply this 25% threshold for significant differences to the ISO 25178 data (5.5 significant differences) we find that it is exceeded by Speedex on the smooth surface, MM913, and Microset 101RF on both surface types, and MM240TV on the rough surface. This is completely different to the pattern seen in the SSFA results, where this threshold is only exceeded by Accutrans on the enameloid surface (1.2 significant differences).

Using SSFA to compare different operators and application methods revealed no difference between application methods.

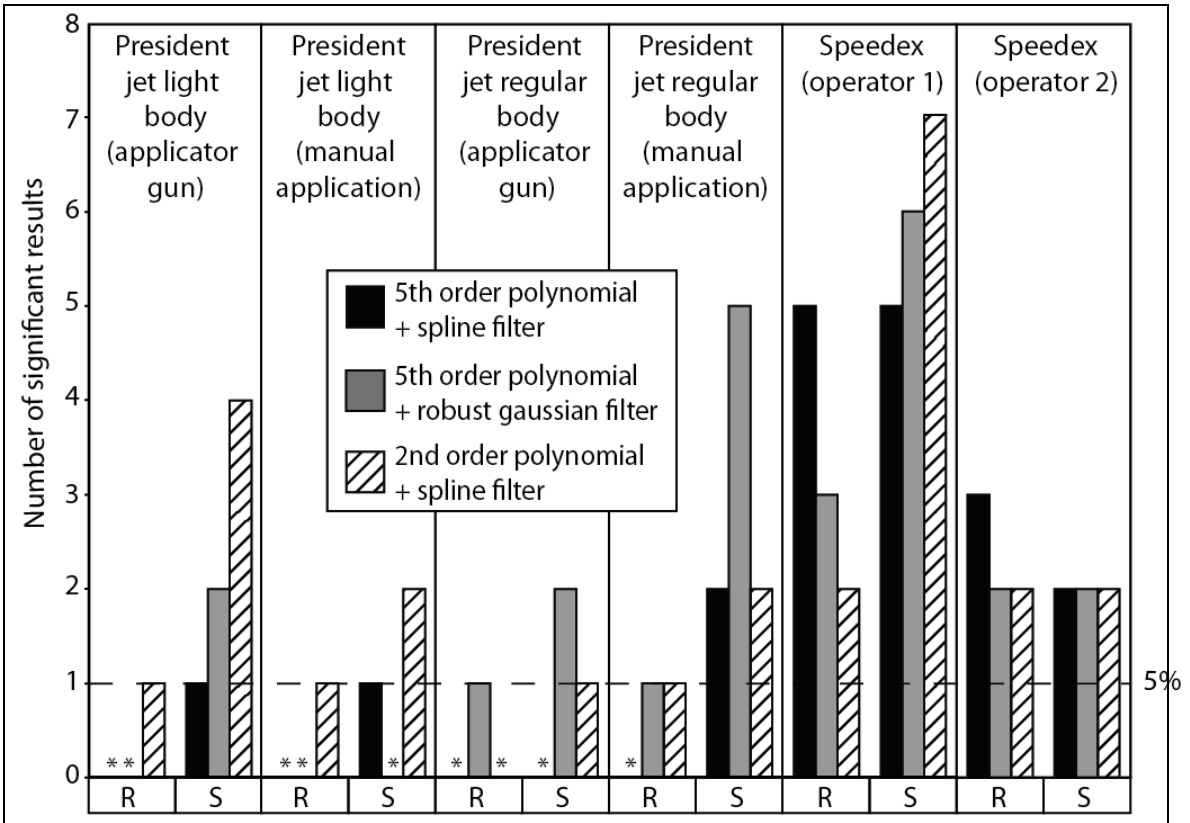

Figure.1.3: *Numbers of significant differences (matched pair t-tests, ISO 25178-2 parameters) between two moulds of the same compound and the original tooth surface. Bars show the number of parameters that differ, (*) represents treatments where no significant results were recorded. Moulds were created using either different operators (Speedex) or application methods (President Jet Light and Regular Body); four quadrants per tooth, broken down by data treatment. R and S indicate whether data were generated from rough or smooth surfaces, respectively. The dotted line on the Y axis (labelled 5%) represents the expected number of false positive results per impression medium based on an average of 20.57 tests per impression medium, and α = 0.05.*

Variability in Precision and Accuracy of Impression Media - ISO 24178-2.

We assess precision in terms of the range of deviations in texture parameter values for each impression medium from the original surface values. Rough and smooth surfaces are compared separately; for each parameter and each medium there are four values (one for each quadrant - see Methods), yielding a range of deviations from the original surface (Fig.1.4). Because these figures are presented to show differences in accuracy and precision between impression media, plots for the rough and smooth surfaces are given at different scales, and although patterns of variation can be compared, absolute values should be taken into account. For the assessment of precision we have only used the data files that have been scale limited using a 5^{th} order of polynomial and a robust Gaussian filter (as in ref.(Purnell et al. 2013)). For clarity, only 13 of the 22 parameters are shown in figure 1.4, all of which represent parameters where at least one significant result was recorded across all impression media on the rough surface. Plots showing data for all remaining parameters can be found in Figure 1.5.

On the rough surface (Fig.1.4 & 1.5 (a)) high viscosity media (MM240TV and Microset 101RF) generally show the greatest range of differences from the original surface and thus the lowest precision. Low viscosity media are split into two levels of precision: Accutrans and MM913 show a similar lack of precision to that shown by high viscosity media; President Jet Light Body and Speedex both show very high levels of precision, with differences clustered much more closely. Finally President Jet Regular Body shows a similarly high level of precision to Speedex and President Jet Light Body, with very little to clearly differentiate the precision of the three compounds. The precision of each impression medium appears to mirror its accuracy on the rough surface, with compounds showing low accuracy also generally showing low precision and vice versa. However, there are two notable exceptions to this pattern, Speedex, which shows high precision, but low accuracy, and Accutrans, which shows high accuracy, but low precision. Microset 101RF shows a much higher level of precision than is typical for this medium in one or two parameters.

On the smooth surface (Fig.1.4 & 1.5 (b)) the pattern of precision is slightly different. The two President Jet compounds and Speedex show a similar high level of precision to that seen on the rough surface. The two high viscosity media (Microset 101RF and MM240TV) again show low levels of precision. However Accutrans and MM913 show much higher levels of precision on the smooth surface, similar to that seen in the two President Jet compounds and Speedex. In most cases, deviations from the original surface values on the smooth surface are smaller in scale than on the rough. However, this is not the case for height parameters, where differences on the smooth surface are similar, and sometimes larger, than those on the rough surface. There appears to be a homogenisation of the precision between the four low viscosity and the one mid viscosity impression media on the smooth surface, making it much harder to determine within these compounds which has the highest precision. For the volume parameters Vmc and Vvc, and the material ratio parameter Sk, all media show a similar level of precision.

On both the rough and smooth surfaces there is a degree of directionality in the error produced by the four least precise media (MM240TV, Microset 101RF, Accutrans and MM913). This is because, for certain parameters, the differences from the original surface are mostly either positive or negative. This implies there is a consistent bias (e.g. a constantly positive bias for parameter Sp would indicate elevated peak heights). However, any bias is not systematic as the order of each quadrant's difference from the original surface is never repeated (i.e. NW quadrant does not consistently have the largest error across all compounds and parameters) (Fig. 1.4 & 1.5). For the results of any parameter to be considered to have positive directionality of error at least three of these four media must show mostly positive differences from the original surface (more than 50% of quadrants in more than 50% of media), and vice versa for negative directionality of error. Both rough and smooth surfaces show an equal degree of directionality, with 12 parameters showing either positive or negative directionality of error on each surface type. There are ten parameters on each of the surface types, in which there is no obvious directionality in differences from the original surface.

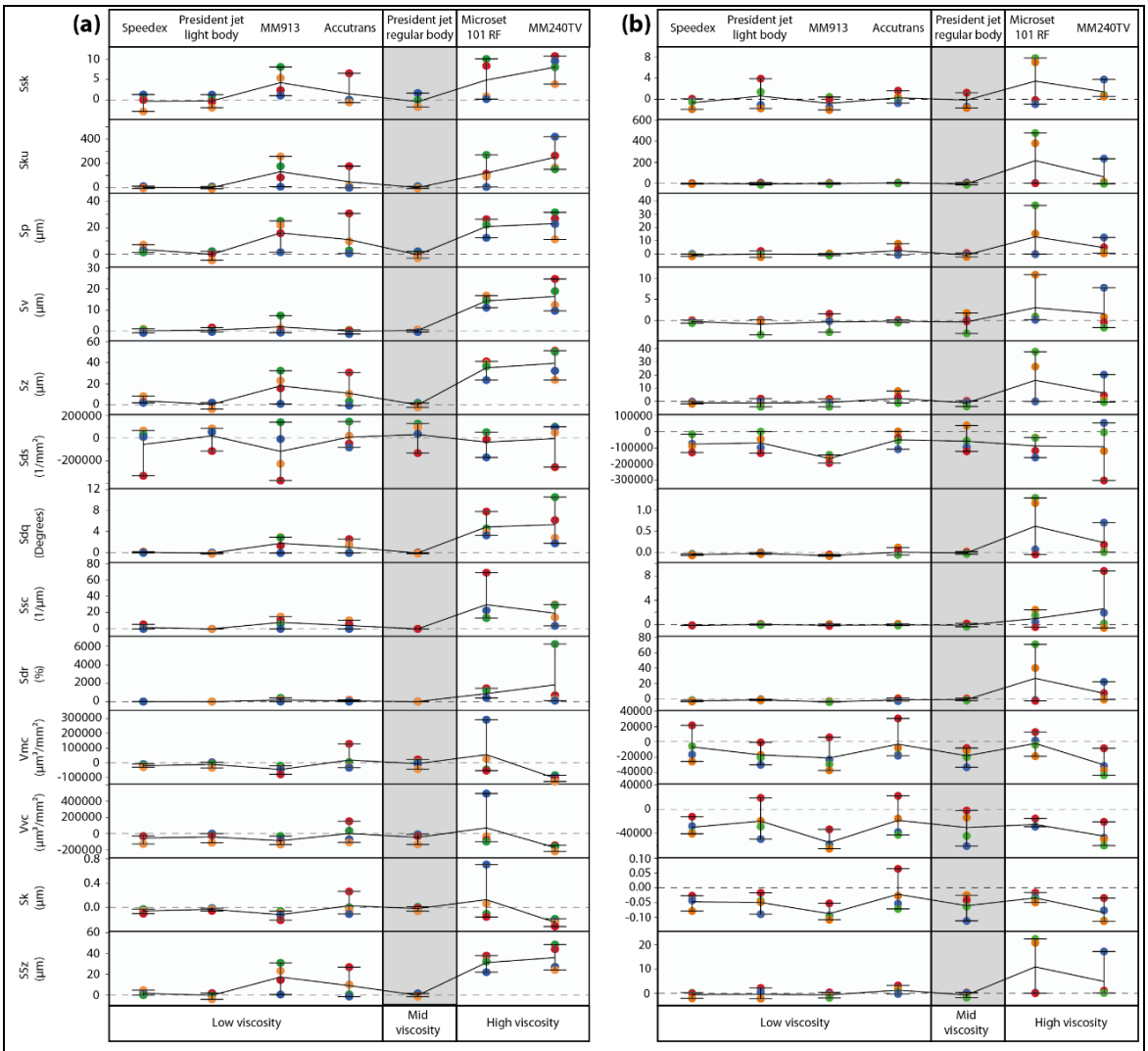

Figure.1.4 *Absolute differences between original surface and each impression medium for the rough surface (a), and the smooth surface (b), generated using the ISO 25178-2 parameterisation method. Points show the actual differences from the original surface, with zero indicating the same value for replica and original surface. Each quadrant has been given a specific colour (NE=Blue, SE=Green, SW=Red, NW=Orange). Lines connecting points horizontally show mean difference. Whiskers represent the range of the data. For convenience, plot shows only data collected using a 5th order of polynomial and a robust Gaussian filter, and only parameters returning significant differences for at least one impression medium on the rough surface. Other data are included in Figure1.5 (below).*

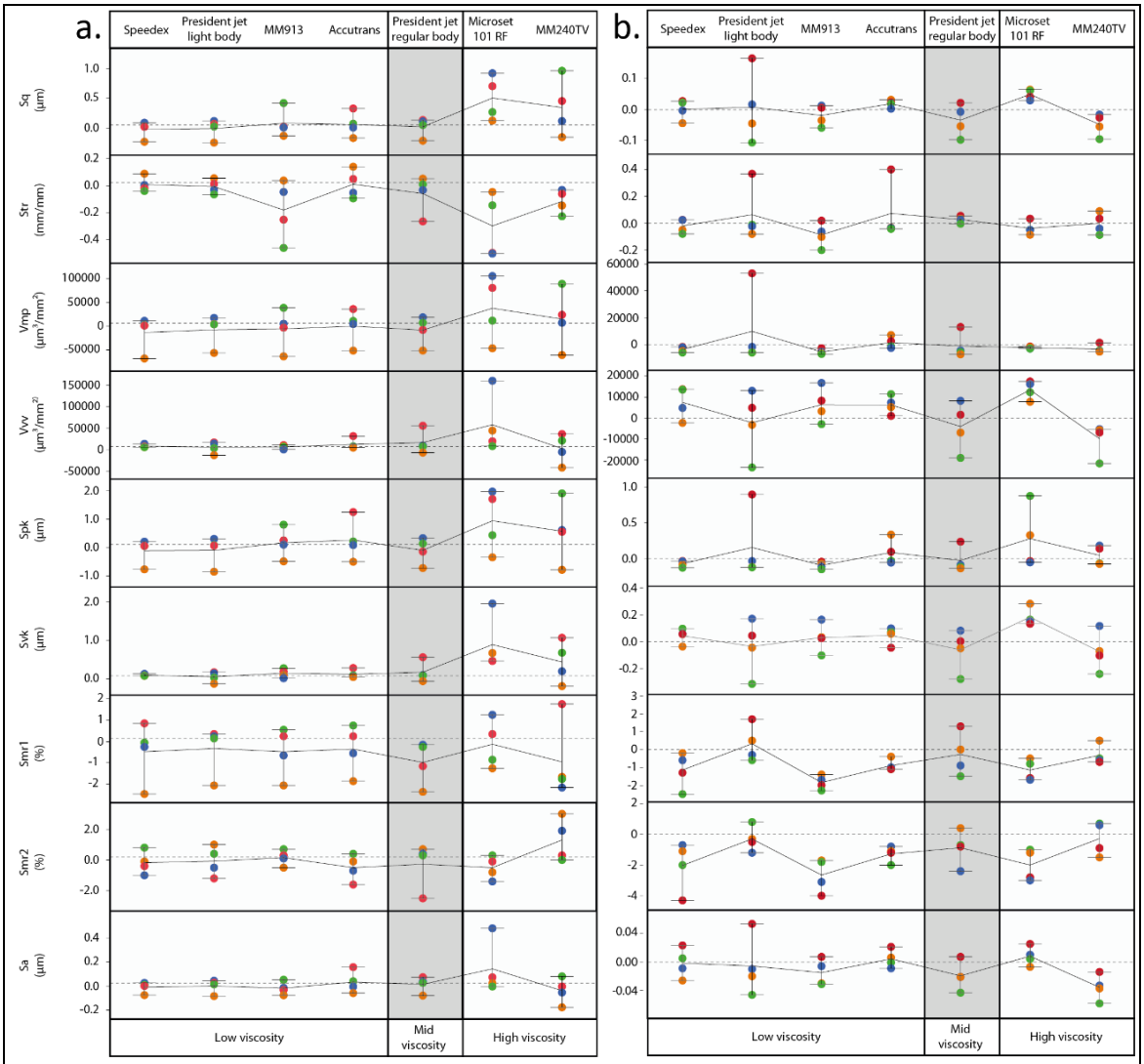

Figure 1.5 *Absolute differences between original surface and each impression medium for the rough surface (a), and the smooth surface (b), generated using the ISO 25178-2 parameterisation method. Points show the actual differences from the original surface, with zero indicating the same value for replica and original surface. Each quadrant has been given a specific colour (NE=Blue, SE=Green, SW=Red, NW=Orange). Lines connecting points horizontally show mean difference. Whiskers represent the range of the data. For convenience, plot shows only data collected using a 5th order of polynomial and a robust Gaussian filter, and only parameters not returning significant differences for at least one impression medium on the rough surface.*

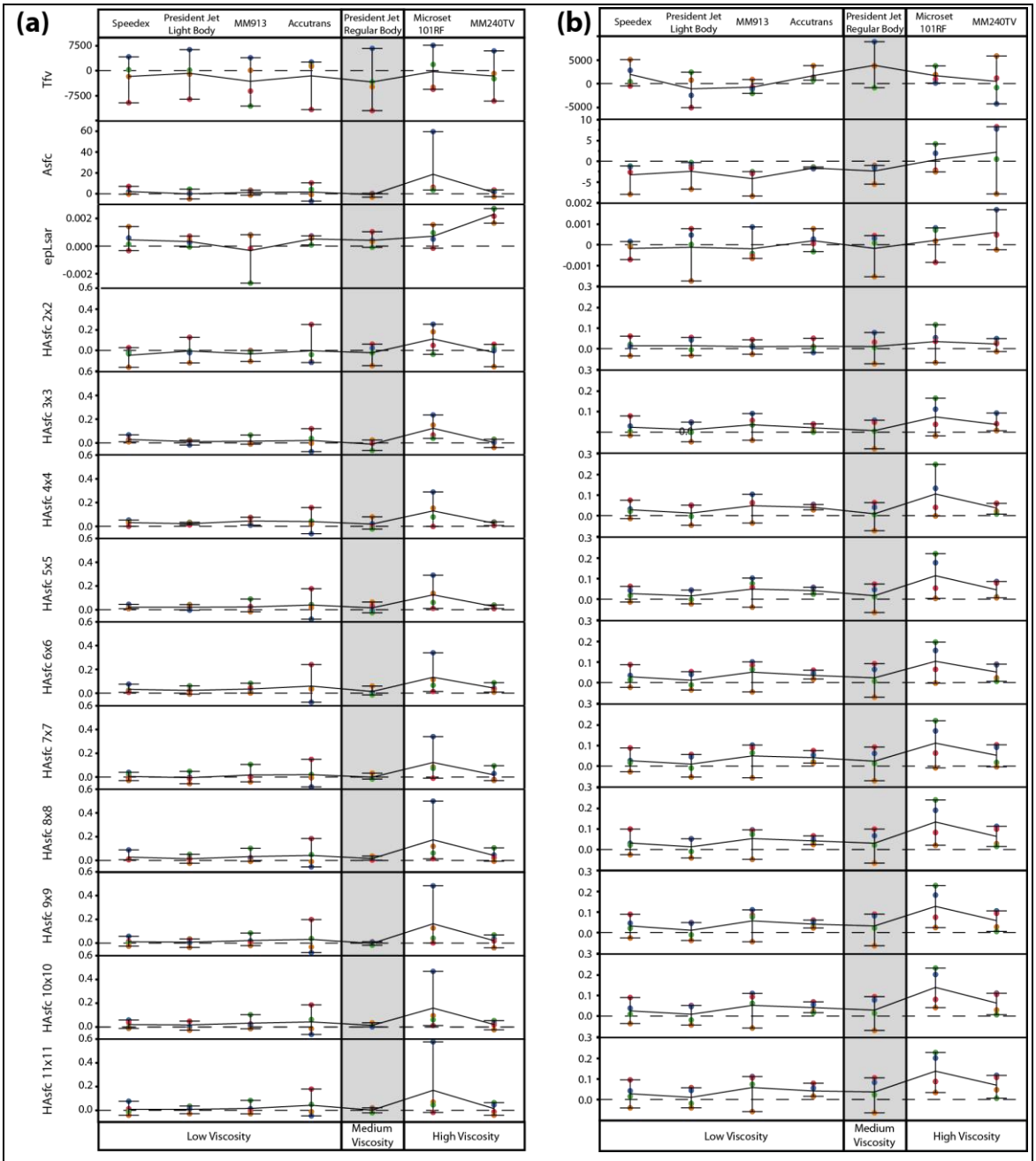

Figure 1.6 *Absolute differences between original surface and each impression medium for the rough surface (a), and the smooth surface (b), generated using the SSFA parameterisation method. Points show the actual differences from the original surface, with zero indicating the same value for replica and original surface. Each quadrant has been given a specific colour (NE=Blue, SE=Green, SW=Red, NW=Orange). Lines connecting points horizontally show mean difference, with all original tooth values set to zero. Whiskers represent the range of the data.*

There are a small number of parameters where the directionality of error is consistent across both surface types. On both the rough and smooth surface there is positive directionality in the Hybrid Parameter Sdr, the Material Ratio Parameter Svk and the Feature Parameter S5z. And there is consistent negatively directionality across both surface types for the Spatial Parameter Str, and the Volume Parameter Vvc. However, most parameters only show directionality of error on one of the two surface types. Positive directionality is also seen on the rough surface in the Height Parameters Ssk, Sku, Sp, Sv, and Sz, and the Hybrid Parameters Sdq and Ssc, and on the smooth surface in the Volume Parameter Vvv. Negative directionality of error is also seen on the smooth surface in the Hybrid Parameter Sds, the Volumetric Parameters Vmp, and Vmc, and the Material Ratio Parameters Sk, Smr1, and Smr2.

Variability in Precision and Accuracy of Impression Media - Scale Sensitive Fractal Analysis.

The precision of impression media when using SSFA parameters was assessed in the same way as with ISO parameters above (Fig.1.6). On both surface types there appear to be different patterns of precision depending on the medium and parameter in question. In some media this pattern is similar across both surface types, however in others the two surface types show very different patterns of precision. This is markedly different to the ISO parameter data, where the patterns were similar across most parameters and across the two surface types. Therefore it appears that in this case differences between media are less systematic when using the SSFA parameterisation method than those detected using the ISO-based analysis.

On the rough surface (Fig.1.6 (a)), Speedex President Jet Light Body and President Jet Regular Body all show very high levels of precision for parameter Asfc (surface complexity), epLsar (anisotropy), and all spits of HAsfc (heterogeneity), but much lower precision for Tfv (textural fill volume), giving them a similar level of precision to all other compounds for this parameter. Low viscosity MM913 shows low precision for Tfv (textural fill volume), and epLsar (anisotropy), but relatively high precision for all other parameters, in line with the precision of Speedex and the two President Jet compounds. However Accutrans is much less precise than all other low

viscosity media for all parameters except epLsar, where it shows precision amongst the highest for all parameters.

Of the two high viscosity media, Microset 101RF shows relatively high precision for all parameters, except Tfv (textural fill volume), whereas MM240TV shows low levels of precision for all parameters.

On the smooth surface (Fig.1.6 (b)) most impression media show medium to low levels of precision for all parameters, without much to separate them. Except in the case of Accutrans, where higher levels of precision can be seen for the parameters Asfc and HAsfc than for the other media.

Although the pattern of precision for the rough surface is similar to that seen when using the ISO parameterisation method, the pattern on the smooth surface is different. On both surface types there is also very little directionality of error evident when using the SSFA parameterisation method.

Magnitude of Differences Between Surfaces: Replicas Compared to Different Diets.

Comparisons of precision and accuracy provide a good test of the fidelity of each of the impression media, but they do not address the question of whether the magnitude of differences that result from using different media would produce erroneous results in a comparative statistical analysis. This kind of analysis is routinely used to investigate dietary differences between species or ecotypes of vertebrates based on differences in 3D microtexture of tooth surfaces. Here we compare the magnitude of the differences in parameter values between different media with the differences obtained from comparing surface textures of teeth from two wild populations of *Archosargus probatocephalus* (Sheepshead Seabream) which exhibit different tooth surface microtextures as a result of dietary differences (this is the same species as that from which our other surface data were acquired). Both populations were collected in Florida (USA) and although they can be considered as dietary generalists with considerable overlap in diet, one population, from Indian River lagoon,

is more herbivorous, while the other, from Port Canaveral lagoon, consumes and crushes more hard-shelled prey, such as bivalves (Darras 2012).

In the dietary analysis, seven ISO 25178-2 parameters (Sdq, Sdr, Vmc, Vvv, Sk, Smr1, and Sa) differed significantly between populations (Darras 2012). Figure 1.7 shows the results of comparing the magnitude of differences between each impression medium, and the original surface with the magnitude of differences between dietary groups for these seven parameters. The parameters listed in each box are those that exhibit a difference between impression media of greater magnitude than would be expected between the different dietary groups.

We find that only two impression media return no differences of greater magnitude than would be expected between dietary groups across both surface types: President Jet Regular Body and President Jet Light Body. All other comparisons between impression media and against the original surface return differences of greater magnitude than would be expected between two dietary populations for at least one parameter, but often more. The number of parameters showing greater magnitude than expected between dietary groups is much smaller on the smooth surface than on the rough surface.

When comparing the magnitude of inter-individual differences within each dietary population to the differences between impression media on the smooth surface we see an almost identical pattern (Figure 1.8) to that shown above.

Discussion

It is clear that different impression media differ significantly in their ability to accurately and precisely replicate surfaces. Accuracy and precision vary between smooth and rough surfaces, between compounds with different levels of viscosity, and between compounds of similar viscosity. A summary of overall accuracy and precision can be seen in Table 1.4.

When using the ISO parameterisation method, high viscosity media (Microset101RF and MM240TV) show the lowest accuracy and precision when replicating a rough surface, at the scale used here, although there is some variation between different data treatments. Many more significant differences are found than low or medium viscosity media in almost all cases, and the magnitude and range of differences from the original surface is much higher than most other media. However MM240TV shows relatively high accuracy on the smooth surface. Comparing profiles across equivalent surfaces produced using different impression media suggests that the higher viscosity of these compounds limits their ability flow into, and thus replicate, the smallest scale features of the surface topology.

Low viscosity media generally replicate a surface more accurately and precisely than high viscosity media, but this is an oversimplification. The number of significant differences and the range of differences from the original surface vary between low viscosity media and between data treatments and the data suggest that all low viscosity compounds are less accurate when replicating a smoother surface at the sub-micrometre scale. On the rough surface President Jet Light Body and Accutrans appear to be the most accurate low viscosity media, showing very few significant differences across all data treatments. However, although President Jet Light Body shows a high level of precision, especially on the rough surface, Accutrans shows much lower precision, similar to the high viscosity media. On the smooth surface both compounds show high levels of precision, with very little difference in precision between these two compounds. Speedex and MM913 appear to be much less accurate on both the rough and smooth surface and show a number of consistent significant differences, across data treatments. On the rough surface, MM913 shows a consistently low level of precision across all parameters, however Speedex is much more precise. On the smooth surface Speedex and MM913 showed a relatively high level of precision in most parameters.

	Specimen	Speedex	President jet light body	MM913	Accutrans	President jet regular body	Microset 101RF	MM240TV
Specimen	-	Smooth Sdr, Sk	Smooth no difference	Smooth Sdr, Vmc, Sk, Smr1, Sa	Smooth Smr1	Smooth no difference	Smooth Sdr	Smooth Sdr, Smr1
Speedex	Rough Sdr, Vmc, Sk	-	Smooth no difference	Smooth Smr1	Smooth Smr1	Smooth Sdr	Smooth Sdr	Smooth Sdr, Smr1
President jet light body	Rough no difference	Rough Sdr, Vvv	-	Smooth Sdr	Smooth Vvv, Smr1	Smooth no difference	Smooth Sdr, Smr1	Smooth Sdr, Smr1
MM913	Rough Sdr, Vmc, Sk, Smr1, Sa	Rough Sdr	Rough Sdr, Vmc, Sk, Sa	-	Smooth Sdr	Smooth Sdr, Smr1	Smooth Sdr	Smooth Sdr
Accutrans	Rough Sdr, Vvv	Rough Sdr, Vvv, Sa	Rough Sdr, Vvv	Rough Sdr, Vmc, Vvv, Sk, Smr1, Sa	-	Smooth no difference	Smooth Sdr	Smooth Sdr
President jet regular body	Rough no difference	Rough Sdr, Vvv	Rough no difference	Rough Sdr, Vvv, Sk, Sa	Rough Sdr, Vvv	-	Smooth Sdr	Smooth Sdr
Microset 101RF	Rough Sdr, Vvv, Sa	Rough Sdr, Vmc, Vvv, Skv, Sa	Rough Sdr, Vmc, Vvv, Sk, Sa	Rough Sdr, Vmc, Vvv, Sk, Sa	Rough Sdr, Vvv, Sk, Sa	Rough Sdr, Vmc, Vvv, Sa	-	Smooth Sdr
MM240TV	Rough Sdr, Vmc, Vvv, Sk, Smr1, Sa	Rough Sdr, Vmc, Vvv, Sk	Rough Sdr, Vmc, Sk	Rough Sdr, Vvv, Sk, Sa	Rough Sdr, Vmc, Sk, Smr1, Sa	Rough Sdr, Vmc, Sk, Sa	Rough Sdr, Vmc, Vvv, Sk, Smr1, Sa	-

Figure.1.7 *Magnitude of differences in texture parameters between impression media compared to the magnitude of differences between dietary ecotypes of Archosargus probatocephalus. Only seven ISO 25178-2 parameters (Sdq, Sdr, Vmc, Vvv, Sk, Smr1, and Sa) were used, as these were the only ones to differ significantly between the two Archosargus probatocephalus dietary populations (Darras 2012). The boxes show those parameters where differences between replica surfaces and the original tooth surfaces exceed those reflecting dietary differences; all possible pairwise comparisons between impression media and the original tooth surfaces were assessed. Whether a parameter value exceeds the dietary difference is calculated by comparing the median value of differences between surfaces (e.g. between the original specimen and Speedex) with the difference between the median value of each the dietary ecotypes. Information towards the lower left shows results for the rough surface, information toward the upper right for the smooth surface. The parameter Sdq is not shown because it exceeds the value for the dietary difference in 27 of 28 comparisons on both surfaces and thus tells us nothing about the relative potential of different impression media to introduce bias into the results of dietary analysis. Highlighted cells represent comparisons where no difference equalled or exceeded that expected from two dietary populations (not including Sdq).*

	Specimen	Speedex	President jet light body	MM913	Accutrans	President jet regular body	Microset 101RF	MM240TV
Specimen	-	PC population Sdr, Sk, Sa	PC population no difference	PC population Sdr, Vmc, Sk, Smr1, Sa	PC population Vvv, Smr1	PC population no difference	PC population Sdr	PC population Sdr, Sk, Smr1, Sa
Speedex	IR population Sdr	-	PC population Sdr	PC population Smr1	PC population Vvv, Smr1	PC population Sdr	PC population Sdr	PC population Sdr
President jet light body	IR population no difference	IR population no difference	-	PC population Sdr, Smr1	PC population Vvv, Smr1	PC population no difference	PC population Sdr, Smr1	PC population Sdr, Smr1
MM913	IR population Sdr, Smr1	IR population Smr1	IR population Sdr, Smr1	-	PC population Sdr, Vvv, Sk, Sa	PC population Sdr, Smr1	PC population Sdr, Sa	PC population Sdr
Accutrans	IR population Smr1	IR population Smr1	IR population Smr1	IR population Sdr	-	PC population no difference	PC population Sdr	PC population Sdr
President jet regular body	IR population no difference	IR population no difference	IR population no difference	IR population Sdr, Smr1	IR population no difference	-	PC population Sdr	PC population Sdr
Microset 101RF	IR population Sdr	IR population Sdr	IR population Sdr, Smr1	IR population Sdr	IR population Sdr	IR population Sdr	-	PC population Sdr
MM240TV	IR population Sdr, Smr1	IR population Sdr	IR population Sdr, Smr1	IR population Sdr	IR population Sdr	IR population Sdr	IR population Sdr	-

Figure 1.8 *Magnitude of differences in texture parameters between impression media compared to the magnitude of differences between individuals in two populations (dietary ecotypes) of Archosargus probatocephalus (compared to smooth tooth surface). The boxes show those parameters where differences between replica surfaces and original tooth surfaces exceed those between individuals in a population; all possible pairwise comparisons between impression media and original tooth surfaces were assessed. Both fish populations are from Florida, USA: Indian River lagoon population is more herbivorous, while Port Canaveral lagoon population consumes and crushes more hard-shelled prey. Only seven ISO 25178-2 parameters (Sdq, Sdr, Vmc, Vvv, Sk, Smr1, and Sa) were compared (the only ones to differ significantly between the two A.probatocephalus populations (Purnell and Darras 2015)). Whether a parameter value exceeds the dietary difference is calculated by comparing the median value of differences between surfaces (e.g. between original specimen and Speedex) with the median value of differences between individuals in each population. Lower left shows results for the comparisons with the Indian River population, upper right for the Port Canaveral population. The parameter Sdq is not shown because it exceeds the value for the dietary difference in almost all comparisons, telling us nothing about the relative potential of different impression media to introduce bias. Highlighted cells represent comparisons where no difference equalled or exceeded that expected from within a wild population (not including Sdq).*

The accuracy of Speedex varied greatly depending on the operator applying the impression medium; both operators were experienced in the use of this compound, and it is unlikely that variation was caused by operator competence; our results therefore suggest there may be issues with using this compound, probably linked to the need to manually measure out and mix imprecise volumes of medium and activator before use. The same might be true of other manually mixed compounds.

President Jet Regular Body, the only mid viscosity impression medium studied, showed the lowest number of significant differences across both surface types and between all data treatments. For President Jet Regular body, given that our multiple comparisons would lead us to expect about one false positive result in every 20 tests, and the fact that there is very little consistency between different data treatments, we would suggest that for the significant differences found when comparing this compound to the original teeth we cannot reject the hypothesis that these are mostly type I errors resulting from multiple comparisons. Also, on the rough surface President Jet Regular Body is one of three compounds showing the highest level of precision, (and shows among the highest levels of precision for most parameters on the smooth surface). It is also one of only 2 compounds not to show any differences from the original surface of a magnitude greater than that seen between different dietary groups. Manual application of President Jet Regular Body produces higher numbers of significant differences on the smooth surface, possibly because the medium is too viscous to be applied consistently in this way.

Rough Tooth	Summary of Results	
Impression Medium	Accuracy	Precision
Speedex	x	✓
President Jet Light Body	✓	✓
MM913	x	x
Accutrans	✓	x
President Jet Regular Body	✓	✓
Microset 101RF	x	x
MM240TV	x	x

Smooth Tooth	Summary of Results	
Impression Medium	Accuracy	Precision
Speedex	x	✓
President Jet Light Body	x	✓
MM913	x	✓
Accutrans	x	✓
President Jet Regular Body	✓	✓
Microset 101RF	x	x
MM240TV	x	x

Table 1.4 *Summary of overall Accuracy and Precision for each impression medium, separated across rough and smooth tooth surfaces. For convenience all treatments of the data are summarised as a single result. Impression media showing high Accuracy (one or fewer significant matched pair T-test results across all treatments of the data) or high Precision (a small range of absolute differences between the original surface and each impression medium) are marked with a (✓). Impression media showing low Accuracy (more than one significant matched pair T-test results across all treatments of the data) or low Precision (a medium to high range of absolute differences between the original surface and each impression medium are marked with an (x). Results are highlighted green for instances where both Accuracy and Precision are shown to be high in a given impression medium.*

When looking at the four media with lowest precision, the directionality of error can tell us something about how the replicated surface differs from the original. Focusing on the parameters that show consistent directionality of error across both surface types, MM913, Accutrans, Microset 101RF, and MM240TV generally over replicate the developed interfacial area ratio (Sdr), the mean depth of valleys below the core material (Svk), and the average value of the five highest and lowest peaks (S5z), and under replicate the surface texture aspect ratio (Str), and the surface core void volume (Vvc) of both smooth and rough surfaces. It is also clear that these compounds generally over replicate most height parameters on the rough surface, and under replicate both peak and valley material portions on the smooth surface. There is also under replication of core void volumes on the rough surface, and over replication of valley void volumes on the smooth surface.

Finally, it appears that there are marked differences between the two surface roughness parameterisation methods currently used in the study of vertebrate diet. The Scale Sensitive Fractal Analysis method produces far fewer significant differences than the ISO 25178-2 method, even when the large difference in numbers of parameters between the two methods is accounted for. The SSFA method also shows no clear pattern on the smooth surface when it comes to understanding the precision of different media. It is unclear whether the differences we see between these methods arise because SSFA is less sensitive, or because the ISO method is exaggerating differences in the surfaces. Further work is needed to understand this.

Given their inaccuracy and imprecision, high viscosity compounds should not be used to replicate surfaces when quantifying 3D areal textures at sub-micrometre scales. Our results also suggest that there are problems with at least two of the low viscosity compounds tested - Speedex and MM913 - on both rough and smooth surfaces. MM913 is slightly less accurate than Speedex on both surfaces, and much less precise on the rough surface, and Speedex shows some potential for operator error to play a part in results. President Jet Light Body may have an issue when studying smooth surfaces, however the level of inaccuracy is very variable and, alongside the generally high precision seen for this compound, it should not be

completely discounted. President Jet Light Body does however have a short cure time, which can cause problems when moulding large surfaces.

Low viscosity Accutrans and mid viscosity President Jet Regular Body show the highest accuracy, producing the lowest number of significant differences across both surface types. However Accutrans shows a low level of precision, especially on the rough surface. The only caveat to using President Jet Regular Body is that manual application will produce less accurate and less precise data, and our results support the use of an applicator gun. On smooth surfaces, President Jet Regular Body shows higher accuracy than Accutrans, and on rough surfaces its shows higher levels of precision.

President Jet Light and Regular Body are also the only two compounds that do not show differences when compared to original surfaces, or to each other, which are greater in magnitude than those found between dietary groups. In the context of dietary analysis based on tooth microwear, we would therefore not recommend that surfaces obtained from impression media other than President Jet Light or Regular body are compared either with each other or with original surfaces. Such comparisons are likely to produce erroneous differences reflecting replication, not ecology.

For most impression media, our results lead to rejection of our null hypothesis that areal texture parameters obtained from replicas do not differ from those obtained from the original surface. Impression media vary in their ability to accurately and precisely reproduce a given surface, with most producing statistically significant differences, and high deviations from true values for areal texture parameters derived from original surfaces, even when false positive results are taken into account. Of the media tested here, President Jet Regular Body produced the most accurate and precise surface replicas.

Chapter 2: Investigating dietary behaviours in pinnipeds and odontocetes using 3D microtextural analysis of tooth wear, and its further application to evolutionary hypotheses in stem cetaceans

Abstract

Understanding the diet of marine mammals is vital for our knowledge of their impacts and interactions on ecosystems, the impact of fisheries on marine mammal populations, and for identifying conservation strategies and the effect of climate change on their ranges and survival. Assessing the diet of any animal feeding in marine habitats is often difficult and costly, so a number of indirect methods have been developed to study diet in marine mammals including stomach contents, faecal pellets, DNA, stable isotope, and quantitative fatty acid signature analysis. However each of these methods has downsides, either in their ability to accurately study long term diet, or identify specific dietary prey items. As such there are still problems with our understanding of marine mammal diet. Here quantitative analysis of tooth microwear at the sub-micron scale is used to differentiate diet in pinnipeds and odontocetes. Dietary classes are separated statistically, while multivariate analysis produces an ordination in which dietary classes inhabit distinct separate distributions. It is also found that dietary signals are stronger than taxonomic signals, so that pinniped and odontocetes displaying the same diet can be grouped, regardless of their tooth morphology or food processing habits. This technique also allows an investigation of the diet of extinct stem cetaceans, by comparing their tooth textures to those of modern pinnipeds and odontocetes. Our analysis shows that several stem cetacean species appear to display the same dietary habits as modern marine mammals, however some individuals possess apparently different diets. Comparing our results to those of previous studies on durophagy, using tooth microtextures, we find that these individuals likely ate harder items than modern marine mammals, however further study is needed. The results of this paper indicate that quantitative analysis of tooth microtextures provides a new way of looking at marine mammal diet that is both sensitive to specific food items, and can study diet over a reasonable time span (up to

a few weeks of feeding). We also find that this technique can be applied to the diet of extinct stem cetaceans and potentially offers a new way to study the diet of these species.

Introduction

Odontocetes (Cetacea: Odontoceti) and pinnipeds (Carnivora: Pinnipedia) are broad groups of active marine mammal predators, containing 75 and 33 species respectively (Berta and Churchill 2012, Perrin 2016), with very different evolutionary histories and morphologies (Uhen 2007).

Understanding the diet of species within odontocetes and pinnipeds is important for a number of reasons. The impact and importance to marine food-webs of both pinniped and odontocete species are thought to be very high (Bowen 1997). Therefore data on their diet are important in understanding these relationships. Individual odontocete and pinniped species have been classed as critically endangered, or endangered (www.iucnredlist.org) (Rosel and Rojas-Bracho 1999, Kovacs et al. 2012, Parrish et al. 2012, Silva 2013), and sometimes extinct (Turvey et al. 2007, Baisre 2013). Part of protecting marine mammal species involves understanding their diet and protecting the environments where their food sources can be found (Hooker and Gerber 2004). Pinnipeds and odontocetes also interact with aquaculture to varying degrees (Trites et al. 1997, Read 2008). This often has negative impacts on the marine mammal species, either by mortality through fisheries bycatch (Dayton et al. 1995, Read et al. 2006, Kiszka et al. 2009, Reeves et al. 2013), or competition between odontocete/pinniped species and fisheries, leading to calls for, or acts of prejudicially culling certain species believed to have impacted fish stocks (Zavala-Gonzalez et al. 1994, DeMaster et al. 2001, Yodzis 2001, Gerber et al. 2009, Loch et al. 2009, Morissette et al. 2012). Species of both pinnipeds and odontocetes are also impacted directly or indirectly by climate change, reducing home ranges, increasing occurrence of disease, affecting migration patterns and habitat ranges, and affecting the distribution of prey species (Simmonds and Isaac 2007, Simmonds and Eliott 2009, Hoegh-Guldberg and Bruno 2010, Doney et al. 2012, Evans and Bjørge 2013). However

the magnitude of this impact will vary by species dependent upon behaviour and habitat. Therefore, greater knowledge of odontocete and pinniped dietary habits has the potential for better understanding of their impacts and interactions on ecosystems, a greater ability to protect endangered species, reduce the impact of fisheries on odontocete and pinniped populations, and go some way toward predicting the effect of climate change on their ranges and survival.

Assessing the diet of any animal feeding in marine habitats is often difficult and costly. Studies using direct observations and captive specimens are used to investigate marine mammal diet (Ainley et al. 2005, Hocking et al. 2013), but a number of indirect methods have been also been developed for both pinnipeds and odontocetes. Unfortunately, each have associated issues hindering their ability to either accurately define long term dietary habits, or identify specific prey items (Bowen and Iverson 2013).

The main destructive sampling method used to study marine mammal diet is stomach contents analysis, often using specimens culled for scientific purposes (Lowry et al. 1988, Mori et al. 2001, Mikkelsen et al. 2002, Yonezaki et al. 2003, Haug et al. 2004), incidentally caught/stranded animals (De Pierrepont et al. 2005, Spitz et al. 2006, Craddock et al. 2009, Spitz et al. 2011, Pate and McFee 2012), or a combination of the two (Lundstrom et al. 2007). Stomachs are dissected and absolute numbers and proportions of prey items are counted based on hard parts. However this approach suffers from two main issues, firstly any observations on diet are restricted to the time over which animals feed, usually 24 to 48 hours (Tollit et al. 2010), secondly the use of hard parts from stomachs is affected by the relative propensity of similar parts of different organisms to resist digestion (Jobling and Breiby 1986). While lethal sampling is also an issue, recently non-lethal methods involving stomach flushing and DNA analysis have been proposed to reduce this issue (Barnett et al. 2010).

Analysis of faecal pellets (scats) is often used as an alternative to stomach contents analysis when studying pinniped diet, as scats can be collected on land at pinniped breeding and resting sites. This technique is non-destructive and uses many

of the same techniques as stomach contents analysis, determining prey items and relative proportions of prey from hard parts in faecal samples (Brown et al. 2001, Sinclair and Zeppelin 2002, Hall-Aspland and Rogers 2004, Gudmundson et al. 2006, Zeppelin and Ream 2006, Trites et al. 2007, McKenzie and Wynne 2008). One major advantage of this technique over stomach contents analysis is the ability to sample a much larger spectrum and number of individuals with more controls over when specimens are collected. However it also suffers from two of the same issues as stomach contents analysis (Cottrell et al. 1996, Tollit et al. 2003); the timescale over which each animal's diet can be measured is still very short, and the differing resistance of animal hard parts to digestion is still a factor, although some suggestions have been made to limit the effect of this second issue (Bowen 2000, Arim and Naya 2003).

Some studies use a combination of both stomach contents and faecal pellet data (Berg et al. 2002), and in both methodologies DNA samples can also be collected and specimens analysed to determine specific prey species (Jarman et al. 2002, Symondson 2002, Deagle et al. 2005, Deagle et al. 2009). This can reduce the problem of differential hard part resistance to digestion, but DNA isolation can be problematic and expensive, false positives and negatives are possible, and methods for determining prey proportions are only just starting to be developed (Bowen and Iverson 2013).

Quantitative fatty acid signature analysis can also be used to identify prey species and proportions of prey items in the diet of marine mammals (Andersen et al. 2004, Iverson et al. 2004). This technique analyses fatty acids stored in the body tissues of animals to determine prey types. While this technique can be used to study diet over a much longer time span than stomach contents and faecal pellet analysis, it is still being developed and the calibration coefficients used to calculate fatty acid signatures must be generated by studying the species in question over long time spans using fixed captive diets, and appear to be heavily effected by phylogeny and prey type (Rosen and Tollit 2012).

Stable isotope data offers another way to study the diet of marine mammals that avoids some of the issues associated with stomach contents and faecal pellet data (Walker and Macko 1999, Lawson and Hobson 2000, Kurle and Worthy 2001, Young et al. 2009, Chambellant et al. 2013). Here carbon and nitrogen isotopes are used to compare species feeding at different trophic levels, assessing diet over a much longer time span than stomach contents or faecal pellet studies, depending on the tissue type used. However, these analyses cannot provide direct evidence of specific food items consumed, meaning it must be combined with other techniques to be most useful (Crawford et al. 2008).

As such there is still much room for improvement when studying marine mammal diets, and our knowledge is hampered by the limitations of current techniques.

Quantitative 3D microtextural analysis of tooth surfaces potentially offers a new way of investigating diet in odontocetes and pinnipeds. This technique is now a well-established means of understanding the dietary ecology of many extant vertebrate groups (Merceron et al. 2010, Schubert et al. 2010, Delezene et al. 2013, Haupt et al. 2013, Purnell et al. 2013, Schulz et al. 2013a, Schulz et al. 2013b, Merceron et al. 2014, Purnell and Darras 2015). It has a number of advantages, including low operator error (Grine et al. 2002, Galbany et al. 2005, Purnell et al. 2006, Mihlbachler et al. 2012, Purnell et al. 2012), its ability to investigate diet over a longer time span than stomach contents or faecal analyses (normally up to a few weeks) (Teaford and Oyen 1989, Calandra and Merceron 2016), but over a short enough time that seasonal variation can still be studied (Merceron et al. 2010), and it is able to transcend morphological similarities (Purnell and Darras 2015).

The objective of this paper is to investigate whether this technique has the ability to differentiate dietary classes in modern marine mammals with known diets. As such we aim to test the hypothesis that microwear textures of tooth surfaces from extant marine mammals reflect their dietary habits, and the subsidiary hypothesis that phylogenetically distinct taxa (species of odontocete and species of pinniped) have

microwear textures that reflect similarities in diet more than similarities in morphological traits associated with feeding.

Quantitative 3D microtextural analysis of tooth surfaces was originally designed to investigate the diet of fossil animals, where ecological observations are not possible (Ungar et al. 2003, Scott et al. 2005, Merceron et al. 2009, Ungar et al. 2010, Winkler et al. 2013, DeSantis and Haupt 2014, Gill et al. 2014). Therefore, results of analysis of extant groups might offer a new approach to analysis of diet in extinct taxa. In the case of odontocetes and pinnipeds the obvious comparison is stem cetaceans (archaeocetes). Stem cetaceans are the paraphyletic stem of crown group Neoceti (mysticete and odontocete whales) (O'Leary and Geisler 1999, O'Leary and Uhen 1999, Gatesy and O'Leary 2001, Gatesy et al. 2013). They first arose in the early Eocene (ca. 54 My) (Bajpai and Gingerich 1998), and preserve direct evidence of the cetacean transition from terrestrial/semi-aquatic forms to obligate aquatic forms (Gingerich et al. 1983, Thewissen and Fish 1997, Spoor et al. 2002, Clementz et al. 2006, Bajpai et al. 2009, Uhen 2010, Hong-Yan and Xi-Jun 2015). Current consensus places stem cetaceans within the Artiodactyla as a sister group to the hippopotamids (Geisler and Uhen 2003, Boisserie et al. 2005, Geisler et al. 2005, Geisler and Theodor 2009, Uhen 2010), although there has been some disagreement about this relationship (Thewissen et al. 2001, Thewissen et al. 2007, Geisler and Theodor 2009, Uhen 2010, Hong-Yan and Xi-Jun 2015).

There are a number of suggestions for the correct phylogenetic relationships within stem cetaceans (Uhen and Gingerich 2001, Geisler et al. 2005, Uhen 2008, Bianucci and Gingerich 2011, Uhen et al. 2011, Gol'din and Zvonok 2013, Gol'din et al. 2014), but no final set of evolutionary relationships at the species level has been agreed upon (Figure 2.1).

Many evolutionary and phylogenetic aspects of this group cannot be widely agreed upon even though studies of stem cetacean evolution are numerous (Gingerich et al. 1983, Fordyce and Barnes 1994, Gingerich 2003, Bajpai et al. 2009, Thewissen et al. 2009, Uhen 2010) and the number of specimens available for study increases every year (West 1980, Gingerich 1992, Gingerich et al. 1995, Bajpai and Thewissen 2000,

Uhen 2008, Uhen and Berndt 2008, Uhen et al. 2011). A number of definite inferences can be made about specific species from exceptional cases. One such example, *Maiacetus inuus*, likely displayed sexual dimorphism, and gave birth on land due to the orientation of foetal remains found with a single female individual (Gingerich et al. 2009), and the likelihood that *Basilosaurus isis* fed on the smaller *Dorudon atrox* (Fahlke 2012, Snively et al. 2015). However this type of material is incredibly rare.

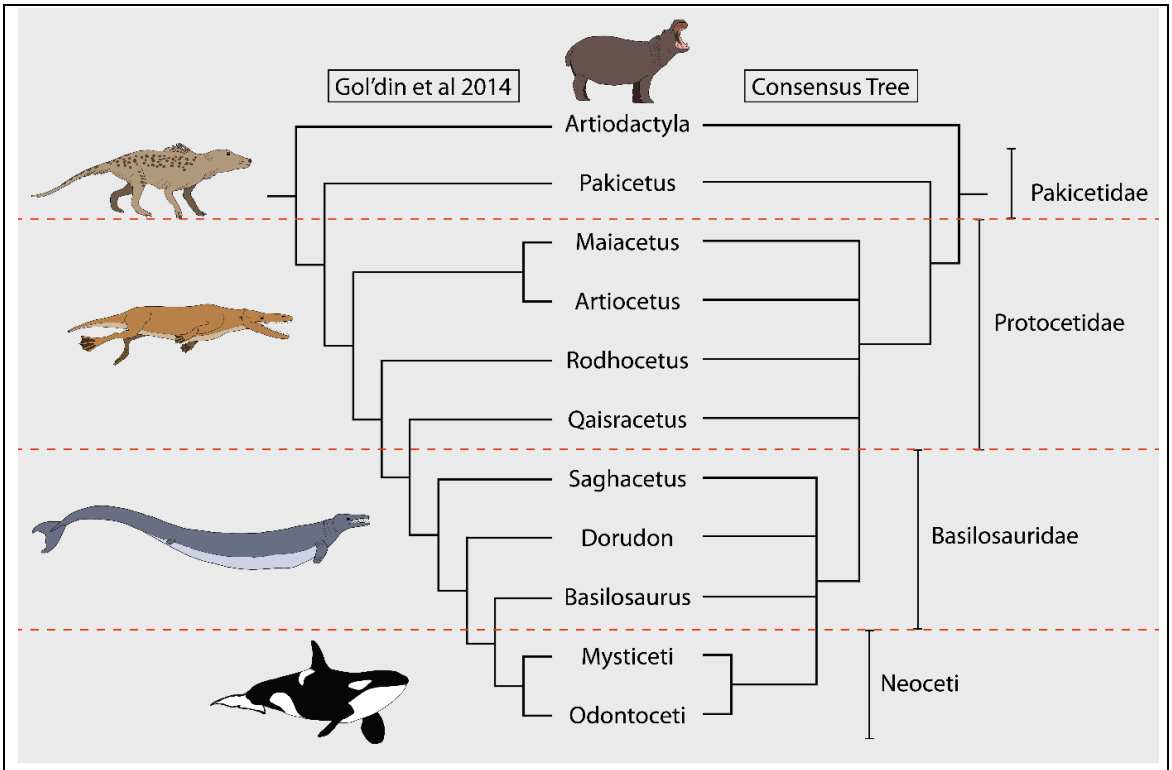

Figure 2.1 *Phylogeny of stem cetacean species included in this paper. Phylogeny on the left reproduced based on Gol'din et al (2014). The phylogeny on the right is a consensus tree based on a number of published phylogenies (Uhen and Gingerich 2001, Geisler et al 2005, Uhen et al 2008, Bianucci and Gingerich 2011, Uhen et al 2011, Gatesy et al 2013, Gol'din et al 2014). Red lines separate stem cetacean "Families".*

Through stem cetacean evolution their morphology underwent a massive degree of change (Thewissen et al. 2009, Uhen 2010). Alongside other adaptations to aquatic living (Gingerich 2003, Buchholtz 2007, Nummela et al. 2007, Fahlke et al. 2011) this involved a marked change in their dentition (Gingerich and Russell 1990,

Maas and Thewissen 1995, Uhen 2000, Thewissen et al. 2011, Gol'din et al. 2014). Stem cetaceans retained a heterodont dentition, but their anterior teeth (incisors and canines) became more morphologically similar to one another, resembling the teeth of modern Odontocetes, while their posterior teeth (pre-molars and molars) developed high crowns and a triangular labio-laterally flattened form to facilitate a shearing motion (Hulbert Jr et al. 1998, Uhen 2010, Thewissen et al. 2011, Gol'din et al. 2014, Snively et al. 2015).

As the earliest forms of the clade, stem cetaceans are of vital importance when trying to understand modern whale and dolphin evolution. Their diet has previously been defined as driving or caused by the evolution to aquatic habitats (Thewissen et al. 2007, Thewissen et al. 2009, Fahlke et al. 2013), so understanding how diet has changed though stem cetacean evolution is of great importance.

However, until recently our knowledge of early cetacean evolution, is almost entirely derived from anatomical studies (Bajpai and Gingerich 1998, Uhen and Berndt 2008, Thewissen et al. 2011, Gol'din et al. 2014), which hypothesise a smooth unidirectional transition in diet through stem cetacean evolution. Very rarely, stomach contents have been preserved in stem cetacean specimens. In these cases it is possible to make direct observations about the short term feeding habits of specific species (Swift and Barnes 1996, Uhen 2004).

Isotopic analyses have also been used to investigate the timing of dietary shifts in stem cetaceans (Clementz et al. 2006, Thewissen et al. 2007, Thewissen et al. 2009). Suggesting a transition from freshwater to shallow marine environments by the early Eocene (Protocetidae), and near-shore marine environments in the late Eocene (Basilosauridae). More recently Thewissen et al. (2011) used isotope data combined with tooth macro wear data from teeth of pakicetids and early protocetids to show that dietary habits were potentially quite homogeneous in the earliest stem cetaceans, and that dietary transitions were not synchronous with adaptation to semi-aquatic environments, disagreeing with both morphological and previous isotope data.

Two-dimensional tooth microwear analysis has also recently been used to investigate diet in stem cetaceans (Fahlke et al. 2013); comparing stem cetaceans with extant odontocetes, pinnipeds and terrestrial carnivores. They found tooth microwear patterns of stem cetaceans differed markedly from terrestrial carnivores and overlap heavily with odontocetes and pinnipeds, although more closely with pinnipeds, suggesting shared dietary habits between these groups. Fahlke et al. (2013) also found that aquatic diets were present in *Pakicetus inachus*, one of the earliest stem cetaceans, but were unable to determine whether this species fed in freshwater, brackish water or marine environments. Almost all stem cetaceans in this study displayed a heterogeneous diet similar to that seen in extant pinniped species. Fahlke et al. (2013) suggest protocetids and *Pakicetus inachus* fed on smaller, less hard items, while basilosaurids, particularly *Basilosaurus isis* fed on marine mammals with large bones due to heavy gouging and coarser wear patterns on their teeth and possibly on sharks due to the similarity between their tooth wear and that of specific *Orcinus orca* individuals (Ford et al. 2011). This would suggest a dietary shift in line with the evolution of obligate aquatic lifestyles.

All of these studies have furthered our understanding of stem cetacean feeding mechanisms, their transition from terrestrial to semi-aquatic to obligate aquatic habitats and indicated changes in diet through their evolution. However they are able to say little about the nature of food items consumed by different species, and disagree to some extent about the homogeneity of diet in the earliest whales, whether the transition of diet through stem cetacean evolution was a smooth or stochastic transition, and whether it was caused by or post-dated their colonization of marine habitats.

Alongside tests of the first hypothesis that microwear textures of tooth surfaces from extant marine mammals reflect their dietary habits, and the subsidiary hypothesis that phylogenetically distinct taxa (species of odontocete and species of pinniped) have microwear textures that reflect similarities in diet more than similarities in morphological traits associated with feeding, this paper also aims to test two further hypotheses; that analysis of microwear texture in stem cetaceans is

comparable to extant marine mammals; and that the hypotheses of diet derived from analysis of microwear texture support hypotheses of a unidirectional dietary transition through the stem cetacean lineage.

Methods

Institutional Abbreviations

CGM, Cairo Geological Museum, Cairo, Egypt; FMNH, Field Museum of Natural History Chicago, USA; GSP, Geological Survey of Pakistan; NHM, Natural History Museum, London, United Kingdom; NMS, National Museums Scotland, Edinburgh, United Kingdom; NMW, Naturhistorisches Museum Wien, Vienna, Austria; UM, University of Michigan Museum of Paleontology, Ann Arbor, USA; UMMZ, University of Michigan Museum of Zoology, Ann Arbor, USA; WH, Wadi Al-Hitan, Egypt (presently curated at the University of Michigan Museum of Paleontology); ZMB_MAM, mammal collection of the Zoological Museum Berlin, Museum für Naturkunde, Berlin, Germany; ZMC, Zoological Museum Copenhagen, University of Copenhagen, Denmark.

Specimens

Seven pinniped and three odontocete species were selected, *Phoca vitulina* (n=5), *Halichoerus grypus* (n=4), *Callorrhinus ursinus* (n=5), *Eumetipias jubatus* (n=4), *Pusa hispida* (n=5), *Pagophilus groenlandicus* (n=5), *Hydrurga leptonyx* (n=7), *Orcinus orca* (n=3), *Tursipos truncatus* (n=3), and *Lagenorhynchus acutus* (n=7). *Orcinus orca* individuals are all from a single North Sea population, known from isotope analysis to eat fish (Foote et al. 2013b).

Thirteen stem cetacean specimens were selected across eight species. This included the families Pakicetidae (n=1, *Pakicetus inachus*), Protocetidae (n=4, one specimen each of *Artiocetus clavis*, *Maiacetus inuus*, *Rodhocetus kasrani*, *Qaisracetus arifi*), and Basilosauridae (n=8, one *Saghacetus osiris*, four *Dorudon atrox*, and three

Basilosaurus isis). The details of all specimens along with collection dates, locations, and host institutions can be found in Table 2.1.

Dietary classes

Odontocetes and pinnipeds display a wide range of dietary habits and feed in both nearshore and open-ocean habitats. From current knowledge, marine mammal diet is made up of many different food types, including fish, cephalopods, other invertebrates and amniotes, and taxonomically distinct groups (pinnipeds and odontocetes) have been suggested to share similar diets, made up of different proportions of these food items (Pauly et al. 1998). Therefore dietary classes containing both pinniped and odontocete species must be defined based on the proportions of food types in their diets rather than sole food items. This approach to dietary classification is supported by work on terrestrial mammals (Pineda-Munoz and Alroy 2014).

Four main dietary classes were identified across species included in this study (Table 2.2). These classes were assembled using stomach contents, and fecal pellet data from a number of published studies on marine mammal diet, (Merrick et al. 1997, Barros and Wells 1998, Pauly et al. 1998, Tollit et al. 1998, Brown et al. 2001, Holst et al. 2001, Santos et al. 2001, Yonezaki et al. 2003, Andersen et al. 2004, Haug et al. 2004, Nilssen et al. 2004, De Pierrepont et al. 2005, Yonezaki et al. 2008, Casaux et al. 2009, Craddock et al. 2009, Chambellant et al. 2013, Foote et al. 2013b). Studies were included where some measure of the proportion of different prey items in the diet, or biomass was available for each species. The dietary classes are; Fish Eaters (>80% of diet made up of fish species), Cephalopod Eaters (>20% of diet made up of cephalopod species), Other Invertebrate Eaters (>20% of diet made up of non-cephalopod invertebrate species, almost all possessing an exoskeleton), and Amniote Eaters (>20% of diet made up of Amniote species, e.g. sea birds and marine mammals). All species studied are known to eat a combination of these four food types. Thus, these dietary classes refer to the relative proportions of food in the diet, and not the sole food type consumed by each species.

Species	Family	Specimen Number	Reported Diet	Tooth Position Used	Moulded by	Locality
Saghacetus osiris	Basilosauridae	UM 83906	-	Lower Right M2	JMF	Fayum, Egypt
Dorudon atrox	Basilosauridae	FMNH P. 12343b	-	Lower Right M2	JMF	Fayum, Egypt
Basilosaurus isis	Basilosauridae	WH 74-0289	-	Right M2	JMF	Wadi al-Hitan, Egypt
Basilosaurus isis	Basilosauridae	WH 2010-001	-	Molar Tooth	JMF	Wadi al-Hitan, Egypt
Basilosaurus isis	Basilosauridae	UM 83901	-	Upper Right PC3	JMF	Egypt
Dorudon atrox	Basilosauridae	UM 97506	-	Lower Left M1	JMF	Wadi al-Hitan, Egypt
Dorudon atrox	Basilosauridae	UM 100146	-	Lower Left M2	JMF	Wadi al-Hitan, Egypt
Dorudon atrox	Basilosauridae	UM 101222	-	Lower Left M2	JMF	Wadi al-Hitan, Egypt
Artiocetus clavis	Protocetidae	GSP-UM 3458	-	Upper Left M2	JMF	Balochistan, Pakistan
Qaisracetus arifi	Protocetidae	GSP-UM 3316	-	Upper Right M2	JMF	Balochistan, Pakistan
Rodhocetus kasrani	Protocetidae	GPS-UM 3012	-	Lower Left M2	JMF	Bozmar Nadi, Punjab, Pakistan
Protocetidae indet.	Protocetidae	GSP-UM 3281	-	Upper Right M2	JMF	Ander Dabh Janubi, Balochistan, Pakistan
Maiacetus inuus	Protocetidae	GSP-UM 3551	-	Lower Left M2	JMF	Pakistan
Protocetidae indet.	Protocetidae	CGM 60581	-	Left M3	JMF	Wadi Rayan (Fayum, Egypt)
Pakicetus inachus	Pakicetidae	GSP-UM 1672	-	Upper M1	JMF	Chorlakki, Pakistan
Lagenorhynchus acutus	Delphinidae	UMMZ 177439	Cephalopods	Cheek Tooth	JMF	Gosnold, Massachusetts
Lagenorhynchus acutus	Delphinidae	UMMZ 177426	Cephalopods	Cheek Tooth	JMF	Wellfleet, Massachusetts
Lagenorhynchus acutus	Delphinidae	UMMZ 176250	Cephalopods	Cheek Tooth	JMF	Unknown
Lagenorhynchus acutus	Delphinidae	NMS Z.2011.41.108	Cephalopods	Lower Left Tooth 20	RHG	Traigh Lar, North Uist
Lagenorhynchus acutus	Delphinidae	NMS Z.2011.41.106	Cephalopods	Lower Left Tooth 22	RHG	South Uist
Lagenorhynchus acutus	Delphinidae	NMS 1956.037	Cephalopods	Lower Right Toth 20	RHG	Bastavoe, Yell, Shetland
Lagenorhynchus acutus	Delphinidae	NMS Z.2011.41.116	Cephalopods	Lower Right Tooth 20	RHG	Eoligarry, Barra
Tursiops truncatus	Delphinidae	ZMB_MAM 66435	Fish	Cheek Tooth	JMF	Unknown
Tursiops truncatus	Delphinidae	NMW 7547	Fish	Cheek Tooth	KAB	Triest (Italy)
Tursiops truncatus	Delphinidae	UMMZ 167402	Fish	Cheek Tooth	JMF	Santa Rosa Beach, Sonora, Mexico
Orcinus orca	Delphinidae	ZMC M1068	Fish	Upper Right Tooth 9	RHG	Mando Island, W Coast of Jutland, Denmark
Orcinus orca	Delphinidae	NHM ZD 1887.5.20.1	Fish	Upper Right Tooth 10	RHG	Bildoen Island
Orcinus orca	Delphinidae	NHM ZD 1886.11.22.1	Fish	Lower Right Tooth 8	RHG	Mouth of the Humber, England
Callorhinus ursinus	Otariidae	ZMB MAM 56761	Cephalopods	Lower Right PC2	JMF	Pribilof Islands, Bering Sea
Callorhinus ursinus	Otariidae	ZMB MAM 60568	Cephalopods	Lower Right PC2	JMF	Alaska
Callorhinus ursinus	Otariidae	ZMB MAM 70669	Cephalopods	Upper Left PC4	JMF	St. Paul Island, Alaska
Callorhinus ursinus	Otariidae	ZMB MAM 5627	Cephalopods	Upper Right PC4	JMF	Pribilof Islands, Bering Sea
Callorhinus ursinus	Otariidae	ZMB MAM 5648	Cephalopods	Upper Left PC4	JMF	Pribilof Islands, Bering Sea
Eumetopias jubatus	Otariidae	ZMB MAM 72816	Cephalopods	Lower Right PC4	JMF	Bering Strait
Eumetopias jubatus	Otariidae	ZMB MAM 2787	Cephalopods	Lower Left PC3	JMF	Kamchatka
Eumetopias jubatus	Otariidae	ZMB MAM 37702	Cephalopods	Lower Left PC3	JMF	Nagai Island, Alaska
Eumetopias jubatus	Otariidae	ZMB MAM 72815	Cephalopods	Upper Right PC5	JMF	St. Paul Island, Alaska
Phoca vitulina	Phocidae	ZMB_MAM 90810	Fish	Upper Left PC5	JMF	Büsum, North Sea
Phoca vitulina	Phocidae	ZMB_MAM 56766	Fish	Upper Right PC4	JMF	North Sea
Phoca vitulina	Phocidae	ZMB_MAM 100997	Fish	Upper Right PC4	JMF	Wangerooge, North Sea
Phoca vitulina	Phocidae	ZMB_MAM 56767	Fish	Upper Right PC4	JMF	North Sea
Phoca vitulina	Phocidae	ZMB_MAM 101271	Fish	Upper Left PC4	JMF	Wangerooge, North Sea
Halichoerus grypus	Phocidae	ZMB_MAM 56786	Fish	Lower Left PC3	JMF	Rügen, Baltic Sea
Halichoerus grypus	Phocidae	ZMB_MAM 70654	Fish	Upper Left PC2	JMF	Oresund, Baltic Sea
Halichoerus grypus	Phocidae	ZMB_MAM 56782	Fish	Upper Left PC3	JMF	Vilm Island, Baltic Sea
Halichoerus grypus	Phocidae	ZMB_MAM 56783	Fish	Upper Left PC3	JMF	Swinouiscie, Poland
Pusa hispida	Phocidae	ZMB_MAM 43743	Invertebrates	Upper Right PC2	JMF	Jameson Land, Greenland
Pusa hispida	Phocidae	ZMB_MAM 43740	Invertebrates	Lower Left PC5	JMF	Scoresby Sund, Eastern Greenland
Pusa hispida	Phocidae	ZMB_MAM 43770	Invertebrates	Lower Left PC5	JMF	Jameson Land, Eastern Greenland
Pusa hispida	Phocidae	ZMB_MAM 43758	Invertebrates	Upper Right PC2	JMF	Jameson Land, Eastern Greenland
Pusa hispida	Phocidae	ZMB_MAM 43763	Invertebrates	Upper Right PC3	JMF	Jameson Land, Greenland
Pagophilus groenlandicus	Phocidae	ZMB_MAM 32569	Invertebrates	Upper Right PC3	JMF	Greenland
Pagophilus groenlandicus	Phocidae	ZMB_MAM 43737	Invertebrates	Upper Left PC2	JMF	Jameson Land, Greenland
Pagophilus groenlandicus	Phocidae	ZMB_MAM 32570	Invertebrates	Upper Right PC3	JMF	Greenland
Pagophilus groenlandicus	Phocidae	ZMB_MAM 43738	Invertebrates	Upper Right PC3	JMF	Jameson Land, Greenland
Pagophilus groenlandicus	Phocidae	ZMB_MAM 56774	Invertebrates	Upper Left PC2	JMF	Greenland
Hydrurga leptonyx	Phocidae	NMS 1996.83.58	Amniotes	Lower Left PC2	RHG	New Zealand, Wellington Harbour
Hydrurga leptonyx	Phocidae	NMS 1948.64	Amniotes	Lower Left PC2	RHG	Unknown
Hydrurga leptonyx	Phocidae	NMS 1921.143.P	Amniotes	Lower Right PC2	RHG	Antarctica
Hydrurga leptonyx	Phocidae	NMS 1905.167.4	Amniotes	Lower Left PC2	RHG	East of South Orkneys
Hydrurga leptonyx	Phocidae	NMS 1921.143.0	Amniotes	Lower Left PC2	RHG	Antarctica
Hydrurga leptonyx	Phocidae	NMS 1822.240.T29	Amniotes	Lower Left PC2	RHG	Unknown
Hydrurga leptonyx	Phocidae	NMS 1960.24	Amniotes	Lower Left PC2	RHG	South Georgia (ex Salvesens)

Table 2.1 *List of all specimens used in this project including Species and Family, plus the institutional specimen number, reported diet, tooth position, and locality for each specimen. For the column "Moulded by", RHG = Robert H Goodall (University of Leicester), JMF = Julia M Fahlke (Museum für Naturkunde, Berlin), KMB = Katharina M Bastl (Medizinische Universität, Vienna*

Multiple *Orcinus orca* ecotypes exist, including Pacific "resident" and "transient" (Ford et al. 1998), and "offshore" (Ford et al. 2011) ecotypes, potential Antarctic ecotypes (Pitman and Ensor 2003), and North Atlantic Fish Eaters and Mammal Eaters (Foote et al. 2013b). The North Atlantic Fish Eating ecotype was used in this study, but could not be included in the table of dietary proportions as the reported diet for this ecotype is based solely on isotope data (Foote et al. 2013b), leaving uncertainty about the proportion of each food type in the diet).

For pinniped dietary classes geographical range was limited as far as possible to remove any intra group dietary bias imposed by access to food types. However, due to their much wider ranges and the relative scarcity of specimens, this was not possible for most Odontocete species. However all *Orcinus orca* specimens are members of a single North Atlantic population. Collection locations for each specimen included in Table 2.1.

	Food Percentages in Diet (%)				
Species	Fish	Cephalopods	Invertebrates	Amniotes	Dietary Class
Pusa Hispida	76.9	0.8	22.2	0.0	Invertebrate Eater
Pagophilus groenlandicus	68.0	1.7	30.3	0.0	Invertebrate Eater
Phoca vitulina	90.4	7.1	2.5	0.0	Fish Eater
Halichoerus grypus	83.6	6.4	7.5	2.5	Fish Eater
Tursiops Truncatus	90.8	9.2	0.0	0.0	Fish Eater
Eumetopias jubatus	69.8	20.2	7.5	2.5	Cephalopod Eater
Callorhinus ursinus	74.6	25.4	0.0	0.0	Cephalopod Eater
Lagenorhynchus acutus	65.6	29.4	5.0	0.0	Cephalopod Eater
Hydrurga Leptonyx	9.5	5.8	40.2	44.5	Amniote Eater

Table 2.2 *Relative proportion of each food type in the diet of all species included in this study (excluding Orcinus orca, as only isotope data was available for this species, which cannot be converted into proportions).*

Data Collection

For all extant specimens a single tooth per individual was sampled from as close to the same region of the jaw as possible (usually using the lower jaw). This selection was complicated somewhat by varying dentitions, and missing teeth in

museum specimens. For Odontocetes, the teeth sampled were equidistant from the distal and mesial ends of the jaw (central cheek teeth). For pinniped specimens post canines two, three, four, and five were used.

For stem cetacean specimens, again a single tooth was sampled, but from the posterior teeth (posterior premolars and molars).

In order to ensure direct comparability with the results of Fahlke et al. (2013) we used the same moulds they used. Tooth locations for all pinniped, odontocete, and stem cetacean specimens used in this study have been included as part of Table 2.1.

Tooth surfaces were replicated using a polyvinylsiloxane moulding compound (President Jet Regular Body, Coltène Whaledent). This compound has been shown to produce highly accurate and precise replicates when moulding tooth surfaces for areal texture analysis (Goodall et al. 2015). Moulding was carried out using an applicator gun, which standardises the mixing of two-components by extruding them through a helical nozzle. Robert Goodall (University of Leicester) produced moulds from *Orcinus orca*, *Hydrurga Leptonyx*, and four of seven *Lagenorhynchus acutus*, Katharina Bastl (Medizinische Universität, Vienna) produced moulds from one of three *Tursiops truncatus* (NMW 7547), and all other moulds were produced by Julia Fahlke (Museum für Naturkunde, Berlin). Casts were made using an epoxy resin containing a black pigment (Epotek 320LV). All casts were placed under 2Bar/30psi of pressure (Protima Pressure Tank 10L, no agitator), for the full duration of their setting (approx. 24hrs) to improve casting fidelity. All casts were gold coated (Emitech K500X sputter coater, four minutes) to optimise data acquisition. This has been shown to produce no difference from original surfaces (Appendix 2: Supplementary Chapter).

Data Acquisition

3D surface texture data were collected from each specimen using focus variation microscopy (Alicona Infinite Focus Microscope, model IFM G4c, software version: 5.1). Data capture followed the methods of previous studies (Purnell et al.

2012, Purnell et al. 2013, Gill et al. 2014, Purnell and Darras 2015) (x100 objective, field of view of 145 x 110 µm, vertical resolution set to 0.02 µm, lateral optical resolution 0.44 µm). All data were collected from tooth enamel. Pinnipeds and odontocetes do not possess faceting teeth, so data were collected from as close to the tooth apex on the labial side as was feasible, as this position is most likely to interact with food items. Data files were only accepted where there was less than 5% missing data. To remove any variation in 3D surfaces arising from manual horizontal positioning of the sample data files were levelled using an all points levelling system (fit to a least squares plane via rotation around all three axes). Surfaces were edited in Surfstand (software version 5.0.0) by manually selecting and replacing data errors with an oblique plane.

3D surface texture data was generated from data files using two different parameterisation methods, one based on ISO 25178-2 (Jiang et al. 2007, International Organization for Standardization 2012), the other using Scale Sensitive Fractal Analysis (SSFA) (Ungar et al. 2003, Scott et al. 2006). For the ISO 25178 method surfaces were scale limited to remove large wavelength information (gross tooth form) using a 5^{th} order of polynomial combined with a spline filter (cut-off wavelength 0.025mm). 22 ISO parameters were then generated automatically from the resulting surfaces. For a full list of parameters see Table 2.3 (See Purnell et al. (2013) and Gill et al. (2014) for more detailed parameter descriptions). Scale Sensitive Fractal Analysis was carried out using the programs SFrax and Toothfrax (Surfract, www.surfract.com). SSFA does not require surfaces to be scale limited, and quantifies five aspects of surface roughness (Table 2.4) in 14 parameters. Settings for all parameters followed those used in previous work (Scott et al. 2006), including the use of scale-sensitive “auto splits” to record Surface Heterogeneity (HAsfc), separating individual scanned sections into increasingly reduced sub-regions (we calculated HAsfc across ten different subdivisions). A scale of observation of 4.4µm was used to calculate epLsar. This differs from previous studies (which used 1.8µm) because this is one order of magnitude higher than the lateral resolution of the microscope being used. Comparability between data collected using different instruments is a concern for 3D microwear analysis, especially when using SSFA parameters, for which settings are intrinsically linked to the limitations of each instrument. Different settings may lead to different

results, reducing the comparability of data collected using different instruments, this variability is experimentally investigated in Chapter 5.

Statistical Analysis

Statistical hypothesis testing was carried out using JMP (Version 11.0.0). The extant marine mammal data were tested for normality (Shapiro Wilks W-test) across each of the four dietary classes. Where data were not normally distributed they were Log transformed (Log_{10}); for the majority of parameters this resulted in normal distributions and data were subjected to parametric tests. The ISO parameter Ssk (Surface Skewness) was excluded as it showed very low levels of normality, and regularly returned a negative value, which could not be Log transformed. The SSFA parameter Smc (Scale of Maximum Complexity) was excluded from all analyses as it either returned the same value for each surface, or a value of zero. The SSFA parameter Tfv was also excluded from further analysis as it returned a value of zero for a number of surfaces. This is due to Tfv calculation being directly linked to the absolute z-range of a surface, which is very variable across the species used in this study.

Microwear parameters were tested for significant differences between the four dietary classes using ANOVA. Variances were tested for equality using O'Brien, Brown-Forsythe, Levene, and Bartlett tests. Where any of these tests returned a significant result Welch ANOVA results are reported. Specific dietary separations between the dietary classes were tested for each parameter using pairwise tests (Tukey-Kramer Honest Significant Difference (HSD) test). These tests assume equal variance in the data, so where data showed unequal variance non parametric Steel-Dwass All Pairs tests were used instead.

Data were also explored using Linear Discriminant Analysis (LDA) (analysis performed in JMP). Potential correlation between the canonical axes of LDA and absolute proportions of food in the diet of extant marine mammals were investigated using Spearman's Rank tests.

Parameter Family	Parameter Name	Definition	Units
Height	Sq	Root Mean Square Height of Surface	µm
	Ssk	Skewness of Height Distribution of Surface	n/a
	Sku	Kurtosis of Height Distribution of Surface	n/a
	Sp	Maximum Peak Height of Surface	µm
	Sv	Maximum Valley Depth of Surface	µm
	Sz	Maximum Height of the Surface (Sp – Sv)	µm
	Sa	Average Height of Surface	µm
Spatial	Str	Surface Texture Aspect Ratio (values range 0-1). Ratio from the distance with the fastest to the distance with the slowest decay of the ACF to the value. 0.2-0.3: surface has a strong directional structure. > 0.5: surface has rather uniform texture.	mm/mm
	Sal	Surface Auto-Correlation Length Horizontal distance of the auto correlation function (ACF) which has the fastest decay to the value 0.2. Large value: surface dominated by low frequencies. Small value: surface dominated by high frequencies.	mm
Hybrid	Ssc	Mean Summit Curvature for Peak Structures	1/µm
	Sds	Density of Summits. Number of summits per unit area making up the surface	$1/mm^2$
	Sdq	Root Mean Square Gradient of the Surface	Degrees
	Sdr	Developed Interfacial Area Ratio of the Surface	%
Volume	Vmp	Surface Peak Material Volume	$\mu m^3/mm^2$
	Vmc	Surface Core Material Volume	$\mu m^3/mm^2$
	Vvc	Surface Core Void Volume	$\mu m^3/mm^2$
	Vvv	Surface Dale Void Volume	$\mu m^3/mm^2$
Material Ratio	Spk	Mean height of the peaks above the core material	µm
	Sk	Core roughness depth, Height of the core material	µm
	Svk	Mean depth of the valleys below the core material	µm
	Smr1	Surface bearing area ratio (the proportion of the surface which consists of peaks above the core material)	%
	Smr2	Surface bearing area ratio (the proportion of the surface which would carry the load)	%
Feature	S5z	Ten Point Height of Surface	µm
Miscellaneous	Std	Texture Direction	Degrees

Table 2.3 *Full list of ISO 25178-2 parameters, including brief descriptions. Parameters Std, Sal, and Ssk were excluded from analyses. For detailed parameter descriptions see Purnell et al (2013) & Gill et al (2014).*

Parameter Name	Acronym	Description
Area Scale Fractal Complexity	Asfc	A measure of the complexity of a surface. Area-scale fractal complexity is a measure of change in roughness with scale. The faster a measured surface area increases with resolution, the more complex the surface.
Exact Proportion Length Scale Anisotropy of Relief	epLsar	A measure of the anisotropy of a surface. Anisotropy is characterized as variation in lengths of transect lines measured at a given scale (we use 3.5 μm) with orientations sampled at 5° intervals across a surface. An anisotropic surface will have shorter transects in the direction of the surface pattern than perpendicular to it (e.g. a transect that cross-cuts parallel scratches must trace the peaks and valleys of each individual feature).
Scale of Maximum Complexity	Smc	The parameter represents the full scale range over which Asfc is calculated. High Smc values should correspond to more complex coarse features.
Textural Fill Volume	Tfv	The total volume filled (Tfv) is a function of two components: 1) the shape of the surface, and 2) the texture of the surface. A more concave or convex surface will have a larger total fill volume than a planar surface even if both surfaces have an identical texture.
Heterogeneity of Area Scale Fractal Complexity	HAsfc	variation of Asfc across a surface (across multiple, equal subdivisions of a surface). High HAsfc values are observed for surfaces that vary in complexity across a facet.

Table 2.4 *Full list of Scale Sensitive Fractal Analysis (SSFA) parameters, including brief descriptions (after refs 16,17). Parameters Tfv and Smc were excluded from analyses. For parameter details and information on methods of calculation see Scott et al (2006).*

Results – Extant Marine Mammals

Verifying the Reliability of Dietary Classes

Proportions of food types in odontocete and pinniped diets (Table 2.2) were compared between each of the expected dietary classes. Due to the lack of normality (Shapiro Wilks W test) and unequal variance (Bartlett, Levene, O'Brien, and Brown Forsythe tests) caused by specimens from the same species all having the same proportion for each food type, rank data was most appropriate. ANOVA were carried out on rank data between the four dietary classes (Table 2.5a). Differences were

evident for comparisons of dietary classes within all of the individual food proportion types. Tukey Honest Significant Difference (HSD) tests and connecting letter reports were used to compare all possible pairs of dietary classes within each of the food proportion types (Table 2.5b). Differences were found between all possible pairs of dietary classes based on cephalopod proportion in the diet. The proportion of fish also differs significantly between dietary classes, except between Invertebrate and Cephalopod Eaters. And for the proportion of invertebrates consumed all dietary classes differ from one another, except Cephalopod and Fish Eaters. The proportion of amniotes consumed differs significantly between comparisons comparing Amniote Eaters with the other dietary classes, but not for comparisons between the other three dietary classes. From these results it is clear that differences in food proportions do exist between the dietary classes. As such they are suitable for testing our hypotheses.

ANOVA results – 3D Microtextural Analysis

ANOVA produced seventeen parameters where differences were recorded between dietary classes (approx. 81% of tests; Table 2.6). These were Height Parameters Sq, Sp, Sv, Sz, Sa, Hybrid Parameters Sdq, Ssc, Sdr, Volume Parameters Vmp, Vmc, Vvc, Vvv, Material Ratio Parameters Spk, Sk, Svk, Smr1, and the Feature Parameter S5z (for parameter abbreviations Table 2.3). Only one out of twelve SSFA parameters (Asfc – Surface complexity) showed a difference between the dietary classes (for parameter abbreviations Table 2.4). These results strongly support the hypothesis that microwear texture in extant Pinnipeds and Odontocetes differs according to diet.

Pairwise test results – 3D Microtextural Data

Where a parameter showed difference between dietary classes (ANOVA), Tukey HSD/Steel Dwass All Pairs tests showed differences between at least one pair of dietary classes. For the ISO 25178-2 parameter Sku difference was found between the Cephalopod and Fish Eating group, where no corresponding difference was found from ANOVA.

A.

	ANOVA		
	F-Ratio	p	d.f
Fish Proportion	58.1155	**<.0001**	3, 41
Cephalopod Proportion	154.8420	**<.0001**	3, 41
Invertebrate Proportion	48.2299	**<.0001**	3, 41
Amniote Proportion	47.2170	**<.0001**	3, 41

B.

	Dietary Classes					
Tukey HSD	Amniote vs Fish Eaters	Invertebrate vs Fish Eaters	Amniote vs Cephalopod Eaters	Invertebrate vs Cephalopod Eaters	Cephalopod vs Fish Eaters	Amniote vs Invertebrate Eaters
	p value	p value	p value	p value	p value	p value
Fish Proportion	**<.0001**	**<.0001**	**0.0003**	0.1326	**<.0001**	**<.0001**
Cephalopod Proportion	**0.0402**	**<.0001**	**<.0001**	**<.0001**	**<.0001**	**0.0005**
Invertebrate Proportion	**<.0001**	**<.0001**	**<.0001**	**<.0001**	0.9475	**0.0207**
Amniote Proportion	**<.0001**	0.1721	**<.0001**	0.3532	0.9355	**<.0001**

Connecting Letters	Fish Proportion	Cephalopod Proportion	Invertebrate Proportion	Amniote Proportion
Fish Eaters	A	A	A	A
Cephalopod Eaters	B	B	B	B
Invertebrate Eaters	B	C	C	B
Amniote Eaters	C	D	C	B

Table 2.5 *ANOVA (A.), and Tukey HSD tests with connecting letter reports (B.) for ranked Proportions of Food tested between the four dietary groups. Significant test results highlighted in bold.*

Tukey HSD/Steel Dwass All Pairs tests between the four dietary classes (Figure 2.2) show that fourteen parameters show a significant differences between Amniote Eaters and Cephalopod Eaters (Sq, Sv, Sz, Sdq, Ssc, Sdr, Vmc, Vvc, Vvv, Sk, Svk, S5z, Sa, and Asfc). This is almost identical to the twelve parameters showing difference between Invertebrate Eaters and Cephalopod Eaters (Sq, Sv, Sz, Sdq, Ssc, Sdr, Vmc, Vvc, Sk, S5z, Sa, and Asfc). A much small number of parameters are able to separate Amniote Eaters and Fish Eaters (Sq, Sv, Sz, Svk, S5z, and Asfc), or Invertebrate Eaters and Fish Eaters (Sz, Spk, S5z). Two parameters (Sku, and Smr1) show a significant difference between Fish Eaters and Cephalopod Eaters. No parameter showed any significant difference between Amniote Eaters and Invertebrate Eaters. For parameter descriptions see Table 2.3 and Table 2.4.

		ANOVA Result		
		F Ratio	p	d.f
ISO 25178 Parameters	**Sq**	**5.6839**	**0.0022**	**3, 44**
	Sku	2.4979*	0.0910*	3, 18.8
	Sp	**3.7303**	**0.0179**	**3, 44**
	Sv	**5.8659**	**0.0018**	**3, 44**
	Sz	**6.9206**	**0.0006**	**3, 44**
	Sds	0.0887	0.9659	3, 44
	Str	0.9708	0.4151	3, 44
	Sdq	**8.2461***	**0.0011***	**3, 18.4**
	Ssc	**6.1826***	**0.0044***	**3, 18.1**
	Sdr	**8.4051***	**0.0010***	**3, 18.4**
	Vmp	**5.0417***	**0.0098***	**3, 19**
	Vmc	**5.7315**	**0.0021**	**3, 44**
	Vvc	**5.6144**	**0.0024**	**3, 44**
	Vvv	**3.4069**	**0.0256**	**3, 44**
	Spk	**5.5263***	**0.0067***	**3, 19.1**
	Sk	**5.5087**	**0.0027**	**3, 44**
	Svk	**3.5720**	**0.0213**	**3, 44**
	Smr1	**4.1720***	**0.0202***	**3, 18.6**
	Smr2	0.1809	0.9088	3, 44
	S5z	**12.1201***	**0.0001***	**3, 19.1**
	Sa	**5.6615**	**0.0023**	**3, 44**
SSFA Parameters	**Asfc**	**8.0023**	**0.0002**	**3, 44**
	epLsar	0.2809*	0.8386*	3, 22.3
	HAsfc 2x2	1.5656	0.2112	3, 44
	HAsfc 3x3	1.0514	0.3794	3, 44
	HAsfc 4x4	1.3787	0.2618	3, 44
	HAsfc 5x5	1.6303	0.1960	3, 44
	HAsfc 6x6	1.4625	0.2378	3, 44
	HAsfc 7x7	1.5414	0.2172	3, 44
	HAsfc 8x8	2.0257	0.1241	3, 44
	HAsfc 9x9	2.2337	0.0976	3, 44
	HAsfc 10x10	2.1425	0.1084	3, 44
	HAsfc 11x11	2.1915	0.1025	3, 44

Table 2.6 *Results of ANOVA carried out between the four dietary classes based on ISO and SSFA parameter values. Bold values indicate significant test results, and * indicate Welch test results. Degrees of freedom presented in column d.f.*

Tukey connecting letter reports (Table. 2.7) indicate that no difference is ever found between Amniote and Invertebrate Eaters, and in most parameters there is no difference between Fish and Cephalopod Eaters (almost always part of the same lettered group). However different parameters suggest slightly different overall separation/lack of separation between dietary classes. Sq, Sv, Sdq, Ssc, Sdr, and Asfc all show no difference between Amniote and Invertebrate Eaters, Invertebrate and Fish Eaters, or Fish and Cephalopod Eaters, but do show differences between Amniote Eaters and Fish Eaters, Amniote Eaters and Cephalopod Eaters, and Invertebrate Eaters and Cephalopod Eaters. Sa, Vmc, Vvc, and Sk suggest a simpler relationship, with Amniote, and Invertebrate Eaters differing from Cephalopod Eaters, but no classes differing from Fish Eaters. Vmp, and Spk separate Fish and Amniote Eaters, but cannot separate Invertebrate or Cephalopod Eaters from any dietary class. Sz, and S5z are able to separate both Amniote and Invertebrate Eaters from Fish and Cephalopod Eaters, but do not show any difference between Amniote and Invertebrate Eaters, or between Fish and Cephalopod Eaters. The remaining parameters (Vvv, Svk, Smr1) each show differences between slightly different dietary classes but with similarities to several of the above. No parameter differs between all four dietary classes (for parameter descriptions see Tables 2.3 & 2.4). There is a general pattern of difference between the dietary classes shown by the results of Tukey HSD and connecting letter reports. There is rarely any difference between Fish and Cephalopod Eaters, and never any difference between Amniote and Invertebrate Eaters. The difference appears to be between the two pairings, so that Fish and Cephalopod Eaters are almost always different from Amniote and Invertebrate Eaters. Some other differences exist, but this pattern of results is the most prevalent.

	Tukey HSD Tests/ Steel Dwass All Pairs Tests		
Dietary Group	**Fish Eaters**	**Cephalopod Eaters**	**Invertebrate Eaters**
Cephalopod Eaters	Sku*, Smr1*		
Invertebrate Eaters	Sz, Spk*, S5z*	Sq, Sv, Sz, Sdq*, Ssc*, Sdr*, Vmc, Vvc, Sk, S5z*, Sa, Asfc	
Amniote Eaters	Sq, Sv, Sz, Svk, S5z*, Asfc	Sq, Sv, Sz, Sdq*, Ssc*, Sdr*, Vmc, Vvc, Vvv, Sk, Svk, S5z*, Sa, Asfc	

Figure 2.2 *Matrix displaying all parameters where pairwise Tukey HSD tests retuned significant results between each combination of dietary classes. Stars represent tests where variances were not equal, and so the results of Steel Dwass All Pairs tests are reported instead. For parameter abbreviations see Table 2.3 and Table 2.4.*

Multivariate Analyses – 3D Microtextural Data

To further test the hypothesis that that microwear textures of tooth surfaces from extant marine mammals reflect their dietary habits, Linear Discriminant Analysis (LDA) was carried out for all odontocete and pinniped species, based on ISO parameter data, using dietary classes as expected groups (Figure 2.3).

Forward stepwise parameter selection using 12 of 21 parameters (Sq, Sku, Sv, Str, Sdq Ssc, Sdr, Vmp, Svk, Smr1, S5z, and Sa) produced an ordination on 3 canonical axes (number of classes tested minus one). Four specimens (8.33%) were misclassified), and the separation of group means along each axis was significant (Wilks' Lambda; p=<0.0001). The average probability of group assignment for correctly classified specimens was 85.4%, however values ranges from 45.8% to 99.9%. All three axes account for a relatively high percentage (minimum 25.48%) of the variance in the data. Selecting a greater number of parameters, using either forward or backward stepwise selection, produced no appreciable difference in the number of misclassified

specimens, (using all 21 ISO parameters three specimens were misclassified). Using fewer parameters resulted in in ordinations with insignificant test results and a greater number of misclassified specimens (e.g when only ten parameters were included eight specimens were misclassified and the test of discriminatory function along axis three was no longer significant). Leave one out cross validation was carried out for the LDA model, repeated for ten random exclusions, in all but one replicate the classification of the excluded specimen did not change from that recorded in the original LDA analysis (Supplementary Table 2.1; see supplementary information at the end of the thesis), suggesting the LDA model is relatively stable.

Parameter Type	Dietary Class	Sq*			Sku	Sp*	Sv*			Sz*		Sa*	
Height	Amniote Eaters	A			A	A	A			A		A	
	Invertebrate Eaters	A	B		A	A	A	B		A		A	
	Fish Eaters		B	C	A	A		B	C		B	A	B
	Cephalopod Eaters			C	A	A			C		B		B
		Sds	Str	Sdq*			Ssc*			Sdr*			
Spatial & Hybrid	Amniote Eaters	A	A	A			A			A			
	Invertebrate Eaters	A	A	A	B		A	B		A	B		
	Fish Eaters	A	A		B	C		B	C		B	C	
	Cephalopod Eaters	A	A			C			C			C	
		Vmp*		Vmc*		Vvc*		Vvv*					
Volume	Amniote Eaters	A		A		A		A					
	Invertebrate Eaters	A	B	A		A		A	B				
	Fish Eaters		B	A	B	A	B	A	B				
	Cephalopod Eaters	A	B		B		B		B				
		Spk*		Sk*		Svk*		Smr1*		Smr2			
Material Ratio	Amniote Eaters	A		A		A		A	B	A			
	Invertebrate Eaters	A	B	A		A	B	A	B	A			
	Fish Eaters		B	A	B		B		B	A			
	Cephalopod Eaters	A	B		B		B	A		A			
		S5z*											
Feature	Amniote Eaters	A											
	Invertebrate Eaters	A											
	Fish Eaters		B										
	Cephalopod Eaters		B										
		Asfc*			epLsar	Hasfc 2x2 - 11x11									
SSFA	Amniote Eaters	A			A	A	A	A	A	A	A	A	A	A	A
	Invertebrate Eaters	A	B		A	A	A	A	A	A	A	A	A	A	A
	Fish Eaters		B	C	A	A	A	A	A	A	A	A	A	A	A
	Cephalopod Eaters			C	A	A	A	A	A	A	A	A	A	A	A

Table 2.7 *Tukey Connecting Letters report for comparisons between dietary classes based on ISO and SSFA parameter values. Connections between dietary classes are displayed as shared letters. Colours indicate parameters displaying exactly the same pattern of differences between dietary classes. Text is pale grey where all classes are connected by the same letter (no difference between classes).*

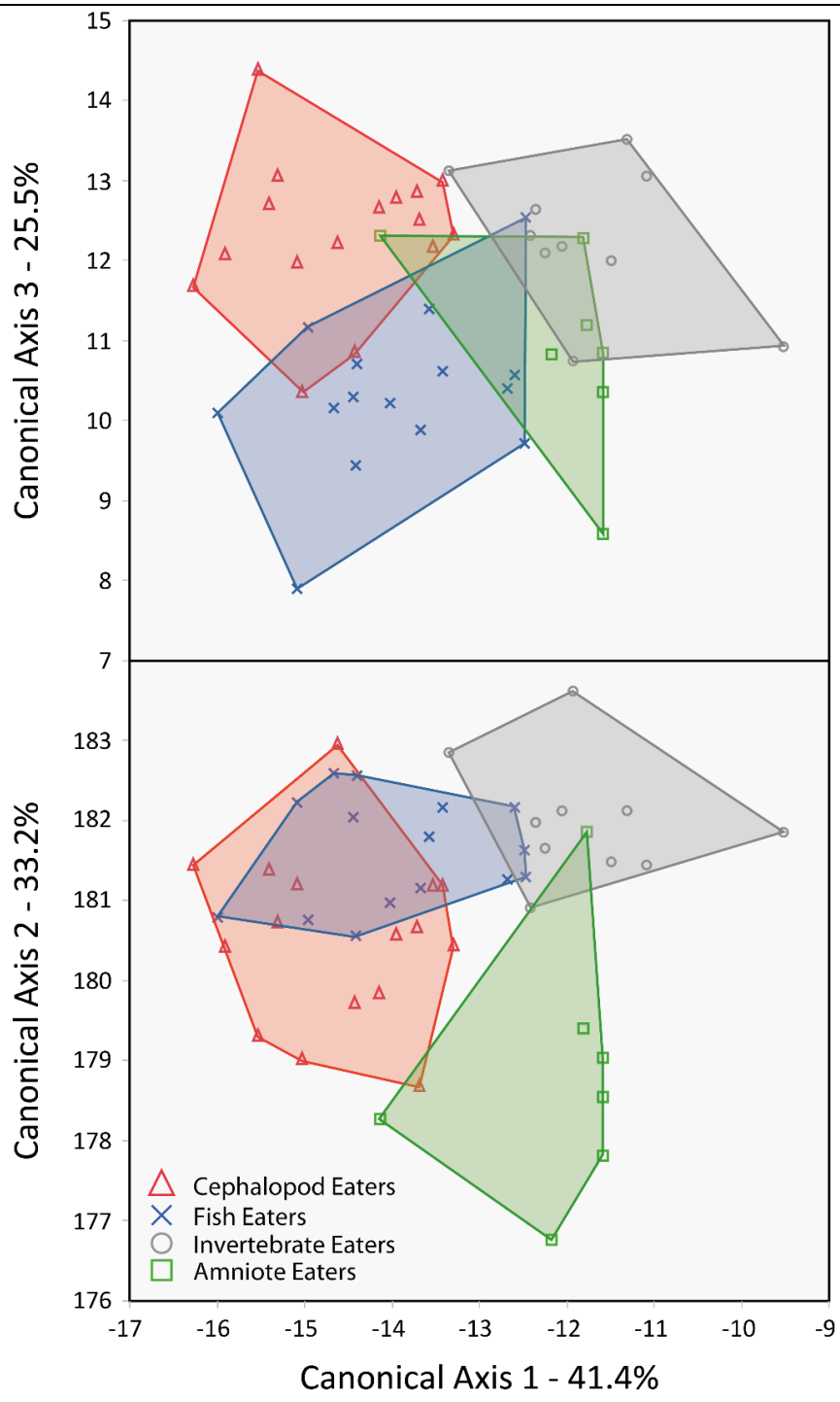

Figure 2.3 *Linear Discriminant Analysis (LDA) for all extant Odontocete and Pinniped specimens. LDA carried out using forward stepwise variable selection, 12 parameters were selected at which point all canonical axes returned significant results for Wilks Lambda tests (CA1 - p=<0.0001, CA2 - p=0.0001, CA3 – p=0.0054). Blue crosses = Fish Eaters, red triangles = Cephalopod Eaters, grey circles = Invertebrate Eaters, and green squares = Amniote Eaters. Convex hull colours correspond to the symbol colour for each dietary class.*

In the 3D multivariate space there are several discreet distributions, corresponding to dietary classes. The distributions of Amniote Eaters and Invertebrate Eaters are almost completely separate from one another and all other dietary classes with only a small degree of overlap. However there is much less difference between the distribution of Fish Eaters and Cephalopod Eaters, with a high degree of overlap between these two classes.

On Canonical Axis 1 (CA1) Fish and Cephalopod Eaters are clearly separated from Invertebrate and Amniote Eaters, with specimens from the latter two classes almost always plotting more positively along CA1 then the former two classes. The parameters with the greatest loading (eigenvectors) on CA1 are Sq (-93.3), S5z (32.8), and Sa (77.7).

Along Canonical Axis 2 (CA2) the separation of classes appears to be between Fish/ Invertebrate Eaters and Cephalopod/Amniote Eaters. However this separation is far less clear due to the high degree of overlap between the Fish Eaters and Cephalopod Eaters. The greatest parameters loadings on CA2 are Sdq (-189.5), and Sdr (95.7).

There is also some degree of separation along Canonical Axis 3 (CA3), with the distributions of Cephalopod/Invertebrate Eaters being quite different from that of Fish/Amniote Eaters. There is much less difference between the distributions of Invertebrate Eaters and Amniote Eaters on this axis, and the Cephalopod and Fish eating classes are separated to a much greater degree than on either of the other two axes. There is no apparent separation on CA3 between Fish Eaters and Higher Vertebrate Eaters, or between Invertebrate Eaters and Fish Eaters. The greatest parameter loading on CA3 are Sq (-355.6), and Sa (310.5).

Dietary Similarity and Tooth Morphology – 3D Microtextural Data

It is interesting to note that although pinnipeds and odontocetes have very different tooth morphologies, those species expected to have the same diet all fall

within the same dietary space. To test whether the impact of diet on surface texture is greater than that of taxonomy, an additional set of ANOVA and Linear Discriminant Analysis were carried out. These used only those dietary classes including both pinniped and odontocete specimens (Fish Eaters and Cephalopod Eaters), but split these two classes into four sub-classes, based on both diet and taxonomy (Fish Eating pinnipeds, Fish Eating odontocetes, Cephalopod Eating pinnipeds, and Cephalopod Eating odontocetes).

ANOVA were carried out between the four sub-classes for all 33 parameters (both SSFA and ISO parameters). It was found that 14 parameters showed differences between the dietary sub-classes (All ANOVA and Tukey HSD test results can be seen in Table 2.8). If diet is the stronger signal we would expect differences from pairwise Tukey HSD tests to be between dietary classes and not taxonomic groups. Eight parameters showed difference between sub-classes based on taxonomy, three between odontocete and pinniped specimens expected to eat fish (Sq, Vvv, and Sa), and five between odontocete and pinniped specimens expected to eat cephalopods (HAsfc 7x7 - 11x11). However, only two of these parameters have previously been found to separate marine mammal dietary classes (Table 2.6). In contrast, 20 differences across 13 parameters were found between dietary sub-classes based on dietary differences, six between Fish and Cephalopod Eating odontocetes (Sq, Vmc, Vvc, Vvv, Sk, and Sa), nine between Fish Eating pinnipeds and Cephalopod Eating odontocetes (Sku, Smr1, HAsfc 5x5 – HAsfc 11x11), and five between Fish Eating odontocetes and Cephalopod Eating pinnipeds (Vmc, Sk, Smr1, HAsfc 9x9, and HAsfc 11x11). Nine of these differences were recorded in parameters previously found to separate marine mammal dietary groups (Table 2.6). The signal between dietary classes therefore appears to be far stronger than that between taxonomic groups, especially for parameters which are informative in regards to marine mammal diet. Tukey connecting letter reports (Table 2.9) for those parameters where dietary sub-classes are found to be different (ANOVA) indicate that no parameter separates sub-classes based solely on taxonomy.

				Tukey Tests					
				Taxonomic Comparisons		Dietary Comparisons			
	ANOVA Result			oFE vs pFE	oCE vs pCE	oFE vs oCE	pFE vs pCE	oFE vs pCE	pFE vs oCE
Parameter	F Ratio	p	d.f	Tukey p	Tukey p	Tukey p	Tukey p	Tukey p	Tukey p
Sq	**4.1251**	**0.0157**	**3, 27**	**0.0273**	0.4441	**0.0199**	0.5889	0.2645	0.9879
Sku	**4.5984**	**0.0234***	**3, 11.8**	0.9293	0.9919	0.6864	0.1254	0.4849	0.2688
Sp	2.1914	0.1121	3, 27	0.9867	0.4912	0.9556	0.5700	0.8403	0.9964
Sv	0.6378	0.5972	3, 27	0.7634	0.7708	0.6583	0.8726	0.9904	0.9940
Sz	1.1085	0.3628	3, 27	0.7607	0.4829	0.7735	0.4446	0.9823	1.0000
Sds	2.5778	0.0744	3, 27	0.0653	0.8036	0.6191	0.9548	0.1626	0.5196
Str	0.6388	0.5966	3, 27	0.7706	0.9982	0.6969	0.9787	0.5602	0.9972
Sdq	1.9378	0.1473	3, 27	0.4510	0.7588	0.1022	0.9997	0.4033	0.7078
Ssc	1.5350	0.2281	3, 27	0.9968	0.9866	0.3681	0.5353	0.4972	0.3917
Sdr	2.0157	0.1354	3, 27	0.4547	0.7779	0.0941	0.9976	0.3626	0.6768
Vmp	2.8337	0.0570	3, 27	0.2507	0.1787	0.9996	0.1103	0.9969	0.3391
Vmc	2.3225	0.1214*	3, 13.4	0.0851	0.9069	**0.0157***	0.9876	**0.0456***	0.7629
Vvc	**2.9667**	**0.0497**	**3, 27**	0.1232	0.8623	**0.0412**	0.9999	0.1396	0.8910
Vvv	**3.9810**	**0.0180**	**3, 27**	**0.0435**	0.2127	**0.0420**	0.2331	0.7169	0.9979
Spk	2.6060	0.0723	3, 27	0.3458	0.1746	0.3996	0.1293	0.9862	1.0000
Sk	2.0511	0.1552*	3, 13.3	0.1073	0.9932	**0.0268***	0.9245	**0.0328***	0.8310
Svk	**3.3631**	**0.0332**	**3, 27**	0.0838	0.2260	0.1119	0.1737	0.9309	1.0000
Smr1	**6.2420**	**0.0023**	**3, 27**	0.9235	0.1819	0.3412	**0.0074**	**0.0040**	0.6145
Smr2	1.9005	0.1533	3, 27	0.8256	0.1487	0.5191	0.3542	0.9174	0.9212
S5z	2.3664	0.0931	3, 27	0.1512	0.4441	0.2298	0.3141	0.9256	0.9991
Sa	**3.9976**	**0.0177**	**3, 27**	**0.0435**	0.6614	**0.0148**	0.9562	0.1129	0.9055
Asfc	1.6781	0.1952	3, 27	0.6286	0.8877	0.1536	0.9677	0.3877	0.6631
epLsar	2.5810	0.0742	3, 27	0.3517	0.1535	0.1201	0.4590	0.9845	0.8572
HAsfc 2x2	1.9582	0.1441	3, 27	0.9554	0.6268	0.9764	0.1122	0.4023	0.7577
HAsfc 3x3	1.7752	0.1757	3, 27	1.0000	0.3669	0.9971	0.2134	0.2990	0.9964
HAsfc 4x4	2.0241	0.1342	3, 27	0.9991	0.4256	0.9519	0.1718	0.2010	0.9711
HAsfc 5x5	**3.8220**	**0.0211**	**3, 27**	0.9999	0.0792	0.9989	**0.0327**	0.0726	0.9963
HAsfc 6x6	**3.3462**	**0.0338**	**3, 27**	0.9952	0.0988	1.0000	**0.0445**	0.1333	0.9972
HAsfc 7x7	**4.1258**	**0.0157**	**3, 27**	0.9928	**0.0443**	0.9969	**0.0249**	0.0909	0.9999
HAsfc 8x8	**4.4272**	**0.0118**	**3, 27**	0.9789	**0.0439**	0.9985	**0.0157**	0.0818	0.9953
HAsfc 9x9	**5.0056**	**0.0069**	**3, 27**	0.9964	**0.0291**	1.0000	**0.0114**	**0.0434**	0.9980
HAsfc 10x10	**4.8461**	**0.0080**	**3, 27**	0.9692	**0.0350**	0.9986	**0.0103**	0.0664	0.9907
HAsfc 11x11	**5.4108**	**0.0048**	**3, 27**	0.9871	**0.0208**	0.9988	**0.0077**	**0.0408**	0.9978

Table 2.8 *ANOVA results for comparisons between dietary sub-classes; odontocete Fish Eater (oFE), odontocete Cephalopod Eater (oCE), pinniped Fish Eater (pFE), and pinniped Cephalopod Eater (pCE), based on ISO and SSFA parameter values. Bold results indicate significant results and * indicate Welch test results (used when variances are unequal). Tukey HSD test results are also shown for all possible combinations of dietary sub groups, broken down into those between sub groups with taxonomic differences (but the same expected diet), and those with dietary differences. * indicate non-parametric Steel Dwass All Pairs results (used when variances are unequal).*

	ISO 25178 Parameters													
Dietary Sub-Class	**Sq**		**Vmc**		**Vvc**		**Vvv**		**Sk**		**Smr1**		**Sa**	
pFE		B	A		A	B		B	A	B		B		B
oFE	A		A	B	A		A		A			B	A	
pCE	A	B		B	A	B	A	B		B	A		A	B
oCE		B		B		B		B		B	A	B		B

	SSFA Parameters													
Dietary Sub-Class	**HAsfc 5x5**		**HAsfc 6x6**		**HAsfc 7x7**		**HAsfc 8x8**		**HAsfc 9x9**		**HAsfc 10x10**		**HAsfc 11x11**	
pFE		B		B		B		B		B		B		B
oFE	A	B	A	B	A	B	A	B		B	A	B		B
pCE	A		A		A		A		A		A		A	
oCE	A	B	A	B		B		B		B		B		B

Table 2.9 *Tukey connecting letters report for comparisons between dietary sub-classes; odontocete Fish Eater (oFE), odontocete Cephalopod Eater (oCE), pinniped Fish Eater (pFE), and pinniped Cephalopod Eater (pCE) based on ISO and SSFA parameter values. Parameter have not been included where no difference between any sub-classes were recorded. Differences/connections between dietary sub-classes are displayed as different/shared letters.*

Linear Discriminant Analysis was carried out to compare the four sub-classes (Fish Eating pinnipeds, Fish Eating odontocetes, Cephalopod Eating pinnipeds, and Cephalopod Eating odontocetes). Forward stepwise variable selection using 18 of the 33 parameters (Sq, Sku, Sv, Sds, Ssc, Sdr, Smr1, S5z, Sa, Asfc, epLsar, HAsfc 4x4 to 7x7, and HAsfc 9x9 to 11x11) produced an ordination on three canonical axes (Figure 2.4). All three axes showed significant discriminatory power between the dietary sub-classes (Wilks' Lambda tests, CA1 p = 0.0023, CA2 p = 0.0121, CA3 p = 0.0416), and there were zero misclassifications. The addition of any further parameters to the analysis resulting in a non-significant Wilks' Lambda test for CA3, and the use of any fewer resulted in a greater level of misclassification. On all three axes dietary sub-classes are separated into discrete clusters with complete separation, except between Cephalopod Eating odontocetes and Fish Eating pinnipeds along CA3. CA1 separates Cephalopod Eating pinnipeds and Fish Eating odontocetes from Cephalopod Eating odontocetes and Fish Eating pinnipeds, the latter have positive values on CA1 while the former have negative values. Scoring coefficients show that Sq (-88.8) and Sa (93.6) have the greatest loading on this axis. CA2 appears to be the axis of dietary

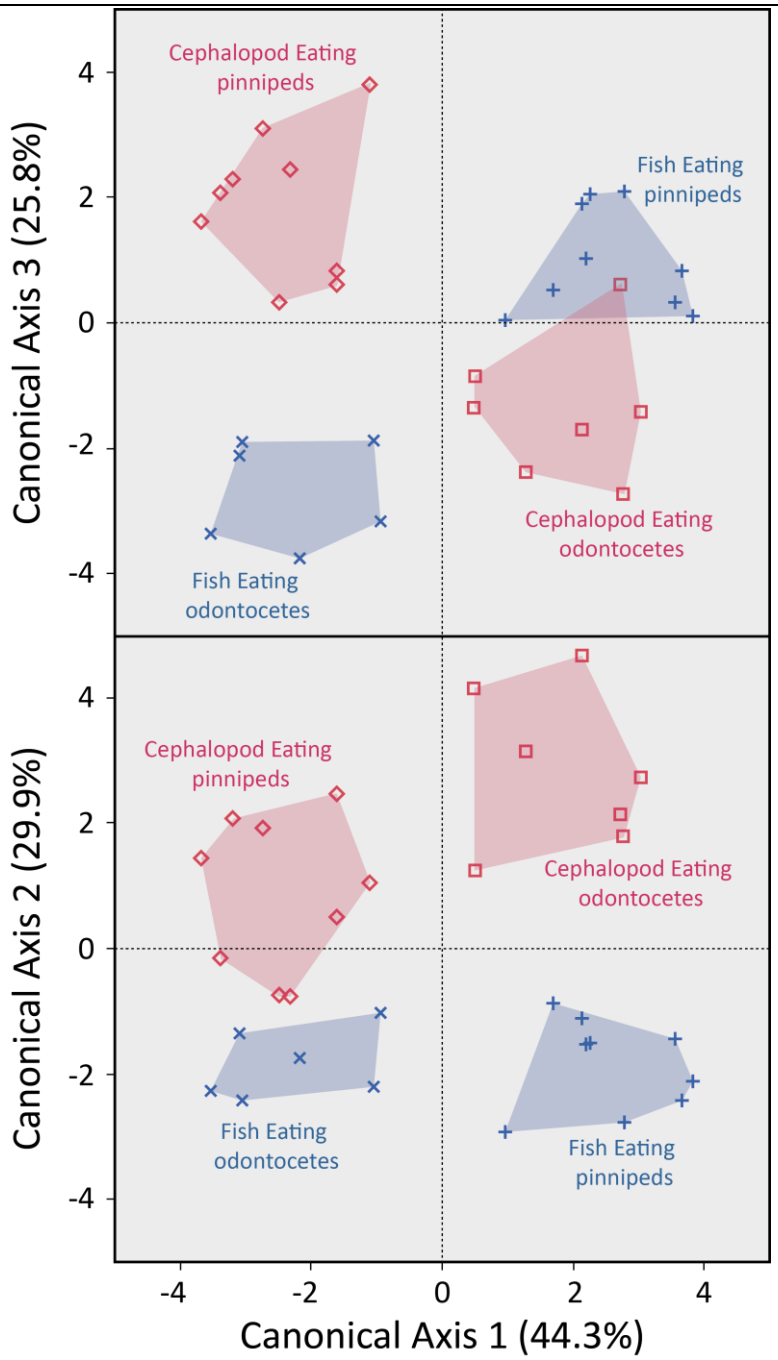

Figure 2.4 *Linear Discriminant Analysis (LDA) comparing 4 dietary sub-groups (Fish Eating pinnipeds, Fish Eating odontocetes, Cephalopod Eating pinnipeds, and Cephalopod Eating odontocetes). CA1 Wilks' Lambda p = 0.0023, CA2 p = 0.0121, CA3 p = 0.0416. Points and convex hulls coloured based on dietary groupings (Red – Cephalopod Eaters, Blue – Fish Eaters). Labels indicate dietary and taxonomic affinities. Parameters with the greatest scoring coefficients for CA1 are Sq -88.8, and Sa 93.6, for CA2 – Sdr -53.2, and Asfc 68.8, and for CA3 – Sq -299.5, Sdr -313.6, Sa 373.8, and Asfc 280.5.*

discrimination, separating Cephalopod Eating classes (mostly positive values on CA2) from Fish Eating classes (negative values on CA2). Scoring coefficients show that Sdr (-53.2) and Asfc (68.8) have the greatest loadings on this axis. CA3 separates classes based on taxonomic groups, showing difference between the pinniped sub-classes (positive values on CA3) and odontocete sub-classes (negative values on CA3). However there is some overlap on this axis between Fish Eating pinnipeds Cephalopod Eating odontocetes. The parameters loading greatest on this axis are Sq (-299.4), Sdr (-313.6), Sa (373.8), and Asfc (280.5).

Extant Marine Mammals: Correlations – 3D Microtextural Data

Spearman's rank correlations were performed between the proportion of food items in the diet of each specimen and their position on Canonical Axes from the LDA containing all extant specimens (Figure 2.3). This tests whether the axes of dietary separation follow the same pattern as the proportions of food in each species' diet.

Canonical Axis 1 is significantly positively correlated with the proportion of non-cephalopod invertebrates in the diet ($R_s = 0.673$, $p = <.0001$), and significantly negatively correlated with the proportion of cephalopods in the diet ($R_s = -0.697$, $p = <.0001$).

Canonical Axis 2 is significantly positively correlated with the proportion of fish in the diet ($R_s = 0.475$, $p = 0.001$), and negatively correlated with both the proportion of cephalopods and amniotes in the diet (respectively $R_s = -0.354$, $p = 0.017$; $R_s = -0.372$, $p = 0.012$).

Canonical Axis 3 is not correlated with any dietary food proportions.

Discussion – Extant Marine Mammals

It is apparent from the results that microwear textures of extant pinniped and odontocete tooth surfaces do reflect their dietary habits. We are able to show statistical differences between dietary classes using ISO 25178 parameters, and further, using 12 of the 21 parameters available we are able to correctly distinguish dietary classes using Linear Discriminant Analysis in over 93% of individuals. This is the first time this technique has been applied to marine mammals and thus it potentially offers a new way to investigate diet in this group.

Scale Sensitive Fractal Analysis appears to be much less sensitive to these dietary differences, showing differences between dietary classes in only one parameter (ANOVA).

ANOVA results show differences between dietary classes in 17 of 33 parameters. Pairwise test results show a strong separation between Fish/Cephalopod Eaters, and Invertebrate/Amniote Eaters. Pairwise tests also suggest a small degree of separation between Fish eaters and Cephalopod eaters, but only in two parameters. There are no parameters that separate Invertebrate eaters from Amniote Eaters in pairwise testing. Given the complex nature and high number of ISO 25178-2 parameters it is difficult to say anything specific about how each type of surface differs in relation to its function; however these results do suggest that differences in 3D tooth texture are between Invertebrate/Amniote Eaters and Fish/Cephalopod Eaters. There is also some evidence for areal texture differences between Fish Eaters and Cephalopod Eaters. This indicates significant differences between certain classes in terms of the surface roughness of their teeth. It is possible these differences are caused by the material properties of food consumed, or by differences in the way each food type is processed. Further work is needed to separate these two possible hypotheses, as little information exists on comparable material properties of the food items consumed by these animals.

The ANOVA and Tukey HSD results are slightly at odds with the overall separation we see in the Linear Discriminant Analysis. The LDA clearly shows that all four dietary classes can be separated graphically along Canonical Axes 1 and 2 using tooth microtextures. CA1 represents the general pattern seen from pairwise tests, with Fish/Cephalopod eaters clearly separated from Invertebrate/Amniote Eaters. Parameters Sa, Sq, and S5z have the greatest loading on this axis and are therefore responsible for the majority of this separation. These are all parameters which return significant differences between Cephalopod Eaters and Invertebrate/Amniote Eaters from pairwise tests, Sq and S5z also return significant differences between Fish Eaters and Amniote Eaters, and S5z shows a significant difference between Fish Eaters and Invertebrate Eaters from pairwise tests. There is obviously a high degree of overlap between Fish eaters and Cephalopod eaters along Canonical Axis 2, and this is to be expected given the low number of pairwise tests that separated these two classes. Surprisingly the LDA almost completely separates Invertebrate eaters and Amniote eaters along Canonical Axis 2. However the parameters with the highest loadings (eigenvectors) on CA2 are Sdq and Sdr, which do not have corresponding pairwise tests to support these results, instead they separate Cephalopod Eaters from Invertebrate/Amniote Eaters. Therefore it appears the LDA is picking up differences not found in the ANOVA and pairwise tests. Further evidence for both these axes being linked to diet comes from the correlation tests between the values of each specimen on the canonical axes and the actual proportions of food in each species diet.

The significant separation of dietary classes on CA1 appears to be linked to the cephalopod and invertebrate proportions in the diet based on correlations. More positive values on CA1 are correlated with a higher proportion of invertebrates in the diet and a lower proportion of cephalopods. This again mirrors the results we see from pairwise tests, and suggests that while the pairwise tests may appear to be separating Fish/Cephalopod Eaters from Invertebrate/Amniote Eaters it is possible that the cephalopod and invertebrate proportions in the diet are playing the largest part in creating these surface texture differences.

The significant separation of classes on CA2 appears to be correlated with fish, cephalopod and higher vertebrate proportions in the diet, so a more positive value along CA2 would suggest a higher proportion of fish in the diet and lower proportion of cephalopods and higher vertebrates. Both Canonical Axis 1 and 2 represent separations in dietary habits recorded in tooth microtextures. However Canonical Axis 3 is likely showing separations based on a different tooth use behaviour (possibly benthic vs pelagic feeding which could not be controlled for in this paper).

From comparisons of dietary sub-classes, where taxonomic separation was compared to dietary separation based on tooth microtextures, we found that many more pairwise tests separated classes based on diet than on taxonomy. This was supported by the LDA of dietary sub-classes where classes could be separated along CA2 based on diet (at an oblique angle). However along CA3 there is a separation between taxonomic groups and there is a weak, taxonomic signal from the Tukey HSD tests, this axis also explains the lowest proportion of variance in the data. For all canonical axes the parameters with the greatest loadings are also parameters useful for separating dietary classes (Table 2.6). It is obvious that CA3 is picking up a taxonomic signal in the data, while CA2 is picking up a dietary signal. The separation on CA1 appears to be linked neither to taxonomy nor diet, and could be picking up a signal produced by other behaviours which could not be controlled for in this paper (again, possibly benthic vs pelagic feeding). Overall the signal from diet appears to be much stronger than that from taxonomy and is more consistent across both LDA and ANOVA.

The results of this study support the hypothesis that the microwear textures of tooth surfaces from extant marine mammals reflect their dietary habits. The results also support our subsidiary hypothesis that phylogenetically distinct taxa have microwear textures that reflect similarities in diet more than phylogenetic relationships. With the caveat that a phylogenetic signal is present in the data, but appears to have a much weaker effect than the dietary signal. It has been clearly demonstrated that dietary classes containing disparate species can be separated using 3D microtextural analysis of tooth surfaces, and this pattern is consistent even across

species with radically different tooth morphologies. However these results also suggest that different methods for generating texture parameters do not show the same sensitivity to these dietary differences.

Results – Stem Cetaceans

Stem Cetacean Diet: Comparison with Data from Extant Marine Mammals

Applying the LDA based on extant marine mammals to stem cetaceans reveals that tooth microwear data for a number of stem cetacean species overlap with the dietary space of modern marine mammals (Figure 2.5). *Pakicetus inachus* plots within the dietary space of both Fish Eaters and Cephalopod Eaters, and *Artiocetus clavis* plots within the dietary space of Fish Eaters. *Rodhocetus kasrani* plots within the dietary space of Amniote Eaters. And *Saghacetus Osiris*, one specimen of *Dorudon atrox*, and one specimen of *Basilosaurus isis* all plot within the dietary space of Invertebrate Eaters.

The remaining specimens (*Maiacetus inuus*, *Qaisracetus arifi*, 2 *Basilosaurus isis* specimens, and 3 *Dorudon atrox* specimens) all plot outside the dietary range of extant marine mammals. Here we find one specimen of *Dorudon Atrox* (UM 101222), previously described as piscivorous from associated stomach contents (Uhen 2004), plotting well outside the range of Fish Eaters, and outside the range of diet for all pinnipeds and odontocetes in this paper. This appears to disagree with the stomach contents data, however our dietary classes are not based on a single prey type and fish make up a sizeable proportion (between 66 and 90%) of the prey items for three of the dietary classes (Fish, Invertebrate, and Invertebrate Eaters), so it is not inconceivable that the diet of this animal contained some proportion of fish. If the breadth of diet in extant marine mammals is any guide however, stomach contents from a single individual are unlikely to allow reliable inference of dietary preferences (Cortés 1997).

This suggests that some stem cetacean species, or individuals had a diet similar to that of extant marine mammals, while others did not fall into any of the four dietary classes in this study.

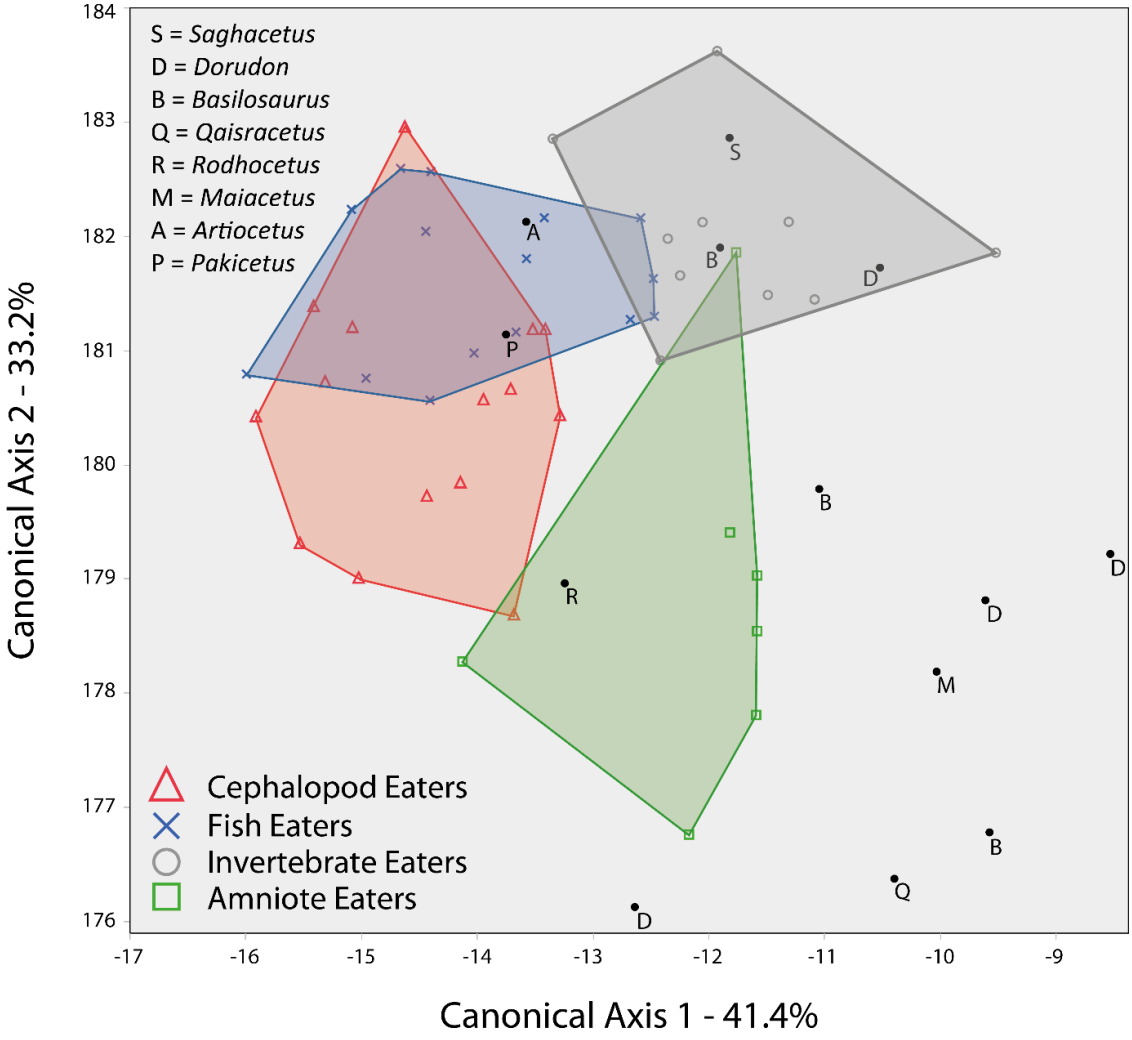

Figure 2.5 *Linear Discriminant Analysis (LDA) for all extant Odontocete and Pinniped specimens with Stem Cetacean specimens projected onto the Canonical Axes. Based on 12 parameters selected using forward stepwise variable selection. Wilks Lambda tests CA1 p=<0.0001, CA2 p=0.0001. Blue crosses = Fish Eaters, red triangles = Cephalopod Eaters, grey circles = Other Invertebrate Eaters, and green squares = Higher Vertebrate Eaters. Convex hulls have been added, with colours corresponding to the symbol colour of each dietary ecotype. Stem Cetacean key - P = Pakicetus inachus, A = Articetus clavis, M = Maiacetus inuus, R = Rodhocetus kasrani, Q = Qaisracetus arifi, S = Saghacetus osiris, D = Dorudon Atrox, and B = Basilosaurus isis.*

There has been previous suggestion, using 2D microwear data, that the species plotting outside the range of pinniped and odontocete diet in our analysis were specialized to feed on harder food items (Fahlke et al. 2013). This can be tested by looking at the parameters that load onto CA1 and CA2 in our analysis of modern marine mammals, and the direction in which each parameter affects the separation of classes. We can compare this to previous work using 3D tooth microtextures to investigate durophagy in aquatic vertebrates (Purnell and Darras 2015).

The group of stem cetaceans plotting outside the range of pinniped and odontocete diet do so along CA1, at a slightly oblique angle. Parameters Sq, S5z, and Sa have the greatest loading on CA1. If we compare this to the results of Purnell and Darras (2015) we see that all three of these parameters are responsible for separating diet based on durophagy. Sa was also found to show a trend of increasing with greater levels of durophagy in the diet, and it was found that stem cetaceans plotting outside the range of pinniped and odontocete diet have among the greatest values for this parameter of all specimens used in this paper.

Discussion – Stem Cetaceans

Comparisons between stem cetacean tooth textures and the relationships of diet in extant marine mammals suggest that analysis of microwear in stem cetaceans is comparable to extant marine mammals. We find that a number of stem cetaceans plot within the dietary classes of modern marine mammals, allowing us to make inferences about the diet of specific species, or individuals within a species.

Pakicetus inachus plots within the same dietary space as the overlap between Fish Eaters and Cephalopod Eaters. This would suggest a combination of both these food items make up a large part of its diet. However given the isotopic evidence (Clementz et al. 2006) linking this species to freshwater habitats it seems very unlikely that cephalopods make up any part of this species' diet.

Artiocetus clavis clearly plots inside the range of the Fish Eating dietary ecotype, suggesting fish made up a large part of this animal's diet. *Rodhocetus kasrani* plots within the dietary range of Amniote Eaters, suggesting higher vertebrates made up more than 20% of this animal's diet. However *Maiacetus inuus*, and *Qaisracetus arifi* both plot outside the dietary range of modern marine mammals, suggesting their diet did not contain the same proportions or types of food items as the extant mammals in this study.

Saghacetus osiris plots within the dietary range of Invertebrate Eaters, as does one specimen of *Basilosaurus isis* (UM 83901) and one specimen of *Dorudon atrox* (UM 100146). This suggests these specimens had a high proportion of non-cephalopod invertebrates in their diet (>20%). However five of eight Basilosauridae specimens do not plot within the dietary range of extant marine mammals; this includes the three remaining *Dorudon atrox* specimens and the remaining two *Basilosaurus isis* specimens. It is also interesting to note that the two Basilosauridae species for which multiple specimens are present (*Basilosaurus isis* and *Dorudon atrox*) occupy a wide dietary space, comparable in size to the large dietary space of the extant species *Hydrurga leptonyx*.

There is evidence that *Hydrurga leptonyx* diet contains a high percentage of krill, and that this is obtained via suction feeding (Hocking et al. 2013). As such we must be aware of the signal this could produce on tooth surfaces, which could be biasing our extant Amniote Eater multivariate distribution toward signals similar to Invertebrate Eaters. However as the labial tooth surface was sampled, which is least likely to contact krill being sieved in the mouth, and most likely to contact larger "pierced" prey items, the impact of this effect is likely to be low.

Based on the work of Purnell and Darras (2015) the results of this paper indicate that stem cetaceans plotting outside the range of pinniped and odontocete diet in our analyses may have been feeding on harder/larger hard items than other stem cetacean species. This supports the work of Fahlke et al. (2013), and potentially adds further weight to their hypothesis that the diet of many Basilosaurids and

Qaisracetus contained more or larger hard items, with a high degree of variability between individuals. However Purnell and Darras (2015) showed that many parameters (19 of 24) were able to separate groups with higher levels of durophagy, and in their study 6 parameters showed a trend of increasing value with increased durophagy, so our single parameter result may simply be down to random chance.

Further comparison between the work here and that of Fahlke et al (2013) is difficult given the different groupings of species between the two papers, and the exclusion of terrestrial predators and inclusion of *Hydrurga leptonyx* in this paper. However it is clear that some consensus is possible; both studies show a high overlap between the diets of modern marine mammals and stem cetaceans, even if specific species or groups of species show differences (such as *Saghacetus osiris* plotting within the range of modern marine mammals in this study and outside in Fahlke et al. (2013)). As such the conclusion that stem cetaceans shared broadly similar diets to those of modern marine mammals is consistent across both studies. However the suggestion of a dietary shift in the basilosaurids in their study, in line with the shift in stem cetaceans to obligate aquatic lifestyles is not supported by our results.

If we compare the predicted diet for each stem cetacean species derived from this paper with the results of previous studies, it is found that the results here do not support previous hypotheses of dietary transition through the cetacean stem (Figure 2.6). This figure is based on the only published phylogeny to include all stem cetacean species in our analyses (Gol'din et al. 2014). From visual inspection of the pattern in our results compared to previous hypotheses dietary habits appear to be independent of phylogenetic relationships.

The results of this paper support the hypothesis that analysis of microwear in stem cetaceans is comparable to extant marine mammals. However they do not support the hypothesis that diet derived from analysis of microwear texture support hypotheses of a unidirectional dietary transition through the stem cetacean lineage. Instead it suggests a more complex pattern of dietary evolution than previously hypothesised. Overall these results indicate that, as stem cetaceans transitioned to

marine environments the diets of different species diverged significantly, suggesting a rapid colonization of most ecological niches.

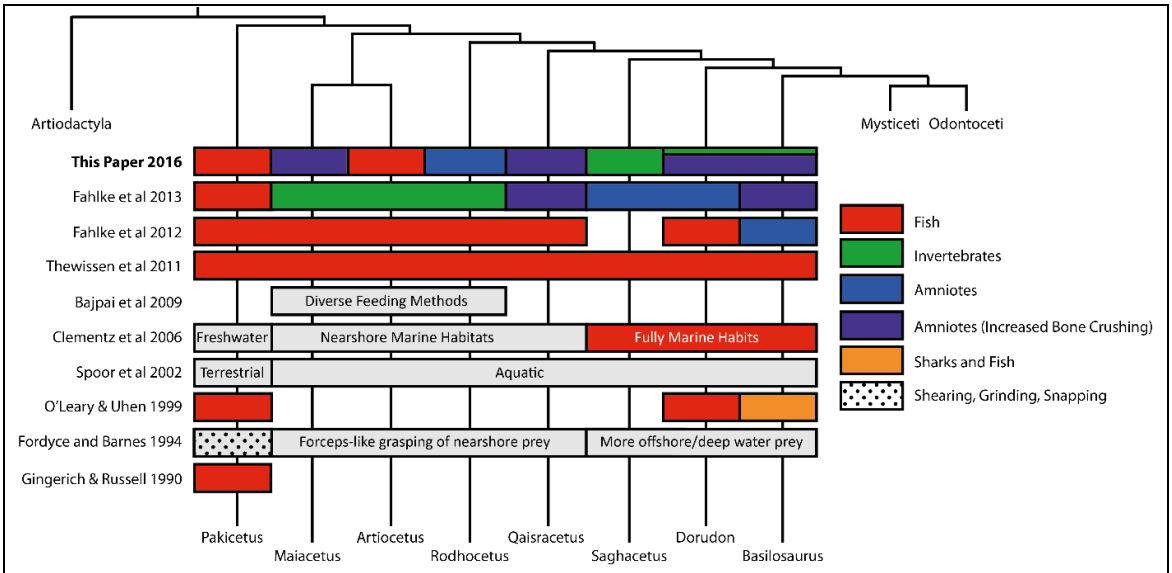

Figure 2.6. *Results of this paper, and several previous papers on stem cetacean dietary evolution, plotted onto their phylogeny (reproduced based on Gol'din et al (2014)). Boxes for each species coloured based on their dietary habits as described by each study (see key).*

Further work is need to explore the diet of those specimens plotting outside the range of modern marine mammals, with a potential focus on modern analogues for marine mammal durophagy, or those consuming large marine vertebrates. But overall our results indicate the potentially positive impact of quantitative 3D tooth surface texture analysis in understanding the diet of stem cetaceans.

Chapter 3: Investigating Dietary Variability between Two North Atlantic Killer Whale (*Orcinus orca*) Populations; Quantitative 3D Microtextural Analysis of Tooth Surfaces

Abstract

As top marine predators with a large impact on marine ecosystems, understanding the dietary habits of *Orcinus orca* (Delphinidae: Odontoceti) is of vital importance to our understanding of top down predator control. The diet of this species has been studied extensively using observational data, stomach contents, isotope data, and DNA analysis, leading to the establishment of a number of wild ecotypes in the North Pacific, North Atlantic, and Antarctic, with some evidence suggesting these groups should now be considered separate species. 3D quantitative analysis of tooth surface texture potentially offers a new way to investigate dietary hypotheses in *Orcinus orca*, and this species presents an interesting case study for the technique. However there is currently no data on the homogeneity of surface texture within and between *Orcinus orca* teeth, which will affect sampling strategies, and how sensitive this technique is to dietary differences between ecotypes. Using populations of *Orcinus orca* from the North Atlantic, where different populations have been shown to feed selectively on herring, or marine mammals, using isotope data, this paper investigates the homogeneity of texture within *Orcinus orca* teeth, and how sensitive 3D tooth surface texture analysis is to dietary differences between ecotypes. It was found that tooth surface textures vary considerably within a tooth, between teeth and between the dentary and maxilla within individual *Orcinus orca* specimens. Some separation is found between dietary ecotypes within this species when using 3D tooth surface texture analysis, but with very low sensitivity. Our results demonstrate the importance of consistent sampling strategies when using tooth surface textures to study diet in *Orcinus orca*, and while this technique appears to be potentially useful when studying dietary differences between *Orcinus orca* ecotypes, further work is needed to understand the absolute relationship between diet and tooth surface textures in this species.

Introduction

Orcinus orca (Killer Whales) are top marine predators, important to a wide range of marine ecosystems (Lopez and Lopez 1985, Simila et al. 1996, de Bruyn et al. 2013). They are members of the family Delphinidae (Cetacea: Odontoceti) and have a global distribution (Ford et al. 2000). *Orcinus orca* are known to feed on many different marine species (e.g. Jefferson et al. 1991, Fertl et al. 1996, Ford et al. 1998, de Bruyn et al. 2013), and their interactions with other marine mammals are notoriously complex (Jefferson et al. 1991). It is clear that *Orcinus orca* are adaptable and display seasonal variability in their diet based on available prey items (Matkin et al. 2007). Due to their position as super predators (de Bruyn et al. 2013), their large effect on marine ecosystems, and their potential effect on large scale habitat changes, such as the North Pacific Sequential Megafaunal Collapse (SMC) (e.g. Springer et al. 2003, DeMaster et al. 2006, Springer et al. 2008, Estes et al. 2009, Wade et al. 2009, Kuker and Barrett-Lennard 2010), it is important that we understand the diet of *Orcinus orca* populations.

Direct observations of dietary habits can provide meaningful data on *Orcinus orca* ecology. Photo identification, observational field studies, DNA analysis, and satellite tracking are often used to study their morphotypes, prey items, and ranges (Baird and Dill 1995, Morin et al. 2006, Matthews et al. 2011, Foote et al. 2013a). It is also possible to observe feeding in Killer Whales (Saulitis et al. 2000, Dahlheim et al. 2008), but this is limited to observable behaviours and requires long time spans. To study diet in obligate marine mammals a number of indirect methods have been developed which can be applied to *Orcinus orca* populations, including stomach contents (Ford et al. 1998), isotope (Krahn et al. 2007), and genetic analysis (Ford et al. 2011). These all provide information on diet, but have a number of drawbacks, including only being able to detect dietary habits over short timescales, or not currently being able to identify specific prey items (Bowen and Iverson 2013).

3D quantitative analysis of tooth surface textures potentially offers a new way of investigating differences between *Orcinus orca* dietary ecotypes, and this species

presents an interesting case study into the effectiveness and resolution of this technique. 3D tooth surface texture analysis has been widely applied to mammal groups (e.g. Schubert et al. 2010, Delezene et al. 2013, Purnell et al. 2013, Schulz et al. 2013a, Merceron et al. 2014), and uses operator independent measures to quantify surface textures. This technique is able to distinguish diet between specimens with morphologically identical dentition (Purnell and Darras 2015), and the signal accumulates over days and weeks (Teaford and Oyen 1989, Calandra and Merceron 2016), providing a longer timescale on dietary habits than stomach contents or DNA analysis, but with a turnover of surface texture that allows seasonal changes in diet to be detected (Merceron et al. 2010).

The broad range of prey items consumed by *Orcinus orca* would suggest a relatively generalist diet across the species, however sympatric dietary ecotypes and potentially distinct genetic species have previously been hypothesised based on ecological data, such as kill observations (Ford et al. 1998), phylogenetic data (Foote et al. 2009, Morin et al. 2010, Foote et al. 2013a), photographic data (Pitman and Ensor 2003), and a combination of macro-scale wear, genetic data and kill observations (Ford et al. 2011). This includes the three 'classic' North Pacific examples, the marine-mammal eating 'transient' type, the fish-eating near shore 'resident' type and an 'offshore' type, (now thought to eat fish but with a potentially significant shark component). Up to five potential distinct ecotypes have also been suggested for Antarctic *Orcinus orca* populations (Pitman and Ensor 2003, Pitman and Durban 2010), and at least two ecotypes have been identified in North Atlantic populations (Foote et al. 2009, Foote et al. 2011). These ecotypes, while still consuming relatively opportunistic diets, appear to favour certain prey groups, even going so far as to select less abundant prey species over more common prey (Ford and Ellis 2006). Although a variety of data supports their recognition, direct evidence and observations of diet are notoriously difficult in cetaceans, especially those that live offshore. This has led to some caution regarding certain ecotypes (de Bruyn et al. 2013).

Orcinus orca individuals have 10 to 14 teeth in their left and right dentary and maxilla. Their teeth are homodont and non-occlusal, with wear facets forming most

regularly on the apical and lateral (mesial and/or distal) tooth surfaces (Loch and Simoes-Lopes 2013). Teeth closest to the mesial and distal ends of the tooth row are much smaller in both length and diameter than teeth in the middle of the jaw (Newsome et al. 2009). *Orcinus orca* have relatively thin (160-230µm), simple bi-layered enamel on their tooth surfaces made up of an inner radial enamel layer and an outer layer of prismless enamel (Loch et al. 2013a), which is worn away very quickly as apical and lateral facets form. Consequently wear facets in this species are almost always composed of dentine. 3D quantitative analysis of tooth surface textures has previously been applied to non occlusal tooth surfaces in new world monkeys (Delezene et al. 2016), this study found that the surface texture of canines (without occlusal surfaces) appear to retain dietary information. Analysis of textures from dentine surfaces in xenarthrans using 3D tooth surface textures (Haupt et al. 2013), found significant differences between dentine and enamel texture. Textural data from dentine tooth surfaces were able to detect dietary differences between species with markedly different diets, but struggled to differentiate those with subtle dietary differences. This suggests that non occlusal teeth with dentine facets in *Orcinus orca* should be suitable for analysis.

The objective of this paper is to determine whether analysis of 3D tooth surface textures can be used to differentiate diet between *Orcinus orca* dietary ecotypes. However as little is known about the variability of surface texture on *Orcinus orca* tooth surfaces, which affects how data is sampled, how tooth surface texture varies within a tooth must also be tested, between teeth, or between maxilla and dentary (left and right) in *Orcinus orca* specimens. We can then use these results to inform sampling strategies when testing the sensitivity of this technique to dietary differences between known ecotypes.

Two null hypotheses are tested here. The first is that the 3D surface texture of *Orcinus orca* teeth does not vary significantly within a single tooth, between teeth from an individual, or between the maxilla and dentary (left and right) within an individual. Using this data to inform our sampling we will then test the null hypothesis

that 3D tooth surface textures cannot differentiate between known dietary ecotypes of *Orcinus orca*.

Methods

Specimens

Eighteen *Orcinus orca* specimens were sampled from three museum collections (NHM, Natural History Museum, London, United Kingdom; NMS, National Museums Scotland, Edinburgh, United Kingdom; ZMC, Zoological Museum Copenhagen, University of Copenhagen, Denmark). A full specimen list including all sampled teeth for each individual can be seen in Table 3.1.

Dietary Groups

Two dietary groups were identified across all *Orcinus orca* specimens, based on isotope data previously published by Foote et al. (2013b). These groups are Herring Eaters and Marine Mammal Eaters (Figure 3.1). Dietary classifications can be seen in Table 3.1. *Orcinus orca* are known to have a fairly opportunistic generalist diet, as such these dietary categories instead refer to the relative proportions of different prey in the diet of each individual. This approach to dietary classification is supported by work on terrestrial mammals (Pineda-Munoz and Alroy 2014). This has also been used previously to explain the variability in isotope values within a dietary population (Foote et al. 2013b). All specimens for which isotope data were not available have not been classified into one of the two dietary groups (instead being classed as having "Unknown" diet).

Specimen Number	Tooth Position	Front/Middle /Rear	Jaw Side	Jaw Type	Expected Diet	Intra-Specimen Tests	Dietary Study
NMS.1956.36.56	2	Front	Left	Dentary	Mammals	✓	✓
	5	Middle	Left	Dentary	Mammals	✓	✓
	8	Rear	Left	Dentary	Mammals	✓	
	2	Front	Right	Dentary	Mammals	✓	
	5	Middle	Right	Dentary	Mammals	✓	
	3	Front	Left	Maxilla	Mammals	✓	
	5	Middle	Left	Maxilla	Mammals	✓	
	3	Front	Right	Maxilla	Mammals	✓	
	6	Middle	Right	Maxilla	Mammals	✓	
ZMC CN89	3	Front	Right	Dentary	Mammals		✓
ZMC 12x	6	Middle	Right	Maxilla	Mammals		✓
ZMC 1x	2	Front	Right	Dentary	Mammals		✓
	5	Middle	Right	Dentary	Mammals		✓
ZMC CN.38x	2	Front	Right	Dentary	Mammals		✓
	6	Middle	Right	Dentary	Mammals		✓
NHM SW 1926.44	5	Middle	Right	Maxilla	Mammals		✓
NHM SW 1943.9	2	Front	Right	Dentary	Mammals		✓
	6	Middle	Right	Dentary	Mammals		✓
NMS 1956.36.57	2	Front	Left	Dentary	Mammals		✓
	6	Middle	Left	Dentary	Mammals		✓
ZMC M1068	2	Front	Right	Maxilla	Herring		✓
	4	Middle	Right	Maxilla	Herring		✓
ZMC 3x	2	Front	Left	Maxilla	Herring		✓
	5	Middle	Left	Maxilla	Herring		✓
NHM ZD.1886.11.22.1	3	Front	Right	Dentary	Herring		✓
	5	Middle	Right	Dentary	Herring		✓
NMS 1990.86	3	Front	Right	Dentary	Herring		✓
	6	Middle	Right	Dentary	Herring		✓
NMS Z.2015.172.48	3	Front	Right	Maxilla	Unknown	✓	✓
	6	Middle	Right	Maxilla	Unknown	✓	✓
	9	Rear	Right	Maxilla	Unknown	✓	
ZMC 24x	3	Front	Left	Dentary	Unknown		✓
	7	Middle	Left	Dentary	Unknown		✓
ZMC M1647	2	Front	Right	Maxilla	Unknown		✓
	6	Middle	Right	Maxilla	Unknown		✓
NHM SW 1943.11	5	Middle	Right	Dentary	Unknown		✓
NMS 1876.11	3	Front	Left	Dentary	Unknown		✓
	6	Middle	Left	Dentary	Unknown		✓

Table 3.1 *List of all Orcinus orca specimens used in this paper, with data on specimen number, tooth position, expected diet, and which tests each specimen was used for, included. Museum collection abbreviations; ZMC = Zoological Museum Copenhagen, NHM = Natural History Museum, London, and NMS = National Museums Scotland, Edinburgh.*

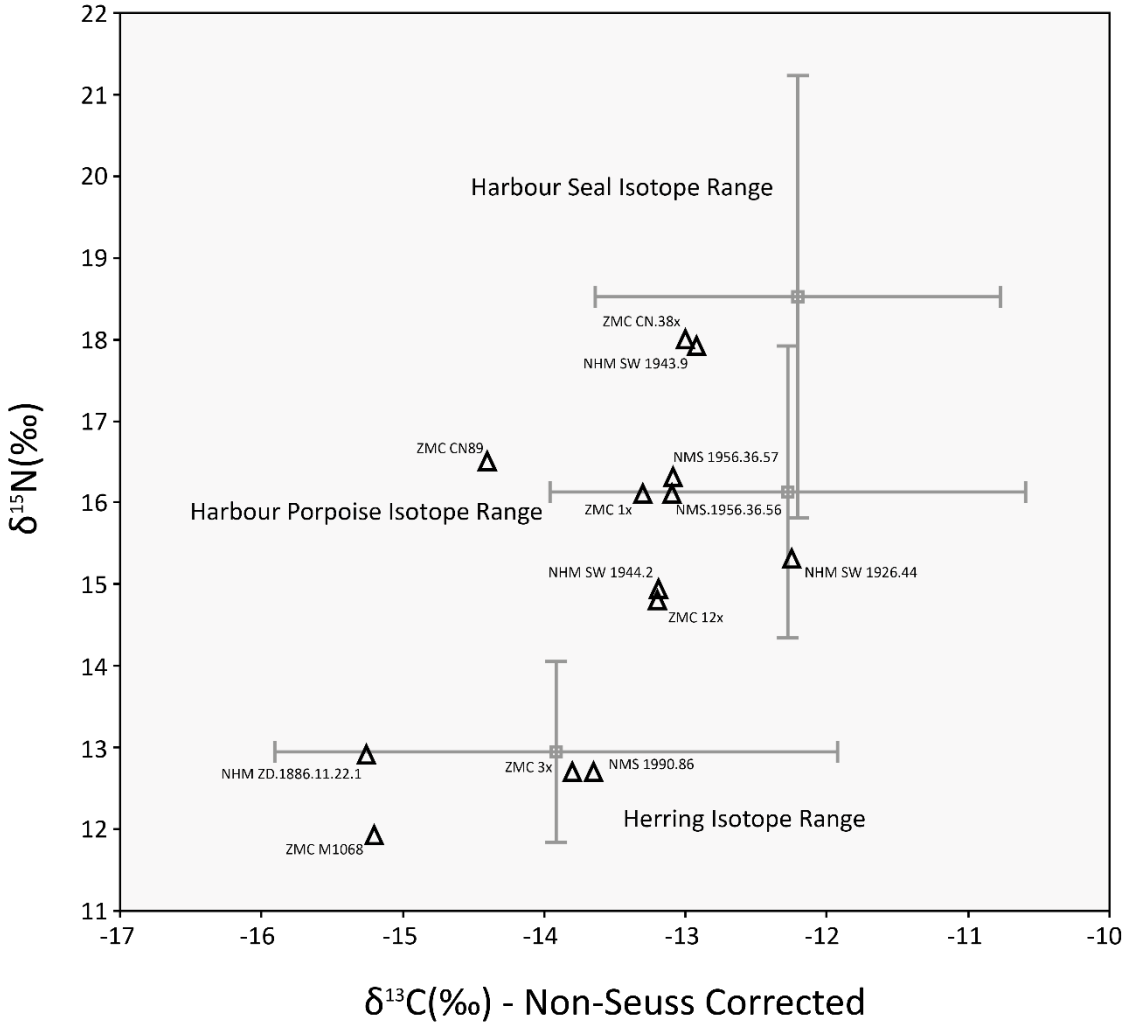

Figure 3.1 *Plot of Nitrogen ($\delta^{15}N$) and Carbon ($\delta^{13}C$) Isotope values for 13 Orcinus orca specimens. $\delta^{13}C$ (non-seuss corrected) is on the X-axis, and $\delta^{15}N$ is on the Y-axis. Both are given in parts per thousand (‰). All specimens are denoted by black triangles, while bars represent the isotope ranges of prey items. Figure modified from Foote et al (2013b).*

Data Collection

All specimens used in this paper had 10 to 13 Tooth Positions in their jaws, and displayed facets consistently on apical tooth surfaces, with different degrees of wear (i.e. just the apical tip worn, to wear present down to the cingulum). Lateral wear facets were present in some individuals, but were not consistent along tooth rows or between individuals. As such apical surfaces were sampled exclusively for this paper

due to their repeatability across all tooth positions within an individual and between specimens.

Jaws were separated into three sections, front, middle, and rear teeth (Figure 3.2). As all *Orcinus orca* individuals have at least 10 teeth in their jaw only the first 10 teeth were counted to ensure comparability across all specimens. All tooth positions were counted from anterior to posterior, and teeth were classed as front teeth (mesial most teeth; positions 1-3), middle teeth (positions 4-7), and rear teeth (distal most teeth; positions 8-10). Rear teeth were relatively rare, and mostly damaged, so could only be sampled from certain specimens.

From every specimen, where possible, one tooth was selected from the front, middle, and rear teeth. Within a specimen teeth were always collected from the same place (left or right, maxilla or dentary). It was not possible to consistently sample teeth from either the maxilla or dentary across all specimens due to the absence of one or the other for certain specimens. As such this variable could not be controlled for in our dataset. For some specimens either the front or middle teeth were available to sample but not both, in these cases only one tooth per specimen was sampled. All information on tooth locations can be found in Table 3.1.

To test the null hypothesis of microtextural variability within teeth, and between teeth along a jaw, two individuals were more intensively sampled. The two specimens were NMS.1956.36.56 (Marine Mammal Eater), and NMS Z.2015.172.48 (Unknown Diet). For these specimens one tooth was selected from each of the front, middle and rear teeth. To test the null hypothesis of variability between Jaw Types, for specimen NMS.1956.36.56 this was replicated for front and middle Teeth across left and right dentary and left and right maxillary teeth. Within this specimen tooth positions on each of these four jaw types were kept as constant as possible.

Where possible teeth were cleaned using standard practice (Williams and Doyle 2010). This involved the application of a solvent gel (ethanol, acetone, and

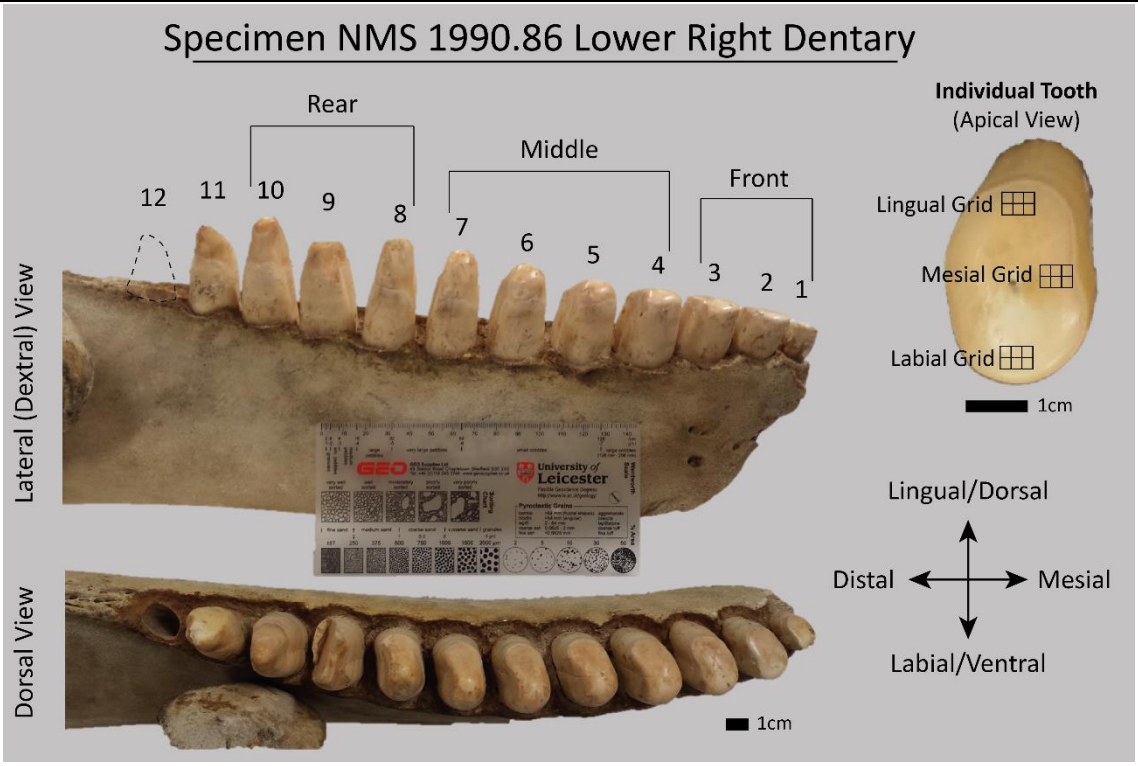

Figure 3.2 *Diagram of Orcinus orca right dentary, and an individual tooth. The jaw, from specimen NMS 1990.86, is shown in both lateral and dorsal views, the individual tooth is shown only in apical view. Tooth positions are numbered along the jaw and teeth up to position 10 are separated into front, middle and rear teeth. Data for comparisons between location within a tooth, tooth position, and jaw type were collected in 3x2 grids as shown on the individual tooth.*

xylene) to the tooth surface, which removes consolidant, dust, and other particles that could obscure microwear textures. Where this was not possible teeth were cleaned using cotton buds and compressed air canisters to remove the majority of dirt. Tooth surfaces were replicated using a polyvinylsiloxane moulding compound (President Jet Regular Body, Coltène Whaledent), which has previously been shown to produce highly accurate and precise surface moulds (Goodall et al. 2015). As per manufacturers guidelines the moulding compound was extruded onto the tooth surface through a helical nozzle, which standardises the mixing of two-components. Casts were produced from these moulds using an epoxy resin containing a black pigment (Epotek 320LV), pressurised to 2Bar/30Psi for the full duration of setting (approx. 24hrs). All casts were

gold coated (Emitech K500X sputter coater, four minutes) to optimise data acquisition using focus variation microscopy. This has been shown to produce no difference in resulting textural data from original surfaces (Appendix 2: Supplementary Chapter).

Data Acquisition

Focus variation microscopy was used to collect surface texture data from specimens (Alicona Infinite Focus Microscope, model IFM G4c, software version: 5.1). Data capture followed Purnell et al. (2013), Gill et al. (2014), and Purnell and Darras (2015) (x100 objective, field of view of 145 x 110 µm, vertical resolution set to 0.02µm, lateral optical resolution 0.44µm).

In all cases apical wear on the *Orcinus orca* teeth had removed all enamel, exposing dentine on the apical facets, therefore all data were collected from tooth dentine, from as close to the outside (nearest the lateral sides) of the apical facet as possible. It was not possible in many specimens to identify post-natal and pre-natal dentine, so this sampling method was used to reduce the effect of sampling different dentine types.

To test the null hypotheses examining data between teeth and between left and right maxilla and dentary, six data files were collected in a 3x2 grid from the labial side of the flattened tooth apex (Figure 3.2). For teeth used to test the null hypothesis of no difference between locations within a tooth data was also collected in the same grid formation from the mesial and lingual sides of the flattened tooth apex (tooth orientation was kept constant for all three areas).

To test the second null hypothesis all specimens were sampled. From each tooth (front, middle, and rear, where present) a single data file was collected from the labial side of the flattened tooth apex (orientation was kept constant across all teeth).

Data files were only accepted where there was less than 5% missing data. Surfaces were edited to remove errors using the Alicona IFM software (version 5.1),

replacing data errors with missing data. To remove any variation in 3D surfaces arising from manual horizontal positioning of the sample data files were levelled using an all points levelling system (fit to a least squares plane via rotation around all three axes). Surfaces were exported to Surfstand (software version 5.0.0) which automatically fills missing data. Any further minor errors were corrected by manually selecting and replacing data errors with an oblique plane. All surfaces were then levelled again (subtraction of least squares plane).

3D surface texture data was generated from data files using two different parameterisation methods; ISO 25178-2 (International Organization for Standardization 2012), and Scale Sensitive Fractal Analysis (SSFA) (Ungar et al. 2003, Scott et al. 2006). For ISO 25178-2 parameter generation surfaces were scale limited to remove large wavelength information (gross tooth form) using a 6^{th} order of polynomial with a spline filter (nesting index 0.025mm). This combination of operator and filter has been shown to produce surfaces with a high level of sensitivity to dietary differences (Chapter 4). 24 ISO parameters were then generated automatically from the resulting surfaces (Table 3.2) (See Purnell et al. (2013) and Gill et al. (2014) for detailed parameter descriptions). Parameters Sal and Std were excluded from further analysis as they almost always produced the same value for all surfaces. Scale Sensitive Fractal Analysis parameters were generated using programs SFrax and Toothfrax (Surfract, www.surfract.com). For the SSFA method surfaces do not need to be scale limited. This method quantifies five surface roughness aspects (Table 3.3) across 14 parameters. Settings followed those used in (Scott et al. 2006) including using scale-sensitive auto splits to record Surface Heterogeneity (HAsfc), separating individual scanned sections into increasingly reduced sub-regions (HAsfc was calculated across ten different subdivisions). A 4.4μm scale of observation was used to calculate parameter epLsar (one order of magnitude higher than the lateral resolution of the microscope being used). Comparability between data collected using different instruments is a concern for 3D microwear analysis, especially when using SSFA parameters, for which settings are intrinsically linked to the limitations of each instrument.

Parameter Family	Parameter Name	Definition	Units
Height	Sq	Root Mean Square Height of Surface	µm
	Ssk	Skewness of Height Distribution of Surface	n/a
	Sku	Kurtosis of Height Distribution of Surface	n/a
	Sp	Maximum Peak Height of Surface	µm
	Sv	Maximum Valley Depth of Surface	µm
	Sz	Maximum Height of the Surface (Sp – Sv)	µm
	Sa	Average Height of Surface	µm
Spatial	Str	Surface Texture Aspect Ratio (values range 0-1). Ratio from the distance with the fastest to the distance with the slowest decay of the ACF to the value. 0.2-0.3: surface has a strong directional structure. > 0.5: surface has rather uniform texture.	mm/mm
Hybrid	Ssc	Mean Summit Curvature for Peak Structures	1/µm
	Sds	Density of Summits. Number of summits per unit area making up the surface	$1/mm^2$
	Sdq	Root Mean Square Gradient of the Surface	Degrees
	Sdr	Developed Interfacial Area Ratio of the Surface	%
Volume	Vmp	Surface Peak Material Volume	$\mu m^3/mm^2$
	Vmc	Surface Core Material Volume	$\mu m^3/mm^2$
	Vvc	Surface Core Void Volume	$\mu m^3/mm^2$
	Vvv	Surface Dale Void Volume	$\mu m^3/mm^2$
Material Ratio	Spk	Mean height of the peaks above the core material	µm
	Sk	Core roughness depth, Height of the core material	µm
	Svk	Mean depth of the valleys below the core material	µm
	Smr1	Surface bearing area ratio (the proportion of the surface which consists of peaks above the core material)	%
	Smr2	Surface bearing area ratio (the proportion of the surface which would carry the load)	%
Feature	S5z	Ten Point Height of Surface	µm

Table 3.2 *Full list of ISO 25178-2 parameters, including brief descriptions. Parameters Std, Sal, and Ssk were excluded from analyses. For detailed parameter descriptions see Purnell et al (2013) & Gill et al (2014).*

Parameter Name	Acronym	Description
Area Scale Fractal Complexity	Asfc	A measure of the complexity of a surface. Area-scale fractal complexity is a measure of change in roughness with scale. The faster a measured surface area increases with resolution, the more complex the surface.
Exact Proportion Length Scale Anisotropy of Relief	epLsar	A measure of the anisotropy of a surface. Anisotropy is characterized as variation in lengths of transect lines measured at a given scale (we use 3.5 μm) with orientations sampled at 5° intervals across a surface. An anisotropic surface will have shorter transects in the direction of the surface pattern than perpendicular to it (e.g. a transect that cross-cuts parallel scratches must trace the peaks and valleys of each individual feature).
Scale of Maximum Complexity	Smc	The parameter represents the full scale range over which Asfc is calculated. High Smc values should correspond to more complex coarse features.
Textural Fill Volume	Tfv	The total volume filled (Tfv) is a function of two components: 1) the shape of the surface, and 2) the texture of the surface. A more concave or convex surface will have a larger total fill volume than a planar surface even if both surfaces have an identical texture.
Heterogeneity of Area Scale Fractal Complexity	HAsfc	variation of Asfc across a surface (across multiple, equal subdivisions of a surface). High HAsfc values are observed for surfaces that vary in complexity across a facet.

Table 3.3 *Full list of Scale Sensitive Fractal Analysis (SSFA) parameters, including brief descriptions (after refs 16,17). Parameter Smc was excluded from analyses. For parameter details and information on methods of calculation see Scott et al (2006).*

Changes in settings could lead to different texture parameter values, reducing comparability between data collected using different instruments, which is experimentally investigated in Chapter 5. SSFA data takes a long time to generate from Alicona IFM data files, due to time constraints SSFA data could not be generated for tests of the first hypothesis (144 data files were used), however SSFA data was included for tests of the dietary hypothesis. SSFA parameter Smc was excluded from analyses as it almost always returned exactly the same value for each surface. SSFA parameter Tfv was also excluded as it regularly returned a zero value for surfaces.

Statistical Analysis

For tests of the first null hypothesis, data files from within each area within a tooth (mesial/distal/labial) were tested for normality using Shapiro Wilks W tests. For tests of the second null hypothes all data from each dietary group was tested for normality by tooth position (i.e. all front tooth data were tested within Herring Eaters separately to front tooth data from Marine Mammal Eaters, and the same for middle tooth data). In all cases $\log_{10}$ transformed data was also tested where data were not normally distributed. For the majority of parameters Log transformed data resulted in normal distributions, therefore this data type was used going forwards, and data were subjected to parametric tests. ISO parameter Ssk was excluded from all analyses as it regularly returns negative values which cannot be log transformed. Although multiple comparisons have been conducted, especially for the tests of the first null hypothesis, we have not used a sequential Bonferroni correction here (Holm 1979), following the reasoning of Goodall et al (2015). Knowing when to use this method is subjective (Cabin and Mitchell 2000) and when used on high numbers of tests, as is the case here, it has been shown to produce many more false negative results (type II errors) than the false positives (type I errors) it seeks to eliminate (Moran 2003, Nakagawa 2004). As such, in not using this technique it must be assumed that false positive results will be present (one of 20 tests if using α =0.05), and this has been accounted for in the interpretations.

To compare surface texture variability within a tooth, and between teeth blocked ANOVA tests were used to determine the effect of changing specific variables, where all variables but the one in question were blocked. ANOVA was used to compare data from left and right maxilla and dentary. Tukey HSD tests and connecting letter reports were used to find specific differences between areas in a tooth, teeth in a jaw, or within and between left and right maxilla and dentary. Following this Two Way ANOVA tests were used to determine whether interaction between variables was present. Principal Component Analysis (PCA) was used to investigate any separation between variables in multivariate space.

T-tests were used to compare the two dietary groups, with Linear Discriminant Analysis (LDA) used to predict the diet of specimens for which there is no isotope data available. These were then classified and added into further analysis. The robustness of the LDA model was tested using leave one out cross validation. LDA and Principal Component analysis were also used to investigate dietary differences between the two *Orcinus orca* populations.

Results – Intra-Individual Variability

Blocked ANOVA – tooth position and location within a tooth

To test the effect of varying location within a tooth, and tooth position separately, blocked ANOVA tests were used, blocking the variable not being tested (i.e. to test the effect of varying location within a tooth, tooth position was blocked). The ANOVA then assumes this variable will change and potentially affect the variable of interest, so removes its effect from the final test result. This means that all data for Location Within a Tooth can be pooled across the three teeth from a specimen, to determine any pattern in the data, without Tooth Position affecting the result, and vice versa.

When testing the effect of varying location within a tooth for all 21 ISO parameters, 16 Parameters return differences between labial, lingual, and mesial tooth facet areas for specimen NMS Z.2015.172.48 (Sku, Sds, Str, Sk, and Smr1 do not separate locations within a tooth), and 17 parameters show differences between locations within a tooth for specimen NMS.1956.36.56 (Sku, Str, Svk, and Smr1 do not separate labial, lingual, and mesial facet areas). Tukey Honest Significant Difference (Tukey HSD) tests and connecting letter reports show that for both specimens these differences are only found between labial vs lingual, and labial vs mesial data (Table 3.4). Suggesting that the labial area of the tooth is significantly different in texture to the mesial and lingual areas.

When testing the effect of varying tooth position for all 21 ISO parameters, 17 parameters show differences between front, middle, and rear teeth, for specimen NMS Z.2015.172.48 (Sku, Str, Smr1, and Smr2 do not show difference), and 19 parameters for specimen NMS.1956.36.56 (Str and Smr2 do not show any difference between tooth positions). Tukey HSD tests and connecting letter reports show that these differences are almost all between front vs middle teeth, and front vs rear teeth (Table 3.5). This suggests that front teeth have different roughness parameter values compared to middle and rear teeth. In a small number of parameters (Sdq, Ssc, and Sdr for specimen NMS Z.2015.172.48, and Str for specimen NMS.1956.36.56) there is a difference between middle and rear teeth, with connecting letters reports separating all three tooth positions into separate groups. Otherwise connecting letter reports always produce one discreet group of Middle and Rear Teeth, and one containing just Front Teeth.

2 Way ANOVA – Interactions between tooth position and location within a tooth

2 Way ANOVA tests were carried out between tooth position and location within a tooth using 21 ISO parameters and two *Orcinus orca* specimens (NMS.1956.36.56, and NMS Z.2015.172.48). For both specimens 18 parameters showed a dependence between tooth position and location within a tooth, so that the value of one was dependant on the value of the other. In both cases parameters Sp, Sv, and Sz showed no dependence between variables. For NMS.1956.36.56 parameter S5z also showed no dependence, and the same for parameter Str in specimen NMS Z.2015.172.48 (For parameter descriptions see Table 3.2).

Tukey HSD tests were carried between all possible combinations of tooth position and locations within a tooth for all parameters in each specimen where dependence was recorded between variables (Figure 3.3). A number of parameters show difference between tooth position and location within a tooth. However for some comparisons only one or zero parameters show differences within and between tooth positions and locations within a tooth. But those comparisons where few or no parameters show difference are not consistent between specimens and do not show any particular

pattern. For example in specimen NMS Z.2015.172.48 the front lingual data shows no difference to front mesial data, but for the middle tooth there are a large number of parameters showing difference between lingual and mesial areas, instead for the middle tooth it is the comparison between mesial and labial data where no parameters showing difference are found.

Intra individual ANOVA – Dentary and Maxillary Teeth

ANOVA were carried out within and between left and right dentary and maxilla for specimen NMS.1956.36.56, separately for front and middle teeth (Table 3.6). A large number of parameters show differences between jaw areas in both front and middle teeth (19 for Front Teeth, 18 for Middle Teeth). But in each case these are not exactly the same parameters (Front Teeth – Sku, Str return non-significant results, Middle Teeth – Sv, Vvv, and Svk return non-significant results). Tukey HSD tests and connecting letter reports show a different pattern for Front Teeth and Middle Teeth. Front Teeth return a much greater number of significant comparisons between Jaw Types, and separation is mainly between Upper and Lower teeth, although there is difference between jaw sides within Upper and Lower teeth, which is much more pronounced between the Lower teeth. For Middle Teeth there are many fewer significant comparisons, with most appearing to separate the Lower Left jaw from all others.

Intra Individual Multivariate Analysis

Principal Component Analysis (PCA) was carried out for each specimen to compare locations within a tooth, tooth positions, and between left and right maxilla and dentary, separately for each variable. This tests whether differences found in the above analyses are based on differences in overlapping data distributions, which would suggest those results were caused by the spread of data rather than actual differences between textures, or whether they are the result of discreet data distributions, indicating a more significant directional shift in data depending on the variable in question.

NMS Z.2015.172.48		Sq	Sp	Sv	Sz	Sdq	Ssc	Sdr	Vmp	Vmc	Vvc	Vvv	Spk	Svk	Smr2	S5z	Sa
A.	Blocked ANOVA p	**0.0005**	**0.0021**	**0.0091**	**0.0002**	**0.0009**	**0.0217**	**0.0006**	**<.0001**	**0.0200**	**0.0104**	**0.0002**	**<.0001**	**0.0004**	**0.0221**	**0.0037**	**0.0030**
	F-Ratio	8.8067	6.9937	5.1790	9.9084	8.1525	4.1449	8.7401	11.2632	4.2409	5.0141	10.3942	11.8154	9.2498	4.1234	6.2754	6.5703
	d.f	2, 49	2, 49	2, 49	2, 49	2, 49	2, 49	2, 49	2, 49	2, 49	2, 49	2, 49	2, 49	2, 49	2, 49	2, 49	2, 49
Connecting Letters	Labial	B	B	B	B	B	B	B	B	B	B	B	B	B	B	B	B
	Lingual	A	A	A	A	A	A	A	A	A	A	A	A	A	A	A	A
	Mesial	A	A B	A B	A	A	A	A	A	A B	A B	A	A	A	A B	A	A B
Tukey Result	Labial/Lingual	**0.0004**	**0.0014**	**0.0089**	**0.0002**	**0.0012**	**0.0426**	**0.0008**	**<.0001**	**0.0150**	**0.0077**	**0.0001**	**<.0001**	**0.0003**	**0.0187**	**0.0036**	**0.0021**
	Labial/Mesial	**0.0290**	0.1570	0.0639	**0.0183**	**0.0081**	**0.0410**	**0.0065**	**0.0369**	0.2359	0.1643	**0.0164**	**0.0263**	**0.0265**	0.6219	**0.0396**	0.0885
	Lingual/Mesial	0.2995	0.1595	0.7124	0.2699	0.7987	0.9999	0.7555	0.0819	0.4264	0.4016	0.2408	0.0868	0.2670	0.1538	0.6422	0.3278

NMS.1956.36.56		Sq	Sp	Sv	Sz	Sds	Sdq	Ssc	Sdr	Vmp	Vmc	Vvc	Vvv	Spk	Sk	Smr2	S5z	Sa
B.	Blocked ANOVA p	**0.0008**	**0.0007**	**0.0338**	**0.0010**	**0.0386**	**0.0007**	**0.0009**	**0.0007**	**0.0003**	**0.0002**	**0.0004**	**0.0197**	**0.0002**	**0.0008**	**0.0186**	**0.0002**	**0.0013**
	F-Ratio	8.2593	8.3801	3.6324	8.0414	3.4814	8.4388	8.0641	8.3670	9.6493	6.8009	9.2096	4.2598	10.3687	8.2595	4.3293	10.3493	7.6837
	d.f	2, 49	2, 49	2, 49	2, 49	2, 49	2, 49	2, 49	2, 49	2, 49	2, 49	2, 49	2, 49	2, 49	2, 49	2, 49	2, 49	2, 49
Connecting Letters	Labial	B	B	B	B	A	B	B	B	B	B	B	A	B	B	A	B	B
	Lingual	A	A	A	A	A B	A	A	A	A	A	A	A B	A	A	A B	A	A
	Mesial	A	A	A B	A	B	A	A	A	A	A	A	B	A	A	B	A	A
Tukey Result	Labial/Lingual	**0.0063**	**0.0028**	**0.0256**	**0.0011**	0.2859	**0.0052**	**0.0011**	**0.0055**	**0.0047**	**0.0097**	**0.0030**	0.1277	**0.0030**	**0.0041**	0.0519	**0.0010**	**0.0076**
	Labial/Mesial	**0.0013**	**0.0022**	0.4003	**0.0121**	**0.0303**	**0.0012**	**0.0124**	**0.0013**	**0.0004**	**0.0049**	**0.0008**	**0.0174**	**0.0002**	**0.0018**	**0.0270**	**0.0006**	**0.0022**
	Lingual/Mesial	0.8552	0.9957	0.3530	0.6876	0.5207	0.8766	0.6736	0.8730	0.6878	0.9679	0.9007	0.6639	0.7012	0.9573	0.9597	0.9840	0.9000

Table 3.4 *Blocked ANOVA and Tukey HSD test results and Connecting Letter Reports for all comparisons between locations within and tooth, presented separately for A. NMS Z.2015.172.48, and B). NMS.1956.36.56. Variable tooth position blocked for all ANOVA tests. Results are only presented for parameters where significant ANOVA results were recorded. Significant results highlighted bold.*

NMS Z.2015.172.48		Sq	Sp	Sv	Sz	Sds	Sdq	Ssc	Sdr	Vmp	Vmc	Vvc	Vvv	Spk	Sk	Svk	S5z	Sa
A.	Blocked ANOVA p	**<.0001**	**0.0005**	**0.0031**	**0.0002**	**<.0001**	**<.0001**	**<.0001**	**<.0001**	**<.0001**	**<.0001**	**<.0001**	**<.0001**	**<.0001**	**<.0001**	**<.0001**	**<.0001**	**<.0001**
	F-Ratio	34.1398	8.9881	6.5215	10.2817	16.1126	45.1453	21.7197	54.1002	22.1599	27.2800	27.5408	35.3686	21.3936	23.4811	25.9042	19.3394	32.6120
	d.f	2, 49	2, 49	2, 49	2, 49	2, 49	2, 49	2, 49	2, 49	2, 49	2, 49	2, 49	2, 49	2, 49	2, 49	2, 49	2, 49	2, 49
Connecting Letters	Front	A	A	A	A	A	A	A	A	A	A	A	A	A	A	A	A	A
	Middle	B	B	B	B	B	B	B	B	B	B	B	B	B	B	B	B	B
	Rear	B	B	B	B	B	C	C	C	B	B	B	B	B	B	B	B	B
Tukey Result	Front / Middle	**<.0001**	**0.0009**	**0.0188**	**0.0006**	**<.0001**	**<.0001**	**0.0012**	**<.0001**	**<.0001**	**<.0001**	**<.0001**	**<.0001**	**<.0001**	**<.0001**	**<.0001**	**0.0007**	**<.0001**
	Front / Read	**<.0001**	**0.0037**	**0.0042**	**0.0011**	**0.0016**	**<.0001**	**<.0001**	**<.0001**	**<.0001**	**<.0001**	**<.0001**	**<.0001**	**<.0001**	**<.0001**	**<.0001**	**<.0001**	**<.0001**
	Middle / Rear	0.7821	0.8842	0.8475	0.9802	0.1549	**0.0101**	**0.0201**	**0.0030**	0.9963	0.7065	0.8936	0.6709	0.9988	0.7577	0.7129	0.0850	0.7849

NMS.1956.36.56		Sq	Sku	Sp	Sv	Sz	Sds	Sdq	Ssc	Sdr	Vmp	Vmc	Vvc	Vvv	Spk	Sk	Svk	Smr1	S5z	Sa
B.	Blocked ANOVA p	**<.0001**	**<.0001**	**<.0001**	**0.0007**	**<.0001**	**<.0001**	**<.0001**	**<.0001**	**<.0001**	**<.0001**	**<.0001**	**<.0001**	**<.0001**	**<.0001**	**<.0001**	**<.0001**	**<.0001**	**<.0001**	**<.0001**
	F-Ratio	35.0621	15.6355	12.2733	8.4341	14.6203	30.9060	40.4796	24.5412	40.7891	28.5586	41.1071	40.4563	20.0407	28.7298	41.4860	11.5699	12.2963	24.6514	38.7294
	d.f	2, 49	2, 49	2, 49	2, 49	2, 49	2, 49	2, 49	2, 49	2, 49	2, 49	2, 49	2, 49	2, 49	2, 49	2, 49	2, 49	2, 49	2, 49	2, 49
Connecting Letters	Front	A	A	A	A	A	A	A	A	A	A	A	A	A	A	A	A	A	A	A
	Middle	B	B	B	B	B	B	B	B	B	B	B	B	B	B	B	B	B	B	B
	Rear	B	B	B	B	B	B	B	C	B	B	B	B	B	B	B	B	B	B	B
Tukey Result	Front / Middle	**<.0001**	**<.0001**	**<.0001**	**0.0138**	**0.0001**	**<.0001**	**<.0001**	**<.0001**	**<.0001**	**<.0001**	**<.0001**	**<.0001**	**<.0001**	**<.0001**	**<.0001**	**0.0013**	**0.0113**	**<.0001**	**<.0001**
	Front / Read	**<.0001**	**0.0012**	**0.0005**	**0.0007**	**<.0001**	**<.0001**	**<.0001**	**0.0002**	**<.0001**	**<.0001**	**<.0001**	**<.0001**	**<.0001**	**<.0001**	**<.0001**	**0.0001**	**<.0001**	**<.0001**	**<.0001**
	Middle / Rear	0.5029	0.2268	0.8926	0.5685	0.9342	0.3211	0.7703	**0.0287**	0.7178	0.1893	0.3421	0.1672	0.9984	0.2201	0.2412	0.7640	0.1471	0.3865	0.3969

Table 3.5 *Blocked ANOVA and Tukey HSD test results and Connecting Letter Reports for all comparisons between tooth positions, presented separately for A. NMS Z.2015.172.48, and B). NMS.1956.36.56. Variable location within a tooth blocked for all ANOVA tests. Results are only presented for parameters where significant ANOVA results were recorded. Significant results highlighted bold.*

Tukey HSD Results		NMS.1956.36.56								
		Front Labial	Front Lingual	Front Mesial	Middle Labial	Middle Lingual	Middle Mesial	Rear Labial	Rear Lingual	Rear Mesial
NMS Z.2015.172.48	Front Labial			Sq, Vmp, Vmc, Vvck, Sk, Sa	Sq, Sku, Sds, Sdq, Ssc, Sdr, Vmp, Vmc, Vvc, Vvvk, Sk, Smr1, Smr2, Sa	Sq, Sku, Sds, Sdq, Sdr, Vmp, Vmc, Vvc, Vvvk, Sk, S5z, Sa	Sq, Sku, Sds, Sdq, Ssc, Sdr, Vmp, Vmc, Vvc, Vvvk, Sk, S5z, Sa	Sq, Sds, Vmp, Vmc, Vvck, Sk, Smr2, Sa	Sq, Sku, Sds, Sdq, Ssc, Sdr, Vmp, Vmc, Vvc, Vvvk, Skk, Smr1, S5z, Sa	Sq, Sds, Sdq, Sdr, Vmp, Vmc, Vvc, Vvvk, Skk, S5z, Sa
	Front Lingual	Sq, Sds, Sdq, Ssc, Sdr, Vmp, Vmc, Vvc, Vvvk, Skk, Sa		Sq, Sds, Sdq, Sdr, Vmp, Vmc, Vvc, Vvvk, Sk, Sa	Sq, Sku, Sds, Sdq, Ssc, Sdr, Vmp, Vmc, Vvc, Vvvk, Skk, Smr1, Sa	Sq, Sku, Sds, Sdq, Sdr, Vmp, Vmc, Vvc, Vvvk, Skk, S5z, Sa	Sq, Sku, Sds, Sdq, Ssc, Sdr, Vmp, Vmc, Vvc, Vvvk, Skk, Smr2, S5z, Sa	Sq, Sku, Sds, Sdq, Sdr, Vmp, Vmc, Vvck, Sk, Sa	Sq, Sku, Sds, Sdq, Ssc, Sdr, Vmp, Vmc, Vvc, Vvvk, Skk, S5z, Sa	Sq, Sds, Sdq, Sdr, Vmp, Vmc, Vvc, Vvvk, Skk, S5z, Sa
	Front Mesial	Sq, Sdq, Ssc, Sdr, Vmp, Vvc, Vvvk, Skk, Sa			Smr1	Sq, Sds, Sdq, Ssc, Sdr, Vmc, Vvc, Sk, Sa	Sq, Sds, Sdq, Sdr, Vmp, Vmc, Vvck, Sk, Smr2, Sa	Sdq	Sq, Sds, Sdq, Ssc, Sdr, Vmp, Vmc, Vvc, Vvvk, Sk, Smr1, S5z, Sa	Sdr
	Middle Labial	Sq, Sds, Sdr, Vmc, Vvc, Vvv, Skk, Sa	Sq, Sds, Sdq, Ssc, Sdr, Vmp, Vmc, Vvc, Vvvk, Skk, Sa	Sq, Sds, Sdq, Ssc, Sdr, Vmp, Vmc, Vvc, Vvvk, Skk, Smr2, Sa		Smr1, Smr2	Sq, Sds, Ssc, Vmp, Vmc, Vvck, Sk, Smr2, Sa		Sq, Sds, Sdq, Ssc, Sdr, Vmp, Vmc, Vvck, Sk, S5z, Sa	
	Middle Lingual		Sq, Sds, Sdq, Sdr, Vmp, Vmc, Vvc, Vvvk, Skk, Sa	Sdq, Ssc, Sdr, Vvvk	Sq, Sds, Sdq, Sdr, Vmp, Vmc, Vvc, Vvvk, Skk, Sa			Sq, Sdq, Sdr, Vmp, Vmc, Vvck, Sk, Smr2, Sa	Sq, Sdq, Sdr, Vmc, Sk, Smr1, Sa	Vvc, Sk
	Middle Mesial	Sds, Vmc, Vvc, Sk, Sa	Sq, Sds, Sdq, Ssc, Sdr, Vmp, Vmc, Vvc, Vvvk, Skk, Sa	Sq, Sds, Sdq, Ssc, Sdr, Vmp, Vmc, Vvc, Vvvk, Skk, Sa	Sds	Sq, Sds, Sdr, Vmc, Vvc, Sa		Sq, Sds, Sdq, Ssc, Sdr, Vmp, Vmc, Vvck, Sk, Smr2, Sa	Smr1	Sq, Sku, Sds, Ssc, Vmp, Vmc, Vvck, Sk, Sa
	Rear Labial	Sdr	Sq, Sds, Sdq, Ssc, Sdr, Vmp, Vmc, Vvc, Vvvk, Skk, Sa	Sds, Sdq, Ssc, Sdr, Vmp, Vmc, Vvc, Vvvk, Skk, Smr2, Sa	Sds	Sk, Sa			Sq, Sds, Sdq, Ssc, Sdr, Vmp, Vmc, Vvc, Vvvk, Skk, S5z, Sa	Sdq, Sdr
	Rear Lingual	Sq, Sds, Sdq, Sdr, Vmc, Vvc, Sk, Smr1, Sa	Sq, Sds, Sdq, Ssc, Sdr, Vmp, Vmc, Vvc, Vvvk, Skk, Sa	Sq, Sds, Sdq, Ssc, Sdr, Vmp, Vmc, Vvc, Vvvk, Skk, Sa	Smr1, Smr2	Sds, Sdq, Sdr, Vmc, Vvc, Vvv, Sk, Smr1, Sa	Sdr	Sds, Vmc, Sk, Smr2		Sq, Sku, Sds, Sdq, Sdr, Vmp, Vmc, Vvck, Sk, Smr1, Sa
	Rear Mesial	Smr1	Sq, Sdq, Ssc, Sdr, Vmp, Vmc, Vvc, Vvvk, Skk, Smr2, Sa	Sq, Sds, Sdq, Ssc, Sdr, Vmp, Vmc, Vvc, Vvvk, Skk, Smr2, Sa	Sds, Vmc, Vvc, Sk	Sq, Sdq, Sdr, Vvvk, Smr2	Sk, Smr1, Smr2		Sds, Vmc, Vvc, Sk, Smr1, Smr2, Sa	

Figure 3.3 *Tukey HSD test results comparing all possible combinations of data by location within a tooth and tooth position, for two <u>Orcinus orca</u> specimens. All data for NMS Z.2015.172.148 can be found on the bottom left of the figure, and all data for NMS 1956.36.56 can be found on the top right. ISO 25178 Parameter abbreviations are given where a significant Tukey HSD result was recorded for the given comparison (α = 0.05). Green boxes denote comparisons where one or fewer significant results across all parameters were recorded.*

For locations within a tooth, and tooth positions, parameters were only used where they returned significant blocked ANOVA results across both specimens (15 parameters when comparing locations within a tooth, and 17 when comparing tooth positions). For dentary and maxilla comparisons all parameters returning significant ANOVA results were used (19 for front teeth, 18 for middle teeth). When comparing locations within a tooth separate PCAs were carried out for each tooth position (Figure 3.4), when comparing tooth position separate PCAs were carried out for each location within a tooth (Figure 3.5), and when comparing dentary and maxilla separate tests were carried out for front and middle teeth (Figure 3.6 and Figure 3.7). Principal Component 1 (PC1) and Principal Component 2 (PC2) are the main axes of separation in all cases, no other axis (PC3 and above) ever produce any appreciable separation between data, nor do they explain significant proportions of variance in the data.

For comparisons between locations within a tooth Principal Component Analyses are able to separate all three areas within the tooth (labial, mesial, and lingual) into relatively discreet distributions across both specimens, with a general separation along PC1, except NMS Z.2015.172.48 rear tooth where the separation appears to be along PC2. The proportion of variance explained by PC1 is relatively consistent between tooth positions for specimen NMS.1956.36.56 (70.5 to 76.1%). For specimen NMS Z.2015.172.48 front and middle teeth show similar proportion of variance explained by PC1 (78.6 and 84.7%), but for the rear tooth this drops to just 45.7%. From parameter loadings (eigenvectors) (Table 3.7) in most cases (except NMS Z.2015.172.48 Rear Tooth) parameters have very similar values for PC1 and no single parameter (or small number of parameters) appears to be responsible for the separation on this axis. For PC2 there are parameters with much higher eigenvectors than others, suggesting these are responsible for the majority of separation on this axis, but they are not consistent between data from different tooth positions, or between specimens.

NMS.1956.36.56 Front Teeth		Sq	Sp	Sv	Sz	Sds	Sdq	Ssc	Sdr	Vmp	Vmc	Vvc	Vvv	Spk	Sk	Svk	Smr1	Smr2	S5z	Sa
A.	ANOVA p	**<.0001**	**<.0001**	**0.0189**	**<.0001**	**<.0001**	**<.0001**	**0.0009**	**<.0001**	**<.0001**	**<.0001**	**<.0001**	**<.0001**	**<.0001**	**<.0001**	**<.0001***	**0.0022**	**<.0001**	**<.0001**	**<.0001**
	F-Ratio	100.56	12.17	4.18	12.41	28.58	60.61	8.30	61.26	36.60	107.26	111.36	84.82	32.18	88.83	55.88	6.92	15.59	24.41	128.67
	d.f	3, 20	3, 20	3, 20	3, 20	3, 20	3, 20	3, 20	3, 20	3, 20	3, 20	3, 20	3, 20	3, 20	3, 20	3, 10.3	3, 20	3, 20	3, 20	3, 20
Tukey Tests	U Right / L Left	**<.0001**	**0.0001**	0.2524	**0.0009**	**<.0001**	**<.0001**	**0.0010**	**<.0001**	**<.0001**	**<.0001**	**<.0001**	**<.0001**	**<.0001**	**<.0001**	**0.0015**	0.3964	0.9363	**0.0003**	**<.0001**
	U Right / U Left	0.3713	0.6141	0.6320	0.9273	**0.0044**	0.9829	0.8980	0.9995	0.4896	0.6563	0.8657	**<.0001**	0.8865	0.1371	**0.0002**	**0.0100**	**0.0001**	0.0540	0.9440
	U Right / L Right	**<.0001**	**0.0090**	0.4217	**0.0073**	**<.0001**	**<.0001**	0.7553	**<.0001**	**0.0002**	**<.0001**	**<.0001**	**<.0001**	**0.0003**	**<.0001**	**0.0012**	0.9275	0.9971	**0.0150**	**<.0001**
	L Right / L Left	**<.0001**	0.2430	0.9841	0.4348	1.0000	**0.0133**	**0.0098**	**0.0137**	0.1124	**<.0001**	**<.0001**	0.2728	0.0974	**<.0001**	0.9995	0.1521	0.8618	0.3465	**<.0001**
	U Left / L Left	**<.0001**	**0.0018**	**0.0255**	**0.0002**	**0.0037**	**<.0001**	**0.0050**	**<.0001**	**<.0001**	**<.0001**	**<.0001**	**<.0001**	**<.0001**	**<.0001**	**<.0001**	0.2447	**<.0001**	**<.0001**	**<.0001**
	U Left / L Right	**0.0029**	0.1172	0.0536	**0.0279**	**0.0039**	**<.0001**	0.9905	**<.0001**	**<.0001**	**<.0001**	**<.0001**	**<.0001**	**<.0001**	**<.0001**	**<.0001**	**0.0025**	**0.0002**	**<.0001**	**<.0001**
Connecting Letters Report	Upper Right	A	A	A	A	A	A	A	A	A	A	A	A	A	A	A	B	A	A	A
	Upper Left	A	A B	A B	A	B	A	A	A	A	A	A	B	A	A	B	A	B	A	A
	Lower Right	B	B C	A B	B	C	B	A	B	B	B	B	C	B	B	C	B	A	B	B
	Lower Left	C	C	B	B	C	C	B	C	B	C	C	C	B	C	C	A B	A	B	C

NMS.1956.36.56 Middle Teeth		Sq	Sku	Sp	Sz	Sds	Str	Sdq	Ssc	Sdr	Vmp	Vmc	Vvc	Spk	Sk	Smr1	Smr2	S5z	Sa
B.	ANOVA p	**0.0231**	**0.0288**	**0.0120**	**0.0098**	**0.0003**	**0.0293***	**0.0012**	**0.0122**	**0.0010**	**0.0073**	**0.0027**	**0.0016**	**0.0053**	**0.0003**	**0.0006**	**<.0001**	**0.0055**	**0.0085**
	F-Ratio	3.95	3.70	4.71	4.97	10.02	4.58	7.80	4.69	8.07	5.33	6.63	7.43	5.74	10.17	8.78	23.25	5.70	5.13
	d.f	3, 20	3, 20	3, 20	3, 20	3, 20	3, 9.92	3, 20	3, 20	3, 20	3, 20	3, 20	3, 20	3, 20	3, 20	3, 20	3, 20	3, 20	3, 20
Tukey Tests	U Right / L Left	**0.0134**	0.8777	**0.0156**	**0.0166**	**0.0004**	0.2878	**0.0006**	**0.0064**	**0.0005**	**0.0251**	**0.0014**	**0.0008**	**0.0177**	**0.0001**	0.5171	**<.0001**	**0.0087**	**0.0043**
	U Right / U Left	0.4642	**0.0249**	0.9881	0.9998	0.9744	1.0000	0.1019	0.3105	0.0986	0.9890	0.0573	0.3013	0.9930	**0.0396**	**0.0324**	0.1207	0.9856	0.1988
	U Right / L Right	0.5465	0.3004	0.9176	0.9541	0.4419	**0.0127**	0.3680	0.3255	0.3188	0.9999	0.0714	0.2645	1.0000	**0.0281**	0.0818	0.1060	0.9748	0.2682
	L Right / L Left	0.1970	0.7171	0.0604	**0.0498**	**0.0135**	0.3968	**0.0272**	0.2214	**0.0273**	**0.0219**	0.3091	0.0518	**0.0175**	0.1022	**0.0041**	**0.0005**	**0.0219**	0.2068
	U Left / L Left	0.2480	0.1123	**0.0313**	**0.0198**	**0.0011**	0.2682	0.1279	0.2332	0.1100	**0.0127**	0.3624	**0.0435**	**0.0098**	0.0745	**0.0014**	**<.0001**	**0.0186**	0.2781
	U Left / L Right	0.9990	0.5576	0.9885	0.9716	0.6907	**0.0115**	0.8651	1.0000	0.8994	0.9943	0.9995	0.9998	0.9934	0.9984	0.9677	0.9999	0.9998	0.9977
Connecting Letters Report	Upper Right	A	B	A	A	A	A	A	A	A	A	A	A	A	A	A	A	A	A
	Upper Left	A B	A	A	A	A	A	A B	A B	A B	A	A B	A	A	B	A C	A	A	A
	Lower Right	A B	A B	A B	A	A	B	A	A B	A	A	A B	A B	A	B	A B	A	A	A
	Lower Left	B	A B	B	B	B	A B	B	B	B	B	B	B	B	B	C	B	B	B

Table 3.6 *ANOVA and Tukey HSD test results and Connecting Letter Reports for all comparisons between dentary and maxilla (specimen NMS.1956.36.56), presented separately for A). front teeth, and B). middle teeth. Results are only presented for parameters where significant ANOVA results were recorded. Significant results*

The Principal Component Analyses comparing tooth position were also able to separate front, middle, and rear teeth into relatively discreet distributions. And again the separation of all three teeth appears to be along PC1 when using data from labial and mesial areas. But when using data from lingual areas the separation is both along PC1 and PC2, and the separation is different for each specimen. The proportion of variance explained by PC1 ranges from 65.2% to 84.1% across all analyses. PCA parameter loadings (Table 3.8) again show that most parameters have a very similar loading on PC1 with little to distinguish their contribution to the separation on this axis. But in PC2 it is clear that specific parameters are responsible for the separation along this axis, and while Sku, Sv, Sz, and S5z are almost always included, the pattern is different between analyses.

PCA between dentary and maxilla (left and right) produce quite different results depending on whether front or middle teeth are used, mirroring the ANOVA and Tukey HSD results. For front teeth (Figure 3.6) all four jaw types fall into discreet distributions, with a clear separation along PC1 between upper and lower teeth. Separation on PC2 is between left and right jaws, with left plotting more positively for both dentary and maxillary teeth. Eigenvectors show little difference in their contribution to the separation along PC1, but on PC2 Smr1 (0.565), and Smr2 (-0.434) appear to be responsible for the greatest proportion of separation. For middle teeth the picture is less clear (Figure 3.7), with much greater overlap between all four jaw types. Upper right teeth seem to be separated from most others along PC2, and lower left teeth show some separation along PC1 from other jaw types. Again most parameters have the same loadings (eigenvectors) on PC1, but Smr1 (0.461), and Sku (0.585) appear to be most responsible for the separation on PC2.

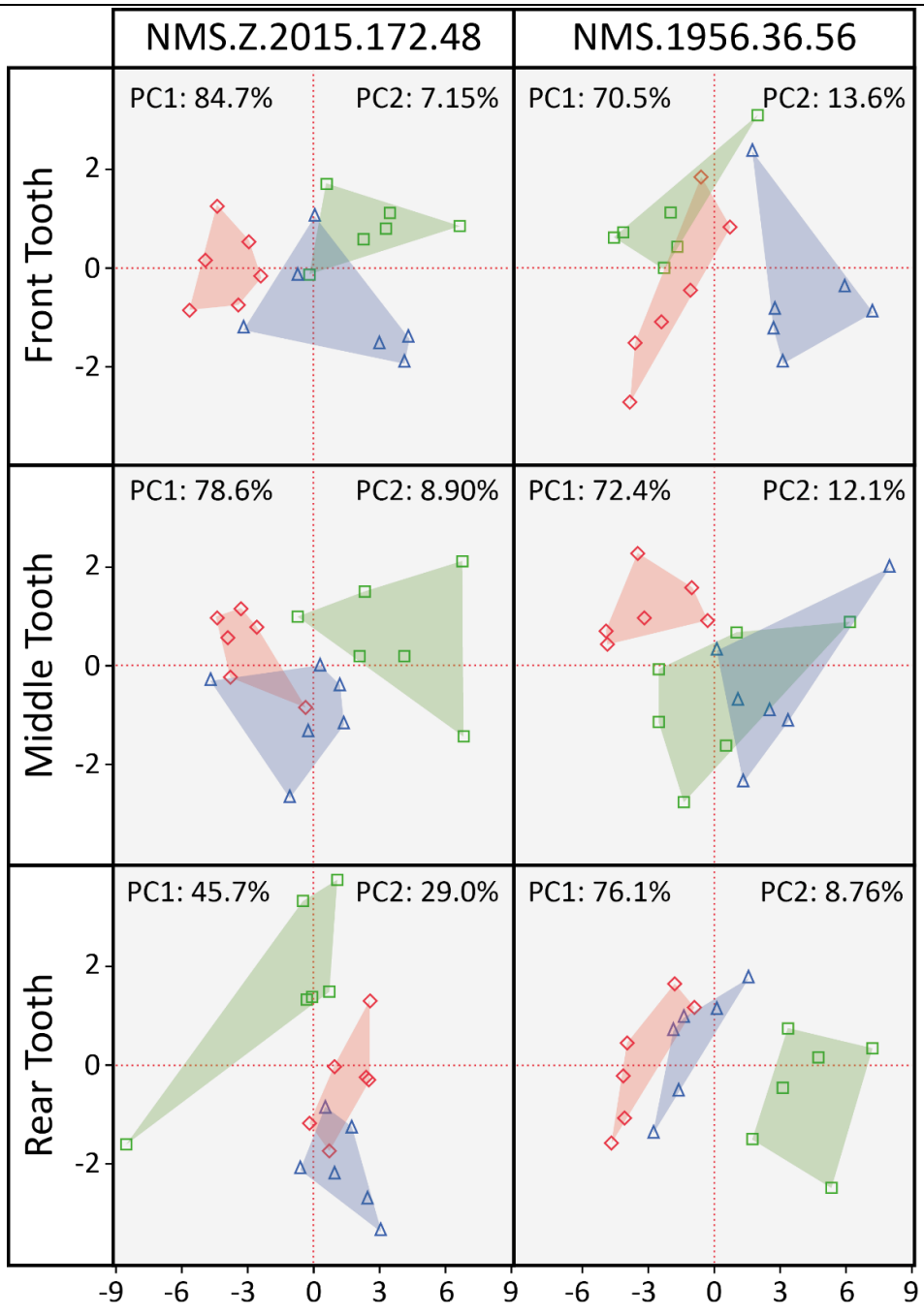

Figure 3.4 *Plots of PCA results (PC1 and PC2) for comparisons between locations within a tooth. Separate PCA are presented for each tooth position and each specimen. Data for NMS Z.2015.172.148 can be seen on the left, and data for NMS 1956.36.56 on the right. Labial area data points are presented as red diamonds, mesial data points as blue triangles, and lingual data points as green squares. Convex hulls are coloured to match that of the data points they represent. PCA for both specimens generated using all parameters returning significant results from Blocked ANOVA tests (Table 3.4).*

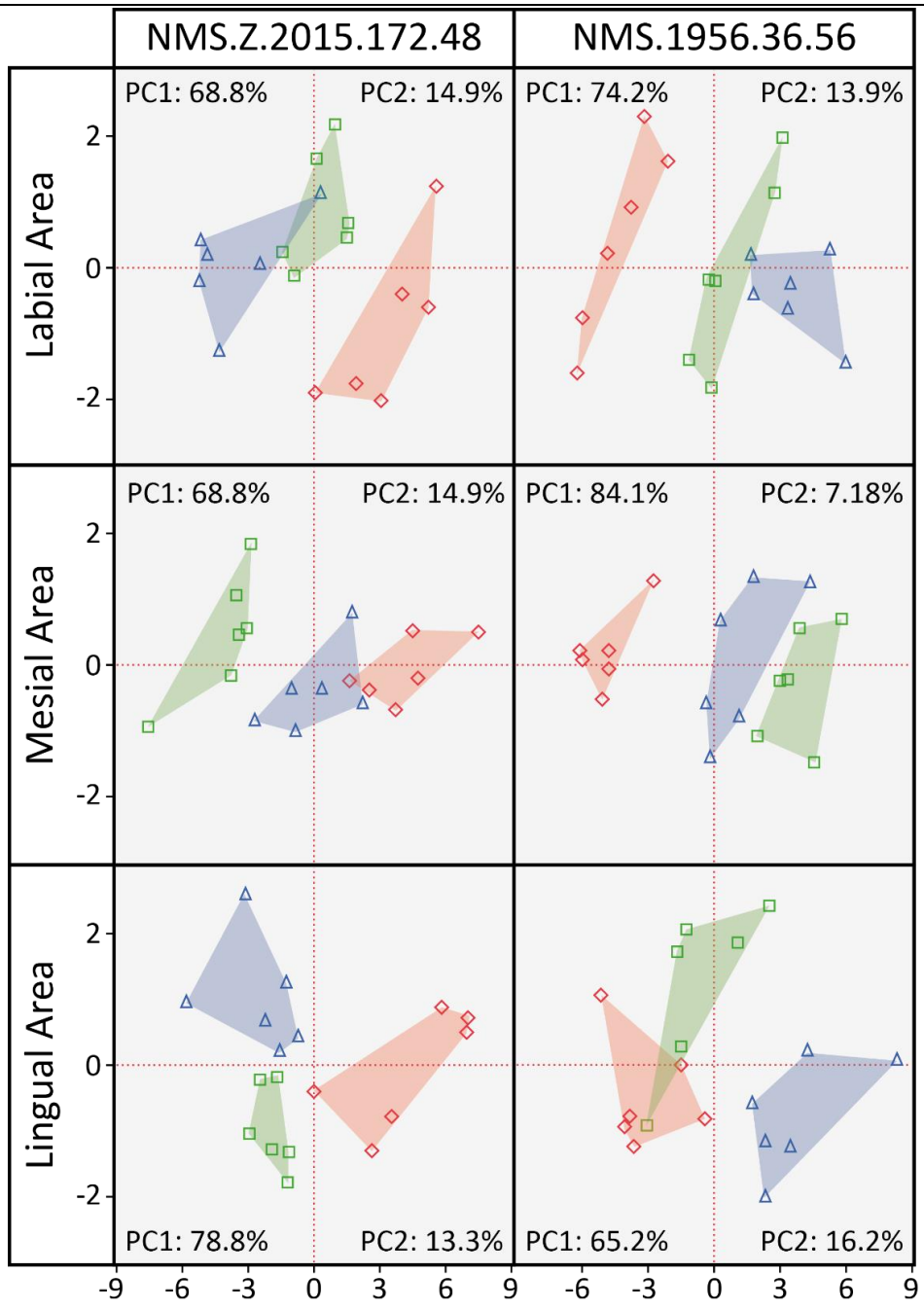

Figure 3.5 *Plots of PCA results (PC1 and PC2) for comparisons between tooth positions. Separate PCA are presented for each location within a tooth and each specimen. Data for NMS Z.2015.172.148 can be seen on the left, and data for NMS 1956.36.56 on the right. Front tooth data points are presented as red diamonds, middle tooth data points as blue triangles, and rear tooth data points as green squares. Convex hulls are coloured to match that of the data points they represent. PCA for both specimens generated using all parameters returning significant results from Blocked ANOVA tests (Table 3.5).*

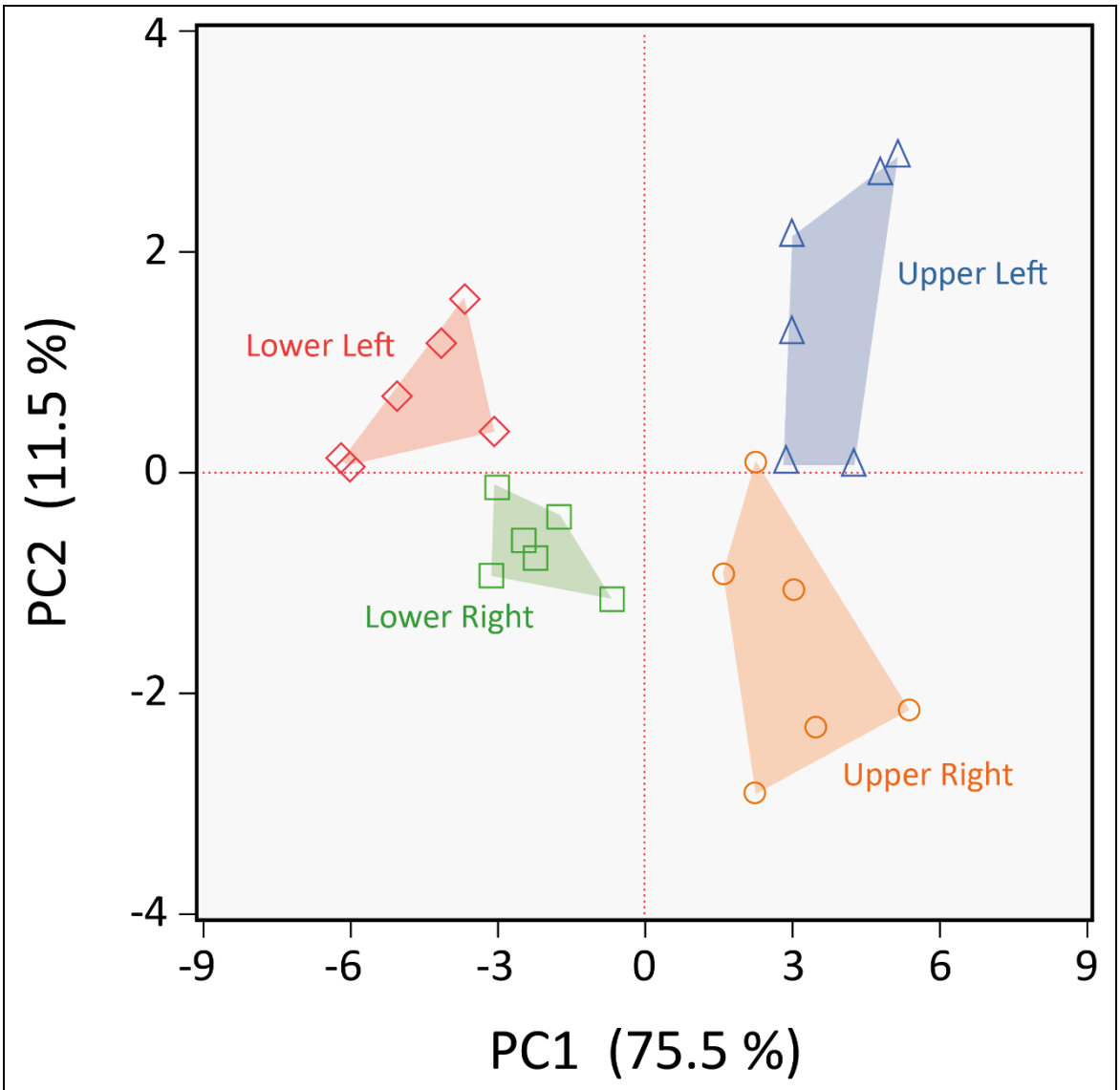

Figure 3.6 *PCA plot for the comparison of jaw types (left, and right, dentary, and maxilla) based on data from front teeth only. Left dentary data points are presented as red diamonds, left maxillary data points as blue triangles, right dentary data points as Green squares, and right maxillary data points as orange circles. Convex hulls are coloured to match that of the data points they represent. PCA based on all parameters returning significant results from ANOVA (Table 3.6.a).*

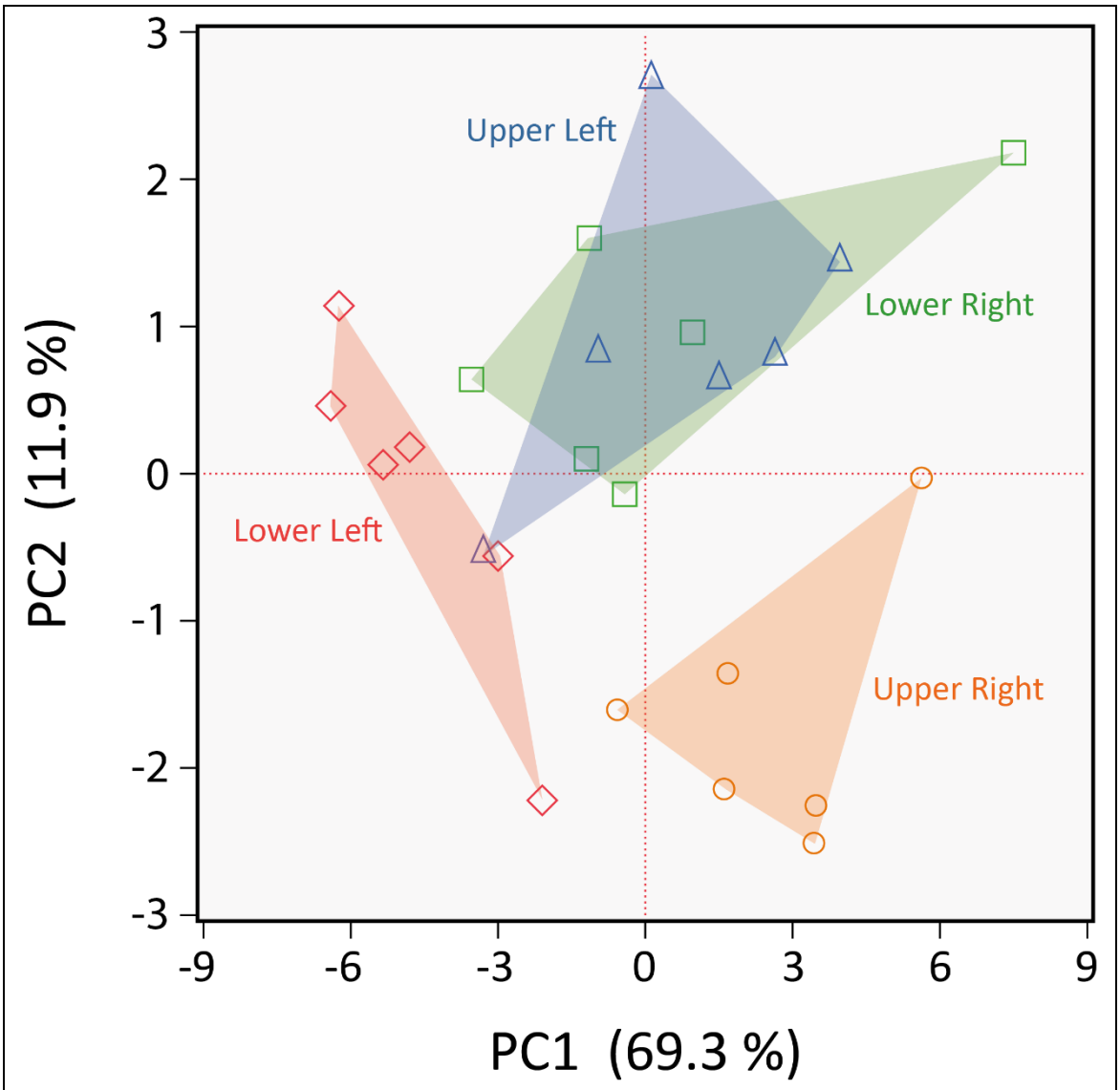

Figure 3.7 *PCA plot for the comparison of jaw types (left, and right, dentary, and maxilla) based on data from middle teeth only. Left dentary data points are presented as red diamonds, left maxillary data points as blue triangles, right dentary data points as Green squares, and right maxillary data points as orange circles. Convex hulls are coloured to match that of the data points they represent. PCA based on all parameters returning significant results from ANOVA (Table 3.6.b).*

A.

NMS Z.2015.172.148 - PCA Between Locations Within a Tooth - Eigenvectors						
	Front Tooth		Middle Tooth		Rear Tooth	
Parameter	PC1	PC2	PC1	PC2	PC1	PC2
Sq	0.2686	0.0780	0.2782	0.1170	**0.3638**	-0.0492
Sp	0.2324	0.2663	0.2271	-0.2111	0.1511	0.0635
Sv	0.2535	-0.1820	0.2332	-0.2666	0.1455	0.2502
Sz	0.2599	0.0566	0.2528	-0.2833	0.2094	0.2389
Sdq	0.2622	-0.0945	0.2675	0.1915	**0.3063**	-0.2454
Ssc	0.2394	-0.1910	0.1928	0.0285	0.0961	-0.0207
Sdr	0.2675	-0.0547	0.2677	0.2055	**0.3045**	-0.2498
Vmp	0.2650	-0.0242	0.2744	-0.0980	0.2268	**0.3298**
Vmc	0.2330	**0.3722**	0.2532	**0.3265**	0.2754	-0.2962
Vvc	0.2451	**0.3275**	0.2569	**0.3237**	0.2957	-0.2722
Vvv	0.2655	-0.1036	0.2751	0.0412	**0.3007**	0.2288
Spk	0.2657	0.0058	0.2733	-0.1147	0.2336	0.2934
Svk	0.2623	-0.1706	0.2702	-0.0388	0.2228	**0.3281**
Smr2	-0.1189	**0.7030**	-0.1072	**0.5551**	0.0480	**-0.4133**
S5z	0.2627	-0.1076	0.2474	**-0.3183**	0.2566	0.1486
Sa	0.2586	0.2152	0.2662	0.2527	**0.3264**	-0.2033

B.

NMS 1956.36.56 - PCA Between Locations Within a Tooth - Eigenvectors						
	Front Tooth		Middle Tooth		Rear Tooth	
Parameter	PC1	PC2	PC1	PC2	PC1	PC2
Sq	0.2865	-0.0408	0.2792	0.1117	0.2739	-0.0443
Sp	0.1977	**0.3217**	0.1617	**-0.4820**	0.2191	0.2152
Sv	0.0856	**0.4628**	0.1556	0.2554	0.1974	**0.4517**
Sz	0.1892	**0.4720**	0.1935	-0.0223	0.2314	**0.3866**
Sds	-0.2088	0.2912	-0.2307	0.2376	-0.2145	0.2441
Sdq	0.2771	-0.1620	0.2648	0.2133	0.2680	-0.0383
Ssc	0.1841	-0.0397	0.2379	0.0902	0.2441	-0.2322
Sdr	0.2771	-0.1659	0.2650	0.2102	0.2683	-0.0411
Vmp	0.2766	0.0849	0.2660	-0.2010	0.2541	-0.0647
Vmc	0.2766	-0.1726	0.2726	0.1083	0.2663	-0.1374
Vvc	0.2777	-0.1684	0.2795	0.0014	0.2686	-0.1795
Vvv	0.2767	-0.0009	0.2140	**0.4222**	0.2474	0.1605
Spk	0.2775	0.1101	0.2568	-0.2642	0.2511	0.0051
Sk	0.2731	-0.1958	0.2759	0.0343	0.2666	-0.1938
Smr2	-0.1332	-0.1153	0.1877	**-0.4663**	0.0490	**-0.4910**
S5z	0.2202	**0.4166**	0.2477	-0.0720	0.2366	**0.3351**
Sa	0.2831	-0.1229	0.2767	0.1062	0.2715	-0.0980

Table 3.7 *PCA eigenvectors for PC1 and PC2 for comparisons of data from different locations within a tooth, presented separately for A). NMS Z.2015.172.148, and B). NMS 1956.36.56. All parameters used in each PCA are included, based on the results of Blocked ANOVA tests (Table 3.4). Values between 0 and 0.2 are light grey text, values between 0.2 and 0.3 are black text, and values above 0.3 are bold black text. Bold parameters represent those contributing the most to the separation on each principal component. Data are separated into front, middle, and rear teeth for each specimen.*

A.

NMS Z.2015.172.148 - Between Teeth PCA - Eigenvectors						
	Labial Area		Mesial Area		Lingual Area	
Parameter	PC1	PC2	PC1	PC2	PC1	PC2
Sq	0.2891	-0.0532	0.2717	-0.0411	0.2582	-0.0549
Sp	0.1886	**0.3678**	0.2084	-0.1710	0.2003	**0.3145**
Sv	0.2326	0.1971	0.1967	**0.3337**	0.2017	**0.4238**
Sz	0.2384	**0.3110**	0.2356	0.1684	0.2222	**0.4590**
Sds	-0.2291	0.1963	-0.1520	**0.5236**	-0.2352	**0.3480**
Sdq	0.2212	-0.2973	0.2652	0.0921	0.2520	-0.1500
Ssc	-0.0131	-0.2455	0.2349	0.2362	0.2328	-0.0198
Sdr	0.2208	**-0.3081**	0.2664	0.0690	0.2528	-0.1910
Vmp	0.2585	0.2287	0.2641	0.1101	0.2462	0.2403
Vmc	0.2561	-0.2624	0.2401	**-0.3028**	0.2499	-0.2392
Vvc	0.2673	-0.2053	0.2473	-0.2674	0.2533	-0.1952
Vvv	0.2826	0.0096	0.2662	0.0820	0.2551	0.0070
Spk	0.2528	0.2685	0.2651	0.0754	0.2466	0.2506
Sk	0.2548	-0.2684	0.2245	**-0.3648**	0.2470	-0.2782
Svk	0.2680	0.1261	0.2585	0.1754	0.2510	0.0900
S5z	0.2398	**0.3074**	0.2314	**0.3204**	0.2530	0.0354
Sa	0.2787	-0.1622	0.2619	-0.1787	0.2551	-0.1573

B.

NMS 1956.36.56 - Between Teeth PCA - Eigenvectors						
	Labial Area		Mesial Area		Lingual Area	
Parameter	PC1	PC2	PC1	PC2	PC1	PC2
Sq	0.2646	-0.0077	0.2815	-0.0339	0.2492	-0.0478
Sku	-0.1562	**0.4667**	-0.1746	**0.3926**	-0.1795	**0.5414**
Sp	0.2170	0.1464	0.1362	0.0627	0.2028	0.2816
Sv	0.1593	**0.3877**	0.1239	**0.4577**	0.1853	**0.4741**
Sz	0.2145	**0.3295**	0.1721	**0.3928**	0.2122	**0.4381**
Sds	-0.1985	**0.3198**	-0.2416	0.1230	-0.2348	0.1532
Sdq	0.2566	-0.0883	0.2747	0.0803	0.2474	-0.0941
Ssc	0.2100	0.0095	0.2354	-0.1650	0.2321	-0.0153
Sdr	0.2565	-0.0907	0.2755	0.0721	0.2474	-0.0936
Vmp	0.2369	0.1380	0.2515	-0.1532	0.2431	0.0291
Vmc	0.2591	-0.1318	0.2750	-0.1299	0.2480	-0.1025
Vvc	0.2604	-0.1123	0.2715	-0.1589	0.2476	-0.0879
Vvv	0.2520	0.0681	0.2314	0.2128	0.2429	-0.0316
Spk	0.2355	0.1459	0.2522	-0.1330	0.2402	0.0741
Sk	0.2575	-0.1456	0.2714	-0.1540	0.2477	-0.0995
Svk	0.2173	0.2359	0.1662	**0.3784**	0.2331	0.0926
Smr1	-0.1770	**0.3598**	-0.0997	-0.0673	-0.1558	0.2598
S5z	0.2189	**0.3098**	0.2063	**0.3399**	0.2310	0.2214
Sa	0.2633	-0.0782	0.2795	-0.0871	0.2487	-0.0825

Table 3.8 *PCA eigenvectors for PC1 and PC2 for comparisons of data from different tooth positions, presented separately for A). NMS Z.2015.172.148, and B). NMS 1956.36.56. All parameters used in each PCA are included, based on the results of Blocked ANOVA tests (Table 3.5). Values between 0 and 0.2 are light grey text, values between 0.2 and 0.3 are black text, and values above 0.3 are bold black text. Bold parameters represent those contributing the most to the separation on each principal component. Data are separated into labial, mesial, and lingual areas of the tooth for each specimen.*

Dietary Analysis – T-tests

To test the null hypothesis that 3D tooth surface textures cannot differentiate between known dietary ecotypes of *Orcinus orca,* data was separated into front teeth and middle teeth, which were tested independently. Within each dataset only labial tooth areas were sampled (a single data file from each tooth, see methods), however we could not control for jaw type (dentary or maxilla, left and right), due to the availability of specimens for study. Due to the high levels of variability seen in the previous analysis teeth with unknown position (i.e. loose teeth) could not be included in the analysis of dietary groups, as they would likely add a high level of noise to the data. Rear teeth were also excluded as they were only available for a small number of specimens so could not be formed into their own dataset.

T-tests were carried out for all specimens where diet was known from Isotope Data. This was done separately for the two datasets, front teeth (four Herring Eaters, six Marine Mammal Eaters) and middle teeth (four Herring Eaters, seven Marine Mammal Eaters). No difference was recorded between the two dietary groups across both datasets in any parameter. This result supports the null hypothesis, however this is a very small sample size, especially for the Herring Eater ecotype. It would be expected that if further data were added there would remain no difference between the two dietary ecotypes if the null hypothesis were true. As such it was decided to include the specimens with unknown diet (those without isotope data), to test whether this result was consistent.

Dietary Analysis – Assigning Specimens with Unknown Diet

In order to include specimens from the Unknown category in the analysis their expected diet had to be predicted using similarities in their tooth surface microtextures to specimens with known diet (as we do not have any other independent variables to use). For this we used Linear Discriminant Analysis (LDA), which was carried out on specimens with known diets for both front and middle teeth datasets. Specimens with unknown diet were excluded from the LDA but left in the

dataset so the analysis could predict their dietary group. Using forward stepwise variable selection an ordination was generated where dietary groups (Herring Eaters and Marine Mammal Eaters) were separated into discreet distributions, no data was misclassified, and the Canonical Axis 1 (CA1) was significant (LDA produces a number of canonical axes equal to the number of tested groups minus one). The classification of specimens with unknown diets was calculated from the resulting analysis.

For front teeth this required four parameters (Sds, Str, Ssc, and Asfc), resulting in zero misclassifications and a significant Wilks' Lambda test result for the Discriminant Function (CA1 p=0.007). Predicted specimen diets were then recorded (Table 3.9.a). The addition of further parameters did not change these predictions. For middle teeth five parameters were required (Str, Ssc, Svk, Smr2, and HAsfc 10x10), this resulted in zero misclassifications and a significant Wilks' Lambda test result for the Discriminant Function (CA1 p=0.026), and again predicted specimen diets were recorded (Table 3.9.b). The addition of further parameters did not change these predictions. The predictions do not agree between front and middle teeth, however it was unclear at this stage which could contain any possible dietary signal, so each set of predictions was used within its respective dataset. Resulting datasets were tested for normality, log transformed (Log_{10}) data were also tested where non-normal distributions were found. In almost all cases log transformed data was normally distributed so parametric statistical tests were appropriate, and this was used going forwards. For the front teeth dataset there are seven Marine Mammal Eaters and seven Herring Eaters, and for the middle teeth dataset there are nine Marine Mammal Eaters and seven Herring Eaters.

New LDA were carried out for both datasets to determine dietary separation and where the specimens with predicted diet plot on the Canonical Axis (we would expect them to plot within their respective dietary groups and not between the dietary groups made up of specimens with known diets). Forward stepwise variable selection was used in both cases to generate an ordination where zero specimens were misclassified and CA1 was significant (number of discriminant functions = number of groups minus one).

A.

	Specimen Number	Expected Diet	Predicted Diet	Probability
Front Teeth	NMS.1956.36.56	Mammals	Mammals	0.9411
	ZMC CN89	Mammals	Mammals	1.0000
	ZMC 1x	Mammals	Mammals	1.0000
	ZMC CN.38x	Mammals	Mammals	1.0000
	NHM SW 1943.9	Mammals	Mammals	0.9972
	NMS 1956.36.57	Mammals	Mammals	0.9997
	ZMC M1068	Fish	Fish	0.9988
	ZMC 3x	Fish	Fish	0.9949
	NHM ZD.1886.11.22.1	Fish	Fish	1.0000
	NMS 1990.86	Fish	Fish	0.9996
	NMS Z.2015.172.48	Unknown	Fish	0.7554
	ZMC 24x	Unknown	Mammals	1.0000
	ZMC M1647	Unknown	Fish	0.9604
	NMS 1876.11	Unknown	Fish	0.9991

B.

	Specimen Number	Expected Diet	Predicted Diet	Probability
Middle Teeth	NMS.1956.36.56	Mammals	Mammals	1.0000
	ZMC 12x	Mammals	Mammals	1.0000
	ZMC 1x	Mammals	Mammals	1.0000
	ZMC CN.38x	Mammals	Mammals	1.0000
	NHM SW 1926.44	Mammals	Mammals	1.0000
	NHM SW 1943.9	Mammals	Mammals	1.0000
	NMS 1956.36.57	Mammals	Mammals	1.0000
	ZMC M1068	Fish	Fish	1.0000
	ZMC 3x	Fish	Fish	1.0000
	NHM ZD.1886.11.22.1	Fish	Fish	1.0000
	NMS 1990.86	Fish	Fish	1.0000
	NMS Z.2015.172.48	Unknown	Mammals	1.0000
	ZMC 24x	Unknown	Fish	1.0000
	ZMC M1647	Unknown	Fish	1.0000
	NHM SW 1943.11	Unknown	Fish	1.0000
	NMS 1876.11	Unknown	Mammals	1.0000

Table 3.9 *Predicted dietary groups for specimens where isotope data was not available, based on the results of LDA carried out on ISO 25178 and SSFA parameters for all specimens with isotope data present, presented separately for A. front teeth dataset, and B). middle teeth dataset. Expected diet is that predicted from isotope data, and predicted diet is that predicted from the LDA. Probability gives the likelihood of each specimen being assigned to its predicted group.*

For the front teeth dataset six parameters (Str, Ssc, Smr1, Smr2, HAsfc 9x9, and HAsfc 10x10) were sufficient to misclassify zero specimens and produce a significant Wilks' Lambda result for CA1 (p=0.002). The resulting ordination (Figure 3.8.a) clearly separates the two dietary groups into discreet distributions along CA1, with all Marine Mammal Eaters plotting below zero, and all Herring Eaters plotting above zero. From scoring coefficients it is clear that Smr2 has the greatest loading on this axis (287.6), meaning it is contributing most to the discriminatory ability of the function (CA1). All but one of the specimens with predicted diet fall well within the range of their dietary group, reinforcing the dietary predictions.

For the middle teeth dataset four parameters (Sq, Str, Ssc, and HAsfc 2x2) were sufficient to misclassify zero specimens and produce a significant Wilks' Lambda result for CA1 (p=0.002). The resulting ordination (Figure 3.8.b) again clearly separates the two dietary groups on CA1, with the same relationship of data as for front teeth, however the distance between the two dietary groups is less. Sq (14.2) and Ssc (-12.3) have the highest loadings (scoring coefficients) on CA1. The specimens that originally had Unknown Diet in this dataset mostly plot as far from the opposing group as possible, or within their predicted group. Again this supports the predictions of diet, but their inclusion on the far reaches of dietary groups mean the proportions of prey types in their diet could be slightly different from the two groups identified using Isotope Data. This cannot be tested here, but must be considered when conclusions are made.

Leave one out cross validation was carried out for the LDA model from both datasets. This is was repeated a total of six times for each dataset (Supplementary Table 3.1 and Supplementary Table 3.2; See supplementary information at the end of the Thesis). In almost all cases excluded specimens were correctly assigned to their dietary group, and the overall misclassification rate did not change. In one case, when specimen ZMC 3x was excluded from the Front Teeth dataset it was misclassified as a Marine Mammal Eater, but this is the only example of any misclassification across all leave one out tests. This suggests both LDA models are relatively robust.

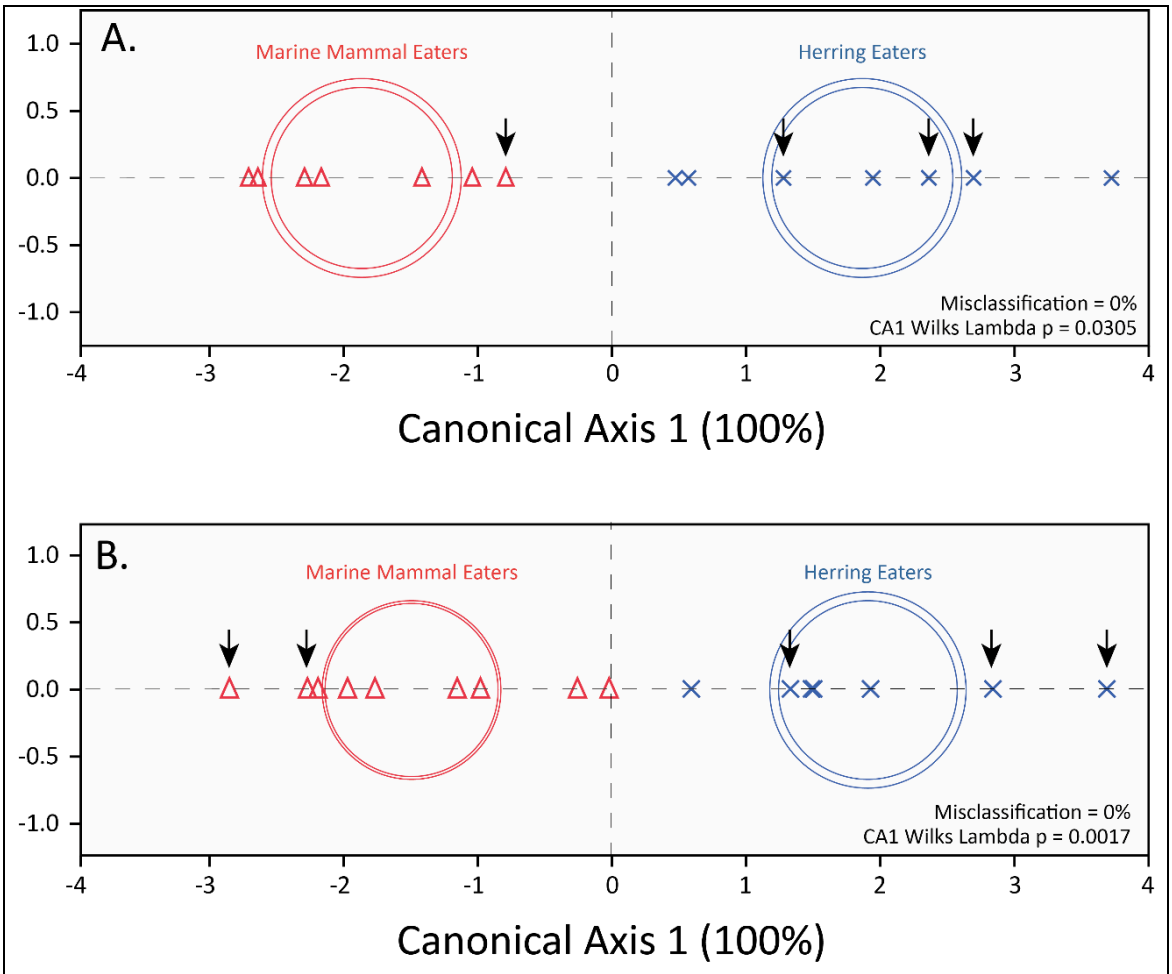

Figure 3.8 *LDA plots of comparisons between Orcinus orca dietary groups for A). front teeth, and B). middle teeth. LDA carried out using stepwise variable selection. Parameters used were A). Str, Ssc, Smr1, Smr2, HAsfc 9x9, and HAsfc 10x10, and B). Sq, Str, Ssc, and HAsfc 2x2 (for all parameter descriptions see Table 3.2 and Table 3.3). For both analyses misclassification was 0%, and Wilks' Lambda test results were p=0.0305 for front teeth, and p=0.0017 for middle teeth. Marine Mammal Eater data points are represented by red triangles, and Herring Eater data points are represented by blue crosses. Two circles are presented for each dietary group, coloured the same as the data points for each. The outer circle represents the normal ellipse region estimated to contain 50% of the population for that group, and the inner circle represents the 95% confidence region to contain the mean of the group. Black arrows point towards those specimens where diet was predicted (i.e. those without associated isotope data).*

Finally a test was carried out to see how well data from the front teeth would predict the dietary group of specimens from the middle teeth, and vice versa (i.e. how much do datasets agree on assignments). This was done by carrying out two further LDA where data from both datasets was present but in each case one of the dietary groups was excluded. For both tests the same parameters were input as for the main dietary LDA for that dataset, and assignment to dietary group and probability of assignment were recorded (Table 3.10). Front teeth were found to misclassify 43.8% of Middle Teeth (7 of 16 specimens) based on their tooth textures. These misclassifications are mostly found in the Marine Mammal Eating ecotype, where 5 specimens have been misclassified as Herring Eaters, however two specimens from those with previously unidentified diet were also misclassified. The middle teeth misclassify a much smaller percentage of front teeth (28.6 %; 4 of 14 specimens). Three of these misclassifications are found in specimens with previously unknown diet. There is also one specimen from the Herring Eating dietary group that the Middle Teeth dataset misclassifies as a Marine Mammal Eater.

T-tests

T-tests were re-run on the new datasets for each of the 33 parameters, with known and predicted diets used as expected diet. For front teeth one parameter showed difference between the two dietary ecotypes (Ssc, p=0.0332). This result is similar to the result from the original datasets and is less than the number we would expect by random chance. For middle teeth four parameters showed a difference between the two dietary ecotypes (Str, p=0.011; Sdq, p=0.018; Sdr, p=0.019; Asfc, p=0.017).

Principal Component Analysis

PCA was carried out for middle teeth using all parameters returning significant results from dietary T-tests. Front teeth were not tested in the same way due to the lack of significant results for this dataset.

It is clear from the PCA (Figure 3.9) that the two dietary groups are separated along Principal Component 1 (PC1 – explains 82.9% of variance in the data). Both groups form discreet distributions in multivariate space, and while there is overlap it is caused by a single outlier Herring Eating specimen. Most Marine Mammal Eaters have negative values for PC1, and all but one Herring Eater have Positive values on PC1.

				Front Teeth Dataset LDA Assignments		Middle Teeth Dataset LDA Assignments	
	Specimen	Tooth Position	Expected Diet	Assignment	Probability	Assignment	Probability
Specimens for which Isotope Data is Available	NMS.1956.36.56	Front	Mammals	Mammals	0.9998	* Mammals	0.9962
	NMS.1956.36.56	Middle	Mammals	* **Herring**	1.0000	Mammals	0.8318
	ZMC CN89	Front	Mammals	Mammals	0.9997	* Mammals	0.9047
	ZMC 12x	Middle	Mammals	* **Herring**	0.9941	Mammals	0.9910
	ZMC 1x	Front	Mammals	Mammals	0.9999	* Mammals	1.0000
	ZMC 1x	Middle	Mammals	* **Herring**	0.9718	Mammals	0.9998
	ZMC CN.38x	Front	Mammals	Mammals	1.0000	* Mammals	1.0000
	ZMC CN.38x	Middle	Mammals	* Mammals	0.9989	Mammals	0.9995
	NHM SW 1926.44	Middle	Mammals	* **Herring**	1.0000	Mammals	0.6928
	NHM SW 1943.9	Front	Mammals	Mammals	0.9797	* Mammals	0.7764
	NHM SW 1943.9	Middle	Mammals	* **Herring**	1.0000	Mammals	0.9989
	NMS 1956.36.57	Front	Mammals	Mammals	0.9950	* Mammals	1.0000
	NMS 1956.36.57	Middle	Mammals	* Mammals	1.0000	Mammals	0.9839
	ZMC M1068	Front	Herring	Herring	0.8930	* Herring	0.7703
	ZMC M1068	Middle	Herring	* Herring	1.0000	Herring	0.9974
	ZMC 3x	Front	Herring	Herring	0.9993	* Herring	0.9996
	ZMC 3x	Middle	Herring	* Herring	1.0000	Herring	0.7888
	NHM ZD.1886.11.22.1	Front	Herring	Herring	1.0000	* **Mammals**	1.0000
	NHM ZD.1886.11.22.1	Middle	Herring	* Herring	1.0000	Herring	0.9884
	NMS 1990.86	Front	Herring	Herring	0.8549	* Herring	0.8980
	NMS 1990.86	Middle	Herring	* Herring	0.9912	Herring	0.9890
Specimens with Originally Unknown Diet	NMS Z.2015.172.48	Front	Herring	Herring	1.0000	* **Mammals**	1.0000
	NMS Z.2015.172.48	Middle	Mammals	* **Herring**	1.0000	Mammals	0.9998
	ZMC 24x	Front	Mammals	Mammals	0.9497	* **Herring**	0.9993
	ZMC 24x	Middle	Herring	* Herring	1.0000	Herring	0.9999
	ZMC M1647	Front	Herring	Herring	0.9998	* Herring	1.0000
	ZMC M1647	Middle	Herring	* Herring	1.0000	Herring	0.9797
	NHM SW 1943.11	Middle	Herring	* **Mammals**	0.9789	Herring	1.0000
	NMS 1876.11	Front	Herring	Herring	0.9917	* **Mammals**	1.0000
	NMS 1876.11	Middle	Mammals	* Mammals	1.0000	Mammals	1.0000

Table 3.10 *Results of LDA carried out to test how well each dataset (front teeth and middle teeth datasets) could assign data from the other. Those specimens predicted (i.e. data from the opposing dataset) are marked with an *. All misclassifications are highlighted in bold. In each case the Assignment gives the group to which the analysis has assigned each specimen, and the probability is the likelihood of that specimen belonging to the assigned group.*

From parameter loadings (eigenvectors) we find that Sdq (0.54), Sdr (0.54), and Asfc (0.54) are responsible for the majority of the separation on PC1, with Str loading highest onto PC2 (0.93).

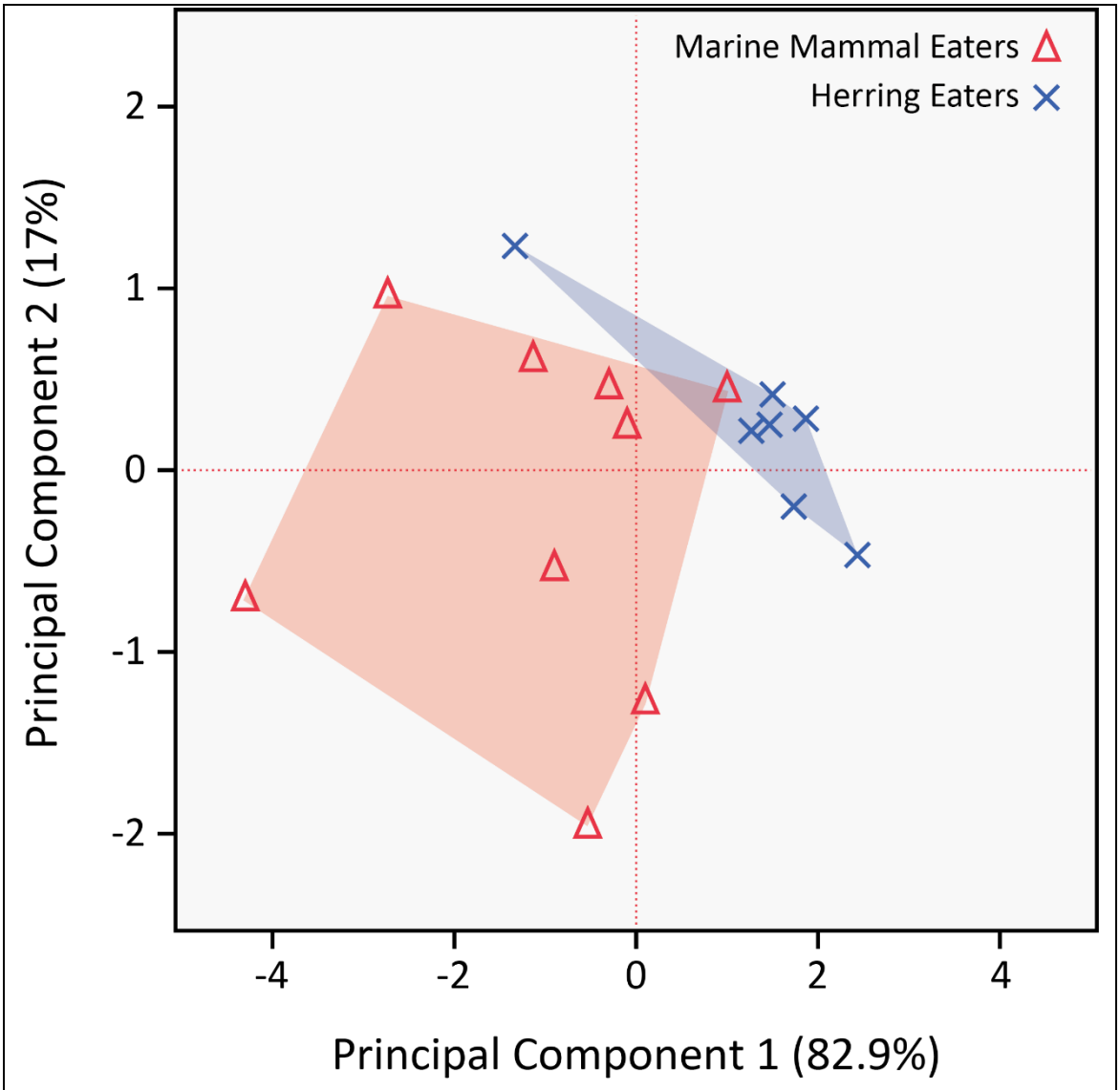

Figure 3.9 *PCA plot comparing Orcinus orca dietary groups, using only data from middle teeth. This figure includes data from specimens where dietary class was predicted using LDA. The PCA is based on parameters Str, Sdq, Sdr, and Asfc (those parameters returning significant results from T-tests between the two dietary groups, using middle teeth data). Marine Mammal Eater data points are represented by red triangles, Herring Eater data points by blue crosses, convex hulls coloured to match the data points their range represents.*

Discussion

Intra-Individual Variability

Within a single tooth, the texture of labial areas of the apical surface appear to significantly differ from mesial and lingual areas. Multivariate analysis however separates all three areas into relatively distinct distributions, without any focus on separating labial areas from mesial or lingual areas. There is almost always some degree of overlap between all three locations in multivariate space. As parameters mostly return similar eigenvectors for PC1 it appear that they are all equally responsible for this separation. Overall this suggests that when each individual tooth is tested separately there are differences in microtexture between all three areas of the apical tooth surface in *Orcinus orca*. But when data for different Tooth Positions is pooled in each analysis the broader difference is only between labial areas and the rest of the tooth. These results are generally consistent across both specimens studied. Multivariate analyses also show that these differences are not caused by broadly overlapping distributions, but by discreet distributions of data, suggesting different areas on the apical surface of *Orcinus orca* teeth have consistently different textures.

Between tooth positions, the apical surface texture of front teeth consistently differs from that of middle and rear teeth, and that while there are some differences between middle and rear teeth they are much more similar in texture to one another than to front teeth. Multivariate analyses separate all three teeth into discreet distributions across both specimens, with only a very small, inconsistent degree of overlap between positions. Again eigenvectors on PC1 are similar for most parameters indicating that they are all responsible for this separation. This shows that if data from all areas within a tooth is pooled that front teeth differ significantly from middle and rear teeth, but when this variable is controlled for all three teeth are significantly different in their surface texture. Again these differences are not caused by broadly overlapping distributions, but by discreet distributions of data, showing that different teeth in the jaw of *Orcinus orca* teeth have consistently different textures.

There is obviously some degree of dependence between locations within a tooth and tooth positions. This can be seen from the PCA analyses where the absolute relationships of one variable are affected by the other (i.e. the separation between tooth position is dependent on the area of the apical tooth facet sampled). This can be seen from the results of the 2 Way ANOVA where for most parameters there is a dependent relationship between these two variables. This makes sampling microtextural data from *Orcinus orca* even more difficult as it suggests any dietary analysis must ideally sample very consistently both within teeth and by tooth position to limit the amount of noise in the data.

For both front and middle teeth here are also clear differences between data from maxillary and dentary teeth, and from left and right jaws within and between the maxilla and dentary.. Front teeth show a very high level of difference between jaw types (Tukey HSD). Differences between the two dentaries appear low, and those between the two maxilla appear very low, with results almost always separating upper from lower areas in the jaw. For middle teeth the difference is much less, and here the main separation appears to be between the lower left jaw and all other jaw types, however there is some difference between each of the jaw types across all parameters. This suggests that middle teeth are potentially less susceptible to variability based on jaw type sampled, but variability does still exist. These results were mirrored in multivariate analysis where, for front teeth, data were separated into distributions of maxillary and dentary data on PC1, and between left and right jaws on PC2. For middle teeth differences between maxillary and dentary data from multivariate analyses are much less clear. However right maxillary teeth separate from all other jaw types along PC2 with parameters Sku and Smr1 most responsible for this separation, which follows the pattern from Tukey tests. And Lower Left data separates along PC1, plotting more negatively than all other Jaw locations (all parameters appear to be contributing to this separation to a relatively similar degree).

Overall it appears that tooth surface texture varies greatly within *Orcinus orca* individuals, such that differences between the textures of areas with a tooth, between teeth, and between left and right maxillary and dentary teeth are found. This suggests

that any analysis of *Orcinus orca* tooth microtextures should be very carefully planned, with an emphasis on consistent sampling strategies. These results mean the first null hypothesis that the 3D surface texture of *Orcinus orca* teeth does not vary significantly within a single tooth, between teeth along a jaw, or between maxillary and dentary teeth (left and right), within an individual must be rejected.

Dietary Comparisons

It was not possible to differentiate dietary groups (T-tests) when using only those specimens with known diet (where isotope data was available). This supports the second null hypothesis, however when specimens with unknown diet have their dietary group predicted some separation is possible when using middle teeth.

For front teeth, when specimens with predicted diet are included in analyses there is still no difference in tooth textures between the two dietary ecotypes, (only one of thirty three parameters shows any difference between ecotypes – T-tests). This difference is so low it is below the level expected by random chance (false positives) and as such should not be taken as any indication of a true difference between the ecotypes. Using LDA dietary ecotypes can be separated using front teeth data, however this requires more parameters than required to separate ecotypes when using middle teeth data and the LDA model is poor at classifying those teeth from the middle teeth dataset into the correct dietary groups.

The middle teeth dataset including specimens with predicted diets appears to be much better at separating *Orcinus orca* dietary ecotypes four parameters show difference between ecotypes – T-tests). While this difference is not large it is greater than we would expect from random chance (1.65 false positives from 33 tests with a 0.05 significance value). Using these same four parameters dietary groups can be clearly separated in multivariate space using PCA, where discreet distributions with only a small degree of overlap are found, along PC1. This separation is due in most part to the effect of three parameters with the highest loadings on PC1 (Sdq, Sdr, and Asfc). It is found that Marine Mammal Eaters have negative values on PC1, while Herring

Eaters have positive values. Linear Discriminant Analysis also correctly assigns specimens to dietary ecotypes when using middle teeth data, when only four parameters are used, with a significant discriminatory function separating the two groups. We also find that the middle teeth dataset including specimens with predicted diet can classify almost all front teeth data into the correct dietary ecotype. However those specimens assigned to dietary groups using LDA are more readily misclassified, which is to be expected due to disagreements between the results for each dataset when assigning these specimens. In all cases middle teeth data reclassify front teeth to match the dietary group of the same specimen in the middle teeth dataset.

Overall, using middle teeth (positions four to seven) it is possible to separate *Orcinus orca* dietary populations using 3D tooth surface texture data from the labial side of apical tooth facets. This data clearly separates those specimen expected to eat herring from those expected to eat marine mammals. However some care must be taken, as this separation is only possible using a very small number of parameters (T-tests), and the multivariate analyses are built upon a similarly small sub-sample of parameters. Front teeth (positions one to three) are much worse at separating *Orcinus orca* dietary groups based on 3D tooth surface texture data, which could indicate a difference in use between teeth in the jaw of *Orcinus orca*, but could also be interpreted as providing doubt on the results from middle teeth. Without data from specimens with predicted diets separation of dietary ecotypes is possible using LDA, but not with statistical tests, indicating separation may be due to the LDA model assumptions rather than any real difference in the data.

From the intra-individual comparisons of data within and between *Orcinus orca* teeth it is clear that tooth surface textures vary considerably within each individual. It is possible the inability to control for jaw type (maxilla and dentary) in both the front and middle datasets has added a large amount of noise to the data and obscures a greater or lesser dietary sensitivity. It is also possible that data from a different region of the apical tooth facet (either mesial, lingual, or distal areas) would be more sensitive to dietary differences, which was not tested here. Rear teeth were also unable to be tested due to a lack of samples, their position in the mouth would suggest a lesser

likelihood of contacting food than other teeth, but this test should not be discounted. It is also possible that dentine is worse at discriminating between dietary ecotypes than enamel in marine mammals. It has previously been shown that tooth enamel can be used to discriminate dietary groups in marine mammals (Chapter 2), but following the results of Haupt et al. (2013) it is possible that dietary differences between the *Orcinus orca* populations tested here are too subtle for dentine surfaces to reliably record. It is also possible that apex tooth facets do not retain much dietary information, so future studies should also investigate the sensitivity of surface texture from lateral tooth facets to dietary differences. This could not be tested here due to a lack of consistency between lateral facets across specimens.

These questions must be addressed in further studies if an understanding of the true sensitivity of 3D tooth surface textures to detect dietary differences between *Orcinus orca* ecotypes is to be reached, with a focus on controlling as many variables as possible in any future work. The results of this paper indicate a possibility that *Orcinus orca* ecotypes could be differentiated using 3D tooth surface texture data from middle teeth (positions four to seven), even if the signal is relatively weak. Therefore the second null hypothesis that 3D tooth surface texture parameters cannot separate known dietary ecotypes of *Orcinus orca* must be rejected, with the caveat that a great deal of further work is needed to investigate the effect of greater controls on variables, different regions within a tooth, and the use of rear teeth on *Orcinus orca* dietary separation.

Chapter 4: Investigating how different methods used to scale limit 3D datafiles affect areal texture parameters and the separation of known dietary groups

Abstract

Quantitative 3D tooth surface texture analysis using ISO 25178-2 areal texture parameters requires large wavelength information to be removed from the 3D surfaces producing scale limited surfaces from which roughness parameter values can be calculated. This is achieved by applying an operator, such as a polynomial of defined order, to the surface, and a filter with a nesting index to define the scale of features to be removed. This removes the form and waviness, leaving a resulting roughness surface. Different studies have used varied operators and filters to scale limit surfaces. However it is unclear at present what effect each combination of operator and filter has on resulting areal parameter values, and what their effect might be on resulting statistical tests carried out to differentiate populations with known textural differences on their tooth surfaces. Here we show the effect of varying the operator and filter applied to surfaces on the absolute areal texture parameter values recorded from resulting scale limited surfaces, and their effect on the sensitivity to statistically differentiate dietary groups from teeth with known textural differences. Different operators, filter types, and nesting indices, have a significant effect on the areal texture parameters recorded from resulting scale limited surfaces, with certain combinations producing surfaces with significantly different parameter values to one another. It is also shown that the sensitivity of resulting analyses to separate groups with known textural differences is highly variable depending on the operator and filter used to scale limit 3D surfaces. Overall our results suggest using a robust Gaussian filter with a nesting index of 0.025mm, combined with a 6^{th} order of polynomial (operator) to scale limit 3D surfaces. These results should inform the use of operator and filters to scale limit 3D surfaces in all future studies using areal texture parameters

Introduction

Quantitative 3D tooth surface texture analysis is increasingly being applied to investigate hypotheses of dietary difference between populations of extant or extinct animals. In such studies the sub-micron roughness of tooth surfaces is parameterised, by collecting 3D data on a suitable microscope and generating parameters from resulting surfaces. One method of parameterisation uses a standardised set of areal texture parameters defined by ISO 25178-2 (International Organization for Standardization 2012) to characterise surface roughness. This produces a range of parameter values, covering aspects of surface roughness including heights, volumes, spatial parameters, and material ratios. This data can then be used to differentiate wear patterns found on tooth surfaces (enamel or dentine) caused by the abrasive effects of processing different food types, this allows for differentiation between dietary habits across populations (Calandra et al. 2012, Purnell et al. 2012, Purnell et al. 2013, Schulz et al. 2013b, Gill et al. 2014, Purnell and Darras 2015). Areal surface roughness parameters are also applied to hypotheses in other disciplines, including engineering, where surfaces are assessed by determining likely wear rates and patterns, and quantifying surface characteristics to determine optimal usage and quality, which allows the function of a surface to be significantly altered (Bruzzone et al. 2008, Leach and Haitjema 2010), and in archaeology, where the roughness of tool surfaces, both lithic and metal, can be investigated to determine their original usage (Evans 2014, Dolfini and Crellin 2016).

3D surfaces are made up of three elements, the largest scale features (low frequency) are called surface form, medium scale features (mid frequency) are termed “waviness” defined as those features whose spacing is of greater magnitude than the roughness sampling distance, and the small scale features (high frequency) are termed “roughness” (Figure 4.1). In order to generate areal texture parameters from 3D datafiles, scanned surfaces must be scale limited (also known as form removal) (Jiang et al. 2007, Giusca et al. 2012, International Organization for Standardization 2012). This involves the removal of large and medium scale wavelength features (form and waviness) from surface texture, leaving only the small scale features (roughness).

Waviness and roughness are defined by the cut-off wavelength of filters used to scale limit a surface. Thus if a roughness filter with a high pass cut-off wavelength of 25µm were applied to a surface then any features with a wavelength greater than this cut off value would be removed and termed “waviness”, while all features with a wavelength lower than this cut-off would remain, and be termed “roughness”. If the surface waviness was required, and roughness were to be removed instead then a low pass filter would be used, removing all wavelengths below the desired cut-off. To remove both the waviness and form, an operator and a filter of defined wavelength must be applied to a 3D surface. An S-filter is also often applied to surfaces in order to remove extremely small surface features (often <2.5 µm) which may represent noise, or microscope error, this produces a surface called a Primary surface (containing form, waviness and roughness). The removal of large scale form involves the application of an operator, termed the F-operator, often a polynomial of defined order (Schulz et al. 2013a), producing a surface containing just roughness and waviness information, called an S-F Surface. To remove waviness from the S-F surface a filter is applied (L-filter), this will have a defined high pass cut-off wavelength (nesting index), so that any features with a greater wavelength than this defined value will be removed, this results in an S-L Surface, also termed a roughness surface (Figure 4.2). From this roughness surface areal texture parameters can be measured.

There are multiple settings for operators and filters that can be applied to scale limit a surface, and while areal surface texture parameters are widely used, the settings used to scale limit surfaces are not standardised. As such different studies use different settings to scale limit surfaces. Operators applied to a surface can be any order of polynomial, and there is currently little information to guide researchers on the use of each. Various options exist for the filters that can be applied to surfaces, including Gaussian, wavelet, and spline filters, again very little information is available to differentiate the use of each.

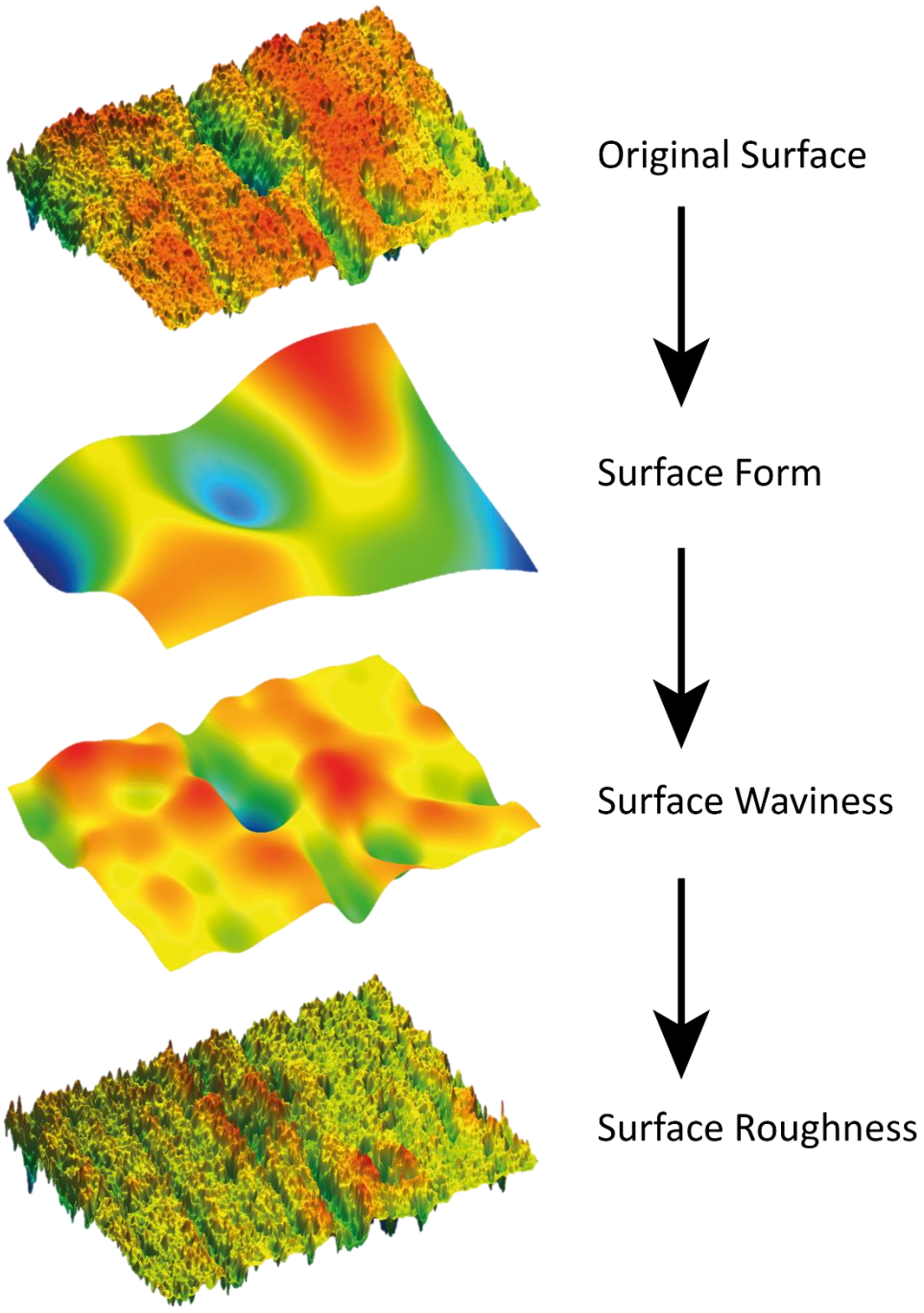

Figure 4.1 *Representation of the elements making up 3D surface texture. The original surface is presented, followed by surface form, then surface waviness, and finally surface roughness. All images are digital elevation models (DEM) of the same surface exported from Surfstand (software version 5.0.0), and imaged in Gwyddion (software version 2.42). The operator used was a 2nd order polynomial, and the filter was a spline filter, with a 0.8mm nesting index for surface waviness, and a 0.025mm nesting index for surface roughness. DEM colours are not at the same scale.*

Many studies have used both an operator and filter in tandem to scale limit surfaces (Schulz et al. 2010, Calandra et al. 2012, Purnell et al. 2013, Schulz et al. 2013a, Schulz et al. 2013b, Gill et al. 2014, Goodall et al. 2015, Purnell and Darras 2015, Gailer et al. 2016). However some studies will not apply an operator, only using a filter with set nesting index (Dunford et al. 2012, Purnell et al. 2012, Nwaogu et al. 2013, Deltombe et al. 2014).

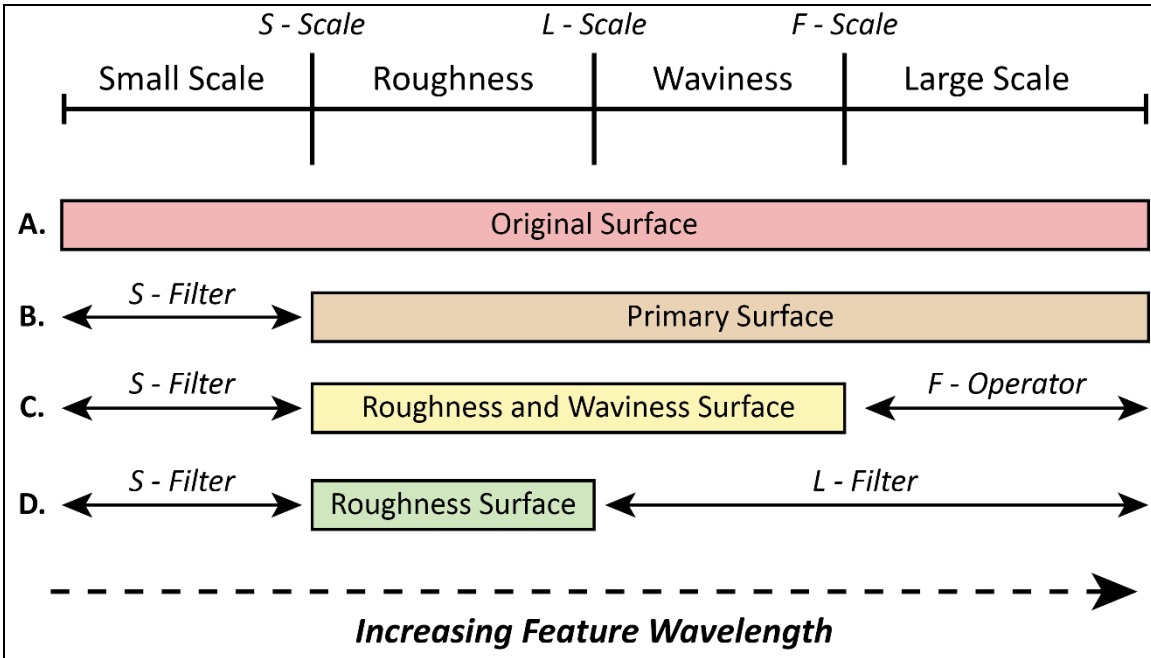

Figure 4.2 *Schematic representation of scale limiting procedures. A. is the original surface with no operators or filters applied. B. Is the primary surface, where extremely small scale features have been removed using an S – Filter. C. is the surface containing both roughness and waviness, where an S –Filter, and a form removing operator have been applied. And D. is the roughness surface produced by applying a filter with set nesting index to the roughness and waviness surface. Surface feature wavelength increases from left to right on the schematic.*

It is not clear what quantifiable effect each scale limiting setting has on a surface, in terms of the way they effect resulting roughness parameter values. The comparability of data generated from surfaces produced using different scale limiting settings is also not clear. This issue affects the choice of operators, filters, and nesting

indices when scale limiting 3D surfaces. Without knowing this information it is impossible to compare current or future studies, and without standardisation this issue will only get worse.

Arman et al. (2016) have approached the use of different filters in their study comparing 3D tooth surface texture data collected using different confocal microscopes. Here surfaces were treated with an operator (2nd order polynomial) to remove surface form prior to thresholding, and then several different approaches were tested for filtering surfaces. The first involved the application of a Gaussian filter (nesting index 2.5 µm), the second approach applied both a Gaussian and robust Gaussian filter to each surface (each with a nesting index of 2.5 µm), and the third involved applying a Gaussian, robust Gaussian, and spline filter to each surface (all with a 2.5 µm nesting index). The effect of these different settings was tested both in terms of how datasets improved the comparability of data from different confocal microscopes, and in how they affected the results of dietary analyses. It was found that all datasets where both the operator and at least one filter were applied showed the lowest difference between microscopes, suggesting these settings increase the comparability of data. In terms of their effect on dietary analyses the study found that, although little difference was detected in the ability of scale limited datasets to differentiate known dietary groups, they were unable to replicate the results of the original study from which the data was taken. This they attribute to the effect of noise being removed from the data by filters, potentially providing a more "pure" dietary signal. However there are serious issues with the way this analysis was performed, which impact the applicability and validity of their results. Firstly this analysis was carried out using a different set of surface texture parameters, called Scale Sensitive Fractal Analysis parameters (SSFA). These parameters were designed to be generated from non-scale limited surfaces (i.e. surfaces where all waviness and roughness information is present). As such applying filters and operators serves only to create uncertainty in the way this affects resulting texture parameter values. Also the nesting index used for all filters is incredibly small, with a 2.5 µm cut-off, meaning all features with a wavelength greater than this (assuming they used a high pass filter) would be removed. This wavelength is so low compared to the field size of data they collected

(220 x 178 µm) it is almost certainly removing most of the surface roughness (which may explain why it lead to greater agreement between data from different microscopes). Another issue is the application of multiple filter types to the same data file, especially as they all have the same nesting index. This appears to create huge redundancy in the methodology, where each filter will simply apply a slightly different shape to the surface, without removing any further information, as all features with a wavelength greater than 2.5 µm will have been removed by the first filter. Other issues are more minor and include unequal sample sizes, and differing data transformation for each dataset, and the editing of datafiles after the application of filters and operators. It is clear therefore that new analyses with a greater control on variables and a focus on avoiding the same pitfalls as Arman et al. (2016) is needed.

In this paper the problem is addressed in a more rigorous way, by testing what effect different settings used to scale limit 3D surfaces have on resulting areal surface texture parameters (using a wide range of operators, filters and nesting indices). This will be investigated by duplicating a set of 3D surfaces and scale limiting each duplicate using a different combination of operator, filter and nesting index. The absolute areal parameter values generated from resulting scale limited surfaces will be statistically compared, based on their absolute differences, and their ability to separate two pairs of dietary groups with known dietary differences (covering multiple tooth, and habitat types). The results of this work will be applicable to all future studies using areal texture parameters, and will help to define comparability between studies and the optimal settings to be used for scale limiting 3D surfaces.

This paper will test a number of null hypotheses;

- Application of different polynomials (operators) to remove long wavelength elements of surface form has no effect on the texture of resulting surfaces (as measured by ISO 25178-2 texture parameters).
- Application of different filter types (robust Gaussian, robust wavelet, and spline) has no effect on the texture of the resulting surface.

- Application of filters with different nesting indices (cut-off wavelengths) has no effect on the texture of the resulting surface.
- When applying different operators, filters, and filters with different nesting indices to a surface, there is no interaction in their effect on resulting texture parameters.
- Application of different filters and operators has no effect on the power of areal microwear texture analyses to detect dietary differences between samples.

It may be obvious to some readers with experience of texture analysis using ISO-based approaches that some of these null hypotheses are very unlikely, but we use them in order to be as transparent as possible in describing our methodology and approach.

Methods

Materials

Twenty individual specimens were selected across two populations (Table 4.1), each population contained two sub-groups known to have textural differences on their tooth surfaces from previous work, and as such each sub-group within a population contained five individuals. This low sample size will affect the results of this study, potentially reducing the likelihood that the data represent the true population mean, and that significant results represent a true effect. However this sample size was chosen to allow a greater number of operators and filters to be tested.

The first population includes ten *Capreolus capreolus* (roe deer) individuals, chosen to represent textural variation within a single species. These include five adult male and five adult female specimens collected from the Dourdan forest (Ile de France, France) February 1989, and held by the Institut National de la Recherche Agronomique (INRA) (Toulouse, France). These specimens have all previously been studied by Merceron et al. (2010), where they were shown to have significantly different tooth

surface textures. Females eat a much higher proportion of bramble leaves, and males eat a high proportion of acorns (Cransac et al. 2001), leading to higher values for complexity and heterogeneity in males, and higher values for anisotropy in females when tested using Scale Sensitive Fractal Analysis (SSFA) (Merceron et al. 2010).

The second population includes five *Pagophilus groenlandicus* (harp seal) and five *Phoca vitulina* (harbour seal) specimens, chosen to represent textural variation between two species. All are pinnipeds from the family Phocidae (hereafter referred to as phocids). All *Pagophilus groenlandicus* specimens were collected from Greenland, and all *Phoca vitulina* specimens were collected from the North Sea. Specimens are held by the mammal collection of the Zoological Museum Berlin (Museum für Naturkunde, Berlin, Germany). From stomach contents analyses these species have been shown to come from two different dietary groups. *Pagophilus groenlandicus* has been shown to consume a high proportion of non-cephalopod invertebrates (Pauly et al. 1998, Haug et al. 2004, Nilssen et al. 2004), while *Phoca vitulina* has been shown to consume a high proportion of fish (Pauly et al. 1998, Tollit et al. 1998, Brown et al. 2001, Andersen et al. 2004). These specific specimens have also been shown to exhibit significantly different 3D areal textures on their tooth surfaces between dietary groups (See Chapter 2).

These two populations present two very different case studies. The *C.capreolus* teeth are occlusal, and feed terrestrially, grinding plant matter between tooth facets. They also represent two sub-groups within a single species, where a more subtle textural difference would be expected. The phocid teeth are non-occlusal, feeding in the marine environment, and piercing prey items with their teeth. This population represents a comparison between two species, and as such a more obvious textural difference would be expected. These two populations allow the hypotheses to be tested on two very different tooth types, representing differing occlusion, habitat, and feeding methods.

	Species	Famliy	Common Name	Sample Number	Host Institution	Diet	Tooth	Locality
Dietary Comparison 1	*Capreolus capreolus*	Cervidae	Roe Deer	INRA 001 126 T	Institut National de la Recherche Agronomique (INRA) (Toulouse, France)	Bramble Leaves	Upper Left M2	Dourdan forest (Ile de France, France)
	Capreolus capreolus	Cervidae	Roe Deer	INRA 002 000 T		Bramble Leaves	Upper Left M2	Dourdan forest (Ile de France, France)
	Capreolus capreolus	Cervidae	Roe Deer	INRA 006 089 T		Bramble Leaves	Upper Left M2	Dourdan forest (Ile de France, France)
	Capreolus capreolus	Cervidae	Roe Deer	INRA 008 076 T		Bramble Leaves	Upper Left M2	Dourdan forest (Ile de France, France)
	Capreolus capreolus	Cervidae	Roe Deer	INRA 014 000 T		Bramble Leaves	Lower Left M2	Dourdan forest (Ile de France, France)
	Capreolus capreolus	Cervidae	Roe Deer	INRA 007 109 T		Acorns	Upper Left M2	Dourdan forest (Ile de France, France)
	Capreolus capreolus	Cervidae	Roe Deer	INRA 004 108 T		Acorns	Upper Left M2	Dourdan forest (Ile de France, France)
	Capreolus capreolus	Cervidae	Roe Deer	INRA 009 085 T		Acorns	Upper Left M2	Dourdan forest (Ile de France, France)
	Capreolus capreolus	Cervidae	Roe Deer	INRA 012 000 T		Acorns	Upper Left M2	Dourdan forest (Ile de France, France)
	Capreolus capreolus	Cervidae	Roe Deer	INRA 013 019 T		Acorns	Upper Left M2	Dourdan forest (Ile de France, France)
Dietary Comparison 2	*Phoca vitulina*	Phocidae	Harbour Seal	ZMB_MAM 90810	Mammal Collection of the Zoological Museum Berlin (Museum für Naturkunde, Berlin, Germany)	Fish	Upper Left PC5	Büsum, North Sea
	Phoca vitulina	Phocidae	Harbour Seal	ZMB_MAM 56766		Fish	Upper Right PC4	North Sea
	Phoca vitulina	Phocidae	Harbour Seal	ZMB_MAM 100997		Fish	Upper Right PC4	Wangerooge, North Sea
	Phoca vitulina	Phocidae	Harbour Seal	ZMB_MAM 56767		Fish	Upper Right PC4	North Sea
	Phoca vitulina	Phocidae	Harbour Seal	ZMB_MAM 101271		Fish	Upper Left PC4	Wangerooge, North Sea
	Pagophilus groenlandicus	Phocidae	Harp Seal	ZMB_MAM 32569		Invertebrates	Upper Right PC3	Greenland
	Pagophilus groenlandicus	Phocidae	Harp Seal	ZMB_MAM 43737		Invertebrates	Upper Left PC2	Jameson Land, Greenland
	Pagophilus groenlandicus	Phocidae	Harp Seal	ZMB_MAM 32570		Invertebrates	Upper Right PC3	Greenland
	Pagophilus groenlandicus	Phocidae	Harp Seal	ZMB_MAM 43738		Invertebrates	Upper Right PC3	Jameson Land, Greenland
	Pagophilus groenlandicus	Phocidae	Harp Seal	ZMB_MAM 56774		Invertebrates	Upper Left PC2	Greenland

Table 4.1 *Full specimen list, including all four dietary groups, taxonomic information, sample numbers, host institutions, dietary categories, tooth position used, and collection locality.*

Data Collection

From each individual specimen a single tooth was selected from which to collect 3D areal texture data.

For all but one *C.capreolus* specimen the upper left second molar (M2) was used. The one exception was INRA 014 000 T, where data had to be collected from the lower left M2, due to the unavailability of the upper dentition. These teeth would be expected to be comparable in their surface texture, as they interact with one another processing the same food item. Data were collected from shearing facet 1 on both upper and lower M2, with teeth consistently orientated (Fig. 4.3).

For *Pagophilus groenlandicus* upper right, or left, Post Canine Tooth 2 or 3 were used, and for *Phoca vitulina* upper right, or left Post Canine Tooth 4 or 5 were used. Phocid tooth locations were less well constrained due to the availability of teeth. All phocid data were collected from as close to the labial apex of the tooth as possible, with teeth consistently orientated (Fig. 4.3).

Tooth surfaces were replicated using polyvinylsiloxane dental moulding compound (President Jet Regular Body, Coltène Whaledent), common practice when using museum or institution specimens which cannot be loaned. It has previously been shown using 3D areal texture analysis that this particular replication compound produces highly accurate and precise moulds (Goodall et al. 2015). The moulding compound was applied as per instructions provided, using an applicator gun, which standardises the mixing of two-components by extruding them through a helical nozzle. An epoxy resin containing a black pigment (Epotek 320LV) was used to produce casts from all resulting moulds. Casts were pressurized (2Bar/30psi), using a Protima Pressure Tank 10L (no agitator), for approximately 24hrs. This reduces the size of any bubbles in the resin, improving the resulting cast fidelity. An Emitech K500X sputter coater was then used to gold coat specimens (four minutes duration) to optimise data acquisition using focus variation microscopy. This has been shown to produce no difference from original surfaces (Appendix 2: Supplementary Chapter).

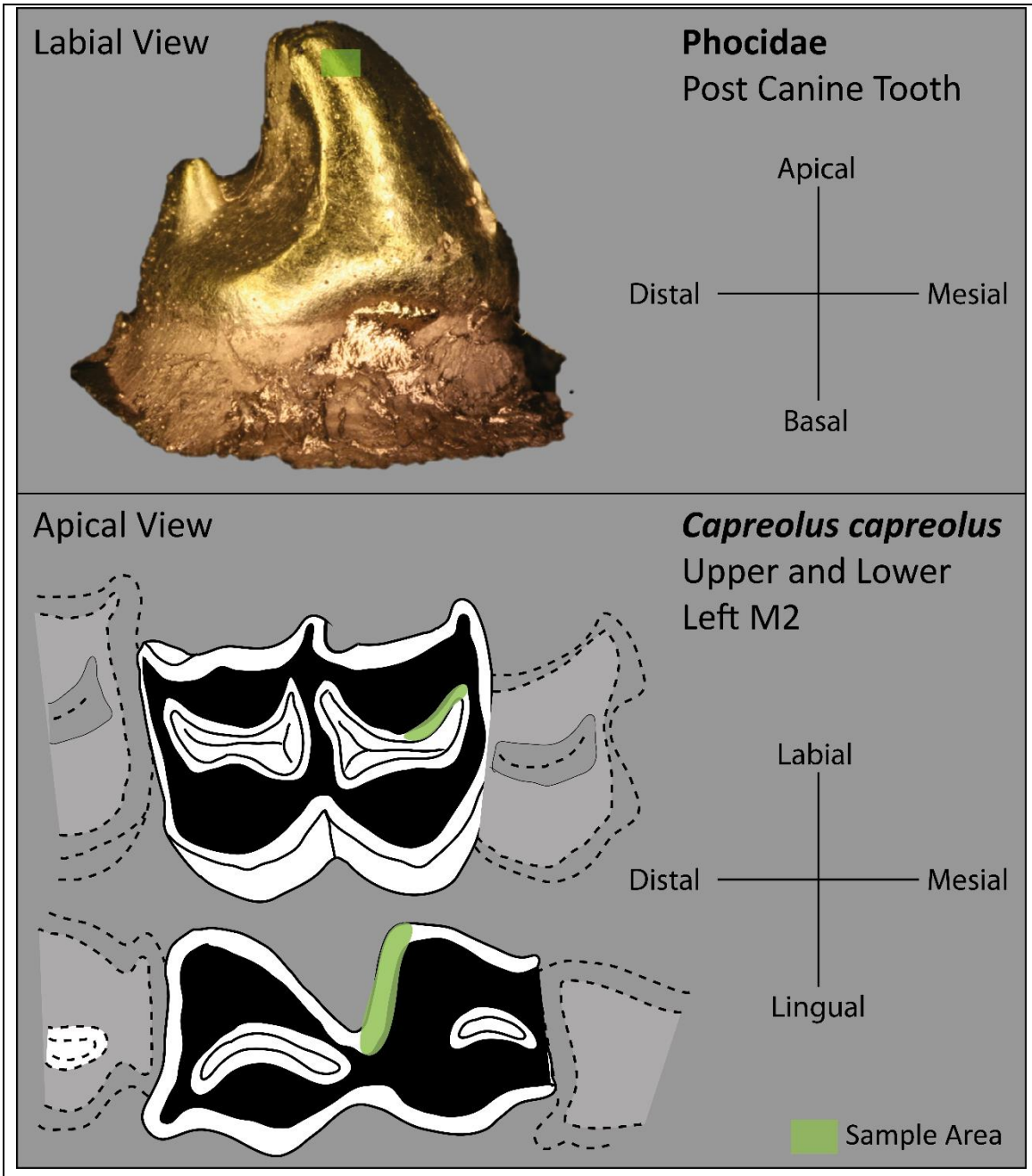

Figure 4.3 *Representations of data collection locations on both phocid and Capreolus capreolus teeth. With orientation information included and sample area highlighted green.*

Data Acquisition

Focus variation microscopy was used to collect 3D surface texture data from each specimen (Alicona Infinite Focus Microscope, model IFM G4c, software version: 5.1). Data capture followed Purnell et al. (2013), Gill et al. (2014), Goodall et al. (2015),

Purnell and Darras (2015) (x100 objective, field of view of 145 x 110 µm, vertical resolution set to 0.02 µm, lateral optical resolution 0.44 µm). All data was collected from tooth enamel. Only data files with less than 5% missing data were accepted. Data files were levelled using an all points levelling system (fit to a least squares plane via rotation around all three axes) to remove any variation in 3D surfaces arising from manual horizontal positioning of the sample. Surfstand (software version 5.0.0) was used to edit resulting data files by manually selecting and replacing data errors with an oblique plane.

Prior to parameter generation surfaces were scale limited using a range of operators and filters. These comprise the removal of a least squares N^{th} order of polynomial (operator), and a filter with a fixed nesting index (cut-off wavelength). 2^{nd} to 11^{th} order polynomials were used, with each removing slightly different form from the surface (Figure 4.4). Filters used were robust Gaussian, robust wavelet, and spline, and nesting index values were 0.025mm and 0.08mm. 40 overall combinations of operator and filter were applied to each surface, producing 40 different scale limited surfaces for each of the 20 specimens. 30 combinations involved the application of all possible pairings of operator and filter together. For all 30 of these settings the nesting index was 0.025mm. The remaining 10 combinations involved all possible pairings of polynomial and a robust Gaussian filter with 0.08mm nesting index. The different nesting indices could not be used across all filter types due to time constraints and the unwieldy nature of the volume of data this would create. The full list of combinations of operator and filter applied to each sample can be seen in Table 4.2.

24 ISO 25178-2 areal texture parameters (International Organization for Standardization 2012) were generated from each of the resulting surfaces using the Surfstand program (software version 5.0.0). For a full list of parameters please see Table 4.3 (See Purnell et al. (2013) and Gill et al. (2014) for more detailed parameter descriptions). Parameter Sal and Std were excluded from further testing as they almost always returned the same value for each surface.

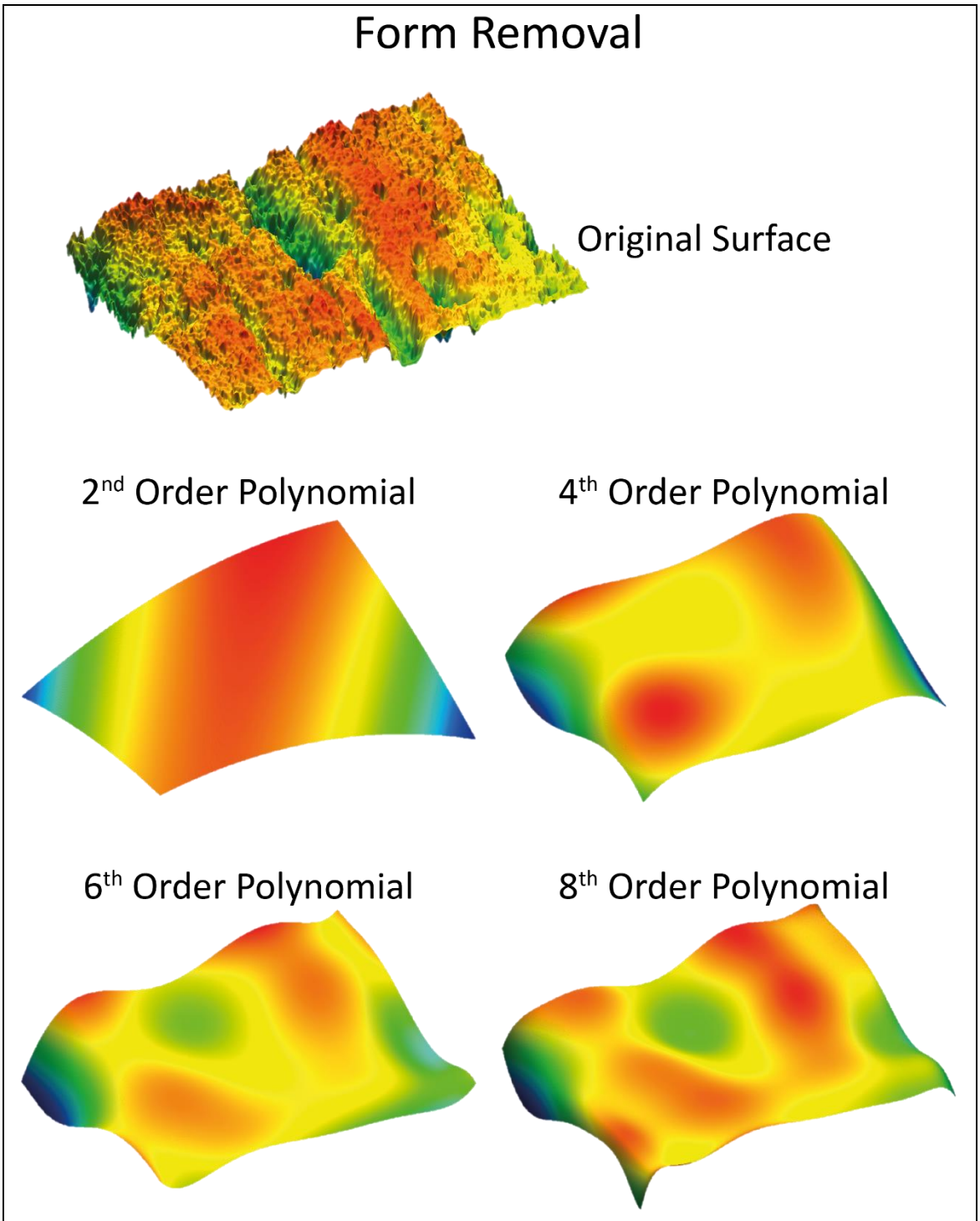

Figure 4.4 *Digital Elevation Models (DEMs) showing the form removed by different operators (orders of polynomial) applied to an original surface. All DEMs were produced in Surfstand (software version 5.0.0), and imaged in Gwyddion (software version 2.42). All images are of the same surface treated in different ways. DEM colours are not all to the same scale.*

Specimen	Dietary Group	Filter	Operator (polynomial)	Resulting Surface
C.capreolus (1)	Bramble Leaves	robust Gaussian, 0.025 mm	2nd order	1bramble_rgp2_0.025
			3rd order	1bramble_rgp3_0.025
			…	…
			11th order	1bramble_rgp11_0.025
		robust Gaussian, 0.08 mm	2nd order	1bramble_rgp2_0.08
			3rd order	1bramble_rgp3_0.08
			…	…
			11th order	1bramble_rgp11_0.08
		robust wavelet, 0.025 mm	2nd order	1bramble_rwp2_0.025
			3rd order	1bramble_rwp3_0.025
			…	…
			11th order	1bramble_rwp11_0.025
		spline, 0.025 mm	2nd order	1bramble_sp2_0.025
			3rd order	1bramble_sp3_0.025
			…	…
			11th order	1bramble_sp11_0.025
C.capreolus (2)	Bramble Leaves	robust Gaussian, 0.025 mm	2nd order	2bramble_rgp2_0.025
			3rd order	2bramble_rgp3_0.025
			…	…
			11th order	2bramble_rgp11_0.025
		robust Gaussian, 0.08 mm	2nd order	2bramble_rgp2_0.08
			3rd order	2bramble_rgp3_0.08
			…	…
			11th order	2bramble_rgp11_0.08
		robust wavelet, 0.025 mm	2nd order	2bramble_rwp2_0.025
			3rd order	2bramble_rwp3_0.025
			…	…
			11th order	2bramble_rwp11_0.025
		spline, 0.025 mm	2nd order	2bramble_sp2_0.025
			3rd order	2bramble_sp3_0.025
			…	…
			11th order	2bramble_sp11_0.025
C.capreolus (3)	Bramble Leaves	robust Gaussian, 0.025 mm	2nd order	3bramble_rgp2_0.025
			3rd order	3bramble_rgp3_0.025
			…	…
			11th order	3bramble_rgp11_0.025
		robust Gaussian, 0.08 mm	2nd order	3bramble_rgp2_0.08
			3rd order	3bramble_rgp3_0.08
			…	…
			11th order	3bramble_rgp11_0.08
		robust wavelet, 0.025 mm	2nd order	3bramble_rwp2_0.025
			3rd order	3bramble_rwp3_0.025
			…	…
			11th order	3bramble_rwp11_0.025
		spline, 0.025 mm	2nd order	3bramble_sp2_0.025
			3rd order	3bramble_sp3_0.025
			…	…
			11th order	3bramble_sp11_0.025
C.capreolus (4)	Bramble Leaves	robust Gaussian, 0.025 mm	2nd order	4bramble_rgp2_0.025
			3rd order	4bramble_rgp3_0.025
			…	…
			11th order	4bramble_rgp11_0.025
		robust Gaussian, 0.08 mm	2nd order	4bramble_rgp2_0.08
			3rd order	4bramble_rgp3_0.08
			…	…
			11th order	4bramble_rgp11_0.08
		robust wavelet, 0.025 mm	2nd order	4bramble_rwp2_0.025
			3rd order	4bramble_rwp3_0.025
			…	…
			11th order	4bramble_rwp11_0.025
		spline, 0.025 mm	2nd order	4bramble_sp2_0.025
			3rd order	4bramble_sp3_0.025
			…	…
			11th order	4bramble_sp11_0.025

C.capreolus (5)	Bramble Leaves	robust Gaussian, 0.025 mm	2nd order	5bramble_rgp2_0.025
			3rd order	5bramble_rgp3_0.025
			…	…
			11th order	5bramble_rgp11_0.025
		robust Gaussian, 0.08 mm	2nd order	5bramble_rgp2_0.08
			3rd order	5bramble_rgp3_0.08
			…	…
			11th order	5bramble_rgp11_0.08
		robust wavelet, 0.025 mm	2nd order	5bramble_rwp2_0.025
			3rd order	5bramble_rwp3_0.025
			…	…
			11th order	5bramble_rwp11_0.025
		spline, 0.025 mm	2nd order	5bramble_sp2_0.025
			3rd order	5bramble_sp3_0.025
			…	…
			11th order	5bramble_sp11_0.025
C.capreolus (6)	Acorns	robust Gaussian, 0.025 mm	2nd order	6acorn_rgp2_0.025
			3rd order	6acorn_rgp3_0.025
			…	…
			11th order	6acorn_rgp11_0.025
		robust Gaussian, 0.08 mm	2nd order	6acorn_rgp2_0.08
			3rd order	6acorn_rgp3_0.08
			…	…
			11th order	6acorn_rgp11_0.08
		robust wavelet, 0.025 mm	2nd order	6acorn_rwp2_0.025
			3rd order	6acorn_rwp3_0.025
			…	…
			11th order	6acorn_rwp11_0.025
		spline, 0.025 mm	2nd order	6acorn_sp2_0.025
			3rd order	6acorn_sp3_0.025
			…	…
			11th order	6acorn_sp11_0.025
C.capreolus (7)	Acorns	robust Gaussian, 0.025 mm	2nd order	7acorn_rgp2_0.025
			3rd order	7acorn_rgp3_0.025
			…	…
			11th order	7acorn_rgp11_0.025
		robust Gaussian, 0.08 mm	2nd order	7acorn_rgp2_0.08
			3rd order	7acorn_rgp3_0.08
			…	…
			11th order	7acorn_rgp11_0.08
		robust wavelet, 0.025 mm	2nd order	7acorn_rwp2_0.025
			3rd order	7acorn_rwp3_0.025
			…	…
			11th order	7acorn_rwp11_0.025
		spline, 0.025 mm	2nd order	7acorn_sp2_0.025
			3rd order	7acorn_sp3_0.025
			…	…
			11th order	7acorn_sp11_0.025
C.capreolus (8)	Acorns	robust Gaussian, 0.025 mm	2nd order	8acorn_rgp2_0.025
			3rd order	8acorn_rgp3_0.025
			…	…
			11th order	8acorn_rgp11_0.025
		robust Gaussian, 0.08 mm	2nd order	8acorn_rgp2_0.08
			3rd order	8acorn_rgp3_0.08
			…	…
			11th order	8acorn_rgp11_0.08
		robust wavelet, 0.025 mm	2nd order	8acorn_rwp2_0.025
			3rd order	8acorn_rwp3_0.025
			…	…
			11th order	8acorn_rwp11_0.025
		spline, 0.025 mm	2nd order	8acorn_sp2_0.025
			3rd order	8acorn_sp3_0.025
			…	…
			11th order	8acorn_sp11_0.025

C.capreolus (9)	Acorns	robust Gaussian, 0.025 mm	2nd order	9acorn_rgp2_0.025
			3rd order	9acorn_rgp3_0.025
			…	…
			11th order	9acorn_rgp11_0.025
		robust Gaussian, 0.08 mm	2nd order	9acorn_rgp2_0.08
			3rd order	9acorn_rgp3_0.08
			…	…
			11th order	9acorn_rgp11_0.08
		robust wavelet, 0.025 mm	2nd order	9acorn_rwp2_0.025
			3rd order	9acorn_rwp3_0.025
			…	…
			11th order	9acorn_rwp11_0.025
		spline, 0.025 mm	2nd order	9acorn_sp2_0.025
			3rd order	9acorn_sp3_0.025
			…	…
			11th order	9acorn_sp11_0.025
C.capreolus (10)	Acorns	robust Gaussian, 0.025 mm	2nd order	10acorn_rgp2_0.025
			3rd order	10acorn_rgp3_0.025
			…	…
			11th order	10acorn_rgp11_0.025
		robust Gaussian, 0.08 mm	2nd order	10acorn_rgp2_0.08
			3rd order	10acorn_rgp3_0.08
			…	…
			11th order	10acorn_rgp11_0.08
		robust wavelet, 0.025 mm	2nd order	10acorn_rwp2_0.025
			3rd order	10acorn_rwp3_0.025
			…	…
			11th order	10acorn_rwp11_0.025
		spline, 0.025 mm	2nd order	10acorn_sp2_0.025
			3rd order	10acorn_sp3_0.025
			…	…
			11th order	10acorn_sp11_0.025
P.vitulina (1)	Fish	robust Gaussian, 0.025 mm	2nd order	1fish_rgp2_0.025
			3rd order	1fish_rgp3_0.025
			…	…
			11th order	1fish_rgp11_0.025
		robust Gaussian, 0.08 mm	2nd order	1fish_rgp2_0.08
			3rd order	1fish_rgp3_0.08
			…	…
			11th order	1fish_rgp11_0.08
		robust wavelet, 0.025 mm	2nd order	1fish_rwp2_0.025
			3rd order	1fish_rwp3_0.025
			…	…
			11th order	1fish_rwp11_0.025
		spline, 0.025 mm	2nd order	1fish_sp2_0.025
			3rd order	1fish_sp3_0.025
			…	…
			11th order	1fish_sp11_0.025
P.vitulina (2)	Fish	robust Gaussian, 0.025 mm	2nd order	2fish_rgp2_0.025
			3rd order	2fish_rgp3_0.025
			…	…
			11th order	2fish_rgp11_0.025
		robust Gaussian, 0.08 mm	2nd order	2fish_rgp2_0.08
			3rd order	2fish_rgp3_0.08
			…	…
			11th order	2fish_rgp11_0.08
		robust wavelet, 0.025 mm	2nd order	2fish_rwp2_0.025
			3rd order	2fish_rwp3_0.025
			…	…
			11th order	2fish_rwp11_0.025
		spline, 0.025 mm	2nd order	2fish_sp2_0.025
			3rd order	2fish_sp3_0.025
			…	…
			11th order	2fish_sp11_0.025

P.vitulina (3)	Fish	robust Gaussian, 0.025 mm	2nd order	3fish_rgp2_0.025
			3rd order	3fish_rgp3_0.025
			…	…
			11th order	3fish_rgp11_0.025
		robust Gaussian, 0.08 mm	2nd order	3fish_rgp2_0.08
			3rd order	3fish_rgp3_0.08
			…	…
			11th order	3fish_rgp11_0.08
		robust wavelet, 0.025 mm	2nd order	3fish_rwp2_0.025
			3rd order	3fish_rwp3_0.025
			…	…
			11th order	3fish_rwp11_0.025
		spline, 0.025 mm	2nd order	3fish_sp2_0.025
			3rd order	3fish_sp3_0.025
			…	…
			11th order	3fish_sp11_0.025
P.vitulina (4)	Fish	robust Gaussian, 0.025 mm	2nd order	4fish_rgp2_0.025
			3rd order	4fish_rgp3_0.025
			…	…
			11th order	4fish_rgp11_0.025
		robust Gaussian, 0.08 mm	2nd order	4fish_rgp2_0.08
			3rd order	4fish_rgp3_0.08
			…	…
			11th order	4fish_rgp11_0.08
		robust wavelet, 0.025 mm	2nd order	4fish_rwp2_0.025
			3rd order	4fish_rwp3_0.025
			…	…
			11th order	4fish_rwp11_0.025
		spline, 0.025 mm	2nd order	4fish_sp2_0.025
			3rd order	4fish_sp3_0.025
			…	…
			11th order	4fish_sp11_0.025
P.vitulina (5)	Fish	robust Gaussian, 0.025 mm	2nd order	5fish_rgp2_0.025
			3rd order	5fish_rgp3_0.025
			…	…
			11th order	5fish_rgp11_0.025
		robust Gaussian, 0.08 mm	2nd order	5fish_rgp2_0.08
			3rd order	5fish_rgp3_0.08
			…	…
			11th order	5fish_rgp11_0.08
		robust wavelet, 0.025 mm	2nd order	5fish_rwp2_0.025
			3rd order	5fish_rwp3_0.025
			…	…
			11th order	5fish_rwp11_0.025
		spline, 0.025 mm	2nd order	5fish_sp2_0.025
			3rd order	5fish_sp3_0.025
			…	…
			11th order	5fish_sp11_0.025
P.groenlandicus (6)	Invertebrates	robust Gaussian, 0.025 mm	2nd order	6invertebrate_rgp2_0.025
			3rd order	6invertebrate_rgp3_0.025
			…	…
			11th order	6invertebrate_rgp11_0.025
		robust Gaussian, 0.08 mm	2nd order	6invertebrate_rgp2_0.08
			3rd order	6invertebrate_rgp3_0.08
			…	…
			11th order	6invertebrate_rgp11_0.08
		robust wavelet, 0.025 mm	2nd order	6invertebrate_rwp2_0.025
			3rd order	6invertebrate_rwp3_0.025
			…	…
			11th order	6invertebrate_rwp11_0.025
		spline, 0.025 mm	2nd order	6invertebrate_sp2_0.025
			3rd order	6invertebrate_sp3_0.025
			…	…
			11th order	6invertebrate_sp11_0.025

P.groenlandicus (7)	Invertebrates	robust Gaussian, 0.025 mm	2nd order	7invertebrate_rgp2_0.025
			3rd order	7invertebrate_rgp3_0.025
			…	…
			11th order	7invertebrate_rgp11_0.025
		robust Gaussian, 0.08 mm	2nd order	7invertebrate_rgp2_0.08
			3rd order	7invertebrate_rgp3_0.08
			…	…
			11th order	7invertebrate_rgp11_0.08
		robust wavelet, 0.025 mm	2nd order	7invertebrate_rwp2_0.025
			3rd order	7invertebrate_rwp3_0.025
			…	…
			11th order	7invertebrate_rwp11_0.025
		spline, 0.025 mm	2nd order	7invertebrate_sp2_0.025
			3rd order	7invertebrate_sp3_0.025
			…	…
			11th order	7invertebrate_sp11_0.025
P.groenlandicus (8)	Invertebrates	robust Gaussian, 0.025 mm	2nd order	8invertebrate_rgp2_0.025
			3rd order	8invertebrate_rgp3_0.025
			…	…
			11th order	8invertebrate_rgp11_0.025
		robust Gaussian, 0.08 mm	2nd order	8invertebrate_rgp2_0.08
			3rd order	8invertebrate_rgp3_0.08
			…	…
			11th order	8invertebrate_rgp11_0.08
		robust wavelet, 0.025 mm	2nd order	8invertebrate_rwp2_0.025
			3rd order	8invertebrate_rwp3_0.025
			…	…
			11th order	8invertebrate_rwp11_0.025
		spline, 0.025 mm	2nd order	8invertebrate_sp2_0.025
			3rd order	8invertebrate_sp3_0.025
			…	…
			11th order	8invertebrate_sp11_0.025
P.groenlandicus (9)	Invertebrates	robust Gaussian, 0.025 mm	2nd order	9invertebrate_rgp2_0.025
			3rd order	9invertebrate_rgp3_0.025
			…	…
			11th order	9invertebrate_rgp11_0.025
		robust Gaussian, 0.08 mm	2nd order	9invertebrate_rgp2_0.08
			3rd order	9invertebrate_rgp3_0.08
			…	…
			11th order	9invertebrate_rgp11_0.08
		robust wavelet, 0.025 mm	2nd order	9invertebrate_rwp2_0.025
			3rd order	9invertebrate_rwp3_0.025
			…	…
			11th order	9invertebrate_rwp11_0.025
		spline, 0.025 mm	2nd order	9invertebrate_sp2_0.025
			3rd order	9invertebrate_sp3_0.025
			…	…
			11th order	9invertebrate_sp11_0.025
P.groenlandicus (10)	Invertebrates	robust Gaussian, 0.025 mm	2nd order	10invertebrate_rgp2_0.025
			3rd order	10invertebrate_rgp3_0.025
			…	…
			11th order	10invertebrate_rgp11_0.025
		robust Gaussian, 0.08 mm	2nd order	10invertebrate_rgp2_0.08
			3rd order	10invertebrate_rgp3_0.08
			…	…
			11th order	10invertebrate_rgp11_0.08
		robust wavelet, 0.025 mm	2nd order	10invertebrate_rwp2_0.025
			3rd order	10invertebrate_rwp3_0.025
			…	…
			11th order	10invertebrate_rwp11_0.025
		spline, 0.025 mm	2nd order	10invertebrate_sp2_0.025
			3rd order	10invertebrate_sp3_0.025
			…	…
			11th order	10invertebrate_sp11_0.025

Table 4.2 *Details of surfaces produced by scale limiting 3D datafiles. Codes are presented for each resulting surface, providing information about the dietary group from which the surface is taken and the operator, filter, and nesting index applied to the surface.*

Parameter Family	Parameter Name	Definition	Units
Height	Sq	Root Mean Square Height of Surface	µm
	Ssk	Skewness of Height Distribution of Surface	n/a
	Sku	Kurtosis of Height Distribution of Surface	n/a
	Sp	Maximum Peak Height of Surface	µm
	Sv	Maximum Valley Depth of Surface	µm
	Sz	Maximum Height of the Surface (Sp – Sv)	µm
	Sa	Average Height of Surface	µm
Spatial	Str	Surface Texture Aspect Ratio (values range 0-1). Ratio from the distance with the fastest to the distance with the slowest decay of the ACF to the value. 0.2-0.3: surface has a strong directional structure. > 0.5: surface has rather uniform texture.	mm/mm
	Sal	Surface Auto-Correlation Length Horizontal distance of the auto correlation function (ACF) which has the fastest decay to the value 0.2. Large value: surface dominated by low frequencies. Small value: surface dominated by high frequencies.	mm
Hybrid	Ssc	Mean Summit Curvature for Peak Structures	1/µm
	Sds	Density of Summits. Number of summits per unit area making up the surface	$1/mm^2$
	Sdq	Root Mean Square Gradient of the Surface	Degrees
	Sdr	Developed Interfacial Area Ratio of the Surface	%
Volume	Vmp	Surface Peak Material Volume	$\mu m^3/mm^2$
	Vmc	Surface Core Material Volume	$\mu m^3/mm^2$
	Vvc	Surface Core Void Volume	$\mu m^3/mm^2$
	Vvv	Surface Dale Void Volume	$\mu m^3/mm^2$
Material Ratio	Spk	Mean height of the peaks above the core material	µm
	Sk	Core roughness depth, Height of the core material	µm
	Svk	Mean depth of the valleys below the core material	µm
	Smr1	Surface bearing area ratio (the proportion of the surface which consists of peaks above the core material)	%
	Smr2	Surface bearing area ratio (the proportion of the surface which would carry the load)	%
Feature	S5z	Ten Point Height of Surface	µm
Miscellaneous	Std	Texture Direction	Degrees

Table 4.3 *Descriptions for all ISO 25178-2 areal texture parameters used in this paper. Parameters Std, and Sal were excluded from analyses as they almost always produced the same value for each surface. Ssk was also excluded as it displayed low normality and regularly returned negative values which could not be log transformed. For detailed parameter descriptions see Purnell et al (2013).*

Statistical Analysis

Statistical hypothesis testing was carried out in the software package JMP Pro (Version 12.1.0). As with previous work (Goodall et al. 2015) a sequential Bonferroni correction was not applied to significant results. This method's application is subjective (Cabin and Mitchell 2000) and when large test numbers are used, as is the case here, it has been shown to produce many more false negative results (type II errors) than the false positives (type I errors) it seeks to eliminate (Moran 2003, Nakagawa 2004). As a consequence of this we would expect a number of type I errors in our results (e.g. we might expect, at $\alpha = 0.05$, one false positive for each 20 tests performed) this will likely bias our results towards incorrectly rejecting null hypotheses, and this has been taken into account when making conclusions

All data were tested for normality within each dietary group, filter type, polynomial order, and nesting index, using Shapiro Wilks W tests. Where data were not normally distributed Log transformed data were also tested for normality. For the majority of parameters Log data resulted in normal distributions, and thus data were subjected to parametric tests. The parameter Ssk was excluded from further analysis, as it almost always returns by a negative value, which cannot be log transformed. Data was considered normally distributed if fewer than one in twenty of the parameters returned a significant Shapiro Wilk's test result, as this takes into account the expected number of type I errors (false positives).

Operators and filters used to scale limit 3D surfaces can be separated into 3 main variables; Polynomial Order, Filter Type, and Nesting Index. We need to understand whether varying each of these affects the ISO 25178-2 parameter values generated from resulting surfaces.

The effect on absolute areal roughness parameter values generated from different scale limited surfaces was tested using ANOVA and T-tests. Following ANOVA, Tukey HSD tests were used to detect specific operators and filters significantly affecting the comparability of data.

To test whether the effect of changing each operator and filter was independent in its effect upon resulting data two way ANOVAs were carried out between parameter values and settings within each of the four sub-groups. The first test included polynomial order and filter type as the dependent variables. For the second test polynomial order and nesting index were the dependent variables. Tests with nesting index and filter type as dependent variables were not possible because nesting index was only varied within a single filter type. Where significant results were recorded (i.e. non-independent variables were found) Tukey Honest Significant Difference (Tukey HSD) tests were used to identify specific surfaces producing significant differences.

To compare the effect of different operators and filters used to scale limited surfaces on their sensitivity to separation between sub-groups with known textural differences, T-tests were carried out separately within each population between dietary groups. This was done separately for surfaces scale limited using each of the 40 combinations of filter type, polynomial order, and nesting index. For each pair of dietary groups Principal Component Analysis (PCA), using parameters returning significant results from T-tests, was used to detect any difference in dietary separation in multivariate space. The magnitude of difference between absolute ISO parameter values was also compared between sub-groups for each parameter where significant T-test results were found, to investigate where the greatest difference in absolute texture values was found

Results

Direct Differences in ISO 25178-2 Parameter Values

In order to test the null hypothesis that different operators have no effect on the texture of the resulting surface, scale limited surfaces were compared where polynomials ranging in order from 2^{nd} to 11^{th} had been applied. Statistical tests (ANOVA, Tukey HSD) were used to test for differences between samples that, other than the application of the operators, should be the same. Sub-groups, and filter type

were kept constant for all tests, so that three sets of tests were carried out for each sub group. One for data scale limited using a robust Gaussian filter, one using a robust wavelet filter and one using a spline filter. In all cases nesting index was constant, set at 0.025mm. So for example, surfaces of male *C.capreolus* teeth to which a robust Gaussian filter and a 2nd order polynomial had been applied were compared with the same surfaces after application of a robust Gaussian filter and all other orders of polynomial. The results of all tests can be seen in Table 4.4. In all cases parameters Sds, Ssc, and Sdr showed differences between surfaces (ANOVA), as did parameter Sdq in most cases (except in the female *C.capreolus* population). When scale limited surfaces are generated using a spline filter parameter Sp also showed difference between surfaces within the *C.capreolus* male population, and when using a robust Gaussian filter this was also the case for parameters Smr1 and Smr2. Data generated using a wavelet filter showed the greatest difference between surfaces for each of the dietary groups. Sp always shows a difference between surfaces scale limited using different orders of polynomial, and a wavelet filter. Other parameters (Sp, Str, Vmp, Vvv, Spk, Svk, Smr2, S5z, and Sa) also show differences between surfaces, depending on the sub-group in question. In order to understand which specific operators were producing this difference Tukey HSD tests were used. All possible pairwise tests were carried out (Figure 4.5 and Figure 4.6). When data is scale limited using a spline or robust Gaussian filter all differences between surfaces are within and between comparisons involving surfaces scale limited using 10th and 11th order polynomials. When using a robust wavelet filter the same is true, but there are also differences for comparisons including a 2nd order polynomial. However this is only for phocid dietary groups.

In order to test the null hypothesis that different filter types have no effect on the texture of the resulting surface we compared scale limited surfaces where robust Gaussian, robust wavelet, and spline filters had been applied (all with 0.025mm nesting index). Statistical tests (ANOVA, Tukey HSD) were used to test for differences between samples that, other than the application of different filter types, should be the same. Sub-groups, and order of polynomial were kept constant for all tests, so that ten sets of tests were carried out for each sub group. One for data scale limited using each order of polynomial (2nd to 11th). So for example, surfaces of male C.capreolus

teeth to which a second order polynomial and a robust Gaussian filter had been applied were compared with the same surfaces after application of a second order of polynomial and all other filter types. The results of all tests can be seen in Table 4.5. Surfaces did not differ consistently in any one parameter across all four dietary groups, and only rarely for surfaces scale limited using specific orders of polynomial.

Filter	Sub-Group	Sq	Sku	Sp	Sv	Sz	Sds	Str	Sdq	Ssc	Sdr	Vmp
Robust Gaussian	Acorns	0.0737	0.9999	**0.0008**	0.8480	0.8444	**<.0001***	0.9971	**0.0082***	**<.0001**	**<.0001**	0.9746
Robust Gaussian	Bramble Leaves	0.7290	0.9998	0.6074	0.9861	0.9354	**<.0001***	1.0000	0.1402*	**<.0001***	**0.0352***	0.9893
Robust Gaussian	Fish	0.8805	0.9993	0.0976	0.6598	0.7875	**<.0001***	0.9977	**0.0048**	**<.0001***	**<.0001**	0.7888
Robust Gaussian	Invertebrates	0.5341	1.0000	0.9835	1.0000	0.9998	**<.0001**	0.6522	**<.0001**	**<.0001**	**<.0001**	0.9638
		Vmc	Vvc	Vvv	Spk	Sk	Svk	Smr1	Smr2	S5z	Sa	**Total**
	Acorns	0.9880	1.0000	0.1869	0.9383	1.0000	0.3609	**0.0380**	**0.0058**	0.8964	0.4236	7
	Bramble Leaves	0.9884	1.0000	0.7121	0.9680	1.0000	0.8427	0.5060	0.9776	0.9448	0.9193	3
	Fish	0.9911	0.9996	0.9957	0.7759	0.9990	0.9994	0.9998	0.9995	0.5344	0.9577	4
	Invertebrates	0.7502	0.9994	0.7563	0.9723	0.9989	0.8987	0.9032	0.5057	0.9808	0.2672	4

Filter	Sub-Group	Sq	Sku	Sp	Sv	Sz	Sds	Str	Sdq	Ssc	Sdr	Vmp
Spline	Acorns	1.0000	1.0000	**0.026***	0.9999	0.3180	**<.0001***	1.0000	**0.0072***	**<.0001**	**<.0001**	0.9785
Spline	Bramble Leaves	1.0000	0.9997	0.4150	0.8668	0.3536	**<.0001***	0.9996	0.1260*	**<.0001***	**0.0312***	0.9994
Spline	Fish	1.0000	0.8790	0.2516*	0.5052	0.0635	**<.0001**	1.0000	**0.0050**	**<.0001***	**0.0001**	1.0000
Spline	Invertebrates	0.9999	0.9999	0.9763	0.9992	0.9888	**<.0001**	0.9909	**<.0001**	**<.0001**	**<.0001**	0.9973
		Vmc	Vvc	Vvv	Spk	Sk	Svk	Smr1	Smr2	S5z	Sa	**Total**
	Acorns	1.0000	1.0000	1.0000	0.7885	1.0000	1.0000	1.0000	0.8664	0.6012	1.0000	5
	Bramble Leaves	1.0000	1.0000	0.9994	0.9796	1.0000	0.9999	1.0000	0.9998	0.9271*	1.0000	3
	Fish	1.0000	1.0000	0.9995	0.9951	1.0000	0.9969	1.0000	0.9999	0.9316	1.0000	4
	Invertebrates	1.0000	1.0000	0.9833	0.9995	1.0000	0.9958	0.9989	0.9087	0.2918	1.0000	4

Filter	Sub-Group	Sq	Sku	Sp	Sv	Sz	Sds	Str	Sdq	Ssc	Sdr	Vmp
Robust Wavelet	Acorns	**0.0111**	0.9996	**0.0007**	0.6815	0.8105	**<.0001***	0.9981	**0.0086***	**<.0001**	**<.0001**	0.9633
Robust Wavelet	Bramble Leaves	**0.0281**	0.8822	0.6421	0.3184	0.9972	**<.0001***	0.9975	0.1457*	**<.0001***	**0.0375***	0.9928
Robust Wavelet	Fish	**0.0031**	0.3749	0.1081*	0.4199	0.2852	**<.0001***	0.9429	**0.0048**	**<.0001***	**<.0001**	**0.0077**
Robust Wavelet	Invertebrates	**0.0299**	1.0000	0.8900	0.9994	0.9896	**<.0001**	**0.0426**	**<.0001**	**<.0001**	**<.0001**	0.1958
		Vmc	Vvc	Vvv	Spk	Sk	Svk	Smr1	Smr2	S5z	Sa	**Total**
	Acorns	0.9368	1.0000	**0.0112**	0.9319	1.0000	**0.0324**	0.4713	**0.0012**	0.7304	0.1161	9
	Bramble Leaves	0.8078	1.0000	**0.0339**	0.9781	1.0000	**0.0413**	0.5721	0.7190	0.3358	0.2014	6
	Fish	0.7274	0.8794	0.2317	**0.0093**	0.9470	0.3469	0.9568	0.9372	**0.0017**	0.0581	8
	Invertebrates	0.0756	0.7813	0.1900	0.2593	0.9153	0.3755	0.9393	0.1655	0.8692	**0.0016**	7

Table 4.4 *ANOVA comparing data from surfaces scale limited using different operators (2^{nd} to 11^{th} polynomial orders). Tests were carried out for each parameter, separately for each of the four dietary groups and within these groups separately for surfaces scale limited using each filter type. Tests results have only been reported where significant results were recorded. Values with a * indicate where variance was unequal (Bartlett, Levene, O'Brien, and Brown-Forsythe tests), therefore a Welch test result is reported instead.*

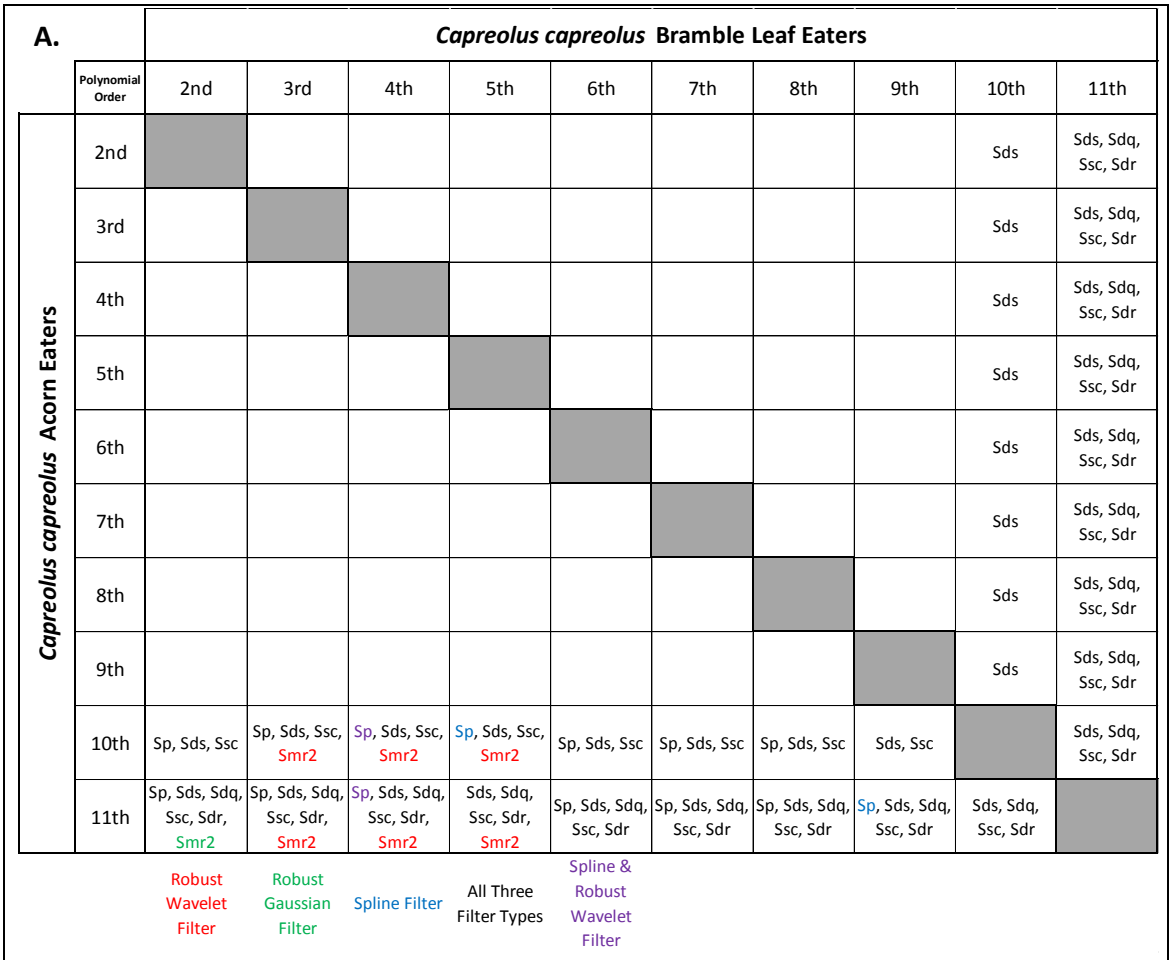

Figure 4.5 *Schematic results of Tukey HSD tests comparing data from C.capreolus surfaces scale limited using different operators (2nd-11th polynomial orders). Parameter abbreviations are given for comparisons where a significant test results was recorded. Parameter abbreviations are coloured based on the settings for which those parameters are significant (see key). Comparisons within bramble leaf eaters – top right, and comparisons within acorn eaters – bottom left.*

Certain parameters regularly show difference between surfaces scale limited using different filter types, except when using higher orders of polynomial, these were Sq, Vvv, Svk, S5z, and Sa. Parameters Sv and Sz also regularly show difference between surfaces across the different orders of polynomial within *C.capreolus* dietary groups. Parameters Sds, Smr1, and Smr2 also often show difference between surfaces when only looking at the *C.capreolus* acorn eating group. Very little difference was found between filter types within the phocid fish eating group (between zero and three

parameters showing differences in most cases), except when data were scale limited using a 2nd (eleven parameters) or 3rd (eight parameters) order of polynomial. Whereas a very high degree and consistency of difference was recorded within the *C.capreolus* acorn eating group. *C.capreolus* bramble leaf eaters, and phocid invertebrate eaters returned a similar degree of difference between surfaces when comparing filter type, falling between the extremes set by the other two dietary groups. Across all four dietary groups there is a pattern in the number of parameters affected, based on the operator used to scale limit the surface.

B.

phocid Fish Eaters \ phocid Invertebrate Eaters	2nd	3rd	4th	5th	6th	7th	8th	9th	10th	11th
2nd							Sa	Sa	Sds	Sds, Sdq, Ssc, Sdr
3rd									Sds	Sds, Sdq, Ssc, Sdr
4th	Vmp, S5z								Sds	Sds, Sdq, Ssc, Sdr
5th									Sds	Sds, Sdq, Ssc, Sdr
6th	Sq, S5z								Sds	Sds, Sdq, Ssc, Sdr
7th	Sq, Vmp, Spk, S5z								Sds	Sds, Sdq, Ssc, Sdr
8th	Sq, Vmp, Spk, S5z								Sds	Sds, Sdq, Ssc, Sdr
9th	Sq, Vmp, Spk, S5z								Sds	Sds, Sdq, Ssc, Sdr
10th	Sq, Sp, Sds, Ssc, Vmp, Spk, S5z	Sp , Sds, Ssc	Sp, Sds, Ssc	Sp , Sds, Ssc	Sp , Sds, Ssc	Sp , Sds, Ssc	Sp , Sds, Ssc	Sds, Ssc		Sds, Sdq, Ssc, Sdr
11th	Sds, Sdq, Ssc, Sdr	Sds, Sdq, Ssc, Sdr	Sds, Sdq, Ssc, Sdr	Sds, Sdq, Ssc, Sdr	Sds, Sdq, Ssc, Sdr	Sds, Sdq, Ssc, Sdr	Sds, Sdq, Ssc, Sdr	Sds, Sdq, Ssc, Sdr	Sds, Sdq, Ssc, Sdr	

Robust Wavelet Filter | Robust Gaussian Filter | Spline Filter | All Three Filter Types | Spline & Robust Wavelet Filter | Spline & Robust Gaussian Filter

Figure 4.6 *Schematic results of Tukey HSD tests comparing data from phocid surfaces scale limited using different operators (2nd-11th polynomial orders). Parameter abbreviations are given for comparisons where a significant test results was recorded. Parameter abbreviations are coloured based on the settings for which those parameters are significant (see key). Comparisons within bramble leaf eaters – top right, and comparisons within acorn eaters – bottom left.*

Polynomial	Dietary Group	Sq	Sku	Sp	Sv	Sz	Sds	Vmp	Vmc	Vvv	Spk	Svk	Smr1	Smr2	S5z	Sa	Total
2nd	Bramble Leaves	**0.0006**	0.0594	0.8492	**0.0025**	**0.0240**	0.3340	0.7546	0.1020	**0.0006**	0.7423	**0.0006**	0.1632	0.0929	**0.0027**	**0.0067**	7
3rd	Bramble Leaves	**0.0010**	0.0755	0.9715	**0.0058**	**0.0274**	0.2972	0.9754	0.0973	**0.0026***	0.9833	**0.0016**	0.1981	0.0970	**0.0044**	**0.0066**	7
4th	Bramble Leaves	**0.0009**	0.1933	0.9898	0.1270	**0.0202**	0.2735	0.9624	0.1203	**0.0024**	0.9616	**0.0045**	0.2297	0.0982	**0.0045**	**0.0078**	6
5th	Bramble Leaves	**0.0055**	0.1263	0.8223	0.0661	**0.0115**	0.3398	0.9570	0.1911	**0.0104***	0.9650	**0.0153**	0.3018	0.1464	**0.0039**	**0.0258**	6
6th	Bramble Leaves	**0.0040**	0.0952	0.6258	0.0650	**0.0025**	0.3829	0.9493	0.2870	**0.0083**	0.9461	**0.0126**	0.2696	0.1508	**0.0013**	**0.0360**	6
7th	Bramble Leaves	**0.0021**	**0.0498**	0.7486	**0.0209**	**0.0213**	0.4057	0.9009	0.3325	**0.0060**	0.9069	**0.0076**	0.3742	0.1970	**0.0011**	**0.0430**	8
8th	Bramble Leaves	**0.0112**	0.0762	0.8226	**0.0225**	0.1589	0.5363	0.8771	0.5036	**0.0129**	0.8896	**0.0113**	0.5986	0.2843	**0.0013**	0.1153	5
9th	Bramble Leaves	**0.0309**	0.0799	0.8017	0.0560*	0.2831	0.9603	0.7881	0.5843	**0.0297**	0.7722	**0.0350**	0.7098	0.3320	**0.0025**	0.1964	4
10th	Bramble Leaves	0.0736	0.0902	0.9958	0.5489	0.7188	0.8560	0.8162	0.6796	**0.0256**	0.8352	**0.0378**	0.9073	0.2737	0.1393	0.2838	2
11th	Bramble Leaves	0.1234	0.1519	0.9968	0.6706	0.9260	0.8775	0.6849	0.7727	**0.0401**	0.7141	0.0704	0.9611	0.3538	0.7650	0.4041	1
2nd	Acorns	**<.0001**	0.1537	0.2345	**0.0169**	**0.0201**	**0.0068**	0.2773	0.1889	**<.0001**	0.3162	**0.0001**	**0.0149**	**0.0001**	**0.0103**	**0.0013**	10
3rd	Acorns	**0.0002**	0.1239	0.9519	**0.0118**	**0.0312**	**0.0134**	0.7964	0.1986	**<.0001**	0.8471	**<.0001**	**0.0047**	**0.0001**	**0.0131**	**0.0023**	10
4th	Acorns	**0.0002**	0.1199	0.7911	**0.0129**	**0.0198**	**0.0189**	0.9804	0.2130	**<.0001**	0.9565	**<.0001**	**0.0057**	**<.0001**	**0.0085**	**0.0032**	10
5th	Acorns	**0.0002**	0.0841	0.7642	**0.0181**	**0.0249**	**0.0223**	0.8993	0.2086	**<.0001**	0.8234	**<.0001**	**0.0051**	**<.0001**	**0.0104**	**0.0031**	10
6th	Acorns	**<.0001**	0.0787	0.9099	**0.0104**	**0.0152**	**0.0147**	0.9058	0.2887	**<.0001**	0.9012	**<.0001**	**0.0416**	**<.0001**	**0.0061**	**0.0028**	10
7th	Acorns	**<.0001**	0.1375	0.9191	**0.0257**	**0.0297**	**0.0277**	0.8227*	0.3459	**<.0001**	0.8216*	**<.0001**	**0.0213**	**<.0001**	**0.0190**	**0.0020**	10
8th	Acorns	**0.0015***	0.1154	0.9983	**0.0324**	**0.0419**	0.0583	0.8224*	0.4551	**<.0001**	0.8874*	**<.0001**	**0.0136**	**<.0001**	**0.0317**	**0.0064**	9
9th	Acorns	**0.0043***	0.0976	0.9322	**0.0288**	0.0623	0.9641	0.7345	0.5020	**<.0001**	0.7502	**<.0001**	0.0883	**<.0001**	**0.0263**	**0.0205**	7
10th	Acorns	**0.0100**	0.2278	0.8597	0.1462*	0.2660	0.9804	0.8222	0.5760	**<.0001**	0.7396	**<.0001**	0.2571	**<.0001**	0.1003	0.0602	4
11th	Acorns	**0.0007**	0.1519	0.9110	0.0520	0.3199	0.7325	0.8336	0.5222	**<.0001**	0.8279	**<.0001**	0.2296	**<.0001**	0.2754	**0.0377**	5
2nd	Fish	**0.0026**	0.0503*	**0.0197**	**0.0272**	**0.0085**	**0.0295**	**0.0043**	0.1409	**0.0417***	**0.0035**	**0.0454***	0.3952	0.2348	**0.0028**	**0.0137**	11
3rd	Fish	**0.0096**	0.2346	0.2462	0.0903	0.0996	**0.0343**	**0.0215**	0.2426	**0.0220**	**0.0331***	**0.0211**	0.7336	0.2491	**0.0283**	**0.0281**	8
4th	Fish	0.0813	0.5320	0.4894	0.4535	0.2001	0.0733	0.2502	0.3547	0.0748	0.2251	0.1121	0.8585	0.3186	**0.0359**	0.1623	1
5th	Fish	**0.0339**	0.4606	0.4787	0.2335	0.3249	0.0584	0.0532	0.4830	0.0841	**0.0265**	0.1187	0.9324	0.3778	**0.0204**	0.1427	3
6th	Fish	**0.0358**	0.6090	0.2765*	0.2938	**0.0206**	0.1202	0.1208	0.5294	0.0680*	0.1156	0.1091*	0.7560	0.5099	**0.0384**	0.1787	3
7th	Fish	0.1983	0.6228	0.8572	0.3507	0.4503	0.1119	0.5756	0.6480	0.0709*	0.6040	0.0831*	0.9064	0.4944	0.1461	0.3647	0
8th	Fish	0.3249	0.8300	0.4961	0.9461	0.8452	0.4818	0.6274	0.7443	0.1293	0.5829	0.2521	0.9385	0.5023*	0.2392	0.5118	0
9th	Fish	0.3116	0.8662	0.8318	0.9678	0.9065	0.9838	0.7431	0.7969	0.1271	0.6312	0.2809	0.9605	0.5140	0.6299	0.5432	0
10th	Fish	0.3143	0.9893	0.9886	0.7332	0.9557	0.9966	0.7267	0.8571	0.0688*	0.7315	0.1192*	0.9906	0.5000	0.5067	0.5686	0
11th	Fish	0.4098	0.6962	0.9653	0.8795	0.8876	0.9650	0.8327	0.8819	0.0901	0.8134	0.1417	0.9883	0.4623	0.7983	0.6529	0
2nd	Invetebrates	**0.0028**	0.2500	0.3567	0.4079	0.2634	0.6284	0.1092	**0.0073**	**0.0103***	0.1262	**0.0150***	0.2148	**0.0348**	0.0774	**0.0012**	6
3rd	Invetebrates	**0.0100**	0.2776*	0.4517	0.4142	0.3301	0.6513	0.2516	**0.0284**	**0.0119***	0.2675	**0.0177***	0.0520	**0.0270**	0.1072	**0.0021**	6
4th	Invetebrates	**0.0097**	0.1857*	0.6966	0.3993	0.3268	0.6395	0.4617	**0.0261**	**0.0128***	0.4898	**0.0166***	0.1899	**0.0348**	0.1272	**0.0034**	6
5th	Invetebrates	**0.0129**	0.2905	0.6140	0.4358	0.4011	0.6747	0.3135	0.0715	**0.0165***	0.3585	**0.0202***	0.2696	0.0673	0.1305	**0.0083**	4
6th	Invetebrates	**0.0121**	0.4149	0.8111	0.7135	0.6372	0.7254	0.4731	0.1751	**0.0157***	0.5049	**0.0260***	0.5451	0.1013	0.1201	**0.0112**	4
7th	Invetebrates	**0.0199**	0.4604	0.9269	0.7013	0.5833	0.7925	0.5846	0.2630	**0.0228**	0.6201	**0.0412**	0.5302	0.1083	0.1189	**0.0234**	4
8th	Invetebrates	**0.0144**	0.3452	0.9407	0.6285	0.5339	0.7523	0.6612	0.3505	**0.0196**	0.6933	**0.0252***	0.5570	0.1129	0.1533	**0.0453**	4
9th	Invetebrates	**0.0259**	0.4722	0.9201	0.8020	0.7199	0.8998	0.7310	0.3961	**0.0250**	0.7462	0.0503	0.3633	0.0986	0.1934	0.0698	2
10th	Invetebrates	**0.0307**	0.3699	0.8632	0.6708	0.5951	0.9346	0.5229	0.4338	**0.0186**	0.5778	**0.0298**	0.4103	0.0794	0.3343	0.0916	3
11th	Invetebrates	**0.0372**	0.4020*	0.9782	0.7982	0.6529	0.9547	0.6340	0.5347	**0.0188**	0.6023	**0.0324**	0.4987	0.0560	0.3284	0.1567	3

Table 4.5 *ANOVA comparing data from surfaces scale limited using different filter types (robust Gaussian, robust wavelet, and spline). Tests were carried out for each parameter, separately for each of the four dietary groups and within these tests were carried out separately for each operator (order of polynomial) used to scale limit the surfaces. Significant results are highlighted in bold. Values with a * indicate where variance was unequal (Bartlett, Levene, O'Brien, and Brown-Forsythe tests), therefore a Welch test result is reported instead.*

In all cases data generated using higher orders of polynomial produce the lowest difference between surfaces when comparing the effect of using different filter types. Whereas data generated using lower orders of polynomial produce the highest. This suggests that certain parameters are more likely to be affected by varying the filter type used to scale limit surface, and that this variability is more pronounced when combined with specific operators (lower orders of polynomial).

A.

Capreolus capreolus Bramble Eaters				
Capreolus capreolus Acorn Eaters	**Filter Type**	Robust Gaussian	Spline	Robust Wavelet
2nd Order Polynomial	Robust Gaussian		Sq, Sv, Vvv, Svk, S5z, Sa	
	Spline	Sq, Sv, Sz, Sds, Vvv, Svk, Smr1, Smr2, S5z, Sa		Sq, Sv, Sz, Vvv, Svk, S5z, Sa
	Robust Wavelet		Sq, Sv, Sz, Sds, Vvv, Svk, Smr2, S5z, Sa	
3rd Order Polynomial	Robust Gaussian		Sq, Sv, Vvv, Svk, S5z, Sa	
	Spline	Sq, Sv, Sds, Vvv, Svk, Smr1, Smr2, S5z, Sa		Sq, Sv, Sz, Vvv, Svk, S5z, Sa
	Robust Wavelet		Sq, Sv, Sds, Vvv, Svk, Smr1, Smr2, S5z, Sa	
4th Order Polynomial	Robust Gaussian		Sq, Vvv, Svk, S5z, Sa	
	Spline	Sq, Sv, Sz, Vvv, Svk, Smr1, Smr2, S5z, Sa		Sq, Sz, Vvv, Svk, S5z, Sa
	Robust Wavelet		Sq, Sv, Sz, Sds, Vvv, Svk, Smr1, Smr2, S5z, Sa	
5th Order Polynomial	Robust Gaussian		Sq, Vvv, S5z	
	Spline	Sq, Sv, Sz, Vvv, Svk, Smr1, Smr2, S5z, Sa		Sq, Sz, Vvv, Svk, S5z, Sa
	Robust Wavelet		Sq, Sv, Sz, Sds, Vvv, Svk, Smr1, Smr2, S5z, Sa	

B.

phocid Invertebrate Eaters				
phocid Fish Eaters	**Filter Type**	Robust Gaussian	Spline	Robust Wavelet
2nd Order Polynomial	Robust Gaussian		Sq, Sa	
	Spline	Sq		Sq, Vmc, Vvv, Svk, Smr2, Sa
	Robust Wavelet	Vmp, Spk	Sq, Sku, Sp, Sv, Sz, Sds, Vmp, Vvv, Spk, Svk, S5z, Sa	
3rd Order Polynomial	Robust Gaussian		Sq, Vmc, Vvv, Smr1, Sa	
	Spline			Sq, Vmc, Vvv, Svk, Smr2, S5z, Sa
	Robust Wavelet		Sq, Sds, Vmp, Vvv, Spk, Svk, S5z, Sa	
4th Order Polynomial	Robust Gaussian		Sq, Vvv, Sa	
	Spline			Sq, Vmc, Vvv, Svk, Smr2, Sa
	Robust Wavelet		Sq, Sds, Vvv, Svk, S5z	
5th Order Polynomial	Robust Gaussian		Sq, Sa	
	Spline	Sq, Spk, S5z		Sq, Vvv, Svk, Sa
	Robust Wavelet		Sq, Spk, S5z	

Capreolus caprеolus Acorn Eaters												
6th Order Polynomial	Robust Gaussian		Sq, Sz, Vvv, Svk, S5z	7th Order Polynomial	Robust Gaussian		Sq, Sz, Vvv, Svk, S5z	8th Order Polynomial	Robust Gaussian		Sq, Sv, Vvv, Svk, S5z	9th Order Polynomial	Robust Gaussian		Sq, Sv, Vvv, S5z
	Spline	Sq, Sv, Sz, Sds, Vvv, Svk, Smr1, Smr2, S5z, Sa			Spline	Sq, Sv, Vvv, Svk, Smr1, Smr2, S5z, Sa			Spline	Sq, Sv, Vvv, Svk, Smr1, Smr2, S5z, Sa			Spline	Sq, Sv, Vvv, Svk, Smr2, S5z, Sa	
	Robust Wavelet		Sq, Sv, Sz, Sds, Vvv, Svk, Smr2, S5z, Sa		Robust Wavelet		Sq, Sv, Sz, Sds, Vvv, Svk, Smr2, S5z, Sa		Robust Wavelet	Sq, Vvv, Svk, Smr2, Sa			Robust Wavelet	Sq, Vvv, Svk, Smr2, Sa	
	Robust Gaussian	Sq, Sz, Vvv, Svk, S5z			Robust Gaussian	Sq, Sv, Sz, Vvv, Svk, S5z			Robust Gaussian	Sq, Sv, Vvv, Svk, S5z			Robust Gaussian	Sq, Sku, Sv, Vvv, S5z	
	Spline		Sq, Sz, Vvv, Svk, S5z, Sa		Spline		Sq, Sv, Sz, Vvv, Svk, S5z		Spline		Sq, Sv, Vvv, Svk, S5z		Spline		Sq, Sv, Vvv, S5z
	Robust Wavelet				Robust Wavelet				Robust Wavelet				Robust Wavelet		

phocid Fish Eaters												
6th Order Polynomial	Robust Gaussian		Sq, Vvv, Sa	7th Order Polynomial	Robust Gaussian		Sq, Vvv	8th Order Polynomial	Robust Gaussian		Sq, Vvv	9th Order Polynomial	Robust Gaussian		Sq, Vvv
	Spline	Sq, Sz			Spline		Sq, Vvv, Sa		Spline				Spline		
	Robust Wavelet		Sq, Sz		Robust Wavelet		Sds		Robust Wavelet				Robust Wavelet		
	Robust Gaussian		Sq, Vvv, Sa		Robust Gaussian				Robust Gaussian		Sq, Vvv		Robust Gaussian		Sq, Vvv
	Spline	Sq, Sz			Spline		Sq, Vvv, Sa		Spline				Spline		
	Robust Wavelet		Sq, Vvv, Svk, Sa		Robust Wavelet				Robust Wavelet				Robust Wavelet		

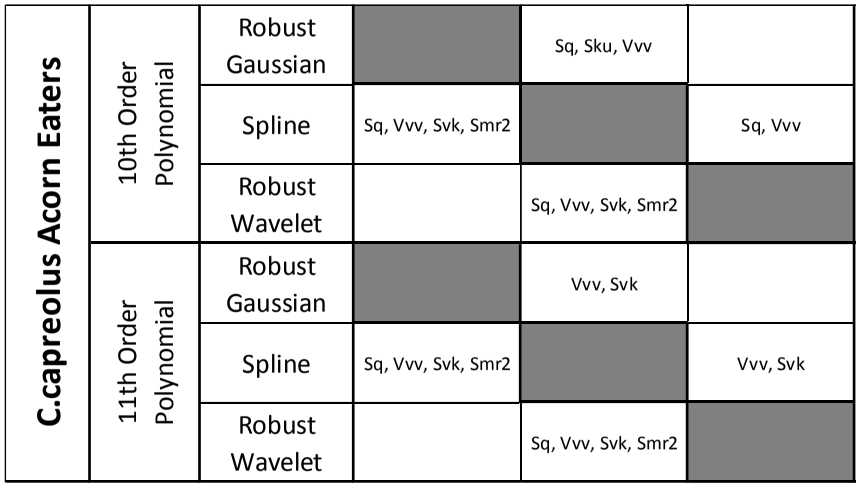

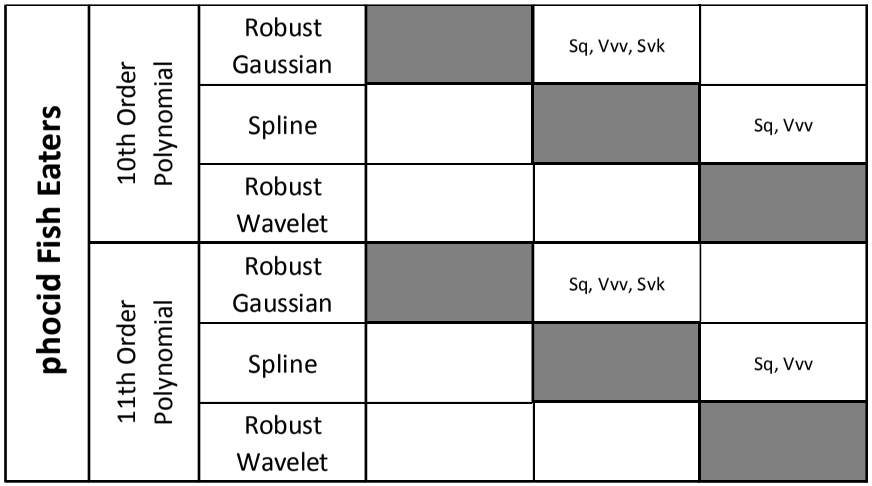

Figure 4.7 *Schematic results of Tukey HSD tests comparing data from surfaces scale limited using different filter types (robust Gaussian, robust wavelet, and spline). Parameter abbreviations are given for comparisons where a significant test results was recorded. Individual schemes are presented separately for data from surfaces scale limited using each operator. Results are presented in two sets of schemes, A.) Capreolus capreolus: comparisons within bramble leaf eaters – top right of each scheme, and comparisons within acorn eaters – bottom left, and B.) Phocids: comparisons within invertebrate eaters – top right of each scheme, and comparisons within fish eaters – bottom left.*

While certain parameters seem to be consistently affected, the scale of difference and numbers of parameters affected depends heavily on the dietary group in question. Resulting Tukey HSD tests (testing all possible pairwise comparisons) show differences within all comparisons where surfaces were scale limited using a spline filter, and only in one case (phocid fish eaters, 2nd order polynomial) between robust Gaussian and robust wavelet filters (Figure 4.7). These differences were negative, so that parameter values generated from surfaces scale limited using a spline filter were consistently lower than those produced when using a robust Gaussian or robust wavelet filter.

In order to test the null hypothesis that scale limiting a surface using filters with different nesting index wavelength cut-off values has no effect on the texture of the resulting surface we compared scale limited surfaces where 0.025mm, and 0.08mm nesting indices had been applied. Statistical tests (T-tests) were used to test for differences between samples that, other than the application of different nesting indices, should be the same. Sub-groups, and order of polynomial were kept constant for all tests, so that ten sets of tests were carried out for each sub-group. One for data scale limited using each order of polynomial (2nd to 11th). So for example, surfaces of male C.capreolus teeth to which a second order polynomial and a robust Gaussian filter with 0.025mm nesting index had been applied were compared with the same surfaces after application of a second order of polynomial, robust Gaussian filter and 0.08mm nesting index. In all tests only surfaces scale limited using a robust Gaussian filter were used, and the results of all tests can be seen in Table 4.6. In more than half of comparisons differences between surfaces are recorded in parameters Sq, Vmc, Vvc, Sk, and Sa. Parameter Sds also shows a difference between surfaces scale limited using different nesting indices within *C.capreolus* acorn eaters and phocid fish eaters (when using a 2nd to 7th order of polynomial). The least difference recorded across parameters is found when comparing nesting indices within *C.capreolus* bramble leaf eaters. Within the other three sub-groups a similar degree of difference between surfaces generated using different nesting indices is found. Again, the number of degree of difference between surfaces is affected by the operator used to scale limit the surface. In two cases (*C.capreolus* bramble leaf eaters, and phocid invertebrate eaters) no

difference is found across all parameters when a higher order of polynomial is used as the operator (bramble leaf eaters, 6^{th}-11^{th} order of polynomial; invertebrate eaters, 8^{th}-11^{th}). These results suggest that varying the nesting index used to scale limit surfaces does affect the resulting roughness parameter values. This affect is greatest when combined with specific operators (lower orders of polynomial), but varies depending on the dietary group in question.

In order to test the null hypothesis that when applying different operators, filters, and filters with different nesting indices to a surface, there is no interaction in their effect on resulting texture parameters we used Two Way ANOVA to compare scale limited surfaces where operator and filter type were dependant variables, and a separate test where nesting index and operator were dependant variables. Where either variable had an effect (showed difference between data from different operators, filters or nesting indices) an interaction test was performed to test whether the effect of one variable was dependent on the value of the other variable. For the two *C.capreolus* sub-groups two way ANOVA tests showed no dependence between data from surfaces scale limited using different operators and those scale limited using different filters. Nor was there any dependence between data from surfaces scale limited using different operators and those scale limited using different nesting indices. For the two phocid groups no dependence was found between data from surfaces scale limited using different operators and those scale limited using different filters. However for two ISO 25178-2 parameters (Sq, and Sa) dependence was found between data from surfaces scale limited using different operators and those scale limited using different nesting indices. In the same test for invertebrate eating phocids four parameters also showed the same dependence (Vmc, Vvc, Sk, and Sa). These results suggest that the effects of the three setting types used in this manuscript are generally independent of one another. However for a small number of parameters there may be some inter dependence between data from surfaces scale limited using different operators and those scale limited using different nesting indices in the phocid populations. To investigate this, for those parameters showing dependence, Tukey HSD tests were used to compare all surfaces produced using all possible combinations of operator and nesting index, separately within each phocid population (Figure 4.8).

Polynomial Order	Dietary Group	Sq	Sds	Vmp	Vmc	Vvc	Vvv	Spk	Sk	Smr2	S5z	Sa	Total
2nd	Acorns	**0.0067**	**0.0029**	0.2055	**0.0275**	**0.0051**	0.3205	0.3031	**0.0027**	0.3276	0.7367	**0.0065**	6
3rd	Acorns	**0.0135**	**0.0019**	0.6275	**0.0284**	**0.0105**	0.3203	0.8381	**0.0037**	0.1578	0.6819	**0.0079**	6
4th	Acorns	**0.0300**	**0.0136**	0.7569	0.0584	**0.0214**	0.3590	0.8850	**0.0083**	0.1924	0.7991	**0.0232**	5
5th	Acorns	0.0711	**0.0224**	0.8149	0.0627	**0.0308**	0.2530	0.9034	**0.0124**	0.1003	0.8224	**0.0375**	4
6th	Acorns	**0.0152**	**0.0236**	0.6398	0.0874	0.0540	0.2693	0.7148	**0.0234**	**0.0015**	0.9230	**0.0308**	5
7th	Acorns	**0.0106**	0.0587	0.4156	0.1218	0.0695	0.3993	0.4874	**0.0315**	**0.0005**	0.8364	**0.0311**	4
8th	Acorns	**0.0161**	0.1179	0.5664	0.1452	0.0722	0.3978	0.7173	**0.0394**	**0.0037**	0.9135	0.0530	3
9th	Acorns	**0.0229**	0.8152	0.3348	0.1360	**0.0454**	0.3965	0.4087	**0.0314**	**0.0177**	0.9356	0.0697	4
10th	Acorns	0.2086	0.9168	0.5542	0.1509	0.0589	0.7098	0.6281	**0.0379**	**0.0283**	0.9692	0.1407	2
11th	Acorns	0.1116	0.8318	0.4177	0.1921	0.0839	0.4222	0.4684	0.0502	**0.0105**	0.9936	0.1333	1
2nd	Bramble Leaves	**0.0186**	0.0783	0.1460	**0.0167**	**0.0346**	0.0773	0.1723	**0.0394**	0.7174	0.1083	**0.0161**	5
3rd	Bramble Leaves	**0.0238**	0.0861	0.3324	**0.0186**	**0.0483**	0.0841	0.4134	**0.0494**	0.8228	0.1992	**0.0181**	5
4th	Bramble Leaves	**0.0246**	0.0829	0.3777	**0.0229**	0.0542	0.0718	0.4744	**0.0416**	0.7740	0.1362	**0.0213**	4
5th	Bramble Leaves	0.0674	0.1149	0.5470	**0.0413**	0.0756	0.1890	0.6247	0.0524	0.6450	0.2121	**0.0454**	2
6th	Bramble Leaves	0.0760	0.1371	0.7489	0.0631	0.0940	0.2149	0.8319	0.0637	0.3915	0.1981	0.0630	0
7th	Bramble Leaves	0.0746	0.1416	0.8034	0.0719	0.1019	0.2103	0.8934	0.0652	0.3787	0.2630	0.0701	0
8th	Bramble Leaves	0.1508	0.2461	0.6752	0.1488	0.1625	0.3303	0.7280	0.1391	0.5574	0.2374	0.1489	0
9th	Bramble Leaves	0.2048	0.7929	0.5620	0.1850	0.1985	0.4362	0.6424	0.1597	0.5513	0.3215	0.1916	0
10th	Bramble Leaves	0.3349	0.8134	0.6171	0.2625	0.2824	0.4083	0.6499	0.2253	0.6378	0.7808	0.2902	0
11th	Bramble Leaves	0.3896	0.8163	0.5718	0.3234	0.3584	0.5862	0.5866	0.3003	0.6515	0.9372	0.3431	0
2nd	Fish	**0.0023**	**0.0002**	**0.0345**	**0.0024**	**0.0037**	**0.0375**	**0.0346**	**0.0025**	0.5370	**0.0384**	**0.0020**	10
3rd	Fish	**0.0049**	**0.0004**	0.0718	**0.0049**	**0.0059**	**0.0440**	0.0731	**0.0041**	0.6851	0.0845	**0.0035**	7
4th	Fish	**0.0114**	**<.0001**	0.1269	**0.0061**	**0.0092**	0.0880	0.1282	**0.0051**	0.5374	**0.0432**	**0.0070**	7
5th	Fish	**0.0133**	**0.0010**	0.1815	**0.0150**	**0.0250**	0.1379	0.1446	**0.0200**	0.8491	0.1197	**0.0123**	6
6th	Fish	**0.0199**	**0.0049**	0.2092	**0.0217**	**0.0335**	0.1976	0.2150	**0.0247**	0.6868	0.1639	**0.0179**	6
7th	Fish	0.0918	**0.0064**	0.5855	0.0518	0.0776	0.3041	0.6332	**0.0497**	0.7882	0.3357	0.0640	2
8th	Fish	0.1349	0.0850	0.5612	0.0999	0.1512	0.3381	0.5742	0.1131	0.9103	0.4847	0.1069	0
9th	Fish	0.1318	0.8340	0.5847	0.1185	0.1928	0.4271	0.5460	0.1432	0.8233	0.7700	0.1103	0
10th	Fish	0.1950	0.9572	0.7376	0.1998	0.2974	0.4298	0.7592	0.2169	0.8281	0.7471	0.1778	0
11th	Fish	0.2628	0.8872	0.7552	0.2624	0.3539	0.4722	0.7611	0.2559	0.7513	0.9312	0.2467	0
2nd	Invertebrates	**0.0035**	0.2286	0.1007	**<.0001**	**<.0001**	0.1542	0.1400	**<.0001**	0.8857	0.3684	**<.0001**	5
3rd	Invertebrates	**0.0097**	0.2794	0.1885	**<.0001**	**<.0001**	0.1807	0.2660	**<.0001**	0.9994	0.3578	**0.0001**	5
4th	Invertebrates	**0.0165**	0.3051	0.2312	**<.0001**	**<.0001**	0.2781	0.3005	**<.0001**	0.9385	0.4370	**0.0004**	5
5th	Invertebrates	**0.0308**	0.3191	0.0577	**0.0001**	**0.0002**	0.3091	0.1169	**0.0003**	0.9626	0.5215	**0.0017**	5
6th	Invertebrates	**0.0319**	0.3224	0.1540	**0.0003**	**0.0003**	0.3764	0.2181	**0.0006**	0.3852	0.6583	**0.0009**	5
7th	Invertebrates	**0.0471**	0.3873	0.2389	**0.0011**	**0.0008**	0.4521	0.3084	**0.0015**	0.2403	0.7489	**0.0023**	5
8th	Invertebrates	**0.0346**	0.3947	0.0934	**0.0032**	**0.0031**	0.4936	0.1733	**0.0048**	0.3570	0.6854	**0.0036**	5
9th	Invertebrates	0.0530	0.6265	0.0931	**0.0052**	**0.0042**	0.5451	0.1326	**0.0061**	0.3472	0.6612	**0.0066**	4
10th	Invertebrates	0.0607	0.7485	0.1069	**0.0066**	**0.0045**	0.5252	0.1718	**0.0057**	0.2879	0.8306	**0.0079**	4
11th	Invertebrates	0.0591	0.8115	0.4112	**0.0238**	**0.0149**	0.5397	0.4434	**0.0139**	0.1908	0.8203	**0.0163**	4

Table 4.6 *T-test results, comparing data from surfaces scale limited using different nesting indices (0.025mm, and 0.08mm). Tests were carried out for each parameter, separately for each of the four dietary groups and within these groups separately for each order of polynomial used to scale limit the surfaces. Only data generated from surfaces scale limited using a robust Gaussian filter have been used. Significant results are highlighted in bold.*

Fish Eaters - Order of Polynomial and Nesting Index	Invertebrate Eaters - Order of Polynomial and Nesting Index																			
		2nd 0.025	3rd 0.025	4th 0.025	5th 0.025	6th 0.025	7th 0.025	8th 0.025	9th 0.025	10th 0.025	11th 0.025	2nd 0.08	3rd 0.08	4th 0.08	5th 0.08	6th 0.08	7th 0.08	8th 0.08	9th 0.08	10th 0.08	11th 0.08
2nd 0.025											Vmc, Vvc, Sk, Sa	Vmc, Vvc, Sk, Sa	Vmc, Vvc, Sk, Sa	Vmc, Vvc, Sk, Sa	Vmc, Vvc, Sk	Vmc, Vvc, Sk	Vvc, Sk			
3rd 0.025											Vmc, Vvc, Sk, Sa	Vmc, Vvc, Sk, Sa	Vmc, Vvc, Sk, Sa	Vmc, Vvc, Sk, Sa	Vmc, Vvc, Sk	Vmc, Vvc, Sk	Vvc, Sk			
4th 0.025											Vmc, Vvc, Sk, Sa	Vmc, Vvc, Sk, Sa	Vmc, Vvc, Sk, Sa	Vmc, Vvc, Sk, Sa	Vmc, Vvc, Sk	Vmc, Vvc, Sk	Vvc, Sk			
5th 0.025											Vmc, Vvc, Sk, Sa	Vmc, Vvc, Sk, Sa	Vmc, Vvc, Sk, Sa	Vmc, Vvc, Sk, Sa	Vmc, Vvc, Sk, Sa	Vmc, Vvc, Sk	Vmc, Vvc, Sk			
6th 0.025											Vmc, Vvc, Sk, Sa	Vmc, Vvc, Sk, Sa	Vmc, Vvc, Sk, Sa	Vmc, Vvc, Sk, Sa	Vmc, Vvc, Sk, Sa	Vmc, Vvc, Sk, Sa	Vmc, Vvc, Sk	Vmc, Sk		
7th 0.025											Vmc, Vvc, Sk, Sa	Vmc, Vvc, Sk, Sa	Vmc, Vvc, Sk, Sa	Vmc, Vvc, Sk, Sa	Vmc, Vvc, Sk, Sa	Vmc, Vvc, Sk, Sa	Vmc, Vvc, Sk	Vmc, Vvc, Sk		
8th 0.025											Vmc, Vvc, Sk, Sa	Vmc, Vvc, Sk, Sa	Vmc, Vvc, Sk, Sa	Vmc, Vvc, Sk, Sa	Vmc, Vvc, Sk, Sa	Vmc, Vvc, Sk, Sa	Vmc, Vvc, Sk, Sa	Vmc, Vvc, Sk		
9th 0.025											Vmc, Vvc, Sk, Sa	Vmc, Vvc, Sk, Sa	Vmc, Vvc, Sk, Sa	Vmc, Vvc, Sk, Sa	Vmc, Vvc, Sk, Sa	Vmc, Vvc, Sk, Sa	Vmc, Vvc, Sk, Sa	Vmc, Vvc, Sk	Vvc	
10th 0.025											Vmc, Vvc, Sk, Sa	Vmc, Vvc, Sk, Sa	Vmc, Vvc, Sk, Sa	Vmc, Vvc, Sk, Sa	Vmc, Vvc, Sk, Sa	Vmc, Vvc, Sk, Sa	Vmc, Vvc, Sk, Sa	Vmc, Vvc, Sk, Sa	Vmc, Vvc	
11th 0.025											Vmc, Vvc, Sk, Sa	Vmc, Vvc, Sk, Sa	Vmc, Vvc, Sk, Sa	Vmc, Vvc, Sk, Sa	Vmc, Vvc, Sk, Sa	Vmc, Vvc, Sk, Sa	Vmc, Vvc, Sk, Sa	Vmc, Vvc, Sk, Sa		
2nd 0.08	Sq, Sa	Sq, Sa	Sq, Sa	Sq, Sa	Sq, Sa	Sq, Sa	Sq, Sa	Sq, Sa	Sq, Sa	Sq, Sa				Vmc	Vmc, Vvc, Sk, Sa	Vmc, Vvc, Sk, Sa	Vmc, Vvc, Sk, Sa	Vmc, Vvc, Sk, Sa	Vmc, Vvc, Sk, Sa	Vmc, Vvc, Sk, Sa
3rd 0.08	Sq, Sa	Sq, Sa	Sq, Sa	Sq, Sa	Sq, Sa	Sq, Sa	Sq, Sa	Sq, Sa	Sq, Sa	Sq, Sa					Vmc	Vmc, Sa	Vmc, Vvc, Sk, Sa	Vmc, Vvc, Sk, Sa	Vmc, Vvc, Sk, Sa	Vmc, Vvc, Sk, Sa
4th 0.08		Sa	Sa	Sa	Sa	Sq, Sa	Sq, Sa	Sq, Sa	Sq, Sa	Sq, Sa						Vmc	Vmc, Sa	Vmc, Sa	Vmc, Vvc, Sk, Sa	Vmc, Vvc, Sk, Sa
5th 0.08									Sa	Sq, Sa								Vmc	Vmc, Sa	Vmc, Sa
6th 0.08																				
7th 0.08											Sq									
8th 0.08											Sq, Sa									
9th 0.08											Sq, Sa	Sq								
10th 0.08											Sq, Sa	Sq, Sa								
11th 0.08											Sq, Sa	Sq, Sa								

Figure 4.8 *Schematic results of Tukey HSD tests for parameters returning significant results from 2-way ANOVA tests between data generated using different nesting indices and data generated using different orders of polynomial. For each possible comparison parameter abbreviations are given when a significant Tukey HSD test results was recorded. All surfaces scale limited using a robust Gaussian filter. Only Phocidae data has been tested, and comparisons within invertebrate eater data are on the top right, and comparisons within fish eater data are on the bottom left.*

It was found that all parameter differences between surfaces involved the use of a 0.08mm nesting index. For the fish eating population, differences between surfaces were restricted to those scale limited using the lowest orders of polynomial (2^{nd} – 4^{th}). For the invertebrate eating population surfaces scale limited using most operators were affected. A greater number of parameters differ in both cases when comparing surfaces scale limited using the 0.08mm nesting index to those scale limited using the 0.025mm nesting index, rather than comparisons of surfaces scale limited using different operators but the same nesting index. No significant results were recorded when comparing surfaces scale limited using a 0.025mm nesting index to other surfaces scale limited using a different operator combined with the same nesting index. This suggests that the effect of the 0.08mm nesting index on resulting parameter values is dependent upon the operator used to scale limit data, but only for a small number of parameters. Overall the effects on resulting data of varying operator, filter and nesting index appear to be relatively independent.

Discriminatory Power between Dietary Groups

The sensitivity of textural parameters – the degree to which they differ between dietary groups of *C.capreolus* – varies with different combinations of operators and filters. T-tests revealed that a maximum of eight parameters differed between the two populations (Sq, Sv, Sz, Sdq, Sdr, Vvv, Svk, and S5z, see Table 4.3 for parameter descriptions). In cases where fewer than eight parameters differ, they are always a subset of these eight (Table 4.7). This suggests variability in the sensitivity to separate the two *C.capreolus* dietary groups, caused by varying the combination of operators and filters used to scale limit surfaces. When looking at the total number of significant results recorded when comparing the two dietary groups (Fig. 4.9b), it is found that the average number of parameters separating the dietary groups is 5.2 across all surfaces. The maximum number is eight (6^{th} order polynomial, spline or robust Gaussian filter, nesting index 0.025mm), and the lowest is two (2^{nd} or 3^{rd} order of polynomial, robust Gaussian filter, nesting index 0.08mm, or robust wavelet filter, nesting index 0.025mm).

Polynomial	Filter	Nesting index	Sq	Sv	Sz	Sdq	Sdr	Vvv	Svk	S5z	Total
2nd	Robust Gaussian	0.025mm	**0.0253**	**0.0175**	**0.0358**	**0.0023**	**0.0058**	0.0697	0.0642	**0.0148**	6
3rd	Robust Gaussian	0.025mm	**0.0404**	**0.0192**	0.0601	**0.0023**	**0.0059**	0.0747	0.0698	**0.0321**	5
4th	Robust Gaussian	0.025mm	**0.0255**	**0.0228**	**0.0120**	**0.0023**	**0.0057**	0.0700	0.0710	**0.0070**	6
5th	Robust Gaussian	0.025mm	**0.0292**	**0.0194**	**0.0146**	**0.0022**	**0.0055**	0.0643	0.0672	**0.0098**	6
6th	Robust Gaussian	0.025mm	**0.0187**	**0.0061**	**0.0040**	**0.0022**	**0.0055**	**0.0455**	**0.0455**	**0.0052**	8
7th	Robust Gaussian	0.025mm	**0.0116**	**0.0190**	0.0591	**0.0023**	**0.0060**	**0.0262**	**0.0289**	**0.0097**	7
8th	Robust Gaussian	0.025mm	**0.0089**	**0.0076**	0.0756	**0.0023**	**0.0064**	**0.0193**	**0.0182**	**0.0030**	7
9th	Robust Gaussian	0.025mm	**0.0083**	**0.0037**	0.1515	**0.0025**	**0.0065**	**0.0108**	**0.0110**	**0.0013**	7
10th	Robust Gaussian	0.025mm	**0.0226**	**0.0361**	**0.0397**	0.2921	0.6619	**0.0074**	**0.0092**	**0.0154**	6
11th	Robust Gaussian	0.025mm	**0.0204**	**0.0025**	**0.0225**	0.5140	0.5510	**0.0046**	**0.0060**	**0.0197**	6
2nd	Robust Gaussian	0.08mm	0.4014	0.0801	0.1065	**0.0034**	**0.0085**	0.3746	0.2476	0.0930	2
3rd	Robust Gaussian	0.08mm	0.4906	0.0836	0.1153	**0.0036**	**0.0087**	0.3939	0.2767	0.0674	2
4th	Robust Gaussian	0.08mm	0.4449	**0.0483**	**0.0254**	**0.0036**	**0.0086**	0.4019	0.2776	**0.0204**	5
5th	Robust Gaussian	0.08mm	0.3970	0.0598	**0.0418**	**0.0036**	**0.0083**	0.2326	0.1701	**0.0265**	4
6th	Robust Gaussian	0.08mm	0.3385	**0.0101**	**0.0228**	**0.0035**	**0.0083**	0.1254	0.0876	**0.0416**	5
7th	Robust Gaussian	0.08mm	0.2292	**0.0294**	0.0802	**0.0036**	**0.0088**	0.0692	**0.0464**	**0.0286**	5
8th	Robust Gaussian	0.08mm	0.1378	**0.0091**	0.0933	**0.0038**	**0.0094**	**0.0262**	**0.0159**	**0.0190**	6
9th	Robust Gaussian	0.08mm	0.0972	**0.0023**	0.1228	**0.0039**	**0.0094**	**0.0094**	**0.0070**	**0.0044**	6
10th	Robust Gaussian	0.08mm	0.1023	**0.0322**	0.0509	0.2932	0.6612	**0.0094**	**0.0042**	**0.0310**	4
11th	Robust Gaussian	0.08mm	0.0795	**0.0030**	**0.0252**	0.5144	0.5509	**0.0020**	**0.0023**	**0.0240**	5
2nd	Spline	0.025mm	**0.0226**	0.0850	0.1653	**0.0026**	**0.0071**	**0.0054**	**0.0119**	**0.0442**	6
3rd	Spline	0.025mm	**0.0287**	0.0852	0.1634	**0.0026**	**0.0071**	**0.0054**	**0.0131**	0.0590	5
4th	Spline	0.025mm	**0.0257**	0.0950	0.1555	**0.0026**	**0.0069**	**0.0068**	**0.0211**	0.0544	5
5th	Spline	0.025mm	**0.0233**	**0.0496**	0.0828	**0.0026**	**0.0068**	**0.0043**	**0.0129**	**0.0222**	7
6th	Spline	0.025mm	**0.0207**	**0.0030**	**0.0138**	**0.0024**	**0.0066**	**0.0035**	**0.0074**	**0.0371**	8
7th	Spline	0.025mm	**0.0250**	**0.0368**	0.1094	**0.0025**	**0.0070**	**0.0039**	**0.0083**	**0.0297**	7
8th	Spline	0.025mm	**0.0326**	0.0747	0.3074	**0.0028**	**0.0073**	**0.0060**	**0.0081**	**0.0336**	6
9th	Spline	0.025mm	**0.0281**	0.0828	0.4453	**0.0026**	**0.0072**	**0.0065**	**0.0090**	**0.0380**	6
10th	Spline	0.025mm	**0.0259**	0.1793	0.1322	0.2999	0.6773	**0.0064**	**0.0168**	0.0916	3
11th	Spline	0.025mm	**0.0273**	0.3028	0.1633	0.5161	0.5517	**0.0027**	**0.0068**	0.1451	3
2nd	Robust Wavelet	0.025mm	0.1619	0.1060	0.1609	**0.0022**	**0.0058**	0.3799	0.3658	0.1109	2
3rd	Robust Wavelet	0.025mm	0.2535	0.1130	0.1714	**0.0024**	**0.0060**	0.3506	0.3263	0.0702	2
4th	Robust Wavelet	0.025mm	0.1004	0.0573	**0.0283**	**0.0023**	**0.0058**	0.2433	0.2381	**0.0115**	4
5th	Robust Wavelet	0.025mm	0.1163	0.0620	**0.0478**	**0.0022**	**0.0057**	0.1926	0.1952	**0.0256**	4
6th	Robust Wavelet	0.025mm	0.0532	**0.0170**	**0.0175**	**0.0021**	**0.0055**	0.0972	0.0976	**0.0297**	5
7th	Robust Wavelet	0.025mm	**0.0143**	**0.0233**	0.0704	**0.0023**	**0.0059**	**0.0474**	**0.0500**	**0.0205**	7
8th	Robust Wavelet	0.025mm	**0.0098**	**0.0065**	0.0843	**0.0024**	**0.0065**	**0.0228**	**0.0202**	**0.0045**	7
9th	Robust Wavelet	0.025mm	**0.0077**	**0.0020**	0.1709	**0.0026**	**0.0067**	**0.0107**	**0.0105**	**0.0011**	7
10th	Robust Wavelet	0.025mm	**0.0205**	**0.0369**	**0.0491**	0.2918	0.6602	**0.0083**	**0.0100**	**0.0167**	6
11th	Robust Wavelet	0.025mm	**0.0162**	**0.0023**	**0.0259**	0.5144	0.5510	**0.0033**	**0.0050**	**0.0240**	6

Table 4.7 *T-test results comparing data from two populations of C.capreolus with known dietary differences (Males - acorn eaters, and Females - bramble leaf eaters) across 21 areal texture parameters. Tests were carried out separately for each combination of operator and filter used to scale limited the 3D surfaces. Significant results are highlighted in bold*

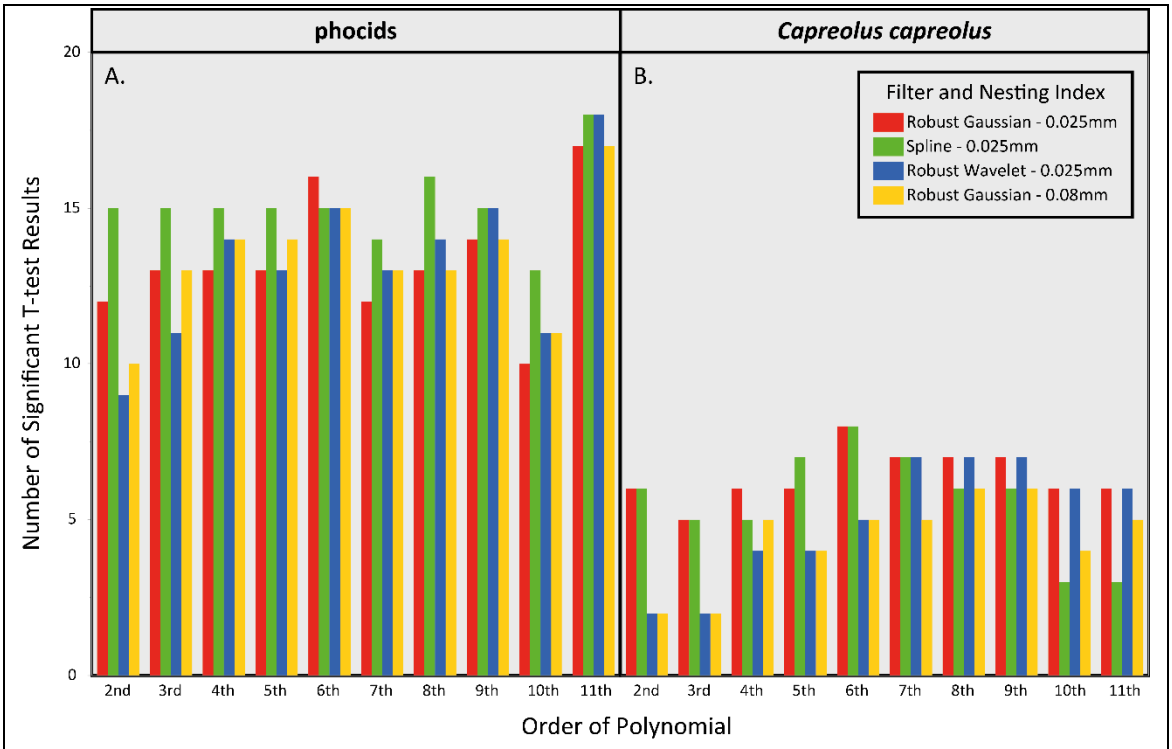

Figure 4.9 *Total numbers of significant T-test results recorded when comparing dietary groups A.) Phocid fish eaters compared to invertebrate eaters, B.)* *Capreolus capreolus* *acorn eaters compared to bramble leaf eaters. Data for each filter type was tested separately and represented by different colours (see key). Data for each order of polynomial was tested separately, represented by the X-axis.*

The sensitivity of textural parameters to detect textural differences between phocid dietary groups also varies with different combinations of operators and filters. T-tests show that a maximum of eighteen parameters differed between the two populations (Sq, Sp, Sv, Sz, Sds, Str, Sdq, Ssc, Sdr, Vmp, Vmc, Vvc, Vvv, Spk, Sk, Svk, S5z, and Sa, see Table 4.3 for parameter descriptions). However two parameters (Sds, and Ssc) only separate dietary groups when an 11^{th} order polynomial is used as the operator.

In all other cases a maximum of sixteen parameters separate the phocid dietary groups. In cases where fewer than eighteen/sixteen parameters differ, they are almost always a subset of these (Table 4.8).

Polynomial	Filter	Nesting index	Sq	Sp	Sv	Sz	Sds	Str	Sdq	Ssc	Sdr	Vmp	Vmc	Vvc	Vvv	Spk	Sk	Svk	Smr2	S5z	Sa	Total
2nd	Robust Gaussian	0.025mm	**0.0008**	0.1522	**0.0036**	**0.0077**	0.6897	0.3297	**0.0108**	0.0866	**0.0121**	0.2106	**0.0008**	**0.0064**	**0.0038**	0.2011	**0.0028**	**0.0051**	0.0939	**0.0025**	**0.0004**	12
3rd	Robust Gaussian	0.025mm	**0.0008**	0.1529	**0.0013**	**0.0031**	0.7417	**0.0499**	**0.0107**	0.0762	**0.0118**	0.1974	**0.0008**	**0.0049**	**0.0027**	0.1705	**0.0027**	**0.0039**	0.0544	**0.0009**	**0.0003**	13
4th	Robust Gaussian	0.025mm	**0.0006**	**0.0070**	**0.0082**	**0.0012**	0.7060	0.0506	**0.0108**	0.0786	**0.0119**	0.0647	**0.0008**	**0.0055**	**0.0034**	0.0606	**0.0029**	**0.0049**	0.0968	**0.0002**	**0.0003**	13
5th	Robust Gaussian	0.025mm	**0.0003**	0.0614	**0.0053**	**0.0078**	0.6806	**0.0090**	**0.0109**	0.0806	**0.0121**	0.0794	**0.0007**	**0.0034**	**0.0031**	0.0718	**0.0028**	**0.0045**	0.1094	**0.0007**	**0.0002**	13
6th	Robust Gaussian	0.025mm	**0.0002**	**0.0007**	**0.0053**	**0.0005**	0.6190	**0.0167**	**0.0106**	0.0781	**0.0117**	**0.0493**	**0.0010**	**0.0037**	**0.0030**	**0.0340**	**0.0029**	**0.0055**	0.1823	**0.0003**	**0.0001**	16
7th	Robust Gaussian	0.025mm	**0.0004**	0.1367	**0.0010**	**0.0012**	0.6903	0.0653	**0.0109**	0.0774	**0.0118**	0.0993	**0.0017**	**0.0055**	**0.0025**	0.1012	**0.0033**	**0.0039**	0.3232	**0.0001**	**0.0003**	12
8th	Robust Gaussian	0.025mm	**0.0003**	**0.0164**	**0.0301**	**0.0062**	0.5490	0.0690	**0.0117**	0.0787	**0.0126**	0.0853	**0.0020**	**0.0089**	**0.0015**	0.0671	**0.0048**	**0.0038**	0.1969	**<.0001**	**0.0004**	13
9th	Robust Gaussian	0.025mm	**0.0002**	**0.0371**	**0.0280**	**0.0080**	0.6089	0.0656	**0.0115**	0.3696	**0.0133**	0.0609	**0.0014**	**0.0072**	**0.0014**	**0.0360**	**0.0039**	**0.0040**	0.1490	**0.0003**	**0.0003**	14
10th	Robust Gaussian	0.025mm	**0.0002**	0.6563	**0.0009**	0.1094	0.6252	0.0578	**0.0454**	0.3054	0.0951	0.0788	**0.0014**	**0.0064**	**0.0008**	0.1430	**0.0027**	**0.0017**	0.1430	**0.0005**	**0.0003**	10
11th	Robust Gaussian	0.025mm	**0.0001**	**0.0370**	**0.0022**	**0.0005**	**0.0428**	0.0596	**0.0131**	**0.0209**	**0.0137**	**0.0334**	**0.0014**	**0.0057**	**0.0007**	**0.0243**	**0.0026**	**0.0014**	0.1515	**0.0001**	**0.0003**	17
2nd	Robust Gaussian	0.08mm	**0.0052**	0.4360	**0.0121**	0.0579	0.7270	0.6472	**0.0100**	0.0995	**0.0107**	0.3513	**0.0022**	**0.0103**	**0.0252**	0.3838	**0.0102**	0.0587	0.0531	**0.0413**	**0.0033**	10
3rd	Robust Gaussian	0.08mm	**0.0036**	0.5905	**0.0007**	**0.0276**	0.7479	0.9343	**0.0097**	0.0824	**0.0105**	0.5928	**0.0028**	**0.0091**	**0.0041**	0.6836	**0.0071**	**0.0061**	**0.0226**	**0.0173**	**0.0021**	13
4th	Robust Gaussian	0.08mm	**0.0013**	**0.0219**	**0.0073**	**0.0027**	0.6790	0.4244	**0.0098**	0.0805	**0.0107**	0.0870	**0.0010**	**0.0043**	**0.0040**	0.1015	**0.0024**	**0.0063**	**0.0057**	**0.0014**	**0.0010**	14
5th	Robust Gaussian	0.08mm	**0.0009**	0.1692	**0.0019**	**0.0082**	0.5720	0.2304	**0.0101**	0.0849	**0.0109**	**0.0123**	**0.0011**	**0.0023**	**0.0038**	**0.0190**	**0.0037**	**0.0054**	0.1044	**0.0019**	**0.0008**	14
6th	Robust Gaussian	0.08mm	**0.0008**	**0.0014**	**0.0036**	**0.0006**	0.5609	0.2720	**0.0101**	0.0769	**0.0108**	**0.0315**	**0.0025**	**0.0039**	**0.0030**	**0.0310**	**0.0054**	**0.0050**	0.3149	**0.0004**	**0.0009**	15
7th	Robust Gaussian	0.08mm	**0.0010**	0.1736	**0.0008**	**0.0016**	0.5267	0.1027	**0.0102**	0.0766	**0.0110**	**0.0462**	**0.0022**	**0.0020**	**0.0042**	0.0637	**0.0027**	**0.0052**	0.8154	**0.0002**	**0.0010**	13
8th	Robust Gaussian	0.08mm	**0.0006**	**0.0125**	**0.0254**	**0.0061**	0.3591	0.1693	**0.0110**	0.0736	**0.0118**	0.0697	**0.0018**	**0.0037**	**0.0020**	0.0650	**0.0030**	**0.0041**	0.5960	**<.0001**	**0.0008**	13
9th	Robust Gaussian	0.08mm	**0.0001**	0.0529	**0.0235**	**0.0084**	0.5357	0.1415	**0.0112**	0.3512	**0.0124**	**0.0234**	**0.0005**	**0.0017**	**0.0012**	**0.0136**	**0.0015**	**0.0034**	0.4391	**0.0002**	**0.0002**	14
10th	Robust Gaussian	0.08mm	**<.0001**	0.7112	**0.0004**	0.0873	0.6664	0.0943	**0.0421**	0.2986	0.0918	**0.0439**	**0.0003**	**0.0013**	**0.0006**	0.0830	**0.0007**	**0.0015**	0.5105	**0.0003**	**0.0001**	11
11th	Robust Gaussian	0.08mm	**<.0001**	**0.0274**	**0.0012**	**0.0003**	**0.0472**	0.0555	**0.0129**	**0.0204**	**0.0136**	**0.0294**	**0.0005**	**0.0016**	**0.0004**	**0.0234**	**0.0007**	**0.0012**	0.5043	**<.0001**	**0.0001**	17
2nd	Spline	0.025mm	**0.0003**	**0.0336**	**0.0004**	**0.0003**	0.9503	0.1895	**0.0125**	0.0683	**0.0136**	**0.0094**	**0.0024**	**0.0064**	**<.0001**	**0.0084**	**0.0045**	**<.0001**	0.1172	**<.0001**	**0.0009**	15
3rd	Spline	0.025mm	**0.0002**	**0.0368**	**0.0006**	**0.0002**	0.9289	0.4037	**0.0125**	0.0627	**0.0135**	**0.0061**	**0.0023**	**0.0050**	**<.0001**	**0.0042**	**0.0043**	**<.0001**	0.0558	**<.0001**	**0.0006**	15
4th	Spline	0.025mm	**0.0004**	**0.0077**	**0.0024**	**0.0004**	0.9496	0.1440	**0.0124**	0.0650	**0.0136**	**0.0117**	**0.0027**	**0.0060**	**<.0001**	**0.0090**	**0.0048**	**<.0001**	0.0794	**<.0001**	**0.0010**	15
5th	Spline	0.025mm	**0.0003**	**0.0268**	**0.0014**	**0.0020**	0.9980	0.0510	**0.0128**	0.0645	**0.0136**	**0.0072**	**0.0026**	**0.0048**	**<.0001**	**0.0042**	**0.0048**	**<.0001**	0.0594	**<.0001**	**0.0010**	15
6th	Spline	0.025mm	**0.0002**	**0.0048**	**0.0009**	**0.0002**	0.9204	0.1238	**0.0122**	0.0622	**0.0131**	**0.0082**	**0.0023**	**0.0044**	**<.0001**	**0.0063**	**0.0040**	**0.0001**	0.1269	**<.0001**	**0.0009**	15
7th	Spline	0.025mm	**0.0004**	0.0746	**0.0009**	**0.0009**	0.8980	0.1251	**0.0121**	0.0618	**0.0131**	**0.0205**	**0.0032**	**0.0063**	**<.0001**	**0.0231**	**0.0041**	**<.0001**	0.2220	**<.0001**	**0.0012**	14
8th	Spline	0.025mm	**0.0009**	**0.0101**	**0.0265**	**0.0055**	0.8160	**0.0309**	**0.0126**	0.0667	**0.0137**	**0.0150**	**0.0040**	**0.0074**	**<.0001**	**0.0096**	**0.0056**	**0.0003**	0.2007	**0.0001**	**0.0020**	16
9th	Spline	0.025mm	**0.0006**	0.0521	**0.0269**	**0.0121**	0.7030	**0.0261**	**0.0128**	0.3515	**0.0145**	**0.0143**	**0.0034**	**0.0066**	**<.0001**	**0.0065**	**0.0052**	**0.0002**	0.0982	**0.0002**	**0.0014**	15
10th	Spline	0.025mm	**0.0006**	0.6126	**0.0005**	0.1438	0.5921	**0.0352**	**0.0472**	0.3034	0.0986	**0.0119**	**0.0034**	**0.0060**	**<.0001**	**0.0336**	**0.0046**	**<.0001**	0.1221	**0.0002**	**0.0013**	13
11th	Spline	0.025mm	**0.0004**	**0.0410**	**0.0014**	**0.0005**	**0.0373**	**0.0363**	**0.0132**	**0.0218**	**0.0138**	**0.0068**	**0.0028**	0.0049	**<.0001**	**0.0044**	**0.0038**	**<.0001**	0.0938	**0.0002**	**0.0013**	18
2nd	Robust Wavelet	0.025mm	**0.0185**	0.8255	**0.0231**	0.1315	0.7882	0.8924	**0.0102**	0.0902	**0.0113**	0.8567	**0.0009**	**0.0151**	**0.0402**	0.7487	**0.0047**	0.0594	0.1111	0.0946	**0.0035**	9
3rd	Robust Wavelet	0.025mm	**0.0087**	0.5942	**0.0026**	0.0551	0.7586	0.2806	**0.0101**	0.0774	**0.0110**	0.7678	**0.0006**	**0.0032**	**0.0077**	0.7188	**0.0027**	**0.0111**	0.0765	**0.0384**	**0.0005**	11
4th	Robust Wavelet	0.025mm	**0.0013**	**0.0182**	**0.0100**	**0.0034**	0.6735	**0.0315**	**0.0101**	0.0797	**0.0112**	0.1311	**0.0003**	**0.0042**	**0.0053**	0.1232	**0.0023**	**0.0072**	0.0652	**0.0011**	**0.0004**	14
5th	Robust Wavelet	0.025mm	**0.0011**	0.0940	**0.0053**	**0.0107**	0.7161	**0.0046**	**0.0103**	0.0843	**0.0114**	0.1011	**0.0005**	**0.0035**	**0.0075**	0.0889	**0.0035**	**0.0105**	0.0765	**0.0020**	**0.0003**	13
6th	Robust Wavelet	0.025mm	**0.0003**	**0.0004**	**0.0052**	**0.0006**	0.6895	**0.0178**	**0.0101**	0.0784	**0.0113**	0.0733	**0.0009**	**0.0042**	**0.0038**	**0.0482**	**0.0040**	**0.0065**	0.1086	**0.0002**	**0.0001**	15
7th	Robust Wavelet	0.025mm	**0.0008**	0.1414	**0.0011**	**0.0015**	0.7663	**0.0127**	**0.0105**	0.0769	**0.0115**	0.1020	**0.0017**	**0.0058**	**0.0043**	0.0994	**0.0038**	**0.0061**	0.2590	**0.0002**	**0.0005**	13
8th	Robust Wavelet	0.025mm	**0.0004**	**0.0111**	**0.0301**	**0.0064**	0.6042	**0.0460**	**0.0110**	0.0783	**0.0123**	0.0953	**0.0026**	**0.0110**	**0.0020**	0.0712	**0.0065**	**0.0046**	0.1559	**0.0001**	**0.0006**	14
9th	Robust Wavelet	0.025mm	**0.0003**	**0.0359**	**0.0283**	**0.0099**	0.6376	**0.0469**	**0.0117**	0.3706	**0.0131**	0.0597	**0.0018**	**0.0080**	**0.0016**	**0.0345**	**0.0050**	**0.0044**	0.1105	**0.0004**	**0.0004**	15
10th	Robust Wavelet	0.025mm	**0.0002**	0.6600	**0.0009**	0.1101	0.5960	**0.0088**	**0.0442**	0.3044	0.0943	0.0776	**0.0018**	**0.0065**	**0.0008**	0.1378	**0.0038**	**0.0018**	0.1074	**0.0005**	**0.0004**	11
11th	Robust Wavelet	0.025mm	**0.0002**	**0.0341**	**0.0020**	**0.0005**	**0.0368**	**0.0453**	**0.0131**	**0.0211**	**0.0136**	**0.0324**	**0.0015**	**0.0049**	**0.0006**	**0.0228**	**0.0030**	**0.0013**	0.0956	**0.0001**	**0.0004**	18

Table 4.8 *T-test results comparing data from two populations of phocids with known dietary differences (Males - acorn eaters, and Females - bramble leaf eaters) across 21 areal texture parameters. Tests were carried out separately for each combination of operator and filter used to scale limited the 3D surfaces. Significant test results have been highlighted bold*

The exception is when using a robust Gaussian filter, nesting index 0.08mm and a 3rd or 4th order of polynomial to scale limit the surfaces, in which cases Smr2 separates the dietary populations. As such only two parameters (Sku, and Smr1) are never able to separate phocid dietary groups. But certain parameters (Sds, Ssc, Smr2) only separate the dietary groups when very specific combinations of operator and filter are applied to the surfaces. Surfaces scale limited using an 11th order polynomial always produce the greatest number of parameters where phocid dietary groups are separated (Fig. 4.9a). However, from statistical comparisons of surfaces scale limited using 10th and 11th orders of polynomial, these settings result in differences between surfaces. It is likely then that the high number of significant T-test results recorded when using an 11th order of polynomial is affected by this noise in the data. The next highest number of parameters separating phocid dietary groups is 16, when using a 6th order polynomial, robust Gaussian filter, and nesting index 0.025mm, and when using an 8th order polynomial, spline filter, and nesting index 0.025mm.

Surfaces producing the greatest magnitude of difference between two dietary populations would be expected to match the surfaces where the greatest number of parameters separating the dietary groups are recorded. If we rank the differences between populations and take a mean rank across all parameters for each combination of operator and filter we can estimate those scale limiting settings producing the greatest overall magnitude of difference between dietary populations (Figure 4.10 & Figure 4.11). The scale limited surfaces producing the greatest magnitude of difference between the *C.capreolus* populations are those produced using a 5th and 6th order polynomial with a robust Gaussian filter and nesting index 0.025mm. The combination of operator and filter using a 6th order polynomial is the same one that produced the greatest number of parameters separating *C.capreolus* dietary groups. However the other combination of filters and operators that produced surfaces where the greatest number of parameters separated *C.capreolus* dietary groups (6th order polynomial with spline filter and nesting index 0.025mm) ranks very low in magnitude of difference. When we look at the magnitude of difference between the two phocid populations the results are quite different. The greatest magnitude of difference between these two dietary groups is found between surfaces scale limiting

using a 4^{th} or 5^{th} order polynomial with a robust Gaussian filter and a nesting index of 0.08mm. While the two combinations of operator and filter producing surfaces where the greatest number of parameters separated the dietary groups show very low magnitude of differences between the groups. However we know from direct comparison of surfaces generated using different nesting indices that a 0.08mm cut-off wavelength generally produces significant differences from surfaces produced using a 0.025mm cut-off and even between combinations of operator and filter using a 0.08mm nesting index. As such it is unclear whether a 0.08mm nesting index is useful for scale limiting 3D surfaces. Overall the magnitude of difference between dietary populations for each set of surfaces produced using different operators and filters potentially calls into question those combinations producing the greatest number of parameters separating dietary groups. The lowest magnitudes of difference between both sets of dietary populations are almost always found for surfaces scale limited using a spline filter.

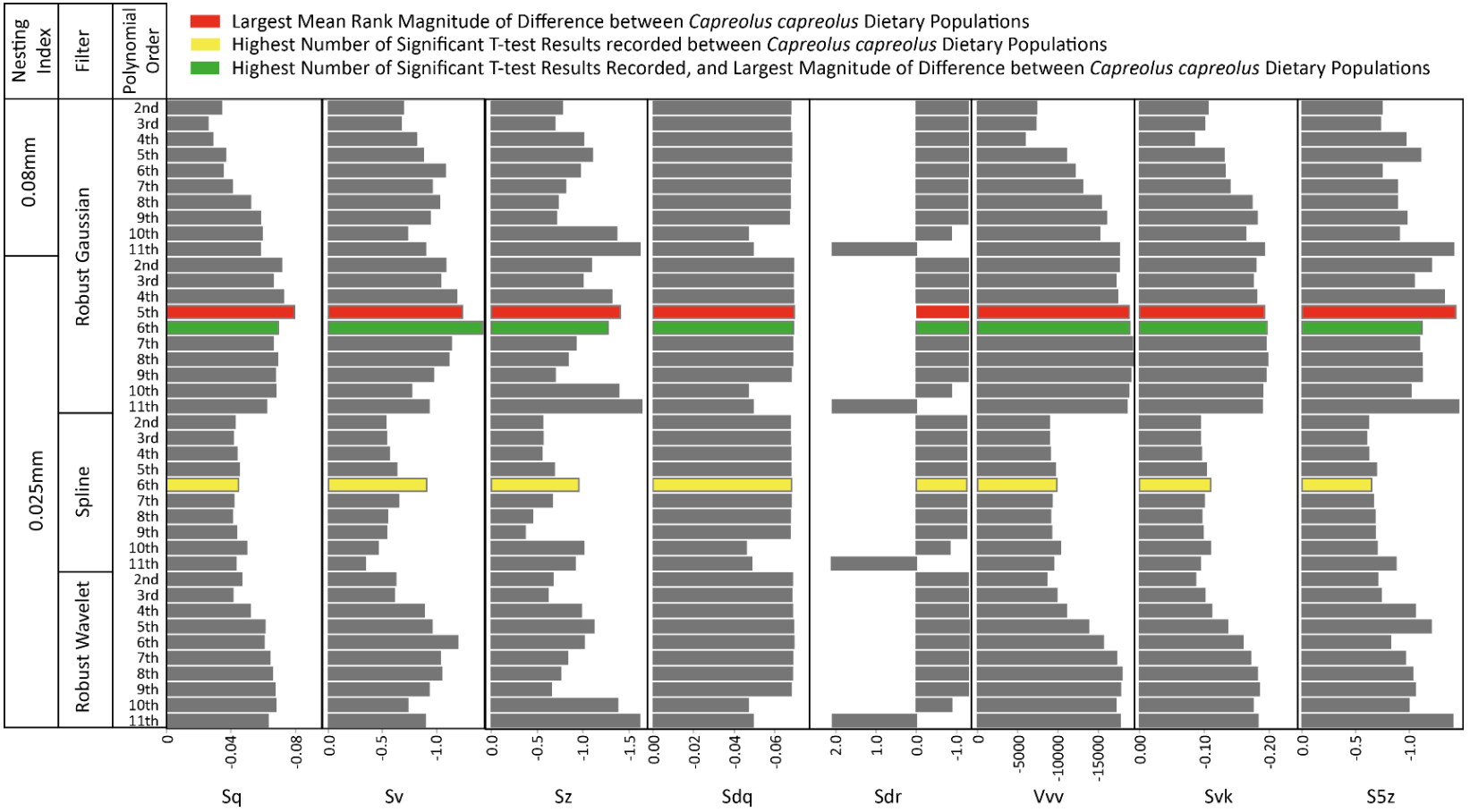

Figure 4.10 *Magnitudes of difference between <u>C.capreolus</u> dietary groups for all eight parameters where significant differences between dietary groups were recorded (T-tests). Data are presented separately for surfaces scale limited using different operators, filters and nesting indices. Surfaces returning the largest rank magnitude of difference across all parameters are highlighted red, and surfaces producing the greatest number parameters showing difference between dietary groups are highlighted yellow. Those surfaces producing both the largest rank magnitude of difference across all parameters, and the greatest number parameters showing difference between dietary groups are highlighted green.*

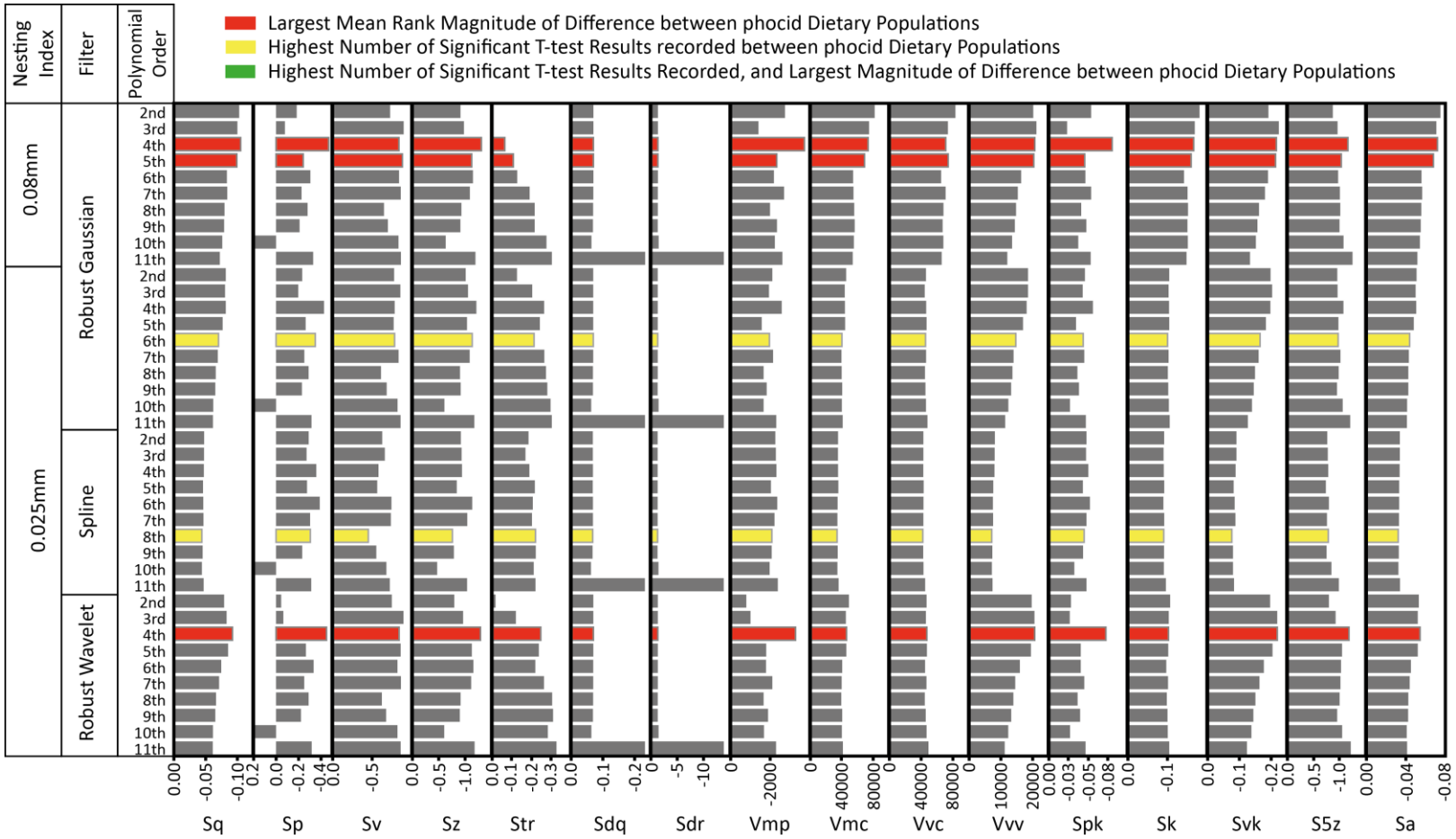

Figure 4.11 *Magnitudes of difference between Phocid dietary groups for all sixteen parameters where significant differences between dietary groups were recorded (T-tests). Parameters are only included where at least one third of surfaces showed a significant difference between dietary groups. Data are presented separately for surfaces scale limited using different operators, filters and nesting indices. Surfaces returning the largest rank magnitude of difference across all parameters are highlighted red, and surfaces producing the greatest number parameters showing difference between dietary groups are highlighted yellow.*

Those parameters statistically separating dietary groups (T-tests) can be used to compare the ability of these same surfaces to separate dietary groups in multivariate space. If we take the maximum possible set of parameters that could separate each dietary group (*C.capreolus* = 8 parameters, Phocidae = 16 parameters excluding data generated using an 11^{th} order polynomial) we can compare the effect of each setting on the multivariate distribution of data without biasing results based on the number of parameters entered into each analysis. For the two dietary comparisons principal component analysis (PCA) was carried out for each of the 40 combinations of operator and filter used to scale limit 3D surface data. A representative selection of PCA analyses can be seen in Figure 4.12 and Figure 4.13, only Principal Component 1 (PC1) and Principal Component 2 (PC2) are shown, as these explain the majority of variance (>79%) in all analyses. Parameter loadings (eigenvectors) for each analysis can been seen in Table 4.9 and Table 4.10. It is clear in all cases, across both phocid and *C.capreolus* dietary comparisons, that separation of dietary groups is most obvious along Principal Component 1 (PC1), and that this general separation is consistent across surfaces generated using each combination of operator and filter. This suggests that, whichever settings are used to scale limit 3D surfaces, dietary groups can be separated to a similar degree using principal component analysis. However the relative position of points and the percentage of variance explained by each axis varies considerably. The eigenvectors also change, although not to the same degree. The biggest difference in relative position of points between analyses can be seen when comparing the multivariate distribution of data from surfaces scale limited using a spline filter to those scale limited using both other filter types. The relationship of points in analyses where a spline filter has been used to scale limit data appears to be the mirror image along Principal Component 2 (PC2) compared to using other filter types. The separation of points along PC2 also appears to be lower when surfaces are scale limited using a spline filter. There appears to be no pattern between data generated from surfaces scale limited using different combinations of operator and filter in the percentage of variance explained by each axis.

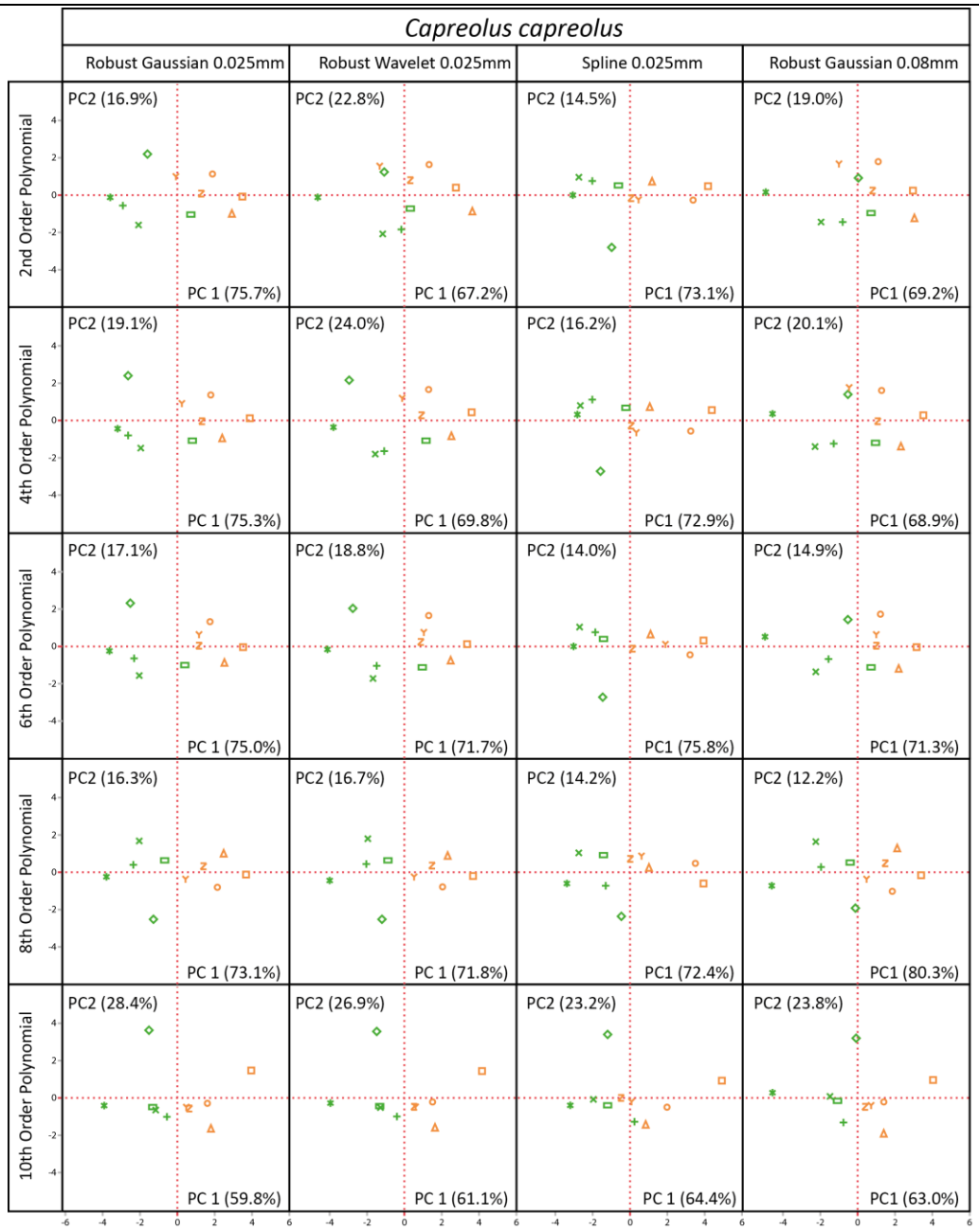

Figure 4.12 *PCA analyses comparing two <u>Capreolus capreolus</u> dietary populations (Acorn Eaters and Bramble Leaf Eaters) using the same parameters for each analysis (Sq, Sv, Sz, Sdq, Sdr, Vvv, Svk, and S5z, for parameter descriptions see Table 4.3). Tests were carried out separately for each surface scale limited using a different combination of operator, filter and nesting index. Points are coloured consistently by dietary group (Acorn eaters – Orange, Bramble Leaf Eaters – Green). Each specimen number is represented by a different symbol, consistent across all tests. Only data from 5 different orders of polynomial across all filter types and nesting indices are shown. Percentage of variance explained by each axes presented for all analyses.*

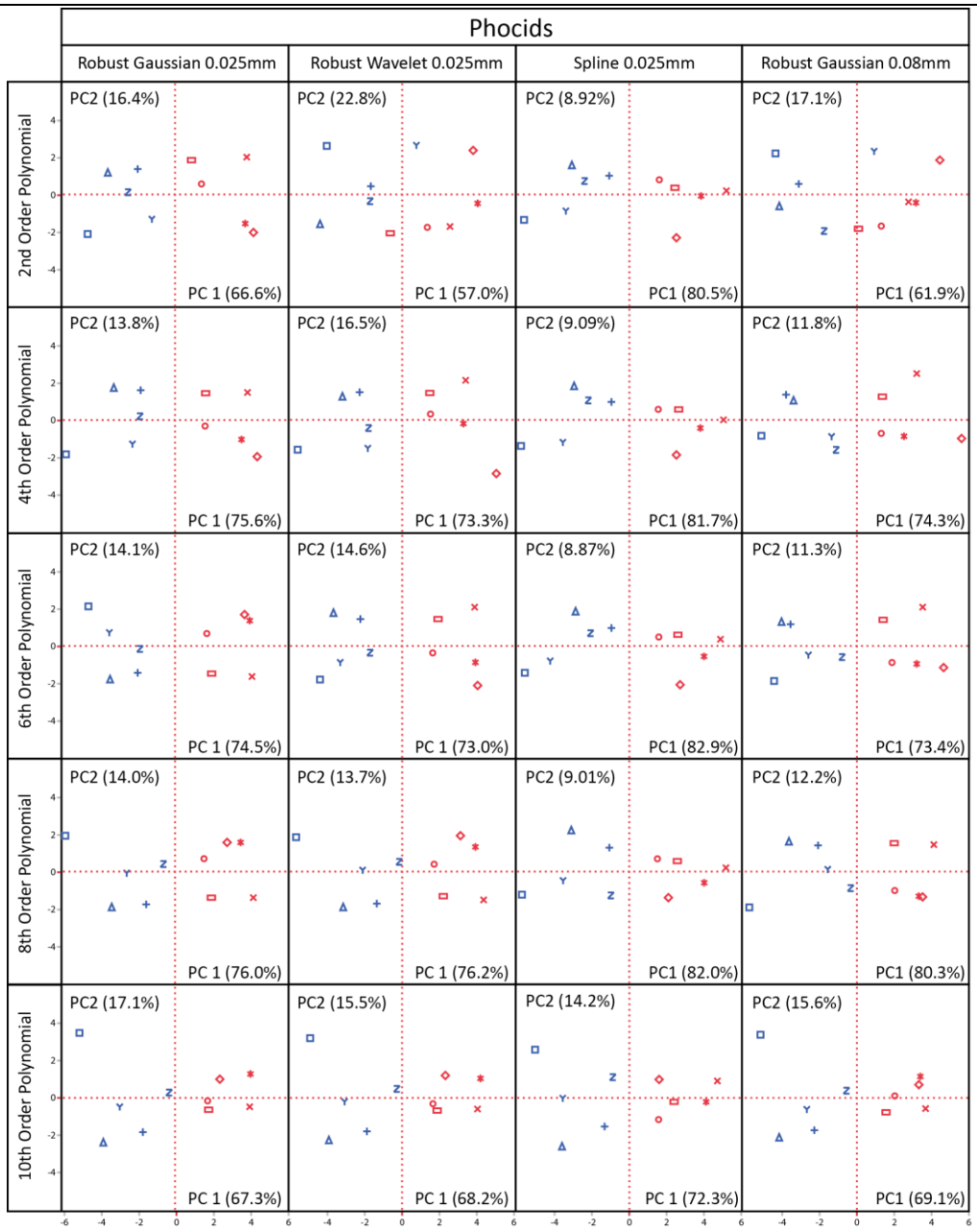

Figure 4.13 *PCA analyses comparing two Phocid dietary populations (Fish Eaters and Invertebrate Eaters) using the same parameters for each analysis (Sq, Sp, Sv, Sz, Str, Sdq, Sdr, Vmp, Vmc, Vvc, Vvv, Spk, Sk, Svk, S5z, and Sa, for parameter descriptions see Table 4.3). Tests were carried out separately for each surface scale limited using a different combination of operator, filter and nesting index. Points are coloured consistently by dietary group (Fish eaters – Blue, Invertebrate Eaters – Red). Each specimen number is represented by a different symbol, consistent across all tests. Only data from 5 different orders of polynomial across all filter types and nesting indices are shown. Percentage of variance explained by each axes presented for all analyses.*

			Polynomial Order									
Filter and Nesting	Index	Parameter	2nd	3rd	4th	5th	6th	7th	8th	9th	10th	11th
Robust Gaussian	0.025	Sq	**0.39312**	**0.39593**	**0.38840**	**0.38407**	**0.38054**	**0.38827**	**0.38957**	**0.38482**	**0.39181**	**0.38609**
Robust Gaussian	0.025	Sv	**0.38910**	**0.39550**	**0.36931**	**0.37395**	**0.37732**	**0.38477**	**0.38938**	**0.39249**	0.33797	**0.40266**
Robust Gaussian	0.025	Sz	0.36528	0.36066	**0.38153**	**0.37937**	**0.37441**	0.34834	0.32043	0.27382	**0.39828**	**0.43781**
Robust Gaussian	0.025	Sdq	0.33060	0.33305	0.31966	0.32479	0.32910	0.33606	0.35976	0.36796	0.27957	0.31604
Robust Gaussian	0.025	Sdr	0.29529	0.29687	0.28295	0.28750	0.29469	0.29511	0.32338	0.34221	0.20829	0.30822
Robust Gaussian	0.025	Vvv	0.32776	0.32383	0.34182	0.34068	0.34329	0.34086	0.31916	0.32949	0.38139	0.24340
Robust Gaussian	0.025	Svk	0.32448	0.32000	0.33530	0.33098	0.33531	0.33178	0.31513	0.31999	0.36854	0.22539
Robust Gaussian	0.025	S5z	**0.38912**	**0.38785**	**0.39457**	**0.39368**	**0.38368**	**0.39189**	**0.39847**	**0.39929**	**0.41329**	**0.43841**
Spline	0.025	Sq	**0.37451**	**0.37470**	**0.36960**	**0.36818**	**0.37060**	**0.37061**	**0.38124**	**0.38263**	0.38948	**0.39363**
Spline	0.025	Sv	0.35019	0.35354	0.34395	0.34392	**0.36686**	0.36222	**0.37651**	**0.36961**	0.34477	0.35159
Spline	0.025	Sz	0.34568	0.35070	0.36038	0.35519	**0.36528**	0.34442	0.30123	0.28085	0.39682	**0.43272**
Spline	0.025	Sdq	**0.37841**	**0.37517**	**0.36675**	**0.37088**	**0.37313**	**0.37749**	**0.38133**	**0.37680**	0.30433	0.32736
Spline	0.025	Sdr	0.34378	0.34005	0.32976	0.33657	0.34470	0.34523	0.35117	0.35988	0.24655	0.31889
Spline	0.025	Vvv	0.34492	0.34577	0.35949	0.35205	0.35085	0.33659	0.33230	0.34389	0.37242	0.27810
Spline	0.025	Svk	0.31015	0.31156	0.31732	0.31367	0.31775	0.31076	0.31597	0.32866	0.35275	0.24665
Spline	0.025	S5z	**0.37560**	**0.37229**	**0.37689**	**0.38320**	0.33547	**0.37586**	**0.37836**	**0.37462**	0.39427	**0.43263**
Robust Wavelet	0.025	Sq	**0.40963**	**0.40775**	**0.40009**	**0.39288**	**0.39174**	**0.39694**	**0.39359**	**0.38942**	**0.39944**	0.39089
Robust Wavelet	0.025	Sv	**0.41122**	**0.41443**	**0.38217**	**0.38301**	**0.37972**	**0.39334**	**0.38708**	**0.39214**	0.34170	**0.40355**
Robust Wavelet	0.025	Sz	0.38273	0.37371	**0.39385**	**0.38843**	**0.37700**	0.35034	0.31982	0.27239	**0.39374**	**0.43051**
Robust Wavelet	0.025	Sdq	0.25001	0.28461	0.27787	0.28252	0.30044	0.31644	0.36084	0.36591	0.28329	0.30401
Robust Wavelet	0.025	Sdr	0.20460	0.23982	0.23500	0.24222	0.26274	0.27544	0.32428	0.34365	0.21546	0.29597
Robust Wavelet	0.025	Vvv	0.34860	0.32626	0.34433	0.35181	0.35790	0.34476	0.31762	0.33113	0.37638	0.26973
Robust Wavelet	0.025	Svk	0.35917	0.33647	0.34767	0.34976	0.35366	0.33992	0.31684	0.31963	0.36343	0.24434
Robust Wavelet	0.025	S5z	**0.40216**	**0.40516**	**0.40850**	**0.40432**	**0.38439**	**0.39317**	**0.39539**	**0.39571**	**0.41018**	**0.43190**
Robust Gaussian	0.08	Sq	0.33722	0.34363	0.32436	0.34328	0.33610	0.34141	0.35474	0.35351	**0.38240**	0.36415
Robust Gaussian	0.08	Sv	**0.38617**	**0.39219**	0.35327	0.36413	0.35720	0.36196	**0.37376**	**0.38127**	0.28687	**0.39051**
Robust Gaussian	0.08	Sz	**0.39876**	**0.40671**	**0.41422**	**0.39779**	**0.38524**	**0.37304**	0.34676	0.30179	0.37679	**0.43382**
Robust Gaussian	0.08	Sdq	0.28609	0.29573	0.31726	0.31280	0.33277	0.33769	0.36074	0.37164	0.33083	0.31499
Robust Gaussian	0.08	Sdr	0.24784	0.25894	0.28084	0.27661	0.30352	0.30168	0.32999	0.35270	0.27012	0.30688
Robust Gaussian	0.08	Vvv	0.37152	0.35569	0.35127	0.36121	0.36635	0.35990	0.34312	0.34737	**0.38819**	0.28864
Robust Gaussian	0.08	Svk	0.36725	0.33462	0.35226	0.35101	0.35725	0.34679	0.32135	0.31379	0.37079	0.24909
Robust Gaussian	0.08	S5z	**0.40247**	**0.41195**	**0.41402**	**0.40411**	**0.38254**	**0.39803**	**0.39267**	**0.39617**	**0.39865**	**0.43353**

Table 4.9 *Loadings (eigenvectors) for each parameter on PC1 and PC2 when comparing C.capreolus dietary populations. PCA carried out using 8 areal texture parameters (Sq, Sv, Sz, Sdq, Sdr, Vvv, Svk, and S5z, for parameter descriptions see Table 4.3), across 40 PCA analyses, each using data from surfaces scale limited using different combinations of operator and filter. Values in bold show the greatest loadings.*

Eigenvectors for each parameter on PC1 are surprisingly similar in all analyses, with no one parameter showing significantly higher values than any other, however some semi-consistently (>50% of operator and filter combinations) weight slightly more heavily along PC1 than others. For comparisons of *C.capreolus* dietary populations these are Sq and S5z, however three other parameters (Sv, Sz, and Sdq) return high eigenvector values when using surfaces scale limited with specific filters or nesting indices. For comparisons of phocid dietary populations the parameters consistently weighting highest on PC1 are Sq, Vmc, Vvc, Sk, S5z, and Sa.

			Polynomial Order									
Filter and Nesting	Index	Parameter	2nd	3rd	4th	5th	6th	7th	8th	9th	10th	11th
Robust Gaussian	0.025	Sq	**0.29444**	**0.29148**	**0.27446**	**0.28548**	**0.27371**	**0.27459**	**0.27371**	**0.27995**	**0.29658**	**0.27874**
Robust Gaussian	0.025	Sp	0.20138	0.17804	0.25004	0.20477	**0.27482**	0.21392	0.22500	0.13615	-0.03545	0.18548
Robust Gaussian	0.025	Sv	**0.27495**	**0.27644**	0.23810	**0.26648**	0.23511	0.24045	0.22701	0.23807	0.25884	0.23704
Robust Gaussian	0.025	Sz	**0.27749**	**0.27870**	**0.26797**	**0.26015**	**0.26712**	**0.27731**	0.25966	0.24372	0.17310	0.25390
Robust Gaussian	0.025	Str	0.05647	0.15610	0.20142	0.21542	0.20745	0.22066	0.22805	0.22735	0.22610	0.20950
Robust Gaussian	0.025	Sdq	0.23570	0.23001	0.23500	0.22970	0.23897	0.23814	0.24187	0.24580	0.24947	0.24948
Robust Gaussian	0.025	Sdr	0.23396	0.22891	0.23412	0.22834	0.23750	0.23717	0.24074	0.24554	0.23374	0.24898
Robust Gaussian	0.025	Vmp	0.18697	0.16344	0.22255	0.19097	0.21604	0.22574	0.23574	0.24097	0.24431	0.23743
Robust Gaussian	0.025	Vmc	**0.28709**	**0.28381**	**0.27647**	**0.27941**	**0.27375**	**0.27918**	**0.28081**	**0.28359**	**0.29536**	**0.27465**
Robust Gaussian	0.025	Vvc	**0.26656**	**0.26551**	**0.26337**	0.25923	**0.26457**	**0.27319**	**0.27277**	**0.27463**	**0.28616**	**0.26835**
Robust Gaussian	0.025	Vvv	**0.26372**	**0.27166**	0.23819	0.25744	0.23187	0.22754	0.22389	0.23208	0.25498	0.24175
Robust Gaussian	0.025	Spk	0.19138	0.17248	0.22512	0.20206	0.22659	0.22687	0.24117	0.24858	0.21619	0.23844
Robust Gaussian	0.025	Sk	**0.27076**	**0.27018**	**0.26505**	**0.26252**	**0.26503**	**0.27325**	**0.27442**	**0.27650**	**0.28830**	**0.27035**
Robust Gaussian	0.025	Svk	0.25622	0.26478	0.22920	0.24910	0.22005	0.21462	0.20899	0.21772	0.23886	0.22923
Robust Gaussian	0.025	S5z	**0.28899**	**0.29219**	**0.27801**	**0.28559**	**0.26521**	**0.27181**	**0.26586**	**0.27974**	**0.27160**	**0.27433**
Robust Gaussian	0.025	Sa	**0.29933**	**0.29966**	**0.28325**	**0.29190**	**0.28402**	**0.28474**	**0.28328**	**0.28800**	**0.30221**	**0.28127**
Spline	0.025	Sq	**0.27437**	**0.27656**	**0.27312**	**0.27386**	**0.27148**	**0.27474**	**0.27398**	**0.27900**	**0.29313**	**0.27294**
Spline	0.025	Sp	0.20803	0.19957	0.24602	0.20585	0.25393	0.22324	0.21307	0.13780	-0.05100	0.17057
Spline	0.025	Sv	0.24137	0.24649	0.21920	0.23558	0.23103	0.22903	0.22076	0.22248	0.24868	0.23430
Spline	0.025	Sz	0.25369	0.25940	0.25329	0.23902	0.25689	0.26386	0.24588	0.22224	0.14380	0.24413
Spline	0.025	Str	0.14388	0.09701	0.15696	0.18372	0.16115	0.15799	0.19528	0.20411	0.19983	0.19888
Spline	0.025	Sdq	0.25336	0.25195	0.25278	0.25108	0.24844	0.24899	0.24604	0.24813	0.24444	0.24432
Spline	0.025	Sdr	0.25233	0.25096	0.25179	0.25028	0.24752	0.24818	0.24493	0.24810	0.22286	0.24284
Spline	0.025	Vmp	0.24906	0.24626	0.24283	0.24340	0.24806	0.24668	0.25355	0.25859	**0.26926**	0.25529
Spline	0.025	Vmc	**0.26896**	**0.26896**	**0.26799**	**0.26873**	**0.26559**	**0.26932**	**0.26953**	**0.27318**	**0.28629**	**0.26748**
Spline	0.025	Vvc	**0.26747**	**0.26809**	**0.26704**	**0.26696**	**0.26590**	**0.27012**	**0.26875**	**0.27184**	**0.28395**	**0.26613**
Spline	0.025	Vvv	0.25169	0.25882	0.25200	0.25624	0.24566	0.25062	0.25412	**0.26075**	**0.27884**	**0.26213**
Spline	0.025	Spk	0.25345	0.25357	0.25041	0.25416	0.25403	0.24820	0.25972	**0.26644**	0.24668	0.25683
Spline	0.025	Sk	**0.26641**	**0.26573**	**0.26533**	**0.26559**	**0.26325**	**0.26864**	**0.26755**	**0.27054**	**0.28363**	**0.26601**
Spline	0.025	Svk	0.23893	0.24799	0.23526	0.24262	0.22944	0.23418	0.23780	0.24392	**0.26259**	0.25069
Spline	0.025	S5z	**0.27166**	**0.27507**	**0.26906**	**0.27149**	**0.26596**	**0.26634**	**0.26020**	**0.27455**	**0.26785**	**0.27247**
Spline	0.025	Sa	**0.27371**	**0.27544**	**0.27258**	**0.27288**	**0.27051**	**0.27449**	**0.27323**	**0.27760**	**0.29114**	**0.27136**
Robust Wavelet	0.025	Sq	**0.32385**	**0.31458**	**0.27857**	**0.28774**	**0.27586**	**0.27448**	**0.27420**	**0.28045**	**0.29605**	**0.27807**
Robust Wavelet	0.025	Sp	0.16525	0.18054	0.25366	0.20614	**0.27606**	0.21302	0.22734	0.13705	-0.02942	0.18530
Robust Wavelet	0.025	Sv	**0.30953**	**0.31080**	0.24909	0.27620	0.24332	0.24317	0.23062	0.24052	0.25949	0.23618
Robust Wavelet	0.025	Sz	**0.29055**	**0.29426**	**0.27443**	**0.26669**	**0.26969**	**0.27805**	0.25994	0.24272	0.17711	0.25254
Robust Wavelet	0.025	Str	-0.11529	0.03590	0.19088	0.21030	0.19051	0.21764	0.22945	0.22997	0.23234	0.21371
Robust Wavelet	0.025	Sdq	0.19408	0.19600	0.22568	0.21839	0.23342	0.23577	0.23729	0.24115	0.24543	0.24754
Robust Wavelet	0.025	Sdr	0.19278	0.19432	0.22399	0.21634	0.23142	0.23484	0.23630	0.24206	0.22902	0.24715
Robust Wavelet	0.025	Vmp	0.15050	0.13845	0.21443	0.19902	0.21116	0.22777	0.23636	0.24383	0.24536	0.24022
Robust Wavelet	0.025	Vmc	**0.28527**	**0.27456**	**0.27576**	**0.27790**	**0.27381**	**0.27895**	**0.28012**	**0.28293**	**0.29305**	**0.27370**
Robust Wavelet	0.025	Vvc	0.24818	0.23556	0.25387	0.24608	0.25926	**0.26998**	**0.27015**	**0.27363**	**0.28422**	**0.26879**
Robust Wavelet	0.025	Vvv	**0.27767**	**0.30559**	0.24994	**0.26272**	0.23918	0.23006	0.22672	0.23346	0.25700	0.24302
Robust Wavelet	0.025	Spk	0.16357	0.14866	0.21724	0.21178	0.22413	0.22981	0.24312	0.25214	0.22030	0.24229
Robust Wavelet	0.025	Sk	0.24753	0.23926	0.25604	0.24930	**0.26019**	**0.26962**	**0.27175**	**0.27458**	**0.28480**	**0.26867**
Robust Wavelet	0.025	Svk	**0.26962**	**0.30015**	0.24347	0.25483	0.22857	0.21800	0.21236	0.21969	0.24200	0.23042
Robust Wavelet	0.025	S5z	**0.30112**	**0.30220**	**0.28133**	**0.28760**	**0.27427**	**0.27306**	**0.26556**	**0.27776**	**0.27339**	**0.27262**
Robust Wavelet	0.025	Sa	**0.32458**	**0.32188**	**0.28818**	**0.29581**	**0.28641**	**0.28572**	**0.28336**	**0.28793**	**0.30042**	**0.28023**
Robust Gaussian	0.08	Sq	**0.31015**	**0.30845**	**0.28296**	**0.28560**	**0.28418**	**0.27813**	**0.27772**	**0.28252**	**0.29575**	**0.27828**
Robust Gaussian	0.08	Sp	0.20032	0.20410	0.25758	0.20377	**0.27292**	0.21370	0.24118	0.14681	-0.02163	0.20274
Robust Gaussian	0.08	Sv	**0.29750**	**0.28022**	0.25289	**0.26963**	0.23990	0.23986	0.23493	0.24224	0.25875	0.23436
Robust Gaussian	0.08	Sz	**0.28402**	**0.29358**	**0.28090**	**0.26657**	**0.26567**	**0.27777**	**0.26440**	0.24821	0.18003	0.25314
Robust Gaussian	0.08	Str	-0.02736	0.03880	0.05464	0.12391	0.09740	0.17026	0.18058	0.18760	0.20510	0.19779
Robust Gaussian	0.08	Sdq	0.18496	0.16175	0.19362	0.19054	0.20427	0.21413	0.22115	0.22954	0.24186	0.24674
Robust Gaussian	0.08	Sdr	0.18422	0.15997	0.19286	0.18934	0.20306	0.21369	0.22121	0.23003	0.22913	0.24675
Robust Gaussian	0.08	Vmp	0.20426	0.18160	0.24335	0.24851	0.24684	0.25439	0.24527	0.25399	0.25381	0.23779
Robust Gaussian	0.08	Vmc	**0.28470**	**0.28728**	**0.27602**	**0.27884**	**0.27343**	**0.27772**	**0.27916**	**0.28117**	**0.29055**	**0.27339**
Robust Gaussian	0.08	Vvc	**0.27690**	**0.27781**	**0.27410**	**0.26673**	**0.26773**	**0.27657**	**0.27449**	**0.27498**	**0.28439**	**0.27011**
Robust Gaussian	0.08	Vvv	**0.27354**	**0.29097**	0.25942	**0.26940**	0.25786	0.24197	0.24026	0.24672	0.26459	0.24703
Robust Gaussian	0.08	Spk	0.19793	0.16855	0.23843	0.25004	0.24756	0.24912	0.24603	0.25949	0.23085	0.23869
Robust Gaussian	0.08	Sk	**0.26580**	**0.27855**	**0.27380**	**0.26264**	**0.26609**	**0.27526**	**0.27423**	**0.27466**	**0.28403**	**0.26985**
Robust Gaussian	0.08	Svk	0.25560	**0.28351**	0.25112	**0.26199**	0.24761	0.23033	0.22587	0.23548	0.25161	0.23472
Robust Gaussian	0.08	S5z	**0.29082**	**0.29865**	**0.28299**	**0.28374**	**0.27583**	**0.27261**	**0.26794**	**0.27932**	**0.27294**	**0.27127**
Robust Gaussian	0.08	Sa	**0.30265**	**0.30384**	**0.28331**	**0.28594**	**0.28430**	**0.28231**	**0.28188**	**0.28503**	**0.29689**	**0.27898**

Table 4.10 *Loadings (eigenvectors) for each parameter on PC1 and PC2 when comparing phocid dietary populations. PCA carried out using 16 areal texture parameters (Sq, Sp, Sv, Sz, Str, Sdq, Sdr, Vmp, Vmc, Vvc, Vvv, Spk, Sk, Svk, S5z, and Sa, for parameter descriptions see Table 4.3), across 40 PCA analyses, each using data from surfaces scale limited using different combinations of operator and filter. Values in bold show the greatest loadings.*

Parameter Sz also weights highly for data generated from surfaces scale limited using most combinations of operator and filter, except when using a spline filter.

It is clear that certain differences exist between multivariate analyses carried out on surfaces scale limited using different combinations of operator and filter. However because we included a constant set of parameters in each analysis when normally we would only use those parameters returning significant results from dietary analyses, it is important to make sure that differences have not been caused by the inclusion of certain parameters. As such we re-ran a subset of the multivariate analyses (five different orders of polynomial with a robust Gaussian filter and nesting index 0.025mm) using the parameters where separation between dietary groups was actually produced (T-tests) and compared them to the results from the original PCA analyses (Figure 4.14). There is little point comparing eigenvectors, given that different number of parameters in different analyses will create incomparable values. We find there is almost no difference in terms of relative position of points, or separation of dietary groups along PC1 between analyses carried out using the maximum possible number of parameters and those using the actual parameters separating dietary groups (T-tests). The only thing affected is the percentage of variance explained by each axis, but this is expected given different numbers of parameters are included in each analysis.

Regardless of the combination of operator and filter used to scale limit 3D surfaces, dietary separation along PC1 is relatively unaffected across multivariate analyses. However this is only seen in the context of individual combinations of operator and filter, and does not tell us whether comparing data from two populations (each scale limited using different combinations of operator and filter) would still produce comparable separations of dietary groups in multivariate space. As such, all data was analysed in two further PCA (one each for comparisons of *C.capreolus*, and phocid dietary groups), which included data for all of the different scale limiting settings.

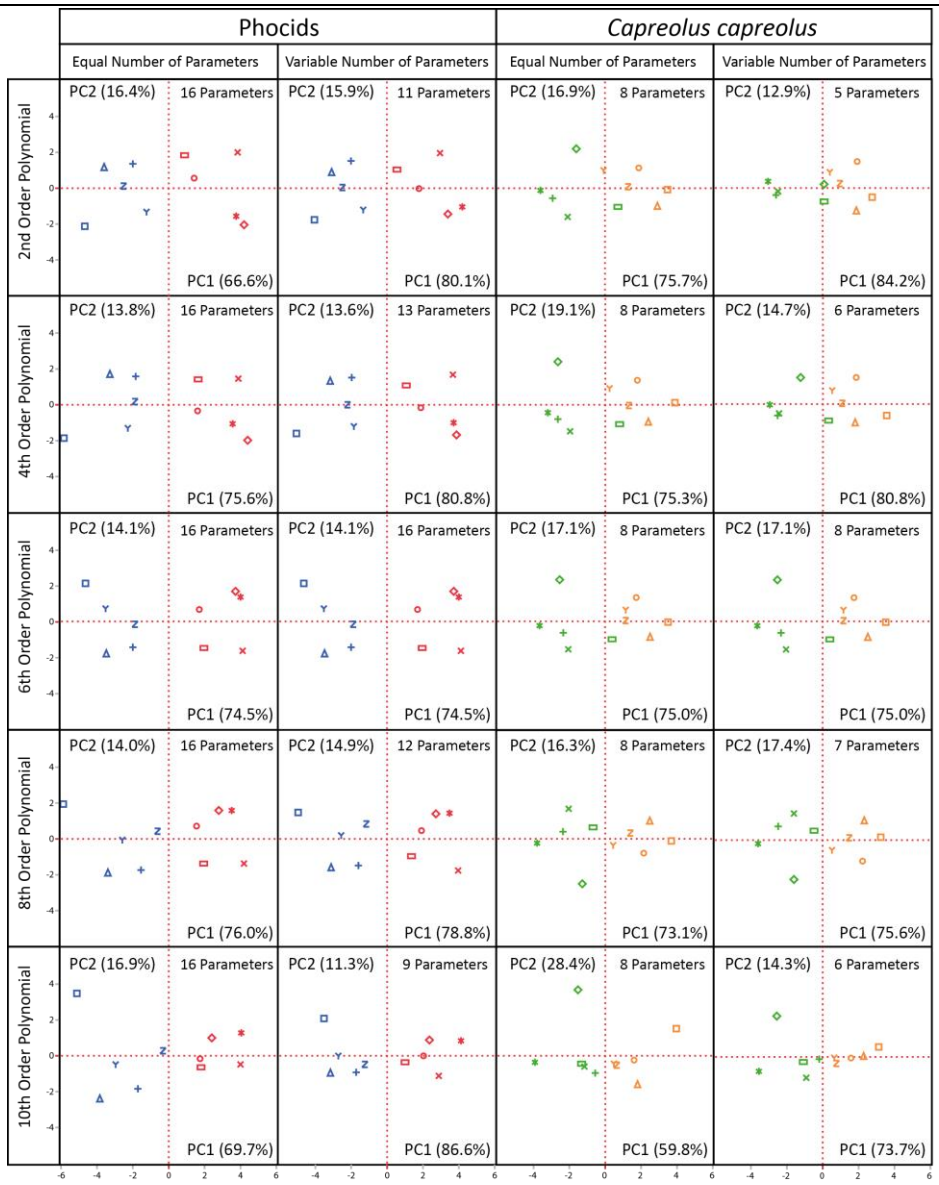

Figure 4.14 *PCA comparing dietary groups, separately for C.capreolus and Phocid populations. For each comparison PCA analyses are split into those containing the maximum number of parameters where significant differences between the dietary populations were recorded, and those using the actual number recorded for each individual surface, so that number of parameters vary between analyses. Tests were carried out separately for each surface scale limited using a different combination of operator, filter and nesting index. Points are coloured consistently by dietary group (C.capreolus: Acorn Eaters – Orange, Bramble Leaf Eaters – Green; Phocid: Fish Eaters – Blue, Invertebrate Eaters – Red). Each specimen number is represented by a different symbol, consistent across all tests within each pair of dietary groups. Only analyses of data from surfaces scale limited using a robust Gaussian filter and 0.025mm nesting index are shown. Percentage of variance explained by each axes presented for each analyses.*

For each pair of dietary groups the maximum number of parameters showing difference between dietary populations (T-tests) was used (eight parameters for *C.capreolus*, and sixteen for phocids). The resulting multivariate analyses can be seen in Figure 4.15 and Figure 4.16. For the PCA analysis between phocid dietary groups we see the same separation along PC1 with very little overlap, suggesting that if data from surfaces scale limited using different combinations of operator and filter were compared, it would still be possible to separate dietary groups in multivariate space. For the *C.capreolus* PCA analysis we again see the same dietary separation along PC1, however there is a greater degree of overlap between the two dietary groups suggesting there would be more difficulty separating them in multivariate space were you to compare data from surfaces scale limited using different combinations of operator and filter. Each individual surface from a single specimen, scale limited using different combinations of operator and filter, appears to show an oblique linear transition along PC1 and PC2. We can test the linearity of the relationship between data from surfaces scale limited using different combinations of operator and filter and their position on PC1 and PC2 using correlations (in the case of operators) and ANOVA tests between the positions of points on each principal component against each combination of operator and filter, separately for each dietary group. For each ANOVA test the variability between individual specimen numbers is blocked, as we would expect this to exceed the variability between combinations of operator and filter. We can then use Tukey HSD tests and group means to determine any trends in multivariate space. Results of ANOVA and Tukey HSD tests can be seen in Table 4.11. The results of Spearman's rank correlations between operator (polynomial order) and the position of points along PC1 and PC2 by filter type can be seen in Table 4.12. We find for both phocid and *C.capreolus* dietary populations that operator (polynomial order) is positively correlated with PC2, and very rarely (3/12 tests) negatively correlated with PC1. This suggests there is likely a consistent directional correlation between the polynomial orders of operators used to scale limit a 3D surface and PC2. This result is supported by ANOVA tests, which only show differences between operator and PC2, never PC1. Resulting Tukey HSD tests and sample means show that this difference is limited to comparisons with surfaces scale limited using 10^{th} and 11^{th} order polynomials, and that these surfaces produce a positive shift in their position

along PC2, with the greatest difference found in surfaces scale limited using an 11th order polynomial.

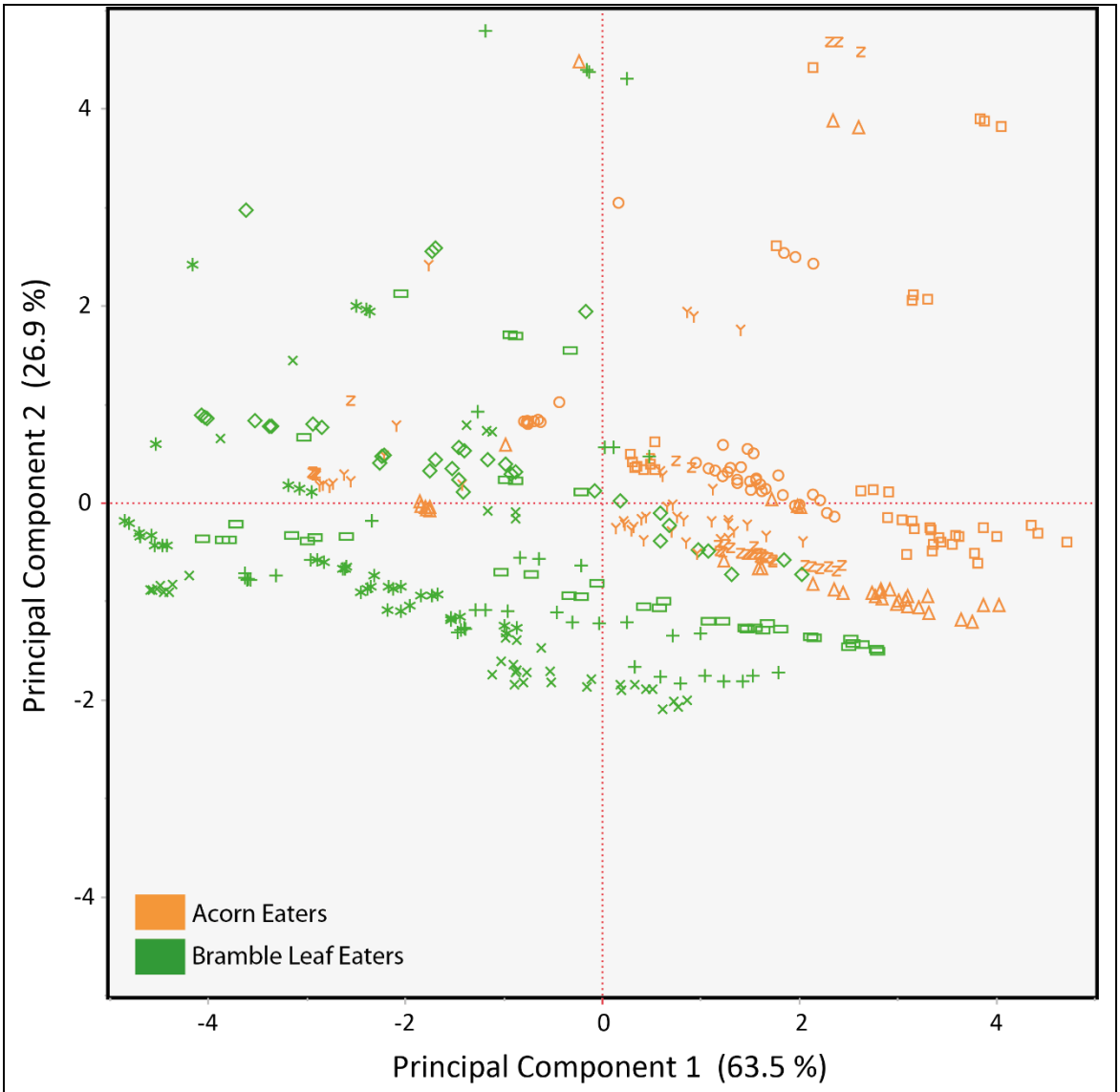

Figure 4.15 *PCA analysis comparing roughness parameter values between C.capreolus dietary groups. PCA is based on eight parameters (Sq, Sv, Sz, Sdq, Sdr, Vvv, Svk, and S5z, for parameter descriptions see Table 4.3). Parameter Data generated from each surface is included for all specimens. Points are coloured consistently by dietary group (Acorn eaters – Orange, Bramble Leaf Eaters – Green). Each specimen number is represented by a different symbol, consistent across all tests.*

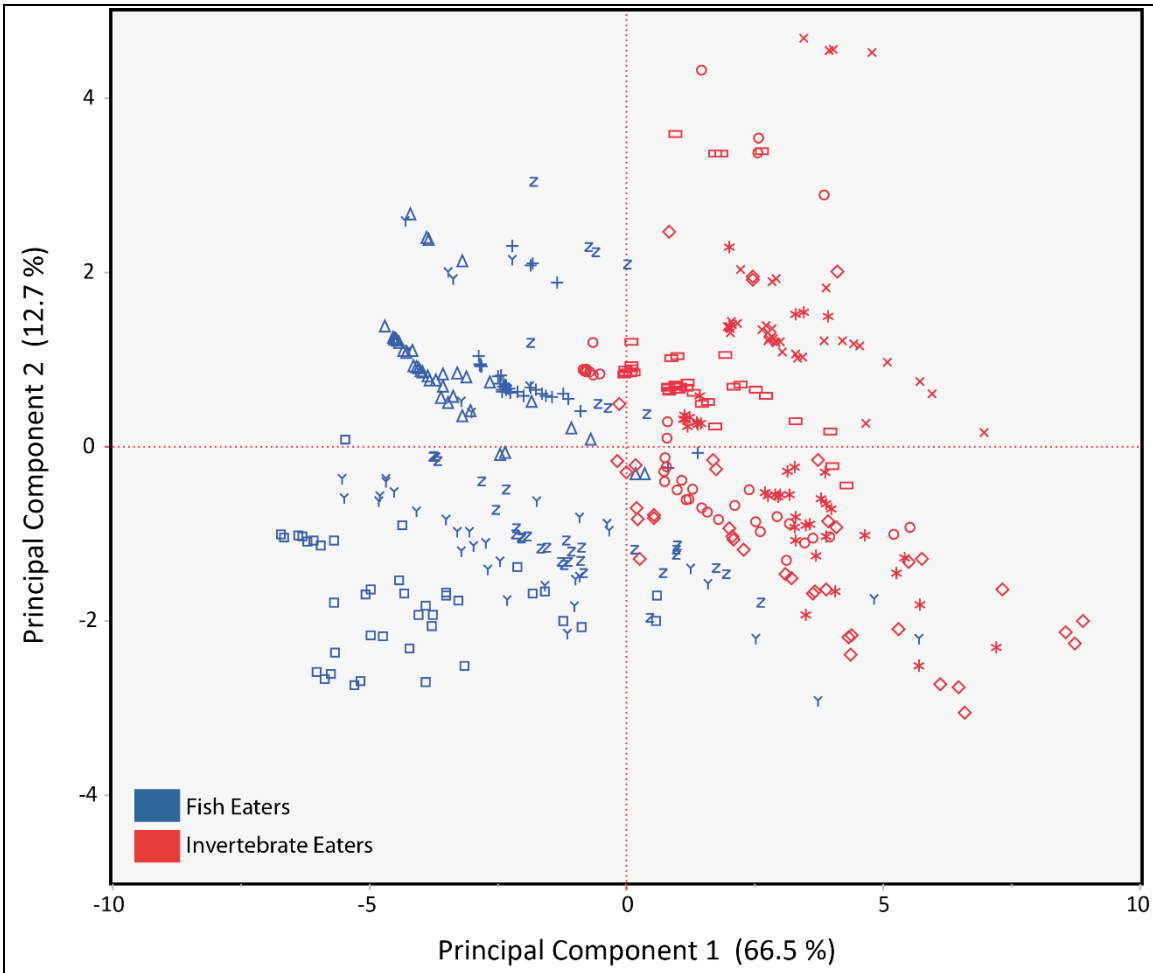

Figure 4.16 *PCA analysis comparing roughness parameter values between phocid dietary groups. PCA is based on sixteen parameters (Sq, Sp, Sv, Sz, Str, Sdq, Sdr, Vmp, Vmc, Vvc, Vvv, Spk, Sk, Svk, S5z, and Sa, for parameter descriptions see Table 4.3). Parameter Data generated from each surface is included for all specimens. Points are coloured consistently by dietary group (Acorn eaters – Orange, Bramble Leaf Eaters – Green). Each specimen number is represented by a different symbol, consistent across all tests.*

This supports the results of our earlier tests, where parameter values from surfaces scale limited using a 10^{th} or 11^{th} order polynomial were found to be different from all surfaces scale limited using different operators. Differences are also found when the same surface is scale limited using different filters. ANOVA tests between filter type and the position of points on each principal component show differences between surfaces treated using different filter types along both PC1 and

Phocids	Fish	ANOVA		Connecting Letters									
		F Ratio	p	2nd	3rd	4th	5th	6th	7th	8th	9th	10th	11th
	PC1 against Polynomial	1.1249	0.3608	A	A	A	A	A	A	A	A	A	A
	PC2 against Polynomial	**29.2450**	**<.0001***	C	C	C	C	C	C	C	C	B	A
	Invertebrates	**ANOVA**		**Connecting Letters**									
		F Ratio	p	2nd	3rd	4th	5th	6th	7th	8th	9th	10th	11th
	PC1 against Polynomial	1.7228	0.1048	A	A	A	A	A	A	A	A	A	A
	PC2 against Polynomial	**95.6308**	**<.0001**	C	C	C	C	C	C	C	C	B	A

Fish	Means									
	2nd	3rd	4th	5th	6th	7th	8th	9th	10th	11th
PC1 against Polynomial	-2.2043	-2.6697	-3.4808	-3.0964	-3.5125	-3.6534	-3.6066	-3.5678	-3.1534	-3.3215
PC2 against Polynomial	-0.9708	-0.8796	-1.0293	-0.8609	-0.8594	-0.9052	-0.8944	-0.5752	1.1747	2.9788
Invertebrates	**Means**									
	2nd	3rd	4th	5th	6th	7th	8th	9th	10th	11th
PC1 against Polynomial	2.7167	2.4823	2.3243	2.1765	1.9062	1.7607	1.4855	1.5144	1.4785	2.3837
PC2 against Polynomial	-0.7103	-0.5960	-0.5933	-0.4671	-0.3355	-0.2718	-0.2192	-0.0638	1.6775	4.6623

Roe Deer	Bramble Leaves	ANOVA		Connecting Letters									
		F Ratio	p	2nd	3rd	4th	5th	6th	7th	8th	9th	10th	11th
	PC1 against Polynomial	0.7585	0.6544	A	A	A	A	A	A	A	A	A	A
	PC2 against Polynomial	**32.7660**	**<.0001***	C	C	C	C	C	C	C	C	B	A
	Acorns	**ANOVA**		**Connecting Letters**									
		F Ratio	p	2nd	3rd	4th	5th	6th	7th	8th	9th	10th	11th
	PC1 against Polynomial	0.5022	0.8709	A	A	A	A	A	A	A	A	A	A
	PC2 against Polynomial	**17.7580**	**<.0001***	C	C	C	C	C	C	C	C	B	A

Bramble Leaves	Means									
	2nd	3rd	4th	5th	6th	7th	8th	9th	10th	11th
PC1 against Polynomial	-0.8921	-0.8782	-1.1875	-1.3075	-1.4781	-1.4682	-1.6492	-1.7000	-1.5431	-0.7992
PC2 against Polynomial	-0.9540	-0.9525	-0.8948	-0.8258	-0.7541	-0.7423	-0.6471	-0.4388	0.7929	3.1786
Acorns	**Means**									
	2nd	3rd	4th	5th	6th	7th	8th	9th	10th	11th
PC1 against Polynomial	1.3125	1.2847	1.3251	1.4422	1.3829	1.1356	0.9638	0.8885	1.1557	2.0121
PC2 against Polynomial	-0.3022	-0.3222	-0.2729	-0.2528	-0.2589	-0.2415	-0.1847	-0.0441	0.7255	3.3918

Table 4.11 *ANOVA results, Tukey tests, connecting letter reports, and group means for all four dietary groups, when comparing data generated for surfaces scale limited using different orders of polynomial against their position along PC1 and PC2. Principal component axis values are taken from PCA performed separately for each comparison of dietary groups (C.capreolus and phocids; Figure 4.15 and Figure 4.16). For the comparison of C.capreolus dietary groups 8 areal texture parameters were included (Sq, Sv, Sz, Sdq, Sdr, Vvv, Svk, and S5z), and for the comparison of phocid groups 16 were used (Sq, Sp, Sv, Sz, Str, Sdq, Sdr, Vmp, Vmc, Vvc, Vvv, Spk, Sk, Svk, S5z, and Sa, for parameter descriptions see Table 4.3). Significant ANOVA results are highlighted bold, and Welch test results from comparisons where variances were unequal are denoted with an *.*

Phocids

Position on PC1 against Polynomial Order				
	Fish		Invertebrates	
	Spearman's p	p	Spearman's p	p
Robust Gaussian	-0.1619	0.2614	-0.2111	0.1411
Robust Wavelet	**-0.4548**	**0.0009**	**-0.3834**	**0.0060**
Spline	0.1764	0.2205	0.1054	0.4662

Position on PC2 against Polynomial Order				
	Fish		Invertebrates	
	Spearman's p	p	Spearman's p	p
Robust Gaussian	**0.4089**	**0.0032**	**0.5329**	**<.0001**
Robust Wavelet	**0.4654**	**0.0007**	**0.5580**	**<.0001**
Spline	**0.4746**	**0.0005**	**0.5498**	**<.0001**

Capreolus capreolus

Position on PC1 against Polynomial Order				
	Bramble Leaves		Acorns	
	Spearman's p	p	Spearman's p	p
Robust Gaussian	-0.0191	0.8955	-0.1098	0.4479
Robust Wavelet	**-0.4220**	**0.0023**	-0.1923	0.1810
Spline	0.2179	0.1286	0.2154	0.1329

Position on PC2 against Polynomial Order				
	Bramble Leaves		Acorns	
	Spearman's p	p	Spearman's p	p
Robust Gaussian	**0.5879**	**<.0001**	**0.5556**	**<.0001**
Robust Wavelet	**0.6656**	**<.0001**	**0.5836**	**<.0001**
Spline	**0.5643**	**<.0001**	**0.6232**	**<.0001**

Table 4.12 *Spearman's rank correlation test results comparing parameter values from surfaces scale limited using different operators, against the position of points along PC1 and PC2. Principal component axis values are taken from PCA performed separately for each comparison of dietary groups (C.capreolus and phocids; Figure 4.15 and Figure 4.16). For the comparison of C.capreolus dietary groups 8 areal texture parameters were included (Sq, Sv, Sz, Sdq, Sdr, Vvv, Svk, and S5z), and for the comparison of phocid groups 16 were used (Sq, Sp, Sv, Sz, Str, Sdq, Sdr, Vmp, Vmc, Vvc, Vvv, Spk, Sk, Svk, S5z, and Sa, for parameter descriptions see Table 4.3). Significant results are highlighted in bold.*

PC2 (except for fish eating phocids, where there is only a difference between surfaces scale limited using different filters and their position on PC1, not PC2). Tukey HSD tests, connecting letter reports and group means show that the difference between surfaces scale limited using different filters along PC1 is the strongest signal (greatest difference in group means), and is consistent across all tests (Table 4.13), but not completely directional, in that data generated from surfaces scale limited using a spline filter will always be more negative than data generated using either of the other filters, but the relationship between surfaces scale limited using robust Gaussian and wavelet filters is not consistently directional. The opposite pattern is found when comparing surfaces scale limited using different filter types with their position on PC2. Here data generated from surfaces scale limited using a spline filter is consistently more positive on PC2 than data generated from surfaces when using either of the other filters. Finally, we carried out T-tests between data from surfaces scale limited using different nesting indices and the position of points on PC1 and PC2, within dietary groups (Table 4.14). The position of points on PC1 is always different for surfaces scale limited using different nesting indices. Data generated from surfaces scale limited using a 0.025mm nesting index are always more negative on PC1 than those generated from surfaces when using a 0.08mm nesting index. No pattern is evident on PC2 and no difference is found between data from surfaces scale limited using the two nesting indices on this axis. This suggests that, when comparing surfaces scale limited using different nesting indices, there are consistent biases in multivariate analyses.

Given that a number of studies only use filters with nesting indices, and not operators to scale limit surfaces (Dunford et al. 2012, Purnell et al. 2012, Nwaogu et al. 2013, Deltombe et al. 2014) it is important to understand whether the orders of polynomial are exaggerating the dietary difference between groups, and whether using just a filter and nesting index without an associated order of polynomial to scale limit surfaces is comparable in terms of its sensitivity to dietary differences. This was investigated by taking the same datafiles used in all tests above and applying only a filter with set nesting index (robust Gaussian, robust wavelet, and spline filters, with nesting indices 0.025mm and 0.08mm) to original data files, producing a new set of

scale limited surfaces. The 0.08mm nesting index was used in combination with all filter types here. ISO 25178-2 parameter data were generated from resulting scale limited surfaces using the same methods described for all other data. Normality of data was tested using Shapiro Wilks W tests and again log transformed data was found to be normally distributed, therefore parametric statistical tests were appropriate. T-tests were carried out between each pair of dietary groups, the results of which can be seen in Table 4.15. T-test results suggest that dietary groups can be separated without using a polynomial to scale limit surfaces.

Phocids		**Fish**		Connecting Letters			Means		
	ANOVA	F Ratio	p	Spline	Gaussian	Wavelet	Spline	Gaussian	Wavelet
	Position on PC1 against Filter	**56.6516**	**<.0001***	C	B	A	-4.3411	-2.9966	-2.3423
	Position on PC2 against Filter	2.5084	0.0850	A	A	A	0.0799	-0.4585	-0.4678
		Invertebrates		Connecting Letters			Means		
	ANOVA	F Ratio	p	Spline	Gaussian	Wavelet	Spline	Gaussian	Wavelet
	Position on PC1 against Filter	**109.9511**	**<.0001***	C	B	A	0.5441	2.5393	2.9853
	Position on PC2 against Filter	**5.9521**	**0.0033**	A	B	B	0.9789	-0.0308	-0.0232
Capreolus capreolus		**Bramble Leaves**		Connecting Letters			Means		
	ANOVA	F Ratio	p	Spline	Gaussian	Wavelet	Spline	Gaussian	Wavelet
	Position on PC1 against Filter	**183.5407**	**<.0001**	C	B	A	-3.2028	-0.6123	-0.0559
	Position on PC2 against Filter	**4.6151**	**0.0114**	A	B	B	0.2510	-0.4006	-0.5218
		Acorns		Connecting Letters			Means		
	ANOVA	F Ratio	p	Spline	Gaussian	Wavelet	Spline	Gaussian	Wavelet
	Position on PC1 against Filter	**337.9172**	**<.0001***	B	A	A	-0.8536	2.3421	2.3825
	Position on PC2 against Filter	**6.3180**	**0.0023**	A	B	B	0.7183	-0.0142	-0.0328

Table 4.13 *ANOVA results, Tukey test connecting letter reports, and group means for all four dietary groups, when comparing data from surfaces scale limited using different filter types based, against their position along PC1 and PC2. Principal component axis values are taken from PCA performed separately for each comparison of dietary groups (C.capreolus and phocids; Figure 4.15 and Figure 4.16). For the comparison of C.capreolus dietary groups 8 areal texture parameters were included (Sq, Sv, Sz, Sdq, Sdr, Vvv, Svk, and S5z), and for the comparison of phocid groups 16 were used (Sq, Sp, Sv, Sz, Str, Sdq, Sdr, Vmp, Vmc, Vvc, Vvv, Spk, Sk, Svk, S5z, and Sa, for parameter descriptions see Table 4.3). Significant ANOVA results are highlighted bold, and Welch test results from comparisons where variances were unequal are denoted with an *.*

Phocids	Fish				Invertebrates			
	T-test		Mean		T-test		Mean	
Test	T-Ratio	p	0.025	0.08	T-Ratio	p	0.025	0.08
PC1 against Nesting Index	**7.9878**	**<.0001**	-3.6815	-1.5299	**10.3142**	**<.0001**	1.5613	3.6501
PC2 against Nesting Index	-0.9787	0.3303	-0.1283	-0.3031	-1.4721	0.1443	0.3839	0.0475

Capreolus capreolus	Bramble Leaves				Acorns			
	T-test		Mean		T-test		Mean	
Test	T-Ratio	p	0.025	0.08	T-Ratio	p	0.025	0.08
PC1 against Nesting Index	**7.6168**	**<.0001**	-2.2983	-0.7390	**4.9062**	**<.0001**	1.2431	1.7942
PC2 against Nesting Index	-1.3292	0.1870	-0.0372	-0.4315	-0.6184	0.5378	0.3133	0.1554

Table 4.14 *T-test results and group means for all four dietary groups, when comparing data from surfaces scale limited using different nesting indices against their position along PC1 and PC2. Principal component axis values are taken from PCA performed separately for each comparison of dietary groups (C.capreolus and phocids; Figure 4.15 and Figure 4.16). For the comparison of C.capreolus dietary groups 8 areal texture parameters were included (Sq, Sv, Sz, Sdq, Sdr, Vvv, Svk, and S5z), and for the comparison of phocid groups 16 were used (Sq, Sp, Sv, Sz, Str, Sdq, Sdr, Vmp, Vmc, Vvc, Vvv, Spk, Sk, Svk, S5z, and Sa, for parameter descriptions see Table 4.3). Significant results are highlighted in bold.*

When comparing phocid dietary groups, surfaces scale limited using a robust Gaussian, or spline filter (and either 0.025mm or 0.08mm nesting index) show the same degree of difference as when also using an operator. When using a robust wavelet filter however there are far fewer parameters showing difference between the two groups, regardless of the nesting index used.

For comparisons of *C.capreolus* six parameters separate the dietary groups, lower than the maximum of 8 we find when an operator is also used to scale limit the surface. Again surfaces scale limited using a spline filter show high sensitivity to dietary difference, as do surfaces scale limited using a robust Gaussian filter with a 0.025mm nesting index. When using a robust Gaussian filter and a 0.08mm nesting index, or a robust wavelet filter with either nesting index setting, surfaces show very low sensitivity to dietary difference (2 parameters). Given that we expect at least one significant result by chance for every 20 tests, we would not consider this a clear

separation of dietary groups. In almost all cases the parameters showing difference between groups are the same ones found when using operators and filters to scale limit surfaces. This suggests that using an operator to scale limit surfaces does not cause random deviations in resulting parameter values. This idea is supported by PCA analyses (Figure 4.17), which are able to separate phocid dietary groups in almost all cases. When using a robust wavelet filter the separation is less good, but still obvious. However the same cannot be said for the multivariate analysis of *C.capreolus* dietary groups. Here separation between dietary groups is found along PC1, but only when a spline filter and a 0.025mm nesting index have been used to scale limit the surfaces. The separation is almost complete when using surfaces scale limited using a robust Gaussian filter and a 0.025mm nesting index, and there is a high degree of overlap between groups in multivariate space when using a robust wavelet filter to scale limit the surfaces.

Filter and Nesting Index		Population	Sq	Sku	Sp	Sv	Sz	Str	Sdq	Ssc	Sdr	Vmp	Vmc	Vvc	Vvv	Spk	Sk	Svk	S5z	Sa
Robust Gaussian	0.025mm	*Capreolus capreolus*	**0.0228**	0.3781	0.4892	**0.0277**	**0.0095**	0.6847	**0.0021**	0.7019	**0.0057**	0.4710	0.3040	0.6527	0.0833	0.3843	0.7493	0.0846	**0.0062**	0.0641
Robust Gaussian	0.08mm	*Capreolus capreolus*	0.8002	0.6394	0.9658	0.1418	0.1850	0.2851	**0.0036**	0.7847	**0.0085**	0.7408	0.8136	0.8631	0.6410	0.8731	0.7924	0.3836	0.1859	0.8748
Spline	0.025mm	*Capreolus capreolus*	**0.0249**	0.5208	0.6068	0.0654	0.1011	0.4454	**0.0025**	0.4435	**0.0070**	0.1596	0.2013	0.2778	**0.0056**	0.1952	0.3956	**0.0202**	**0.0353**	0.0948
Spline	0.08mm	*Capreolus capreolus*	0.3985	0.4595	0.8216	**0.0278**	**0.0288**	0.7301	**0.0033**	0.7339	**0.0085**	0.7872	0.6441	0.9117	0.1714	0.7506	0.9937	0.1185	**0.0339**	0.5744
Robust Wavelet	0.025mm	*Capreolus capreolus*	0.6518	0.8095	0.8316	0.2296	0.4890	0.2750	**0.0026**	0.6616	**0.0069**	0.6904	0.4736	0.8369	0.9246	0.7889	0.9450	0.9236	0.5904	0.9226
Robust Wavelet	0.08mm	*Capreolus capreolus*	0.6766	0.7735	0.8155	0.1384	0.1259	0.3801	**0.0033**	0.7862	**0.0084**	0.8996	0.6275	0.9540	0.7178	0.7815	0.9074	0.5132	0.1442	0.7251
Robust Gaussian	0.025mm	Phocids	**0.0003**	0.0816	**0.0030**	**0.0113**	**0.0016**	0.0624	**0.0111**	0.0832	**0.0124**	0.1686	**0.0006**	**0.0070**	**0.0012**	0.1303	**0.0031**	**0.0015**	**0.0002**	**0.0002**
Robust Gaussian	0.08mm	Phocids	**<.0001**	0.8183	**0.0041**	**0.0113**	**0.0011**	0.9783	**0.0097**	0.0785	**0.0110**	0.1065	**0.0011**	**0.0054**	**0.0057**	0.1243	**0.0050**	**0.0036**	**0.0003**	**0.0002**
Spline	0.025mm	Phocids	**0.0009**	0.1879	**0.0072**	**0.0021**	**0.0004**	**0.0298**	**0.0128**	0.0653	**0.0138**	**0.0157**	**0.0045**	**0.0084**	**<.0001**	**0.0117**	**0.0064**	**0.0002**	**<.0001**	**0.0018**
Spline	0.08mm	Phocids	**0.0006**	**0.0345**	**0.0017**	**0.0043**	**0.0015**	0.9156	**0.0103**	0.0861	**0.0112**	0.0564	**0.0004**	**0.0023**	**0.0016**	0.0651	**0.0010**	**0.0011**	**0.0004**	**0.0005**
Robust Wavelet	0.025mm	Phocids	**0.0091**	0.8949	0.0817	0.0787	**0.0208**	0.9647	**0.0101**	0.0657	**0.0110**	0.5366	**0.0010**	**0.0271**	0.2790	0.5112	**0.0084**	0.2923	**0.0119**	**0.0109**
Robust Wavelet	0.08mm	Phocids	**0.0181**	0.4008	**0.0171**	0.4974	0.0843	0.6148	**0.0097**	0.0776	**0.0107**	0.1899	**0.0009**	**0.0016**	0.3044	0.1876	**0.0014**	0.3096	**0.0337**	**0.0093**

Table 4.15 *T-test results comparing C.capreolus data from surfaces scale limited using only a filter and nesting index. Tests were carried out separately, across 21 areal texture parameters, for each combination of filter type, and nesting index applied to surfaces. Tests results have only been reported where significant results were recorded.*

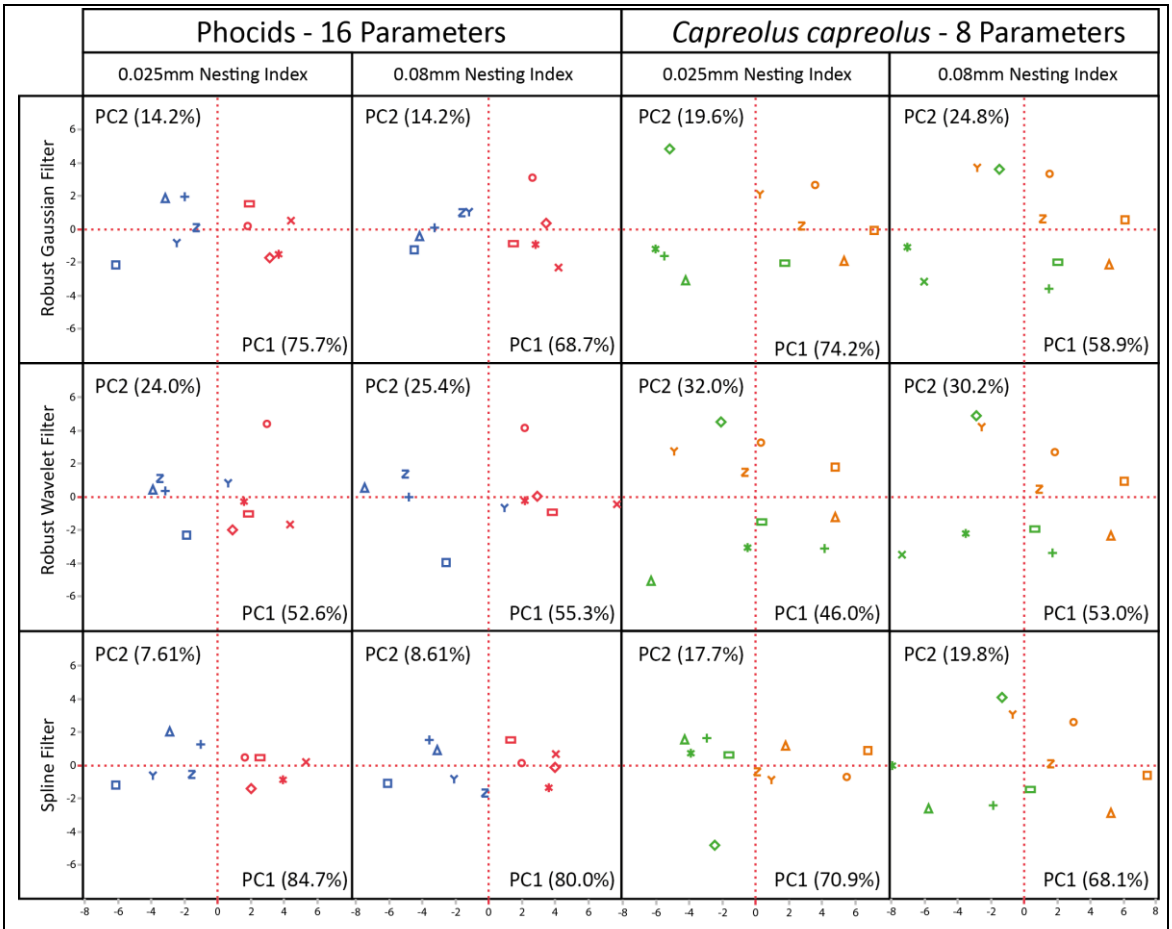

Figure 4.17 *PCA analyses comparing dietary groups, separately for Phocids and C.capreolus. Surfaces were only scale limited using a filter and nesting index, without a polynomial. Tests carried out separately for each surface. C.capreolus PCA is based on eight parameters (Sq, Sv, Sz, Sdq, Sdr, Vvv, Svk, and S5z), and Phocid PCA is based on sixteen (Sq, Sp, Sv, Sz, Str, Sdq, Sdr, Vmp, Vmc, Vvc, Vvv, Spk, Sk, Svk, S5z, and Sa, for parameter descriptions see Table 4.3). Points are coloured by dietary group (C.capreolus: Acorn Eaters – Orange, Bramble Leaf Eaters – Green; Phocids: Fish Eaters – Blue, Invertebrate Eaters – Red). Within each dietary group specimen numbers are represented by different symbols, consistently across all tests. Axes are consistent across PCA analyses within each dietary pair. Percentage of variance explained by each axes presented for all analyses.*

DISCUSSION

Scale limited surfaces generated using different combinations of operators and filters differ from one another, and in their ability to discriminate between dietary groups. However the effect of using different operators and filters on resulting parameter values is not consistent, and not all operators and filters show the same propensity to affect resulting areal roughness parameter values in the same direction or to the same magnitude. These effects also appear to be independent of one another in almost all cases. Differences between surfaces scale limited using different operators and filters are generally restricted to specific parameters, this suggests that the effect caused by varying operators and filters is not random, but consistently affects specific aspects of surface roughness.

Scale limiting surfaces using different operators leads to significant differences between resulting parameter values, meaning the null hypothesis that application of different polynomials (operators) to remove long wavelength elements of surface form has no effect on the texture of resulting surfaces (as measured by ISO 25178-2 texture parameters) must be rejected. Scale limiting surfaces using different operators almost always affects mean summit curvature for peak structures (Ssc), summit density (Sds), root mean square gradient of the surface (Sdq), and the developed interfacial area ratio of the surface (Sdr). Tukey tests show that these differences are restricted to surfaces scale limited using a 10^{th} or 11^{th} order polynomial to remove surface form. Less consistently, root mean square height of the surface (Sq), surface dale void volume (Vvv), and mean depth of valleys below the core material (Svk) also significantly differ between surfaces scale limited using these two operators. However these parameters are only affected when operators are combined with a robust wavelet filter, suggesting that treating surfaces with a combination of this filter and specific operators leads to further deviations in surface texture. Of those parameters affected, five are also found to be useful for separating dietary groups in dietary comparisons of both *C.capreolus* and phocids (Sq, Sdq, Sdr, Vvv, and Svk). As such changes in these parameters could lead to reduced sensitivity to dietary differences.

Varying the filter type used to scale limit surfaces also produces significant differences between the resulting areal roughness parameter values. This means the null hypothesis that application of different filter types (robust Gaussian, robust wavelet, and spline) has no effect on the texture of the resulting surface must also be rejected. It is clear from the ANOVA and Tukey HSD tests that where a spline filter has been used, the parameter values produced from scale limited surfaces are significantly different to those produced from surfaces treated with a robust Gaussian or robust wavelet filter. However, this difference is not consistent for any parameter across the whole range of dietary groups. This is mostly due to the very low level of difference between surfaces scale limited using different filter types within the phocid fish eaters, as the effect of varying the filter type used to scale limit surfaces is apparently much lower for this group. Among the remaining three dietary groups several parameters do consistently show differences between surfaces treated with different filter types. These include the root mean square height of the surface (Sq), the surface dale void volume (Vvv), the mean depth of valleys below the core material (Svk), and the average height of the surface (Sa). This indicates that spline filters often affect valley features when used to scale limit surfaces, compared to the effect of robust Gaussian or robust wavelet filters. Sq, Vvv, and Svk are also parameters useful for separating dietary groups in dietary comparisons of both *C.capreolus* and phocids, and Sa is shown to separate phocid dietary groups. As such changes in these parameter values could lead to a reduced sensitivity to dietary differences between populations. Differences between surfaces scale limited using different filter types were more prevalent within *C.capreolus* populations, returning consistent differences between surfaces for parameters associated with surface valleys. However care must be taken when making inferences from this result, as they are all parameters easily affected by individual valley structures.

There are also differences between resulting areal texture parameters when comparing 3D surfaces scale limited using different nesting indices. This means the null hypothesis that the application of filters with different nesting indices (cut-off wavelengths) has no effect on the texture of the resulting surface, must also be rejected. The use of different nesting indices appears to affect the root mean square

height of the surface (Sq) in most cases, but not when also using the highest orders of polynomial (operators) to scale limit the surface. No other parameter consistently shows differences between surfaces treated with different nesting indices. Differences are also restricted to those combinations of operator and filter including the lower orders of polynomial (variable depending on the dietary group). Within *C.capreolus* groups Sq is the only affected parameter that is also shown to separate dietary groups. Surfaces within the phocid populations are similarly affected, but here most parameters showing differences between surfaces treated with different nesting indices are also found to separate dietary groups. Therefore the variation in roughness parameters due to the application of different nesting indices appears likely to have a greater effect on the sensitivity to dietary differences between phocids. However this is to be expected due to the much greater number of parameters separating these dietary groups.

Use of the highest orders of polynomial (10^{th} and 11^{th}) appears likely to affect peak structures. The use of a spline filter appears to produce increases in the depth of valleys compared to surfaces scale limited using other filters (only consistent across three of the four dietary groups). We also find that varying the nesting index used to scale limit surfaces has an effect on the surface core material, however there is no consistent directionality in this effect. It is also clear that there is no interaction between the effect of different operators and filter types on surface texture, and there is very little interaction between the effect of operators and nesting indices on surface texture (and any effect is restricted to phocid data). This means the results of this paper support the null hypothesis that when applying different operators, filters, and filters with different nesting indices to a surface, there is no interaction in their effect on resulting texture parameters. With the clarification that there is a very small degree of interaction for a limited number of parameters within the phocid data.

The results presented here show the sensitivity of surfaces scale limited using different combinations of operator and filter to known dietary differences varies significantly. This means the hypothesis that application of different filters and operators has no effect on the power of areal microwear texture analyses to detect

dietary differences between samples must be rejected. Also, those surfaces showing the greatest sensitivity to separations between dietary groups do not necessarily show the greatest magnitude of difference between dietary groups. A comparatively low number of parameters are able to separate dietary groups when surfaces are scale limited using those operators with the lowest (2nd and 3rd) and highest (10th and 11th) orders of polynomial. When comparing *C.capreolus* dietary groups we find that using a robust Gaussian filter with a 0.025mm nesting index to scale limit surfaces results in the greatest comparability between parameters separating dietary groups, across all operators with which it is paired. The same is true when phocid tooth surfaces are scale limited using a spline filter with a 0.025mm nesting index. However, the magnitude of difference between dietary groups is consistently lowest when using a spline filter, even though the statistical difference is high (except for *C.capreolus* where the difference is relatively low when also using the highest and lowest orders of polynomial). Surfaces producing the greatest magnitude of difference are not comparable between phocid and *C.capreolus* dietary groups. For the latter the greatest magnitude of difference is found when using surfaces scale limited with a 5th or 6th order polynomial and a robust Gaussian filter (0.025mm nesting index), while for the former the greatest magnitude of differences is recorded between surfaces scale limited using either a 4th or 5th order polynomial with robust Gaussian filter and 0.08mm nesting index, or a 4th order polynomial, wavelet filter, and 0.025mm nesting index. There appears to be little difference in the ability of multivariate analysis (PCA) to separate dietary groups regardless of the surface in question. While the variance explained by each axis does vary, the ability of multivariate analyses to discriminate dietary groups does not appear to be highly affected by changing the operator and filter used to scale limit 3D surfaces.

In both the PCA analysis where all *C.caproelus* data is included, and the PCA analysis where all phocid data is included, there is a directional correlation between the position of points on PC2 and the operator used to scale limit surfaces. This corresponds to a positive linear shift in parameter values for only those surfaces scale limited using a 10th or 11th order polynomial. As this shift is along PC2, which is not the axis of dietary separation, this effect has little impact on the ability of multivariate

analyses to distinguish dietary groups. So, even though the effect of these high orders of polynomial appears to be detrimental, it is unclear whether these settings alone would actually effect the sensitivity of subsequent multivariate analyses to separate dietary groups. However there is also a linear directional change in the position of points on PC1 depending on the filter type used to scale limit the surface. Those surfaces scale limited using a spline filter always plot more negatively on this axis than surfaces scale limited using any other filter type. Additionally we find a difference between robust wavelet and robust Gaussian filter types on PC1, but this is not directionally consistent. Varying the nesting index used to scale limit surfaces appears to produce a similar pattern along PC1, with those surfaces scale limited using a 0.025mm nesting index consistently plotting in a more negative position to those scale limited using a 0.08mm nesting index. As these differences are found along PC1, which is the main axis of dietary separation, significant reductions in sensitivity to dietary differences are much more likely if data from surfaces scale limited using two different settings are compared.

The absolute comparability of data and the sensitivity of tests to dietary differences are obviously affected by the operator and filter chosen to scale limit surfaces. Therefore comparing data generated using different scale limiting settings generally appears to be unwise. Spline filters, and 0.08mm nesting indices produce surfaces with significantly different roughness parameter values to surfaces generated using all other filters (when the same operator is used). There is a lack of comparability between surfaces scale limited using a 10^{th} or 11^{th} order polynomial and all surfaces scale limited using other operators. When performing dietary analyses we find that surfaces scale limited using either wavelet filters or 0.08mm nesting indices produce highly variable results. We also find that when spline filters are used the lowest magnitude of difference between dietary groups is recorded, however surfaces are still highly sensitive to dietary differences. Surfaces scale limited using a robust Gaussian filter and 0.025mm nesting index produce parameters with high consistency in their sensitivity to differences between dietary groups regardless of the operator used (excluding 10^{th} and 11^{th} order polynomials). Surfaces scale limited with this filter also produce the greatest number of parameters separating dietary groups, and the

greatest magnitude of difference between dietary groups (when comparing *C.capreolus* populations). As such it is possible to make certain inferences from these results about comparability and suitability of different settings to areal texture analysis.

From a combination of direct comparisons of parameter values and sensitivity to dietary differences in both statistical testing and multivariate space, it appears advisable not to use a 0.08mm nesting index, and 10^{th} or 11^{th} order polynomial to scale limit 3D surfaces. It also appears that the robust wavelet filter is not consistent when separating dietary groups, depending on the operator with which it is combined, and in multivariate space produces differences from surfaces scale limited using a robust Gaussian filter, in a non-linear direction. Therefore, parameters generated from surfaces scale limited using this filter would not be comparable to data generated from surfaces where other filters had been used. While a spline filter produces significantly different parameter values to those of other filter types, and in multivariate space produces data that is consistently more negative than other filter types, it is harder to dismiss this filter for use in areal texture analysis as surfaces it produced return a high number of parameters separating dietary groups, in line with the best performing settings. However surfaces scale limited using a robust Gaussian filter produce much higher magnitudes of difference, and highly consistent separation when comparing dietary groups, regardless of the operator with which it was combined (excluding 10^{th} and 11^{th} order polynomials). As such the results of this chapter would suggest the use of a robust Gaussian filter with a nesting index of 0.025mm for all future areal surface texture analyses. Data generated from surfaces scale limited using this filter should also be relatively comparable with any surfaces scale limited using the same filter and nesting index combined with a number of different operators (2^{nd} to 7^{th} order polynomial). However surfaces scale limited using a 6^{th} order polynomial combined with a robust Gaussian filter and 0.025mm nesting index separates dietary groups in the greatest number of parameters, and in the case of *C.capreolus* populations produces the greatest magnitude of difference between dietary groups, making this combination of settings ideal for future studies using areal texture analysis.

Chapter 5: Testing the Effect of Different Instruments Used to Collect 3D Microtextural Data from Tooth Surfaces

Abstract

Quantitative analysis of 3D tooth surface texture is now a widely used technique for testing hypotheses of dietary difference between populations (extinct or extant). This technique requires the use of a suitable microscope/instrument to capture 3D surface data, from which roughness parameters are calculated via two separate automated methods. Many different groups of vertebrates have now been studied using 3D tooth surface texture data and the comparability of these studies is becoming more important. However several models of microscope/instrument, including several different technologies are employed for this purpose. While some work has been done to compare microscopes, no study has yet compared how different models and technologies replicate surfaces using the full suite of roughness parameters utilised for quantitative analysis of 3D tooth surface texture. Here it is shown that data files generated using different microscope models and technologies can produce very different results. Quantitatively comparing roughness parameters generated from data files collected using different microscopes, it was found that significant differences exist when scanning exactly the same location on a surface. And while data collected from each microscope produces correlated roughness parameter values there are big differences between the effects on different surface parameterisation methods. We also show that these differences appear to affect the results of dietary analyses, using specimen sets from previously published 3D tooth surface texture analyses. In each case resampling data to the lowest µm/pixel and field size across all data files collected from each microscope has little effect on this difference. Our results show how differences in methodologies can have a profound impact on the results of subsequent analyses. This has wide reaching implications for the comparability of studies using 3D surface texture data, and further work is needed to explore the reasons behind these differences and methods for reducing their impact on comparability.

Introduction

In any discipline, understanding the variability potential of analytical techniques is of vital importance. This is even more important for newer techniques, where a greater number of variables have the potential to affect analyses. And any variability in analytical techniques will obviously affect the comparability of studies carried out in the same field using different methods.

Quantitative analysis of 3D tooth surface textures (also known as Dental Microwear Texture Analysis; DMTA) (Calandra and Merceron 2016) is a relatively new technique. Developed in 2003 (Ungar et al. 2003) and advanced in 2006 (Scott et al. 2006), it has been widely applied to populations where dietary differences have been hypothesised, especially fossil hominids (Ungar et al. 2008, Merceron et al. 2009, Ungar et al. 2010, Ungar and Sponheimer 2011), but also in many other groups, both extinct and extant (Schubert et al. 2010, Haupt et al. 2013, Gill et al. 2014, Merceron et al. 2014). This technique measures the patterns of wear on tooth surfaces, caused by the interaction of teeth and food items to determine differences in diet between populations. This is based on surface roughness, which is assessed using two main parameterisation methods, Scale Sensitive Fractal Analysis (SSFA) (Ungar et al. 2003, Scott et al. 2006), and an International Standards approach using areal surface texture parameters (ISO 25178-2) (International Organization for Standardization 2012). Tooth surfaces are imaged using non-contact optical microscopy techniques, producing a 3D surface topography of the area of interest from which parameters can be calculated, explaining the texture of the surface. Originally 3D microtextural analysis of tooth surface textures was developed using confocal microscopy (tandem laser scanning, and white light) (Ungar et al. 2003, Scott et al. 2005, Scott et al. 2006). This technique has continued to be used in a wide range of studies, using either white light scanning confocal profilometers (e.g. Merceron et al. 2009, Ungar et al. 2010, Delezene et al. 2013, DeSantis and Haupt 2014), or a confocal disk scanning 3D surface measurement system (Schulz et al. 2010, Calandra et al. 2012, Schulz et al. 2013a, Winkler et al. 2013, Gailer et al. 2016). However other surface measurement technologies have now been applied to dietary analyses using tooth surface roughness. Focus variation

microscopy has been used to collect data in a number of studies investigating dietary hypotheses in terrestrial (Purnell et al. 2013, Gill et al. 2014), and aquatic vertebrates (Purnell et al. 2012, Purnell and Darras 2015). And interferometric approaches have also been applied to studies of dental microwear (Estebaranz et al. 2007, Merceron et al. 2014). As such understanding the variability in surface texture recorded by each of these methods is vital to understanding the comparability between different studies.

3D surface texture measurement has also been applied in other fields, including traffic wear on road stones (Dunford et al. 2012), surface roughness on castings (Nwaogu et al. 2013), and wear on axe heads as part of an archaeological study (Dolfini and Crellin 2016) which all used focus variation microscopy. Confocal microscopy has been used to investigate lithic microwear on stone tools (Evans et al. 2014), engineered surfaces (Jordan et al. 1998), and on dental ceramics (Al-Shammery et al. 2007), and Interferometry has been used to investigate roughness on semi-conductor wafers (Blunt 2006), and the roughness of grinding wheels (Yan et al. 2011). These are just examples and many more studies have been carried out using these techniques.

Laser, white light scanning, and disk scanning confocal profilometry all employ confocal microscopy, which uses point illumination and an optically conjugate plane, with a pinhole in it, to prevent out of focus signal reaching the detector. The detector can therefore only receive reflected light from close to the focal plane, improving the optical resolution compared to microscopes with wide-field detectors (Webb 1996). Focus variation microscopy by comparison uses multiple optics of different objectives (lens systems) providing measurements at different resolutions. Light emerging from a source is projected into the optical path via a beam splitting mirror, and the objective focuses it onto the specimen, with reflected light caught by a sensor placed behind the beam splitting mirror. Data is captured continually as the optic moves vertically bringing different elements of the surface into focus (Danzl et al. 2011). Interferometry involves splitting a beam of light into two, reflecting one off the surface to be measured and passing the other along a known constant path. Both beams are then passed through another splitter which combines them creating an interference pattern, which is magnified and picked up by a sensor. By moving the objective lens

vertically a point of greatest brightness can be achieved, and as this point is known, the surface form can be mapped (Blunt 2006). However interferometry suffers from not being able to replicate surfaces with a high degree of slope, something often present on tooth surfaces. All of these methods use white light, but in most cases different microscopes, even different models which use the same technology will collect data using different field sizes (the area of data being collected), and different sampling resolutions.

Several studies have already been carried out to investigate the effect of using different instruments to collect surface data. Many are simply comparisons of how well classical stylus profilometry, where a physical stylus is drawn across a surface to measure profiles, compares to optical surface profilometry (Vorburger et al. 2007, Jouini et al. 2009, Heurich et al. 2010, Passos et al. 2013). Or investigate variation between optical instruments where resulting data is assessed manually, such as when studying the thickness of enamel/dentin from transverse tooth sections (Schwendicke et al. 2014). However two recent studies have gone further and compared the variability between different optical non-contact instruments using surface texture parameters associated with DMTA.

(Tosello et al. 2016) studied the effect of using multiple optical instruments to measure polymer artefacts, characterising surface roughness using areal texture parameters (ISO 25178-2). Sixteen instruments were used across thirteen laboratories, investigating all microscope technologies described above, and found that some agreement between confocal microscopy/interferometry instruments and a reference surface measured using atomic force microscopy could be reached, so long as certain guidelines were followed and the performance characteristics of each instrument were understood. However they also found that focus variation microscopy performed very poorly compared to other techniques due to the very low roughness values on the measured surfaces. While this study is important and highlights issues with comparisons of optical surface measurements to reference surfaces, it is of limited use to the issues faced in dietary analyses using these same techniques. Firstly for DMTA it is not a question of whether each microscope compares well to a reference plane, but

whether each optical microscope produces data comparable to other optical microscopes. Secondly their study used only three areal texture parameters, whereas this chapter is interested in the effect of different microscopes on a much wider range of parameters (24 x ISO 25178 parameters; 14 x SSFA parameters). Finally the surfaces Tosello et al (2016) are testing have very low roughness (flat polymer surfaces), which is not comparable to the type of data collected for DMTA, where roughness is much greater and surface texture more variable.

A recent study by Arman et al. (2016) has approached the effect of variable microscopes in a way that corresponds to the type of data expected in DMTA. Here the authors investigated the effect of using multiple, different confocal microscopy instruments, most made by the same company (Solarius, Inc., San Jose, CA, USA). Four extant, and one extinct, kangaroo (Marsupialia: Macropodoidea) species were used, and differences in tooth texture between these species were based on dietary interpretations from a range of sources, including gut and faecal contents, stable isotopes, and ecological observation. Multiple instruments were used to scan identical regions of tooth surfaces, and agreement between resulting data was statistically compared. Two SSFA parameters were used in this study, measuring the anisotropy and complexity of the scanned tooth surfaces. It was found that most microscopes did not agree, displaying significant differences in resulting texture parameters. But that agreement could be produced by processing data using surface filters (polynomial order operators, and spline, Gaussian and robust Gaussian filters). This paper is the first evidence that differences between microscopes used to collect 3D surface data for dietary analyses can produce significantly different results, and as such begins to address questions of comparability between methods. However a number of issues with the methodologies used in this publication mean that some of the results could be suspect. The samples they have used include a range of dietary habits within kangaroo species, but are based on a continuum of dietary difference, rather than specifically different food items, this means that any difference may be obscured by the noise between groups. Also the specimens in question have not previously been studied using any DMTA techniques, meaning the authors cannot know what result comparing their diet using these techniques would have, this in turn means that the

assumption underpinning their study is not based on the same data being used. Also the use of only two parameters from the fourteen possible means it is difficult to know how this result effects the full range of SSFA parameters, and impossible to know how it will effect ISO parameters (they do make clear that this must be studied in further work). The paper focusses only on confocal microscopy, and while it is interesting to know how differences in microscope model (using the same technique) can drastically alter surface texture measurements, it is important to understand how this pattern compares to a wider range of technologies. Finally in performing this study the authors also add some variables to the analysis that should otherwise be controlled, such as data transformation (they have used multiple transformation types but not consistently across all microscopes), and sample sizes (due to differing performance of microscopes some were able to scan more samples than others). Therefore, while this study opens up the problem of differences between microscopes a great deal of further work is needed to understand the true pattern of difference between microscopes, using a greater range of microscopy techniques and surface roughness parameters, and much greater controls on variables, especially with a focus on using datasets previously studied via DMTA so that expected outcomes are already known.

Here is presented the first study comparing the effect of using different microscope technologies to collect quantitative surface roughness data from specific repeatable areas of tooth surfaces, sourced from populations with known dietary difference, previously studied using DMTA techniques. The aim is to apply three microscope technologies, confocal microscopy, focus variation microscopy, and point autofocus microscopy (which is akin to stylus profilometry, but carried out using a non-contact laser method, scanning surfaces as profiles every 0.1µm, which are then processed into a 3D surface by software algorithms). It was unfortunately not possible to include Interferometry in this study, due to its inability to accurately replicate surfaces with moderate slopes, and the time constraints on this study. Two confocal microscopes have been included (both used by Arman et al. (2016)) to test the relative difference between microscopes using the same technique, and different technologies to capture 3D data. This paper will compare both the absolute difference between data generated from each microscope, and how the use of different microscopes

affects the results of dietary analyses, which have an expected outcome. These effects will also be tested on different types of diet and tooth interaction.

This paper aims to test a number of hypotheses:

- That using different microscopes/instruments to collect 3D tooth surface data will result in significantly different roughness parameter values (ISO 25178, and SSFA) recorded from resulting surfaces.
- That any differences in 3D texture produced by using different microscopes/instruments are caused in large part by the effect of each microscope collecting data at different sampling resolutions and field size, thus resampling datafiles collected from each microscope down to the lowest µm/pixel value across all microscopes and then reducing the field of view to the lowest across all microscopes will eliminate this difference.
- That when comparing dietary groups with known variation in the texture of their tooth surfaces, the sensitivity of data collected using different microscopes varies in its ability to detect this variation, so that certain microscopes are more sensitive than others to significant textural differences.
- That any differences between the sensitivity to dietary differences of data collected using different microscopes/instruments are eliminated by resampling the data down to the lowest µm/pixel resolution and field size.

Methods

Materials

In order to test the hypotheses set out by this paper two populations of specimens were selected. Each population contained two groups with known differences in surface texture (based on the results of previously published studies). In each case the difference in texture is related to a dietary difference between populations. A full list of all specimens used in this paper can be seen in Table 5.1.

The first population contains two groups of *Capreolus capreolus* (roe deer, Cervidae; Artiodactyla) originally published in (Merceron et al. 2010) where textural differences were found between groups using Scale Sensitive Fractal Analysis (SSFA). Both dietary groups in this population were collected from the Dourdan Forest (Ile de France, France), in February (winter) 1989, and are held by the Institut National de la Recherche Agronomique (INRA) (Toulouse, France). One dietary group is made up of males (n=5), and one of females (n=5). The male population is known to eat a much higher proportion of acorns in winter than females, leading to greater complexity and heterogeneity of texture on their tooth surfaces. Females are known to eat a much higher proportion of bramble leaves than males in winter leading to greater levels of anisotropy on their tooth surfaces. From each specimen a single tooth was selected from the jaw. In all cases this was Molar position two (M2), as per the methods of Merceron et al. (2010). For nine of the ten specimens M2 was selected from the upper left jaw. For one specimen no upper left jaw was available, therefore the lower left M2 was used instead. From all teeth data were collected from shearing facet one (Scott et al. 2006, Merceron et al. 2010). These facets connect between shearing facet one on upper and lower teeth retaining the same dietary signal for both upper and lower M2.

The second population contained two *Archosargus probatocephalus* (sheepshead seabream, Sparidae; Perciformes) dietary groups. These specimens were published in Purnell and Darras (2015), where areal texture parameters were used to test for textural differences between populations based on the degree to which they engaged in durophagy. Specimens were collected from the Indian River Lagoon, Florida, USA: The first population (IR-herb, n=5) was collected from the southern area of the lagoon, and the second (PC-duro, n=5) from the northern area (close to Port Canaveral). The PC-duro population is known to consume a much greater proportion of hard shelled prey than the IR-herb population, this leads to greater values for a number of textural parameters on their tooth surfaces. *Archosargus probatocephalus* teeth are all molariform and domed in shape, they do not have specific positions, do not occlude, and vary in size and number between individuals. As such for all specimens the most worn tooth in the right maxilla was used.

Specimen Number	Species	Tooth Used	Collection Location	Gender	Diet	Collection	Date of Death
INRA 001 126 T	*Capreolus capreolus*	Upper M2 left	Massif de Dourdan, France	Female	Bramble Leaves	INRA Toulouse, France	01/02/1989
INRA 002 000 T	*Capreolus capreolus*	Upper M2 left	Massif de Dourdan, France	Female	Bramble Leaves	INRA Toulouse, France	02/02/1989
INRA 006 089 T	*Capreolus capreolus*	Upper M2 left	Massif de Dourdan, France	Female	Bramble Leaves	INRA Toulouse, France	07/02/1989
INRA 008 076 T	*Capreolus capreolus*	Upper M2 left	Massif de Dourdan, France	Female	Bramble Leaves	INRA Toulouse, France	08/02/1989
INRA 014 000 T	*Capreolus capreolus*	Lower M2 Left	Massif de Dourdan, France	Female	Bramble Leaves	INRA Toulouse, France	13/02/1989
INRA 004 108 T	*Capreolus capreolus*	Upper M2 left	Massif de Dourdan, France	Male	Acorns	INRA Toulouse, France	03/02/1989
INRA 007 109 T	*Capreolus capreolus*	Upper M2 left	Massif de Dourdan, France	Male	Acorns	INRA Toulouse, France	08/02/1989
INRA 009 085 T	*Capreolus capreolus*	Upper M2 left	Massif de Dourdan, France	Male	Acorns	INRA Toulouse, France	09/02/1989
INRA 012 000 T	*Capreolus capreolus*	Upper M2 left	Massif de Dourdan, France	Male	Acorns	INRA Toulouse, France	13/02/1989
INRA 013 019 T	*Capreolus capreolus*	Upper M2 left	Massif de Dourdan, France	Male	Acorns	INRA Toulouse, France	13/02/1989
SH-IR-01	*Archosargus probatocephalus*	Right Maxilla Worn Tooth	Southern Indian River Lagoon	-	Herbivorous	University of Leicester, UK	-
SH-IR-02	*Archosargus probatocephalus*	Right Maxilla Worn Tooth	Southern Indian River Lagoon	-	Herbivorous	University of Leicester, UK	-
SH-IR-03	*Archosargus probatocephalus*	Right Maxilla Worn Tooth	Southern Indian River Lagoon	-	Herbivorous	University of Leicester, UK	-
SH-IR-04	*Archosargus probatocephalus*	Right Maxilla Worn Tooth	Southern Indian River Lagoon	-	Herbivorous	University of Leicester, UK	-
SH-IR-05	*Archosargus probatocephalus*	Right Maxilla Worn Tooth	Southern Indian River Lagoon	-	Herbivorous	University of Leicester, UK	-
SH-IR-06	*Archosargus probatocephalus*	Right Maxilla Worn Tooth	Southern Indian River Lagoon	-	Herbivorous	University of Leicester, UK	-
SH-PC-01	*Archosargus probatocephalus*	Right Maxilla Worn Tooth	Northern Indian River Lagoon	-	Durophagus	University of Leicester, UK	-
SH-PC-02	*Archosargus probatocephalus*	Right Maxilla Worn Tooth	Northern Indian River Lagoon	-	Durophagus	University of Leicester, UK	-
SH-PC-03	*Archosargus probatocephalus*	Right Maxilla Worn Tooth	Northern Indian River Lagoon	-	Durophagus	University of Leicester, UK	-
SH-PC-04	*Archosargus probatocephalus*	Right Maxilla Worn Tooth	Northern Indian River Lagoon	-	Durophagus	University of Leicester, UK	-
SH-PC-05	*Archosargus probatocephalus*	Right Maxilla Worn Tooth	Northern Indian River Lagoon	-	Durophagus	University of Leicester, UK	-
SH-PC-06	*Archosargus probatocephalus*	Right Maxilla Worn Tooth	Northern Indian River Lagoon	-	Durophagus	University of Leicester, UK	-

Table 5.1 *Full specimen list, including all specimen numbers, taxonomic information, teeth used, collection locations, gender (where known), dietary categories, host institutions, and date of death (where known).*

These two specimen sets represent very different dentitions (heterodont occlusal versus homodont non-occlusal), feeding modes, and terrestrial versus aquatic feeding environment. These specimens were chosen specifically to make the results of this paper applicable to as wide a range of dietary studies as possible.

Specimen Preparation and Data Collection

In order to control as many variables as possible, all specimens (both *Capreolus capreolus* and *Archosargus probatocephalus*) were prepared in exactly the same way. This involved cleaning the tooth surfaces using cotton buds, acetone, and a pressurised air canister. The cotton buds were dipped in acetone, which was then carefully applied to tooth surfaces, to remove dirt, dust and any other particles that could affect tooth surface texture. Once dry compressed air was blown over tooth surfaces to remove any loose remaining dirt.

Moulds of all teeth were then taken using a polyvinylsiloxane dental impression media (President Jet Regular Body, Coltène Whaledent). This moulding compound has been shown to produce highly accurate and precise replicas of tooth surfaces (Goodall et al. 2015). The first mould taken from each tooth was discarded as a "cleaning mould". The second mould was kept and used to test our hypotheses. All moulds were applied as per manufacturer's guidelines, using an applicator gun which automatically mixes the two parts of the moulding compound by extruding them through a helical nozzle. This process produced negative moulds of the tooth surfaces. Positive casts were produced from resulting moulds using an epoxy resin containing a black pigment (Epotek 320LV). While setting, casts were pressurised to 2Bar (30psi) in a Protima Pressure Tank (10L, no agitator) for approximately 24 hours. This process reduces the size of any bubbles in the resulting casts. After casts were removed from moulds they were gold coated using an Emitech K500X sputter coater for four minutes, to optimise data acquisition across all microscopes used in this paper and provide a consistent surface, measurable by all instruments. This has been shown to produce no difference from original surfaces (Appendix 2: Supplementary Chapter).

Gold coated casts were mounted on an epoxy putty base (Milliput® standard yellow-grey, The Milliput Co.). This putty is made by mixing two parts in equal measure to produce a yellow compound which sets over 24 hours. Once mixed, casts were imbedded in the putty under a stereoscopic light microscope and then left to set. This process allowed specimens to be imbedded with the area of interest on each tooth positioned horizontally, which means data could be collected on each microscope from teeth with identical horizontal positioning. When completely set, marks were made on the putty base, which could be aligned identically on each instrument, allowing data to be collected from exactly the same orientation across all instruments. Finally, data areas were imaged as 2D photographs at 100x, 50x, 20x, 10x, and 5x magnification, producing a set of images from which sample areas could be replicated across all instruments.

Data Acquisition

3D surface data were collected using four different microscope models, comprising three different data collection methods. The first method was Focus Variation Microscopy (FVM), which was carried out on an Alicona Infinite Focus Microscope (Department of Geology, University of Leicester, Leicester, UK; model IFM G4c), for this instrument data collection followed previously published methods from Purnell et al. (2013), Gill et al. (2014), Purnell and Darras (2015) (x100 objective, field of view of 145 x 110 µm, vertical resolution set to 0.02 µm, lateral optical resolution 0.44 µm). The second method was White Light Scanning Confocal Profilometry (WLSCP), carried out on two instruments, a Sensofar model Plµ, and a Sensofar model Plµ neox (University of Arkansas, Anthropology Department, Arkansas, USA, Solarius, Inc.). For the Sensofar Plµ data was collected at 100x objective, field of view 140 x 103 µm, vertical resolution 0.005 µm, lateral optical resolution 0.18 µm. For the Sensofar Plµ neox data was collected at 100x resolution, field of view 128 x 96 µm, vertical resolution 0.001 µm, and lateral optical resolution 0.17 µm. This generally followed the methods of previous studies (Scott et al. 2006, Arman et al. 2016), however to match our data collection on the Alicona IFM, rather than collect a stitched/patched file made of four connected data files, a single data file was instead collected on both

instruments at the given field sizes. The final method was Point Autofocus Microscopy (PAFM) carried out on a Mitaka microscope/probe (Department of Mechanical, Materials and Manufacturing Engineering, University of Nottingham, Nottingham, UK; Mitaka model MLP-3SP). On the Mitaka PAFM data was collected at 100x resolution, field of view 160 x 120 µm, lateral resolution 0.1 µm.

Data were collected from specific locations on the surface of each tooth. These locations were replicated across all four microscopes, using the marks on putty bases to orientate specimens, and photographs of surfaces at multiple resolutions to replicate areas. Resulting datafiles were exported into the software package MountainsMap® Premium version 7.2.7368 (www.digitalsurf.com). This allowed all following processes to be standardised across files from all four microscopes. Datafiles were first levelled using an all points levelling system (fit to a least squares plane via rotation around all three axes). This accounted for any error in horizontal mounting of the specimens on putty bases. Each data file from the two Sensofar Microscopes is made up of a topography layer and an intensity layer, the topography layer alone was extracted for use in our analyses (matching the format of files from both other instruments). Any errors on the surface were manually edited using a 1 x 1 µm tool to replace errors with non-measured data points. Non-measured data points were then filled using a smooth shape calculated from neighbouring points. It has been shown that filling non-measured points reduces differences between raw files extracted topography layers when using Sensofar microscopes (Arman et al. 2016). All data files were again levelled using the same method as above and exported as .sur files. These files were classed as Non-Resampled Datafiles and had different vertical and lateral resolutions, and fields of view, based on the settings used for each microscope.

Surface texture parameters were generated from Non-Resampled Datafiles using two parameterisation methods. The first was areal texture parameters ISO 25178-2 (International Organization for Standardization 2012), for this method datafiles were imported into the program Surfstand (software version 5.0.0). Surfaces were scale limited using a 6^{th} order Polynomial and a Robust Gaussian Filter with a nesting index of 0.025mm. This removes the large scale waviness of the surface,

leaving only the roughness surface with a maximum feature wavelength defined by the nesting index. 24 ISO 25178 parameters were generated from the resulting surfaces (Table 5.2, for more detailed parameter descriptions see Purnell et al. (2013), and Gill et al. (2014)). Parameters Std (surface texture direction), and Sal (surface autocorrelation length) returned almost identical values for all surfaces and so were excluded from analyses. The second parameterisation method was Scale Sensitive Fractal Analysis (SSFA), for which surfaces do not need to be scale limited (Ungar et al. 2003, Scott et al. 2006). SSFA quantifies five aspects of surface roughness (Table 5.3) in 14 parameters. To generate SSFA parameters datafiles were imported into the programs SFrax and Toothfrax (Surfract, www.surfract.com). Settings followed those used in previous work (Scott et al. 2006), including the use of scale-sensitive "auto splits" to record Surface Heterogeneity (HAsfc), separating individual scanned sections into increasingly reduced sub-regions (we calculated HAsfc across ten different subdivisions). Parameter epLsar (exact proportion length scale anisotropy of relief) was calculated separately for data from each microscope using a scale of observation one order of magnitude greater than the lateral sampling resolution of the microscope in question (e.g. data from Sensofar Plμ neox lateral sampling resolution = 0.17 μm, therefore epLsar setting = 1.7 μm). Parameter Smc (scale of maximum complexity) was excluded from further analysis as it almost always returned the same parameter values for files collected on the Alicona IFM.

All datafiles were duplicated and resampled to the same lateral resolution and field size, using the program Gwyddion (version 2.42; http://gwyddion.net). Each file was down-sampled using linear interpolation to the coarsest μm/pixel resolution across all four microscopes (0.18 μm; Sensofar Plμ). Each file was then cropped to the lowest field size across all microscopes (128 x 96 μm; Sensofar Plμ neox), making sure the final area of the surface was the same for each data file from each microscope. This produced a second set of data, referred to hereafter as Resampled Datafiles. ISO and SSFA parameters were then generated from all Resampled Datafiles in exactly the same way as described above for Non-Resampled Datafiles.

Parameter Family	Parameter Name	Definition	Units
Height	Sq	Root Mean Square Height of Surface	µm
	Ssk	Skewness of Height Distribution of Surface	n/a
	Sku	Kurtosis of Height Distribution of Surface	n/a
	Sp	Maximum Peak Height of Surface	µm
	Sv	Maximum Valley Depth of Surface	µm
	Sz	Maximum Height of the Surface (Sp – Sv)	µm
	Sa	Average Height of Surface	µm
Spatial	Str	Surface Texture Aspect Ratio (values range 0-1). Ratio from the distance with the fastest to the distance with the slowest decay of the ACF to the value. 0.2-0.3: surface has a strong directional structure. > 0.5: surface has rather uniform texture.	mm/mm
	Sal	Surface Auto-Correlation Length Horizontal distance of the auto correlation function (ACF) which has the fastest decay to the value 0.2. Large value: surface dominated by low frequencies. Small value: surface dominated by high frequencies.	mm
Hybrid	Ssc	Mean Summit Curvature for Peak Structures	1/µm
	Sds	Density of Summits. Number of summits per unit area making up the surface	$1/mm^2$
	Sdq	Root Mean Square Gradient of the Surface	Degrees
	Sdr	Developed Interfacial Area Ratio of the Surface	%
Volume	Vmp	Surface Peak Material Volume	$\mu m^3/mm^2$
	Vmc	Surface Core Material Volume	$\mu m^3/mm^2$
	Vvc	Surface Core Void Volume	$\mu m^3/mm^2$
	Vvv	Surface Dale Void Volume	$\mu m^3/mm^2$
Material Ratio	Spk	Mean height of the peaks above the core material	µm
	Sk	Core roughness depth, Height of the core material	µm
	Svk	Mean depth of the valleys below the core material	µm
	Smr1	Surface bearing area ratio (the proportion of the surface which consists of peaks above the core material)	%
	Smr2	Surface bearing area ratio (the proportion of the surface which would carry the load)	%
Feature	S5z	Ten Point Height of Surface	µm
Miscellaneous	Std	Texture Direction	Degrees

Table 5.2 *Descriptions for all ISO 25178-2 areal texture parameters used in this paper. Parameters Sal and Std were excluded from analyses as they rarely produced normally distributed data even when log transformed. Ssk was also excluded as it displayed low normality and regularly returned negative values which could not be log transformed. For detailed parameter descriptions see Purnell et al (2013).*

Parameter Name	Acronym	Description
Area Scale Fractal Complexity	Asfc	A measure of the complexity of a surface. Area-scale fractal complexity is a measure of change in roughness with scale. The faster a measured surface area increases with resolution, the more complex the surface.
Exact Proportion Length Scale Anisotropy of Relief	epLsar	A measure of the anisotropy of a surface. Anisotropy is characterized as variation in lengths of transect lines measured at a given scale (we use 3.5 µm) with orientations sampled at 5° intervals across a surface. An anisotropic surface will have shorter transects in the direction of the surface pattern than perpendicular to it (e.g. a transect that cross-cuts parallel scratches must trace the peaks and valleys of each individual feature).
Scale of Maximum Complexity	Smc	The parameter represents the full scale range over which Asfc is calculated. High Smc values should correspond to more complex coarse features.
Textural Fill Volume	Tfv	The total volume filled (Tfv) is a function of two components: 1) the shape of the surface, and 2) the texture of the surface. A more concave or convex surface will have a larger total fill volume than a planar surface even if both surfaces have an identical texture.
Heterogeneity of Area Scale Fractal Complexity	HAsfc	variation of Asfc across a surface (across multiple, equal subdivisions of a surface). High HAsfc values are observed for surfaces that vary in complexity across a facet.

Table 5.3 *Full list of Scale Sensitive Fractal Analysis (SSFA) parameters, including brief descriptions (after Ungar et al (2003) and Scott et al (2006)). Parameter Smc was excluded from analyses. For parameter details and information on methods of calculation see Scott et al (2006).*

Here parameter epLsar was generated for all datafiles using the same scale of observation (1.8 µm; one order of magnitude greater than the lateral sampling resolution), as all Resampled Datafiles have the same µm/pixel lateral resolution.

All of these processes have resulted in four complete datasets, *Capreolus capreolus* Non-Resampled, *Capreolus capreolus* Resampled, *Archosargus probatocephalus* Non-Resampled, and *Archosargus probatocephalus* Resampled. Within each of these four datasets are two dietary group datasets (for *C.capreolus* = Acorn Eaters, and Bramble Leaf Eaters; for *A.probatocephalus* = IR-Herb, and IR-Duro).

This obviously lends its self to confusion, as such we have given each dataset, and sub-dataset a logical code (Table 5.4), for which they will be referred to throughout the remainder of this paper.

Species	Diet	Resampled?	Dataset	Code	Sub Dataset	Code
C.capreolus	Bramble Leaves	No	*C.capreolus* Non-Resampled	C.c-NonRes	*C.capreolus* Bramble Leaf Eaters Non-Resampled	C.c-BLE-NonRes
C.capreolus	Acorns	No			*C.capreolus* Acorn Eaters Non-Resampled	C.C-AE-NonRes
A.probatocephalus	Herbivorous	No	*A.probatocephalus* Non-Resampled	A.p-NonRes	*A.probatocephalus* IR-Herb Non-Resampled	A.p-IRH-NonRes
A.probatocephalus	Durophagus	No			*A.probatocephalus* PC-Duro Non-Resampled	A.p-PCD-NonRes
C.capreolus	Bramble Leaves	Yes	*C.capreolus* Resampled	C.c-Res	*C.capreolus* Bramble Leaf Eaters Resampled	C.c-BLE-Res
C.capreolus	Acorns	Yes			*C.capreolus* Acorn Eaters Resampled	C.C-AE-Res
A.probatocephalus	Herbivorous	Yes	*A.probatocephalus* Resampled	A.p-Res	*A.probatocephalus* IR-Herb Resampled	A.p-IRH-Res
A.probatocephalus	Durophagus	Yes			*A.probatocephalus* PC-Duro Resampled	A.p-PCD-Res

Table 5.4 *Codes for Non-Resampled and Resampled datasets and sub-datasets used in this paper.*

To make sure using linear interpolation did not lead different parameter values compared to other forms of resampling interpolation, we duplicated one Non-Resampled sub-dataset (*Archosargus probatocephalus* IR-Herb population, n=6) seven times and applied a different interpolation method to each. Interpolation methods used were Round, Linear, Key, BSpline, O-MOMS, NNA, and Schaum interpolation. Details of these interpolation methods can be seen in Table 5.5. Surfaces were scale limited and ISO 25178 parameters were generated for all 42 datafiles using the same methods described above for all datafiles. All data were tested for normality using Shapiro Wilks W tests, and all original data was found to be normally distributed, except for parameters Sp (maximum peak height of surface), Ssc (mean summit curvature for peak structures), and Smr2 (surface bearing area ratio 2). Log transformed data did not improve normality and so these parameters were not included in this analysis. ANOVA, Tukey Honest Significant Difference (Tukey HSD), and Student's Each Pair T-tests were carried out in JMP Pro (Version 12.1.0) between data from the seven interpolation methods to determine any significant difference in resulting parameter values. There were no significant results recorded for any statistical test, and almost all parameter values were identical between interpolation methods. As such there is no bias introduced by using linear interpolation in our methods.

Interpolation Method	Description
Round	Also known as nearest neighbourhood interpolation. This is the simplest method possible – it takes rounded values of the expected position and finds the closest data value at the integer position
Linear	A linear interpolation between the two closest data values. Caluculated from z=(1-x)z0+xz1, where z0 and z1 are values at the preceding and following points, respectively. It is identical to the 2nd order BSpline
Key	Makes use of values in the before-preceding and after-following points z_{-1} and z_2, respectively. In other words it has support of length 4
Schaum	Fourth-order Schaum also has a support length of 4 but uses different weights to calculate points compared to Key Interpolation
NNA	Nearest neighbour approximation is calculated from the closest four data values but unlike all others it is not piecewise-polynomial.
BSpline	Calculated weights are not used with direct function values as above, but with interpolation coefficients calculated from function values
O-MOMS	Similar to BSpline but uses different weightings to calculate points

Table 5.5 *Descriptions of all seven interpolation methods tested for resampling the µm/pixel values of datafiles (further information can be found at http://gwyddion.net/documentation/user-guide-en/interpolation.html).*

Statistical Analysis

All statistical hypothesis testing was carried out in software package JMP Pro (Version 12.1.0). All data were tested for normality by dietary groups using Shapiro Wilks W-tests, and where data were not normally distributed Log transformed data were also tested for normality. In all cases original data showed a low degree of normality, whereas log data showed a relatively high degree of normality, as such log data were exclusively used going forwards. ISO 25178 parameter Ssk (surface skewness) was excluded from further analysis as negative values were regularly returned for this parameter, which could not be log transformed. With all parameter exclusions this left data from 13 SSFA, and 21 ISO 25178 parameters for our analyses.

Although multiple comparisons are conducted throughout our analyses, we have chosen not to use a sequential Bonferroni correction (Holm 1979), following the reasoning of (Goodall et al. 2015). The application of this method is subjective (Cabin and Mitchell 2000) and when used on large test numbers, as we have done here, it has been shown to produce many more false negative results (type II errors) than the false positives (type I errors) it seeks to eliminate (Moran 2003, Nakagawa 2004). Instead we have used a less conservative approach, the Benjamini–Hochberg procedure (Benjamini and Hochberg 1995). This approach ranks the p-values from a set of tests and applies a critical value based on the rank of the p-value, the total number of tests, and the assumed false discovery rate (here our false discovery rate would be one in twenty, 0.05). This critical value is calculated separately for each p-value, and any p-value exceeding its calculated critical value is considered non-significant, and a false positive result. This procedure has been applied to all significant results reported in this manuscript.

To test our first hypotheses Non-Resampled Data from each microscope were compared using ANOVA and Tukey Honest Significant Difference (HSD) tests. All Non-Resampled Data were then combined and tested using Linear Discriminant Analysis (LDA) to determine how easily data could be separated based on the microscope from which it was collected. Linear Regressions were also used on this combined dataset to test the linear relationship between data from each microscope. Finally Bland Altman Plots were used on collections of parameters from this combined dataset to test the relative similarity between the signals from each microscope. To test our second hypothesis the same tests were carried out in exactly the same way on Resampled Datasets.

To test our third and fourth hypotheses (the effect on varying microscope on dietary separation) ANOVA and Tukey HSD tests were carried out between dietary groups for each Dataset (separately for both Non-Resampled and Resampled Data). Parameters showing difference were then put into separate Principal Component Analyses (PCA) for each dataset. Both these tests allow us to determine the relative sensitivity to dietary differences of data from surfaces generated using each

microscope both in their original Non-Resampled form, and when resampled to the same µm/pixel resolution and field size.

Results

Direct Comparison of Microscopes – ANOVA and Tukey HSD

Direct comparison of parameter values generated from surfaces collected using different microscopes was carried out using ANOVA, separately for each sub-dataset (dietary group), and separately for Non-Resampled Data, and Resampled Data. This means a total of eight sub-datasets were tested (Table 5.4). Within each sub-dataset data from different microscopes was compared by parameter for a total of 34 separate tests within each sub-dataset. Equality of variance was tested using Levene, Bartlett, O-Brien, and Brown-Forsythe tests. Where any of these tests returned significant results variances were not equal, and as such Welch test results were reported instead. These analyses test the hypotheses that using different microscopes/instruments to collect 3D tooth surface data will result in significantly different roughness parameter values (ISO 25178, and SSFA) recorded from resulting surfaces, and that any differences in 3D texture produced by using different microscopes/instruments are caused in large part by the effect of each microscope collecting data at different sampling resolutions and field size, thus resampling datafiles collected from each microscope down to the lowest µm/pixel value across all microscopes and then reducing the field of view to the lowest across all microscopes will eliminate this difference.

The results of ANOVA for Non-Resampled Data can be seen in Table 5.6. In all dietary groups SSFA parameter values show difference between surfaces from separate microscopes. However HAsfc 2x2, and HAsfc 3x3 only show differences between microscope data in two datasets each (C.c-BLE-NonRes/A.p-IRH-NonRes and A.p-PCD-NonRes/A.p-IRH-NonRes respectively). And parameter Tfv shows difference between microscope data in three of the sub-datasets (for full parameter descriptions see Table 5.3). As a proportion there are many fewer ISO 25178 parameters showing

differences between data collected using separate microscopes, however this is not a consistent pattern across all four Non-Resampled sub-datasets. The greatest difference between microscope data were recorded within A.p-PCD-NonRes.

		Non-Resampled Data											
		Capreolus capreolus						*Archosargus probatocephalus*					
		Acorns			Bramble Leaves			Durophagus			Herbivorous		
		F Ratio	p	d.f	F Ratio	p	d.f	F Ratio	p	d.f	F Ratio	p	d.f
SSFA	Tfv	**8.0717**	**0.0017**	**3, 16**	1.9271	0.1659	3, 16	**4.4540**	**0.0149**	**3, 16**	**7.7147**	**0.0013**	**3, 16**
	Asfc	**49.2311**	**<.0001**	**3, 16**	**142.9144**	**<.0001***	**3, 8.62**	**33.4924**	**<.0001**	**3, 16**	**16.8090**	**<.0001**	**3, 16**
	epLsar	**16.0892**	**<.0001**	**3, 16**	**9.0041**	**0.0058***	**3, 8.12**	3.1870	0.0460	3, 16	**4.3496**	**0.0163**	**3, 16**
	HAsfc 2x2	2.5757	0.0901	3, 16	**10.9827**	**0.0033***	**3, 7.98**	1.1791	0.3427	3, 16	**12.0391**	**0.0001**	**3, 16**
	HAsfc 3x3	2.6066	0.0875	3, 16	2.5448	0.0926	3, 16	**7.0133**	**0.0021**	**3, 16**	**7.6332**	**0.0014**	**3, 16**
	HAsfc 4x4	**5.1367**	**0.0112**	**3, 16**	**11.6949**	**0.0003**	**3, 16**	**6.0116**	**0.0043**	**3, 16**	**8.0624**	**0.0010**	**3, 16**
	HAsfc 5x5	**5.8374**	**0.0068**	**3, 16**	**9.3741**	**0.0064***	**3, 7.47**	**8.5500**	**0.0007**	**3, 16**	**8.3896**	**0.0008**	**3, 16**
	HAsfc 6x6	**6.7663**	**0.0037**	**3, 16**	**11.8899**	**0.0002**	**3, 16**	**10.7085**	**0.0002**	**3, 16**	**11.1030**	**0.0002**	**3, 16**
	HAsfc 7x7	**11.5893**	**0.0003**	**3, 16**	**13.5580**	**0.0001**	**3, 16**	**10.7396**	**0.0002**	**3, 16**	**13.0340**	**<.0001**	**3, 16**
	HAsfc 8x8	**8.4029**	**0.0014**	**3, 16**	**17.5829**	**<.0001**	**3, 16**	**10.8658**	**0.0002**	**3, 16**	**14.6140**	**<.0001**	**3, 16**
	HAsfc 9x9	**10.0689**	**0.0006**	**3, 16**	**23.5604**	**<.0001**	**3, 16**	**12.0464**	**0.0001**	**3, 16**	**18.5755**	**<.0001**	**3, 16**
	HAsfc 10x10	**10.8014**	**0.0004**	**3, 16**	**16.9785**	**<.0001**	**3, 16**	**13.4399**	**<.0001**	**3, 16**	**20.1107**	**<.0001**	**3, 16**
	HAsfc 11x11	**11.8988**	**0.0002**	**3, 16**	**19.0138**	**<.0001**	**3, 16**	**17.3348**	**<.0001**	**3, 16**	**21.2012**	**<.0001**	**3, 16**
ISO 25178	Sq	**7.4217**	**0.0025**	**3, 16**	**5.8959**	**0.0066**	**3, 16**	**11.0358**	**0.0002**	**3, 16**	1.3684	0.2811	3, 16
	Sku	0.2243	0.8781	3, 16	0.1161	0.9493	3, 16	1.7407	0.1910	3, 16	1.0378	0.3973	3, 16
	Sp	3.3307	0.0462	3, 16	0.3057	0.8209	3, 16	0.7725	0.5229	3, 16	**3.6240**	**0.0308**	**3, 16**
	Sv	**5.7539**	**0.0072**	**3, 16**	**4.4335**	**0.0189**	**3, 16**	**6.0425**	**0.0042**	**3, 16**	3.2506	0.0434	3, 16
	Sz	**7.4673**	**0.0024**	**3, 16**	**4.0986**	**0.0246**	**3, 16**	3.0335	0.0531	3, 16	**3.9744**	**0.0226**	**3, 16**
	Sds	**215.6210**	**<.0001***	**3, 8.27**	**18.3753**	**<.0001**	**3, 16**	**112.0516**	**<.0001***	**3, 16**	**50.2020**	**<.0001***	**3, 9.89**
	Str	0.7851	0.5196	3, 16	0.1061	0.9553	3, 16	**8.7513**	**0.0007**	**3, 16**	0.3546	0.7863	3, 16
	Sdq	**36.5393**	**<.0001**	**3, 16**	**99.8536**	**<.0001**	**3, 16**	**17.5994**	**<.0001**	**3, 16**	**11.2904**	**0.0001**	**3, 16**
	Ssc	**88.5470**	**<.0001**	**3, 16**	**20.5714**	**0.0004***	**3, 7.86**	**6.7188**	**0.0085***	**3, 9.84**	**5.3740**	**0.0071**	**3, 16**
	Sdr	**50.1548**	**<.0001**	**3, 16**	**99.9914**	**<.0001**	**3, 16**	**21.1778**	**<.0001**	**3, 16**	**12.8995**	**<.0001**	**3, 16**
	Vmp	0.3394	0.7971	3, 16	0.0771	0.9715	3, 16	**7.4351**	**0.0016**	**3, 16**	1.7617	0.1869	3, 16
	Vmc	**3.9295**	**0.0281**	**3, 16**	2.8057	0.0731	3, 16	**11.8182**	**0.0001**	**3, 16**	**4.3395**	**0.0165**	**3, 16**
	Vvc	**4.6351**	**0.0162**	**3, 16**	1.6784	0.2116	3, 16	**13.0002**	**<.0001**	**3, 16**	2.0172	0.1707*	3, 10.9
	Vvv	3.2481	0.0496	3, 16	1.4060	0.2775	3, 16	**4.3282**	**0.0166**	**3, 16**	0.4943	0.6903	3, 16
	Spk	0.4103	0.7478	3, 16	0.0713	0.9745	3, 16	**7.0651**	**0.0020**	**3, 16**	2.1066	0.1315	3, 16
	Sk	**5.9964**	**0.0061**	**3, 16**	2.1137	0.1387	3, 16	**8.9847**	**0.0006**	**3, 16**	3.3813	0.0584*	3, 10.9
	Svk	**4.1077**	**0.0244**	**3, 16**	1.8234	0.1835	3, 16	**3.8144**	**0.0260**	**3, 16**	0.4356	0.7299	3, 16
	Smr1	0.8386	0.4923	3, 16	0.2940	0.8292	3, 16	0.1193	0.9477	3, 16	1.2345	0.3234	3, 16
	Smr2	1.2825	0.3142	3, 16	0.2950	0.8285	3, 16	0.5266	0.6691	3, 16	0.3703	0.7752	3, 16
	S5z	**7.4516**	**0.0024**	**3, 16**	**17.3136**	**<.0001**	**3, 16**	**8.8079**	**0.0006**	**3, 16**	**5.4219**	**0.0068**	**3, 16**
	Sa	**5.4019**	**0.0092**	**3, 16**	**4.4750**	**0.0183**	**3, 16**	**12.8056**	**<.0001**	**3, 16**	1.9878	0.1483	3, 16

Table 5.6 *ANOVA carried out separately on each Non-Resampled sub-dataset for all SSFA and ISO 25178 parameters. F Ratio and p values are given for each test, and results are only reported where significant (α=0.05). All significant results were tested using the Benjimini-Hochberg method.*

For this dataset all but five ISO parameters (Sku, Sp, Sz, Smr1, and Smr2) showed differences between data from separate microscopes (for parameter descriptions see Table 5.2). A similar difference was found between data from separate microscopes for sub-dataset C.c-AE-NonRes where eight parameters did not show any difference (Sku, Sp, Str, Vmp, Vvv, Spk, Smr1, and Smr2). Within the remaining two sub-datsets a much lower degree of difference was found between data from separate microscopes. Across tests for all four sub-datasets three ISO parameters never showed any difference between data from surfaces generated using different microscopes (Sku, Smr1, and Smr2), and two parameters were only able to separate microscopes within a single sub-dataset (A.p-PCD-NonRes; Vmp, and Str).

To test which microscopes were producing these differences Tukey Honest Significant Difference (HSD) tests were carried out for all parameters within each Non-Resampled sub-dataset where significant results were recorded from ANOVA tests (Table 5.7). Data from every possible pair of microscopes was tested within each sub-dataset using a significance test and connecting letter reports, grouping microscopes based on similarities in data means. Across all four Non-Resampled sub-datasets there appears to be a loose pattern of similarity/difference in the data. Data from the two Sensofar microscopes are almost always connected and only very rarely show differences from one another. Based on the number of parameters showing differences between specific microscopes across Tukey HSD tests, by far the greatest difference is between the Sensofar Plμ and Mitaka PAFM data. Followed closely by the difference between the Sensofar Plμ neox and Mitaka PAFM data. Alicona IFM data is often different to data from both the Sensofar Plμ and Mitaka PAFM data, but more so compared to the former than the latter, and in neither case is this difference as great as when comparing the Mitaka PAFM to either of the Sensofar microscopes. Data from the Alicona IFM shows some difference to that from the Sensofar Plμ neox, but this is much lower, and there is almost no difference when comparing data from the two Sensofar microscopes. Between sub-datasets the pattern of which parameters produce these various differences is not absolutely consistent, however for almost all parameters across all four sub datasets the two Sensofar microscopes are grouped by connecting letter reports, and the Alicona IFM and Mitaka PAFM are often connected.

However this is not the case when looking at the HAsfc parameters for sub-dataset A.p-PCD-NonRes where the Sensofar Plμ data is separated from all other microscopes. Alicona IFM and Sensofar Plμ neox data are sometimes grouped, but this is not a consistent pattern. In only one case (parameter Sds; C.c-AE-NonRes) are all four microscopes separated into four distinct groups with significant differences between all comparisons.

When ANOVA are carried out on Resampled sub-datasets in exactly the same way as for Non-Resampled data we find a slight reduction in the difference between data from separate microscopes, with an overall lower number of parameters showing difference between microscopes within each sub-dataset, but this reduction is within ISO parameters only, not SSFA parameters (Table 5.8). Six ISO parameters show no difference between microscopes across any sub dataset (Sku, Sp, Vmp, Spk, Smr1, and Smr2), and for parameter Str difference is only found between microscope data within sub-dataset A.p-PCD-Res.

Again Tukey HSD tests were carried out on data from all Resampled sub-datasets, producing test results for each comparison and connecting letter reports (Table 5.9). While there are obviously fewer parameters tested than for Non-Resampled data the pattern for Resampled data is the same. Again data from the Alicona IFM and Mitaka PAFM are often grouped together, and data form the two Sensofar microscopes are almost always grouped together. The proportion of significant results is also the same for each comparison, with the Mitaka PAFM – Sensofar Plμ comparison producing the greatest difference, and the Sensofar Plμ - Sensofar Plμ neox comparison showing almost no difference. Differences between microscopes are most evident between the PAFM/IFM and both Sensofar microscopes.

			Tfv	Asfc	epLsar	HAsfc 4x4	HAsfc 5x5	HAsfc 6x6	HAsfc 7x7	HAsfc 8x8	HAsfc 9x9	HAsfc 10x10	HAsfc 11x11	Sq
Acorn Eaters	PAFM	Plu Neox	**0.0016**	**<.0001**	**0.0003**	0.1576	0.1216	0.0468	**0.0222**	0.0294	**0.0147**	**0.0140**	**0.0096**	**0.0060**
	PAFM	Plu	**0.0072**	**<.0001**	**<.0001**	**0.0161**	**0.0080**	**0.0076**	**0.0005**	**0.0028**	**0.0012**	**0.0008**	**0.0005**	**0.0036**
	PAFM	IFM	0.0847	**<.0001**	0.0600	0.9753	0.9087	0.9567	0.9214	0.9373	0.8972	0.8945	0.9091	0.0266
	IFM	Plu	0.2296	0.0229	**0.0144**	0.0367	0.0304	**0.0210**	**0.0016**	**0.0090**	**0.0048**	**0.0032**	**0.0020**	0.7555
	IFM	Plu Neox	0.6039	**0.0006**	0.0702	0.3027	0.3488	0.1193	0.0749	0.0885	0.0579	0.0560	**0.0362**	0.8816
	Plu Neox	Plu	0.8776	0.3103	0.8484	0.6315	0.5157	0.7981	0.2609	0.6554	0.6103	0.5026	0.4999	0.9937
	Connecting Letters	PAFM	A	A	A	A	A	A	A	A	A	A	A	A
		IFM	A B	B	A B	A	A	A B	A B	A B	A B	A B	A	B
		Plu Neox	B	C	B C	A B	A B	B C	B C	B C	B C	B C	B	B
		Plu	B	C	C	B	B	C	C	C	C	C	B	B

			Sv	Sz	Sds	Sdq	Ssc	Sdr	Vmc	Vvc	Sk	Svk	S5z	Sa
Acorn Eaters	PAFM	Plu Neox	**0.0077**	**0.0039**	**<.0001**	**<.0001**	**<.0001**	**<.0001**	0.0635	0.0388	**0.0186**	0.0568	**0.0033**	0.0217
	PAFM	Plu	**0.0198**	**0.0052**	**<.0001**	**<.0001**	**<.0001**	**<.0001**	0.0361	**0.0211**	**0.0075**	0.0449	**0.0058**	**0.0106**
	PAFM	IFM	0.0806	0.0251	**<.0001**	**0.0003**	**0.0079**	**<.0001**	0.5913	0.4822	0.3307	0.0480	0.0392	0.1966
	IFM	Plu	0.8855	0.8650	**<.0001**	**0.0037**	**<.0001**	**0.0005**	0.3298	0.2917	0.2080	1.0000	0.7787	0.4340
	IFM	Plu Neox	0.6391	0.7941	**<.0001**	0.0402	**<.0001**	**0.0129**	0.4822	0.4430	0.3997	0.9997	0.6180	0.6406
	Plu Neox	Plu	0.9649	0.9988	**0.0002**	0.6476	0.0879	0.3831	0.9908	0.9894	0.9691	0.9993	0.9921	0.9839
	Connecting Letters	PAFM	A	A	A	A	A	A	A	A	A	A	A	A
		IFM	A B	B	B	B	B	B	A B	A B	A B	B	B	A B
		Plu Neox	B	B	C	C	C	C	A B	B	B	A B	B	B
		Plu	B	B	D	C	C	C	B	B	B	B	B	B

			Asfc	epLsar	HAsfc 2x2	HAsfc 4x4	HAsfc 5x5	HAsfc 6x6	HAsfc 7x7	HAsfc 8x8	HAsfc 9x9	HAsfc 10x10	HAsfc 11x11
Bramble Leaf Eaters	PAFM	Plu Neox	**<.0001**	0.0404	0.1221	**0.0055**	**0.0188**	**0.0050**	**0.0037**	**0.0019**	**0.0002**	**0.0008**	**0.0012**
	PAFM	Plu	**<.0001**	**0.0168**	0.1751	**0.0050**	**0.0064**	**0.0031**	**0.0010**	**0.0002**	**<.0001**	**0.0006**	**0.0003**
	PAFM	IFM	**0.0014**	0.9982	0.8961	0.9807	0.9919	0.9980	1.0000	1.0000	0.9990	0.9984	0.9731
	IFM	Plu	**<.0001**	0.0236	0.0497	**0.0023**	**0.0036**	**0.0022**	**0.0010**	**0.0002**	**<.0001**	**0.0005**	**0.0001**
	IFM	Plu Neox	**<.0001**	0.0561	0.0330	**0.0025**	**0.0107**	**0.0035**	**0.0038**	**0.0019**	**0.0002**	**0.0006**	**0.0005**
	Plu Neox	Plu	0.1417	0.9700	0.9965	1.0000	0.9492	0.9949	0.9103	0.6512	0.9641	0.9990	0.8817
	Connecting Letters	PAFM	A	A	A B	A	A	A	A	A	A	A	A
		IFM	B	A B	A	A	A	A	A	A	A	A	A
		Plu Neox	C	B C	B	B	B	B	B	B	B	B	B
		Plu	C	C	B	B	B	B	B	B	B	B	B

			Sq	Sv	Sz	Sds	Sdq	Ssc	Sdr	S5z	Sa
Bramble Leaf Eaters	PAFM	Plu Neox	**0.0095**	0.0744	0.1722	**0.0002**	**<.0001**	**0.0005**	**<.0001**	**<.0001**	0.0279
	PAFM	Plu	**0.0182**	0.0409	0.0313	**<.0001**	**<.0001**	**<.0001**	**<.0001**	**0.0001**	0.0300
	PAFM	IFM	0.0293	0.0252	0.0416	0.0548	**<.0001**	0.1854	**<.0001**	**0.0028**	0.0964
	IFM	Plu	0.9949	0.9945	0.9988	**0.0053**	**<.0001**	**0.0060**	**<.0001**	0.4135	0.9261
	IFM	Plu Neox	0.9417	0.9423	0.8620	0.0606	**0.0091**	0.0397	**0.0044**	0.1505	0.9134
	Plu Neox	Plu	0.9880	0.9888	0.7911	0.6195	0.1137	0.7830	0.1137	0.9069	1.0000
	Connecting Letters	PAFM	A	A	A	A	A	A	A	A	A
		IFM	B	B	B	A B	B	A	B	B	A B
		Plu Neox	B	A B	A B	B C	C	B	C	B	B
		Plu	B	B	B	C	C	B	C	B	B

			Tfv	Asfc	HAsfc 3x3	HAsfc 4x4	HAsfc 5x5	HAsfc 6x6	HAsfc 7x7	HAsfc 8x8	HAsfc 9x9	HAsfc 10x10	HAsfc 11x11	Sq	Sv
Durophagus Population	PAFM	Plu Neox	**0.0171**	**<.0001**	0.5265	0.6757	0.2165	0.1314	0.1457	0.1447	0.1247	0.0582	0.0587	**0.0009**	**0.0024**
	PAFM	Plu	0.4104	**<.0001**	**0.0066**	**0.0077**	**0.0014**	**0.0002**	**0.0002**	**0.0002**	**0.0001**	**<.0001**	**<.0001**	**0.0004**	0.0540
	PAFM	IFM	0.9839	**0.0038**	0.9736	1.0000	0.2558	0.3728	0.8654	0.9244	0.8487	0.8040	0.8458	**0.0015**	0.1248
	IFM	Plu	0.6185	**0.0003**	**0.0025**	**0.0073**	**0.0018**	**0.0011**	**0.0012**	**0.0009**	**0.0007**	**0.0004**	**<.0001**	0.9201	0.9722
	IFM	Plu Neox	0.0367	**0.0067**	0.3011	0.6589	0.9996	0.9156	0.4731	0.3867	0.4454	0.2923	0.2582	0.9972	0.2768
	Plu Neox	Plu	0.3384	0.5033	0.1192	0.0850	0.1114	0.0419	0.0325	0.0353	**0.0201**	0.0241	**0.0047**	0.9713	0.4984
	Connecting Letters	PAFM	A	A	A	A	A	A	A	A	A	A	A	A	A
		IFM	A	B	A	A	A	A	A	A	A	A	A	B	A B
		Plu Neox	A B	C	A B	A B	A B	A	A	A	A	A	A	B	B
		Plu	B	C	B	B	B	B	B	B	B	B	B	B	A B

			Sds	Str	Sdq	Ssc	Sdr	Vmp	Vmc	Vvc	Vvv	Spk	Sk	Svk	S5z	Sa
Durophagus Population	PAFM	Plu Neox	**<.0001**	**0.0021**	**<.0001**	**0.0172**	**<.0001**	**0.0112**	**0.0009**	**0.0006**	0.0492	**0.0132**	**0.0041**	0.0716	**0.0005**	**0.0004**
	PAFM	Plu	**<.0001**	**0.0089**	**<.0001**	**0.0075**	**<.0001**	**0.0088**	**0.0001**	**<.0001**	0.0607	**0.0112**	**0.0005**	0.1179	**0.0049**	**<.0001**
	PAFM	IFM	**<.0001**	**0.0012**	**0.0042**	0.8978	**0.0033**	**0.0019**	0.0281	**0.0171**	**0.0208**	**0.0024**	0.0879	0.0267	**0.0178**	**0.0034**
	IFM	Plu	**<.0001**	0.8067	0.0823	0.0341	**0.0214**	0.9062	0.0938	0.0842	0.9552	0.9043	0.1204	0.8798	0.9362	0.3841
	IFM	Plu Neox	**0.0004**	0.9940	0.1733	0.0736	0.1085	0.8616	0.4403	0.4527	0.9764	0.8750	0.4988	0.9629	0.4281	0.7867
	Plu Neox	Plu	0.4459	0.9169	0.9770	0.9812	0.8551	0.9995	0.7768	0.7334	0.9996	0.9999	0.7931	0.9936	0.7690	0.8969
	Connecting Letters	PAFM	A	A	A	A	A	A	A	A	A	A	A	A	A	A
		IFM	B	B	B	A B	B	B	B	B	B	B	A B	B	B	B
		Plu Neox	C	B	B	B C	B C	B	B	B	B	B	B	A B	B	B
		Plu	C	B	B	C	C	B	B	B	A B	B	B	A B	B	B

			Tfv	Asfc	epLsar	HAsfc 2x2	HAsfc 3x3	HAsfc 4x4	HAsfc 5x5	HAsfc 6x6	HAsfc 7x7	HAsfc 8x8	HAsfc 9x9	HAsfc 10x10	HAsfc 11x11
Herbivorous Population	PAFM	Plu Neox	**0.0016**	**<.0001**	0.3374	**0.0030**	**0.0127**	0.0339	**0.0270**	**0.0058**	**0.0060**	**0.0027**	**0.0011**	**0.0011**	**0.0007**
	PAFM	Plu	**0.0044**	**<.0001**	0.3258	**0.0005**	**0.0024**	**0.0016**	**0.0012**	**0.0002**	**<.0001**	**<.0001**	**<.0001**	**<.0001**	**<.0001**
	PAFM	IFM	0.0797	**0.0006**	**0.0087**	0.9381	0.6870	0.8716	0.8273	0.5764	0.6235	0.5910	0.5661	0.6747	0.5649
	IFM	Plu	0.5430	0.3693	0.2755	**0.0018**	0.0290	**0.0088**	**0.0085**	**0.0045**	**0.0012**	**0.0008**	**0.0002**	**<.0001**	**<.0001**
	IFM	Plu Neox	0.3009	0.7722	0.2654	**0.0109**	0.1248	0.1501	0.1470	0.0908	0.0804	0.0438	**0.0202**	**0.0143**	**0.0143**
	Plu Neox	Plu	0.9684	0.8962	1.0000	0.8594	0.8832	0.5275	0.5253	0.5086	0.2573	0.2923	0.1677	0.1064	0.0956
	Connecting Letters	PAFM	A	A	A	A	A	A	A	A	A	A	A	A	A
		IFM	A B	B	B	A	A B	A B	A B	A B	A B	A	A	A	A
		Plu Neox	B	B	A B	B	B C	B C	B C	B C	B C	B	B	B	B
		Plu	B	B	A B	B	C	C	C	C	C	B	B	B	B

			Sp	Sz	Sds	Sdq	Ssc	Sdr	Vmc	S5z
Herbivorous Population	PAFM	Plu Neox	0.1059	0.0694	**<.0001**	**0.0006**	0.0258	**0.0003**	0.0457	**0.0141**
	PAFM	Plu	0.0464	0.0398	**<.0001**	**0.0003**	**0.0069**	**0.0001**	**0.0164**	**0.0186**
	PAFM	IFM	0.0551	0.0423	**0.0001**	**0.0020**	0.2685	**0.0015**	0.1269	**0.0211**
	IFM	Plu	0.9998	1.0000	**0.0075**	0.8547	0.2878	0.6734	0.7483	0.9999
	IFM	Plu Neox	0.9868	0.9947	**0.0167**	0.9406	0.6122	0.8949	0.9525	0.9977
	Plu Neox	Plu	0.9748	0.9926	0.9835	0.9956	0.9318	0.9723	0.9622	0.9993
	Connecting Letters	PAFM	A	A	A	A	A	A	A	A
		IFM	A B	B	B	B	A B	B	A B	B
		Plu Neox	A B	A B	C	B	B	B	B	B
		Plu	B	B	C	B	B	B	B	B

Table 5.7 *Tukey HSD tests carried out separately on each Non-Resampled sub-dataset for all SSFA and ISO 25178 parameters. p values and connecting letters reports are given for each test, parameters are only reported where significant ANOVA results were recorded (Table 5.6). All significant results were tested using the Benjimini-Hochberg method.*

		Resampled Data											
		Capreolus capreolus						*Archosargus probatocephalus*					
		Acorns			Bramble Leaves			Durophagus			Herbivorous		
		F Ratio	p	d.f	F Ratio	p	d.f	F Ratio	p	d.f	F Ratio	p	d.f
SSFA	Tfv	**4.3699**	**0.0199**	**3, 16**	0.5345	0.6652	3, 16	0.3479	0.7910	3, 16	0.6220	0.6090	3, 16
	Asfc	**55.6864**	**<.0001**	**3, 16**	**126.1553**	**<.0001**	**3, 16**	**30.6456**	**<.0001**	**3, 16**	**15.7315**	**<.0001**	**3, 16**
	epLsar	4.5504	0.0352*	3, 8.61	**13.2752**	**0.0001**	**3, 16**	2.9123	0.0596	3, 16	0.9857	0.4195	3, 16
	HAsfc 2x2	3.0076	0.0611	3, 16	**5.1676**	**0.0270***	**3, 8.24**	0.8948	0.4610	3, 16	**6.2946**	**0.0035**	**3, 16**
	HAsfc 3x3	3.3132	0.0469	3, 16	2.8602	0.0697	3, 16	3.2460	0.0436	3, 16	3.5650	0.0325	3, 16
	HAsfc 4x4	2.5940	0.0886	3, 16	**5.5393**	**0.0084**	**3, 16**	**4.6744**	**0.0124**	**3, 16**	**4.6621**	**0.0126**	**3, 16**
	HAsfc 5x5	**5.3723**	**0.0094**	**3, 16**	**5.7390**	**0.0073**	**3, 16**	**4.4815**	**0.0146**	**3, 16**	**6.3547**	**0.0033**	**3, 16**
	HAsfc 6x6	**5.8220**	**0.0069**	**3, 16**	**9.4632**	**0.0008**	**3, 16**	**5.1980**	**0.0081**	**3, 16**	**7.9444**	**0.0011**	**3, 16**
	HAsfc 7x7	**6.5008**	**0.0044**	**3, 16**	**7.8076**	**0.0020**	**3, 16**	**5.4317**	**0.0067**	**3, 16**	**8.7334**	**0.0007**	**3, 16**
	HAsfc 8x8	**6.1020**	**0.0057**	**3, 16**	**9.2547**	**0.0009**	**3, 16**	**7.2603**	**0.0018**	**3, 16**	**9.2313**	**0.0005**	**3, 16**
	HAsfc 9x9	**8.4754**	**0.0013**	**3, 16**	**9.1368**	**0.0009**	**3, 16**	**8.2697**	**0.0009**	**3, 16**	**12.5979**	**<.0001**	**3, 16**
	HAsfc 10x10	**7.8828**	**0.0019**	**3, 16**	**10.0236**	**0.0006**	**3, 16**	**8.0614**	**0.0010**	**3, 16**	**14.2748**	**<.0001**	**3, 16**
	HAsfc 11x11	**9.1887**	**0.0009**	**3, 16**	**12.7871**	**0.0002**	**3, 16**	**9.2508**	**0.0005**	**3, 16**	**14.4724**	**<.0001**	**3, 16**
ISO 25178	Sq	**11.5421**	**0.0003**	**3, 16**	**6.0529**	**0.0059**	**3, 16**	**6.0021**	**0.0043**	**3, 16**	1.0198	0.4048	3, 16
	Sku	0.3269	0.8059	3, 16	0.6084	0.6192	3, 16	1.1053	0.3702	3, 16	1.2248	0.3267	3, 16
	Sp	0.7651	0.5301	3, 16	0.1313	0.9401	3, 16	0.3275	0.8055	3, 16	2.7794	0.0925*	3, 10.7
	Sv	**8.4469**	**0.0014**	**3, 16**	2.8076	0.0730	3, 16	**4.3604**	**0.0162**	**3, 16**	1.8632	0.1684	3, 16
	Sz	**4.8879**	**0.0134**	**3, 16**	1.4442	0.2671	3, 16	1.8813	0.1653	3, 16	2.0246	0.1702*	3, 10.7
	Sds	**142.7678**	**<.0001**	**3, 16**	**14.2816**	**<.0001**	**3, 16**	**79.5598**	**<.0001***	**3, 9.74**	**37.8975**	**<.0001***	**3, 9.19**
	Str	0.6723	0.5814	3, 16	0.1257	0.9435	3, 16	**6.8885**	**0.0023**	**3, 16**	0.0865	0.9666	3, 16
	Sdq	**35.0610**	**<.0001**	**3, 16**	**86.4381**	**<.0001**	**3, 16**	**16.9383**	**<.0001**	**3, 16**	**9.3669**	**0.0005**	**3, 16**
	Ssc	**63.8616**	**<.0001**	**3, 16**	**24.3645**	**0.0002***	**3, 8**	**6.1051**	**0.0040**	**3, 16**	**5.7695**	**0.0052**	**3, 16**
	Sdr	**45.1319**	**<.0001**	**3, 16**	**87.0477**	**<.0001**	**3, 16**	**19.6454**	**<.0001**	**3, 16**	**10.8094**	**0.0002**	**3, 16**
	Vmp	0.4842	0.6980	3, 16	0.0521	0.9837	3, 16	1.8000	0.1796	3, 16	1.0267	0.4019	3, 16
	Vmc	**4.5696**	**0.0170**	**3, 16**	3.2233	0.0507	3, 16	**7.0009**	**0.0021**	**3, 16**	2.5589	0.0839	3, 16
	Vvc	**4.8734**	**0.0136**	**3, 16**	1.7130	0.2045	3, 16	**7.0619**	**0.0020**	**3, 16**	1.3661	0.3047*	10.9000
	Vvv	**4.6878**	**0.0156**	**3, 16**	1.2521	0.3240	3, 16	3.4546	0.0360	3, 16	0.3621	0.7810	3, 16
	Spk	0.4459	0.7236	3, 16	0.0873	0.9660	3, 16	1.7318	0.1927	3, 16	1.3806	0.2775	3, 16
	Sk	**6.1299**	**0.0056**	**3, 16**	2.4544	0.1007	3, 16	**5.5047**	**0.0064**	**3, 16**	2.0606	0.1643*	3, 10.9
	Svk	**6.0615**	**0.0059**	**3, 16**	1.5699	0.2356	3, 16	3.0532	0.0522	3, 16	0.3469	0.7917	3, 16
	Smr1	0.1672	0.9169	3, 16	0.2737	0.8435	3, 16	0.5049	0.6833	3, 16	0.5077	0.6814	3, 16
	Smr2	0.8921	0.4665	3, 16	0.2753	0.8423	3, 16	0.6970	0.5648	3, 16	0.4458	0.7229	3, 16
	S5z	**7.3069**	**0.0026**	**3, 16**	**9.8855**	**0.0006**	**3, 16**	**6.2777**	**0.0035**	**3, 16**	2.4806	0.0906	3, 16
	Sa	**8.4781**	**0.0013**	**3, 16**	**4.8035**	**0.0143**	**3, 16**	**7.0457**	**0.0020**	**3, 16**	1.2917	0.3046	3, 16

Table 5.8 *ANOVA carried out separately on each Resampled sub-dataset for all SSFA and ISO 25178 parameters. F Ratio and p values are given for each test, and results are only reported where significant (α=0.05). All significant results were tested using the Benjimini-Hochberg method.*

			Tfv	Asfc	HAsfc 5x5	HAsfc 6x6	HAsfc 7x7	HAsfc 8x8	HAsfc 9x9	HAsfc 10x10	HAsfc 11x11	Sq	Sv	Sz
Acorn Eaters	PAFM	Plu Neox	0.0381	**<.0001**	0.1862	0.1112	0.1026	0.0905	0.0481	0.0988	0.0392	**0.0005**	**0.0034**	0.0209
	PAFM	Plu	0.0246	**<.0001**	**0.0102**	**0.0075**	**0.0059**	**0.0084**	**0.0016**	**0.0024**	**0.0011**	**0.0007**	**0.0032**	0.0224
	PAFM	IFM	0.1201	**0.0004**	0.9272	0.8636	0.9405	0.9463	0.8226	0.9431	0.8005	**0.0066**	**0.0067**	0.0829
	IFM	Plu	0.8363	**<.0001**	0.0348	0.0355	**0.0185**	0.0254	**0.0091**	**0.0076**	**0.0067**	0.6883	0.9844	0.9034
	IFM	Plu Neox	0.9256	**0.0009**	0.4502	0.3791	0.2636	0.2296	0.2229	0.2518	0.2019	0.5898	0.9876	0.8900
	Plu Neox	Plu	0.9960	0.4872	0.4436	0.5261	0.4841	0.6295	0.3548	0.2803	0.3122	0.9983	1.0000	1.0000
	Connecting Letters	PAFM	A	A	A	A	A	A	A	A	A	A	A	A
		IFM	A B	B	A	A	A	A	A B	A	A B	B	B	A B
		Plu Neox	B	C	A B	A B	A B	A B	B C	A B	B C	B	B	B
		Plu	B	C	B	B	B	B	C	B	C	B	B	B

			Sds	Sdq	Ssc	Sdr	Vmc	Vvc	Vvv	Sk	Svk	S5z	Sa
Acorn Eaters	PAFM	Plu Neox	**<.0001**	**<.0001**	**<.0001**	**<.0001**	0.0345	0.0294	0.0285	**0.0149**	**0.0123**	**0.0046**	**0.0027**
	PAFM	Plu	**<.0001**	**<.0001**	**<.0001**	**<.0001**	0.0253	0.0194	0.0405	**0.0080**	**0.0146**	**0.0062**	**0.0023**
	PAFM	IFM	**<.0001**	**0.0005**	**<.0001**	**0.0002**	0.4886	0.4468	0.0343	0.3497	**0.0178**	**0.0178**	0.0794
	IFM	Plu	**<.0001**	**0.0051**	**<.0001**	**0.0010**	0.3268	0.3015	0.9998	0.2055	0.9996	0.9532	0.3174
	IFM	Plu Neox	**0.0094**	**0.0169**	**0.0004**	**0.0071**	0.4050	0.4017	0.9997	0.3258	0.9977	0.9091	0.3559
	Plu Neox	Plu	**0.0006**	0.9345	0.8437	0.7637	0.9985	0.9967	0.9979	0.9898	0.9998	0.9989	0.9998
	Connecting Letters	PAFM	A	A	A	A	A	A	A	A	A	A	A
		IFM	B	B	B	B	A B	A B	B	A B	B	B	A B
		Plu Neox	C	C	C	C	B	B	B	B	B	B	B
		Plu	D	C	C	C	B	B	B	B	B	B	B

			Asfc	epLsar	HAsfc 2x2	HAsfc 4x4	HAsfc 5x5	HAsfc 6x6	HAsfc 7x7	HAsfc 8x8	HAsfc 9x9
Bramble Leaf Eaters	PAFM	Plu Neox	**<.0001**	**0.0006**	0.1150	0.1122	0.0640	0.0376	0.0560	0.0509	0.0357
	PAFM	Plu	**<.0001**	**0.0001**	0.1182	0.0529	0.0343	**0.0030**	**0.0081**	**0.0042**	**0.0054**
	PAFM	IFM	**<.0001**	**0.0095**	0.9951	0.9695	0.9999	0.9999	0.9993	0.9925	0.9933
	IFM	Plu	**<.0001**	0.1926	0.0769	**0.0221**	0.0303	**0.0027**	**0.0063**	**0.0024**	**0.0031**
	IFM	Plu Neox	**<.0001**	0.5469	0.0747	0.0491	0.0569	0.0336	0.0440	0.0298	0.0212
	Plu Neox	Plu	0.0820	0.8716	1.0000	0.9765	0.9878	0.6057	0.7662	0.6057	0.7836
	Connecting Letters	PAFM	A	A	A	A B	A B	A	A B	A B	A
		IFM	B	B	A	A	A	A	A	A	A
		Plu Neox	C	B	A	B	B	B	B C	B C	B
		Plu	C	B	A	B	B	B	C	C	B

			HAsfc 10x10	HAsfc 11x11	Sq	Sds	Sdq	Ssc	Sdr	S5z	Sa
Bramble Leaf Eaters	PAFM	Plu Neox	0.0283	**0.0081**	**0.0135**	**0.0006**	**<.0001**	**0.0008**	**<.0001**	**0.0048**	0.0258
	PAFM	Plu	**0.0050**	**0.0016**	**0.0124**	**<.0001**	**<.0001**	**0.0004**	**<.0001**	**0.0006**	0.0214
	PAFM	IFM	0.9643	0.9888	0.0198	**0.0081**	**<.0001**	**0.0185**	**<.0001**	**0.0069**	0.0747
	IFM	Plu	**0.0019**	**0.0008**	0.9954	0.1273	**0.0002**	0.2533	**0.0001**	0.6280	0.9161
	IFM	Plu Neox	**0.0110**	**0.0043**	0.9973	0.5906	**0.0073**	0.4432	**0.0038**	0.9976	0.9450
	Plu Neox	Plu	0.8279	0.8508	1.0000	0.7076	0.2983	0.9770	0.2937	0.7368	0.9997
	Connecting Letters	PAFM	A	A	A	A	A	A	A	A	A
		IFM	A	A	B	B	B	B	B	B	A B
		Plu Neox	B	B	B	B	C	B	C	B	B
		Plu	B	B	B	B	C	B	C	B	B

			Asfc	HAsfc 4x4	HAsfc 5x5	HAsfc 6x6	HAsfc 7x7	HAsfc 8x8	HAsfc 9x9	HAsfc 10x10	HAsfc 11x11	Sq
Durophagus Population	PAFM	Plu Neox	**<.0001**	0.6610	0.6834	0.5152	0.4767	0.4760	0.5730	0.4771	0.4908	**0.0149**
	PAFM	Plu	**<.0001**	**0.0125**	**0.0180**	**0.0087**	**0.0075**	**0.0018**	**0.0011**	**0.0017**	**0.0007**	**0.0060**
	PAFM	IFM	**0.0053**	0.9646	0.9959	0.9734	0.9767	0.9199	0.9477	0.9987	0.9911	0.0257
	IFM	Plu	**0.0004**	0.0345	0.0292	0.0221	**0.0183**	**0.0074**	**0.0036**	**0.0024**	**0.0014**	0.9102
	IFM	Plu Neox	**0.0106**	0.9020	0.8081	0.7666	0.7186	0.8391	0.8717	0.5661	0.6654	0.9942
	Plu Neox	Plu	0.5155	0.1330	0.1678	0.1533	0.1530	0.0449	0.0198	0.0433	0.0190	0.9761
	Connecting Letters	PAFM	A	A	A	A	A	A	A	A	A	A
		IFM	B	A	A	A	A	A	A	A	A	B
		Plu Neox	C	A B	A B	A B	A B	A	A	A	A	B
		Plu	C	B	B	B	B	B	B	B	B	B

			Sv	Sds	Str	Sdq	Ssc	Sdr	Vmc	Vvc	Sk	S5z	Sa
Durophagus Population	PAFM	Plu Neox	**0.0148**	**<.0001**	**0.0106**	**<.0001**	**0.0037**	**<.0001**	**0.0165**	**0.0151**	0.0436	**0.0039**	**0.0098**
	PAFM	Plu	0.0481	**<.0001**	0.0209	**<.0001**	0.0192	**<.0001**	**0.0016**	**0.0016**	**0.0048**	**0.0111**	**0.0019**
	PAFM	IFM	0.1931	**<.0001**	**0.0026**	**0.0075**	0.2261	**0.0070**	0.1560	0.1806	0.3225	0.0668	0.0449
	IFM	Plu	0.8814	**0.0092**	0.7859	0.0594	0.5950	**0.0188**	0.1678	0.1468	0.1818	0.8312	0.4914
	IFM	Plu Neox	0.5791	0.0620	0.9224	0.1520	0.2189	0.0962	0.6839	0.6082	0.6883	0.5685	0.8938
	Plu Neox	Plu	0.9442	0.8080	0.9893	0.9595	0.8790	0.8567	0.7244	0.7530	0.7466	0.9667	0.8826
	Connecting Letters	PAFM	A	A	A	A	A	A	A	A	A	A	A
		IFM	A B	B	B	B	A B	B	A B	A B	A B	A B	B
		Plu Neox	B	B C	B	B	B	B C	B	B	B	B	B
		Plu	B	C	B	B	B	C	B	B	B	B	B

			Asfc	HAsfc 2x2	HAsfc 4x4	HAsfc 5x5	HAsfc 6x6	HAsfc 7x7	HAsfc 8x8
Herbivorous Population	PAFM	Plu Neox	**<.0001**	**0.0207**	0.1453	0.0906	0.0401	0.0495	0.0456
	PAFM	Plu	**<.0001**	**0.0105**	0.0201	**0.0064**	**0.0014**	**0.0013**	**0.0010**
	PAFM	IFM	**0.0016**	0.8990	0.9769	0.9846	0.8240	0.9702	0.9818
	IFM	Plu	0.3019	0.0465	0.0474	**0.0140**	**0.0100**	**0.0035**	**0.0024**
	IFM	Plu Neox	0.5530	0.0863	0.2847	0.1724	0.2057	0.1176	0.0956
	Plu Neox	Plu	0.9654	0.9893	0.7596	0.6046	0.4537	0.3721	0.3471
	Connecting Letters	PAFM	A	A	A	A	A	A	A
		IFM	B	A B	A	A	A B	A B	A B
		Plu Neox	B	B C	A B	A B	B C	B C	B C
		Plu	B	C	B	B	C	C	C

			HAsfc 9x9	HAsfc 10x10	HAsfc 11x11	Sds	Sdq	Ssc	Sdr
Herbivorous Population	PAFM	Plu Neox	0.0218	**0.0136**	**0.0100**	**<.0001**	**0.0013**	**0.0089**	**0.0007**
	PAFM	Plu	**0.0002**	**<.0001**	**<.0001**	**<.0001**	**0.0013**	0.0338	**0.0004**
	PAFM	IFM	0.9569	0.8990	0.8974	**<.0001**	**0.0032**	**0.0117**	**0.0025**
	IFM	Plu	**0.0005**	**0.0003**	**0.0003**	0.6915	0.9809	0.9605	0.8722
	IFM	Plu Neox	0.0624	0.0590	0.0450	0.5276	0.9790	0.9993	0.9438
	Plu Neox	Plu	0.1568	0.1059	0.1347	0.9927	1.0000	0.9268	0.9970
	Connecting Letters	PAFM	A	A	A	A	A	A	A
		IFM	A B	A B	A	B	B	B	B
		Plu Neox	B C	B C	B	B	B	B	B
		Plu	C	C	B	B	B	B	B

Table 5.9 *Tukey HSD tests carried out separately on each Resampled sub-dataset for all SSFA and ISO 25178 parameters. p values and connecting letters reports are given for each test, parameters are only reported where significant ANOVA results were recorded (Table 5.8). All significant results were tested using the Benjimini-Hochberg method.*

Direct Comparison of Microscopes – Linear Discriminant Analysis

All Non-Resampled sub-datasets were combined into one large Non-Resampled dataset. Linear Discriminant Analysis was carried out on this dataset to test how easily data from the four microscopes could be separated into discreet distributions in multivariate space, regardless of differences in diet between sub-datasets (i.e. is there an overriding difference between data from each microscope whatever dataset is used). LDA was performed using forward stepwise variable selection, where parameters are added one by one to the analysis based on their ability to discriminate the desired groups (in this case data from each microscope). At no point did misclassification reach zero percent, the lowest was four misclassified specimens (4/88; 4.55%). This was found when 18 of 34 parameters were used (Tfv, epLsar, HAsfc3x3, HAsfc 5x5, HAsfc6x6, HAsfc11x11, Sp, Sv, Sds, Str, Sdq, Ssc, Sdr, Vvv, Svk, Smr1, Smr2, S5z), at this stage discriminatory power of all three canonical axes were also significant (Wilks Lambda test – CA1 p=<.0001; CA2 p=<.0001; CA3 p=0.0406). The addition of any further parameters via stepwise variable selection did not reduce the misclassification rate and only led to non-significant Wilks Lambda test results for Canonical Axis 3 (CA3). Using 18 parameters an ordination was produced on three Canonical Axes (one fewer than the number of groups tested), which can be seen in Figure 5.1. CA3 is not included in the figure, as it shows no obvious separation between any of the microscope data and it explains only 2.2% of variance in the data. On Canonical Axis 1 (CA1) and Canonical Axis 2 (CA2) data from the Alicona IFM and Mitaka PAFM clearly form their own discreet distributions, with no overlap to any other microscope. The distribution of Alicona IFM data is much closer to that of the two Sensofar microscopes than that of the Mitaka PAFM. The distributions of both Sensofar Microscopes overlap heavily, and this is where all misclassifications are recorded. The main axis of separation between microscopes is CA1, which is able to separate data from the Mitaka PAFM from all other microscopes, with all data points possessing highly positive values for CA1. The Alicona IFM data is also separated on this axis from all other microscope data, falling between the Mitaka PAFM and Sensofar data, with all points plotting close to the zero line. All Sensofar data (both Plμ

and Plμ neox) plots with negative values on CA1, with Sensofar Plμ data plotting slightly more negatively on CA1.

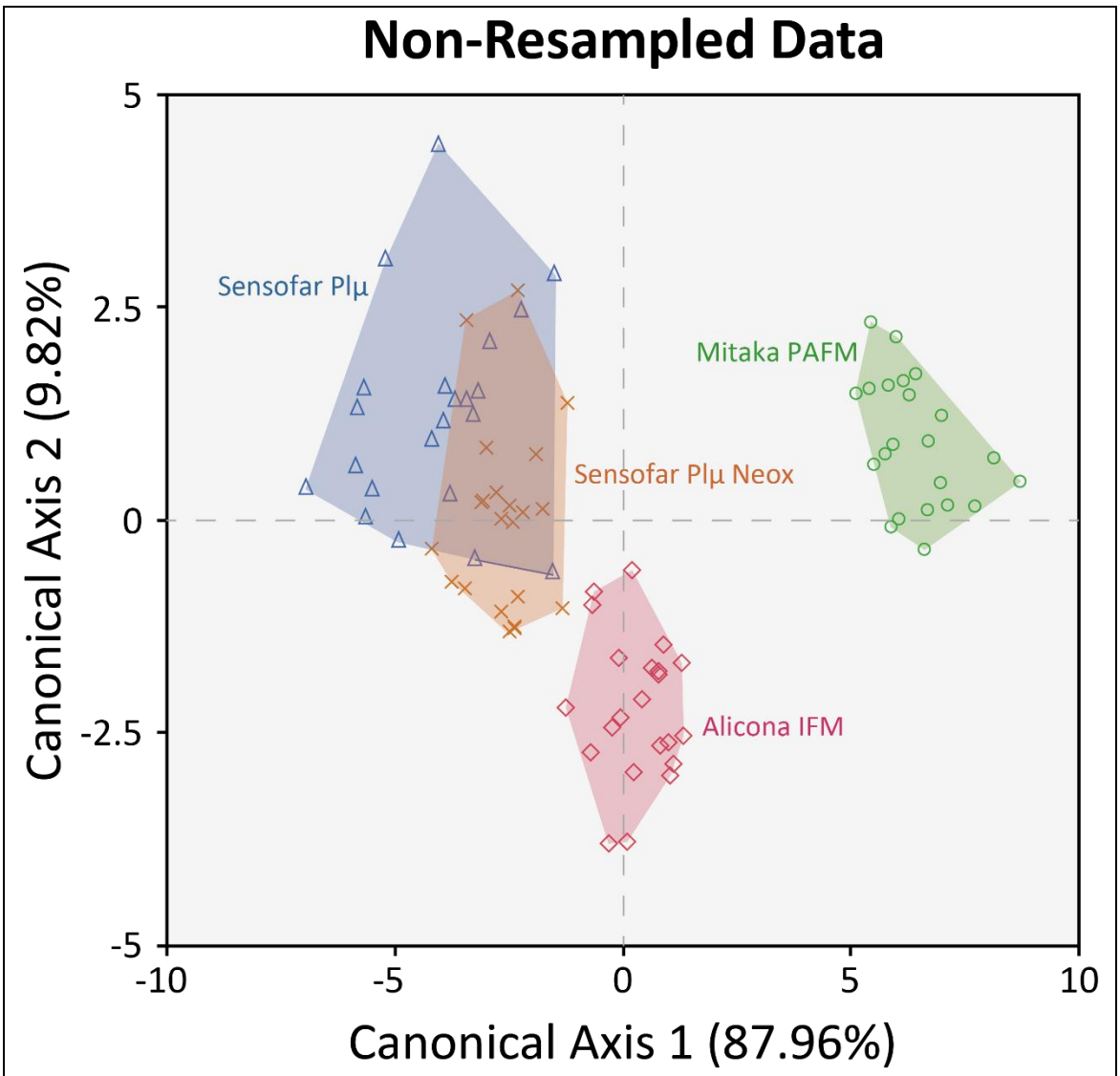

Figure 5.1 *Linear Discriminant Analysis for all Non-Resampled data, produced using eighteen 3D roughness parameters (Tfv, epLsar, HAsfc3x3, HAsfc 5x5, HAsfc6x6, HAsfc11x11, Sp, Sv, Sds, Str, Sdq, Ssc, Sdr, Vvv, Svk, Smr1, Smr2, S5z). Canonical Axis 1 (CA1, explains 87.96% of variance) and Canonical Axis 2 (CA2, explains 9.82% of variance) are shown. Points represent each specimen replicated for each of the four microscopes. For each microscope points, convex hulls and labels are consistently coloured. Sensofar Plμ = Blue Triangles, Sensofar Plμ neox = Orange Crosses, Alicona IFM = Pink Diamonds, and Mitaka PAFM = Green Circles. Misclassification is 4/88 samples (4.55%), Wilks Lambda test results for CA1 and CA2 = <.0001 in both cases.*

CA2 separates the Alicona IFM data from all other microscopes to some degree, with Alicona IFM data plotting negatively on this axis, while most other data plots positively or at least near the zero line. Leave one out cross validation was carried out for the LDA model, with a total of ten replicates performed. At no point did the misclassification rate or axis significance change when any data files were excluded, indicating the LDA model is relatively robust.

LDA was also carried out on Resampled data, however in this case stepwise variable selection wasn't used, instead it was run by simply using the same parameters as were used for the Non-Resampled Data. This tests whether the same model performs better or worse on Resampled Data, giving an indication of any improvement in the similarity of data from different microscopes when datafiles are resampled. LDA using 18 parameters (Tfv, epLsar, HAsfc3x3, HAsfc 5x5, HAsfc6x6, HAsfc11x11, Sp, Sv, Sds, Str, Sdq, Ssc, Sdr, Vvv, Svk, Smr1, Smr2, S5z) produced an ordination on three Canonical Axes (Figure 5.2). Five specimens were misclassified (5/88; 5.68%), and only CA1 and CA2 returned significant results for Wilks Lambda tests (CA1 p=<.0001; CA2 p=0.0005; CA3 p=0.8879). The distribution of Mitaka PAFM data is still discreet and completely separate from all other microscopes. Whereas there is now some overlap between the Alicona IFM data and the Sensofar Plμ neox data. There is still overlap between the two Sensofar clusters, but it is much less than when using Non-Resampled Data. The separation is again mostly along CA1 with the relative position of groups almost identical to the Non-Resampled data. Along PC2 again the Alicona IFM data is separated From the Sensofar Plμ data and Mitaka PAFM data, plotting more negatively than either, but the Sensofar Plμ neox data is now also plotting relatively negatively on this axis and overlapping much more with the Alicona IFM data. In the LDA produced from Resampled data there appears to be two groups of data points, one made up of data from the Mitaka PAFM, and one made up of all three other instruments. Their distributions only slightly overlap, but they are much closer to one another than any are to the Mitaka PAFM data. Again leave one out cross validation was performed in the same way as for Non-Resampled data, with 10 replicates used. Six of the ten replicates showed no difference in misclassification, two replicates reduced the misclassification rate (4/87, 4.59%; 3/87, 3.45% respectively), and two

replicates increased the misclassification rate ((6/87, 6.90%; 7/87, 8.05% respectively). This shows the LDA model is less robust when used on Resampled data, but overall is still relatively robust.

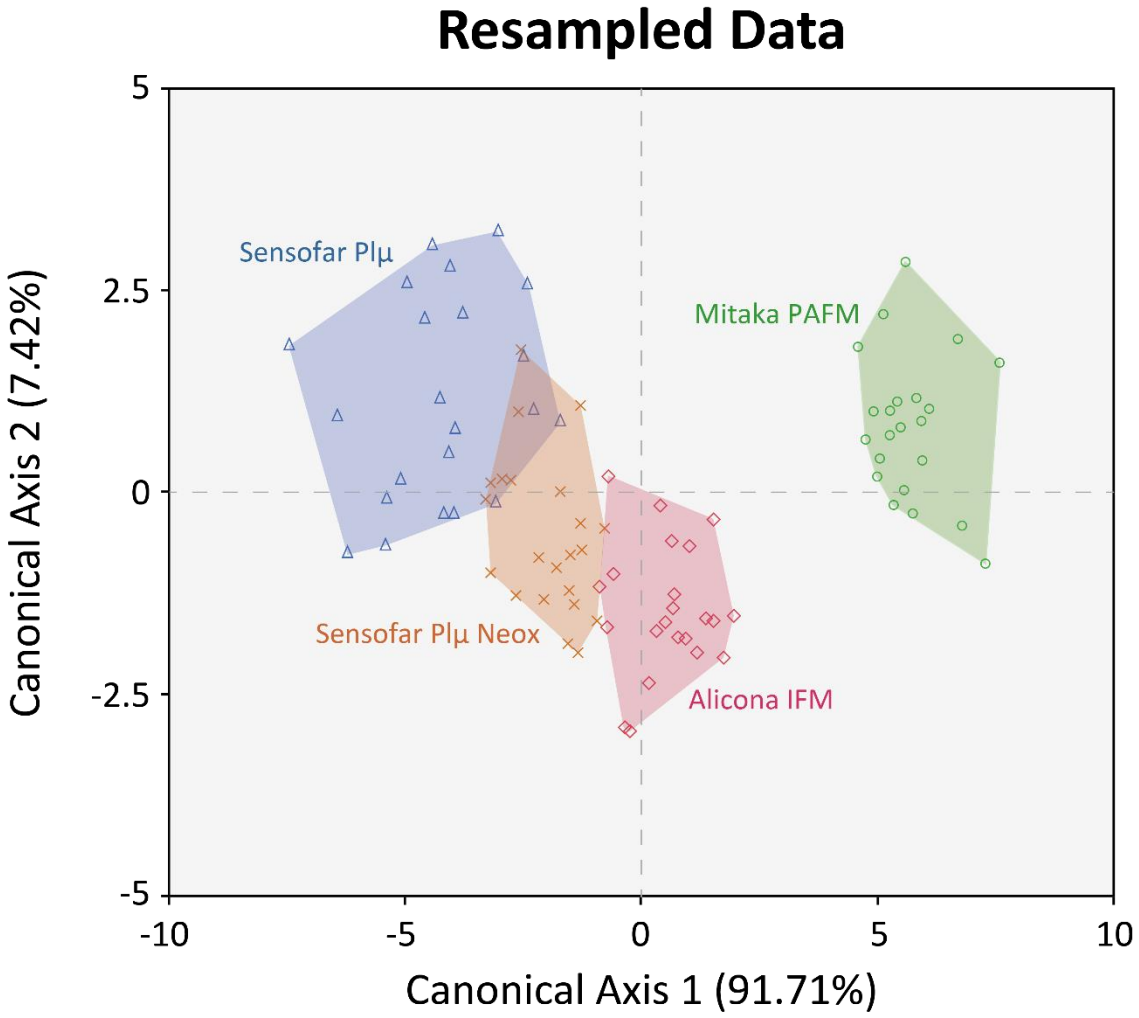

Figure 5.2 *Linear Discriminant Analysis for all Resampled data, produced using eighteen 3D roughness parameters (Tfv, epLsar, HAsfc3x3, HAsfc 5x5, HAsfc6x6, HAsfc11x11, Sp, Sv, Sds, Str, Sdq, Ssc, Sdr, Vvv, Svk, Smr1, Smr2, S5z), stepwise parameter selection was not used. Canonical Axis 1 (CA1, explains 91.71% of variance) and Canonical Axis 2 (CA2, explains 7.42% of variance) are shown. Points represent each specimen replicated for each of the four microscopes. For each microscope points, convex hulls and labels are consistently coloured. Sensofar Plμ = Blue Triangles, Sensofar Plμ neox = Orange Crosses, Alicona IFM = Pink Diamonds, and Mitaka PAFM = Green Circles. Misclassification is 5/88 samples (5.68%), Wilks Lambda test results for CA1 and CA2 = <.0001 and 0.0005 respectively.*

Direct Comparison of Microscopes – Correlation and Regression

There are obviously differences between data from different microscopes, however there may still be a linear relationship between data collected using different microscopes. To test whether any linear relationship exists linear regression was performed on the Non Resampled dataset, for each parameter. The R^2 value, intercept and regression significance are recorded in Table 5.10. The results show that for almost all comparisons there is a linear correlation between microscopes when using ISO 25178 parameters. However parameter Sds shows only one comparison where a microscope data is correlated (Sensofar Plμ against Sensofar Plμ neox). For SSFA parameters most comparisons with data collected using the Mitaka PAFM do not show any correlation. And for parameter Asfc all comparisons with data from the Alicona IFM do not show correlation. Some intercept tests are also significant, indicating a bias in the relationship between data from different microscopes, however these results are not consistent within a parameter (i.e. not recorded for comparisons with a certain microscope/s), or between parameters, indicating a non-consistent bias.

When the same tests were carried out for Resampled data (Table 5.11), the results were almost identical for ISO 25178 parameters, but for SSFA parameters more comparisons showed correlation than when using Non-Resampled Data, with parameters Tfv, and Asfc in particular showing much greater levels of correlation between data from different microscopes. Again significant results for intercept were recorded, and while the pattern is not identical to when using Non-Resampled data, it is very similar, with the same level of non-consistent bias.

To determine whether correlation was still strong when the effect of all four microscopes was taken into account in a single correlation, Intraclass Correlations were carried out on both Non-Resampled and Resampled datasets separately. Here data are grouped within each dataset into their sub-datasets (dietary groups), and tested across all four microscopes, to determine whether units within the same group (data points within a dietary group) resemble one another across all microscopes. The results of this test for both Datasets can be seen in Table 5.12. Data are classified as

having Poor, Fair, Good, or Excellent correlation based on the correlation value and interpretation is based on Cicchetti (1994). We find that for Non-Resampled Data all SSFA parameters show poor intraclass correlation. Nine ISO 25178 parameters also show poor intraclass correlation for this dataset (Sv, Sz, Sds, Sdq, Ssc, Sdr, Vvv, Svk, and S5z), while nine other ISO parameters show Fair correlation (Sq, Sku, Sp, Str, Vmc, Sk, Smr1, Smr2, and Sa), and finally three parameters show Good correlation (Vmp, Vvc, and Spk). The results of the same test on the Resampled dataset show a relatively similar pattern, and certain parameters have had their correlation improved, going from Poor to Fair (Tfv, epLsar, Ssc, and S5z). However three parameters have also had their correlation reduced from Good to Fair (Vmp, and Spk), and from Fair to Poor (Sku).

Direct Comparison of Microscopes – Bland Altman Plots

Overall agreement between microscopes across multiple parameters was tested using Bland Altman plots. This plots the mean of data from two instruments (X axis) against the difference between the methods (Y axis). Absolute agreement between two methods would lead to a perfect zero line and disagreement between methods leads to a line closer to 1. A significant intercept indicates a bias in data from one of the two microscopes. This is the opposite of linear regression where a significant regression test would indicate agreement between two methods, here a significant result indicates no agreement between methods.

For this test parameters were divided into groups based on those with the same units and similar scales, leading to three obvious groups. The first contains only the ten SSFA HAsfc parameters (that is HAsfc2x2 to HAsfc11x11) and will be referred to as the Heterogeneity of Complexity group. The second group is made up of all ISO parameters measured in µm with similar scales (Sq, Sp, Sv, Sz, Sa, Spk, Sk, Svk, and S5z), which will be referred to as the Height group. And finally a group was made from all volumetric ISO parameters (Vmp, Vmc, Vvc, Vvv), which will be referred to as the Volume group. All other parameters did not share units or similar scale and so could not be grouped.

For Non-Resampled Data Bland Altman plots can be seen in Figure 5.3, Figure 5.4, and Figure 5.5 respectively for each of the parameter groups in order. Six plots have been made for each group to test all possible comparisons of microscopes. The Heterogeneity of complexity group shows no agreement between data from different microscopes (ordinary least square regression), except for one comparison (comparison of Alicona IFM and Mitaka PAFM data). In all cases there is a significant bias in the data (intercept test) indicating the line of fit does not pass through zero. Comparisons within the Height group show much higher levels of agreement between microscopes, with three non-significant regression test results for comparisons between the Alicona IFM and each Sensofar microscope, and the comparison of both Sensofar microscopes. All comparisons with the Mitaka PAFM data showed no agreement. Again most intercept tests were significant, except for the comparisons of both Sensofar microscopes, where differences have a much more linear relationship than any other comparison along the zero line. Finally, comparisons within the Volume group show the same level of agreement (non-significant regression results) between data from different microscopes as the Height group, but for mostly different comparisons (when comparing the Mitaka PAFM data with Alicona IFM data and Sensofar Plμ neox data, and when comparing the two Sensofar instruments to one another). Only two intercepts showed bias between instruments and these were for the comparisons between data from the Alicona IFM and each Sensofar instrument.

For Resampled data exactly the same tests were carried out, for the same groupings of parameters, the results of which can be seen in Figure 5.6, Figure 5.7, and Figure 5.8 respectively. Comparisons between microscopes within the Heterogeneity of Complexity group show the same pattern of results as Non-Resampled data, with very little agreement between microscopes, except for the comparison between Alicona IFM and Mitaka PAFM data, and all intercepts do not pass through zero. Comparisons of resampled data within the Height group also exactly mirror the results of Non-Resampled data.

Bivariate Fit of			Parameter	R^2	Parameter Estimates			
					Intercept		Variable	
					t Ratio	p	t Ratio	p
Sensofar Plμ	by	Sensofar Plμ Neox	Tfv	0.8917	0.69	0.4968	12.83	<.0001
Sensofar Plμ	by	Alicona IFM	Tfv	0.8997	-4.93	<.0001	13.39	<.0001
Sensofar Plμ	by	Mitaka PAFM	Tfv	0.1522	-0.71	0.4845	1.89	0.0727
Sensofar Plμ Neox	by	Alicona IFM	Tfv	0.9253	-5.89	<.0001	15.74	<.0001
Sensofar Plμ Neox	by	Mitaka PAFM	Tfv	0.1574	-0.74	0.4667	1.93	0.0675
Alicona IFM	by	Mitaka PAFM	Tfv	0.2050	-0.23	0.8220	2.27	0.0344
Sensofar Plμ	by	Sensofar Plμ Neox	Asfc	0.9043	-4.27	0.0004	13.75	<.0001
Sensofar Plμ	by	Alicona IFM	Asfc	0.0861	-0.01	0.9919	1.37	0.1849
Sensofar Plμ	by	Mitaka PAFM	Asfc	0.6359	-4.61	0.0002	5.91	<.0001
Sensofar Plμ Neox	by	Alicona IFM	Asfc	0.1391	0.47	0.6454	1.80	0.0874
Sensofar Plμ Neox	by	Mitaka PAFM	Asfc	0.7480	-5.20	<.0001	7.70	<.0001
Alicona IFM	by	Mitaka PAFM	Asfc	0.0952	1.26	0.2207	1.45	0.1623
Sensofar Plμ	by	Sensofar Plμ Neox	epLsar	0.8550	0.34	0.7340	10.86	<.0001
Sensofar Plμ	by	Alicona IFM	epLsar	0.1624	-1.60	0.1255	1.97	0.0630
Sensofar Plμ	by	Mitaka PAFM	epLsar	0.1180	-3.76	0.0012	-1.64	0.1176
Sensofar Plμ Neox	by	Alicona IFM	epLsar	0.2740	-1.54	0.1397	2.75	0.0124
Sensofar Plμ Neox	by	Mitaka PAFM	epLsar	0.1184	-4.01	0.0007	-1.64	0.1169
Alicona IFM	by	Mitaka PAFM	epLsar	0.1100	-4.46	0.0002	-1.57	0.1316
Sensofar Plμ	by	Sensofar Plμ Neox	HAsfc 2x2	0.4216	-1.81	0.0848	3.82	0.0011
Sensofar Plμ	by	Alicona IFM	HAsfc 2x2	0.4513	-0.67	0.5131	4.06	0.0006
Sensofar Plμ	by	Mitaka PAFM	HAsfc 2x2	0.0676	-2.33	0.0305	1.20	0.2427
Sensofar Plμ Neox	by	Alicona IFM	HAsfc 2x2	0.1719	-1.82	0.0833	2.04	0.0550
Sensofar Plμ Neox	by	Mitaka PAFM	HAsfc 2x2	0.2638	-1.44	0.1663	2.68	0.0145
Alicona IFM	by	Mitaka PAFM	HAsfc 2x2	0.0180	-3.73	0.0013	0.61	0.5519
Sensofar Plμ	by	Sensofar Plμ Neox	HAsfc 3x3	0.6011	-0.18	0.8554	5.49	<.0001
Sensofar Plμ	by	Alicona IFM	HAsfc 3x3	0.4616	1.43	0.1690	4.14	0.0005
Sensofar Plμ	by	Mitaka PAFM	HAsfc 3x3	0.0356	-0.68	0.5032	0.86	0.4004
Sensofar Plμ Neox	by	Alicona IFM	HAsfc 3x3	0.3572	0.31	0.7628	3.33	0.0033
Sensofar Plμ Neox	by	Mitaka PAFM	HAsfc 3x3	0.0480	-0.92	0.3684	1.00	0.3271
Alicona IFM	by	Mitaka PAFM	HAsfc 3x3	0.0255	-2.77	0.0119	0.72	0.4777
Sensofar Plμ	by	Sensofar Plμ Neox	HAsfc 4x4	0.6584	1.85	0.0796	6.21	<.0001
Sensofar Plμ	by	Alicona IFM	HAsfc 4x4	0.4872	2.73	0.0129	4.36	0.0003
Sensofar Plμ	by	Mitaka PAFM	HAsfc 4x4	0.0797	0.23	0.8201	1.32	0.2030
Sensofar Plμ Neox	by	Alicona IFM	HAsfc 4x4	0.4897	1.45	0.1618	4.38	0.0003
Sensofar Plμ Neox	by	Mitaka PAFM	HAsfc 4x4	0.1675	-0.11	0.9163	2.01	0.0586
Alicona IFM	by	Mitaka PAFM	HAsfc 4x4	0.1278	-2.70	0.0137	1.71	0.1024
Sensofar Plμ	by	Sensofar Plμ Neox	HAsfc 5x5	0.7113	3.21	0.0044	7.02	<.0001
Sensofar Plμ	by	Alicona IFM	HAsfc 5x5	0.5993	4.23	0.0004	5.47	<.0001
Sensofar Plμ	by	Mitaka PAFM	HAsfc 5x5	0.1336	1.16	0.2594	1.76	0.0944
Sensofar Plμ Neox	by	Alicona IFM	HAsfc 5x5	0.5345	2.03	0.0559	4.79	0.0001
Sensofar Plμ Neox	by	Mitaka PAFM	HAsfc 5x5	0.2475	0.89	0.3863	2.57	0.0185
Alicona IFM	by	Mitaka PAFM	HAsfc 5x5	0.2839	-1.31	0.2055	2.82	0.0107
Sensofar Plμ	by	Sensofar Plμ Neox	HAsfc 6x6	0.6561	2.50	0.0212	6.18	<.0001
Sensofar Plμ	by	Alicona IFM	HAsfc 6x6	0.5642	4.18	0.0005	5.09	<.0001
Sensofar Plμ	by	Mitaka PAFM	HAsfc 6x6	0.0684	0.80	0.4322	1.21	0.2399
Sensofar Plμ Neox	by	Alicona IFM	HAsfc 6x6	0.4561	2.18	0.0410	4.10	0.0006
Sensofar Plμ Neox	by	Mitaka PAFM	HAsfc 6x6	0.1423	0.69	0.4976	1.82	0.0835
Alicona IFM	by	Mitaka PAFM	HAsfc 6x6	0.1333	-1.88	0.0742	1.75	0.0948
Sensofar Plμ	by	Sensofar Plμ Neox	HAsfc 7x7	0.6934	4.75	0.0001	6.73	<.0001
Sensofar Plμ	by	Alicona IFM	HAsfc 7x7	0.6351	5.66	<.0001	5.90	<.0001
Sensofar Plμ	by	Mitaka PAFM	HAsfc 7x7	0.1222	1.62	0.1200	1.67	0.1107
Sensofar Plμ Neox	by	Alicona IFM	HAsfc 7x7	0.4364	2.06	0.0523	3.94	0.0008
Sensofar Plμ Neox	by	Mitaka PAFM	HAsfc 7x7	0.1346	0.46	0.6501	1.76	0.0931
Alicona IFM	by	Mitaka PAFM	HAsfc 7x7	0.1760	-2.27	0.0346	2.07	0.0519
Sensofar Plμ	by	Sensofar Plμ Neox	HAsfc 8x8	0.6864	4.29	0.0004	6.62	<.0001
Sensofar Plμ	by	Alicona IFM	HAsfc 8x8	0.5161	4.44	0.0003	4.62	0.0002
Sensofar Plμ	by	Mitaka PAFM	HAsfc 8x8	0.1071	1.52	0.1450	1.55	0.1370
Sensofar Plμ Neox	by	Alicona IFM	HAsfc 8x8	0.5159	2.82	0.0106	4.62	0.0002
Sensofar Plμ Neox	by	Mitaka PAFM	HAsfc 8x8	0.1476	0.76	0.4587	1.86	0.0775
Alicona IFM	by	Mitaka PAFM	HAsfc 8x8	0.1990	-2.01	0.0586	2.23	0.0374

Bivariate Fit of			Parameter	R^2	Parameter Estimates			
					Intercept		Variable	
					t Ratio	p	t Ratio	p
Sensofar Plμ	by	Sensofar Plμ Neox	HAsfc 9x9	0.6100	4.46	0.0002	5.59	<.0001
Sensofar Plμ	by	Alicona IFM	HAsfc 9x9	0.5439	5.19	<.0001	4.88	<.0001
Sensofar Plμ	by	Mitaka PAFM	HAsfc 9x9	0.0551	1.37	0.1852	1.08	0.2929
Sensofar Plμ Neox	by	Alicona IFM	HAsfc 9x9	0.3771	2.28	0.0339	3.48	0.0024
Sensofar Plμ Neox	by	Mitaka PAFM	HAsfc 9x9	0.1474	1.04	0.3120	1.86	0.0778
Alicona IFM	by	Mitaka PAFM	HAsfc 9x9	0.1450	-2.17	0.0423	1.84	0.0804
Sensofar Plμ	by	Sensofar Plμ Neox	HAsfc 10x10	0.6036	4.83	0.0001	5.52	<.0001
Sensofar Plμ	by	Alicona IFM	HAsfc 10x10	0.5094	5.13	<.0001	4.56	0.0002
Sensofar Plμ	by	Mitaka PAFM	HAsfc 10x10	0.1399	2.28	0.0335	1.80	0.0864
Sensofar Plμ Neox	by	Alicona IFM	HAsfc 10x10	0.4484	2.91	0.0087	4.03	0.0007
Sensofar Plμ Neox	by	Mitaka PAFM	HAsfc 10x10	0.2617	1.85	0.0791	2.66	0.0149
Alicona IFM	by	Mitaka PAFM	HAsfc 10x10	0.2417	-1.92	0.0691	2.52	0.0201
Sensofar Plμ	by	Sensofar Plμ Neox	HAsfc 11x11	0.5266	5.67	<.0001	4.72	0.0001
Sensofar Plμ	by	Alicona IFM	HAsfc 11x11	0.5515	6.27	<.0001	4.96	<.0001
Sensofar Plμ	by	Mitaka PAFM	HAsfc 11x11	0.0727	2.25	0.0360	1.25	0.2251
Sensofar Plμ Neox	by	Alicona IFM	HAsfc 11x11	0.4655	3.36	0.0031	4.17	0.0005
Sensofar Plμ Neox	by	Mitaka PAFM	HAsfc 11x11	0.2248	1.84	0.0812	2.41	0.0258
Alicona IFM	by	Mitaka PAFM	HAsfc 11x11	0.1157	-2.71	0.0133	1.62	0.1214
Sensofar Plμ	by	Sensofar Plμ Neox	Sq	0.8936	-0.19	0.8503	12.96	<.0001
Sensofar Plμ	by	Alicona IFM	Sq	0.9311	0.59	0.5593	16.44	<.0001
Sensofar Plμ	by	Mitaka PAFM	Sq	0.6210	-4.65	0.0002	5.72	<.0001
Sensofar Plμ Neox	by	Alicona IFM	Sq	0.9118	-0.19	0.8515	14.38	<.0001
Sensofar Plμ Neox	by	Mitaka PAFM	Sq	0.6246	-5.07	<.0001	5.77	<.0001
Alicona IFM	by	Mitaka PAFM	Sq	0.6047	-5.36	<.0001	5.53	<.0001
Sensofar Plμ	by	Sensofar Plμ Neox	Sku	0.6358	0.96	0.3486	5.91	<.0001
Sensofar Plμ	by	Alicona IFM	Sku	0.8756	2.03	0.0562	11.86	<.0001
Sensofar Plμ	by	Mitaka PAFM	Sku	0.6605	1.58	0.1305	6.24	<.0001
Sensofar Plμ Neox	by	Alicona IFM	Sku	0.5307	2.87	0.0095	4.76	0.0001
Sensofar Plμ Neox	by	Mitaka PAFM	Sku	0.4028	2.62	0.0164	3.67	0.0015
Alicona IFM	by	Mitaka PAFM	Sku	0.6382	0.95	0.3547	5.94	<.0001
Sensofar Plμ	by	Sensofar Plμ Neox	Sp	0.7492	-0.47	0.6442	7.73	<.0001
Sensofar Plμ	by	Alicona IFM	Sp	0.6214	-0.22	0.8318	5.73	<.0001
Sensofar Plμ	by	Mitaka PAFM	Sp	0.6052	-2.16	0.0431	5.54	<.0001
Sensofar Plμ Neox	by	Alicona IFM	Sp	0.5520	0.85	0.4069	4.96	<.0001
Sensofar Plμ Neox	by	Mitaka PAFM	Sp	0.4181	-0.60	0.5555	3.79	0.0011
Alicona IFM	by	Mitaka PAFM	Sp	0.4653	-0.67	0.5081	4.17	0.0005
Sensofar Plμ	by	Sensofar Plμ Neox	Sv	0.3865	0.83	0.4166	3.55	0.0020
Sensofar Plμ	by	Alicona IFM	Sv	0.7629	-0.22	0.8317	8.02	<.0001
Sensofar Plμ	by	Mitaka PAFM	Sv	0.7075	-1.69	0.1059	6.96	<.0001
Sensofar Plμ Neox	by	Alicona IFM	Sv	0.3112	2.72	0.0132	3.01	0.0070
Sensofar Plμ Neox	by	Mitaka PAFM	Sv	0.3935	1.02	0.3188	3.60	0.0018
Alicona IFM	by	Mitaka PAFM	Sv	0.5561	-0.03	0.9777	5.01	<.0001
Sensofar Plμ	by	Sensofar Plμ Neox	Sz	0.5891	0.70	0.4914	5.36	<.0001
Sensofar Plμ	by	Alicona IFM	Sz	0.6728	0.58	0.5714	6.41	<.0001
Sensofar Plμ	by	Mitaka PAFM	Sz	0.6272	-0.04	0.9695	5.80	<.0001
Sensofar Plμ Neox	by	Alicona IFM	Sz	0.4355	2.14	0.0451	3.93	0.0008
Sensofar Plμ Neox	by	Mitaka PAFM	Sz	0.3493	1.70	0.1055	3.28	0.0038
Alicona IFM	by	Mitaka PAFM	Sz	0.4734	1.15	0.2654	4.24	0.0004
Sensofar Plμ	by	Sensofar Plμ Neox	Sds	0.7151	-2.34	0.0300	7.09	<.0001
Sensofar Plμ	by	Alicona IFM	Sds	0.0099	1.80	0.0865	-0.45	0.6596
Sensofar Plμ	by	Mitaka PAFM	Sds	0.0309	1.04	0.3095	0.80	0.4343
Sensofar Plμ Neox	by	Alicona IFM	Sds	0.0731	1.22	0.2379	1.26	0.2235
Sensofar Plμ Neox	by	Mitaka PAFM	Sds	0.1730	1.47	0.1569	2.05	0.0542
Alicona IFM	by	Mitaka PAFM	Sds	0.1231	4.74	0.0001	1.68	0.1093
Sensofar Plμ	by	Sensofar Plμ Neox	Str	0.9007	-0.64	0.5312	13.47	<.0001
Sensofar Plμ	by	Alicona IFM	Str	0.9458	-1.02	0.3218	18.68	<.0001
Sensofar Plμ	by	Mitaka PAFM	Str	0.2176	-1.45	0.1620	2.36	0.0286
Sensofar Plμ Neox	by	Alicona IFM	Str	0.8663	-0.99	0.3329	11.39	<.0001
Sensofar Plμ Neox	by	Mitaka PAFM	Str	0.2201	-1.42	0.1699	2.38	0.0276
Alicona IFM	by	Mitaka PAFM	Str	0.2384	-1.24	0.2287	2.50	0.0211

Bivariate Fit of			Parameter	R^2	Parameter Estimates			
					Intercept		Variable	
					t Ratio	p	t Ratio	p
Sensofar Plμ	by	Sensofar Plμ Neox	Sdq	0.9148	1.38	0.1826	14.66	<.0001
Sensofar Plμ	by	Alicona IFM	Sdq	0.6635	-0.33	0.7476	6.28	<.0001
Sensofar Plμ	by	Mitaka PAFM	Sdq	0.6960	-8.64	<.0001	6.77	<.0001
Sensofar Plμ Neox	by	Alicona IFM	Sdq	0.6639	-1.34	0.1955	6.28	<.0001
Sensofar Plμ Neox	by	Mitaka PAFM	Sdq	0.7873	-12.61	<.0001	8.60	<.0001
Alicona IFM	by	Mitaka PAFM	Sdq	0.5682	-9.71	<.0001	5.13	<.0001
Sensofar Plμ	by	Sensofar Plμ Neox	Ssc	0.9406	-1.99	0.0608	17.80	<.0001
Sensofar Plμ	by	Alicona IFM	Ssc	0.6567	-7.87	<.0001	6.18	<.0001
Sensofar Plμ	by	Mitaka PAFM	Ssc	0.6064	-8.58	<.0001	5.55	<.0001
Sensofar Plμ Neox	by	Alicona IFM	Ssc	0.6493	-6.91	<.0001	6.08	<.0001
Sensofar Plμ Neox	by	Mitaka PAFM	Ssc	0.6630	-8.91	<.0001	6.27	<.0001
Alicona IFM	by	Mitaka PAFM	Ssc	0.5063	-3.05	0.0064	4.53	0.0002
Sensofar Plμ	by	Sensofar Plμ Neox	Sdr	0.9356	-5.20	<.0001	17.05	<.0001
Sensofar Plμ	by	Alicona IFM	Sdr	0.6569	-3.75	0.0013	6.19	<.0001
Sensofar Plμ	by	Mitaka PAFM	Sdr	0.7137	-5.77	<.0001	7.06	<.0001
Sensofar Plμ Neox	by	Alicona IFM	Sdr	0.7032	-2.71	0.0135	6.88	<.0001
Sensofar Plμ Neox	by	Mitaka PAFM	Sdr	0.7902	-6.19	<.0001	8.68	<.0001
Alicona IFM	by	Mitaka PAFM	Sdr	0.5927	-1.85	0.0795	5.40	<.0001
Sensofar Plμ	by	Sensofar Plμ Neox	Vmp	0.9145	0.22	0.8271	14.62	<.0001
Sensofar Plμ	by	Alicona IFM	Vmp	0.9284	-2.24	0.0370	16.10	<.0001
Sensofar Plμ	by	Mitaka PAFM	Vmp	0.7260	1.27	0.2192	7.28	<.0001
Sensofar Plμ Neox	by	Alicona IFM	Vmp	0.8612	-0.88	0.3893	11.14	<.0001
Sensofar Plμ Neox	by	Mitaka PAFM	Vmp	0.6877	1.61	0.1230	6.64	<.0001
Alicona IFM	by	Mitaka PAFM	Vmp	0.7090	3.01	0.0068	6.98	<.0001
Sensofar Plμ	by	Sensofar Plμ Neox	Vmc	0.9500	0.94	0.3566	19.49	<.0001
Sensofar Plμ	by	Alicona IFM	Vmc	0.9029	-1.51	0.1467	13.64	<.0001
Sensofar Plμ	by	Mitaka PAFM	Vmc	0.7093	0.84	0.4118	6.99	<.0001
Sensofar Plμ Neox	by	Alicona IFM	Vmc	0.9549	-3.16	0.0049	20.58	<.0001
Sensofar Plμ Neox	by	Mitaka PAFM	Vmc	0.7665	0.44	0.6645	8.10	<.0001
Alicona IFM	by	Mitaka PAFM	Vmc	0.7236	2.26	0.0352	7.24	<.0001
Sensofar Plμ	by	Sensofar Plμ Neox	Vvc	0.9830	0.69	0.4959	33.98	<.0001
Sensofar Plμ	by	Alicona IFM	Vvc	0.9311	-1.46	0.1596	16.44	<.0001
Sensofar Plμ	by	Mitaka PAFM	Vvc	0.8072	0.30	0.7701	9.15	<.0001
Sensofar Plμ Neox	by	Alicona IFM	Vvc	0.9641	-2.66	0.0150	23.17	<.0001
Sensofar Plμ Neox	by	Mitaka PAFM	Vvc	0.8014	0.22	0.8306	8.98	<.0001
Alicona IFM	by	Mitaka PAFM	Vvc	0.7816	1.63	0.1177	8.46	<.0001
Sensofar Plμ	by	Sensofar Plμ Neox	Vvv	0.9092	0.11	0.9099	14.15	<.0001
Sensofar Plμ	by	Alicona IFM	Vvv	0.8439	-0.17	0.8668	10.40	<.0001
Sensofar Plμ	by	Mitaka PAFM	Vvv	0.4359	0.44	0.6621	3.93	0.0008
Sensofar Plμ Neox	by	Alicona IFM	Vvv	0.8509	0.20	0.8402	10.68	<.0001
Sensofar Plμ Neox	by	Mitaka PAFM	Vvv	0.4174	0.69	0.4962	3.79	0.0012
Alicona IFM	by	Mitaka PAFM	Vvv	0.4317	0.93	0.3657	3.90	0.0009
Sensofar Plμ	by	Sensofar Plμ Neox	Spk	0.8985	-0.46	0.6523	13.31	<.0001
Sensofar Plμ	by	Alicona IFM	Spk	0.9147	1.59	0.1266	14.65	<.0001
Sensofar Plμ	by	Mitaka PAFM	Spk	0.7132	-3.54	0.0020	7.05	<.0001
Sensofar Plμ Neox	by	Alicona IFM	Spk	0.8509	0.71	0.4851	10.69	<.0001
Sensofar Plμ Neox	by	Mitaka PAFM	Spk	0.6669	-3.59	0.0018	6.33	<.0001
Alicona IFM	by	Mitaka PAFM	Spk	0.6855	-5.14	<.0001	6.60	<.0001
Sensofar Plμ	by	Sensofar Plμ Neox	Sk	0.9694	-3.50	0.0023	25.18	<.0001
Sensofar Plμ	by	Alicona IFM	Sk	0.9267	-4.67	0.0001	15.90	<.0001
Sensofar Plμ	by	Mitaka PAFM	Sk	0.7396	-9.82	<.0001	7.54	<.0001
Sensofar Plμ Neox	by	Alicona IFM	Sk	0.9609	-3.00	0.0071	22.18	<.0001
Sensofar Plμ Neox	by	Mitaka PAFM	Sk	0.7662	-8.45	<.0001	8.10	<.0001
Alicona IFM	by	Mitaka PAFM	Sk	0.7189	-6.38	<.0001	7.15	<.0001
Sensofar Plμ	by	Sensofar Plμ Neox	Svk	0.9132	1.50	0.1482	14.51	<.0001
Sensofar Plμ	by	Alicona IFM	Svk	0.8236	0.56	0.5824	9.66	<.0001
Sensofar Plμ	by	Mitaka PAFM	Svk	0.5223	-4.01	0.0007	4.68	0.0001
Sensofar Plμ Neox	by	Alicona IFM	Svk	0.8137	-0.90	0.3773	9.35	<.0001
Sensofar Plμ Neox	by	Mitaka PAFM	Svk	0.4560	-5.07	<.0001	4.09	0.0006
Alicona IFM	by	Mitaka PAFM	Svk	0.5101	-5.14	<.0001	4.56	0.0002

Bivariate Fit of			Parameter	R^2	Parameter Estimates			
					Intercept		Variable	
					t Ratio	p	t Ratio	p
Sensofar Plμ	by	Sensofar Plμ Neox	Smr1	0.8737	0.37	0.7142	11.76	<.0001
Sensofar Plμ	by	Alicona IFM	Smr1	0.8888	-1.48	0.1539	12.64	<.0001
Sensofar Plμ	by	Mitaka PAFM	Smr1	0.4268	0.82	0.4226	3.86	0.0010
Sensofar Plμ Neox	by	Alicona IFM	Smr1	0.7915	-0.26	0.7939	8.71	<.0001
Sensofar Plμ Neox	by	Mitaka PAFM	Smr1	0.3723	1.19	0.2482	3.44	0.0026
Alicona IFM	by	Mitaka PAFM	Smr1	0.4738	1.62	0.1202	4.24	0.0004
Sensofar Plμ	by	Sensofar Plμ Neox	Smr2	0.9584	1.83	0.0822	21.47	<.0001
Sensofar Plμ	by	Alicona IFM	Smr2	0.8658	1.87	0.0767	11.36	<.0001
Sensofar Plμ	by	Mitaka PAFM	Smr2	0.3718	1.78	0.0900	3.44	0.0026
Sensofar Plμ Neox	by	Alicona IFM	Smr2	0.8858	1.04	0.3109	12.46	<.0001
Sensofar Plμ Neox	by	Mitaka PAFM	Smr2	0.4240	1.30	0.2096	3.84	0.0010
Alicona IFM	by	Mitaka PAFM	Smr2	0.4390	1.14	0.2658	3.96	0.0008
Sensofar Plμ	by	Sensofar Plμ Neox	S5z	0.6738	0.96	0.3489	6.43	<.0001
Sensofar Plμ	by	Alicona IFM	S5z	0.8523	-2.18	0.0418	10.74	<.0001
Sensofar Plμ	by	Mitaka PAFM	S5z	0.6693	-0.52	0.6088	6.36	<.0001
Sensofar Plμ Neox	by	Alicona IFM	S5z	0.6074	-0.05	0.9631	5.56	<.0001
Sensofar Plμ Neox	by	Mitaka PAFM	S5z	0.5548	0.30	0.7649	4.99	<.0001
Alicona IFM	by	Mitaka PAFM	S5z	0.6109	1.70	0.1049	5.60	<.0001
Sensofar Plμ	by	Sensofar Plμ Neox	Sa	0.9451	-0.54	0.5952	18.55	<.0001
Sensofar Plμ	by	Alicona IFM	Sa	0.9226	0.21	0.8329	15.44	<.0001
Sensofar Plμ	by	Mitaka PAFM	Sa	0.6843	-4.05	0.0006	6.58	<.0001
Sensofar Plμ Neox	by	Alicona IFM	Sa	0.9647	0.85	0.4072	23.39	<.0001
Sensofar Plμ Neox	by	Mitaka PAFM	Sa	0.7159	-4.11	0.0005	7.10	<.0001
Alicona IFM	by	Mitaka PAFM	Sa	0.6841	-4.63	0.0002	6.58	<.0001

Table 5.10 *Linear Regression tests comparing all possible pairs of microscopes for all Non-Resampled data. Data for each parameter is tested separately and t-ratio and p values are given for the intercept and regression line of each comparison within each parameter. R^2 values are also reported for each comparisons within each parameter. Significant p values (α=0.05) are highlighted in red, and all significant results were tested using the Benjimini-Hochberg method.*

Finally the results of comparisons between Resampled data from different microscopes within the Volume group show no agreement between microscopes for any comparison involving the Sensofar Plμ instrument. However comparisons between the Alicona IFM and each of the Sensofar Plμ neox and Mitaka PAFM data and the comparison between Sensofar Plμ neox and Mitaka PAFM data all show agreement between the different instruments. Only two intercepts do not pass through zero, which are for the comparisons between data from the Sensofar Plμ instrument and the Sensofar Plμ neox and Alicona IFM.

Bivariate Fit of			Parameter	R^2	Parameter Estimates			
					Intercept		Variable	
					t Ratio	p	t Ratio	p
Sensofar Plμ	by	Sensofar Plμ Neox	Tfv	0.9369	-0.46	0.6535	17.23	<.0001
Sensofar Plμ	by	Alicona IFM	Tfv	0.8888	-2.90	0.0088	12.64	<.0001
Sensofar Plμ	by	Mitaka PAFM	Tfv	0.7069	-3.83	0.0010	6.95	<.0001
Sensofar Plμ Neox	by	Alicona IFM	Tfv	0.9703	-5.56	<.0001	25.57	<.0001
Sensofar Plμ Neox	by	Mitaka PAFM	Tfv	0.5500	-2.28	0.0337	4.94	<.0001
Alicona IFM	by	Mitaka PAFM	Tfv	0.4554	-0.94	0.3567	4.09	0.0006
Sensofar Plμ	by	Sensofar Plμ Neox	Asfc	0.9023	-3.80	0.0011	13.59	<.0001
Sensofar Plμ	by	Alicona IFM	Asfc	0.4674	-2.30	0.0326	4.19	0.0005
Sensofar Plμ	by	Mitaka PAFM	Asfc	0.6946	-5.23	<.0001	6.74	<.0001
Sensofar Plμ Neox	by	Alicona IFM	Asfc	0.6063	-2.21	0.0390	5.55	<.0001
Sensofar Plμ Neox	by	Mitaka PAFM	Asfc	0.7812	-5.73	<.0001	8.45	<.0001
Alicona IFM	by	Mitaka PAFM	Asfc	0.4836	-0.56	0.5811	4.33	0.0003
Sensofar Plμ	by	Sensofar Plμ Neox	epLsar	0.9643	-1.82	0.0844	23.24	<.0001
Sensofar Plμ	by	Alicona IFM	epLsar	0.9051	-0.20	0.8429	13.81	<.0001
Sensofar Plμ	by	Mitaka PAFM	epLsar	0.0027	-2.83	0.0102	-0.23	0.8169
Sensofar Plμ Neox	by	Alicona IFM	epLsar	0.9617	1.58	0.1309	22.40	<.0001
Sensofar Plμ Neox	by	Mitaka PAFM	epLsar	0.0077	-2.85	0.0098	-0.39	0.6972
Alicona IFM	by	Mitaka PAFM	epLsar	0.0099	-3.15	0.0050	-0.45	0.6601
Sensofar Plμ	by	Sensofar Plμ Neox	HAsfc 2x2	0.5410	-1.36	0.1903	4.86	<.0001
Sensofar Plμ	by	Alicona IFM	HAsfc 2x2	0.3679	-1.03	0.3155	3.41	0.0028
Sensofar Plμ	by	Mitaka PAFM	HAsfc 2x2	0.0795	-1.89	0.0728	1.31	0.2035
Sensofar Plμ Neox	by	Alicona IFM	HAsfc 2x2	0.2425	-1.68	0.1092	2.53	0.0199
Sensofar Plμ Neox	by	Mitaka PAFM	HAsfc 2x2	0.3001	-0.97	0.3421	2.93	0.0083
Alicona IFM	by	Mitaka PAFM	HAsfc 2x2	0.1404	-2.35	0.0291	1.81	0.0857
Sensofar Plμ	by	Sensofar Plμ Neox	HAsfc 3x3	0.6913	1.80	0.0870	6.69	<.0001
Sensofar Plμ	by	Alicona IFM	HAsfc 3x3	0.2408	0.42	0.6795	2.52	0.0204
Sensofar Plμ	by	Mitaka PAFM	HAsfc 3x3	0.1438	0.24	0.8160	1.83	0.0817
Sensofar Plμ Neox	by	Alicona IFM	HAsfc 3x3	0.1816	-1.26	0.2214	2.11	0.0480
Sensofar Plμ Neox	by	Mitaka PAFM	HAsfc 3x3	0.2653	-0.27	0.7892	2.69	0.0142
Alicona IFM	by	Mitaka PAFM	HAsfc 3x3	0.3703	-1.10	0.2827	3.43	0.0027
Sensofar Plμ	by	Sensofar Plμ Neox	HAsfc 4x4	0.7402	2.10	0.0486	7.55	<.0001
Sensofar Plμ	by	Alicona IFM	HAsfc 4x4	0.3722	1.24	0.2311	3.44	0.0026
Sensofar Plμ	by	Mitaka PAFM	HAsfc 4x4	0.1680	0.56	0.5844	2.01	0.0581
Sensofar Plμ Neox	by	Alicona IFM	HAsfc 4x4	0.4092	-0.02	0.9847	3.72	0.0013
Sensofar Plμ Neox	by	Mitaka PAFM	HAsfc 4x4	0.3668	0.59	0.5624	3.40	0.0028
Alicona IFM	by	Mitaka PAFM	HAsfc 4x4	0.3239	-1.07	0.2971	3.10	0.0057
Sensofar Plμ	by	Sensofar Plμ Neox	HAsfc 5x5	0.5853	2.18	0.0411	5.31	<.0001
Sensofar Plμ	by	Alicona IFM	HAsfc 5x5	0.5195	3.18	0.0047	4.65	0.0002
Sensofar Plμ	by	Mitaka PAFM	HAsfc 5x5	0.0929	0.71	0.4852	1.43	0.1678
Sensofar Plμ Neox	by	Alicona IFM	HAsfc 5x5	0.4900	1.07	0.2989	4.38	0.0003
Sensofar Plμ Neox	by	Mitaka PAFM	HAsfc 5x5	0.1922	0.20	0.8400	2.18	0.0413
Alicona IFM	by	Mitaka PAFM	HAsfc 5x5	0.2284	-1.40	0.1772	2.43	0.0245
Sensofar Plμ	by	Sensofar Plμ Neox	HAsfc 6x6	0.7384	4.31	0.0003	7.51	<.0001
Sensofar Plμ	by	Alicona IFM	HAsfc 6x6	0.4808	3.49	0.0023	4.30	0.0003
Sensofar Plμ	by	Mitaka PAFM	HAsfc 6x6	0.0903	1.07	0.2964	1.41	0.1743
Sensofar Plμ Neox	by	Alicona IFM	HAsfc 6x6	0.4465	1.23	0.2312	4.02	0.0007
Sensofar Plμ Neox	by	Mitaka PAFM	HAsfc 6x6	0.1908	0.54	0.5953	2.17	0.0421
Alicona IFM	by	Mitaka PAFM	HAsfc 6x6	0.2358	-1.17	0.2540	2.48	0.0220
Sensofar Plμ	by	Sensofar Plμ Neox	HAsfc 7x7	0.7051	4.75	0.0001	6.92	<.0001
Sensofar Plμ	by	Alicona IFM	HAsfc 7x7	0.5354	4.38	0.0003	4.80	0.0001
Sensofar Plμ	by	Mitaka PAFM	HAsfc 7x7	0.0619	1.06	0.3015	1.15	0.2640
Sensofar Plμ Neox	by	Alicona IFM	HAsfc 7x7	0.3995	1.16	0.2597	3.65	0.0016
Sensofar Plμ Neox	by	Mitaka PAFM	HAsfc 7x7	0.1210	0.05	0.9639	1.66	0.1127
Alicona IFM	by	Mitaka PAFM	HAsfc 7x7	0.1862	-1.80	0.0868	2.14	0.0449
Sensofar Plμ	by	Sensofar Plμ Neox	HAsfc 8x8	0.7037	4.82	0.0001	6.89	<.0001
Sensofar Plμ	by	Alicona IFM	HAsfc 8x8	0.5424	4.63	0.0002	4.87	<.0001
Sensofar Plμ	by	Mitaka PAFM	HAsfc 8x8	0.1404	1.80	0.0865	1.81	0.0858
Sensofar Plμ Neox	by	Alicona IFM	HAsfc 8x8	0.4162	1.50	0.1497	3.78	0.0012
Sensofar Plμ Neox	by	Mitaka PAFM	HAsfc 8x8	0.2171	0.81	0.4247	2.36	0.0288
Alicona IFM	by	Mitaka PAFM	HAsfc 8x8	0.2622	-1.45	0.1638	2.67	0.0148

Bivariate Fit of			Parameter	R^2	Parameter Estimates			
					Intercept		Variable	
					t Ratio	p	t Ratio	p
Sensofar Plμ	by	Sensofar Plμ Neox	HAsfc 9x9	0.5923	5.32	<.0001	5.39	<.0001
Sensofar Plμ	by	Alicona IFM	HAsfc 9x9	0.5005	5.19	<.0001	4.48	0.0002
Sensofar Plμ	by	Mitaka PAFM	HAsfc 9x9	0.0459	1.62	0.1206	0.98	0.3381
Sensofar Plμ Neox	by	Alicona IFM	HAsfc 9x9	0.3539	1.62	0.1203	3.31	0.0035
Sensofar Plμ Neox	by	Mitaka PAFM	HAsfc 9x9	0.1756	0.86	0.3989	2.06	0.0522
Alicona IFM	by	Mitaka PAFM	HAsfc 9x9	0.2575	-1.63	0.1186	2.63	0.0159
Sensofar Plμ	by	Sensofar Plμ Neox	HAsfc 10x10	0.6324	5.73	<.0001	5.87	<.0001
Sensofar Plμ	by	Alicona IFM	HAsfc 10x10	0.5703	6.04	<.0001	5.15	<.0001
Sensofar Plμ	by	Mitaka PAFM	HAsfc 10x10	0.0616	1.85	0.0788	1.15	0.2652
Sensofar Plμ Neox	by	Alicona IFM	HAsfc 10x10	0.4167	2.15	0.0444	3.78	0.0012
Sensofar Plμ Neox	by	Mitaka PAFM	HAsfc 10x10	0.1718	1.02	0.3189	2.04	0.0551
Alicona IFM	by	Mitaka PAFM	HAsfc 10x10	0.2708	-1.37	0.1850	2.73	0.0130
Sensofar Plμ	by	Sensofar Plμ Neox	HAsfc 11x11	0.6130	6.20	<.0001	5.63	<.0001
Sensofar Plμ	by	Alicona IFM	HAsfc 11x11	0.5876	6.93	<.0001	5.34	<.0001
Sensofar Plμ	by	Mitaka PAFM	HAsfc 11x11	0.0704	2.38	0.0273	1.23	0.2329
Sensofar Plμ Neox	by	Alicona IFM	HAsfc 11x11	0.4354	2.64	0.0158	3.93	0.0008
Sensofar Plμ Neox	by	Mitaka PAFM	HAsfc 11x11	0.1330	1.06	0.3029	1.75	0.0951
Alicona IFM	by	Mitaka PAFM	HAsfc 11x11	0.2837	-1.30	0.2070	2.81	0.0107
Sensofar Plμ	by	Sensofar Plμ Neox	Sq	0.9585	-0.23	0.8207	21.50	<.0001
Sensofar Plμ	by	Alicona IFM	Sq	0.9139	0.39	0.7028	14.57	<.0001
Sensofar Plμ	by	Mitaka PAFM	Sq	0.5318	-5.15	<.0001	4.77	0.0001
Sensofar Plμ Neox	by	Alicona IFM	Sq	0.9541	0.76	0.4565	20.40	<.0001
Sensofar Plμ Neox	by	Mitaka PAFM	Sq	0.5530	-5.28	<.0001	4.97	<.0001
Alicona IFM	by	Mitaka PAFM	Sq	0.4292	-5.72	<.0001	3.88	0.0009
Sensofar Plμ	by	Sensofar Plμ Neox	Sku	0.9245	1.62	0.1208	15.65	<.0001
Sensofar Plμ	by	Alicona IFM	Sku	0.7984	1.17	0.2569	8.90	<.0001
Sensofar Plμ	by	Mitaka PAFM	Sku	0.4029	2.87	0.0095	3.67	0.0015
Sensofar Plμ Neox	by	Alicona IFM	Sku	0.8113	0.52	0.6059	9.27	<.0001
Sensofar Plμ Neox	by	Mitaka PAFM	Sku	0.3772	2.54	0.0193	3.48	0.0024
Alicona IFM	by	Mitaka PAFM	Sku	0.4594	2.67	0.0147	4.12	0.0005
Sensofar Plμ	by	Sensofar Plμ Neox	Sp	0.8854	-0.54	0.5921	12.43	<.0001
Sensofar Plμ	by	Alicona IFM	Sp	0.7572	-1.44	0.1649	7.90	<.0001
Sensofar Plμ	by	Mitaka PAFM	Sp	0.5148	-1.05	0.3074	4.61	0.0002
Sensofar Plμ Neox	by	Alicona IFM	Sp	0.7436	-0.77	0.4499	7.62	<.0001
Sensofar Plμ Neox	by	Mitaka PAFM	Sp	0.5686	-0.90	0.3772	5.13	<.0001
Alicona IFM	by	Mitaka PAFM	Sp	0.5854	0.13	0.8953	5.31	<.0001
Sensofar Plμ	by	Sensofar Plμ Neox	Sv	0.7231	0.58	0.5674	7.23	<.0001
Sensofar Plμ	by	Alicona IFM	Sv	0.7206	1.27	0.2187	7.18	<.0001
Sensofar Plμ	by	Mitaka PAFM	Sv	0.3392	1.16	0.2609	3.20	0.0045
Sensofar Plμ Neox	by	Alicona IFM	Sv	0.6310	2.07	0.0519	5.85	<.0001
Sensofar Plμ Neox	by	Mitaka PAFM	Sv	0.2375	1.88	0.0755	2.50	0.0214
Alicona IFM	by	Mitaka PAFM	Sv	0.1878	1.72	0.1009	2.15	0.0439
Sensofar Plμ	by	Sensofar Plμ Neox	Sz	0.7872	0.51	0.6164	8.60	<.0001
Sensofar Plμ	by	Alicona IFM	Sz	0.7366	1.06	0.3004	7.48	<.0001
Sensofar Plμ	by	Mitaka PAFM	Sz	0.4912	1.55	0.1365	4.39	0.0003
Sensofar Plμ Neox	by	Alicona IFM	Sz	0.6176	1.82	0.0833	5.68	<.0001
Sensofar Plμ Neox	by	Mitaka PAFM	Sz	0.4510	2.02	0.0574	4.05	0.0006
Alicona IFM	by	Mitaka PAFM	Sz	0.4605	1.73	0.0988	4.13	0.0005
Sensofar Plμ	by	Sensofar Plμ Neox	Sds	0.6685	-2.01	0.0586	6.35	<.0001
Sensofar Plμ	by	Alicona IFM	Sds	0.0013	0.90	0.3779	0.16	0.8731
Sensofar Plμ	by	Mitaka PAFM	Sds	0.0517	0.72	0.4808	1.04	0.3087
Sensofar Plμ Neox	by	Alicona IFM	Sds	0.1099	0.44	0.6628	1.57	0.1318
Sensofar Plμ Neox	by	Mitaka PAFM	Sds	0.1629	1.38	0.1823	1.97	0.0625
Alicona IFM	by	Mitaka PAFM	Sds	0.0621	6.31	<.0001	1.15	0.2635
Sensofar Plμ	by	Sensofar Plμ Neox	Str	0.9142	-0.93	0.3656	14.60	<.0001
Sensofar Plμ	by	Alicona IFM	Str	0.9501	-1.52	0.1433	19.52	<.0001
Sensofar Plμ	by	Mitaka PAFM	Str	0.3121	-1.30	0.2087	3.01	0.0069
Sensofar Plμ Neox	by	Alicona IFM	Str	0.9162	-0.98	0.3392	14.79	<.0001
Sensofar Plμ Neox	by	Mitaka PAFM	Str	0.3693	-1.00	0.3314	3.42	0.0027
Alicona IFM	by	Mitaka PAFM	Str	0.3407	-0.95	0.3556	3.21	0.0043

Bivariate Fit of			Parameter	R^2	Parameter Estimates			
					Intercept		Variable	
					t Ratio	p	t Ratio	p
Sensofar Plμ	by	Sensofar Plμ Neox	Sdq	0.9090	1.78	0.0896	14.14	<.0001
Sensofar Plμ	by	Alicona IFM	Sdq	0.5657	-0.20	0.8463	5.10	<.0001
Sensofar Plμ	by	Mitaka PAFM	Sdq	0.7418	-7.47	<.0001	7.58	<.0001
Sensofar Plμ Neox	by	Alicona IFM	Sdq	0.5982	-1.16	0.2591	5.46	<.0001
Sensofar Plμ Neox	by	Mitaka PAFM	Sdq	0.8223	-12.09	<.0001	9.62	<.0001
Alicona IFM	by	Mitaka PAFM	Sdq	0.4619	-8.90	<.0001	4.14	0.0005
Sensofar Plμ	by	Sensofar Plμ Neox	Ssc	0.9216	2.84	0.0101	15.33	<.0001
Sensofar Plμ	by	Alicona IFM	Ssc	0.6527	-0.82	0.4221	6.13	<.0001
Sensofar Plμ	by	Mitaka PAFM	Ssc	0.6725	-9.86	<.0001	6.41	<.0001
Sensofar Plμ Neox	by	Alicona IFM	Ssc	0.6495	-2.67	0.0147	6.09	<.0001
Sensofar Plμ Neox	by	Mitaka PAFM	Ssc	0.6728	-12.02	<.0001	6.41	<.0001
Alicona IFM	by	Mitaka PAFM	Ssc	0.4486	-7.24	<.0001	4.03	0.0007
Sensofar Plμ	by	Sensofar Plμ Neox	Sdr	0.9224	-4.00	0.0007	15.42	<.0001
Sensofar Plμ	by	Alicona IFM	Sdr	0.5579	-2.93	0.0083	5.02	<.0001
Sensofar Plμ	by	Mitaka PAFM	Sdr	0.7436	-6.18	<.0001	7.62	<.0001
Sensofar Plμ Neox	by	Alicona IFM	Sdr	0.6322	-2.41	0.0259	5.86	<.0001
Sensofar Plμ Neox	by	Mitaka PAFM	Sdr	0.8075	-6.61	<.0001	9.16	<.0001
Alicona IFM	by	Mitaka PAFM	Sdr	0.4723	-0.94	0.3562	4.23	0.0004
Sensofar Plμ	by	Sensofar Plμ Neox	Vmp	0.9607	-0.08	0.9333	22.11	<.0001
Sensofar Plμ	by	Alicona IFM	Vmp	0.9318	-2.27	0.0348	16.53	<.0001
Sensofar Plμ	by	Mitaka PAFM	Vmp	0.5385	1.67	0.1111	4.83	0.0001
Sensofar Plμ Neox	by	Alicona IFM	Vmp	0.9331	-1.95	0.0651	16.70	<.0001
Sensofar Plμ Neox	by	Mitaka PAFM	Vmp	0.5737	1.74	0.0979	5.19	<.0001
Alicona IFM	by	Mitaka PAFM	Vmp	0.5604	2.94	0.0080	5.05	<.0001
Sensofar Plμ	by	Sensofar Plμ Neox	Vmc	0.9673	1.69	0.1059	24.31	<.0001
Sensofar Plμ	by	Alicona IFM	Vmc	0.8803	-1.19	0.2473	12.13	<.0001
Sensofar Plμ	by	Mitaka PAFM	Vmc	0.6086	1.05	0.3049	5.58	<.0001
Sensofar Plμ Neox	by	Alicona IFM	Vmc	0.9274	-2.64	0.0159	15.98	<.0001
Sensofar Plμ Neox	by	Mitaka PAFM	Vmc	0.6539	0.55	0.5853	6.15	<.0001
Alicona IFM	by	Mitaka PAFM	Vmc	0.5643	2.34	0.0299	5.09	<.0001
Sensofar Plμ	by	Sensofar Plμ Neox	Vvc	0.9849	1.75	0.0948	36.14	<.0001
Sensofar Plμ	by	Alicona IFM	Vvc	0.9184	-1.46	0.1591	15.00	<.0001
Sensofar Plμ	by	Mitaka PAFM	Vvc	0.7272	0.43	0.6697	7.30	<.0001
Sensofar Plμ Neox	by	Alicona IFM	Vvc	0.9532	-3.00	0.0071	20.18	<.0001
Sensofar Plμ Neox	by	Mitaka PAFM	Vvc	0.7295	0.12	0.9056	7.34	<.0001
Alicona IFM	by	Mitaka PAFM	Vvc	0.6645	1.77	0.0920	6.29	<.0001
Sensofar Plμ	by	Sensofar Plμ Neox	Vvv	0.9664	-0.29	0.7730	23.97	<.0001
Sensofar Plμ	by	Alicona IFM	Vvv	0.8578	0.18	0.8579	10.98	<.0001
Sensofar Plμ	by	Mitaka PAFM	Vvv	0.4511	1.19	0.2486	4.05	0.0006
Sensofar Plμ Neox	by	Alicona IFM	Vvv	0.8939	0.33	0.7446	12.98	<.0001
Sensofar Plμ Neox	by	Mitaka PAFM	Vvv	0.4439	1.37	0.1864	4.00	0.0007
Alicona IFM	by	Mitaka PAFM	Vvv	0.3559	1.82	0.0844	3.32	0.0034
Sensofar Plμ	by	Sensofar Plμ Neox	Spk	0.9561	-0.52	0.6064	20.87	<.0001
Sensofar Plμ	by	Alicona IFM	Spk	0.9357	1.19	0.2482	17.06	<.0001
Sensofar Plμ	by	Mitaka PAFM	Spk	0.5624	-3.33	0.0034	5.07	<.0001
Sensofar Plμ Neox	by	Alicona IFM	Spk	0.9343	1.24	0.2279	16.87	<.0001
Sensofar Plμ Neox	by	Mitaka PAFM	Spk	0.6020	-3.29	0.0036	5.50	<.0001
Alicona IFM	by	Mitaka PAFM	Spk	0.5786	-4.24	0.0004	5.24	<.0001
Sensofar Plμ	by	Sensofar Plμ Neox	Sk	0.9828	-5.51	<.0001	33.81	<.0001
Sensofar Plμ	by	Alicona IFM	Sk	0.9258	-4.17	0.0005	15.80	<.0001
Sensofar Plμ	by	Mitaka PAFM	Sk	0.6902	-8.47	<.0001	6.68	<.0001
Sensofar Plμ Neox	by	Alicona IFM	Sk	0.9539	-1.67	0.1108	20.34	<.0001
Sensofar Plμ Neox	by	Mitaka PAFM	Sk	0.7024	-6.67	<.0001	6.87	<.0001
Alicona IFM	by	Mitaka PAFM	Sk	0.6258	-5.50	<.0001	5.78	<.0001
Sensofar Plμ	by	Sensofar Plμ Neox	Svk	0.9572	1.44	0.1648	21.15	<.0001
Sensofar Plμ	by	Alicona IFM	Svk	0.8328	0.81	0.4275	9.98	<.0001
Sensofar Plμ	by	Mitaka PAFM	Svk	0.4783	-4.28	0.0004	4.28	0.0004
Sensofar Plμ Neox	by	Alicona IFM	Svk	0.8607	0.08	0.9332	11.12	<.0001
Sensofar Plμ Neox	by	Mitaka PAFM	Svk	0.4354	-4.92	<.0001	3.93	0.0008
Alicona IFM	by	Mitaka PAFM	Svk	0.3693	-5.37	<.0001	3.42	0.0027

Bivariate Fit of			Parameter	R^2	Parameter Estimates			
					Intercept		Variable	
					t Ratio	p	t Ratio	p
Sensofar Plμ	by	Sensofar Plμ Neox	Smr1	0.9030	0.61	0.5505	13.65	<.0001
Sensofar Plμ	by	Alicona IFM	Smr1	0.8993	-1.32	0.2023	13.37	<.0001
Sensofar Plμ	by	Mitaka PAFM	Smr1	0.3994	1.18	0.2515	3.65	0.0016
Sensofar Plμ Neox	by	Alicona IFM	Smr1	0.8916	-1.13	0.2713	12.83	<.0001
Sensofar Plμ Neox	by	Mitaka PAFM	Smr1	0.4096	1.18	0.2518	3.72	0.0013
Alicona IFM	by	Mitaka PAFM	Smr1	0.4890	1.75	0.0954	4.37	0.0003
Sensofar Plμ	by	Sensofar Plμ Neox	Smr2	0.9802	1.65	0.1140	31.44	<.0001
Sensofar Plμ	by	Alicona IFM	Smr2	0.9053	1.68	0.1076	13.83	<.0001
Sensofar Plμ	by	Mitaka PAFM	Smr2	0.4468	1.51	0.1479	4.02	0.0007
Sensofar Plμ Neox	by	Alicona IFM	Smr2	0.9195	1.03	0.3150	15.11	<.0001
Sensofar Plμ Neox	by	Mitaka PAFM	Smr2	0.4911	1.13	0.2703	4.39	0.0003
Alicona IFM	by	Mitaka PAFM	Smr2	0.5302	0.87	0.3972	4.75	0.0001
Sensofar Plμ	by	Sensofar Plμ Neox	S5z	0.8702	-1.36	0.1890	11.58	<.0001
Sensofar Plμ	by	Alicona IFM	S5z	0.7204	-0.74	0.4665	7.18	<.0001
Sensofar Plμ	by	Mitaka PAFM	S5z	0.6254	-0.56	0.5834	5.78	<.0001
Sensofar Plμ Neox	by	Alicona IFM	S5z	0.6962	0.72	0.4819	6.77	<.0001
Sensofar Plμ Neox	by	Mitaka PAFM	S5z	0.5725	0.75	0.4610	5.18	<.0001
Alicona IFM	by	Mitaka PAFM	S5z	0.3559	1.86	0.0775	3.32	0.0034
Sensofar Plμ	by	Sensofar Plμ Neox	Sa	0.9695	-1.37	0.1850	25.23	<.0001
Sensofar Plμ	by	Alicona IFM	Sa	0.9040	-0.01	0.9918	13.73	<.0001
Sensofar Plμ	by	Mitaka PAFM	Sa	0.5572	-4.12	0.0005	5.02	<.0001
Sensofar Plμ Neox	by	Alicona IFM	Sa	0.9471	1.10	0.2835	18.93	<.0001
Sensofar Plμ Neox	by	Mitaka PAFM	Sa	0.5807	-3.78	0.0012	5.26	<.0001
Alicona IFM	by	Mitaka PAFM	Sa	0.4756	-4.54	0.0002	4.26	0.0004

Table 5.11 *Linear Regression tests comparing all possible pairs of microscopes for all Resampled data. Data for each parameter is tested separately and t-ratio and p values are given for the intercept and regression line of each comparison within each parameter. R^2 values are also reported for each comparions within each parameter. Significant p values (α=0.05) are highlighted in red, and all significant results were tested using the Benjimini-Hochberg method.*

	A. Non-Resampled Data			**B.** Resampled Data		
	Probable Error	Intraclass Correlation	Interpretation	Probable Error	Intraclass Correlation	Interpretation
Tfv	0.2524	0.3939	Poor	0.2713	0.5515	Fair
Asfc	0.1200	0.1783	Poor	0.1153	0.1999	Poor
epLsar	0.1736	0.2411	Poor	0.1496	0.4382	Fair
HAsfc 2x2	0.1333	0.0784	Poor	0.1229	0.1502	Poor
HAsfc 3x3	0.1332	0.0661	Poor	0.1571	0.0834	Poor
HAsfc 4x4	0.1196	0.0819	Poor	0.1284	0.0977	Poor
HAsfc 5x5	0.1190	0.1113	Poor	0.1292	0.0950	Poor
HAsfc 6x6	0.1129	0.0606	Poor	0.1233	0.1026	Poor
HAsfc 7x7	0.1044	0.0908	Poor	0.1210	0.0970	Poor
HAsfc 8x8	0.1033	0.0851	Poor	0.1113	0.1149	Poor
HAsfc 9x9	0.0982	0.0865	Poor	0.1107	0.0968	Poor
HAsfc 10x10	0.0963	0.0963	Poor	0.1091	0.1141	Poor
HAsfc 11x11	0.0965	0.0865	Poor	0.1057	0.1169	Poor
Sq	0.0610	0.4744	Fair	0.0647	0.4514	Fair
Sku	0.1301	0.4542	Fair	0.1262	0.3683	Poor
Sp	0.1155	0.5624	Fair	0.1439	0.4413	Fair
Sv	0.0898	0.2335	Poor	0.0818	0.2850	Poor
Sz	0.0811	0.3596	Poor	0.0858	0.3584	Poor
Sds	0.0726	0.0000	Poor	0.0715	0.0000	Poor
Str	0.1359	0.5408	Fair	0.1330	0.5646	Fair
Sdq	0.0707	0.2797	Poor	0.0720	0.2578	Poor
Ssc	0.1220	0.3998	Poor	0.1155	0.4035	Fair
Sdr	0.1262	0.2659	Poor	0.1298	0.2486	Poor
Vmp	0.1231	0.6373	Good	0.1344	0.5614	Fair
Vmc	0.0673	0.5225	Fair	0.0702	0.4872	Fair
Vvc	0.0738	0.6397	Good	0.0766	0.6098	Good
Vvv	0.0879	0.2532	Poor	0.0914	0.2642	Poor
Spk	0.1194	0.6339	Good	0.1322	0.5456	Fair
Sk	0.0747	0.5923	Fair	0.0768	0.5662	Fair
Svk	0.0902	0.2849	Poor	0.0910	0.2949	Poor
Smr1	0.0446	0.5100	Fair	0.0454	0.4930	Fair
Smr2	0.0090	0.5427	Fair	0.0091	0.5511	Fair
S5z	0.0702	0.3406	Poor	0.0710	0.4158	Fair
Sa	0.0592	0.5228	Fair	0.0632	0.4813	Fair

Table 5.12 *Intraclass Correlation tests comparing all possible pairs of microscopes for Non-Resampled (A.) and Resampled (B.) data. Data for each parameter is tested separately and probable error, intraclass correlation and interpretation are given in each case. The interpretation provides a measure of how well the classes are correlated (Cicchetti 1994), with classes based on the correlation result (Poor = 0 to 0.4, Fair = 0.4 to 0.59, Good = 0.6 to 0.74, and Excellent = 0.75 to 1).*

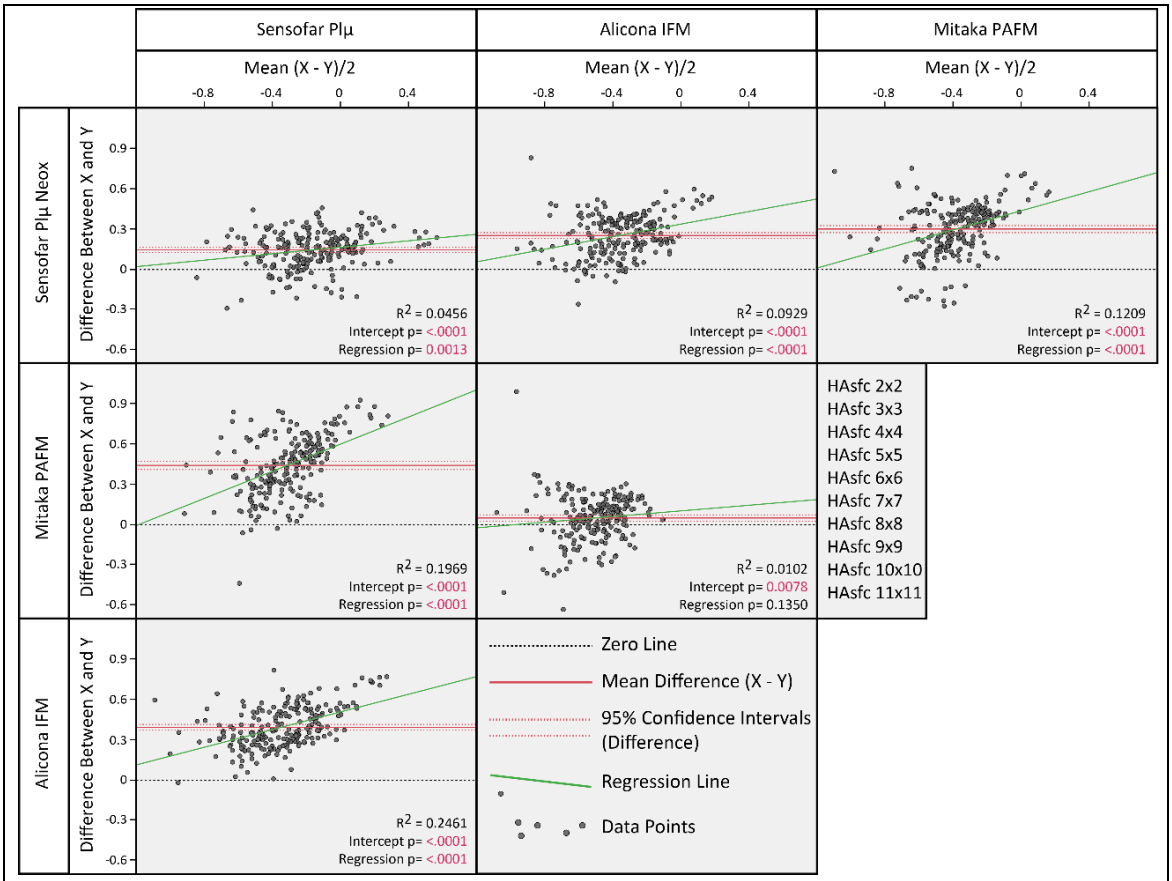

Figure 5.3 *Bland-Altman plots of 3D roughness parameter data, comparing pairs of microscopes. All Non-Resampled data for parameters HAsfc2x2 to HAsfc 11x11 are included. X-axis shows the mean of each datafile collected on the two microscopes. Y-axis shows the difference between each datafile. Microscope names at the top are compared to microscope names on the right hand side, with figures representing their comparison where the two cross. The R^2, intercept and Regression test results are given for each plot, black dashed line = zero line, solid red line = mean of Y-axis, dashed red line = 95% confidence intervals of mean, green line = regression line.*

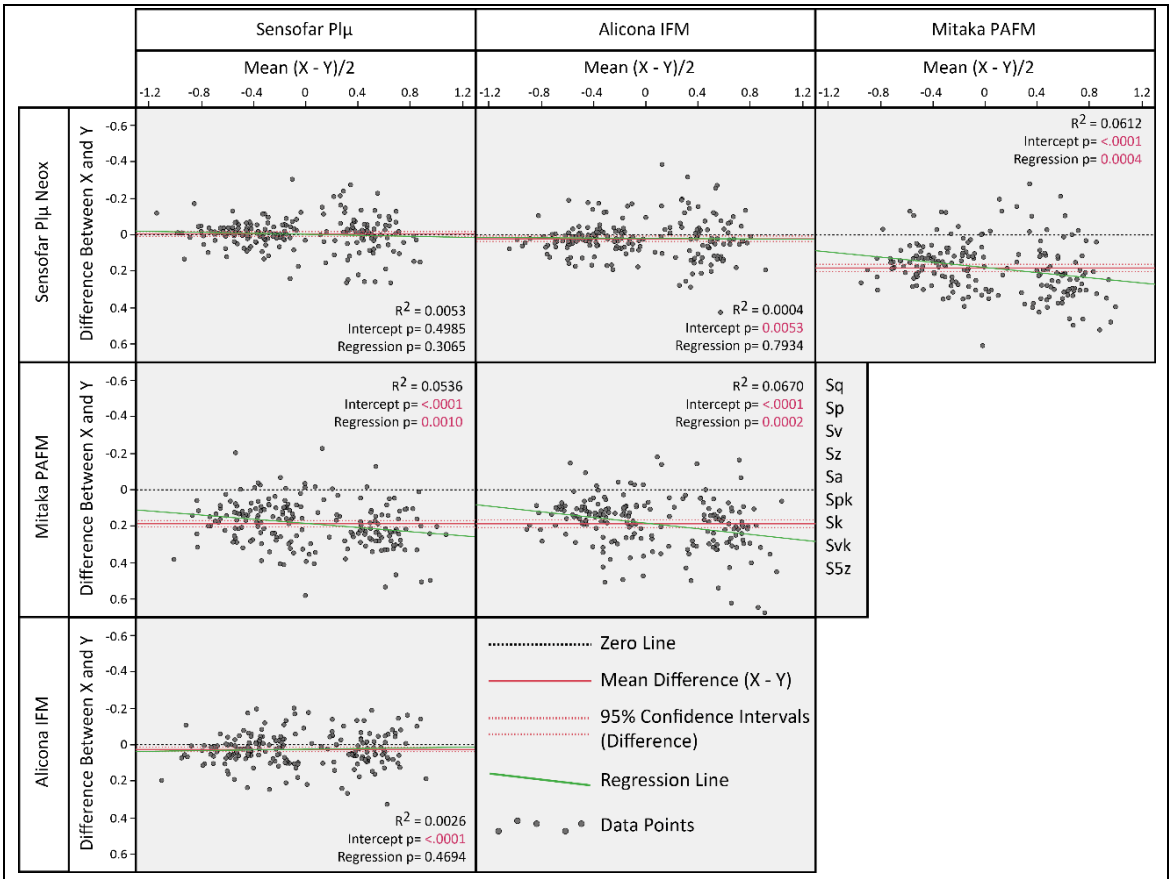

Figure 5.4 *Bland-Altman plots of 3D roughness parameter data, comparing pairs of microscopes. All Non-Resampled data for parameters Sq, Sp, Sv, Sa, Spk, Sk, Svk, S5z are included. X-axis shows the mean of each datafile collected on the two microscopes. Y-axis shows the difference between each datafile. Microscope names at the top are compared to microscope names on the right hand side, with figures representing their comparison where the two cross. The R^2, intercept and Regression test results are given for each plot, black dashed line = zero line, solid red line = mean of Y-axis, dashed red line = 95% confidence intervals of mean, green line = regression line.*

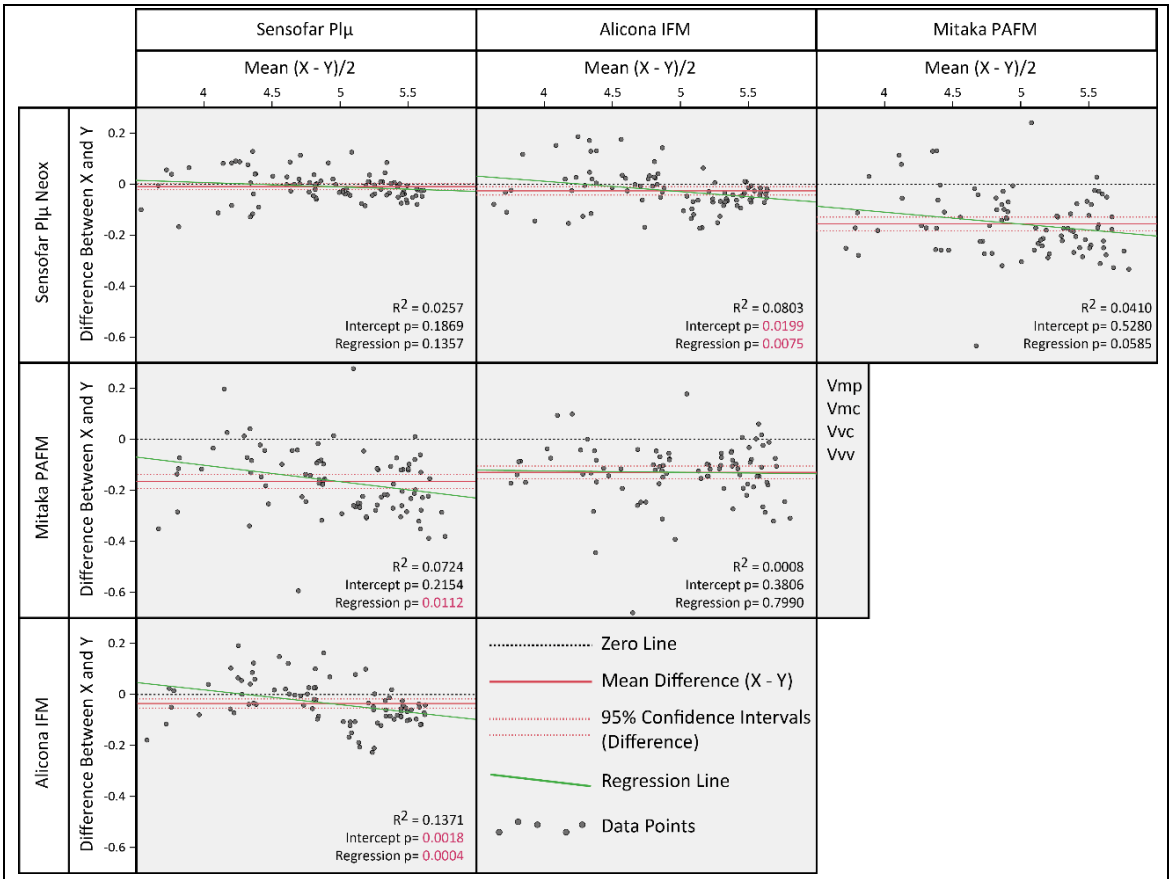

Figure 5.5 *Bland-Altman plots of 3D roughness parameter data, comparing pairs of microscopes. All Non-Resampled data for parameters Vmp, Vmc, Vvc, Vvv are included. X-axis shows the mean of each datafile collected on the two microscopes. Y-axis shows the difference between each datafile. Microscope names at the top are compared to microscope names on the right hand side, with figures representing their comparison where the two cross. The R^2, intercept and Regression test results are given for each plot, black dashed line = zero line, solid red line = mean of Y-axis, dashed red line = 95% confidence intervals of mean, green line = regression line.*

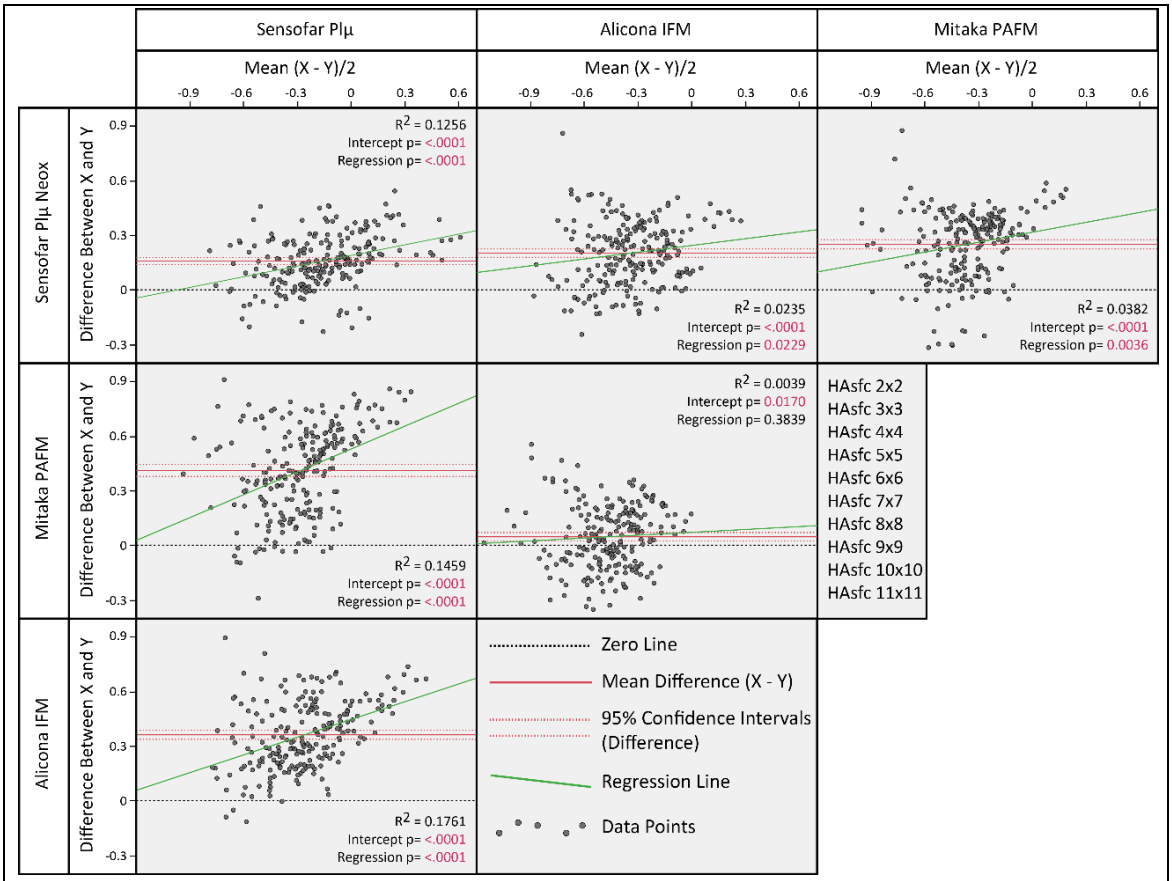

Figure 5.6 *Bland-Altman plots of 3D roughness parameter data, comparing pairs of microscopes. All Resampled data for parameters HAsfc2x2 to HAsfc 11x11 are included. X-axis shows the mean of each datafile collected on the two microscopes. Y-axis shows the difference between each datafile. Microscope names at the top are compared to microscope names on the right hand side, with figures representing their comparison where the two cross. The R^2, intercept and Regression test results are given for each plot, black dashed line = zero line, solid red line = mean of Y-axis, dashed red line = 95% confidence intervals of mean, green line = regression line.*

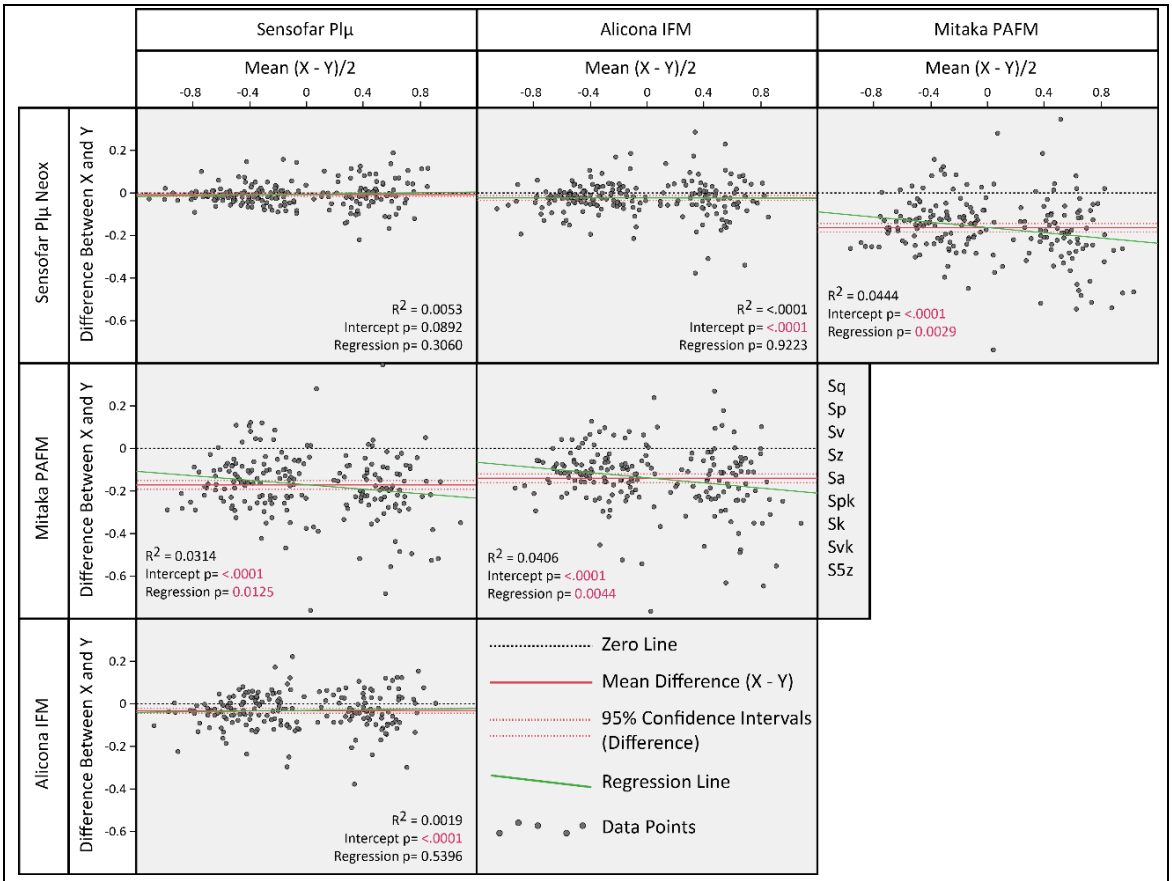

Figure 5.7 *Bland-Altman plots of 3D roughness parameter data, comparing pairs of microscopes. All Resampled data for parameters Sq, Sp, Sv, Sa, Spk, Sk, Svk, S5z are included. X-axis shows the mean of each datafile collected on the two microscopes. Y-axis shows the difference between each datafile. Microscope names at the top are compared to microscope names on the right hand side, with figures representing their comparison where the two cross. The R^2, intercept and Regression test results are given for each plot, black dashed line = zero line, solid red line = mean of Y-axis, dashed red line = 95% confidence intervals of mean, green line = regression line.*

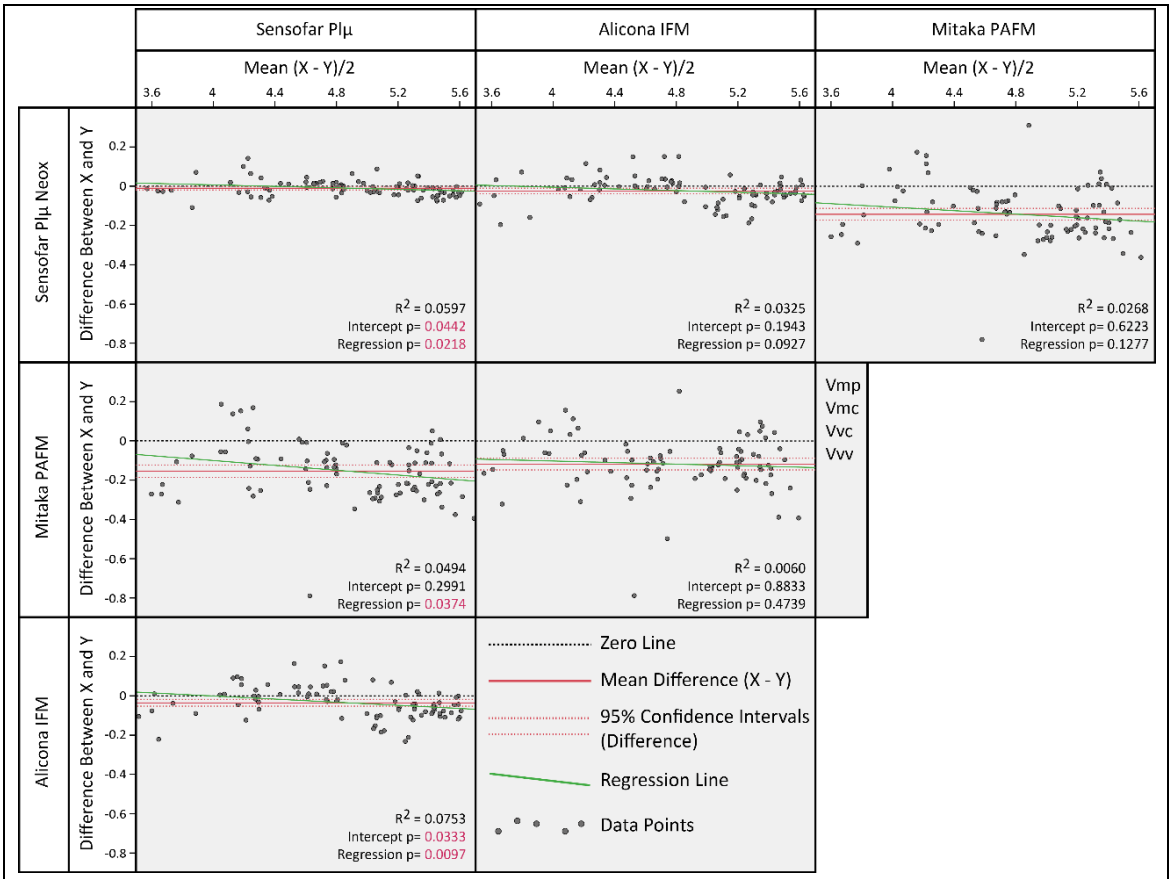

Figure 5.8 *Bland-Altman plots of 3D roughness parameter data, comparing pairs of microscopes. All Resampled data for parameters Vmp, Vmc, Vvc, Vvv are included. X-axis shows the mean of each datafile collected on the two microscopes. Y-axis shows the difference between each datafile. Microscope names at the top are compared to microscope names on the right hand side, with figures representing their comparison where the two cross. The R^2, intercept and Regression test results are given for each plot, black dashed line = zero line, solid red line = mean of Y-axis, dashed red line = 95% confidence intervals of mean, green line = regression line.*

Dietary Comparison – T-tests

To test the third and fourth hypotheses, that when comparing dietary groups with known variation in the texture of their tooth surfaces, the sensitivity of data collected using different microscopes varies in its ability to detect this variation, so that certain microscopes are more sensitive than other to significant textural differences,

and that differences between the sensitivity of data collected using different microscopes/instruments are eliminated by resampling the data down to the lowest µm/pixel resolution and field size, T-tests were performed between dietary groups for data from each of the microscopes. Because the cost of false negatives in these results is so high, and it is known that a dietary difference exists in these populations, the Benjamini-Hochberg Procedure (Benjamini and Hochberg 1995) has not been used on these results. Instead it is assumed that a fixed false discovery rate is inherent in the results (for α=0.05 this would be one in twenty test results).

For Non-Resampled data from each microscope dataset C.c-AE-NonRes was compared to dataset C.c-BLE-NonRes (Table 5.13), and dataset A.p-IRH-NonRes was compared to dataset A.p-PCD-NonRes (Table 5.14). For comparisons of *Capreolus capreolus* dietary groups the sensitivity to dietary differences is very low when using SSFA parameters (only 1 significant result across all tests for all microscopes; Asfc Mitaka PAFM), however the sensitivity is much greater when using ISO 25178 parameters, and greatest for data from the Alicona IFM and Mitaka PAFM (eight and seven parameters showing difference between the dietary groups respectively). The sensitivity to dietary difference is only slightly lower for data from the Sensofar Plµ neox (five parameters), but much lower for data from the Sensofar Plµ (3 parameters). Significant results are only ever recorded in 10 of the 34 parameters across all microscopes, suggesting a consistent pattern. For comparisons between the *Archosargus probatocephalus* populations the overall sensitivity to dietary difference is much lower, and only high when using data from a single microscope (Sensofar Plµ neox) where twelve parameters show difference between the two dietary groups. All other microscopes show no sensitivity to dietary differences, with a single significant result returned for each instrument, and from different parameters in each case. For the *A.probatocephalus* populations it appears SSFA parameters are better at discriminating dietary differences than ISO parameters, with a 13 SSFA parameters showing difference between dietary groups across all microscopes, while only 3 ISO parameters ever show any difference between these groups.

	Tfv		Asfc		epLsar		HAsfc 2x2		HAsfc 3x3		HAsfc 4x4		HAsfc 5x5	
Dataset	T-Ratio	p	T-Ratio	p	T-Ratio	p	T-Ratio	p	T-Ratio	p	T-Ratio	p	T-Ratio	p
Non-Res Plμ *C.capreolus*	0.3426	0.7407	-1.2222	0.2564	-0.4063	0.6952	-1.6213	0.1436	-1.0372	0.3300	-1.5725	0.1545	-1.5323	0.1640
Non-Res Plμ Neox *C.capreolus*	0.9575	0.3664	-1.7679	0.1151	-0.3525	0.7336	-0.0754	0.9417	-0.4865	0.6397	-0.4243	0.6825	-0.5782	0.5791
Non-Res IFM *C.capreolus*	0.8662	0.4116	0.9232	0.3829	-1.2892	0.2334	-0.9071	0.3909	-0.6953	0.5066	-0.9280	0.3805	-1.3390	0.2174
Non-Res PAFM *C.capreolus*	0.3305	0.7495	**-2.3072**	**0.0499**	-0.3580	0.7296	0.2626	0.7995	0.1168	0.9099	-0.1410	0.8914	-0.1747	0.8657

	HAsfc 6x6		HAsfc 7x7		HAsfc 8x8		HAsfc 9x9		HAsfc 10x10		HAsfc 11x11	
Dataset	T-Ratio	p	T-Ratio	p	T-Ratio	p	T-Ratio	p	T-Ratio	p	T-Ratio	p
Non-Res Plμ *C.capreolus*	-1.1482	0.2841	-2.0038	0.0800	-1.3124	0.2258	-1.4873	0.1753	-1.7440	0.1193	-1.5694	0.1552
Non-Res Plμ Neox *C.capreolus*	-0.5473	0.5991	-0.8426	0.4239	-0.9665	0.3621	-0.5360	0.6066	-0.4321	0.6771	-0.8169	0.4377
Non-Res IFM *C.capreolus*	-0.8413	0.4246	-0.8220	0.4349	-0.8195	0.4363	-1.0238	0.3359	-1.1831	0.2707	-1.1354	0.2891
Non-Res PAFM *C.capreolus*	0.1424	0.8903	0.0582	0.9550	0.0622	0.9519	0.1464	0.8872	-0.0050	0.9961	0.3127	0.7625

	Sq		Sku		Sp		Sv		Sz		Sds		Str	
Dataset	T-Ratio	p	T-Ratio	p	T-Ratio	p	T-Ratio	p	T-Ratio	p	T-Ratio	p	T-Ratio	p
Non-Res Plμ *C.capreolus*	-1.9161	0.0917	-1.1092	0.2996	-0.1151	0.9112	-2.1528	0.0635	-1.8238	0.1056	0.7177	0.4933	1.0123	0.3410
Non-Res Plμ Neox *C.capreolus*	**-3.1901**	**0.0128**	-1.1364	0.2887	0.3126	0.7626	**-2.6691**	**0.0284**	-0.8638	0.4129	0.1941	0.8510	0.4262	0.6812
Non-Res IFM *C.capreolus*	**-2.9219**	**0.0192**	-1.1619	0.2788	0.2851	0.7828	**-3.5781**	**0.0072**	**-4.0563**	**0.0037**	0.0850	0.9344	0.2147	0.8354
Non-Res PAFM *C.capreolus*	**-3.3046**	**0.0108**	-1.4395	0.1880	**-2.9224**	**0.0192**	**-2.9692**	**0.0179**	**-4.0989**	**0.0034**	-0.5195	0.6175	-0.5579	0.5922

	Sdq		Ssc		Sdr		Vmp		Vmc		Vvc		Vvv	
Dataset	T-Ratio	p	T-Ratio	p	T-Ratio	p	T-Ratio	p	T-Ratio	p	T-Ratio	p	T-Ratio	p
Non-Res Plμ *C.capreolus*	-1.5971	0.1489	0.9516	0.3691	-1.4213	0.1930	-0.0835	0.9355	-0.0458	0.9646	0.3581	0.7295	**-2.5090**	**0.0364**
Non-Res Plμ Neox *C.capreolus*	-2.0883	0.0702	0.7467	0.4766	-2.0056	0.0798	0.2604	0.8011	-0.2578	0.8031	0.3319	0.7485	**-3.3901**	**0.0095**
Non-Res IFM *C.capreolus*	**-3.8848**	**0.0046**	-0.3965	0.7021	**-3.4943**	**0.0081**	-0.3287	0.7509	-1.1864	0.2695	-0.5750	0.5811	**-2.3620**	**0.0458**
Non-Res PAFM *C.capreolus*	**-3.2489**	**0.0117**	0.1099	0.9152	**-3.0109**	**0.0168**	-0.3331	0.7476	-0.8859	0.4015	-0.1168	0.9099	-1.9978	0.0808

	Spk		Sk		Svk		Smr1		Smr2		S5z		Sa	
Dataset	T-Ratio	p	T-Ratio	p	T-Ratio	p	T-Ratio	p	T-Ratio	p	T-Ratio	p	T-Ratio	p
Non-Res Plμ *C.capreolus*	-0.1542	0.8813	0.4889	0.6381	**-2.5322**	**0.0351**	-0.0208	0.9839	1.6978	0.1280	**-2.5388**	**0.0348**	-0.8164	0.4379
Non-Res Plμ Neox *C.capreolus*	0.0889	0.9314	0.2391	0.8171	**-3.5054**	**0.0080**	1.0055	0.3441	1.3867	0.2029	**-3.8526**	**0.0049**	-1.4438	0.1868
Non-Res IFM *C.capreolus*	-0.3314	0.7488	-0.4748	0.6476	**-2.3575**	**0.0461**	-0.0098	0.9924	1.3349	0.2186	**-3.7645**	**0.0055**	-2.1130	0.0676
Non-Res PAFM *C.capreolus*	-0.6794	0.5160	-0.0105	0.9919	-1.9206	0.0910	0.7805	0.4575	1.5003	0.1719	**-3.3126**	**0.0107**	-1.6919	0.1291

Table 5.13 *T-tests comparing Capreolus capreolus dietary groups, using only Non-Resampled data. Tests were carried out separately for each SSFA and ISO 25178 parameter, significant results are highlighted in bold*

For Resampled data exactly the same tests were carried out; results of T-test comparisons between datasets C.c-AE-Res and C.c-BLE-Res can be seen in Table 5.15, and comparisons between A.p-IRH-Res and A.p-PCD-Res can be seen in Table 5.16. In both cases the sensitivity to dietary separation is almost identical to that for Non-Resampled data, and only slight improvement or reduction in sensitivity is seen.

Dietary Comparison – Principal Component Analysis

The sensitivity of microscopes to textural differences was also tested using Principal Component Analysis (PCA). Separate tests were carried out for data captured by each microscope. For Non-Resampled data dataset C.c-AE-NonRes was compared to dataset C.c-BLE-NonRes, and dataset A.p-IRH-NonRes was compared to dataset

A.p-PCD-NonRes, all PCA analyses can be seen in Figure 5.9. The analyses were based on data from parameters returning significant results from dietary T-tests for at least one microscope. Therefore for Non-Resampled datasets the PCA for *Capreolus capreolus* populations used ten parameters Asfc, Sq, Sp, Sv, Sz, Sdq, Sdr, Vvv, Svk, and S5z, and the PCA for *Archosargus probatocephalus* populations used fourteen parameters epLsar, HAsfc2x2 to HAsfc11x11, Sku, Sv, and Str. Principal Component 1 (PC1) and Principal Component 2 (PC2) are presented, with no separation of groups found on any other axis.

	Tfv		Asfc		epLsar		HAsfc 2x2		HAsfc 3x3		HAsfc 4x4		HAsfc 5x5	
Dataset	T-Ratio	p	T-Ratio	p	T-Ratio	p	T-Ratio	p	T-Ratio	p	T-Ratio	p	T-Ratio	p
Non-Res Plμ *A.probatocephalus*	-0.7164	0.4901	1.0725	0.3087	1.4330	0.1824	**2.6993**	**0.0223**	1.3806	0.1975	0.9864	0.3472	1.2525	0.2389
Non-Res Plμ Neox *A.probatocephalus*	0.5477	0.5959	0.8472	0.4167	**2.2356**	**0.0494**	**3.2281**	**0.0090**	**2.8071**	**0.0186**	**2.7245**	**0.0214**	**2.6228**	**0.0255**
Non-Res IFM *A.probatocephalus*	-0.2350	0.8189	-1.5694	0.1476	0.6020	0.5606	1.3005	0.2226	**2.2425**	**0.0488**	1.4706	0.1722	1.8162	0.0994
Non-Res PAFM *A.probatocephalus*	1.7622	0.1085	0.6179	0.5505	1.4785	0.1701	0.1978	0.8472	0.1525	0.8818	0.3200	0.7556	0.6484	0.5313

	HAsfc 6x6		HAsfc 7x7		HAsfc 8x8		HAsfc 9x9		HAsfc 10x10		HAsfc 11x11	
Dataset	T-Ratio	p	T-Ratio	p	T-Ratio	p	T-Ratio	p	T-Ratio	p	T-Ratio	p
Non-Res Plμ *A.probatocephalus*	0.9891	0.3460	1.2846	0.2279	1.6879	0.1223	1.5196	0.1596	1.5353	0.1557	1.2602	0.2362
Non-Res Plμ Neox *A.probatocephalus*	**2.4397**	**0.0349**	**2.5158**	**0.0306**	**2.6527**	**0.0242**	**3.1315**	**0.0107**	**3.1808**	**0.0098**	**3.1254**	**0.0108**
Non-Res IFM *A.probatocephalus*	1.2582	0.2369	1.4092	0.1891	1.2218	0.2498	1.2002	0.2577	1.1902	0.2614	1.2780	0.2301
Non-Res PAFM *A.probatocephalus*	0.2587	0.8011	0.7068	0.4958	0.2687	0.7936	0.5194	0.6148	0.8316	0.4251	0.5381	0.6023

	Sq		Sku		Sp		Sv		Sz		Sds		Str	
Dataset	T-Ratio	p	T-Ratio	p	T-Ratio	p	T-Ratio	p	T-Ratio	p	T-Ratio	p	T-Ratio	p
Non-Res Plμ *A.probatocephalus*	1.1803	0.2652	-0.0107	0.9917	0.3112	0.7621	0.4616	0.6542	0.4559	0.6582	1.0838	0.3039	-1.4689	0.1726
Non-Res Plμ Neox *A.probatocephalus*	0.9284	0.3751	0.3291	0.7489	0.2076	0.8397	**2.4257**	**0.0357**	1.2420	0.2426	0.7460	0.4728	-1.5204	0.1594
Non-Res IFM *A.probatocephalus*	0.9548	0.3622	1.1414	0.2803	-0.2987	0.7713	0.2070	0.8402	-0.0324	0.9748	-1.0350	0.3251	-1.7368	0.1131
Non-Res PAFM *A.probatocephalus*	0.7351	0.4792	**2.6958**	**0.0225**	1.9073	0.0856	1.2962	0.2240	1.7153	0.1171	0.0872	0.9323	**-2.4109**	**0.0366**

	Sdq		Ssc		Sdr		Vmp		Vmc		Vvc		Vvv	
Dataset	T-Ratio	p	T-Ratio	p	T-Ratio	p	T-Ratio	p	T-Ratio	p	T-Ratio	p	T-Ratio	p
Non-Res Plμ *A.probatocephalus*	0.8969	0.3908	0.8815	0.3987	0.9822	0.3492	1.5624	0.1493	0.3315	0.7471	1.3511	0.2064	1.1482	0.2776
Non-Res Plμ Neox *A.probatocephalus*	1.0451	0.3206	1.3165	0.2174	0.9962	0.3427	0.9334	0.3726	0.2030	0.8432	0.8233	0.4295	0.8730	0.4032
Non-Res IFM *A.probatocephalus*	-0.2998	0.7705	-0.1564	0.8788	-0.4685	0.6494	1.2885	0.2266	-0.2731	0.7904	0.2672	0.7947	1.1411	0.2804
Non-Res PAFM *A.probatocephalus*	1.1255	0.2867	1.4718	0.1718	1.0034	0.3393	0.6716	0.5171	0.3789	0.7127	0.3292	0.7488	0.8652	0.4072

	Spk		Sk		Svk		Smr1		Smr2		S5z		Sa	
Dataset	T-Ratio	p	T-Ratio	p	T-Ratio	p	T-Ratio	p	T-Ratio	p	T-Ratio	p	T-Ratio	p
Non-Res Plμ *A.probatocephalus*	1.4500	0.1777	-0.0968	0.9248	1.2828	0.2285	1.9391	0.0812	-0.3911	0.7039	0.6365	0.5388	1.0592	0.3144
Non-Res Plμ Neox *A.probatocephalus*	0.8483	0.4161	-0.0729	0.9434	1.2012	0.2574	1.5538	0.1513	-0.2884	0.7789	1.3393	0.2101	0.7224	0.4866
Non-Res IFM *A.probatocephalus*	1.1516	0.2763	-0.3170	0.7578	1.2294	0.2471	1.7623	0.1085	-0.0477	0.9629	0.4148	0.6870	0.5750	0.5780
Non-Res PAFM *A.probatocephalus*	0.8204	0.4311	0.2350	0.8190	0.9699	0.3550	0.7237	0.4858	-0.5610	0.5871	1.8110	0.1002	0.5026	0.6261

Table 5.14 *T-tests comparing Archosargus probatocephalus dietary groups, using only Non-Resampled data. Tests were carried out separately for each SSFA and ISO 25178 parameter, significant results are highlighted in bold*

Across all microscopes PCA of Non-resampled *Capreolus capreolus* data show discreet distributions for each dietary group, and a separation of dietary groups along PC1. However the degree of separation and position of specific specimens in

multivariate space is very different. However data from the Sensofar Plμ does produce a slight overlap in distributions between the dietary groups. The eigenvectors (parameter loadings) for these PCA analyses can be seen in Table 5.17a. We see that no one parameter ever has the greatest loading on PC1 except for when using Sensofar Plμ neox data, when S5z has a much greater loading than any other parameter, and that the parameters with the highest loadings vary depending on the microscope.

	Tfv		Asfc		epLsar		HAsfc 2x2		HAsfc 3x3		HAsfc 4x4		HAsfc 5x5	
Dataset	T-Ratio	p	T-Ratio	p	T-Ratio	p	T-Ratio	p	T-Ratio	p	T-Ratio	p	T-Ratio	p
Res Plμ *C.capreolus*	0.9901	0.3511	-1.2878	0.2338	-0.3455	0.7386	-2.1974	0.0592	-1.3866	0.2030	-0.8522	0.4189	-1.9222	0.0908
Res Plμ Neox *C.capreolus*	1.0068	0.3435	-1.6637	0.1347	-0.4956	0.6335	-0.1147	0.9115	-0.5606	0.5904	-0.6145	0.5559	-0.4623	0.6562
Res IFM *C.capreolus*	1.4632	0.1816	**-3.0131**	**0.0167**	-0.0962	0.9257	-0.8604	0.4146	-0.9101	0.3894	-1.1963	0.2658	-0.5696	0.5846
Res PAFM *C.capreolus*	0.2077	0.8406	**-2.5683**	**0.0332**	-0.0407	0.9685	0.1454	0.8880	0.0259	0.9800	-0.0053	0.9959	0.3531	0.7331

	HAsfc 6x6		HAsfc 7x7		HAsfc 8x8		HAsfc 9x9		HAsfc 10x10		HAsfc 11x11	
Dataset	T-Ratio	p	T-Ratio	p	T-Ratio	p	T-Ratio	p	T-Ratio	p	T-Ratio	p
Res Plμ *C.capreolus*	-1.3438	0.2159	-1.3987	0.1995	-1.1908	0.2679	-1.5230	0.1663	-1.5416	0.1617	-2.0616	0.0732
Res Plμ Neox *C.capreolus*	-0.6317	0.5452	-0.9808	0.3554	-0.9379	0.3757	-0.5480	0.5987	-0.4424	0.6699	-0.8946	0.3971
Res IFM *C.capreolus*	-0.6942	0.5072	-0.5786	0.5788	-0.7938	0.4502	-1.0101	0.3420	-1.0062	0.3438	-1.2178	0.2580
Res PAFM *C.capreolus*	0.4815	0.6431	0.2779	0.7881	0.1527	0.8824	0.3510	0.7347	0.1543	0.8812	0.2389	0.8172

	Sq		Sku		Sp		Sv		Sz		Sds		Str	
Dataset	T-Ratio	p	T-Ratio	p	T-Ratio	p	T-Ratio	p	T-Ratio	p	T-Ratio	p	T-Ratio	p
Res Plμ *C.capreolus*	**-2.8830**	**0.0204**	-1.2636	0.2420	0.2903	0.7790	-2.0218	0.0778	-0.9684	0.3612	0.7505	0.4744	0.6563	0.5301
Res Plμ Neox *C.capreolus*	**-3.2137**	**0.0124**	-1.1650	0.2776	0.3853	0.7101	**-2.8283**	**0.0222**	-0.8294	0.4309	0.1837	0.8588	0.4409	0.6710
Res IFM *C.capreolus*	**-4.1968**	**0.0030**	-1.0726	0.3147	-0.3849	0.7103	**-3.0677**	**0.0154**	-2.0709	0.0721	0.1900	0.8541	0.0532	0.9588
Res PAFM *C.capreolus*	**-4.4721**	**0.0021**	-2.2714	0.0528	-0.2734	0.7915	**-3.9266**	**0.0044**	**-2.9760**	**0.0177**	-0.3747	0.7176	-0.8363	0.4272

	Sdq		Ssc		Sdr		Vmp		Vmc		Vvc		Vvv	
Dataset	T-Ratio	p	T-Ratio	p	T-Ratio	p	T-Ratio	p	T-Ratio	p	T-Ratio	p	T-Ratio	p
Res Plμ *C.capreolus*	-1.6722	0.1330	0.6581	0.5290	-1.4718	0.1793	-0.0548	0.9576	-0.1800	0.8616	0.4132	0.6903	**-3.2877**	**0.0111**
Res Plμ Neox *C.capreolus*	-2.0118	0.0791	0.8270	0.4322	-1.9494	0.0871	0.2581	0.8029	-0.2622	0.7998	0.3411	0.7418	**-3.3677**	**0.0098**
Res IFM *C.capreolus*	**-4.4430**	**0.0022**	-0.5657	0.5871	**-3.7962**	**0.0053**	-0.2111	0.8381	-1.2163	0.2585	-0.4111	0.6918	**-3.2884**	**0.0110**
Res PAFM *C.capreolus*	**-3.4868**	**0.0082**	0.0870	0.9328	**-3.2594**	**0.0115**	-0.5776	0.5794	-1.1779	0.2727	-0.1320	0.8982	**-2.6327**	**0.0301**

	Spk		Sk		Svk		Smr1		Smr2		S5z		Sa	
Dataset	T-Ratio	p	T-Ratio	p	T-Ratio	p	T-Ratio	p	T-Ratio	p	T-Ratio	p	T-Ratio	p
Res Plμ *C.capreolus*	-0.2023	0.8447	0.3840	0.7110	**-3.3191**	**0.0106**	0.8476	0.4213	1.8116	0.1076	**-3.5435**	**0.0076**	-1.2924	0.2323
Res Plμ Neox *C.capreolus*	0.0841	0.9350	0.2545	0.8055	**-3.4627**	**0.0085**	1.0709	0.3155	1.4405	0.1877	**-3.5266**	**0.0078**	-1.4781	0.1776
Res IFM *C.capreolus*	-0.3972	0.7016	-0.4157	0.6886	**-3.1905**	**0.0128**	0.8826	0.4032	1.5035	0.1711	**-4.9680**	**0.0011**	**-2.7352**	**0.0256**
Res PAFM *C.capreolus*	-0.6216	0.5515	<.0001	1.0000	**-2.5106**	**0.0363**	0.4165	0.6880	1.7959	0.1102	**-4.2490**	**0.0028**	**-2.7985**	**0.0233**

Table 5.15 *T-tests comparing Capreolus capreolus dietary groups, using only Resampled data. Tests were carried out separately for each SSFA and ISO 25178 parameter, significant results are highlighted in bold*

On PC2 Sp has the greatest loading when using Alicona IFM data, Asfc, Sdq, and Sdr when using Mitaka PAFM data, and Sp, Vvv, and Svk when using Sensofar Plμ and Plμ neox data. For Non-Resampled *Archosargus probatocephalus* data we see a much

more variable pattern of dietary separation in multivariate space depending on the microscope in question. When using data from the Sensofar Plμ dietary separation appears to be along PC2 with discreet distributions for each population. A similar distribution is found when using Mitaka PAFM data, with separation obviously being along PC2, however there is significant overlap between the distributions for each population.

	Tfv		Asfc		epLsar		HAsfc 2x2		HAsfc 3x3		HAsfc 4x4		HAsfc 5x5	
Dataset	T-Ratio	p	T-Ratio	p	T-Ratio	p	T-Ratio	p	T-Ratio	p	T-Ratio	p	T-Ratio	p
Res Plμ *A.probatocephalus*	0.2940	0.7747	1.2631	0.2352	2.1044	0.0616	**2.9844**	**0.0137**	1.1078	0.2939	1.0436	0.3212	1.2534	0.2386
Res Plμ Neox *A.probatocephalus*	-0.1741	0.8652	0.8757	0.4017	**2.2927**	**0.0448**	**3.3901**	**0.0069**	**2.7411**	**0.0208**	**2.8386**	**0.0176**	**2.6009**	**0.0265**
Res IFM *A.probatocephalus*	0.4715	0.6474	-1.1547	0.2751	**2.9153**	**0.0154**	0.5206	0.6140	0.2854	0.7812	0.7767	0.4553	0.5422	0.5996
Res PAFM *A.probatocephalus*	0.4234	0.6809	0.6110	0.5548	1.2096	0.2543	0.2814	0.7842	0.6704	0.5178	0.7686	0.4599	0.4455	0.6655

	HAsfc 6x6		HAsfc 7x7		HAsfc 8x8		HAsfc 9x9		HAsfc 10x10		HAsfc 11x11	
Dataset	T-Ratio	p	T-Ratio	p	T-Ratio	p	T-Ratio	p	T-Ratio	p	T-Ratio	p
Res Plμ *A.probatocephalus*	1.0949	0.2992	1.3416	0.2094	1.2805	0.2293	1.2495	0.2399	1.4802	0.1696	1.4169	0.1869
Res Plμ Neox *A.probatocephalus*	**2.5137**	**0.0307**	**2.5327**	**0.0297**	**2.9149**	**0.0154**	**3.2767**	**0.0083**	**3.0017**	**0.0133**	**3.3423**	**0.0075**
Res IFM *A.probatocephalus*	0.9964	0.3426	0.6561	0.5266	0.5397	0.6012	0.5561	0.5904	0.9004	0.3891	0.6741	0.5155
Res PAFM *A.probatocephalus*	0.5727	0.5795	0.5795	0.5751	0.7969	0.4440	0.5574	0.5895	0.3547	0.7302	0.1892	0.8537

	Sq		Sku		Sp		Sv		Sz		Sds		Str	
Dataset	T-Ratio	p	T-Ratio	p	T-Ratio	p	T-Ratio	p	T-Ratio	p	T-Ratio	p	T-Ratio	p
Res Plμ *A.probatocephalus*	0.9835	0.3486	-0.2363	0.8179	0.0079	0.9938	1.3778	0.1983	0.6248	0.5461	1.1166	0.2903	-1.6830	0.1233
Res Plμ Neox *A.probatocephalus*	0.9041	0.3872	0.2861	0.7806	0.2118	0.8365	**2.4259**	**0.0357**	1.2317	0.2463	0.7243	0.4855	-1.5143	0.1609
Res IFM *A.probatocephalus*	0.5217	0.6132	1.5194	0.1596	-0.0464	0.9639	1.3185	0.2167	0.7175	0.4895	-1.1640	0.2715	-1.7632	0.1083
Res PAFM *A.probatocephalus*	0.6454	0.5332	2.1138	0.0607	**2.4267**	**0.0356**	0.7139	0.4916	1.6791	0.1241	0.0165	0.9872	-1.0839	0.3038

	Sdq		Ssc		Sdr		Vmp		Vmc		Vvc		Vvv	
Dataset	T-Ratio	p	T-Ratio	p	T-Ratio	p	T-Ratio	p	T-Ratio	p	T-Ratio	p	T-Ratio	p
Res Plμ *A.probatocephalus*	1.0987	0.2976	0.9228	0.3779	1.1191	0.2893	0.7977	0.4436	0.4130	0.6883	0.9083	0.3851	0.9004	0.3891
Res Plμ Neox *A.probatocephalus*	1.0536	0.3169	1.7124	0.1176	1.0045	0.3388	0.8693	0.4051	0.1925	0.8512	0.7938	0.4458	0.8694	0.4050
Res IFM *A.probatocephalus*	-0.6891	0.5064	-0.5829	0.5729	-0.8135	0.4349	0.8885	0.3951	-0.5622	0.5864	-0.1827	0.8587	0.7025	0.4984
Res PAFM *A.probatocephalus*	0.9098	0.3843	1.2385	0.2438	0.8363	0.4225	0.9884	0.3463	0.2978	0.7720	0.4605	0.6550	0.4051	0.6939

	Spk		Sk		Svk		Smr1		Smr2		S5z		Sa	
Dataset	T-Ratio	p	T-Ratio	p	T-Ratio	p	T-Ratio	p	T-Ratio	p	T-Ratio	p	T-Ratio	p
Res Plμ *A.probatocephalus*	0.6332	0.5408	-0.0026	0.9980	1.0352	0.3250	1.0140	0.3345	-0.5435	0.5987	0.9580	0.3606	0.8802	0.3994
Res Plμ Neox *A.probatocephalus*	0.8184	0.4322	-0.0810	0.9370	1.2042	0.2562	1.5587	0.1501	-0.2752	0.7888	1.5711	0.1472	0.7044	0.4972
Res IFM *A.probatocephalus*	0.6589	0.5249	-0.6364	0.5388	0.9380	0.3704	2.1220	0.0598	-0.1417	0.8901	0.3464	0.7362	0.1639	0.8731
Res PAFM *A.probatocephalus*	1.0948	0.2993	0.3024	0.7685	0.5515	0.5934	1.2921	0.2254	0.3866	0.7072	1.0452	0.3205	0.4338	0.6737

Table 5.16 *T-tests comparing Archosargus probatocephalus dietary groups, using only Resampled data. Tests were carried out separately for each SSFA and ISO 25178 parameter, significant results are highlighted in bold*

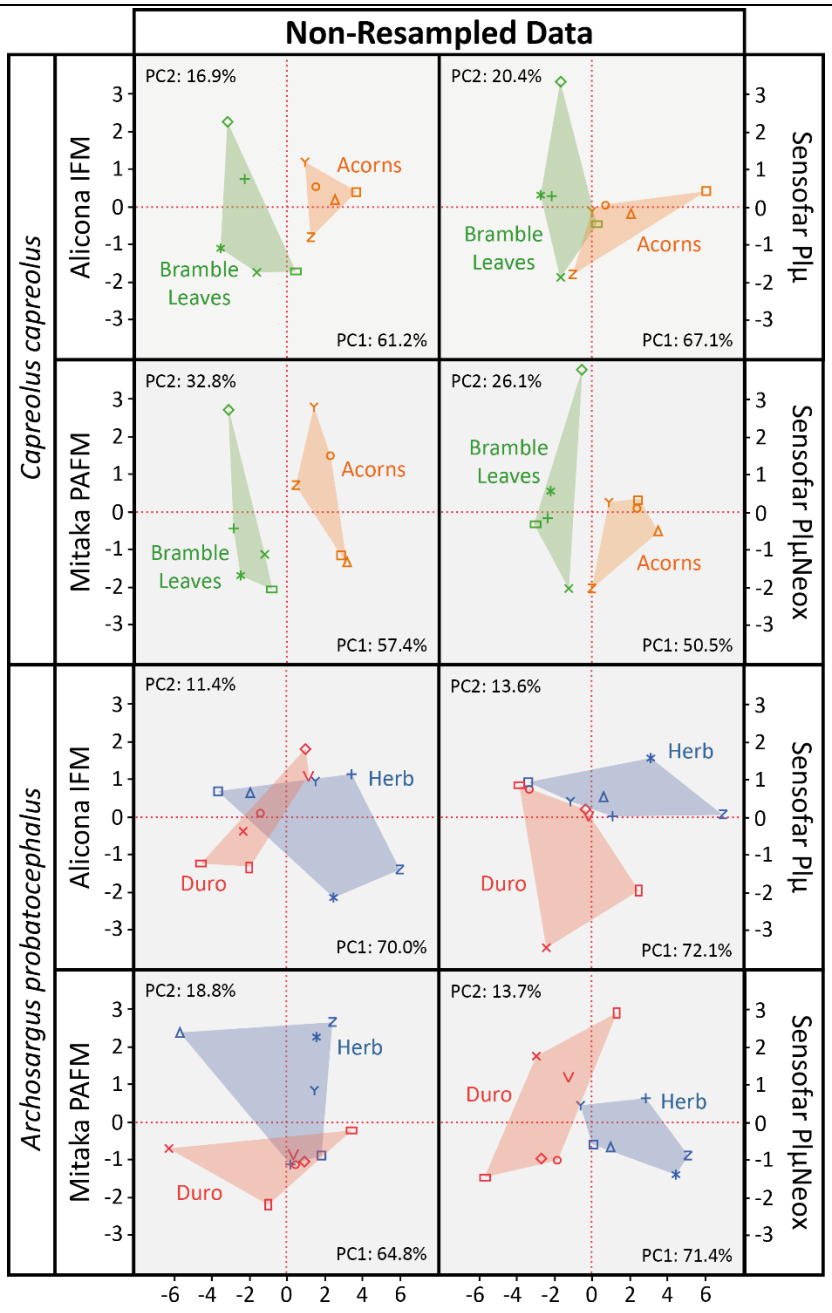

Figure 5.9 *Principal Component Analysis (PCA) carried out on Non-Resampled data. Top four PCA carried out on Capreolus capreolus Non-Resampled data, separately for data from each microscope, using parameters Asfc, Sq, Sp, Sv, Sz, Sdq, Sdr, Vvv, Svk, and S5z (parameters showing significant difference between dietary groups). Bottom four PCA carried out on Archosargus probatocephalus Non-Resampled data, separately for data from each microscope, using parameters epLsar, HAsfc2x2 to HAsfc11x11, Sku, Sv, and Str. For all PCA analyses the proportion of variance explained by each axis is presented within the graph, and dietary groups have points, convex hulls and labels with consistent colour coding.*

		Non-Resampled Data							
	A.	Alicona IFM		Mitaka PAFM		Sensofar Plμ		Sensofar Plμ Neox	
	Parameter	PC1	PC2	PC1	PC2	PC1	PC2	PC1	PC2
Capreolus capreolus	Asfc	-0.1488	-0.3109	0.1766	**0.4808**	0.3257	0.2977	0.2973	0.2556
	Sq	0.3668	0.1664	0.3821	-0.0562	0.3466	0.0329	0.3871	0.0163
	Sp	-0.1291	**0.6472**	0.2206	0.3887	0.1264	**0.5257**	0.0219	**0.5068**
	Sv	0.3814	-0.1814	0.3776	-0.2171	0.3289	-0.3141	0.3175	-0.2600
	Sz	0.3723	0.1257	0.3973	-0.1078	0.3607	0.0206	0.2263	0.3223
	Sdq	0.2853	0.3133	0.2436	**0.4364**	0.3306	0.2539	0.3724	0.2000
	Sdr	0.2548	0.3213	0.2273	**0.4503**	0.3140	0.3201	0.3579	0.2497
	Vvv	0.3603	-0.2935	0.3307	-0.2421	0.2939	**-0.4244**	0.2896	**-0.4510**
	Svk	0.3541	-0.3232	0.3256	-0.2790	0.2952	**-0.4325**	0.2971	**-0.4461**
	S5z	0.3756	0.1267	0.3840	-0.1619	0.3717	-0.0295	**0.4128**	0.0377

	B.	Alicona IFM		Mitaka PAFM		Sensofar Plμ		Sensofar Plμ Neox	
	Parameter	PC1	PC2	PC1	PC2	PC1	PC2	PC1	PC2
Archosargus probatocephalus	epLsar	0.0469	0.0808	-0.1010	**0.4419**	0.0951	**0.6530**	0.0836	**-0.6687**
	HAsfc 2x2	0.2004	0.3872	0.2413	0.0469	0.1417	**0.5741**	0.2234	-0.3657
	HAsfc 3x3	0.2844	0.1411	0.3022	0.0539	0.2911	0.0987	0.2895	-0.0743
	HAsfc 4x4	0.3104	0.1173	0.3207	0.0079	0.2981	-0.0638	0.3018	-0.0416
	HAsfc 5x5	0.3138	0.0156	0.3165	0.0208	0.3033	-0.0692	0.3019	0.0570
	HAsfc 6x6	0.3103	0.0708	0.3244	-0.0283	0.3089	-0.0503	0.3100	0.0832
	HAsfc 7x7	0.3133	0.0717	0.3252	0.0668	0.3046	0.0346	0.3085	0.0760
	HAsfc 8x8	0.3159	-0.0088	0.3242	-0.0083	0.3070	-0.0299	0.3108	0.0341
	HAsfc 9x9	0.3112	0.0542	0.3179	0.0535	0.3084	-0.0322	0.3071	0.0826
	HAsfc 10x10	0.3126	0.1076	0.3159	0.0470	0.3052	-0.0318	0.3053	0.0950
	HAsfc 11x11	0.3071	0.0706	0.3182	0.0613	0.2988	-0.1562	0.3044	0.0502
	Sku	0.2114	**-0.5363**	0.0557	**0.5674**	0.2087	-0.3040	0.1385	**0.4718**
	Sv	0.1691	**-0.5032**	-0.0836	**0.5340**	0.2436	-0.1768	0.2230	0.1458
	Str	-0.1601	**0.4890**	0.0953	**-0.4218**	-0.2062	-0.2659	-0.2003	0.3641

Table 5.17 *Eigenvectors for PC1 and PC2 from the Principal Component Analyses comparing dietary groups within each microscope, using only Non-Resampled data. Results are given separately for A. Capreolus capreolus data, and B. Archosargus probatocephalus data. Eigenvecors are coloured light grey where below 0.3, black between 0.3 and 0.4 and highlighted bold when above 0.4.*

Data from the Alicona IFM do not appear to separate *A.probatocephalus* populations well at all, with a high degree of overlap between groups, but with some separation along PC1. And finally Sensofar Plμ neox data appears to separate populations well along PC1 with discreet distributions and no overlap. Eigenvectors for

the A.probatocephalus Non-Resampled Data PCAs can be seen in Table 5.17b. We find the greatest loadings for PC1 are always within the HAsfc parameters (consistently for HAsfc5x5 to HAsfc 10x10). For PC2 the parameters with greatest loadings when using Alicona IFM data are Sku, Sv, and Str, when using Mitaka PAFM data they are epLsar, Sku, Sv, and Str, when using Sensofar Plμ data they are epLsar and HAsfc 2x2, and finally when using Sensofar Plμ neox data they are epLsar, and Sku.

Resampled data were tested in the same way using PCA, however the parameters were slightly different, due to minor differences between parameters returning significant results for Resampled and Non-Resampled data. Here *Capreolus capreolus* populations were compared using ten parameters Asfc, Sq, Sv, Sz, Sdq, Sdr, Vvv, Svk, S5z, and Sa. And *Archosargus probatocephalus* populations were compared using 13 parameters, epLsar, Hasfc2x2 to HAsfc11x11, Sp, and Sv. All PCA analyses using Resampled Data can be seen in Figure 5.10. PCA analyses of *C.capreolus* populations show a very similar separation to that seen when using Non-Resampled data, however the separation is much greater when using Resampled data from the Sensofar Plμ and the distributions no longer overlap. The relative position of specimens has however changed quite drastically. Parameter loadings (eigenvectors, Table 5.18a), show that several parameters have the greatest loadings on PC1 for all microscopes, but that these are not the same parameters for data from each microscope. For PC2 again different parameter show the greatest loadings but in the case of this axis they are specific parameters (Alicona IFM, Asfc, Sv; Mitaka PAFM, Asfc, Sdr; Sensofar Plμ, Sv, Vvv, Svk; Sensofar Plμ neox, Asfc, Vvv, Svk). For PCA carried out on Resampled *A.probatocephalus* data we find separation between dietary groups along PC2 for data from three of the microscopes (Alicona IFM, Mitaka PAFM, and Sensofar Plμ), with separation of populations along PC1 for data from the Sensofar Plμ neox. In almost all cases the separation is better (less overlap of data) than when using Non-Resampled data, but there is some overlap between dietary groups when using data from each of the four microscopes. Eigenvectors (Table 5.18b) show that parameters HAsfc4x4 to HAsfc11x11 load greatest on PC1 in all cases with HAsfc3x3 loading to the same degree when using data from the two Sensofar microscopes.

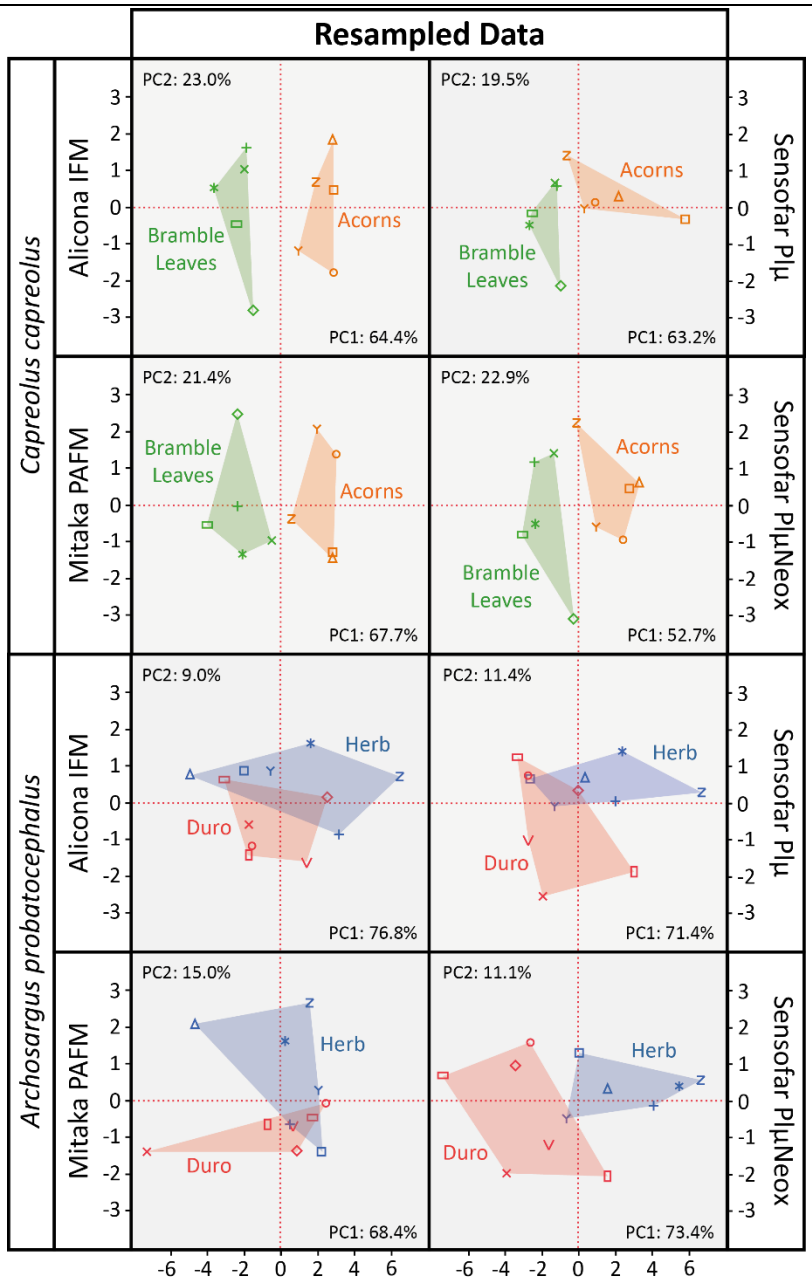

Figure 5.10 *Principal Component Analysis (PCA) carried out on Resampled data. Top four PCA carried out on Capreolus capreolus Resampled data, separately for data from each microscope, using parameters Asfc, Sq, Sv, Sz, Sdq, Sdr, Vvv, Svk, S5z, and Sa (parameters showing significant difference between dietary groups). Bottom four PCA carried out on Archosargus probatocephalus Resampled data, separately for data from each microscope, using parameters epLsar, Hasfc2x2 to HAsfc11x11, Sp, and Sv. For all PCA analyses the proportion of variance explained by each axis is presented within the graph, and dietary groups have points, convex hulls and labels with consistent colour coding.*

		Resampled Data							
	A.	Alicona IFM		Mitaka PAFM		Sensofar Plμ		Sensofar Plμ Neox	
	Parameter	PC1	PC2	PC1	PC2	PC1	PC2	PC1	PC2
Capreolus capreolus	Asfc	0.2831	**-0.4233**	0.2550	**0.4898**	0.3304	-0.3442	0.2885	**-0.4101**
	Sq	0.3717	-0.0272	0.3751	-0.0637	0.3711	0.0238	0.3885	0.0653
	Sv	0.2875	**0.4200**	0.3429	-0.2891	0.2566	**0.4443**	0.3022	0.3863
	Sz	0.2523	0.3004	0.3137	-0.1911	0.2940	-0.0311	0.2288	-0.1018
	Sdq	0.3428	-0.3088	0.3135	0.3701	0.3468	-0.2933	0.3580	-0.3110
	Sdr	0.3219	-0.3651	0.3036	**0.4030**	0.3311	-0.3579	0.3477	-0.3541
	Vvv	0.3112	0.3261	0.2926	-0.3237	0.2777	**0.4626**	0.2731	**0.4568**
	Svk	0.3005	0.3591	0.2880	-0.3662	0.2791	**0.4704**	0.2793	**0.4638**
	S5z	0.3520	0.1061	0.3552	-0.1694	0.3625	0.0344	0.3946	0.0408
	Sa	0.3216	-0.2797	0.3052	0.2625	0.2905	-0.1789	0.2547	-0.1430

	B.	Alicona IFM		Mitaka PAFM		Sensofar Plμ		Sensofar Plμ Neox	
	Parameter	PC1	PC2	PC1	PC2	PC1	PC2	PC1	PC2
Archosargus probatocephalus	epLsar	0.0657	**0.7352**	-0.1686	**0.4998**	0.0793	**0.7561**	0.0948	**0.7112**
	HAsfc 2x2	0.2854	0.0378	0.2404	0.0549	0.2183	**0.4537**	0.2343	0.2923
	HAsfc 3x3	0.2919	-0.0676	0.2749	-0.0344	0.3005	0.1288	0.3004	0.1320
	HAsfc 4x4	0.3062	-0.0317	0.3022	0.0867	0.3168	-0.0399	0.3088	0.1177
	HAsfc 5x5	0.3010	-0.1419	0.3317	0.0494	0.3044	0.0105	0.3120	0.0164
	HAsfc 6x6	0.3107	0.0113	0.3217	0.1162	0.3165	-0.0713	0.3177	-0.0545
	HAsfc 7x7	0.3119	-0.0522	0.3238	0.0465	0.3232	-0.0767	0.3164	-0.0728
	HAsfc 8x8	0.3073	-0.0245	0.3178	0.1167	0.3233	-0.0756	0.3175	-0.0316
	HAsfc 9x9	0.3123	-0.0155	0.3207	0.1042	0.3224	-0.0594	0.3175	-0.0356
	HAsfc 10x10	0.3089	0.0276	0.3149	0.0821	0.3174	-0.1027	0.3132	-0.1099
	HAsfc 11x11	0.3059	-0.0581	0.3094	0.0259	0.3207	-0.0549	0.3126	-0.0522
	Sp	0.2475	-0.0526	-0.0579	**0.6678**	0.0408	-0.3849	0.0699	**-0.5057**
	Sv	0.0930	**0.6495**	-0.1629	**0.4925**	0.2107	-0.1494	0.2232	-0.3102

Table 5.18 *Eigenvectors for PC1 and PC2 from the Principal Component Analyses comparing dietary groups within each microscope, using only Resampled data. Results are given separately for A. Capreolus capreolus data, and B. Archosargus probatocephalus data. Eigenvecors are coloured light grey where below 0.3, black between 0.3 and 0.4 and highlighted bold when above 0.4.*

For PC2 parameter epLsar always has one of the greatest loadings when using data from each microscope, along with Sv for Alicona IFM data, Sv, and Sp when using Mitaka PAFM data, HAsfc2x2 when using Sensofar Plμ data, and Sp when using Sensofar Plμ neox data.

Dietary Comparison – Magnitudes of Difference

A final test was carried out for each parameter, to compare the magnitude of difference between each of the dietary groups with the magnitude of difference between microscopes. This tests whether the difference between microscopes is greater than the difference between populations with known dietary differences, which would very likely affect the results of dietary analyses. This was done separately for each dietary comparison and for Resampled and Non-Resampled data. In each case parameters were only used where a corresponding significant dietary T-test result was recorded. Thus parameters used are different for the comparison of *C.caproelus* dietary groups and the comparisons of *A.probatocephalus* dietary groups.

The results of comparisons between magnitudes of difference for Non-Resampled and Resampled *C.capreolus* data can be seen in Figure 5.11. For each comparison between microscopes parameters are displayed where the difference exceeds that between *C.capreolus* dietary groups. We find that all comparisons between data from the Mitaka PAFM and other microscopes produce six parameters with greater difference than found between dietary groups. For comparisons between the Alicona IFM and the Sensofar microscopes this number drops to two/three depending on the comparison, and no differences for any parameters exceed the difference between dietary groups when comparing the two Sensofar microscopes. The same exact pattern is found when using Resampled data. Differences between microscopes for parameters Vvv, and Sq never exceed the difference between dietary groups.

For *A.probatocephalus* datasets the results of comparisons between magnitudes of difference for microscopes and dietary groups can be seen in Figure 5.12. Again both Resampled and Non-Resampled data are presented in the same figure. A very different pattern is found for *A.probatocephalus* data to the *C.capreolus* data, with all comparisons except the one between the Alicona IFM and the Mitaka PAFM showing many parameters exceeding the difference between dietary groups when microscopes are compared. The comparison between the Alicona IFM and

Mitaka PAFM only returns parameter Sv as having a greater magnitude of difference between data from these two microscopes than between dietary groups. The pattern is almost the same for Resampled data, however the comparison between the Alicona IFM and Sensofar Plμ neox shows fewer parameters with greater magnitude of difference between microscopes than between dietary groups, and for the comparison between Alicona IFM data and Mitaka PAFM data parameter epLsar has a greater magnitude of difference between microscopes than between dietary groups, which it did not when using Non-Resampled data.

		***Capreolus capreolus* Resampled Dataset**			
		Sensofar Plμ	Sensofar Plμ Neox	Alicona IFM	Mitaka PAFM
***Capreolu capreolus* Non-Resampled Dataset**	Sensofar Plμ			Asfc, Sdq, Sdr	Asfc, Sq, Sv, Sz, Sdq, Sdr, S5z
	Sensofar Plμ Neox			Asfc, Sdq	Asfc, Sq, Sv, Sz, Sdq, Sdr, S5z
	Alicona IFM	Asfc, Sdq, Sdr	Asfc, Sdq		Asfc, Sq, Sv, Sz, Sdq, Sdr, S5z
	Mitaka PAFM	Asfc, Sv, Sz, Sdq, Sdr, S5z	Asfc, Sv, Sz, Sdq, Sdr, S5z	Asfc, Sv, Sz, Sdq, Sdr, S5z	

Figure 5.11 *Comparisons of the magnitude of difference between microscopes with the known magnitude of difference between Capreolus capreolus dietary groups. For each comparison of microscopes, where the difference for a specific parameter exceeds the difference between dietary groups that parameter is listed. Results on the bottom left are for Non-Resampled data, results on the top right are for Resampled data. Only parameters where significant differences between dietary groups were recorded for both Non-Resampled and Resampled data have been tested (Table 5.15 and Table 5.17).*

		Archosargus probatocephalus Resampled Dataset			
		Sensofar Plμ	Sensofar Plμ Neox	Alicona IFM	Mitaka PAFM
Archosargus probatocephalus Non-Resampled Dataset	Sensofar Plμ		HAsfc3x3, HAsfc5x5, HAsfc6x6, HAsfc7x7, HAsfc8x8, HAsfc9x9, HASfc10x10, HAsfc11x11	HAsfc2x2, HAsfc3x3, HAsfc4x4, HAsfc5x5, HAsfc6x6, HAsfc7x7, HAsfc8x8, HAsfc9x9, HASfc10x10, HAsfc11x11	HAsfc2x2, HAsfc3x3, HAsfc4x4, HAsfc5x5, HAsfc6x6, HAsfc7x7, HAsfc8x8, HAsfc9x9, HASfc10x10, HAsfc11x11, Sv
	Sensofar Plμ Neox	HAsfc3x3, HAsfc4x4, HAsfc5x5, HAsfc6x6, HAsfc7x7, HAsfc8x8, HAsfc9x9, HAsfc10x10, HAsfc11x11		HASfc10x10, HAsfc11x11	HAsfc2x2, HAsfc3x3, HAsfc4x4, HAsfc5x5, HAsfc6x6, HAsfc7x7, HAsfc8x8, HAsfc9x9, HASfc10x10, HAsfc11x11, Sv
	Alicona IFM	HAsfc2x2, HAsfc3x3, HAsfc4x4, HAsfc5x5, HAsfc6x6, HAsfc7x7, HAsfc8x8, HAsfc9x9, HAsfc10x10, HAsfc11x11	HAsfc3x3, HAsfc5x5, HAsfc6x6, HAsfc7x7, HAsfc8x8, HAsfc9x9, HAsfc10x10, HAsfc11x11		epLsar, Sv
	Mitaka PAFM	HAsfc2x2, HAsfc3x3, HAsfc4x4, HAsfc5x5, HAsfc6x6, HAsfc7x7, HAsfc8x8, HAsfc9x9, HAsfc10x10, HAsfc11x11, Sv	HAsfc3x3, HAsfc5x5, HAsfc6x6, HAsfc7x7, HAsfc8x8, HAsfc9x9, HAsfc10x10, HAsfc11x11, Sv	Sv	

Figure 5.12 *Comparisons of the magnitude of difference between microscopes with the known magnitude of difference between Archosargus probatocephalus dietary groups. For each comparison of microscopes, where the difference for a specific parameter exceeds the difference between dietary groups that parameter is listed. Results on the bottom left are for Non-Resampled data, results on the top right are for Resampled data. Only parameters where significant differences between dietary groups were recorded for both Non-Resampled and Resampled data have been tested (Table 5.16 and Table 5.18).*

Discussion

It is clear that significant variability exists between 3D microtextural data collected using different instruments. This variability is not consistent when comparing every possible pair of microscopes, with data from one instrument more similar to data from specific instruments than others. However there is a high degree of linear correlation between data collected from most instruments. We also find that data collected using different instruments varies considerably in its sensitivity to differences between populations with known variation in tooth surface textures, with data from certain instruments showing high sensitivity, and data from other instruments showing very low sensitivity, and the magnitude of difference between data from specific instruments in many cases exceeds the difference between dietary populations. None of these effects appear to be mitigated by resampling the data down to the lowest µm/pixel resolution and lowest field size across all instruments, with only slight variation in results recorded.

There is a great deal of absolute difference between parameter values calculated from datafiles generated by each microscope (ANOVA). These differences are more pronounced within certain sub-datasets than others. There is a proportionally much greater difference between microscopes when using SSFA parameters than ISO 25178 parameters (i.e. almost all SSFA parameters show differences between microscopes). While for ISO parameters many fewer parameters (as a proportion) show differences between data from separate microscopes, and there are several ISO parameters where no difference is ever recorded between microscopes across all sub-datasets. When data is resampled this pattern does not change, however the absolute difference (number of parameters where microscopes differ) is reduced slightly, and a greater number of ISO parameters show no difference between microscopes across all datasets than when using Non-Resampled data. Tukey HSD tests and connecting letter reports indicate a very specific set of differences, which are relatively consistent across datasets. It is clear that the two Sensofar instruments very rarely produce surfaces with different parameter values to each

other. There is also relatively little difference between datafiles generated from the Alicona IFM and Mitaka PAFM. The biggest difference appears to be between these two groups, however the Mitaka PAFM appears to show greater difference from the Alicona than the two Sensofar instruments are to each other. Again the same pattern is shown when using resampled data, indicating very little difference between the two types of data. This would indicate a relationship between data from different microscopes, where both Sensofar instruments produce relatively similar data to one another, the Alicona IFM produces data which is slightly different to these two instruments, and the Mitaka PAFM produces data different to all microscopes, but closer to that of the Alicona IFM than any other instrument. We see this same relationship from the LDA of Non-Resampled data and the LDA of Resampled data. Here the Mitaka PAFM data is separated from all other microscopes along PC1, but closest to the Alicona IFM data, while the distribution of Alicona IFM data is close to an overlapping distribution made up of data from both Sensofar microscopes. This is almost the same for Non-Resampled and Resampled data, however for Resampled data there is less overlap between data from the two Sensofar instruments, and Alicona IFM data now overlaps with that of the Sensofar Plμ neox.

From Linear Regression analysis it was found that data from almost all microscopes is correlated, and that this correlation is always positive, so as parameter values increase on surface data from one microscope they also increase on all other microscopes. However there is disparity between parameter types, with ISO 25178 parameters showing a much greater level of correlation than SSFA parameters, where certain comparisons, especially those with data from the Mitaka PAFM, rarely or never show correlation. The significance of certain intercepts in the regression analysis indicates some bias in this relationship, which appears to be relatively random given the lack of consistency between which comparisons show significant intercepts for each parameter. Again when we resample data there is apparently very little improvement in the correlation between microscopes, except for the textural fill volume (Tfv), and complexity (Asfc) of surfaces, which show correlation in all comparisons for Resampled data, but only in about half of comparisons for Non-Resampled data. Parameter Sds (Density of Summits) shows very little correlation

between microscopes for both data types, and separates all four microscopes into distinct groups in Tukey connecting letter reports (again for both data types). This suggests there is something fundamentally different about the density of summits on each microscope, which is not solved by resampling the data. Datafiles from the Mitaka PAFM show the largest Sds values, followed by the Alicona IFM, then the Sensofar Plμ neox, and finally the Sensofar Plμ. There is no obvious pattern to this relationship, and further work would be needed to investigate the reasons for this difference.

The Bland-Altman plots indicate that these relationships are not so consistent when measured across multiple parameters simultaneously. The difference between microscopes is clear from the significant regression results, which test whether the relationship of points is significantly different from zero (absolute agreement between data from each microscope). The Heterogeneity of Complexity parameter group shows little to no agreement between microscopes for either Resampled or Non-Resampled data. This is not surprising as SSFA parameters have performed consistently poorly, showing greater proportions of parameters differing, and worse correlation between microscopes. The only improvement indicated by Resampling data is a non-significant regression test between data collected on the Alicona IFM and the Mitaka PAFM, however the spread of the data, and significant intercept indicate bias in the comparison. Comparisons within the two parameters groups using ISO 25178 parameters show a much greater level of agreement between data from different microscopes. The Height group shows that data from the Alicona IFM, Sensofar Plμ, and Sensofar Plμ neox all agree, with some bias in their relationship, however comparisons of all microscopes with data form the Mitaka PAFM do not agree; this pattern is identical for Resampled and Non-Resampled data. While for the Volume group the pattern is less clear cut, with certain comparisons showing agreement, and others showing no agreement between microscopes, without any consistent pattern of specific microscopes which agree. The pattern is slightly different for Resampled data, but with the same lack of consistency.

Overall this indicates that surface data collected by different microscopes produces significantly different texture parameter values. Especially when using SSFA parameters, which show much lower levels of correlation between data. Resampling data does however appear to improve the comparability of certain SSFA parameters (Tfv, and Asfc). ISO parameter data on the other hand shows much greater correlation and agreement between microscopes, despite the differences between absolute texture values, with only parameter Sds consistently showing no agreement between the results of different microscopes. It is possible that the better overall performance of ISO parameters is due to the filtering that has been carried out on these surfaces to remove large wavelength information, which would support the work of Arman et al (2016), which showed greater parity of data between microscopes when surface filters were applied, however further investigation to confirm this would be needed.

These results all support the first hypothesis that using different microscopes/instruments to collect 3D tooth surface data will result in significantly different roughness parameter values (ISO 25178, and SSFA) recorded from resulting surfaces. With the caveat that parameter types appear to be affected differently, and that there is a high degree of correlation between data from different microscopes. However these results do not support the second hypothesis, that any differences in 3D texture produced by using different microscopes/instruments are caused in large part by the effect of each microscope collecting data at different sampling resolutions and field size, thus resampling datafiles collected from each microscope down to the lowest µm/pixel value across all microscopes and then reducing the field of view to the lowest across all microscopes will eliminate this difference. We see very little evidence for any reduction in difference, or improvement in correlation, outside a few select parameters. However, while we must reject this hypothesis there is a small reduction in difference between microscopes when using Resampled data (ANOVA) suggesting at least a small effect.

Dietary tests between populations with known textural differences return very different results depending on which microscope the data was collected, but this is not consistent across the two dietary comparisons. From T-tests we find that data from the

Alicona IFM and Mitaka PAFM are most sensitive to differences between *Capreolus capreolus* dietary populations, with data collected on the Sensofar Plμ performing worst. PCA analyses between *Capreolus capreolus* populations show a high degree of separation between distributions along PC1, but with some overlap between dietary groups when using data from the Sensofar Plμ, which support the T-tests results. Resampling data appears to have little effect on most comparisons, but does improve the PCA results for data collected using the Sensofar Plμ, with complete separation of groups. Eigenvectors indicate inconsistent results for parameters loading onto each axis depending on which microscope is used and whether data has been resampled. For comparisons of *Archosargus probatocephalus* populations we find a stark contrast between data collected using the Sensofar Plμ neox, which shows very high sensitivity to textural differences between these populations, and data from all other microscopes, which shows very little/no sensitivity between known groups. PCA between these populations show a much more complicated picture, with complete separation of group distributions when using data from the Sensofar Plμ and Sensofar Plμ Neox, but not along the same plane of separation, and a high degree of overlap between dietary groups when using the other two microscopes. Resampling data has little effect on T-test results, but appears to reduce the separation between groups in PCA analyses, especially for data collected either of the two Sensofar microscopes. Eigenvectors suggest any separation along PC1 being caused by the effect of HAsfc splits, but along PC1 the pattern is not clear.

Finally we find that the magnitude of difference between dietary groups is often exceeded by the difference between pairs of microscopes. For *Capreolus capreolus* populations, differences between microscopes exceed dietary differences in most parameters when data collected from the Mitaka PAFM is compared to data from other microscopes, and far fewer or none when other comparisons are carried out. This suggests that differences between the Mitaka PAFM and other microscopes would likely obscure dietary differences if compared together. For the *Archosargus probatocephalus* populations comparisons produce a different pattern, with magnitudes of difference between microscopes exceeding differences between dietary populations for many parameters in all but one comparison (Mitaka PAFM data against

Alicona IFM data). This would suggest that only the comparison between data from these two microscopes would not obscure dietary differences, while all other comparisons would. Resampling data has no effect on magnitudes of difference for the *Capreolus capreolus* populations, but does improve the picture for *Archosargus probatocephalus* populations with three comparisons showing fewer parameters with greater magnitudes of difference between microscopes than between dietary groups.

It is clear from all of these results that the sensitivity of data collected using different microscopes to known textural difference between dietary populations is highly variable, and as such using different microscopes will produce different results when comparing the same dietary groups. However the magnitude of this effect appears variable depending on the comparison in question, with *Capreolus capreolus* populations showing less variability than *Archosargus probatocephalus* populations. This may have something to do with the nature of the teeth in question, as *C.capreolus* are terrestrial with occlusal tooth facets which grind food, while *A.probatocephalus* are aquatic and do not have occlusal facets. This could lead to stronger dietary signals on *C.capreolus* teeth, with greater roughness, which would be less likely to be obscured by variation between data from difference microscopes. Resampling data does not appear to improve this pattern in any way, except for slight improvements in PCA results for *C.capreolus* populations when using Sensofar Plμ data, and slight reductions in magnitude of difference between microscopes when using *A.probatocephalus* tooth surfaces.

These results support the third hypothesis, that when comparing dietary groups with known variation in the texture of their tooth surfaces, the sensitivity of data collected using different microscopes varies in its ability to detect this variation, so that certain microscopes are more sensitive than others to significant textural differences. But the fourth hypothesis, that differences between the sensitivity of data collected using different microscopes/instruments are eliminated by resampling the data down to the lowest μm/pixel resolution and field size, must be rejected. The reason for these differences are unclear, whether it is an artefact of how each instrument fills data between measurement locations, or something more

fundamental about how each methodology captures a surface will need further investigation. However the implications of these differences are clear, that data collected by different microscopes, especially those which use different methods to scan a surface, while apparently correlated, is significantly different, and produces varied sensitivity to textural differences from populations with different diets. The absolute solution to this problem (until further study has been carried out) would be to collect data from multiple instruments when testing hypotheses of textural difference. However this would be very costly and potentially prohibitively time consuming. As such, until the reasons for, and solutions to these differences are discovered, care must be taken when comparing results of dietary hypotheses tested using different microscopes.

Conclusions

This PhD set out to investigate two overarching topics, the effect of varying methodologies on the results of quantitative 3D tooth surface texture analysis when it is used to differentiate diet, and the utility of this technique for studying the diet of marine mammals, both extant and extinct. Within these topics a number of hypotheses have been experimentally tested, which has led to a set of conclusions summing up the results of this PhD.

The accuracy and precision of different silicon based moulding compounds, when replicating tooth surface textures prior to data collection, was tested in **Chapter One** by comparing the values of surface roughness parameters generated from scans of original tooth surfaces and those of casts produced using different moulding compounds. It was found that significant differences exist between the accuracy and precision of a range of compounds and that those differences were most pronounced in high viscosity compounds, likely due to their inability to flow into and thus replicate small scale features of surface texture. The mid viscosity compound President Jet Regular Body (Coltène Whaledent) showed the highest precision and accuracy of all moulding compounds, with little difference evident from the original surface in all but a very small number of parameters. The null hypothesis that areal texture parameters obtained from replicas do not differ from those obtained from the original surface was rejected. Therefore it is of vital importance that the same moulding compound is employed for all studies of diet using 3D tooth surface roughness parameters. These results support the use of President Jet Regular Body for this purpose.

In **Chapter Two** the ability of 3D tooth surface texture analysis to separate diet in modern marine mammals was tested, along with a subsequent test comparing the textures on fossil whale teeth to those of modern marine mammals to determine whether this technique could be used to differentiate diet in extinct stem cetaceans. It was found that dietary groups in modern marine mammals could be separated via univariate and multivariate statistical analysis, using roughness parameters generated

from scans of labial-apical enamel from post canine teeth in pinnipeds and cheek teeth in odontocetes. The sensitivity to this difference was high (ANOVA) and the dietary signal was stronger even than the taxonomic signal between species expected to eat the same food type, but with radically different dentitions. However a phylogenetic signal was present in the data. The tooth texture of stem cetaceans were found to overlap heavily with those of modern marine mammals, suggesting a parity of diet between certain extinct species and modern pinnipeds and odontocetes. However some species were found to fall outside the range of modern marine mammal diet. From a previously published analysis it was found that the parameter separating this group of stem cetaceans from all other specimens in multivariate space was also one that is correlated with increased durophagy, suggesting a potential dietary hypotheses towards increased consumption of hard food items in these individuals. These results all support the hypotheses that the microwear textures of tooth surfaces from extant marine mammals reflect their dietary habits, and that phylogenetically distinct taxa have microwear textures that reflect similarities in diet more than phylogenetic relationships. They also support the hypothesis that analysis of microwear in stem cetaceans is comparable to extant marine mammals. But when comparing the dietary habits of stem cetaceans to their phylogeny the data does not support the hypothesis that diet derived from analysis of microwear texture support hypotheses of a unidirectional dietary transition through the stem cetacean lineage. Instead it paints a picture of a much more complex evolution.

Quantitative analysis of 3D tooth surface texture was also applied to populations of killer whales (*Orcinus orca*) from the North Atlantic, hypothesised to eat different diets from isotope analysis. The aim of **Chapter Three** was to determine the variability of texture within and between teeth from an individual, and the sensitivity of 3D tooth surface texture analysis to known dietary differences in *Orcinus orca* (defined by isotope data), using dentine tooth surfaces. Statistical comparisons of roughness parameter data within an individual showed that tooth textures varied significantly within and between teeth from the same individual, and between jaw types (upper, lower, left, right). This implies that analyses using 3D surface textures from *Orcinus orca* tooth dentine should take care when sampling data locations and

tooth positions, with a focus on extreme consistency in data collection. This also means the null hypothesis that the 3D surface texture of *Orcinus orca* teeth does not vary significantly within a single tooth, between teeth along a jaw from an individual, or between Jaw Types must be rejected. The comparison of *Orcinus orca* dietary groups showed very little sensitivity to dietary differences, with separation of groups only possible when the diet of specimens without isotope data was predicted using their tooth surface roughness parameter values. When this data was included, Middle Teeth analysed using univariate and multivariate statistics do show a difference between dietary groups, however this difference is small. It is unclear what has caused this low sensitivity to dietary differences, but it is possible that the inability to control for jaw type and exact tooth position may have added enough variability to the data to partly obscure the dietary signal, or it may be that the labial side of apical facets are not the best source of dietary information in *Orcinus orca*. This data means the null hypothesis that 3D tooth surface texture parameters cannot separate known dietary ecotypes of *Orcinus orca* must be rejected, however this includes the caveat that sensitivity to this separation was low, and only found using Middle Teeth and when diet was predicted for specimens with no isotope data.

Chapter Four focussed on testing the effect of different operators and filters used to scale limit 3D surfaces on resulting areal roughness parameter values. Ten different operators and three different filters (one filter with two separate nesting index cut-off wavelengths) were tested, comparing the absolute resulting parameter values produced from surfaces using each scale limiting setting, and their sensitivity to detect differences between known dietary groups. It was found that significant differences exist between settings in all categories (operator, filter, and nesting index). For operators this difference was restricted of the effect of 10^{th} and 11^{th} order polynomials, which produce surfaces with significantly different roughness values to those produced using any other setting. Tests comparing surfaces produced using different filters show that spline filters produce surfaces with significantly different roughness values to those produced using either robust Gaussian or robust wavelet filters. And tests between surfaces produced using different nesting indices indicate that a 0.08mm cut-off produces different roughness values from surfaces treated with

a 0.025mm cut-off, and from other surfaces where a 0.08mm setting was also used. When testing the sensitivity to dietary differences of surfaces produced using different scale limiting settings, within two dietary groups of roe deer and two dietary groups of phocids, it was found that scale limited surfaces vary considerably in their sensitivity depending on the operator, filter, and nesting index used. In all cases surfaces treated with a robust Gaussian filter, or spline filter (0.025mm nesting index) and a 2^{nd} to 7^{th} order polynomial showed the greatest sensitivity to dietary difference when testing with univariate analyses, however the greatest magnitude of difference between dietary groups was highly variable, and only coincided with the greatest sensitivity for surfaces scale limited using a 6^{th} order polynomial and a robust Gaussian filter (0.025mm nesting index), and only in one of the two dietary comparisons. Multivariate analyses were able to separate the distributions of each dietary group in all cases, but showed variability in the relationship of each specimen in multivariate space. Overall the results of this chapter lead us to reject the null hypotheses that application of different polynomials (operators) to remove long wavelength elements of surface form has no effect on the texture of resulting surfaces (as measured by ISO 25178-2 texture parameters); that application of different filter types (robust Gaussian, robust wavelet, and spline) has no effect on the texture of the resulting surface; that application of filters with different nesting indices (cut-off wavelengths) has no effect on the texture of the resulting surface; and that application of different filters and operators has no effect on the power of areal microwear texture analyses to detect dietary differences between samples. However the results support the null hypothesis that when applying different operators, filters, and filters with different nesting indices to a surface, there is no interaction in their effect on resulting texture parameters. The results of this chapter support the use of a 6^{th} order polynomial and a robust Gaussian filter (0.025mm nesting index) to scale limit 3D surfaces for areal texture parameter generation, and therefore should be recommended for use in all future analyses using 3D areal texture parameters.

Chapter Five investigated the effect of using different microscopes to collect 3D texture data from the same location on tooth surfaces, and the effect this has on resulting dietary analyses, using groups where differences in diet have previously been

confirmed. This test used four microscopes, covering 3 technologies, comparing roughness parameters (both ISO 25178 and SSFA) generated from surfaces captured using each microscope. Univariate and multivariate analysis found large differences between different microscopes, with those employing the same technology showing the least difference, and the greatest degree of similarity in multivariate space. However data from surfaces generated using different microscopes was directionally and linearly correlated to a high degree. Bland-Altman plots show that this correlation still exists to some degree (except when using SSFA parameters), even when multiple parameters sharing units and scale are included in the same plot. In all cases SSFA parameter values were more affected by varying the microscope used to collect data than ISO 25178 parameters. The sensitivity to dietary differences was shown to be highly variable depending on the microscope used to collect data, but was not consistent across two separate dietary comparisons. In both direct comparisons and dietary tests, resampling data to the lowest µm/pixel and field size slightly reduces the scale of difference, but has no appreciable effect. These results support the hypotheses that using different Microscopes will result in statistically significant differences in 3D microtextural parameter values (ISO 25178, and SSFA), and that when comparing dietary groups with known variation in the texture of their tooth surfaces, the sensitivity of data collected using different microscopes varies in its ability to detect this variation, so that certain microscopes are more sensitive than other to significant textural differences. However we must reject both hypotheses that differences and sensitivity can be improved by resampling data to the lowest µm/pixel and field size.

The work in this PhD has shown that methodological variability is incredibly important for quantitative 3D microtextural analysis of tooth surfaces. The choice of moulding compound used to produce tooth replicas, microscope used to collect data files, and settings used to scale limit surfaces for ISO parameter generation all significantly affect the results of subsequent analyses. The results of this PhD show that one specific moulding compound is more accurate and precise than any others, producing replicas with no difference to the original surface, and should be used in all future studies. When scale limiting surfaces one combination of operator, filter and

nesting index, shows the greatest sensitivity to dietary difference and the lowest difference from other surfaces so this should again be used when areal texture parameters (ISO 25178) are employed. The results also show that different microscopes capturing data from the same location on a tooth surface can result in significantly different roughness parameter values, and while we are not able to suggest a gold standard going forwards, this is at least an important factor to be considered for all future work. This PhD has also shown that quantitative 3D microtextural analysis of tooth surfaces can be employed to differentiate diet in modern marine mammals, especially when using enamel tooth surfaces, but also potentially when using dentine. The diet of extinct cetacean species can be illuminated using this technique, producing a much more complex picture of dietary evolution in these early whales than previously hypothesised.

It is clear from the results of this PhD that differences in diet between marine mammal species, even those that are very taxonomically dissimilar, can be detected using 3D microtextural analysis of tooth surfaces. This is also true for stem cetacean dietary analyses. It is also found that dietary information may be preserved in tooth dentine from *Orcinus orca*, however this result is much less convincing. Methodologically, a number of recommendations can be made from the results of this PhD for future analyses using 3D microtextural analysis of tooth surfaces. Firstly, the mid viscosity moulding compound President Jet Regular Body should be used to replicate tooth surfaces in all future studies, due to the compound showing the highest accuracy and greatest precision of any compound tested. Secondly it appears that a 6^{th} order polynomial, alongside a robust Gaussian filter with a nesting index of 0.025mm should be used in all future work to scale limit 3D surfaces prior to parameter generation. This setting showed very high sensitivity to dietary differences, and includes those settings least likely to produce deviations in surface texture when compared to data generated using other settings. It is also the only combination of operator and filter where the greatest sensitivity to dietary difference corresponds to the greatest magnitude of difference between dietary populations. Recommendations for the use of different microscopes in future studies are much more difficult. It is unclear from the analyses carried out in this PhD whether one microscope is

consistently more sensitive to dietary differences than another, but it appears that the Mitaka point autofocus microscope shows the greatest propensity to produce radically different data compared to the infinite focus microscope, or either of the confocal microscopes. Unfortunately, this pattern is variable depending on the dietary groups analysed. However, the linear correlation of much of the data from different microscopes, and the ability of each microscope to separate dietary groups in multivariate space relatively equally, suggests that while absolute data values are different they are producing the same pattern of results, potentially implying that the use of different microscopes is more of a problem when comparing absolute values than when comparing their ability to separate dietary groups.

There are several clear implications for both past and future studies using 3D microtextural analysis that come out of this PhD. The comparability of analyses carried out using different methodologies is likely to be low, and the need to standardise methodologies across research groups is shown to be great. Across all methods tested there are high levels of variability when methodological parameters are changed. Standardisation following the suggestions of this PhD could go some way towards ameliorating variability when selecting moulding compounds and settings used to scale limit data files, however there appears to be no “best” methodology when it comes to choosing which microscope to use when collecting data. This obviously presents a serious problem, and one that is likely to impact the comparability of studies until a solution can be found. This certainly impacts the ability to compare those studies already carried out using different methodologies, but is unlikely to invalidate the results of previous studies, as the relative ability of microscope to separate groups in multivariate space was high, and the linear relationships in the data suggest a consistent pattern regardless of the microscope used. It does however mean that studies carried out using methodologies found to be less than optimum, such as using a less accurate/precise moulding compound (e.g. Purnell and Darras 2015), or a different scale limiting setting (e.g. Schulz et al 2013a), must be scrutinised and the potential need to test the repeatability of these analyses is high. Regarding the results of dietary tests between marine mammal species, this PhD provides evidence that 3D microtextural analysis of tooth surfaces is a robust and sensitive technique that can be

added to the current suite of quantitative methodologies used to study marine mammal diet (stomach contents/faecal data, DNA, Isotopes, quantitative fatty acid data), which overcomes many of the drawbacks of these techniques, and is able to traverse taxonomic boundaries. Therefore, it may be possible to use 3D microtextural analysis of tooth surfaces to inform conservation strategies, the likely impact of climate change, and inform calls to cull specific marine mammal species based on their competition with fisheries resources. It will certainly make the study of diets that are otherwise very hard to quantify much easier. The technique is also shown to be applicable to future studies of diet in stem cetaceans, and potentially other fossil marine mammal species. It offers a new powerful tool to study the diet of these animals, where previously morphological analysis and rare stomach contents and species interaction evidence provided the only data for studying stem cetacean diet. This has the potential to radically affect our ability to understand the diet of these extinct species, and the evidence provided here for a more complex evolution of diet in stem cetaceans than previously hypothesised offers a new hypothesis for the drivers behind stem cetacean evolution. One of greater niche exploitation that previously thought. The potential for answering further questions about stem cetacean diet are very positive, and with increased sample sizes and data from a greater range of modern analogues it is likely trends in diet can be even further illuminated in these extinct species.

For all this, much further work is needed to investigate certain hypotheses and issues, brought to light by this PhD. More work is needed to explore the diet of stem cetaceans, with a focus on modern analogues for diets including hard food items in modern marine mammals, as this may help elucidate the dietary habits of those stem cetaceans plotting outside the range of modern marine mammal diet. There should also be a focus on increased sample size for the stem cetaceans with multiple specimens for each species and a greater number of species. While this will not be possible in all cases due to the rarity of fossil specimens it should at least be attempted. In a similar vein a great deal of further work is needed to determine the true sensitivity of 3D tooth surface texture analysis to dietary difference in killer whales. We now know that variability in tooth surface texture is high, so future work

can take these results into account, and improve on this study by including an even greater control on the variables, especially jaw type and exact tooth position. Both mesial and lingual data (from the tooth apex) and data from lateral tooth facets should be tested to determine whether these areas are better at recording data than the labial tooth apex. An obvious improvement in future work would also be to increase the sample size for specimens with known isotopic data, which would reduce the need to predict diet. For the methodological areas of study further work is need to determine the root cause of the differences produced by varying the microscope used to collect data. Any future work should aim to use larger sample sizes, as the small sample sizes used in this PhD will likely have some effect on the variability in data and could explain the different results produced for each dietary comparison.

Appendix 1: Supplementary Figures and Tables

Supplementary Table 2.1 *Results of "Leave One Out" validation of the LDA model from Fig 2.3. Specimen number and expected dietary groupings for each specimen are given from Table 2.2, as are the results of the LDA from Figure 2.3, including dietary group predictions, probability of prediction, Wilk's Lambda test results for each axis, and misclassification rates. These same statistics are then also provided for all ten "Leave One Out" replicates, with the specimen left out highlighted in grey. Bold text indicates misclassified specimens, and red text indicates significant Wilks' Lambda test results.*

				Leave on Out Replicate 1		Leave on Out Replicate 2	
		Original LDA (Figure 3)		Specimen Excluded NMS_1905.167.4		Specimen Excluded NMS_Z.2011.41.108	
Specimen Number	Expected Dietary Group	Dietary Group Predicted from LDA	Probability of Prediction	Dietary Group Predicted from LDA	Probability of Prediction	Dietary Group Predicted from LDA	Probability of Prediction
UMMZ 177439	Cephalopods	Cephalopods	0.9878	Cephalopods	0.9886	Cephalopods	0.9873
UMMZ 177426	Cephalopods	Cephalopods	0.8328	Cephalopods	0.9424	Cephalopods	0.8105
UMMZ 176250	Cephalopods	Cephalopods	0.5870	Cephalopods	0.8337	Cephalopods	0.6309
Z.2011.41.108	Cephalopods	Cephalopods	0.9508	Cephalopods	0.9363	Cephalopods	0.7375
Z.2011.41.106	Cephalopods	Cephalopods	0.8742	Cephalopods	0.8222	Cephalopods	0.7934
1956.037	Cephalopods	Cephalopods	0.5527	Cephalopods	0.8076	Cephalopods	0.5786
Z.2011.41.116	Cephalopods	Cephalopods	0.8399	Cephalopods	0.9234	Cephalopods	0.8705
ZMB 66435	Fish	Fish	0.9728	Fish	0.9885	Fish	0.9657
NMW 7547	Fish	Fish	0.9471	Fish	0.9650	Fish	0.9442
UMMZ 167402	Fish	Fish	0.8794	Fish	0.8765	Fish	0.8659
M1068	Fish	Fish	0.8807	Fish	0.8955	Fish	0.8761
ZD 1887.5.20.1	Fish	Fish	0.9477	Fish	0.9646	Fish	0.9443
ZD 1886.11.22.1	Fish	**Invertebrates**	**0.8313**	**Invertebrates**	**0.8711**	**Invertebrates**	**0.7754**
ZMB_MAM_90810	Fish	Fish	0.6317	Fish	0.6855	Fish	0.6302
ZMB_MAM_56766	Fish	Fish	0.7463	Fish	0.6805	Fish	0.7305
ZMB_MAM_100997	Fish	Fish	0.9466	Fish	0.9681	Fish	0.9446
ZMB_MAM_56767	Fish	Fish	0.8923	Fish	0.9062	Fish	0.8862
ZMB ?? => I1271	Fish	**Cephalopods**	**0.6080**	**Cephalopods**	**0.7639**	**Cephalopods**	**0.6740**
ZMB_MAM_43743	Invertebrates	Invertebrates	0.8113	Invertebrates	0.7840	Invertebrates	0.8015
ZMB_MAM_43740	Invertebrates	Invertebrates	0.9976	Invertebrates	0.9975	Invertebrates	0.9974
ZMB_MAM_43770	Invertebrates	Invertebrates	0.8968	Invertebrates	0.8959	Invertebrates	0.8749
ZMB_MAM_43758	Invertebrates	Invertebrates	0.9630	Invertebrates	0.9690	Invertebrates	0.9606
ZMB_MAM_43763	Invertebrates	Invertebrates	0.7298	Invertebrates	0.7717	Invertebrates	0.7552
ZMB_MAM_56786	Fish	Fish	0.9995	Fish	0.9997	Fish	0.9992
ZMB_MAM_70654	Fish	Fish	0.6551	Fish	0.6504	Fish	0.6549
ZMB_MAM_56782	Fish	Fish	0.7522	Fish	0.7330	Fish	0.7617
ZMB_MAM_56783	Fish	Fish	0.9265	Fish	0.9418	Fish	0.9216
ZMB_MAM_56761	Cephalopods	Cephalopods	0.4585	**Fish**	**0.6276**	Cephalopods	0.4775
ZMB_MAM_60568	Cephalopods	Cephalopods	0.5644	Cephalopods	0.6653	Cephalopods	0.6289
ZMB_MAM_70669	Cephalopods	Cephalopods	0.9996	Cephalopods	0.9999	Cephalopods	0.9994
ZMB_MAM_5627	Cephalopods	Cephalopods	0.6633	Cephalopods	0.8680	Cephalopods	0.7119
ZMB_MAM_5648	Cephalopods	Cephalopods	0.9180	Cephalopods	0.9667	Cephalopods	0.9267
ZMB_MAM_72816	Cephalopods	Cephalopods	0.9572	Cephalopods	0.9911	Cephalopods	0.9577
ZMB_MAM_2787	Cephalopods	Cephalopods	0.6845	Cephalopods	0.7736	Cephalopods	0.6925
ZMB_MAM_37702	Cephalopods	Cephalopods	0.5903	Cephalopods	0.9566	**Amniotes**	**0.5358**
ZMB_MAM_72815	Cephalopods	Cephalopods	0.9629	Cephalopods	0.9800	Cephalopods	0.9626
ZMB_MAM_32569	Invertebrates	Invertebrates	0.8395	Invertebrates	0.8883	Invertebrates	0.8320
ZMB_MAM_43737	Invertebrates	Invertebrates	0.9405	Invertebrates	0.9682	Invertebrates	0.9598
ZMB_MAM_32570	Invertebrates	Invertebrates	0.9581	Invertebrates	0.9691	Invertebrates	0.9573
ZMB_MAM_43738	Invertebrates	Invertebrates	0.9929	Invertebrates	0.9945	Invertebrates	0.9913
ZMB_MAM_56774	Invertebrates	Invertebrates	0.9873	Invertebrates	0.9603	Invertebrates	0.9858
NMS_1996.83.58	Amniotes	Amniotes	0.8713	Amniotes	0.7874	Amniotes	0.9134
NMS_1948.64	Amniotes	**Invertebrates**	**0.8788**	**Invertebrates**	**0.8908**	**Invertebrates**	**0.8781**
NMS_1921.143.P	Amniotes	Amniotes	0.9999	Amniotes	1.0000	Amniotes	0.9998
NMS_1905.167.4	Amniotes	**Cephalopods**	**0.6163**	**Cephalopods**	**0.9991**	**Cephalopods**	**0.7182**
NMS_1921.143.0	Amniotes	Amniotes	0.9997	Amniotes	0.9999	Amniotes	0.9998
NMS_1822.240.T29	Amniotes	Amniotes	0.9976	Amniotes	0.9978	Amniotes	0.9970
NMS_1960.24	Amniotes	Amniotes	0.9935	Amniotes	0.9936	Amniotes	0.9922
Wilks Lambda Test	CA1	<.0001		<.0001		<.0001	
	CA2	0.0001		0.0003		0.0002	
	CA3	0.0054		0.0043		0.0081	
Misclassified	Number	4		4		5	
	Percentage	8.33		8.51		10.64	

Leave on Out Replicate 3		Leave on Out Replicate 4		Leave on Out Replicate 5		Leave on Out Replicate 6	
Specimen Excluded ZMB_MAM_66435		Specimen Excluded ZMB_MAM_5627		Specimen Excluded ZMB_MAM_32570		Specimen Excluded ZMB_MAM_43740	
Dietary Group Predicted from LDA	Probability of Prediction	Dietary Group Predicted from LDA	Probability of Prediction	Dietary Group Predicted from LDA	Probability of Prediction	Dietary Group Predicted from LDA	Probability of Prediction
Cephalopods	0.9898	Cephalopods	0.9925	Cephalopods	0.9864	Cephalopods	0.9836
Cephalopods	0.8031	Cephalopods	0.8767	Cephalopods	0.8283	Cephalopods	0.8644
Cephalopods	0.5548	Cephalopods	0.4553	Cephalopods	0.5586	Cephalopods	0.6022
Cephalopods	0.9403	Cephalopods	0.9623	Cephalopods	0.9479	Cephalopods	0.9484
Cephalopods	0.8733	Cephalopods	0.8763	Cephalopods	0.8837	Cephalopods	0.8649
Cephalopods	0.5183	Cephalopods	0.638	Cephalopods	0.5479	Cephalopods	0.5282
Cephalopods	0.8530	Cephalopods	0.7989	Cephalopods	0.8347	Cephalopods	0.8346
Fish	0.9544	Fish	0.9647	Fish	0.9713	Fish	0.9760
Fish	0.9519	Fish	0.9287	Fish	0.9429	Fish	0.9470
Fish	0.8868	Fish	0.8713	Fish	0.8637	Fish	0.8552
Fish	0.8800	Fish	0.8756	Fish	0.8692	Fish	0.8587
Fish	0.9429	Fish	0.9412	Fish	0.9435	Fish	0.9510
Invertebrates	**0.8232**	**Invertebrates**	**0.8829**	**Invertebrates**	**0.8189**	**Invertebrates**	**0.8225**
Fish	0.6401	Fish	0.6567	Fish	0.6419	Fish	0.6104
Fish	0.7311	Fish	0.7651	Fish	0.7432	Fish	0.7774
Fish	0.9380	Fish	0.9285	Fish	0.9433	Fish	0.9441
Fish	0.8915	Fish	0.9059	Fish	0.8889	Fish	0.8963
Cephalopods	**0.5967**	**Cephalopods**	**0.5897**	**Cephalopods**	**0.6059**	**Cephalopods**	**0.6272**
Invertebrates	0.8015	Invertebrates	0.8788	Invertebrates	0.8037	Invertebrates	0.7839
Invertebrates	0.9971	Invertebrates	0.9986	Invertebrates	0.9979	Invertebrates	0.9948
Invertebrates	0.8898	Invertebrates	0.9062	Invertebrates	0.8931	Invertebrates	0.9092
Invertebrates	0.9571	Invertebrates	0.9861	Invertebrates	0.9505	Invertebrates	0.9697
Invertebrates	0.7202	Invertebrates	0.8332	Invertebrates	0.6718	Invertebrates	0.7689
Fish	0.9992	Fish	0.9993	Fish	0.9994	Fish	0.9995
Fish	0.6780	Fish	0.5293	Fish	0.6957	Fish	0.6132
Fish	0.7569	Fish	0.7958	Fish	0.7436	Fish	0.7184
Fish	0.9220	Fish	0.9186	Fish	0.9217	Fish	0.9127
Cephalopods	0.5021	**Fish**	**0.5205**	Cephalopods	0.4706	Cephalopods	0.4746
Cephalopods	0.5834	Cephalopods	0.6042	Cephalopods	0.5604	Cephalopods	0.5173
Cephalopods	0.9996	Cephalopods	0.9997	Cephalopods	0.9996	Cephalopods	0.9996
Cephalopods	0.6391	**Invertebrates**	**0.8046**	Cephalopods	0.7055	Cephalopods	0.6599
Cephalopods	0.9043	Cephalopods	0.8973	Cephalopods	0.9079	Cephalopods	0.9162
Cephalopods	0.9479	Cephalopods	0.9591	Cephalopods	0.9540	Cephalopods	0.9655
Cephalopods	0.6835	Cephalopods	0.7336	Cephalopods	0.6744	Cephalopods	0.6535
Cephalopods	0.5806	Cephalopods	0.6525	Cephalopods	0.5845	Cephalopods	0.6118
Cephalopods	0.9610	Cephalopods	0.9477	Cephalopods	0.9599	Cephalopods	0.9526
Invertebrates	0.8381	Invertebrates	0.8308	Invertebrates	0.8332	Invertebrates	0.8537
Invertebrates	0.9353	Invertebrates	0.9028	Invertebrates	0.9368	Invertebrates	0.9309
Invertebrates	0.9544	Invertebrates	0.974	Invertebrates	0.9413	Invertebrates	0.9619
Invertebrates	0.9925	Invertebrates	0.9932	Invertebrates	0.9934	Invertebrates	0.9900
Invertebrates	0.9848	Invertebrates	0.9883	Invertebrates	0.9870	Invertebrates	0.9867
Amniotes	0.8545	Amniotes	0.8868	Amniotes	0.8730	Amniotes	0.8410
Invertebrates	**0.8761**	**Invertebrates**	**0.856**	**Invertebrates**	**0.8623**	**Invertebrates**	**0.9013**
Amniotes	0.9998	Amniotes	0.9998	Amniotes	0.9998	Amniotes	0.9998
Amniotes	0.5191	**Cephalopods**	**0.5477**	**Cephalopods**	**0.6046**	**Cephalopods**	**0.6284**
Amniotes	0.9997	Amniotes	0.9996	Amniotes	0.9996	Amniotes	0.9996
Amniotes	0.9972	Amniotes	0.9973	Amniotes	0.9973	Amniotes	0.9971
Amniotes	0.9933	Amniotes	0.9932	Amniotes	0.9923	Amniotes	0.9930
<.0001		<.0001		<.0001		<.0001	
0.0003		0.0002		0.0002		0.0003	
0.0092		0.0086		0.0073		0.0091	
3		5		4		4	
6.38		10.64		8.51		8.51	

Leave on Out Replicate 7		Leave on Out Replicate 8		Leave on Out Replicate 9		Leave on Out Replicate 10	
Specimen Excluded ZMB_MAM_43763		Specimen Excluded ZMB_MAM_56782		Specimen Excluded ZMB_MAM_72816		Specimen Excluded ZMB_MAM_90810	
Dietary Group Predicted from LDA	Probability of Prediction	Dietary Group Predicted from LDA	Probability of Prediction	Dietary Group Predicted from LDA	Probability of Prediction	Dietary Group Predicted from LDA	Probability of Prediction
Cephalopods	0.9865	Cephalopods	0.9864	Cephalopods	0.9906	Cephalopods	0.9910
Cephalopods	0.8083	Cephalopods	0.7756	Cephalopods	0.7810	Cephalopods	0.9219
Cephalopods	0.6057	Cephalopods	0.5945	Cephalopods	0.5482	Cephalopods	0.6053
Cephalopods	0.9550	Cephalopods	0.9522	Cephalopods	0.9523	Cephalopods	0.9580
Cephalopods	0.9081	Cephalopods	0.8724	Cephalopods	0.8848	Cephalopods	0.8729
Cephalopods	0.5617	Cephalopods	0.5675	Cephalopods	0.5789	Cephalopods	0.5797
Cephalopods	0.8399	Cephalopods	0.8072	Cephalopods	0.8272	Cephalopods	0.7537
Fish	0.9727	Fish	0.9710	Fish	0.9670	Fish	0.9758
Fish	0.9345	Fish	0.8931	Fish	0.9697	Fish	0.9751
Fish	0.8899	Fish	0.9180	Fish	0.8698	Fish	0.8802
Fish	0.8869	Fish	0.9124	Fish	0.8797	Fish	0.9274
Fish	0.9458	Fish	0.9556	Fish	0.9306	Fish	0.9102
Invertebrates	**0.8427**	**Invertebrates**	**0.8730**	**Invertebrates**	**0.8180**	**Invertebrates**	**0.8180**
Fish	0.6586	Fish	0.6881	Fish	0.5978	**Invertebrates**	**0.3923**
Fish	0.7116	Fish	0.7728	Fish	0.7313	Fish	0.7653
Fish	0.9486	Fish	0.9451	Fish	0.9411	Fish	0.8972
Fish	0.8811	Fish	0.8952	Fish	0.8787	Fish	0.8827
Cephalopods	**0.5918**	**Cephalopods**	**0.5837**	**Cephalopods**	**0.6038**	**Cephalopods**	**0.4988**
Invertebrates	0.8411	Invertebrates	0.7913	Invertebrates	0.8121	Invertebrates	0.8293
Invertebrates	0.9987	Invertebrates	0.9978	Invertebrates	0.9975	Invertebrates	0.9974
Invertebrates	0.8649	Invertebrates	0.9134	Invertebrates	0.8909	Invertebrates	0.9033
Invertebrates	0.9192	Invertebrates	0.9553	Invertebrates	0.9539	Invertebrates	0.9771
Invertebrates	0.4825	Invertebrates	0.7283	Invertebrates	0.7103	Invertebrates	0.7454
Fish	0.9994	Fish	0.9996	Fish	0.9993	Fish	0.9998
Fish	0.6895	Fish	0.6635	Fish	0.6534	Fish	0.5428
Fish	0.7574	Fish	0.4278	Fish	0.7766	Fish	0.8155
Fish	0.9279	Fish	0.9129	Fish	0.9369	Fish	0.9019
Fish	**0.4711**	Cephalopods	0.4622	**Fish**	**0.4531**	**Fish**	**0.5291**
Cephalopods	0.5739	Cephalopods	0.5956	Cephalopods	0.5702	Cephalopods	0.5160
Cephalopods	0.9996	Cephalopods	0.9996	Cephalopods	0.9996	Cephalopods	0.9995
Cephalopods	0.7976	Cephalopods	0.7104	Cephalopods	0.6725	Cephalopods	0.6643
Cephalopods	0.9163	Cephalopods	0.9169	Cephalopods	0.9140	Cephalopods	0.9296
Cephalopods	0.9538	Cephalopods	0.9613	Cephalopods	0.9041	Cephalopods	0.9504
Cephalopods	0.7119	Cephalopods	0.6693	Cephalopods	0.7002	Cephalopods	0.7015
Cephalopods	0.5887	Cephalopods	0.6533	Cephalopods	0.6497	Cephalopods	0.5789
Cephalopods	0.9680	Cephalopods	0.9563	Cephalopods	0.9583	Cephalopods	0.9784
Invertebrates	0.8951	Invertebrates	0.8973	Invertebrates	0.8254	Invertebrates	0.8507
Invertebrates	0.9468	Invertebrates	0.9235	Invertebrates	0.9309	Invertebrates	0.9452
Invertebrates	0.9399	Invertebrates	0.9616	Invertebrates	0.9541	Invertebrates	0.9675
Invertebrates	0.9963	Invertebrates	0.9935	Invertebrates	0.9926	Invertebrates	0.9899
Invertebrates	0.9917	Invertebrates	0.9863	Invertebrates	0.9860	Invertebrates	0.9887
Amniotes	0.9306	Amniotes	0.8683	Amniotes	0.8841	Amniotes	0.8656
Invertebrates	**0.8203**	**Invertebrates**	**0.9259**	**Invertebrates**	**0.8718**	**Invertebrates**	**0.9044**
Amniotes	0.9998	Amniotes	0.9999	Amniotes	0.9998	Amniotes	0.9998
Cephalopods	**0.6103**	**Cephalopods**	**0.6387**	**Cephalopods**	**0.6762**	**Cephalopods**	**0.6144**
Amniotes	0.9997	Amniotes	0.9996	Amniotes	0.9997	Amniotes	0.9996
Amniotes	0.9974	Amniotes	0.9988	Amniotes	0.9984	Amniotes	0.9958
Amniotes	0.9914	Amniotes	0.9947	Amniotes	0.9951	Amniotes	0.9932
<.0001		<.0001		<.0001		<.0001	
0.0001		0.0002		0.0002		0.0001	
0.0075		0.0079		0.0083		0.0037	
5		4		5		5	
10.64		8.51		10.64		10.64	

Supplementary Table 3.1 *Results from Leave One Out cross validation test of the LDA model from Figure 3.8.a, for the front teeth dataset. First column gives specimen number, second gives expected diet from both isotope data and the predictive LDA, and third and fourth column give the results for the original LDA. All subsequent pairs of columns give each replicate of the Leave One Out test. In each case a random sample was excluded (highlighted in grey) and the LDA run to test its robustness. Misclassified specimens are highlighted with bold text. In each case the Assignment gives the group to which the analysis has assigned each specimen, and the probability is the likelihood of that specimen belonging to the assigned group.*

Front Teeth				Replicate 1		Replicate 2		Replicate 3	
Specimen	Expected Diet	Original LDA Assignment	Probability	Assignment	Probability	Assignment	Probability	Assignment	Probability
NMS.1956.36.56	Mammals	Mammals	0.9998	Mammals	0.9995	Mammals	0.9997	Mammals	0.9996
ZMC CN89	Mammals	Mammals	0.9997	Mammals	0.9988	Mammals	0.9997	Mammals	0.9993
ZMC 1x	Mammals	Mammals	0.9999	Mammals	0.9999	Mammals	0.9999	Mammals	0.9999
ZMC CN.38x	Mammals	Mammals	1.0000	Mammals	0.9999	Mammals	1.0000	Mammals	0.9999
NHM SW 1943.9	Mammals	Mammals	0.9797	Mammals	0.9824	Mammals	0.9808	Mammals	0.9691
NMS 1956.36.57	Mammals	Mammals	0.9950	Mammals	0.9929	Mammals	0.9971	Mammals	0.9913
ZMC M1068	Herring	Herring	0.8930	Herring	0.8724	Herring	0.8463	Herring	0.8885
ZMC 3x	Herring	Herring	0.9993	Herring	0.9986	Herring	0.9988	Herring	0.9989
NHM ZD.1886.11.22.1	Herring	Herring	1.0000	Herring	1.0000	Herring	1.0000	Herring	1.0000
NMS 1990.86	Herring	Herring	0.8549	Herring	0.8235	Herring	0.8827	Herring	0.8538
NMS Z.2015.172.48	Herring	Herring	1.0000	Herring	0.9999	Herring	0.9999	Herring	0.9999
ZMC 24x	Mammals	Mammals	0.9497	Mammals	0.9332	Mammals	0.9537	Mammals	0.9266
ZMC M1647	Herring	Herring	0.9998	Herring	0.9997	Herring	0.9996	Herring	0.9997
NMS 1876.11	Herring	Herring	0.9917	Herring	0.9827	Herring	0.9761	Herring	0.9896

Replicate 4		Replicate 5		Replicate 6	
Assignment	Probability	Assignment	Probability	Assignment	Probability
Mammals	1.0000	Mammals	0.9999	Mammals	1.0000
Mammals	0.9999	Mammals	0.9997	Mammals	1.0000
Mammals	0.9999	Mammals	0.9998	Mammals	1.0000
Mammals	1.0000	Mammals	0.9998	Mammals	1.0000
Mammals	0.9997	Mammals	0.9841	Mammals	0.9958
Mammals	0.9995	Mammals	0.9608	Mammals	0.9984
Herring	0.9553	Herring	0.9441	Herring	1.0000
Mammals	**1.0000**	Herring	0.9994	Herring	1.0000
Herring	1.0000	Herring	1.0000	Herring	1.0000
Herring	0.9938	Herring	0.6989	Herring	0.9932
Herring	1.0000	Herring	1.0000	Herring	1.0000
Mammals	0.8624	Mammals	0.9806	Mammals	0.9988
Herring	0.9993	Herring	0.9998	Herring	1.0000
Herring	0.9997	Herring	0.9930	Herring	0.9994

Supplementary Table 3.2 *Results from Leave One Out cross validation test of the LDA model from Figure 3.8.b, for the middle teeth dataset. First column gives specimen number, second gives expected diet from both isotope data and the predictive LDA, and third and fourth column give the results for the original LDA. All subsequent pairs of columns give each replicate of the Leave One Out test. In each case a random sample was excluded (highlighted in grey) and the LDA run to test its robustness. Misclassified specimens are highlighted with bold text. In each case the Assignment gives the group to which the analysis has assigned each specimen, and the probability is the likelihood of that specimen belonging to the assigned group.*

Middle Teeth				Replicate 1		Replicate 2		Replicate 3	
Specimen	Expected Diet	Original LDA Assignment	Probability	Assignment	Probability	Assignment	Probability	Assignment	Probability
NMS.1956.36.56	Mammals	Mammals	1.0000	Mammals	0.8127	Mammals	0.7702	Mammals	0.8615
ZMC 12x	Mammals	Mammals	1.0000	Mammals	0.9845	Mammals	0.9560	Mammals	0.9911
ZMC 1x	Mammals	Mammals	1.0000	Mammals	0.9995	Mammals	0.9995	Mammals	0.9998
ZMC CN.38x	Mammals	Mammals	1.0000	Mammals	0.9991	Mammals	0.9992	Mammals	0.9995
NHM SW 1926.44	Mammals	Mammals	1.0000	Mammals	0.7269	Mammals	0.8736	Mammals	0.7554
NHM SW 1943.9	Mammals	Mammals	1.0000	Mammals	0.9983	Mammals	0.9990	Mammals	0.9984
NMS 1956.36.57	Mammals	Mammals	1.0000	Mammals	0.9790	Mammals	0.9786	Mammals	0.9792
ZMC M1068	Herring	Herring	1.0000	Herring	0.9957	Herring	0.9957	Herring	0.9960
ZMC 3x	Herring	Herring	1.0000	Herring	0.7412	Herring	0.6128	Herring	0.7548
NHM ZD.1886.11.22.1	Herring	Herring	1.0000	Herring	0.9847	Herring	0.9912	Herring	0.9783
NMS 1990.86	Herring	Herring	1.0000	Herring	0.9865	Herring	0.9945	Herring	0.9829
NMS Z.2015.172.48	Mammals	Mammals	1.0000	Mammals	0.9997	Mammals	0.9997	Mammals	0.9999
ZMC 24x	Herring	Herring	1.0000	Herring	0.9998	Herring	0.9999	Herring	0.9998
ZMC M1647	Herring	Herring	1.0000	Herring	0.9732	Herring	0.9800	Herring	0.9708
NHM SW 1943.11	Herring	Herring	1.0000	Herring	1.0000	Herring	1.0000	Herring	1.0000
NMS 1876.11	Mammals	Mammals	1.0000	Mammals	0.9999	Mammals	0.9999	Mammals	0.9999

Replicate 4		Replicate 5		Replicate 6	
Assignment	Probability	Assignment	Probability	Assignment	Probability
Mammals	0.8400	Mammals	0.8310	Mammals	0.8588
Mammals	0.9890	Mammals	0.9887	Mammals	0.9919
Mammals	0.9994	Mammals	0.9996	Mammals	0.9997
Mammals	0.9993	Mammals	0.9992	Mammals	0.9996
Mammals	0.6600	Mammals	0.7017	Mammals	0.7222
Mammals	0.9966	Mammals	0.9983	Mammals	0.9987
Mammals	0.9832	Mammals	0.9809	Mammals	0.9877
Herring	0.9959	Herring	0.9957	Herring	0.9966
Herring	0.7716	Herring	0.7542	Herring	0.7478
Herring	0.9812	Herring	0.9825	Herring	0.9851
Herring	0.9822	Herring	0.9834	Herring	0.9858
Mammals	0.9997	Mammals	0.9997	Mammals	0.9998
Herring	0.9998	Herring	0.9998	Herring	0.9999
Herring	0.9701	Herring	0.9707	Herring	0.9737
Herring	1.0000	Herring	1.0000	Herring	1.0000
Mammals	0.9999	Mammals	1.0000	Mammals	1.0000

Appendix 2: Supplementary Chapter - Investigating the Effect of Gold Coating Surfaces on Resulting 3D Roughness Parameters

Reasoning and Methods

Gold coating a surface improves data capture times and quality of data collected when using Focus Variation Microscopy, and is therefore very useful for all analyses collecting data using this technique. It is important to understand how gold coating a sample effects roughness parameters generated from 3D surfaces, as bias could be introduced into studies if parameter values are significantly affected. This methodology will be used throughout this PhD, and as such knowing whether it has biased resulting parameter values is of the utmost importance.

The hypothesis was tested that gold coating surfaces produces significant differences between roughness parameters generated before and after gold coats are applied.

For this test metal Scanning Electron Microscopy (SEM) stubbs were used. These stubbs are flat metal circles, normally used to mount specimens on before placing them within an SEM, however they present a good opportunity to test the effect of gold coating on a flat surface where surface texture can be produced manually. Four stubbs were used, and each represents a replication of the hypothesis test. Each stubb was manually worn using a sheet of p400 glass paper, by rubbing the stubb surface, face down, on the glass paper for 2 minutes in a consistent clockwise circular pattern. A pressurised air canister was used to remove any loose metal from the surfaces after wearing. This produced a relatively consistent texture on the surface of each stubb.

3D surface data was acquired from each stubb using focus variation microscopy (Alicona Infinite Focus Microscope, model IFM G4c, software version 2.1.2). Data capture followed the methods of Purnell et al (2013) (x100 objective, field of view of

145x110 µm, vertical resolution set to 0.02 µm, lateral optical resolution equivalent to 0.35 - 0.4 µm). Data was collected from ten random locations on the surface of each stubb.

All stubbs were then gold coated using an Emitech K500X sputter coater, for four minutes. And 3D surface data was acquired again in exactly the same way as described above (IFM, x100 objective, field of view of 145x110 µm, vertical resolution set to 0.02 µm, lateral optical resolution equivalent to 0.35 - 0.4 µm). Again data was collected from ten random locations on each stubb. For each of the four stubbs this meant there were ten data files collected from the surface before gold coating and ten collected after gold coating, 80 data files in total.

All resulting datafiles were levelled on the Alicona software (version 2.1.2), using all points levelling (fit to a least squares plane via rotation around all three axes, to remove any variation in the surface caused by manual horizontal positioning of the sample under the objective). Datafiles were then exported as .sur files into the program Surfstand (version 5.0.0). Errors in data collection (e.g. data spikes) were manually deleted and replaced with a mean surface value. Surface roughness parameters were quantified from each datafile using 24 ISO 25178 areal texture parameters (Table A), which require surfaces to be scale limited prior to parameter generation, to remove large wavelength information, producing a roughness surface (International Organisation for Standardization 2012). Surfaces were scale limited using a 2^{nd} order polynomial (0.025mm nesting index) and a spline filter. Parameters Str and Sal were excluded as they almost always produced identical values for each surface.

Resulting parameter values were tested for normality within each parameter by stubb and by original and gold coated surfaces (Shapiro Wilks W test), meaning eight tests were carried out for each parameter, two for each stubb, one containing original surface data and one containing gold coated surface data. Almost all data was found to be normally distributed and therefore parametric statistical tests were appropriate.

Parameter Family	Parameter Name	Definition	Units
Height	Sq	Root Mean Square Height of Surface	µm
	Ssk	Skewness of Height Distribution of Surface	n/a
	Sku	Kurtosis of Height Distribution of Surface	n/a
	Sp	Maximum Peak Height of Surface	µm
	Sv	Maximum Valley Depth of Surface	µm
	Sz	Maximum Height of the Surface (Sp – Sv)	µm
	Sa	Average Height of Surface	µm
Spatial	Str	Surface Texture Aspect Ratio (values range 0-1). Ratio from the distance with the fastest to the distance with the slowest decay of the ACF to the value. 0.2-0.3: surface has a strong directional structure. > 0.5: surface has rather uniform texture.	mm/mm
	Sal	Surface Auto-Correlation Length Horizontal distance of the auto correlation function (ACF) which has the fastest decay to the value 0.2. Large value: surface dominated by low frequencies. Small value: surface dominated by high frequencies.	mm
Hybrid	Ssc	Mean Summit Curvature for Peak Structures	1/µm
	Sds	Density of Summits. Number of summits per unit area making up the surface	$1/mm^2$
	Sdq	Root Mean Square Gradient of the Surface	Degrees
	Sdr	Developed Interfacial Area Ratio of the Surface	%
Volume	Vmp	Surface Peak Material Volume	$\mu m^3/mm^2$
	Vmc	Surface Core Material Volume	$\mu m^3/mm^2$
	Vvc	Surface Core Void Volume	$\mu m^3/mm^2$
	Vvv	Surface Dale Void Volume	$\mu m^3/mm^2$
Material Ratio	Spk	Mean height of the peaks above the core material	µm
	Sk	Core roughness depth, Height of the core material	µm
	Svk	Mean depth of the valleys below the core material	µm
	Smr1	Surface bearing area ratio (the proportion of the surface which consists of peaks above the core material)	%
	Smr2	Surface bearing area ratio (the proportion of the surface which would carry the load)	%
Feature	S5z	Ten Point Height of Surface	µm
Miscellaneous	Std	Texture Direction	Degrees

Table A *ISO 25178-2 parameters used, including brief descriptions. Parameter Sal was excluded from analyses, as it only produced normally distributed data in one of the three data treatments, even when using log_{10} values. For detailed parameter descriptions see Purnell et al (2013).*

T-tests were used to compare each stubb before and after gold coating. Tests of the hypothesis have not been carried out where non-normal distributions were found.

Although multiple comparisons were carried out, a sequential Bonferroni correction (Holm 1979) was not applied, because the use of this method is subjective in most cases (Cabin and Mitchell 2000), and the correction has been shown to produce more type II error (false negatives) than the type I error (false positives) it seeks to remove (Moran 2003, Nakagawa 2004). Choosing not to use a Bonferroni correction will bias our results towards incorrectly accepting the hypothesis of differences between surfaces before and after gold coating (i.e. the likelihood of type I errors will be increased). This has been taken into account when drawing conclusions (e.g. it might be expected expect, at $\alpha = 0.05$, one false positive for every 20 tests).

Results and Discussion

To test the hypothesis T-tests were carried out for each stubb between data from the original surface and data from the gold coated surface (Table B).

It is clear that very little differences is evident between surfaces before and after gold coating is applied. For one stubb no difference is found at all. For stubb 1 difference is only found between gold coated and uncoated surfaces for parameter Sku, for stubb 2 there are two parameters showing difference between original and gold coated surfaces (Ssc, and Sdr), and for stubb 3 there is one parameter showing differences between original and gold coated surfaces (Sds). A total of 81 tests were carried out across all four stubbs, therefore four significant results is below the number expected by random chance (false positives).

It is clear from these results that there is no difference between surfaces before and after gold coating, as such the hypothesis that gold coating surfaces produces significant differences between roughness parameters generated before and after gold

coats are applied must be rejected. This means that this technique is suitable to use in all analyses of 3D tooth surface textures.

t Test comparisons											
Stubb 1			Stubb 2			Stubb 3			Stubb 4		
Parameter	t-ratio	t	Parameter	t-ratio	t	Parameter	t-ratio	t	Parameter	t-ratio	t
Sq	0.8861	0.3873	Sq	-0.5583	0.5835	Sq	1.0559	0.305	Sq	-0.7156	0.4834
Ssk	-	-	Ssk	0.2560	0.8009	Ssk	1.9324	0.0692	Ssk	0.0719	0.9435
Sku	**-2.2916**	**0.0342**	Sku	0.4450	0.6617	Sku	0.3697	0.7159	Sku	0.9756	0.3422
Sp	-0.0990	0.9223	Sp (log)	0.7279	0.476	Sp	1.1308	0.273	Sp (log)	0.0363	0.9714
Sv	-	-	Sv	-1.0721	0.2979	Sv	-0.1005	0.921	Sv (log)	-1.1329	0.2721
Sz	-1.1426	0.2682	Sz	-	-	Sz	0.6881	0.5002	Sz	-	-
Sds	-0.8180	0.4241	Sds	1.5070	0.1492	Sds	**-3.5274**	**0.0024**	Sds	-1.9944	0.0615
Str	-0.3141	0.7571	Str	0.5448	0.5926	Str	0.5413	0.5949	Str	0.4494	0.6585
Sal (log)	0.1548	0.8787	Sal (log)	-1.3414	0.1965	Sal	1.7909	0.0901	Sal	-0.8024	0.4328
Sdq (log)	-1.3797	0.1846	Sdq	-1.5551	0.1373	Sdq (log)	-1.1710	0.2569	Sdq (log)	-1.3860	0.1827
Ssc	-	-	Ssc	**-6.2002**	**0.0001**	Ssc	-	-	Ssc	-	-
Sdr (log)	-1.2765	0.218	Sdr	**-2.2318**	**0.0386**	Sdr	-1.5685	0.1342	Sdr (log)	-1.6340	0.1196
Vmp	1.0817	0.2937	Vmp	-0.4697	0.6442	Vmp (log)	1.7154	0.1034	Vmp	-0.1456	0.8858
Vmc	1.4975	0.1516	Vmc	-0.4854	0.6332	Vmc (log)	0.8532	0.4047	Vmc	-0.9304	0.3645
Vvc	1.3307	0.1999	Vvc	-0.9091	0.3753	Vvc	1.6067	0.1255	Vvc	-0.9469	0.3562
Vvv	-0.6810	0.5046	Vvv	-0.2128	0.8339	Vvv	-0.1947	0.8478	Vvv	-0.1830	0.8568
Spk	0.7016	0.4919	Spk	-0.4720	0.6426	Spk (log)	1.6790	0.1104	Spk (log)	0.2529	0.8032
Sk	1.4116	0.1751	Sk	-0.7613	0.4563	Sk	-	-	Sk	-0.8363	0.4139
Svk	0.4975	0.6248	Svk	-0.5269	0.6047	Svk	-0.6306	0.5362	Svk	0.1687	0.8679
Smr1	-	-	Smr1 (log)	0.7861	0.442	Smr1	-0.3673	0.7177	Smr1	0.4076	0.6884
Smr2	1.5378	0.1415	Smr2	-0.1613	0.8737	Smr2	1.0266	0.3182	Smr2	-	-
S5z	-1.0451	0.3098	S5z	-	-	S5z	1.4875	0.1542	S5z (log)	-0.5901	0.5624
Sa	1.1022	0.2849	Sa	-0.5197	0.6096	Sa	1.0911	0.2896	Sa	-0.8913	0.3845

Table B *T-tests carried out between ten surfaces collected from an SEM stubb before and after gold coating for four minutes. This has been repeated four times, each time using a different stubb. Tests with a – represent parameters where non normal distributions were found in the data, and all significant results are highlighted bold.*

Appendix 3: List of Planned Publications

1. **Goodall**, **R**. **H**., **Fahlke**, **J**. **M**., **Bastl**, **K**. **A**., **Purnell**, **M**. **A**. *Investigating dietary behaviours in pinnipeds and odontocetes using 3D microtextural analysis of tooth wear and its further application to evolutionary hypotheses regarding stem cetaceans*.

Author Contributions: M.A.P and R.H.G conceived research programme. R.H.G, J.M.F and K.A.B collected tooth moulds. R.H.G generated and analysed data. R.H.G and M.A.P interpreted results. R.H.G wrote the main manuscript and prepared all figures and tables. All authors reviewed the manuscript.

2. **Goodall**, **R**. **H**., **Foote**, **A**., **Purnell**, **M**. **A**. *Dietary Variability between Two North Atlantic Killer Whale (Orcinus orca) Populations; Quantitative 3D Microtextural Analysis of Tooth Surfaces*.

Author Contributions: M.A.P conceived research programme. A.F generated isotope data. R.H.G collected tooth moulds, generated 3D microwear data, and analysed data. R.H.G and M.A.P interpreted results. R.H.G wrote the main manuscript and prepared all figures and tables. All authors reviewed the manuscript.

3. **Goodall**, **R**. **H**., **Purnell**, **M**. **A**. *Investigating how different methods used to scale limit 3D datafiles affect areal texture parameters and the separation of known dietary groups*.

Author Contributions: M.A.P conceived research programme. R.H.G collected tooth moulds, generated, and analysed data. R.H.G and M.A.P interpreted results. R.H.G wrote the main manuscript and prepared all figures and tables. All authors reviewed the manuscript.

4. **Goodall**, **R**. **H**., **Ungar**, **P**. **S**., **Leach**, **R**. **K**., **Merceron**, **G**., **Livengood**, **S**., **Syam**, **W**., **Feng**, **X**. *Testing the Effect of Different Instruments Used to Collect 3D Microtextural Data from Tooth Surface.*

Author Contributions: M.A.P conceived research programme. R.H.G and G.M collected tooth moulds. R.H.G generated, and analysed data. P.S.U and S.L assisted with data generation on one instrument. W.S and X.F generated data on one instrument with assistance and advice from R.K.L. R.H.G and M.A.P interpreted results. R.H.G wrote the main manuscript and prepared all figures and tables. All authors reviewed the manuscript.

Appendix 4: Chapter 1 - Publication

Goodall, **R**. **H**., **Darras**, **L**. **P**., **& Purnell**, **M**. **A**. (2015). Accuracy and precision of silicon based impression media for quantitative areal texture analysis. *Scientific reports*, *5*.

Author Contributions
M.A.P conceived and designed research programme. R.H.G and M.A.P wrote the main manuscript text. R.H.G and L.P.D generated data. M.A.P and R.H.G analysed and interpreted results. R.H.G and M.A.P prepared all figures and tables. All authors reviewed the manuscript.

Supplementary information accompanies this paper at http://www.nature.com/srep

This paper and all supplementary information is fully reproduced following this page.

SCIENTIFIC REPORTS

OPEN

Accuracy and Precision of Silicon Based Impression Media for Quantitative Areal Texture Analysis

Received: 08 October 2014
Accepted: 29 April 2015
Published: 20 May 2015

Robert H. Goodall, Laurent P. Darras & Mark A. Purnell

Areal surface texture analysis is becoming widespread across a diverse range of applications, from engineering to ecology. In many studies silicon based impression media are used to replicate surfaces, and the fidelity of replication defines the quality of data collected. However, while different investigators have used different impression media, the fidelity of surface replication has not been subjected to quantitative analysis based on areal texture data. Here we present the results of an analysis of the accuracy and precision with which different silicon based impression media of varying composition and viscosity replicate rough and smooth surfaces. Both accuracy and precision vary greatly between different media. High viscosity media tested show very low accuracy and precision, and most other compounds showed either the same pattern, or low accuracy and high precision, or low precision and high accuracy. Of the media tested, mid viscosity President Jet Regular Body and low viscosity President Jet Light Body (Coltène Whaledent) are the only compounds to show high levels of accuracy and precision on both surface types. Our results show that data acquired from different impression media are not comparable, supporting calls for greater standardisation of methods in areal texture analysis.

Analysis and quantification of natural and manufactured surfaces at micrometric and sub-micrometric scales is becoming widespread. Applications range from engineering[1] and superconductor technologies in particle accelerators[1–4], to archaeology[5–7], human skin surface topography[8,9], and biomimetics (e.g. antifouling properties of bivalve shells[10]). In particular, quantitative areal surface texture analysis is increasingly applied to analysis of tooth wear as a tool for dietary niche separation (e.g. refs 11-21).

In many cases, rather than direct analysis of a surface, replicas are used. Often this is for methodological reasons: some samples cannot be transported to the analytical facility, and some are too large to be accommodated by the measuring instruments; some types of surface are prone to movement during measurement (e.g. *in vivo* skin measurements); the properties of some surfaces (e.g. highly transparent or highly reflective) are unsuited for data collection using certain instruments. It is also possible for surface replication to be the solution to certain problems in dentistry caused by the inability of intra-oral dental scanners to collect data at high enough resolution[22]. When replicas are used, data is acquired either from the replica or from a cast made using the replica. Obviously, the quality of data acquired in this way is entirely dependent on the fidelity of surface replication, with significant implications for the accuracy and precision of resulting measurements. Furthermore, if impression media differ in fidelity, this will preclude comparisons between studies based on data acquired using different media.

Clearly, investigations into the precision and accuracy of impression media used are important, but only a few such studies have been conducted[5,9,10,23–32], and none have undertaken systematic, statistical comparisons of areal textural parameters acquired from sub-micrometre resolution replicas, produced using a range of impression media with different properties.

Four studies have undertaken qualitative evaluations of impression media used to replicate tooth surfaces for microwear analysis. Two of these[24,25] concluded from visual inspection of SEM images that low

University of Leicester, Department of Geology, Leicester, UK LE1 7RH. Correspondence and requests for materials should be addressed to M.A.P. (email: mark.purnell@le.ac.uk)

viscosity polyvinylsiloxane impression media produced the highest fidelity of replication. Another used similar methods to investigate the fidelity of three moulding compounds of varying viscosity from the President Jet product line (Coltène Whaledent)[30], concluding that both the low and mid viscosity compounds showed high levels of accuracy. A forth study, investigating accuracy in replicating skin surface textures[9], used a small number of different impression media, and included no information about the media used. However, none of these studies quantified the variation in resulting surfaces.

Of the remaining studies, very few have directly compared the fidelity with which multiple different compounds replicate the same surface. Most have focussed on a small number of compounds, either to examine the most basic questions of whether a surface can be replicated accurately in the first place[10,28,31], or to make recommendations for standard laboratory procedures[23]. Others examined replication at far too coarse a scale (e.g. refs [26,27]) to be of use in quantitative areal texture analysis. Analysis of the accuracy of different impression media at replicating sub-micrometre scale surface structure of cuts to bones and tooth surfaces created by tool use in early humans[5] did not investigate compounds of different viscosity, used only two different impression media, and compared only four parameters (angles within cut marks, derived from 2D profile data). Rodriquez *et al.*[32] collected 2D profile data to investigate the influence of colour and transparency in a number of impression materials on the accuracy of surface reproduction.

Nilsson and Ohlsson[29] investigated a range of impression media at the sub-micrometre scale using three dimensional surface texture data, comparing original surfaces to replicas. This study was limited to only three media types, and fidelity was tested only using percentage deviations in surface texture, with no statistical testing of the significance of the differences.

Here we present the results of a quantitative analysis, based on 3D areal texture analysis (see Methods), of the variation in accuracy and precision between seven different silicon based impression media of varying composition and viscosity, investigating their ability to replicate rough and smooth surfaces. For each medium, we present statistical tests of the null hypothesis that areal texture parameters obtained from replicas do not differ from those obtained from the original surface.

Accuracy refers to the degree to which replica surfaces made using different impression media differ from the original surface. We test this through analysis of the number of areal texture parameters that differ significantly when replica and original surfaces are compared. Precision refers to the magnitude of differences for textural parameter values between replicas and original surfaces, and between replicas made using different impression media. As part of this we also test the degree to which differences between original and replica surfaces are systematic rather than random (i.e. do particular impression media consistently increase or decrease parameter values). A moulding compound that produces surfaces with a large number of differences from the original, but all of small magnitude, is inaccurate but relatively precise. An ideal moulding compound would produce surfaces with few significant differences, all of which would be small in magnitude - it would be both accurate and precise. Importantly, we also assess the degree to which imprecision and inaccuracy in replication arising from different moulding compounds are likely to bias the results of analysis. If inaccuracies and imprecision are large in relation to the number and magnitude of differences arising because of variation between different types of original surface under investigation, then their impact on analysis is likely to be significant.

Results

Accuracy of Impression Media - ISO 24178-2. For each impression medium, the null hypothesis of no difference from the original surface was rejected for at least one parameter, but the number of parameters that differed ranged widely: between media, between rough (dentine) and smooth (enameloid) surfaces, and between modes of application (Fig. 1 (a)). To simplify discussion, we report here the average number of significant differences across all three scale limiting settings for each replicating medium, but Fig. 1 (a) shows all differences. For low and mid viscosity media, smooth surfaces exhibited a greater number of significant differences than rough. However the opposite is true for high viscosity media (Microset 101RF and MM240TV).

On the rough surface high viscosity Microset 101RF, and MM240TV produce the greatest number of significant differences, with an average of eight for Microset 101RF, and 10.66 for MM240TV. In MM240TV we also see the largest variation in significant differences between the two surfaces, with an average of 10.66 significant differences on the rough surface, but an average of only 2.33 on the smooth surface. Microset 101RF also displays the highest variability on the smooth surface between results recorded using each of the methods for scale limiting surfaces, varying between two significant differences when using a 2nd order of polynomial and a spline filter, and seven significant differences when using a 5th order of polynomial and a robust Gaussian filter.

The two low viscosity media, MM913 and Speedex, both show high numbers of significant differences across both surface types. They produce smaller numbers of significant differences than high viscosity media in almost all cases (except MM240TV on the smooth surface), but much higher numbers of significant differences than the remaining three low and mid viscosity compounds. The greatest number of significant differences across all impression media on the smooth surface is found in MM913, with an average of nine. The two remaining low viscosity impression media (President Jet Light Body, and Accutrans), along with the mid viscosity President Jet Regular Body, produce the smallest number of significant differences across both surface types with an average of 0.33 significant differences for each

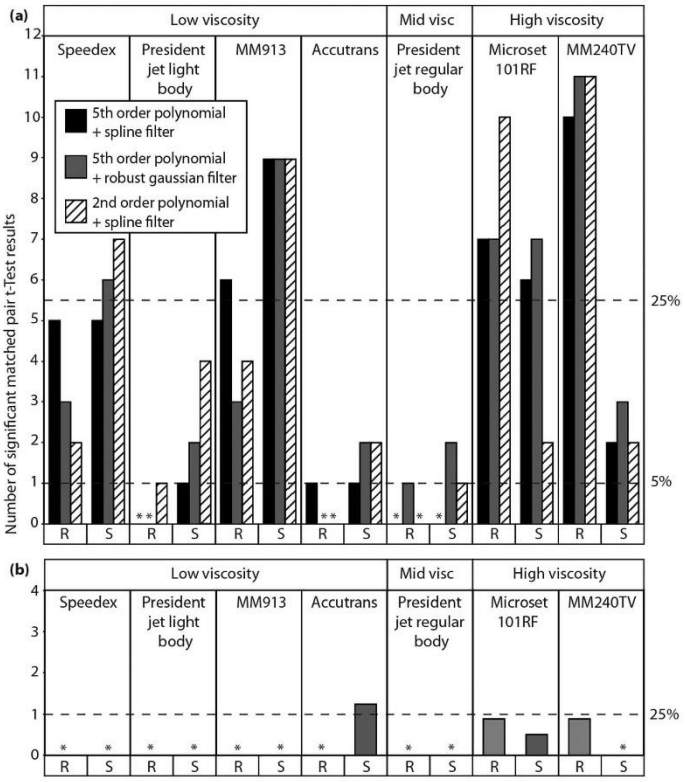

Figure 1. Numbers of significant differences (matched pair t-tests) between impression media and original tooth surfaces. With (**a**) data generated using ISO 25178-2 method and (**b**) data generated using SSFA method. Bars show the number of parameters that differ, (*) represents treatments where no significant results were recorded. For (**a**) data treatments (polynomial/spline/Gaussian filter) reflect different approaches to generation of scale-limited surfaces from which texture parameters are generated. R and S indicate whether data were generated from rough or smooth surfaces, respectively. The dashed line on the Y axis labelled 5% represents the expected number of false positive results per impression medium based on an average of 20.57 tests per impression medium, and $\alpha = 0.05$. The dashed lines on the Y axes labelled 25% serve to compare numbers of significant results produced using the two different roughness parameterisation methods (ISO & SSFA).

of the three compounds on the rough surface, and averages of one significant difference for President Jet Regular Body, 2.33 for President Jet Light Body, and 1.66 for Accutrans on the smooth surface.

Looking at the effect of operator and mode of application (Fig. 2), Speedex shows a great deal of variation in the number of significant differences recorded on both the rough and smooth surfaces, depending on the operator, with moulds produced by operator 1 exhibiting more differences. Comparing applicator gun and manual application, both modes of application of President Jet Light Body to rough surfaces produce few differences. For the smooth surfaces, use of the applicator gun produces a greater number of significant differences than manual application. The converse is true of President Jet regular Body, with manual application to smooth surfaces producing more than twice the number of significant differences compared to using the applicator gun across all scale limiting settings. Manual application to the rough surface also proved less accurate than using the applicator gun, however the difference was only a single significant result in one of the scale limiting settings (2nd order of polynomial with a spline filter).

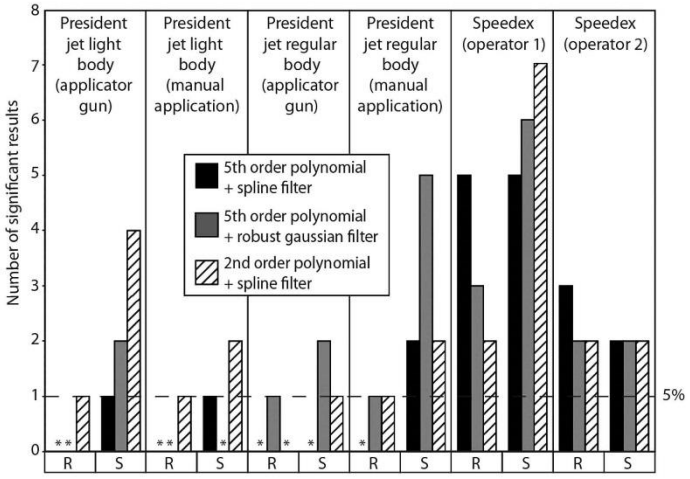

Figure 2. Numbers of significant differences (matched pair t-tests, ISO 25178-2 parameters) between two moulds of the same compound and the original tooth surface. Bars show the number of parameters that differ, (*) represents treatments where no significant results were recorded. Moulds were created using either different operators (Speedex) or application methods (President Jet Light and Regular Body); four quadrants per tooth, broken down by data treatment. R and S indicate whether data were generated from rough or smooth surfaces, respectively. The dashed line on the Y axis (labelled 5%) represents the expected number of false positive results per impression medium based on an average of 20.57 tests per impression medium, and $\alpha = 0.05$.

Accuracy of Impression Media - Scale Sensitive Fractal Analysis. Comparing impression media to the original surfaces using SSFA parameters yields fewer significant differences (matched pair t-tests) than comparisons using the ISO 25178 method (Fig. 1 (b)). This is partly because SSFA generates fewer parameters. HAsfc is recorded here as a fraction, due to this parameter being calculated across ten different subdivisions (splits) of the sample area.

On the rough surface significant differences were recorded only in the two high viscosity impression media (Microset 101RF & MM240TV), and only in the parameter HAsfc (Surface Heterogeneity; significant differences were recorded in eight of the ten "splits" used to calculate this parameter for each of these impression media).

On the smooth surface there were even fewer significant differences, but they were found in more than one media viscosity level. Again high viscosity Microset 101RF showed significant differences for the parameter HAsfc (in four of the ten "splits" used), however MM240TV recorded no significant differences in any parameter. Significant differences were also found when using low viscosity Accutrans, in the parameters HAsfc (2/10 "splits"), and Asfc (Surface Complexity).

However if we consider the percentage of significant differences, as opposed to the overall number, it may give us a better comparison between the SSFA and ISO 25178 results. In this situation one significant result using SSFA parameters is 25% of the total possible significant differences. If we apply this 25% threshold for significant differences to the ISO 25178 data (5.5 significant differences) we find that it is exceeded by Speedex on the smooth surface, MM913, and Microset 101RF on both surface types, and MM240TV on the rough surface. This is completely different to the pattern seen in the SSFA results, where this threshold is only exceeded by Accutrans on the enameloid surface (1.2 significant differences).

Using SSFA to compare different operators and application methods revealed no difference between application methods.

Variability in Precision and Accuracy of Impression Media - ISO 24178-2. We assess precision in terms of the range of deviations in texture parameter values for each impression medium from the original surface values. Rough and smooth surfaces are compared separately; for each parameter and each medium there are four values (one for each quadrant - see Methods), yielding a range of deviations from the original surface (Fig. 3). Because these figures are presented to show differences in accuracy and precision between impression media, plots for the rough and smooth surfaces are given at different

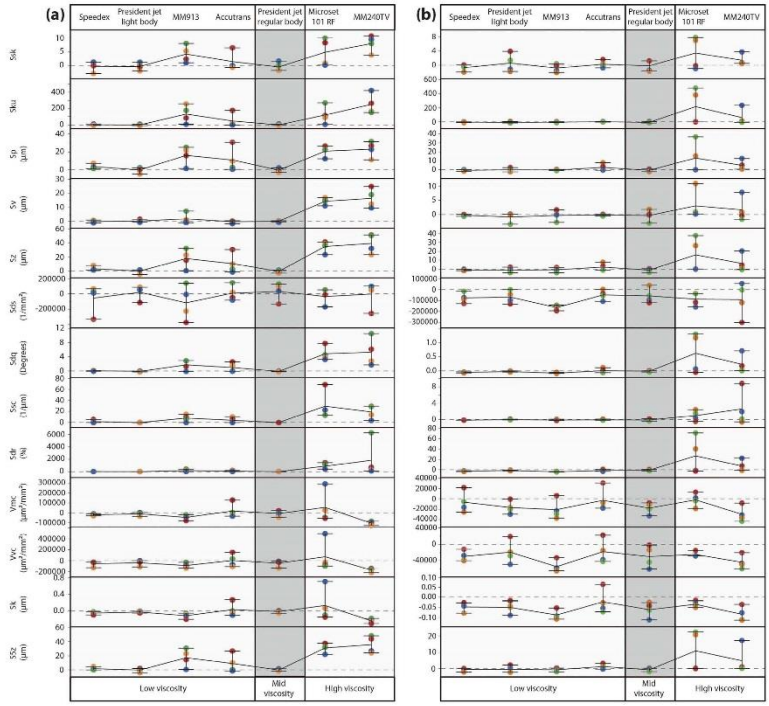

Figure 3. Absolute differences between original surface and each impression medium for the rough surface (a), and the smooth surface (b), generated using the ISO 25178-2 parameterisation method. Points show the actual differences from the original surface, with zero indicating the same value for replica and original surface. Each quadrant has been given a specific colour (NE = Blue, SE = Green, SW = Red, NW = Orange). Lines connecting points horizontally show mean difference. Whiskers represent the range of the data. For convenience, plot shows only data collected using a 5th order of polynomial and a robust Gaussian filter, and only parameters returning significant differences for at least one impression medium on the rough surface. Other data are included in Supplementary Fig. S1.

scales, and although patterns of variation can be compared, absolute values should be taken into account. For the assessment of precision we have only used the data files that have been scale limited using a 5th order of polynomial and a robust Gaussian filter (as in ref. 20). For clarity, only 13 of the 22 parameters are shown in Fig. 3, all of which represent parameters where at least one significant result was recorded across all impression media on the rough surface. Plots showing data for all remaining parameters are included as Supplementary Fig. S1.

On the rough surface (Fig. 3 (a)) high viscosity media (MM240TV and Microset 101RF) generally show the greatest range of differences from the original surface and thus the lowest precision. Low viscosity media are split into two levels of precision: Accutrans and MM913 show a similar lack of precision to that shown by high viscosity media; President Jet Light Body and Speedex both show very high levels of precision, with differences clustered much more closely. Finally President Jet Regular Body shows a similarly high level of precision to Speedex and President Jet Light Body, with very little to clearly differentiate the precision of the three compounds. The precision of each impression medium appears to mirror its accuracy on the rough surface, with compounds showing low accuracy also generally showing low precision and vice versa. However, there are two notable exceptions to this pattern, Speedex, which shows high precision, but low accuracy, and Accutrans, which shows high accuracy, but low precision. Microset 101RF shows a much higher level of precision than is typical for this medium in one or two parameters.

On the smooth surface (Fig. 3 (b)) the pattern of precision is slightly different. The two President Jet compounds and Speedex show a similar high level of precision to that seen on the rough surface. The

two high viscosity media (Microset 101RF and MM240TV) again show low levels of precision. However Accutrans and MM913 show much higher levels of precision on the smooth surface, similar to that seen in the two President Jet compounds and Speedex. In most cases, deviations from the original surface values on the smooth surface are smaller in scale than on the rough. However, this is not the case for height parameters, where differences on the smooth surface are similar, and sometimes larger, than those on the rough surface. There appears to be a homogenisation of the precision between the four low viscosity and the one mid viscosity impression media on the smooth surface, making it much harder to determine within these compounds which has the highest precision. For the volume parameters Vmc and Vvc, and the material ratio parameter Sk, all media show a similar level of precision.

On both the rough and smooth surfaces there is a degree of directionality in the error produced by the four least precise media (MM240TV, Microset 101RF, Accutrans and MM913). This is because, for certain parameters, the differences from the original surface are mostly either positive or negative. This implies there is a consistent bias (e.g. a constantly positive bias for parameter Sp would indicate elevated peak heights). However, any bias is not systematic as the order of each quadrant's difference from the original surface is never repeated (i.e. NW quadrant does not consistently have the largest error across all compounds and parameters) (Fig. 3). For the results of any parameter to be considered to have positive directionality of error at least three of these four media must show mostly positive differences from the original surface (more than 50% of quadrants in more than 50% of media), and vice versa for negative directionality of error. Both rough and smooth surfaces show an equal degree of directionality, with 12 parameters showing either positive or negative directionality of error on each surface type. There are ten parameters on each of the surface types, in which there is no obvious directionality in differences from the original surface.

There is a small number of parameters where the directionality of error is consistent across both surface types. On both the rough and smooth surface there is positive directionality in the Hybrid Parameter Sdr, the Material Ratio Parameter Svk and the Feature Parameter S5z. And there is consistent negatively directionality across both surface types for the Spatial Parameter Str, and the Volume Parameter Vvc.

However, most parameters only show directionality of error on one of the two surface types. Positive directionality is also seen on the rough surface in the Height Parameters Ssk, Sku, Sp, Sv, and Sz, and the Hybrid Parameters Sdq and Ssc, and on the smooth surface in the Volume Parameter Vvv. Negative directionality of error is also seen on the smooth surface in the Hybrid Parameter Sds, the Volumetric Parameters Vmp, and Vmc, and the Material Ratio Parameters Sk, Smr1, and Smr2.

Variability in Precision and Accuracy of Impression Media - Scale Sensitive Fractal Analysis. The precision of impression media when using SSFA parameters was assessed in the same way as with ISO parameters above (Fig. 4). On both surface types there appear to be different patterns of precision depending on the medium and parameter in question. In some media this pattern is similar across both surface types, however in others the two surface types show very different patterns of precision. This is markedly different to the ISO parameter data, where the patterns were similar across most parameters and across the two surface types. Therefore it appears that in this case differences between media are less systematic when using the SSFA parameterisation method than those detected using the ISO-based analysis.

On the rough surface (Fig. 4 (a)), Speedex, President Jet Light Body and President Jet Regular Body all show very high levels of precision for parameter Asfc (surface complexity), and HAsfc (heterogeneity), but much lower precision for epLsar (anisotropy) and Tfv (textural fill volume), giving them a similar level of precision to Accutrans for these two parameters. Accutrans is less precise than Speedex and President Jet media for other parameters, but in all but one case precision is better than the remaining three media (the exception is HAsfc, with Accutrans showing the lowest levels of precision of any media on the rough surface).

Low viscosity MM913, and the two high viscosity media (Microset 101RF and MM240TV), all generally show very low levels of accuracy on the rough surface. However MM913 shows much higher levels of precision for the parameter Asfc, similar to the precision seen in the President Jet media and Speedex.

On the smooth surface (Fig. 4 (b)) all impression media show low levels of precision for parameters Asfc, epLsar, Tfv, and HAsfc, without much to separate them. Except in the case of Accutrans, where higher levels of precision can be seen for the parameters Asfc and HAsfc than for the other media.

Although the pattern of precision for the rough surface is similar to that seen when using the ISO parameterisation method, the pattern on the smooth surface is different. On both surface types there is also very little directionality of error evident when using the SSFA parameterisation method.

Magnitude of Differences Between Surfaces: Replicas Compared to Different Diets. Comparisons of precision and accuracy provide a good test of the fidelity of each of the impression media, but they do not address the question of whether the magnitude of differences that result from using different media would produce erroneous results in a comparative statistical analysis. This kind of analysis is routinely used to investigate dietary differences between species or ecotypes of vertebrates based on differences in 3D microtexture of tooth surfaces. Here we compare the magnitude of the differences in parameter values between different media with the differences obtained from comparing surface

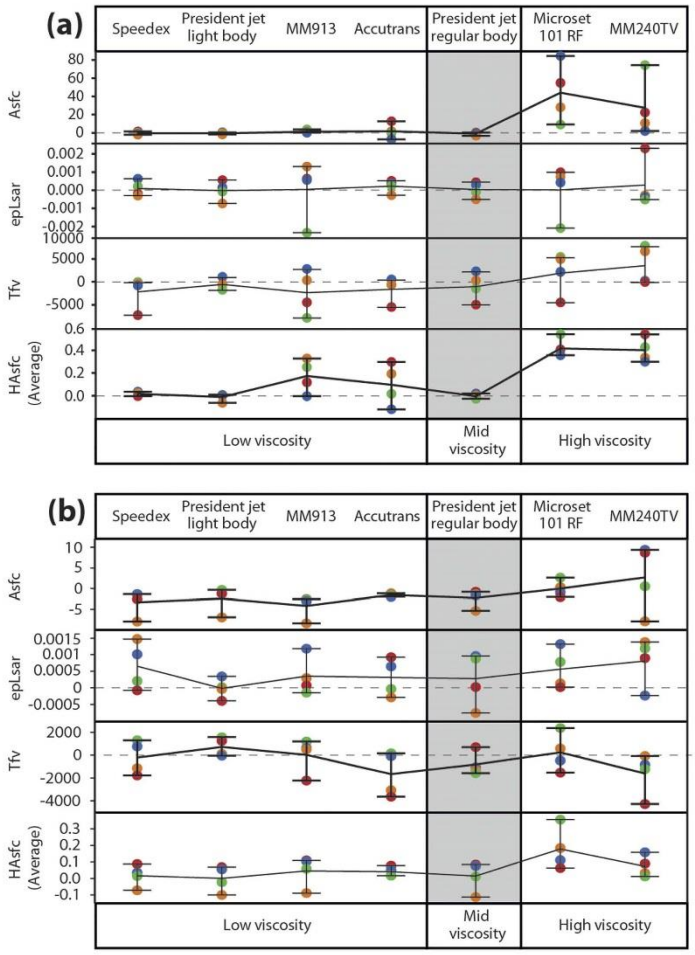

Figure 4. Absolute differences between original surface and each impression medium for the rough surface (a), and the smooth surface (b), generated using the SSFA parameterisation method. Points show the actual differences from the original surface, with zero indicating the same value for replica and original surface. Each quadrant has been given a specific colour (NE = Blue, SE = Green, SW = Red, NW = Orange). Lines connecting points horizontally show mean difference. Whiskers represent the range of the data.

textures of teeth from two wild populations of *Archosargus probatocephalus* (Sheepshead Seabream) which exhibit different tooth surface microtextures as a result of dietary differences (this is the same species as that from which our other surface data were acquired). Both populations were collected in Florida (USA) and although they can be considered as dietary generalists with considerable overlap in diet, one population, from Indian River lagoon, is more herbivorous, while the other, from Port Canaveral lagoon, consumes and crushes more hard-shelled prey, such as bivalves[33].

In the dietary analysis, seven ISO 25178-2 parameters (Sdq, Sdr, Vmc, Vvv, Sk, Smr1, and Sa) differed significantly between populations[33]. Figure 5 shows the results of comparing the magnitude of differences

	Specimen	Speedex	President jet light body	MM913	Accutrans	President jet regular body	Microset 101RF	MM240TV
Specimen	-	Smooth Sdr, Sk	Smooth no difference	Smooth Sdr, Vmc, Sk, Smr1, Sa	Smooth Smr1	Smooth no difference	Smooth Sdr	Smooth Sdr, Smr1
Speedex	Rough Sdr, Vmc, Sk	-	Smooth no difference	Smooth Smr1	Smooth Smr1	Smooth Sdr	Smooth Sdr	Smooth Sdr, Smr1
President jet light body	Rough no difference	Rough Sdr, Vvv	-	Smooth Sdr	Smooth Vvv, Smr1	Smooth no difference	Smooth Sdr, Smr1	Smooth Sdr, Smr1
MM913	Rough Sdr, Vmc, Sk, Smr1, Sa	Rough Sdr	Rough Sdr, Vmc, Sk, Sa	-	Smooth Sdr	Smooth Sdr, Smr1	Smooth Sdr	Smooth Sdr
Accutrans	Rough Sdr, Vvv	Rough Sdr, Vvv, Sa	Rough Sdr, Vvv	Rough Sdr, Vmc, Vvv, Sk, Smr1, Sa	-	Smooth no difference	Smooth Sdr	Smooth Sdr
President jet regular body	Rough no difference	Rough Sdr, Vvv	Rough no difference	Rough Sdr, Vvv, Sk, Sa	Rough Sdr, Vvv	-	Smooth Sdr	Smooth Sdr
Microset 101RF	Rough Sdr, Vvv, Sa	Rough Sdr, Vmc, Vvv, Skv, Sa	Rough Sdr, Vmc, Vvv, Sk, Sa	Rough Sdr, Vmc, Vvv, Sk, Sa	Rough Sdr, Vvv, Sk, Sa	Rough Sdr, Vmc, Vvv, Sa	-	Smooth Sdr
MM240TV	Rough Sdr, Vmc, Vvv, Sk, Smr1, Sa	Rough Sdr, Vmc, Vvv, Sk	Rough Sdr, Vmc, Sk	Rough Sdr, Vvv, Sk, Sa	Rough Sdr, Vmc, Sk, Smr1, Sa	Rough Sdr, Vmc, Sk, Sa	Rough Sdr, Vmc, Vvv, Sk, Smr1, Sa	-

Figure 5. Magnitude of differences in texture parameters between impression media compared to the magnitude of differences between dietary ecotypes of *Archosargus probatocephalus*. Only seven ISO 25178-2 parameters (Sdq, Sdr, Vmc, Vvv, Sk, Smr1, and Sa) were used, as these were the only ones to differ significantly between the two *Archosargus probatocephalus* dietary populations[33]. The boxes show those parameters where differences between replica surfaces and the original tooth surfaces exceed those reflecting dietary differences; all possible pairwise comparisons between impression media and the original tooth surfaces were assessed. Whether a parameter value exceeds the dietary difference is calculated by comparing the median value of differences between surfaces (e.g. between the original specimen and Speedex) with the difference between the median value of each the dietary ecotypes. Information towards the lower left shows results for the rough surface, information toward the upper right for the smooth surface. The parameter Sdq is not shown because it exceeds the value for the dietary difference in 27 of 28 comparisons on both surfaces and thus tells us nothing about the relative potential of different impression media to introduce bias into the results of dietary analysis. Highlighted cells represent comparisons where no difference equalled or exceeded that expected from two dietary populations (not including Sdq).

between each impression medium, and the original surface with the magnitude of differences between dietary groups for these seven parameters. The parameters listed in each box are those that exhibit a difference between impression media of greater magnitude than would be expected between the different dietary groups.

We find that only two impression media return no differences of greater magnitude than would be expected between dietary groups across both surface types: President Jet Regular Body and President Jet Light Body. All other comparisons between impression media and against the original surface return differences of greater magnitude than would be expected between two dietary populations for at least one parameter, but often more. The number of parameters showing greater magnitude than expected between dietary groups is much smaller on the smooth surface than on the rough surface.

When comparing the magnitude of inter-individual differences within each dietary population to the differences between impression media on the smooth surface we see an almost identical pattern (Supplementary Fig. S2) to that shown above.

Discussion

It is clear that different impression media differ significantly in their ability to accurately and precisely replicate surfaces. Accuracy and precision vary between smooth and rough surfaces, between compounds with different levels of viscosity, and between compounds of similar viscosity.

When using the ISO parameterisation method, high viscosity media (Microset101RF and MM240TV) show the lowest accuracy and precision when replicating a rough surface, at the scale used here, although there is some variation between different data treatments. Many more significant differences are found than low or medium viscosity media in almost all cases, and the magnitude and range of differences from the original surface is much higher than most other media. However MM240TV shows relatively high accuracy on the smooth surface. Comparing profiles across equivalent surfaces produced using different impression media suggests that the higher viscosity of these compounds limits their ability flow into, and thus replicate, the smallest scale features of the surface topology.

Impression Media	Application	Viscosity Level	Manufacturer	Colour
Speedex Light Body	Manual	Low	Coltène-Whaledent	Blue
President Jet Light Body	Applicator Gun	Low	Coltène-Whaledent	Green
MM913	Manual	Low	ACC Silicones	Transparent
Accutrans	Applicator Gun	Low	Coltène-Whaledent	Brown
President Jet Regular Body	Applicator Gun	Medium	Coltène-Whaledent	Blue
Microset 101RF	Applicator Gun	High	Microset Products Ltd	Black
MM240TV	Manual	High	ACC Silicones	Light Blue

Table 1. Details of all seven silicon based impression media used in this study. Speedex, President Jet Light and Regular Body, and Accutrans are polyvinylsiloxane compounds. MM913 and MM240TV are room temperature vulcanising (RTV) rubber compounds, and Microset 101RF is a heat accelerated RTV rubber compound.

Low viscosity media generally replicate a surface more accurately and precisely than high viscosity media, but this is an oversimplification. The number of significant differences and the range of differences from the original surface vary between low viscosity media and between data treatments and the data suggest that all low viscosity compounds are less accurate when replicating a smoother surface at the sub-micrometre scale. On the rough surface President Jet Light Body and Accutrans appear to be the most accurate low viscosity media, showing very few significant differences across all data treatments. However, although President Jet Light Body shows a high level of precision, especially on the rough surface, Accutrans shows much lower precision, similar to the high viscosity media. On the smooth surface both compounds show high levels of precision, with very little difference in precision between these two compounds. Speedex and MM913 appear to be much less accurate on both the rough and smooth surface and show a number of consistent significant differences, across data treatments. On the rough surface, MM913 shows a consistently low level of precision across all parameters, however Speedex is much more precise. On the smooth surface Speedex and MM913 showed a relatively high level of precision in most parameters. The accuracy of Speedex varied greatly depending on the operator applying the impression medium; both operators were experienced in the use of this compound, and it is unlikely that variation was caused by operator competence; our results therefore suggest there may be issues with using this compound, probably linked to the need to manually measure out and mix imprecise volumes of medium and activator before use. The same might be true of other manually mixed compounds.

President Jet Regular Body, the only mid viscosity impression medium studied, showed the lowest number of significant differences across both surface types and between all data treatments. For President Jet Regular body, given that our multiple comparisons would lead us to expect about one false positive result in every 20 tests, and the fact that there is very little consistency between different data treatments, we would suggest that for the significant differences found when comparing this compound to the original teeth we cannot reject the hypothesis that these are mostly type I errors resulting from multiple comparisons. Also, on the rough surface President Jet Regular Body is one of three compounds showing the highest level of precision, (and shows among the highest levels of precision for most parameters on the smooth surface). It is also one of only two compounds not to show any differences from the original surface of a magnitude greater than that seen between different dietary groups. Manual application of President Jet Regular Body produces higher numbers of significant differences on the smooth surface, possibly because the medium is too viscous to be applied consistently in this way.

When looking at the four media with lowest precision, the directionality of error can tell us something about how the replicated surface differs from the original. Focusing on the parameters that show consistent directionality of error across both surface types, MM913, Accutrans, Microset 101RF, and MM240TV generally over replicate the developed interfacial area ratio (Sdr), the mean depth of valleys below the core material (Svk), and the average value of the five highest and lowest peaks (S5z), and under replicate the surface texture aspect ratio (Str), and the surface core void volume (Vvc) of both smooth and rough surfaces. It is also clear that these compounds generally over replicate most height parameters on the rough surface, and under replicate both peak and valley material portions on the smooth surface. There is also under replication of core void volumes on the rough surface, and over replication of valley void volumes on the smooth surface.

Finally, it appears that there are marked differences between the two surface roughness parameterisation methods currently used in the study of vertebrate diet. The Scale Sensitive Fractal Analysis method produces far fewer significant differences than the ISO 25178-2 method, even when the large difference in numbers of parameters between the two methods is accounted for. The SSFA method also shows no clear pattern on the smooth surface when it comes to understanding the precision of different media. It is unclear whether the differences we see between these methods arise because SSFA is less sensitive, or

Parameter Family	Parameter Name	Definition	Units
Height	Sq	Root Mean Square Height of Surface	μm
	Ssk	Skewness of Height Distribution of Surface	n/a
	Sku	Kurtosis of Height Distribution of Surface	n/a
	Sp	Maximum Peak Height of Surface	μm
	Sv	Maximum Valley Depth of Surface	μm
	Sz	Maximum Height of the Surface (Sp – Sv)	μm
	Sa	Average Height of Surface	μm
Spatial	Str	Surface Texture Aspect Ratio (values range 0-1). Ratio from the distance with the fastest to the distance with the slowest decay of the ACF to the value. 0.2–0.3: surface has a strong directional structure. >0.5: surface has rather uniform texture.	mm/mm
	Sal	Surface Auto-Correlation Length Horizontal distance of the auto correlation function (ACF) which has the fastest decay to the value 0.2. Large value: surface dominated by low frequencies. Small value: surface dominated by high frequencies.	mm
Hybrid	Ssc	Mean Summit Curvature for Peak Structures	1/μm
	Sds	Density of Summits. Number of summits per unit area making up the surface	$1/mm^2$
	Sdq	Root Mean Square Gradient of the Surface	Degrees
	Sdr	Developed Interfacial Area Ratio of the Surface	%
Volume	Vmp	Surface Peak Material Volume	$\mu m^3/mm^2$
	Vmc	Surface Core Material Volume	$\mu m^3/mm^2$
	Vvc	Surface Core Void Volume	$\mu m^3/mm^2$
	Vvv	Surface Dale Void Volume	$\mu m^3/mm^2$
Material Ratio	Spk	Mean height of the peaks above the core material	μm
	Sk	Core roughness depth, Height of the core material	μm
	Svk	Mean depth of the valleys below the core material	μm
	Smr1	Surface bearing area ratio (the proportion of the surface which consists of peaks above the core material)	%
	Smr2	Surface bearing area ratio (the proportion of the surface which would carry the load)	%
Feature	S5z	Ten Point Height of Surface	μm
Miscellaneous	Std	Texture Direction	Degrees

Table 2. ISO 25178-2 parameters used, including brief descriptions. Parameter Sal was excluded from analyses, as it only produced normally distributed data in one of the three data treatments, even when using $\log_{10}$ values. For detailed parameter descriptions see refs. 17,20.

because the ISO method is exaggerating differences in the surfaces. Further work is needed to understand this.

Given their inaccuracy and imprecision, high viscosity compounds should not be used to replicate surfaces when quantifying 3D areal textures at sub-micrometre scales. Our results also suggest that there are problems with at least two of the low viscosity compounds tested - Speedex and MM913 - on both rough and smooth surfaces. MM913 is slightly less accurate than Speedex on both surfaces, and much less precise on the rough surface, and Speedex shows some potential for operator error to play a part in results. President Jet Light Body may have an issue when studying smooth surfaces, however the level of inaccuracy is very variable and, alongside the generally high precision seen for this compound, it should not be completely discounted. President Jet Light Body does however have a short cure time, which can cause problems when moulding large surfaces.

Low viscosity Accutrans and mid viscosity President Jet Regular Body show the highest accuracy, producing the lowest number of significant differences across both surface types. However Accutrans shows a low level of precision, especially on the rough surface. The only caveat to using President Jet Regular Body is that manual application will produce less accurate and less precise data, and our results support the use of an applicator gun. On smooth surfaces, President Jet Regular Body shows higher accuracy than Accutrans, and on rough surfaces its shows higher levels of precision.

President Jet Light and Regular Body are also the only two compounds that do not show differences when compared to original surfaces, or to each other, that are greater in magnitude than those found

between dietary groups. In the context of dietary analysis based on tooth microwear, we would therefore not recommend that surfaces obtained from impression media other than President Jet Light or Regular body are compared either with each other or with original surfaces. Such comparisons are likely to produce erroneous differences reflecting replication, not ecology.

For most impression media, our results lead to rejection of our null hypothesis that areal texture parameters obtained from replicas do not differ from those obtained from the original surface. Impression media vary in their ability to accurately and precisely reproduce a given surface, with most producing statistically significant differences, and high deviations from true values for areal texture parameters derived from original surfaces, even when false positive results are taken into account. Of the media tested here, President Jet Regular Body produced the most accurate and precise surface replicas.

Methods

Materials. The lower right jaw (dentary) of an adult specimen of *Archosargus probatocephalus* (Perciformes: Sparidae) was dissected and mounted on a temporary base to facilitate manipulation. Two worn teeth with obvious variation in surface texture were selected from among the molariform teeth of the jaw: one exhibiting little wear, with a relatively smooth, enameloid surface; the other, more worn, with a relatively rough surface of exposed dentine (the enameloid having been worn away). A needle was used to scratch two intersecting perpendicular lines across the centre of each tooth surface, dividing it into quadrants. Within each quadrant a relocatable $100 \times 145\,\mu m$ area was identified, based on recognisable surface features, so that data could be collected from the same location on the replicated surfaces (Supplementary Fig. S3; areas designated NE, SE, SW, NW). Before the moulds used in this study were collected, tooth surfaces were cleaned by applying a random light body impression medium to the surfaces, which was then discarded.

Seven impression media were selected, representing different viscosity levels (Table 1). Four are polyvinylsiloxane compounds, two room temperature vulcanising (RTV) rubber compounds, and one heat accelerated RTV compound. Moulds were taken using each of the different media in a random order. Some media allow use of an applicator gun, which standardizes the mixing of two-components by extruding them through a helical nozzle; others required the body and activator components to be mixed and applied manually.

For each medium we tested accuracy and precision of replication, and for three media we also tested the effect of how they were applied (manual versus applicator gun, and application by different operators). The latter test was based on moulds taken using three different impression media, representing the compounds currently used in dietary microwear analysis: two moulds of manually mixed Speedex, each made by a different operator, to test for effects of variability between operators; two moulds of President Jet Light Body, one applied to the surface using the applicator gun, the other applied manually; two moulds of President Jet Regular Body, one applied to the surface using the applicator gun, the other applied manually. Manual versus applicator comparison was not possible with Speedex, because an applicator version is not available.

Epoxy casts were produced from each mould using EpoTek 320LV. In many studies, particularly of tooth microwear, transparent/translucent epoxy casting material is used, but in order to optimise data acquisition (using focus variation microscopy; see below) we used the black pigmented EpoTek 320LV, which in other respects has similar properties to the commonly used transparent EpoTek 301. After all moulds were taken, data were acquired from the original tooth surfaces (gold coated, using an Emitech K500X sputter coater, for three minutes to optimise data acquisition). Throughout the text, each cast is referred to by the name of the impression media from which it was created.

Data Acquisition. 3D surface texture data were collected using focus variation microscopy (Alicona Infinite Focus Microscope, model IFM G4c, software version: 2.1.2). Data capture followed the methods of previous studies[13,20,21] (x100 objective, field of view of $145 \times 110\,\mu m$, vertical resolution set to $0.02\,\mu m$, lateral optical resolution equivalent to $0.35–0.4\,\mu m$). Data were captured from exactly the same fields of view across all replicas, and from the original tooth surfaces, so that for each quadrant (NE, SE, SW, and NW), there is an identical sample area for the original surface and each replica (see Supplementary Fig. S3 for examples of 3D surface data).

The resulting data files were investigated using two different approaches to surface texture analysis: one based on ISO 25178-2[1,34], the other using Scale Sensitive Fractal Analysis. In the first, data files were levelled using all points levelling (fit to a least squares plane via rotation around all three axes) to remove any variation in the 3D surface arising from manual horizontal positioning of the sample. Files were then transferred to SurfStand software (Version: 5.0.0) for further processing. Errors in data collection (e.g. data spikes) were manually deleted and replaced with a mean surface value point. Surface roughness was quantified using ISO 25178-2 texture parameters (Table 2) which requires generation of scale-limited surfaces[34] (for detailed parameter descriptions see refs [17,20]). Scale limited surfaces were generated through application of a robust polynomial (which finds and removes the Least Squares polynomial surface for the levelled data) combined with either a spline or a robust Gaussian wavelength filter (to remove long wavelength features of the tooth surface; gross tooth form). Three different settings were used, producing three complete datasets of eight samples: a 2nd order polynomial with a spline filter, a

Parameter Name	Acronym	Description
Area Scale Fractal Complexity	Asfc	A measure of the complexity of a surface. Area-scale fractal complexity is a measure of change in roughness with scale. The faster a measured surface area increases with resolution, the more complex the surface.
Exact Proportion Length Scale Anisotropy of Relief	epLsar	A measure of the anisotropy of a surface. Anisotropy is characterized as variation in lengths of transect lines measured at a given scale (we use 3.5 μm) with orientations sampled at 5° intervals across a surface. An anisotropic surface will have shorter transects in the direction of the surface pattern than perpendicular to it (e.g. a transect that cross-cuts parallel scratches must trace the peaks and valleys of each individual feature)
Scale of Maximum Complexity	Smc	The parameter represents the full scale range over which Asfc is calculated. High Smc values should correspond to more complex coarse features
Textural Fill Volume	Tfv	The total volume filled (Tfv) is a function of two components: 1) the shape of the surface, and 2) the texture of the surface. A more concave or convex surface will have a larger total fill volume than a planar surface even if both surfaces have an identical texture
Heterogeneity of Area Scale Fractal Complexity	HAsfc	Variation of Asfc across a surface (across multiple, equal subdivisions of a surface). High HAsfc values are observed for surfaces that vary in complexity across a facet

Table 3. Scale Sensitive Fractal Analysis (SSFA) parameters used, including brief descriptions (after refs. 16,17). Smc was excluded from statistical analyses as it was rarely normally distributed and almost always returned the same value for each surface. For parameter details and information on methods of calculation see ref. 17.

5th order polynomial with a spline filter, and a 5th order polynomial with a robust Gaussian filter, all with the wavelength cut-off for the filter set to 0.025 mm. This allowed us to account for differences in the process of generating scale-limited surfaces causing variation in assessments of accuracy and precision. Two of the three settings also correspond to previous work carried out on dietary analysis based on ISO texture parameters[20,33].

Scale Sensitive Fractal Analysis (SSFA)[16,17] was carried out using the programs ToothFrax and SFrax (Surfract, www.surfract.com). SSFA does not require surfaces to be scale limited, and quantifies five aspects of surface roughness (Table 3). Settings for all parameters followed those used in previous work[17], including the use of scale-sensitive "auto splits" to record Surface Heterogeneity (HAsfc), separating individual scanned sections into increasingly reduced sub-regions (we calculated HAsfc across ten different subdivisions). As a small deviation from the published method we used a single data file location for each sampled surface, rather than four adjoining locations normally used. This was necessary in order for us to directly compare the same locations from which ISO parameter data were calculated. Also, rather than a setting of 1.8 μm[17], we used a 3.5 μm scale of observation to calculate the parameter epLsar[35] (this value being based on the lateral resolution of the microscope being used).

Statistical Analysis. Statistical hypothesis testing was carried out using JMP (Version 10.0.0). Data acquired from rough and smooth surfaces were analysed separately. Data sets were tested for normality (Shapiro Wilks W test; by parameter and impression medium); the majority of data were normally distributed so parametric statistical tests were appropriate. Log_{10} data were used for parameters where this produced a greater number of normally distributed media. For each parameter either original data or log_{10} data were used across all media, never a combination of the two. The ISO 25178-2 parameter Sal (Auto-Correlation Length), and the SSFA parameter Smc (Scale of Maximum Complexity) were found rarely to be normally distributed in any impression medium and were excluded from further analysis.

Because data were collected from exactly the same eight locations on the two teeth and each set of replicas, our replica datasets can be considered as 'treatments' of the original surfaces. Consequently we tested for differences using matched pair t-tests, so that rather than treating the data from a replica as a general sample population, the same quadrants are compared (e.g. comparing the Microset replica with the original surface, Microset data for the NE quadrant are compared with original data for the NE quadrant, Microset SE compared with original SE etc.)

Although we conducted multiple comparisons, a sequential Bonferroni correction[36] was not applied, because knowing when to use this method is difficult and in most cases subjective[37]; when used on test numbers as large as ours, the correction has been shown to produce more type II error (false negatives) than the type I error (false positives) it removes[38,39]. Choosing not to use a Bonferroni correction will bias our results towards incorrectly rejecting the null hypothesis of no difference between moulding compounds (i.e. it will increase the likelihood of type I errors), and this is taken into account when drawing our conclusions (e.g. given that an average of 20.57 tests were performed for each impression medium using the ISO 25178-2 data, we might expect, at $\alpha = 0.05$, one false positive for each medium).

References

1. Jiang, X., Scott, P. J., Whitehouse, D. J. & Blunt, L. Paradigm shifts in surface metrology. Part II. The current shift. *Proc. Roy. Soc A* **463**, 2071–2099, DOI:10.1098/rspa.2007.1873 (2007).

2. Leach, R. Characterisation of Areal Surface Texture. (Springer, 2013).
3. Ge, M. *et al.* Routine characterization of 3D profiles of SRF cavity defects using replica techniques. *Supercond. Sci. Technol.* **24,** 035002, DOI:10.1088/0953-2048/24/3/035002 (2011).
4. Xu, C., Reece, C. & Kelley, M. Characterization of Nb SRF cavity materials by white light interferometry and replica techniques. *Appl. Surf. Sci.* **274,** 15–21, DOI:10.1016/j.apsusc.2013.02.006 (2013).
5. Bello, S. M., Verveniotou, E., Cornish, L. & Parfitt, S. A. 3-dimensional microscope analysis of bone and tooth surface modifications: comparisons of fossil specimens and replicas. *Scanning* **33,** 316–324, DOI:10.1002/sca.20248 (2011).
6. Bello, S. M., Parfitt, S. A. & Stringer, C. Quantitative micromorphological analyses of cut marks produced by ancient and modern handaxes. *J. Archaeol. Sci.* **36,** 1869–1880, DOI:10.1016/j.jas.2009.04.014 (2009).
7. Evans, A. A., Lerner, H., Macdonald, D. A., Stemp, W. J. & Anderson, P. C. Standardization, calibration and innovation: a special issue on lithic microwear method. *J. Archaeol. Sci.*, DOI:10.1016/j.jas.2014.03.002 (2014).
8. Nardin, P., Nita, D. & Mignot, J. Automation of a series of cutaneous topography measurements from silicon rubber replicas. *Skin. Res. Technol.* **8,** 112–117, DOI:10.1034/j.1600-0846.2002.00309.x (2002).
9. Rosén, B. G., Blunt, L. & Thomas, T. R. On *in vivo* skin topography metrology and replication techniques. *J. Phys.: Conf. Ser.* **13,** 325–329, DOI:10.1088/1742-6596/13/1/076 (2005).
10. Bai, X. Q. *et al.* Study on biomimetic preparation of shell surface microstructure for ship antifouling. *Wear* **306,** 285–295, DOI:10.1016/j.wear.2012.11.020 (2013).
11. Ungar, P. S., Grine, F. E. & Teaford, M. F. Dental microwear and diet of the Plio-Pleistocene hominin *Paranthropus boisei*. *PloS One* **3,** e2044, DOI:10.1371/journal.pone.0002044 (2008).
12. Calandra, I., Schulz, E., Pinnow, M., Krohn, S. & Kaiser, T. M. Teasing apart the contributions of hard dietary items on 3D dental microtextures in primates. *J. Hum. Evol.* **63,** 85–98, DOI:10.1016/j.jhevol.2012.05.001 (2012).
13. Purnell, M., Seehausen, O. & Galis, F. Quantitative three-dimensional microtextural analyses of tooth wear as a tool for dietary discrimination in fishes. *J. R. Soc., Interface* **9,** 2225–2233, DOI:10.1098/rsif.2012.0140 (2012).
14. Scott, R. S. *et al.* Dental microwear texture analysis shows within-species diet variability in fossil hominins. *Nature* **436,** 693–695, DOI:10.1038/nature03822 (2005).
15. Schulz, E. *et al.* Dietary abrasiveness is associated with variability of microwear and dental surface texture in rabbits. *PloS One* **8,** e56167, DOI:10.1371/journal.pone.0056167 (2013).
16. Ungar, P. S., Brown, C. A., Bergstrom, T. S. & Walker, A. Quantification of dental microwear by tandem scanning confocal microscopy and scale-sensitive fractal analysis. *Scanning* **25,** 185–193, DOI:10.1002/sca.4950250405 (2003).
17. Scott, R. S. *et al.* Dental microwear texture analysis: technical considerations. *J. Hum. Evol.* **51,** 339–349, DOI:10.1016/j.jhevol.2006.04.006 (2006).
18. Ungar, P. S., Scott, R. S., Grine, F. E. & Teaford, M. F. Molar microwear textures and the diets of *Australopithecus anamensis* and *Australopithecus afarensis*. *Philos. Trans. R. Soc., B* **365,** 3345–3354, DOI:10.1098/rstb.2010.0033 (2010).
19. Merceron, G., Escarguel, G., Angibault, J. & Verheyden-Tixier, H. Can dental microwear textures record inter-individual dietary variations? *PloS One* **5,** DOI:10.1371/journal.pone.0009542.g001 (2010).
20. Purnell, M. A., Crumpton, N., Gill, P. G., Jones, G. & Rayfield, E. J. Within-guild dietary discrimination from 3-D textural analysis of tooth microwear in insectivorous mammals. *J. Zool.* **291,** 249–257, DOI:10.1111/jzo.12068 (2013).
21. Gill, P. G. *et al.* Dietary specializations and diversity in feeding ecology of the earliest stem mammals. *Nature* **512,** 303–305, DOI:10.1038/nature13622 (2014).
22. Austin, R. S., Mullen, F. & Bartlett, D. W. Surface texture measurement for dental wear applications. *Surf. Topogr.: Metrol. Prop.* **3,** 023002, DOI:10.1088/2051-672x/3/2/023002 (2015).
23. Fiorenza, L., Benazzi, S. & Kullmer, O. Morphology, wear and 3D digital surface models: materials and techniques to create high-resolution replicas of teeth. *J. Anthropol. Sci.* **87,** 211–218 (2009).
24. Galbany, J. *et al.* Comparative analysis of dental enamel polyvinylsiloxane impression and polyurethane casting methods for SEM research. *Microsc. Res. Tech.* **69,** 246–252, DOI:10.1002/jemt.20296 (2006).
25. Williams, V. S., Purnell, M. & Gabbott, S. Dental microwear in dinosaurs: a comparative analysis of polysiloxane replication. *Dent. Pract.* **44,** 22–23 (2006).
26. Chee, W. W. L. & Donovan, T. E. Polyvinyl siloxane impression materials: a review of properties and techniques. *J. Prosthet. Dent.* **68,** 728–732, DOI:10.1016/0022-3913(92)90192-D (1992).
27. DeLong, R., Pintado, M. R., Ko, C.-C., Hodges, J. S. & Douglas, W. H. Factors influencing optical 3D scanning of vinyl polysiloxane impression materials. *J. Prosthodontics* **10,** 78–85, DOI:10.1053/jpro.2001.24718 (2001).
28. Chung, S., Im, Y., Kim, H., Jeong, H. & Dornfeld, D. A. Evaluation of micro-replication technology using silicone rubber molds and its applications. *Int. J. Mach. Tools. Manuf.* **43,** 1337–1345, DOI:10.1016/s0890-6955(03)00164-0 (2003).
29. Nilsson, L. & Ohlsson, R. Accuracy of replica materials when measuring engineering surfaces. *Int. J. Mach. Tools. Manuf.* **41,** 2139–2145, DOI:10.1016/S0890-6955(01)00080-3 (2001).
30. Galbany, J., Martínez, L. M. & Perez-Perez, A. Tooth replication techniques, SEM imaging and microwear analysis in primates: methodological obstacles. *Anthropologie* **42,** 5–12 (2004).
31. Xia, Y. *et al.* Complex optical surfaces formed by replica molding against elastomeric masters. *Science* **273,** 347–349, DOI:10.1126/science.273.5273.347 (1996).
32. Rodriguez, J. M., Curtis, R. V. & Bartlett, D. W. Surface roughness of impression materials and dental stones scanned by non-contacting laser profilometry. *Dent. Mater.* **25,** 500–505, DOI:10.1016/j.dental.2008.10.003 (2009).
33. Darras, L. P. G. The evolution and macroecological consequences of grazing and shell crushing in fishes PhD thesis, University of Leicester, (2012).
34. International Organization for Standardization. Geometrical product specifications (GPS) - Surface texture: Areal - Part 2: Terms, definitions and surface texture parameters (ISO 25178-2). 1–42 (2012).
35. Merceron, G., Hofman-Kamińska, E. & Kowalczyk, R. 3D dental microwear texture analysis of feeding habits of sympatric ruminants in the Białowieża Primeval Forest, Poland. *For. Ecol. Manage.* **328,** 262–269, DOI:10.1016/j.foreco.2014.05.041 (2014).
36. Holm, S. A simple sequentially rejective multiple test procedure. *Scand. J. Statist.* **6,** 65–70 (1979).
37. Cabin, R. J. & Mitchell, R. J. To Bonferroni or not to Bonferroni: When and how are the questions. *Bull. Ecol. Soc. Am.* **81,** 246–248 (2000).
38. Moran, M. D. Arguments for rejecting the sequential Bonferroni in ecological studies. *Oikos* **100,** 403–405, DOI:10.1034/j.1600-0706.2003.12010.x (2003).
39. Nakagawa, S. A farewell to Bonferroni: the problems of low statistical power and publication bias. *Behav. Ecol.* **15,** 1044–1045, DOI:10.1093/beheco/arh107 (2004).

Acknowledgements

We thank John Larkham at Coltène Whaledent Ltd., ACC Silicones Ltd. and Microset Products Ltd. for supplying impression media. Funded by NERC grants NE/G018189/1 and NE/J017728/1 (to M.A.P).

Author Contributions

M.A.P conceived and designed research programme. R.H.G and M.A.P wrote the main manuscript text. R.H.G and L.P.D generated data. M.A.P and R.H.G analysed and interpreted results. R.H.G and M.A.P prepared all figures and tables. All authors reviewed the manuscript.

Additional Information

Supplementary information accompanies this paper at http://www.nature.com/srep

Competing financial interests: The authors declare no competing financial interests.

How to cite this article: Goodall, R. H. *et al.* Accuracy and Precision of Silicon Based Impression Media for Quantitative Areal Texture Analysis. *Sci. Rep.* **5**, 10800; doi: 10.1038/srep10800 (2015).

ACCURACY AND PRECISION OF SILICON BASED IMPRESSION MEDIA FOR QUANTITATIVE AREAL SURFACE TEXTURE ANALYSIS

Goodall, Robert. H.[1], Darras, Laurent. P.[1], *Purnell, Mark. A.[1]
[1]University of Leicester, Department of Geology, Leicester, UK LE1 7RH
* Correspondence to mark.purnell@le.ac.uk

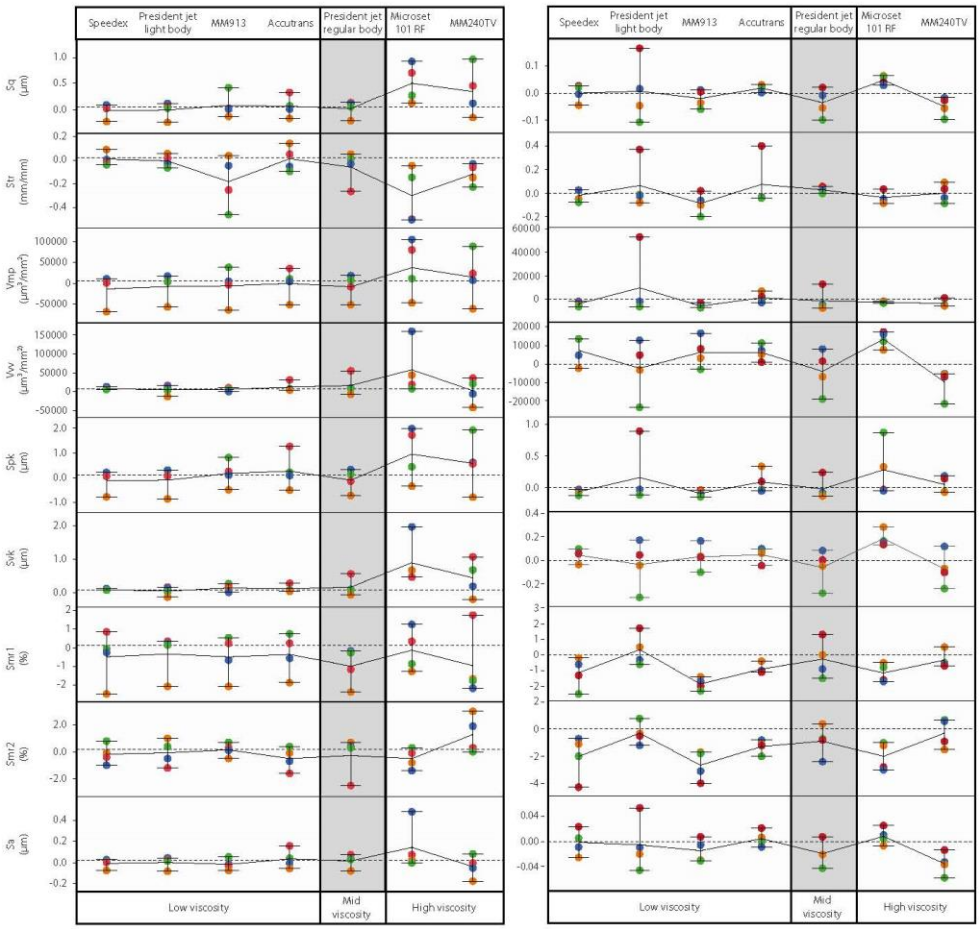

Supplementary Figure S1. Absolute differences between original surface and each impression medium for the rough surface (a), and the smooth surface (b), generated using the ISO 25178-2 parameterisation method. Points show the actual differences from the original surface, with zero indicating the same value for replica and original surface. Each quadrant has been given a specific colour (NE=Blue, SE=Green, SW=Red, NW=Orange). Lines connecting points horizontally show mean difference. Whiskers represent the range of the data. For convenience, plot shows only data collected using a 5th order of polynomial and a robust Gaussian filter, and only parameters not returning significant differences for at least one impression medium on the rough surface.

	Specimen	Speedex	President Jet light body	MM913	Accutrans	President Jet regular body	Microset 101RF	MM240TV
Specimen	-	PC population Sdr, Sk, Sa	PC population no difference	PC population Sdr, Vmc, Sk, Smr1, Sa	PC population Vvv, Smr1	PC population no difference	PC population Sdr	PC population Sdr, Sk, Smr1, Sa
Speedex	IR population Sdr	-	PC population Sdr	PC population Smr1	PC population Vvv, Smr1	PC population Sdr	PC population Sdr	PC population Sdr
President Jet light body	IR population no difference	IR population no difference	-	PC population Sdr, Smr1	PC population Vvv, Smr1	PC population no difference	PC population Sdr, Smr1	PC population Sdr, Smr1
MM913	IR population Sdr, Smr1	IR population Smr1	IR population Sdr, Smr1	-	PC population Sdr, Vvv, Sk, Sa	PC population Sdr, Smr1	PC population Sdr, Sa	PC population Sdr
Accutrans	IR population Smr1	IR population Smr1	IR population Smr1	IR population Sdr	-	PC population no difference	PC population Sdr	PC population Sdr
President Jet regular body	IR population no difference	IR population no difference	IR population no difference	IR population Sdr, Smr1	IR population no difference	-	PC population Sdr	PC population Sdr
Microset 101RF	IR population Sdr	IR population Sdr	IR population Sdr, Smr1	IR population Sdr	IR population Sdr	IR population Sdr	-	PC population Sdr
MM240TV	IR population Sdr, Smr1	IR population Sdr	IR population Sdr, Smr1	IR population Sdr	IR population Sdr	IR population Sdr	IR population Sdr	-

Supplementary Figure S2. Magnitude of differences in texture parameters between impression media compared to the magnitude of differences between individuals in two populations (dietary ecotypes) of Archosargus probatocephalus (compared to smooth tooth surface). The boxes show those parameters where differences between replica surfaces and the original tooth surfaces exceed those between individuals in a population; all possible pairwise comparisons between impression media and the original tooth surfaces were assessed. Both fish populations are from Florida, USA: the Indian River lagoon population is more herbivorous, while the Port Canaveral lagoon population consumes and crushes more hard-shelled prey, such as bivalves. Only seven ISO 25178-2 parameters (Sdq, Sdr, Vmc, Vvv, Sk, Smr1, and Sa) were compared, as these were the only ones to differ significantly between the two A. probatocephalus populations 31. Whether a parameter value exceeds the dietary difference is calculated by comparing the median value of differences between surfaces (e.g. between the original specimen and Speedex) with the median value of differences between individuals in each population. Information towards the lower left shows results for the comparisons with the Indian River population, information toward the upper right for the Port Canaveral population. The parameter Sdq is not shown because it exceeds the value for the dietary difference in almost all comparisons and thus tells us nothing about the relative potential of different impression media to introduce bias. Highlighted cells represent comparisons where no difference equalled or exceeded that expected from within a wild population (not including Sdq).

Rough Tooth	Summary of Results	
Impression Medium	Accuracy	Precision
Speedex	x	✓
President Jet Light Body	✓	✓
MM913	x	x
Accutrans	✓	x
President Jet Regular Body	✓	✓
Microset 101RF	x	x
MM240TV	x	x

Smooth Tooth	Summary of Results	
Impression Medium	Accuracy	Precision
Speedex	x	✓
President Jet Light Body	x	✓
MM913	x	✓
Accutrans	x	✓
President Jet Regular Body	✓	✓
Microset 101RF	x	x
MM240TV	x	x

Supplementary Figure S3. Summary of overall Accuracy and Precision for each impression medium, separated across rough and smooth tooth surfaces. For convenience all treatments of the data are summarised as a single result. Impression media showing high Accuracy (one or fewer significant matched pair T-test results across all treatments of the data) or high Precision (a small range of absolute differences between the original surface and each impression medium) are marked with a (✓). Impression media showing low Accuracy (more than one significant matched pair T-test results across all treatments of the data) or low Precision (a medium to high range of absolute differences between the original surface and each impression mediumare marked with an (x). Results are highlighted green for instances where both Accuracy and Precision are shown to be high in a given impression medium.

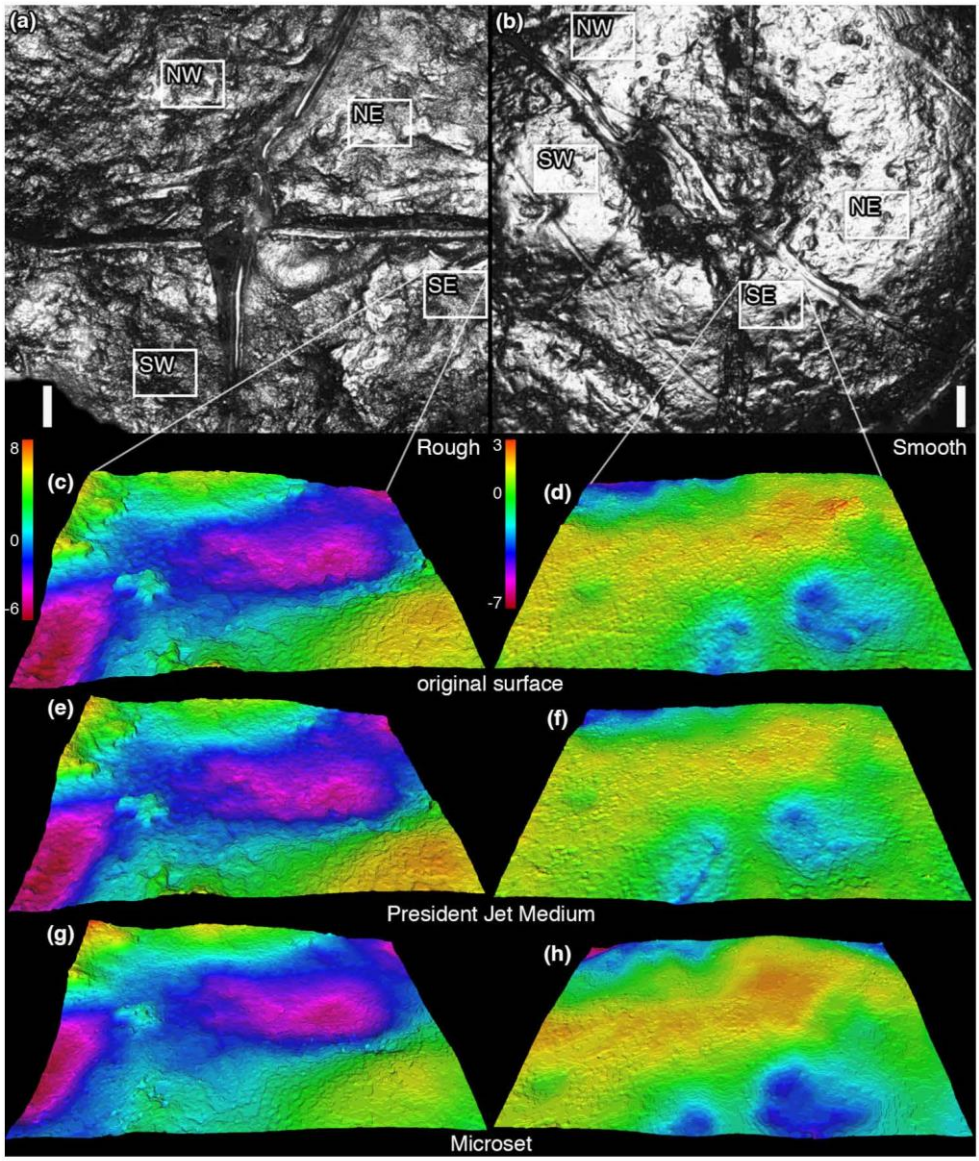

Supplementary Figure S4. Sample locations of four quadrants from the rough (a) and smooth (b) tooth surfaces (optical images). (c) - (h), digital elevation models of levelled surface data from original surface and examples of replicas made using different impresion media for SE quadrant, for rough (c, e, g) and smooth (d, f, h) surfaces. (c) and (d) original surfaces; (e) and (f) replicas, President Jet medium body impression medium; (g) and (h) replicas, Microset impression medium. Scale bars in (a) and (b), 100μm. Digital elevation models all 110 x 145 μm. Vertical scales in μm.

References

Ainley, D. G., G. Ballard, B. Karl, J., and K. M. Dugger. 2005. Leopard seal predation rates at penguin colonies of different size. Antarctic Science **17**:335-340.doi: 10.1017/S0954102005002750

Al-Shammery, H. A., N. L. Bubb, C. C. Youngson, D. J. Fasbinder, and D. J. Wood. 2007. The use of confocal microscopy to assess surface roughness of two milled CAD-CAM ceramics following two polishing techniques. Dental Materials **23**:736-741.doi: 10.1016/j.dental.2006.06.012

Andersen, S. M., C. Lydersen, O. Grahl-Nielsen, and K. M. Kovacs. 2004. Autumn diet of harbour seals (*Phoca vitulina*) at Prins Karls Forland, Svalbard, assessed via scat and fatty-acid analyses. Canadian Journal of Zoology **82**:1230-1245.doi: 10.1139/z04-093

Arim, M., and D. E. Naya. 2003. Pinniped diets inferred from scats: analysis of biases in prey occurrence. Canadian Journal of Zoology **81**:67-73.doi: 10.1139/z02-221

Arman, S. D., P. S. Ungar, C. A. Brown, L. R. G. DeSantis, C. Schmidt, and G. J. Prideaux. 2016. Minimizing inter-microscope variability in dental microwear texture analysis. Surface Topography: Metrology and Properties **4**:024007.doi: 10.1088/2051-672x/4/2/024007

Austin, R. S., F. Mullen, and D. W. Bartlett. 2015. Surface texture measurement for dental wear applications. Surface Topography: Metrology and Properties **3**:023002.doi: 10.1088/2051-672x/3/2/023002

Bai, X. Q., G. T. Xie, H. Fan, Z. X. Peng, C. Q. Yuan, and X. P. Yan. 2013. Study on biomimetic preparation of shell surface microstructure for ship antifouling. Wear **306**:285-295.doi: 10.1016/j.wear.2012.11.020

Baird, R. W., and L. M. Dill. 1995. Occurrence and behaviour of transient killer whales: seasonal and pod-specific variability, foraging behaviour, and prey handling. Canadian Journal of Zoology **73**:1300-1311,

Baisre, J. A. 2013. Shifting baselines and the extinction of the Caribbean monk seal. Conservation Biology **27**:927-935.doi: 10.1111/cobi.12107

Bajpai, S., and P. D. Gingerich. 1998. A new Eocene archaeocete (Mammalia, Cetacea) from India and the time of origin of whales. Proceedings of the National Academy of Sciences **95**:15464-15468.doi: 10.1073/pnas.95.26.15464

Bajpai, S., and J. G. M. Thewissen. 2000. A new, diminutive Eocene whale from Kachchh (Gujarat, India) and its implications for locomotor evolution of cetaceans. Current Science **79**:1478-1482,

Bajpai, S., J. G. M. Thewissen, and A. Sahni. 2009. The origin and early evolution of whales: macroevolution documented on the Indian Subcontinent. Journal of Biosciences **34**:673-686.doi: 10.1007/s12038-009-0060-0

Barnett, A., K. S. Redd, S. D. Frusher, J. D. Stevens, and J. M. Semmens. 2010. Non-lethal method to obtain stomach samples from a large marine predator and the use of DNA analysis to improve dietary information. Journal of Experimental Marine Biology and Ecology **393**:188-192.doi: 10.1016/j.jembe.2010.07.022

Barros, N. B., and R. S. Wells. 1998. Prey and feeding patterns of resident bottlenose dolphins (*Tursiops truncatus*) in Sarasota Bay, Florida. Journal of Mammalogy **79**:1045-1059.doi: 10.2307/1383114

Bello, S. M., S. A. Parfitt, and C. Stringer. 2009. Quantitative micromorphological analyses of cut marks produced by ancient and modern handaxes. Journal of Archaeological Science **36**:1869-1880.doi: 10.1016/j.jas.2009.04.014

Bello, S. M., E. Verveniotou, L. Cornish, and S. A. Parfitt. 2011. 3-dimensional microscope analysis of bone and tooth surface modifications: comparisons of fossil specimens and replicas. Scanning **33**:316-324.doi: 10.1002/sca.20248

Benjamini, Y., and Y. Hochberg. 1995. Controlling the false discovery rate: a practical and powerful approach to multiple testing. Journal of the royal statistical society. Series B (Methodological) **57**:289-300,

Berg, I., T. Haug, and K. T. Nilssen. 2002. Harbour seal (*Phoca vitulina*) diet in Vesteralen, North Norway. Sarsia **87**:451-461.doi: 10.1080/0036482021000155735

Berta, A., and M. Churchill. 2012. Pinniped taxonomy: review of currently recognized species and subspecies, and evidence used for their description. Mammal Review **42**:207-234.doi: 10.1111/j.1365-2907.2011.00193.x

Bianucci, G., and P. D. Gingerich. 2011. *Aegyptocetus tarfa*, N. Gen. Et Sp. (Mammalia, Cetacea), from the Middle Eocene of Egypt: clinorhynchy, olfaction, and hearing

in a protocetid whale. Journal of Vertebrate Paleontology **31**:1173-1188.doi: 10.1080/02724634.2011.607985

Blunt, R. T. 2006. White light interferometry - a production worthy technique for measuring surface roughness on semiconductor wafers. CS MANTECH Conference. IQE (Europe) Ltd, Vancouver, British Columbia, Canada,

Boisserie, J. R., F. Lihoreau, and M. Brunet. 2005. The position of Hippopotamidae within Cetartiodactyla. Proceedings of the National Academy of Sciences **102**:1537-1541.doi: 10.1073/pnas.0409518102

Bowen, W. D. 1997. Role of marine mammals in aquatic ecosystems. Marine Ecological Progress Series **158**:267-274.doi: 10.3354/meps158267

Bowen, W. D. 2000. Reconstruction of pinniped diets: accounting for complete digestion of otoliths and cephalopod beaks. Canadian Journal of Fisheries and Aquatic Sciences **57**:898-905.doi: 10.1139/f00-032

Bowen, W. D., and S. J. Iverson. 2013. Methods of estimating marine mammal diets: A review of validation experiments and sources of bias and uncertainty. Marine Mammal Science:n/a-n/a.doi: 10.1111/j.1748-7692.2012.00604.x

Brown, E. G., G. J. Pierce, J. R. G. Hislop, and M. B. Santos. 2001. Interannual variation in the summer diets of harbour seals *Phoca vitulina* at Mousa, Shetland (UK). Journal of the Marine Biological Association of the United Kingdom **81**:325-337.doi: 10.1017/S0025315401003812

Bruzzone, A. A. G., H. L. Costa, P. M. Lonardo, and D. A. Lucca. 2008. Advances in engineered surfaces for functional performance. CIRP Annals - Manufacturing Technology **57**:750-769.doi: 10.1016/j.cirp.2008.09.003

Buchholtz, E. A. 2007. Modular evolution of the cetacean vertebral column. Evolution & Development **9**:278-289.doi: 10.1111/j.1525-142X.2007.00160.x

Cabin, R. J., and R. J. Mitchell. 2000. To Bonferroni or not to Bonferroni: When and how are the questions. Bulletin of the Ecological Society of America **81**:246-248,

Calandra, I., and G. Merceron. 2016. Dental microwear texture analysis in mammalian ecology. Mammal Review doi: 10.1111/mam.12063

Calandra, I., E. Schulz, M. Pinnow, S. Krohn, and T. M. Kaiser. 2012. Teasing apart the contributions of hard dietary items on 3D dental microtextures in primates. Journal of Human Evolution **63**:85-98.doi: 10.1016/j.jhevol.2012.05.001

Caporale, S. S., and P. S. Ungar. 2016. Rodent incisor microwear as a proxy for ecological reconstruction. Palaeogeography, Palaeoclimatology, Palaeoecology **446**:225-233.doi: 10.1016/j.palaeo.2016.01.013

Casaux, R., A. Baroni, A. Ramón, A. Carlini, M. Bertolin, and C. Y. DiPrinzio. 2009. Diet of the leopard seal *Hydrurga leptonyx* at the Danco Coast, Antarctic Peninsula. Polar Biology **32**:307-310.doi: 10.1007/s00300-008-0567-0

Chambellant, M., I. Stirling, and S. H. Ferguson. 2013. Temporal variation in western Hudson Bay ringed seal *Phoca hispida* diet in relation to environment. Marine Ecology Progress Series **481**:269-287.doi: 10.3354/meps10134

Chee, W. W. L., and T. E. Donovan. 1992. Polyvinyl siloxane impression materials: a review of properties and techniques. Journal of Prosthetic Dentistry **68**:728-732.doi: 10.1016/0022-3913(92)90192-D

Chung, S., Y. Im, H. Kim, H. Jeong, and D. A. Dornfeld. 2003. Evaluation of micro-replication technology using silicone rubber molds and its applications. International Journal of Machine Tools and Manufacture **43**:1337-1345.doi: 10.1016/s0890-6955(03)00164-0

Cicchetti, D. V. 1994. Guidelines, criteria, and rules of thumb for evaluating normed and standardized assessment instruments in psychology. Psychological Assessment **6**:284-290.doi: 10.1037/1040-3590.6.4.284

Clementz, M. T., A. Goswami, P. D. Gingerich, and P. L. Koch. 2006. Isotopic records from early whales and sea cows: contrasting patterns of ecological transition. Journal of Vertebrate Paleontology **26**:355-370.doi: 10.1671/0272-4634(2006)26[355:irfewa]2.0.co;2

Cortés, E. 1997. A critical review of methods of studying fish feeding based on analysis of stomach contents: application to elasmobranch fishes. Canadian Journal of Fisheries and Aquatic Sciences **54**:726-738.doi: 10.1139/f96-316

Cottrell, P. E., A. W. Trites, and E. H. Miller. 1996. Assessing the use of hard parts in faeces to identify harbour seal prey: results of captive-feeding trials. Canadian Journal of Zoology **74**:875-880.doi: 10.1139/z96-101

Craddock, J. E., P. T. Polloni, B. Hayward, and F. Wenzel. 2009. Food habits of Atlantic white-sided dolphins (*Lagenorhynchus acutus*) off the coast of New England. Fishery Bulletin **107**:384-394,

Cransac, N., C. Cibien, J. M. Angibault, N. Morrelet, and J. P. Vincent. 2001. Variations saisonnie`res du re´gime alimentaire du chevreuil (*Capreolus capreolus*) selon le sexe en milieu forestier a` forte densite´ (foreˆt domaniale de Dourdan). Mammalia **65**:1-12,

Crawford, K., R. A. McDonald, and S. Bearhop. 2008. Applications of stable isotope techniques to the ecology of mammals. Mammal Review **38**:87-107.doi: 10.1111/j.1365-2907.2008.00120.x

Daegling, D. J., S. Judex, E. Ozcivici, M. J. Ravosa, A. B. Taylor, F. E. Grine, M. F. Teaford, and P. S. Ungar. 2013. Viewpoints: feeding mechanics, diet, and dietary adaptations in early hominins. American Journal of Physical Anthropology **151**:356-371.doi: 10.1002/ajpa.22281

Dahlberg, A. A., and W. Kinzey. 1962. Etude microscopique de l'abrasion et de l'attrition sur la surface des dents. Bulletin du Groupement International pour la Recherche Scientifique en Stomatologie et Odontologie (Bruxelles) **5**:242-251,

Dahlheim, M. E., A. Schulman-Janiger, N. A. Black, R. Ternullo, and D. Ellifrit. 2008. Eastern temperate North Pacific offshore killer whales (*Orcinus orca*): Occurrence, movements, and insights into feeding ecology. Publications, Agencies and Staff of the U.S. Department of Commerce. **Paper 169**.doi: 10.1111/j.1748-7692.2008.00206.x

Danzl, R., F. Helmli, and S. Scherer. 2011. Focus variation – a robust technology for high resolution optical 3D surface metrology. Strojniški vestnik – Journal of Mechanical Engineering **2011**:245-256.doi: 10.5545/sv-jme.2010.175

Darras, L. P. G. 2012. The evolution and macroecological consequences of grazing and shell crushing in fishes. University of Leicester.

Dayton, P. K., S. F. Thrush, M. Tundi Agardy, and R. J. Hofman. 1995. Environmental effects of marine fishing. Aquatic Conservation: Marine and Freshwater Ecosystems **5**:205-232.doi: 10.1002/aqc.3270050305

de Bruyn, P. J., C. A. Tosh, and A. Terauds. 2013. Killer whale ecotypes: is there a global model? Biological Reviews of the Cambridge Philosophical Society **88**:62-80.doi: 10.1111/j.1469-185X.2012.00239.x

De Pierrepont, J. F., B. Dubois, S. Desormonts, M. B. Santos, and J. P. Robin. 2005. Stomach contents of English Channel cetaceans stranded on the coast of

Normandy. Journal of the Marine Biological Association of the United Kingdom **85**:1539-1546.doi: 10.1017/S0025315405012762

Deagle, B. E., R. Kirkwood, and S. N. Jarman. 2009. Analysis of Australian fur seal diet by pyrosequencing prey DNA in faeces. Molecular Ecology **18**:2022-2038.doi: 10.1111/j.1365-294X.2009.04158.x

Deagle, B. E., D. J. Tollit, S. N. Jarman, M. A. Hindell, A. W. Trites, and N. J. Gales. 2005. Molecular scatology as a tool to study diet: analysis of prey DNA in scats from captive Steller sea lions. Molecular Ecology **14**:1831-1842.doi: 10.1111/j.1365-294X.2005.02531.x

Delezene, L. K., M. F. Teaford, and P. S. Ungar. 2016. Canine and incisor microwear in pitheciids and *Ateles* reflects documented patterns of tooth use. American Journal of Physical Anthropology **161**:6-25.doi: 10.1002/ajpa.23002

Delezene, L. K., M. S. Zolnierz, M. F. Teaford, W. H. Kimbel, F. E. Grine, and P. S. Ungar. 2013. Premolar microwear and tooth use in *Australopithecus afarensis*. Journal of Human Evolution **65**:282-293.doi: 10.1016/j.jhevol.2013.06.001

DeLong, R., M. R. Pintado, C.-C. Ko, J. S. Hodges, and W. H. Douglas. 2001. Factors influencing optical 3D scanning of vinyl polysiloxane impression materials. Journal of Prosthodontics **10**:78-85.doi: 10.1053/jpro.2001.24718

Deltombe, R., K. J. Kubiak, and M. Bigerelle. 2014. How to select the most relevant 3D roughness parameters of a surface. Scanning **36**:150-160.doi: 10.1002/sca.21113

DeMaster, D. P., C. W. Fowler, S. L. Perry, and M. F. Richlen. 2001. Predation and competition: the impact of fisheries on marine-mammal populations over the next one hundred years. Journal of Mammalogy **82**:641-651.doi: 10.1644/1545-1542(2001)082<0641:PACTIO>2.0.CO;2

DeMaster, D. P., A. W. Trites, P. Clapham, S. Mizroch, P. Wade, R. J. Small, and J. V. Hoef. 2006. The sequential megafaunal collapse hypothesis: testing with existing data. Progress in Oceanography **68**:329-342.doi: 10.1016/j.pocean.2006.02.007

DeSantis, L. R., and R. J. Haupt. 2014. Cougars' key to survival through the Late Pleistocene extinction: insights from dental microwear texture analysis. Biology Letters **10**:20140203.doi: 10.1098/rsbl.2014.0203

DeSantis, L. R., J. R. Scott, B. W. Schubert, S. L. Donohue, B. M. McCray, C. A. Van Stolk, A. A. Winburn, M. A. Greshko, and M. C. O'Hara. 2013. Direct comparisons of 2D and 3D dental microwear proxies in extant herbivorous and carnivorous mammals. PLoS One **8**:e71428.doi: 10.1371/journal.pone.0071428

DeSantis, L. R. G., B. W. Schubert, J. R. Scott, and P. S. Ungar. 2012. Implications of diet for the extinction of sabre-toothed cats and American lions. PLoS One **7**.doi: 10.1371/journal.pone.0052453.g001

Dolfini, A., and R. J. Crellin. 2016. Metalwork wear analysis: The loss of innocence. Journal of Archaeological Science **66**:78-87.doi: 10.1016/j.jas.2015.12.005

Doney, S. C., M. Ruckelshaus, J. E. Duffy, J. P. Barry, F. Chan, C. A. English, H. M. Galindo, J. M. Grebmeier, A. B. Hollowed, N. Knowlton, J. Polovina, N. N. Rabalais, W. J. Sydeman, and L. D. Talley. 2012. Climate change impacts on marine ecosystems. Annual Review of Marine Science **4**:11-37.doi: 10.1146/annurev-marine-041911-111611

Donohue, S. L., L. R. G. DeSantis, B. W. Schubert, and P. S. Ungar. 2013. Was the giant short-faced bear a hyper scavenger? A new approach to the dietary study of ursids using dental microwear textures. PLoS One **8**:e77531. doi:77510.71371/journal.pone.0077531.doi: 10.1371/journal.pone.0077531.g001

Dunford, A. M., A. R. Parry, P. H. Shipway, and H. E. Viner. 2012. Three-dimensional characterisation of surface texture for road stones undergoing simulated traffic wear. Wear **292-293**:188-196.doi: 10.1016/j.wear.2012.05.010

El Zaatari, S., and J. J. Hublin. 2014. Diet of upper paleolithic modern humans: Evidence from microwear texture analysis. American Journal of Physical Anthropology **153**:570-581.doi: 10.1002/ajpa.22457

Estebaranz, F., J. Galbany, L. M. Martinez, and A. Perez-Perez. 2007. 3-D interferometric microscopy applied to the study of buccal enamel microwear. Dental Perspectives on Human Evolution:391-403.doi: 10.1007/978-1-4020-5845-5_25

Estes, J. A., D. F. Doak, A. M. Springer, T. M. Williams, and G. B. van Vliet. 2009. Trend data do support the sequential nature of pinniped and sea otter declines in the North Pacific Ocean, but does it really matter? Marine Mammal Science **25**:748-754.doi: 10.1111/j.1748-7692.2009.00322.x

Evans, A. A. 2014. On the importance of blind testing in archaeological science: the example from lithic functional studies. Journal of Archaeological Science **48**:5-14.doi: 10.1016/j.jas.2013.10.026

Evans, A. A., H. Lerner, D. A. Macdonald, W. J. Stemp, and P. C. Anderson. 2014. Standardization, calibration and innovation: a special issue on lithic microwear method. Journal of Archaeological Science.doi: 10.1016/j.jas.2014.03.002

Evans, P. G. H., and A. Bjørge. 2013. Impacts of climate change on marine mammals. Marine Climate Change Impacts Partnership: Science Review 2013:134-148.doi: 10.1016/b978-012374473-9.00685-8

Fahlke, J. M. 2012. Bite marks revisited – evidence for middle-to-late Eocene *Basilosaurus isis* predation on *Dorudon atrox* (both Cetacea, Basilosauridae). Palaeontologia Electronica **15**,

Fahlke, J. M., K. A. Bastl, G. M. Semprebon, and P. D. Gingerich. 2013. Paleoecology of archaeocete whales throughout the Eocene: Dietary adaptations revealed by microwear analysis. Palaeogeography, Palaeoclimatology, Palaeoecology **386**:690-701.doi: 10.1016/j.palaeo.2013.06.032

Fahlke, J. M., P. D. Gingerich, R. C. Welsh, and A. R. Wood. 2011. Cranial asymmetry in Eocene archaeocete whales and the evolution of directional hearing in water. Proceedings of the National Academy of Sciences **108**:14545-14548.doi: 10.1073/pnas.1108927108

Fertl, D., A. Acevedo-Gutierrez, and F. L. Darby. 1996. A report of killer whales (*Orcinus orca*) feeding on a carcharhinid shark in Costa Rica. Marine Mammal Science **12**:606-611,

Fiorenza, L., S. Benazzi, and O. Kullmer. 2009. Morphology, wear and 3D digital surface models: materials and techniques to create high-resolution replicas of teeth. Journal of Anthropological Sciences **87**:211-218,

Foote, A. D., P. A. Morin, R. L. Pitman, M. C. Ávila-Arcos, J. W. Durban, A. Helden, M. S. Sinding, and M. T. P. Gilbert. 2013a. Mitogenomic insights into a recently described and rarely observed killer whale morphotype. Polar Biology:1-5.doi: 10.1007/s00300-013-1354-0

Foote, A. D., J. Newton, M. C. Avila-Arcos, M. L. Kampmann, J. A. Samaniego, K. Post, A. Rosing-Asvid, M. H. Sinding, and M. T. Gilbert. 2013b. Tracking niche variation

over millennial timescales in sympatric killer whale lineages. Proceedings of the Royal Society B: Biological Sciences **280**:20131481.doi: 10.1098/rspb.2013.1481

Foote, A. D., J. Newton, S. B. Piertney, E. Willerslev, and M. T. P. Gilbert. 2009. Ecological, morphological and genetic divergence of sympatric North Atlantic killer whale populations. Molecular Ecology **18**:5207-5217.doi: 10.1111/j.1365-294X.2009.04407.x

Foote, A. D., J. T. Vilstrup, R. De Stephanis, P. Verborgh, S. C. Abel Nielsen, R. Deaville, L. Kleivane, V. Martin, P. J. Miller, N. Oien, M. Perez-Gil, M. Rasmussen, R. J. Reid, K. M. Robertson, E. Rogan, T. Simila, M. L. Tejedor, H. Vester, G. A. Vikingsson, E. Willerslev, M. T. Gilbert, and S. B. Piertney. 2011. Genetic differentiation among North Atlantic killer whale populations. Molecular Ecology **20**:629-641.doi: 10.1111/j.1365-294X.2010.04957.x

Ford, J. K. B., and G. M. Ellis. 2006. Selective foraging by fish-eating killer whales *Orcinus orca* in British Columbia. Marine Ecology Progress Series **316**:185-199.doi: 10.3354/meps316185

Ford, J. K. B., G. M. Ellis, and K. C. Balcomb. 2000. Killer whales. UBC Press, Vancouver, Canada.

Ford, J. K. B., G. M. Ellis, L. G. Barrett-Lennard, A. B. Morton, R. S. Palm, and K. C. Balcomb. 1998. Dietary specialization in two smpatric populations of killer whales (*Orcinus orca*) in coastal British Columbia and adjacent waters. Canadian Journal of Zoology **76**:1456-1471,

Ford, J. K. B., G. M. Ellis, C. O. Matkin, M. H. Wetklo, L. G. Barrett-Lennard, and R. E. Withler. 2011. Shark predation and tooth wear in a population of northeastern Pacific killer whales. Aquatic Biology **11**:213-224.doi: 10.3354/ab00307

Fordyce, R. E., and L. G. Barnes. 1994. The evolutionary history of whales and dolphins. Annual Review of Earth and Planetary Sciences **22**:419-455,

Gailer, J. P., I. Calandra, E. Schulz-Kornas, and T. M. Kaiser. 2016. Morphology is not destiny: discrepancy between form, function and dietary adaptation in Bovid cheek teeth. Journal of Mammalian Evolution.doi: 10.1007/s10914-016-9325-1

Galbany, J., F. Estebaranz, L. M. Martinez, A. Romero, J. De Juan, D. Turbon, and A. Perez-Perez. 2006. Comparative analysis of dental enamel polyvinylsiloxane impression

and polyurethane casting methods for SEM research. Microscopy Research and Technique **69**:246-252.doi: 10.1002/jemt.20296

Galbany, J., L. M. Martinez, H. M. Lopez-Amor, V. Espurz, O. Hiraldo, A. Romero, J. De Juan, and A. Perez-Perez. 2005. Error rates in buccal-dental microwear quantification using scanning electron microscopy. Scanning **27**:23-29.doi: 10.1002/sca.4950270105

Galbany, J., L. M. Martinez, and A. Perez-Perez. 2004. Tooth replication techniques, SEM imagine and microwear analysis in primates: methodological obstacles. Anthopologie **42**:5-12,

Gatesy, J., J. H. Geisler, J. Chang, C. Buell, A. Berta, R. W. Meredith, M. S. Springer, and M. R. McGowen. 2013. A phylogenetic blueprint for a modern whale. Molecular Phylogenetics and Evolution **66**:479-506.doi: 10.1016/j.ympev.2012.10.012

Gatesy, J., and M. A. O'Leary. 2001. Deciphering whale origins with molecules and fossils. TRENDS in Ecology & Evolution **16**:562-570.doi: 10.1016/S0169-5347(01)02236-4

Ge, M., G. Wu, D. Burk, J. Ozelis, E. Harms, D. Sergatskov, D. Hicks, and L. D. Cooley. 2011. Routine characterization of 3D profiles of SRF cavity defects using replica techniques. Superconductor Science and Technology **24**:035002.doi: 10.1088/0953-2048/24/3/035002

Geisler, J. H., A. E. Sanders, and Z. Luo. 2005. A new protocetid whale (Cetacea: Archaeoceti) from the Late Middle Eocene of South Carolina. American Museum Novitates **3480**:1.doi: 10.1206/0003-0082(2005)480[0001:anpwca]2.0.co;2

Geisler, J. H., and J. M. Theodor. 2009. Hippopotamus and whale phylogeny. Nature **458**:E1-4; discussion E5.doi: 10.1038/nature07776

Geisler, J. H., and M. D. Uhen. 2003. Morphological support for a close relationship between hippos and whales. Journal of Vertebrate Paleontology **23**:991-996.doi: 10.1671/32

Gerber, L. R., L. Morisette, K. Kaschner, and D. Pauly. 2009. Should whales be culled to increase fishery yield? Science **323**:880-881.doi: 10.1126/science.1169981

Gill, P. G., M. A. Purnell, N. Crumpton, K. Robson Brown, N. J. Gostling, M. Stamponi, and E. J. Rayfield. 2014. Dietary specializations and diversity in feeding ecology of the earliest stem mammals. Nature **512**:303-305.doi: 10.1038/nature13622

Gingerich, P. D. 1992. Marine mammals (Cetacea and Sirenia) from the Eocene in Gebel Mokattam and Fayum, Egypt: stratigraphy, age, and paleoenvironments. Papers on Palaeontology, University of Michigan **30**,

Gingerich, P. D. 2003. Land-to-sea transition in early whales: evolution of Eocene Archaeoceti (Cetacea) in relation to skeletal proportions and locomotion of living semiaquatic mammals. Paleobiology **29**:429-454.doi: 10.1666/0094-8373(2003)029<0429:ltiewe>2.0.co;2

Gingerich, P. D., M. Arif, and W. C. Clyde. 1995. New archaeocetes (Mammalia, Cetacea) from the Middle Eocene Domanda Formation of the Sulaiman Range, Punjab (Pakistan). Contributions from the Museum of Paleontology **29**:291-330,

Gingerich, P. D., and D. E. Russell. 1990. Dentition of Early Eocene *Pakicetus* (Mammalia, Cetacea). Contributions from the Museum of Paleontology **28**:1-20,

Gingerich, P. D., M. Ul-Haq, W. von Koenigswald, W. J. Sanders, B. H. Smith, and I. S. Zalmout. 2009. New protocetid whale from the Middle Eocene of Pakistan: birth on land, precocial development, and sexual dimorphism. PLoS One **4**:e4366.doi: 10.1371/journal.pone.0004366

Gingerich, P. D., N. A. Wells, D. E. Russell, and S. M. I. Shah. 1983. Origin of whales in epicontinental remnant seas: new evidence from the Early Eocene of Pakistan. Science **220**:403-406,

Giusca, C. L., R. K. Leach, F. Helary, T. Gutauskas, and L. Nimishakavi. 2012. Calibration of the scales of areal surface topography-measuring instruments: part 1. Measurement noise and residual flatness. Measurement Science and Technology **23**:035008.doi: 10.1088/0957-0233/23/3/035008

Gogarten, J. F., and F. E. Grine. 2013. Seasonal mortality patterns in primates: implications for the interpretation of dental microwear. Evolutionary Anthropology **22**:9-19.doi: 10.1002/evan.21338

Gol'din, P., and E. Zvonok. 2013. *Basilotritus uheni*, a new Cetacean (Cetacea, Basilosauridae) from the Late Middle Eocene of Eastern Europe. Journal of Paleontology **87**:254-268.doi: 10.1666/12-080r.1

Gol'din, P., E. Zvonok, L. Rekovets, A. Kovalchuk, and T. Krakhmalnaya. 2014. *Basilotritus* (Cetacea: Pelagiceti) from the Eocene of Nagornoye (Ukraine): New data on

anatomy, ontogeny and feeding of early basilosaurids. Comptes Rendus Palevol **13**:267-276.doi: 10.1016/j.crpv.2013.11.002

Goodall, R. H., L. P. Darras, and M. A. Purnell. 2015. Accuracy and precision of silicon based impression media for quantitative areal texture analysis. Scientific Reports **5**:10800.doi: 10.1038/srep10800

Green, J. L. 2009a. Dental microwear in the orthodentine of the Xenarthra (Mammalia) and its use in reconstructing the palaeodiet of extinct taxa: the case study of *Nothrotheriops shastensis* (Xenarthra, Tardigrada, Nothrotheriidae). Zoological Journal of the Linnean Society **156**:201-222.doi: 10.1111/j.1096-3642.2008.00486.x

Green, J. L. 2009b. Intertooth variation of orthodentine microwear in Armadillos (Cingulata) and Tree Sloths (Pilosa). Journal of Mammalogy **90**:768-778.doi: 10.1644/08-mamm-a-257r1.1

Grine, F. E., P. S. Ungar, and M. F. Teaford. 2002. Error rates in dental microwear quantification using scanning electron microscopy. Scanning **24**:144-153.doi: 10.1002/sca.4950240307

Gudmundson, C. J., T. K. Zeppelin, and R. R. Ream. 2006. Application of two methods for determining diet of northern fur seals (*Callorhinus ursinus*). Fisheries Bulletin **104**:445-455,

Hall-Aspland, S. A., and T. L. Rogers. 2004. Summer diet of leopard seals (*Hydrurga leptonyx*) in Prydz Bay, Eastern Antarctica. Polar Biology **27**:729-734.doi: 10.1007/s00300-004-0662-9

Haug, T., K. T. Nilssen, and L. Lindblom. 2004. Feeding habits of harp and hooded seals in drift ice waters along the east coast of Greenland in summer and winter. Polar Research **23**:35-42.doi: 10.1111/j.1751-8369.2004.tb00127.x

Haupt, R. J., L. R. G. DeSantis, J. L. Green, and P. S. Ungar. 2013. Dental microwear texture as a proxy for diet in xenarthrans. Journal of Mammalogy **94**:856-866.doi: 10.1644/12-mamm-a-204.1

Heurich, E., M. Beyer, K. D. Jandt, J. Reichert, V. Herold, M. Schnabelrauch, and B. W. Sigusch. 2010. Quantification of dental erosion--a comparison of stylus profilometry and confocal laser scanning microscopy (CLSM). Dental Materials **26**:326-336.doi: 10.1016/j.dental.2009.12.001

Hocking, D. P., A. R. Evans, and E. M. G. Fitzgerald. 2013. Leopard seals (*Hydrurga leptonyx*) use suction and filter feeding when hunting small prey underwater. Polar Biology **36**:211-222.doi: 10.1007/s00300-012-1253-9

Hoegh-Guldberg, O., and J. F. Bruno. 2010. The impact of climate change on the world's marine ecosystems. Science **328**:1523-1528.doi: 10.1126/science.1189930

Holm, S. 1979. A simple sequentially rejective multiple test procedure. Scandinavian Journal of Statistics **6**:65-70,

Holst, M., I. Striling, and K. A. Hobson. 2001. Diet of ringed seals (*Phoca hispida*) on the east and west sides of the North Water Polynya, Northern Baffin Bay. Marine Mammal Science **17**:888-908.doi: 10.1111/j.1748-7692.2001.tb01304.x

Hong-Yan, G., and N. Xi-Jun. 2015. Diverse stem cetaceans and their phylogentic relationships with mesonychids and artiodactyls. Vertebrata PalAsiatica **53**:153-176,

Hooker, S. K., and L. R. Gerber. 2004. Marine reserves as a tool for ecosystem-based management: The Potential Importance of Megafauna. Bioscience **54**:27-39.doi: 10.1641/0006-3568(2004)054%5B0027:MRAATF%5D2.0.CO;2

Hulbert Jr, R. C., R. M. Petkewich, G. A. Bishop, D. Bukry, and D. P. Aleshire. 1998. A new Middle Eocene protocetid whale (Mammalia: Cetacea: Archaeoceti) and associated biota from Georgia. Journal of Paleontology **72**:907-927,

International Organization for Standardization. 2012. Geometrical product specifications (GPS) - Surface texture: Areal - Part 2: Terms, definitions and surface texture parameters (ISO 25178-2).

Iverson, S. J., C. Field, W. D. Bowen, and W. Blanchard. 2004. Quantitative fatty acid signature analysis: a new method of estimating predator diets. Ecological Monographs **74**:211-235.doi: 10.1890/02-4105

Jarman, S. N., N. J. Gales, M. Tierney, P. C. Gill, and N. G. Elliott. 2002. A DNA-based method for identification of krill species and its application to analysing the diet of marine vertebrate predators. Molecular Ecology **11**:2679-2690.doi: 10.1046/j.1365-294X.2002.01641.x

Jefferson, T. A., P. J. Stacey, and R. W. Baird. 1991. A review of killer whale interactions with other marine mammals: predation to co-existence. Mammal Review **21**:151-180.doi: 10.1111/j.1365-2907.1991.tb00291.x

Jiang, X., P. J. Scott, D. J. Whitehouse, and L. Blunt. 2007. Paradigm shifts in surface metrology. Part II. The current shift. Proceedings of the Royal Society A: Mathematical, Physical and Engineering Sciences **463**:2071-2099.doi: 10.1098/rspa.2007.1873

Jobling, M., and A. Breiby. 1986. The use and abuse of fish otoliths in studies of feeding habits of marine piscivores. Sarsia **71**:265-274.doi: 10.1080/00364827.1986.10419696

Jordan, H. J., M. Wegner, and H. Tziani. 1998. Highly accurate non-contact characterization of engineering surfaces using confocal microscopy. Measurement Science and Technology **9**:1142-1151.10.1088/0957-0233/9/7/023

Jouini, N., A. Gautier, P. Revel, P.-E. Mazeran, and M. Bigerelle. 2009. Multi-scale analysis of high precision surfaces by stylus profiler, scanning white-light interferometry and atomic force microscopy. International Journal of Surface Science and Engineering **3**:310-327.doi: 10.1504/IJSURFSE.2009.027418

Keeley, L. H. 1974. Technique and methodology in microwear studies: A critical review. World Archaeology **5**:323-336,

Kiszka, J., C. Muir, C. Poonian, T. M. Cox, O. A. Amir, J. Bourjea, Y. Razafindrakoto, N. Wambitji, and N. Bristol. 2009. Marine mammal bycatch in the Southwest Indian Ocean: review and need for a comprehensive status assessment. Western Indian Ocean Journal Marine Science **7**:119-136,

Kovacs, K. M., A. Aguilar, D. Aurioles, V. Burkanov, C. Campagna, N. Gales, T. Gelatt, S. D. Goldsworthy, S. J. Goodman, G. J. G. Hofmeyr, T. Härkönen, L. Lowry, C. Lydersen, J. Schipper, T. Sipilä, C. Southwell, S. Stuart, D. Thompson, and F. Trillmich. 2012. Global threats to pinnipeds. Marine Mammal Science **28**:414-436.doi: 10.1111/j.1748-7692.2011.00479.x

Krahn, M. M., D. P. Herman, C. O. Matkin, J. W. Durban, and L. Barrett-Lennard. 2007. Use of chemical tracers in assessing the diet and foraging regions of eastern North Pacific killer whales. Marine Environmental Research **63**:91-114.doi: 10.1016/j.marenvres.2006.07.002

Krueger, K. L., and P. S. Ungar. 2012. Anterior dental microwear texture analysis of the Krapina Neandertals. Central European Journal of Geosciences **4**:651-662.doi: 10.2478/s13533-012-0111-1

Kuker, K., and L. Barrett-Lennard. 2010. A re-evaluation of the role of killer whales (*Orcinus orca*) in a population decline of sea ottersEnhydra lutrisin the Aleutian Islands and a review of alternative hypotheses. Mammal Review **40**:103-124.doi: 10.1111/j.1365-2907.2009.00156.x

Kurle, C. M., and G. A. J. Worthy. 2001. Stable isotope assessment of temporal and geographic differences in feeding ecology of northern fur seals (*Callorhinus ursinus*) and their prey. Oecologia **126**:254-265.doi: 10.1007/s004420000518

Lawson, J. W., and K. A. Hobson. 2000. Diet of harp seals (*Pagophilus groenlandicus*) in nearshore Northeast Newfoundland: inferences from stable-carbon (δ13C) and nitrogen (δ15N) isotope analyses. Marine Mammal Science **16**:578-591.doi: 10.1111/j.1748-7692.2000.tb00953.x

Leach, R. 2013. Characterisation of Areal Surface Texture. Springer.

Leach, R., and H. Haitjema. 2010. Bandwidth characteristics and comparisons of surface texture measuring instruments. Measurement Science and Technology **21**:079801.doi: 10.1088/0957-0233/21/7/079801

Loch, C., W. Duncan, P. C. Simões-Lopes, J. A. Kieser, and R. E. Fordyce. 2013a. Ultrastructure of enamel and dentine in extant dolphins (Cetacea: Delphinoidea and Inioidea). Zoomorphology **132**:215-225.doi: 10.1007/s00435-012-0180-1

Loch, C., L. J. Grando, D. R. Schwass, J. A. Kieser, R. E. Fordyce, and P. C. Simões-Lopes. 2013b. Dental erosion in South Atlantic dolphins (Cetacea: Delphinidae): A macro and microscopic approach. Marine Mammal Science **29**:338-347.doi: 10.1111/j.1748-7692.2012.00562.x

Loch, C., M. Marmontel, and P. C. Simões-Lopes. 2009. Conflicts with fisheries and intentional killing of freshwater dolphins (Cetacea: Odontoceti) in the Western Brazilian Amazon. Biodiversity and Conservation **18**:3979-3988.doi: 10.1007/s10531-009-9693-4

Loch, C., and P. C. Simoes-Lopes. 2013. Dental wear in dolphins (Cetacea: Delphinidae) from southern Brazil. Archives of Oral Biology **58**:134-141.doi: 10.1016/j.archoralbio.2012.08.002

Lopez, J. C., and D. Lopez. 1985. Killer whales (*Orcinus orca*) of Patagonia, and their behavior of intentional stranding while hunting nearshore. Journal of Mammalogy **66**:181-183,

Lowry, L. F., J. W. Testa, and W. Calvert. 1988. Notes on winter feeding of crabeater and leopard seals near the Antarctic Peninsula. Polar Biology **8**:475-478,

Lucas, P. W., R. Omar, K. Al-Fadhalah, A. S. Almusallam, A. G. Henry, S. Michael, L. A. Thai, J. Watzke, D. S. Strait, and A. G. Atkins. 2013. Mechanisms and causes of wear in tooth enamel: implications for hominin diets. Journal of the Royal Society Interface **10**:20120923.doi: 10.1098/rsif.2012.0923

Lundstrom, K., O. Hjerne, K. Alexandersson, and O. Karlsson. 2007. Estimation of grey seal (*Halichoerus grypus*) diet composition in the Baltic Sea. NAMMCO Scientific Publications **6**:177-196.doi: 10.7557/3.2733

Maas, M. C., and J. G. M. Thewissen. 1995. Enamel microstructure of *Pakicetus* (Mammalia: Archaeoceti). Journal of Paleontology **69**:1154-1163.doi: 10.1017/S0022336000038130

Matkin, C. O., L. G. Barrett-Lennard, H. Yurk, D. Ellifrit, and A. W. Trites. 2007. Ecotypic variation and predatory behavior among killer whales (*Orcinus orca*) off the eastern Aleutian Islands, Alaska. Fishery Bulletin **105**:74-88,

Matthews, C. J. D., S. P. Luque, S. D. Petersen, R. D. Andrews, and S. H. Ferguson. 2011. Satellite tracking of a killer whale (*Orcinus orca*) in the eastern Canadian Arctic documents ice avoidance and rapid, long-distance movement into the North Atlantic. Polar Biology **34**:1091-1096.doi: 10.1007/s00300-010-0958-x

McKenzie, J., and K. M. Wynne. 2008. Spatial and temporal variation in the diet of Steller sea lions in the Kodiak Archipelago, 1999 to 2005. Marine Ecology Progress Series **360**:265-283.doi: 10.3354/meps07383

Merceron, G., G. Escarguel, J. Angibault, and H. Verheyden-Tixier. 2010. Can dental microwear textures record inter-individual dietary variations? PLoS One **5**.doi: 10.1371/journal.pone.0009542.g001

Merceron, G., E. Hofman-Kamińska, and R. Kowalczyk. 2014. 3D dental microwear texture analysis of feeding habits of sympatric ruminants in the Białowieża Primeval Forest, Poland. Forest Ecology and Management **328**:262-269.doi: 10.1016/j.foreco.2014.05.041

Merceron, G., J. Scott, R. S. Scott, D. Geraads, N. Spassov, and P. S. Ungar. 2009. Folivory or fruit/seed predation for *Mesopithecus*, an earliest colobine from the late Miocene of Eurasia? Journal of Human Evolution **57**:732-738.doi: 10.1016/j.jhevol.2009.06.009

Merceron, G., S. Taylor, R. Scott, Y. Chaimanee, and J. J. Jaeger. 2006. Dietary characterization of the hominoid *Khoratpithecus* (Miocene of Thailand): evidence from dental topographic and microwear texture analyses. Naturwissenschaften **93**:329-333.doi: 10.1007/s00114-006-0107-0

Merrick, R. L., M. K. Chumbley, and G. V. Byrd. 1997. Steller sea lions (*Eumetopias jubatus*) and their population decline in Alaska: a potential relationship. Canadian Journal of Fisheries and Aquatic Sciences **54**:1342-1348.doi: 10.1139/f97-037

Mihlbachler, M. C., B. L. Beatty, A. Caldera-Siu, D. Chan, and R. Lee. 2012. Error rates and observer bias in dental microwear analysis using light microscopy. Palaeontologia Electronica **15**:12A,22p,

Mikkelsen, B., T. Haug, and K. T. Nilssen. 2002. Summer diet of Grey Seals (*Halichoerus grypus*) in Faroese waters. Sarsia **87**:462-471.doi: 10.1080/00364820210001557 45

Moran, M. D. 2003. Arguments for rejecting the sequential bonferroni in ecological studies. Oikos **100**:403-405.doi: 10.1034/j.1600-0706.2003.12010.x

Mori, J., T. Kubodera, and N. Baba. 2001. Squid in the diet of northern fur seals, *Callorhinus ursinus*, caught in the Western and Central North Pacific Ocean. Fisheries Research **52**:91-97.doi: 10.1016/S0165-7836(01)00233-8

Morin, P. A., F. I. Archer, A. D. Foote, J. Vilstrup, E. E. Allen, P. Wade, J. Durban, K. Parsons, R. Pitman, L. Li, P. Bouffard, S. C. Abel Nielsen, M. Rasmussen, E. Willerslev, M. T. Gilbert, and T. Harkins. 2010. Complete mitochondrial genome phylogeographic analysis of killer whales (*Orcinus orca*) indicates multiple species. Genome Res **20**:908-916.doi: 10.1101/gr.102954.109

Morin, P. A., R. G. LeDuc, K. M. Robertson, N. M. Hedrick, W. F. Perrin, M. Etnier, P. Wade, and B. L. Taylor. 2006. Genetic analysis of killer whale (*Orcinus Orca*) historical bone and tooth samples to identify Western U.S. ecotypes. Marine Mammal Science **22**:897-909.doi: 10.1111/j.1748-7692.2006.00070.x

Morissette, L., V. Christensen, and D. Pauly. 2012. Marine mammal impacts in exploited ecosystems: would large scale culling benefit fisheries? PLoS One **7**:e43966.doi: 10.1371/journal.pone.0043966

Nakagawa, S. 2004. A farewell to Bonferroni: the problems of low statistical power and publication bias. Behavioral Ecology **15**:1044-1045.doi: 10.1093/beheco/arh107

Nardin, P., D. Nita, and J. Mignot. 2002. Automation of a series of cutaneous topography measurements from silicon rubber replicas. Skin Research and Technology **8**:112-117.doi: 10.1034/j.1600-0846.2002.00309.x

Newsome, S. D., M. A. Etnier, D. H. Monson, and M. L. Fogel. 2009. Retrospective characterization of ontogenetic shifts in killer whale diets via δ13C and δ15N analysis of teeth. Marine Ecology Progress Series **374**:229-242.doi: 10.3354/meps07747

Nilssen, K. T., O. Pedersen, L. P. Folkow, and T. Haug. 2004. Food consumption estimates of Barents Sea harp seals. NAMMCO Scientific Publications **2**:9-27.doi: 10.7557/3.2968

Nilsson, L., and R. Ohlsson. 2001. Accuracy of replica materials when measuring engineering surfaces. International Journal of Machine Tools and Manufacture **41**:2139-2145.doi: 10.1016/S0890-6955(01)00080-3

Nummela, S., J. G. Thewissen, S. Bajpai, T. Hussain, and K. Kumar. 2007. Sound transmission in archaic and modern whales: anatomical adaptations for underwater hearing. The Anatomical Record **290**:716-733.doi: 10.1002/ar.20528

Nwaogu, U. C., N. S. Tiedje, and H. N. Hansen. 2013. A non-contact 3D method to characterize the surface roughness of castings. Journal of Materials Processing Technology **213**:59-68.doi: 10.1016/j.jmatprotec.2012.08.008

O'Leary, M. A., and J. H. Geisler. 1999. The position of Cetacea within Mammalia: phylogenetic analysis of morphological data from extinct and extant taxa. Systematic Biology **48**:455-490.doi: 10.1080/106351599260102

O'Leary, M. A., and M. D. Uhen. 1999. The time of origin of whales and the role of behavioral changes in the terrestrial-aquatic transition. Paleobiology **25**:534-556.doi: 10.1017/S0094837300020376

Odell, G. H. 1975. Micro-wear in perspective: a sympathetic response to Lawrence H. Keeley. World Archaeology **7**:226-240,

Parrish, F. A., E. A. Howell, G. A. Antonelis, S. J. Iverson, C. L. Littnan, J. D. Parrish, and J. J. Polovina. 2012. Estimating the carrying capacity of French frigate shoals for the endangered Hawaiian monk seal using ecopath with ecosim. Marine Mammal Science **28**:522-541.doi: 10.1111/j.1748-7692.2011.00502.x

Passos, V. F., M. A. Melo, A. A. Vasconcellos, L. K. Rodrigues, and S. L. Santiago. 2013. Comparison of methods for quantifying dental wear caused by erosion and abrasion. Microscopy Research and Technique **76**:178-183.doi: 10.1002/jemt.22150

Pate, S. M., and W. E. McFee. 2012. Prey species of bottlenose dolphins (*Tursiops truncatus*) from South Carolina waters. Southeastern Naturalist **11**:1-22.doi: 10.1656/058.011.0101

Pauly, D., A. W. Trites, E. Capuli, and V. Christensen. 1998. Diet composition and trophic levels of marine mammals. ICES Journal of Marine Science **55**:467-481.doi: 10.1006/jmsc.1997.0280

Perrin, W. F. 2016. World Cetacea Database. Accessed at http://www.marinespecies.org/cetacea.

Pineda-Munoz, S., and J. Alroy. 2014. Dietary characterization of terrestrial mammals. Proceedings of the Royal Society of London B: Biological Sciences **281**:20141173.doi: 10.1098/rspb.2014.1173

Pitman, R. L., and J. W. Durban. 2010. Killer whale predation on penguins in Antarctica. Polar Biology **33**:1589-1594.doi: 10.1007/s00300-010-0853-5

Pitman, R. L., and P. Ensor. 2003. Three forms of killer whales (*Orcinus orca*) in Antarctic waters. Journal of Cetacean Research and Management **5**:131-139,

Purnell, M., O. Seehausen, and F. Galis. 2012. Quantitative three-dimensional microtextural analyses of tooth wear as a tool for dietary discrimination in fishes. Journal of the Royal Society, Interface **9**:2225-2233.10.1098/rsif.2012.0140

Purnell, M. A., N. Crumpton, P. G. Gill, G. Jones, and E. J. Rayfield. 2013. Within-guild dietary discrimination from 3-D textural analysis of tooth microwear in insectivorous mammals. Journal of Zoology **291**:249-257.doi: 10.1111/jzo.12068

Purnell, M. A., and L. P. G. Darras. 2015. 3D tooth microwear texture analysis in fishes as a test of dietary hypotheses of durophagy. Surface Topography: Metrology and Properties **4**:014006.doi: 10.1088/2051-672x/4/1/014006

Purnell, M. A., P. J. B. Hart, D. C. Baines, and M. A. Bell. 2006. Quantitative analysis of dental microwear in threespine stickleback: a new approach to analysis of trophic ecology in aquatic vertebrates. Journal of Animal Ecology **75**:967-977.doi: 10.1111/j.1365-2656.2006.01116.x

Read, A. J. 2008. The looming crisis: interactions between marine mammals and fisheries. Journal of Mammalogy **89**:541-548.doi: 10.1644/07-MAMM-S-315R1.1

Read, A. J., P. Drinker, and S. Northridge. 2006. Bycatch of marine mammals in U.S. and global fisheries. Conservation Biology **20**:163-169.doi: 10.1111/j.1523-1739.2006.00338.x

Reeves, R. R., K. McClellan, and T. B. Werner. 2013. Marine mammal bycatch in gillnet and other entangling net fisheries, 1990 to 2011. Endangered Species Research **20**:71-97.doi: 10.3354/esr00481

Rodriguez, J. M., R. V. Curtis, and D. W. Bartlett. 2009. Surface roughness of impression materials and dental stones scanned by non-contacting laser profilometry. Dental Materials **25**:500-505.doi: 10.1016/j.dental.2008.10.003

Rosel, P. E., and L. Rojas-Bracho. 1999. Mitochondrial DNA variation in the critically endangered vaquita *Phocoena sinus* Norris and MacFarland, 1958. Marine Mammal Science **15**:990-1003.doi: 10.1111/j.1748-7692.1999.tb00874.x

Rosén, B. G., L. Blunt, and T. R. Thomas. 2005. On in-vivo skin topography metrology and replication techniques. Journal of Physics: Conference Series **13**:325-329.doi: 10.1088/1742-6596/13/1/076

Rosen, D. A. S., and D. J. Tollit. 2012. Effects of phylogeny and prey type on fatty acid calibration coefficients in three pinniped species: implications for the QFASA dietary quantification technique. Marine Ecology Progress Series **467**:263-276.doi: 10.3354/meps09934

Santos, M. B., G. J. Pierce, R. J. Reid, I. A. P. Patterson, H. M. Ross, and E. Mente. 2001. Stomach contents of bottlenose dolphins (*Tursiops truncatus*) in Scottish waters. Journal of the Marine Biological Association of the United Kingdom **81**:873-878.doi: 10.1017/S0025315401004714

Saulitis, E., C. Matkin, L. Barrett-Lennard, K. Heise, and G. Ellis. 2000. Foraging strategies of sympatric killer whale (*Orcinus orca*) populations in Prince William Sound,

Alaska. Marine Mammal Science **16**:94-109.doi: 10.1111/j.1748-7692.2000.tb00906.x

Schubert, B. W., P. S. Ungar, and L. R. G. DeSantis. 2010. Carnassial microwear and dietary behaviour in large carnivorans. Journal of Zoology **280**:257-263.doi: 10.1111/j.1469-7998.2009.00656.x

Schulz, E., I. Calandra, and T. M. Kaiser. 2010. Applying tribology to teeth of hoofed mammals. Scanning **32**:162-182.doi: 10.1002/sca.20181

Schulz, E., I. Calandra, and T. M. Kaiser. 2013a. Feeding ecology and chewing mechanics in hoofed mammals: 3D tribology of enamel wear. Wear **300**:169-179.doi: 10.1016/j.wear.2013.01.115

Schulz, E., V. Piotrowski, M. Clauss, M. Mau, G. Merceron, and T. M. Kaiser. 2013b. Dietary abrasiveness is associated with variability of microwear and dental surface texture in rabbits. PLoS One **8**:e56167.doi: 10.1371/journal.pone.0056167

Schwendicke, F., G. Felstehausen, C. Carey, and C. Dorfer. 2014. Comparison of four methods to assess erosive substance loss of dentin. PLoS One **9**:e108064.doi: 10.1371/journal.pone.0108064

Scott, J. R., L. R. Godfrey, W. L. Jungers, R. S. Scott, E. L. Simons, M. F. Teaford, P. S. Ungar, and A. Walker. 2009. Dental microwear texture analysis of two families of subfossil lemurs from Madagascar. Journal of Human Evolution **56**:405-416.doi: 10.1016/j.jhevol.2008.11.003

Scott, R. S., M. F. Teaford, and P. S. Ungar. 2012. Dental microwear texture and anthropoid diets. American Journal of Physical Anthropology **147**:551-579.doi: 10.1002/ajpa.22007

Scott, R. S., P. S. Ungar, T. S. Bergstrom, C. A. Brown, B. E. Childs, M. F. Teaford, and A. Walker. 2006. Dental microwear texture analysis: technical considerations. Journal of Human Evolution **51**:339-349.doi: 10.1016/j.jhevol.2006.04.006

Scott, R. S., P. S. Ungar, T. S. Bergstrom, C. A. Brown, F. E. Grine, M. F. Teaford, and A. Walker. 2005. Dental microwear texture analysis shows within-species diet variability in fossil hominins. Nature **436**:693-695.doi: 10.1038/nature03822

Shearer, B. M., P. S. Ungar, K. P. McNulty, W. E. Harcourt-Smith, H. M. Dunsworth, and M. F. Teaford. 2015. Dental microwear profilometry of African non-

cercopithecoid catarrhines of the Early Miocene. Journal of Human Evolution **78**:33-43.doi: 10.1016/j.jhevol.2014.08.011

Silva, I. 2013. Short note: presence and distribution of Hawaiian false killer whales (*Pseudorca crassidens*) in Maui County waters: a historical perspective. Aquatic Mammals **39**:409-414.doi: 10.1578/am.39.4.2013.409

Simila, T., J. C. Holst, and I. Christensen. 1996. Occurrence and diet of killer whales in northern Norway: seasonal patterns relative to the distribution and abundance of Norwegian spring-spawning herring. Canadian Journal of Fisheries and Aquatic Sciences **53**:769-779.doi: 10.1139/f95-253

Simmonds, M. P., and W. J. Eliott. 2009. Climate change and cetaceans: concerns and recent developments. Journal of the Marine Biological Association of the United Kingdom **89**:203.doi: 10.1017/s0025315408003196

Simmonds, M. P., and S. J. Isaac. 2007. The impacts of climate change on marine mammals: early signs of significant problems. Oryx **41**:19.doi: 10.1017/s0030605307001524

Simpson, G. G. 1926. Mesozoic mammalia. IV. the multituberculates as living animals. American Journal of Science **63**:228-250,

Sinclair, E. H., and T. K. Zeppelin. 2002. Seasonal and spatial differences in diet in the western stock of steller sea lions (*Eumetopias jubatus*). Journal of Mammalogy **83**:973-990.doi: 10.1644/1545-1542(2002)083<0973:SASDID>2.0.CO;2

Snively, E., J. M. Fahlke, and R. C. Welsh. 2015. Bone-breaking bite force of *Basilosaurus isis* (Mammalia, Cetacea) from the late Eocene of Egypt estimated by finite element analysis. PLoS One **10**:e0118380.doi: 10.1371/journal.pone.0118380

Spitz, J., Y. Cherel, S. Bertin, J. Kiszka, A. Dewez, and V. Ridoux. 2011. Prey preferences among the community of deep-diving odontocetes from the Bay of Biscay, Northeast Atlantic. Deep Sea Research Part I: Oceanographic Research Papers **58**:273-282.doi: 10.1016/j.dsr.2010.12.009

Spitz, J., Y. Rousseau, and V. Ridoux. 2006. Diet overlap between harbour porpoise and bottlenose dolphin: An argument in favour of interference competition for food? Estuarine, Coastal and Shelf Science **70**:259-270.doi: 10.1016/j.ecss.2006.04.020

Spoor, F., S. Bajpai, S. T. Hussain, K. Kumar, and J. G. M. Thewissen. 2002. Vestibular evidence for the evolution of aquatic behaviour in early Cetaceans. Nature **417**:163-166.doi: 10.1038/417163a

Springer, A. M., J. A. Estes, G. B. van Vliet, T. M. Williams, D. F. Doak, E. M. Danner, K. A. Forney, and B. Pfister. 2003. Sequential megafaunal collapse in the North Pacific Ocean: an ongoing legacy of industrial whaling? Proceedings of the National Academy of Sciences **100**:12223-12228.doi: 10.1073/pnas.1635156100

Springer, A. M., J. A. Estes, G. B. van Vliet, T. M. Williams, D. F. Doak, E. M. Danner, and B. Pfister. 2008. Mammal-eating killer whales, industrial whaling, and the sequential megafaunal collapse in the North Pacific Ocean: A reply to critics of Springer et al. 2003. Marine Mammal Science **24**:414-442.doi: 10.1111/j.1748-7692.2008.00185.x

Swift, C. C., and L. G. Barnes. 1996. Stomach contents of *Basilosaurus cetoides*: implications for the evolution of cetacean feeding behavior, and evidence for vertebrate fauna of epicontinental seas. Paleontological Society Special Publication **8**:380,

Symondson, W. O. C. 2002. Molecular identification of prey in predator diets. Molecular Ecology **11**:627-641.doi: 10.1046/j.1365-294X.2002.01471.x

Teaford, M. F., and O. J. Oyen. 1989. In vivo and in vitro turnover in dental microwear. American Journal of Physical Anthropology **80**:447-460.doi: 10.1002/ajpa.1330800405

Thewissen, J. G., L. N. Cooper, M. T. Clementz, S. Bajpai, and B. N. Tiwari. 2007. Whales originated from aquatic artiodactyls in the Eocene epoch of India. Nature **450**:1190-1194.doi: 10.1038/nature06343

Thewissen, J. G. M., L. N. Cooper, J. C. George, and S. Bajpai. 2009. From land to water: the origin of whales, dolphins, and porpoises. Evolution: Education and Outreach **2**:272-288.doi: 10.1007/s12052-009-0135-2

Thewissen, J. G. M., and F. E. Fish. 1997. Locomotor evolution in the earliest Cetaceans: functional model, modern analogues, and paleontological evidence. Paleobiology **23**:482-490.doi: 10.1017/S0094837300019850

Thewissen, J. G. M., J. D. Sensor, M. T. Clementz, and S. Bajpai. 2011. Evolution of dental wear and diet during the origin of whales. Paleobiology **37**:655-669.doi: 10.1666/10038.1

Thewissen, J. G. M., E. M. Williams, L. J. Roe, and S. T. Hussain. 2001. Skeletons of terrestrial cetaceans and the relationship of whales to artiodactyls. Nature **413**:277-281.doi: 10.1038/35095005

Tollit, D. J., A. D. Black, P. M. Thompson, A. Mackay, H. M. Corpe, B. Wilson, S. M. Van Parijs, K. Grellier, and S. Parlane. 1998. Variations in harbour seal *Phoca vitulina* diet and dive-depths in relation to foraging habitat. Journal of Zoology **244**:209-222.doi: 10.1111/j.1469-7998.1998.tb00026.x

Tollit, D. J., G. J. Pierce, K. A. Hobson, W. D. Bowen, and S. J. Iverson. 2010. Diet. Pages 191-221 *in* I. L. Boyd, W. D. Bowen, and S. J. Iverson, editors. Marine mammal ecology and conservation: a handbook of techniques. Oxford University Press, Oxford.

Tollit, D. J., M. Wong, A. J. Winship, D. A. S. Rosen, and A. W. Trites. 2003. Quantifying errors associated with using prey skeletal structures from fecal samples to detirmine the diet of steller's sea lion (*Eumetopias jubatus*). Marine Mammal Science **19**:724-744.doi: 10.1111/j.1748-7692.2003.tb01127.x

Tosello, G., H. Haitjema, R. K. Leach, D. Quagliotti, S. Gasparin, and H. N. Hansen. 2016. An international comparison of surface texture parameters quantification on polymer artefacts using optical instruments. CIRP Annals - Manufacturing Technology **65**:529-532.doi: 10.1016/j.cirp.2016.04.003

Trites, A. W., D. G. Calkins, and A. J. Winship. 2007. Diets of Steller sea lions (*Eumetopias jubatus*) in Southeast Alaska, 1993−1999. Fisheries Bulletin **105**:234-248,

Trites, A. W., V. Christensen, and D. Pauly. 1997. Competition between fisheries and marine mammals for prey and primary production in the Pacific Ocean. Journal of Northwest Atlantic Fishery Science **22**:173-187,

Turvey, S. T., R. L. Pitman, B. L. Taylor, J. Barlow, T. Akamatsu, L. A. Barrett, X. Zhao, R. R. Reeves, B. S. Stewart, K. Wang, Z. Wei, X. Zhang, L. T. Pusser, M. Richlen, J. R. Brandon, and D. Wang. 2007. First human-caused extinction of a cetacean species? Biology Letters **3**:537-540.doi: 10.1098/rsbl.2007.0292

Uhen, M. D. 2000. Replacement of deciduous first premolars and dental eruption in archaeocete whales. American Society of Mammalogists **81**:123-133.doi: 10.1093/jmammal/81.1.123

Uhen, M. D. 2004. Form, function, and anatomy of *Dorudon atrox* (Mammalia, Cetacea): an archaeocete from the Middle to Late Eocene of Egypt. University of Michigan. Papers on Palaeontology **34**:1-222,

Uhen, M. D. 2007. Evolution of marine mammals: back to the sea after 300 million years. The Anatomical Record **290**:514-522.doi: 10.1002/ar.20545

Uhen, M. D. 2008. New protocetid whales from Alabama and Mississippi, and a new Cetacean clade, Pelagiceti. Journal of Vertebrate Paleontology **28**:589-593.doi: 10.1671/0272-4634(2008)28%5B589:NPWFAA%5D2.0.CO;2

Uhen, M. D. 2010. The origin(s) of whales. Annual Review of Earth and Planetary Sciences **38**:189-219.doi: 10.1146/annurev-earth-040809-152453

Uhen, M. D., and H.-J. Berndt. 2008. First record of the archaeocete whale family Protocetidae from Europe. Fossil Record **11**:57-60.doi: 10.1002/mmng.200800001

Uhen, M. D., and P. D. Gingerich. 2001. New genus of Dorudontine archaeocete (Cetacea) from the Middle-to-Late Eocene of South Carolina. Marine Mammal Science **17**:1-34.doi: 10.1111/j.1748-7692.2001.tb00979.x

Uhen, M. D., N. D. Pyenson, T. J. Devries, M. Urbina, and P. R. Renne. 2011. New Middle Eocene whales from the Pisco Basin of Peru. Journal of Paleontology **85**:955-969.doi: 10.1666/10-162.1

Ungar, P. S. 1996. Dental microwear of european Miocene Catarrhines: evidence for diets and tooth Use. Journal of Human Evolution **31**:335-366.doi: 10.1006/jhev.1996.0065

Ungar, P. S., C. A. Brown, T. S. Bergstrom, and A. Walker. 2003. Quantification of dental microwear by tandem scanning confocal microscopy and scale-sensitive fractal analysis. Scanning **25**:185-193.doi: 10.1002/sca.4950250405

Ungar, P. S., F. E. Grine, and M. F. Teaford. 2008. Dental microwear and diet of the Plio-Pleistocene hominin *Paranthropus boisei*. PLoS One **3**:e2044.doi: 10.1371/journal.pone.0002044

Ungar, P. S., G. Merceron, and R. S. Scott. 2007. Dental microwear texture analysis of Varswater Bovids and Early Pliocene paleoenvironments of Langebaanweg, Western Cape Province, South Africa. Journal of Mammalian Evolution **14**:163-181.doi: 10.1007/s10914-007-9050-x

Ungar, P. S., R. S. Scott, F. E. Grine, and M. F. Teaford. 2010. Molar microwear textures and the diets of *Australopithecus anamensis* and *Australopithecus afarensis*. Philosophical Transactions of the Royal Society, B: Biological Sciences **365**:3345-3354.doi: 10.1098/rstb.2010.0033

Ungar, P. S., and M. Sponheimer. 2011. The diets of early hominins. Science **334**:190-193.doi: 10.1126/science.1207701

Vorburger, T. V., H. G. Rhee, T. B. Renegar, J. F. Song, and A. Zheng. 2007. Comparison of optical and stylus methods for measurement of surface texture. The International Journal of Advanced Manufacturing Technology **33**:110-118.doi: 10.1007/s00170-007-0953-8

Wade, P. R., J. M. Ver Hoef, and D. P. DeMaster. 2009. Mammal-eating killer whales and their prey-trend data for pinnipeds and sea otters in the North Pacific Ocean do not support the sequential megafaunal collapse hypothesis. Marine Mammal Science **25**:737-747.doi: 10.1111/j.1748-7692.2009.00282.x

Walker, A., H. N. Hoeck, and L. Perez. 1978. Microwear of mammalian teeth as an indicator of diet. Science **201**:908-910.doi: 10.1126/science.684415

Walker, J. L., and S. A. Macko. 1999. Dietary studies of marine mammals using stable carbon and nitrogen isotopic ratios of teeth. Marine Mammal Science **15**:314-334.doi: 10.1111/j.1748-7692.1999.tb00804.x

Webb, R. H. 1996. Confocal optical microscopy. Reports on Progress in Physics **59**:427-471.doi: 10.1088/0034-4885/59/3/003

West, R. M. 1980. Middle eocene large mammal assemblage with Tethyan affinities, Ganda Kas Region, Pakistan. Journal of Paleontology **54**:508-533,

Whitlock, J. A. 2011. Inferences of diplodocoid (Sauropoda: Dinosauria) feeding behavior from snout shape and microwear analyses. PLoS One **6**:e18304.doi: 10.1371/journal.pone.0018304

Williams, F. L. 2013. Enamel microwear texture properties of IGF 11778 (*Oreopithecus bambolii*) from the late Miocene of Baccinello, Italy. Journal of Anthropological Sciences **91**:201-217.doi: 10.4436/jass.89003

Williams, V. S., P. M. Barrett, and M. A. Purnell. 2009. Quantitative analysis of dental microwear in hadrosaurid dinosaurs, and the implications for hypotheses of jaw mechanics and feeding. Proceedings of the National Academy of Sciences **106**:11194-11199.doi: 10.1073/pnas.0812631106

Williams, V. S., and A. M. Doyle. 2010. Cleaning fossil tooth surfaces for microwear analysis: Use of solvent gels to remove resistant consolidant. Palaeontologia Electronica **13**:2T:12p,

Williams, V. S., M. Purnell, and S. Gabbott. 2006. Dental microwear in dinosaurs: a comparative analysis of polysiloxane replication. Dental Practice **44**:22-23,

Winkler, D. E., E. Schulz, I. Calandra, J.-P. Gailer, C. Landwehr, and T. M. Kaiser. 2013. Indications for a dietary change in the extinct Bovid genus *Myotragus* (Plio-Holocene, Mallorca, Spain). Geobios **46**:143-150.doi: 10.1016/j.geobios.2012.10.010

Wood, B. 2013. Gritting their teeth. Nature **493**:486-487.doi: 10.1038/493486a

Wroe, S., T. L. Ferrara, C. R. McHenry, D. Curnoe, and U. Chamoli. 2010. The craniomandibular mechanics of being human. Proceedings of the Royal Society B: Biological Sciences **277**:3579-3586.doi: 10.1098/rspb.2010.0509

Xia, J., J. Zheng, D. Huang, Z. R. Tian, L. Chen, Z. Zhou, P. S. Ungar, and L. Qian. 2015. New model to explain tooth wear with implications for microwear formation and diet reconstruction. Proceedings of the National Academy of Sciences **112**:10669-10672.doi: 10.1073/pnas.1509491112

Xia, Y., E. Kim, Z. Xiao-Mei, J. A. Rogers, M. Prentiss, and G. M. Whitesides. 1996. Complex optical surfaces formed by replica molding against elastomeric masters. Science **273**:347-349.doi: 10.1126/science.273.5273.347

Xu, C., C. Reece, and M. Kelley. 2013. Characterization of Nb SRF cavity materials by white light interferometry and replica techniques. Applied Surface Science **274**:15-21.doi: 10.1016/j.apsusc.2013.02.006

Yan, L., Y. M. Rong, F. Jiang, and Z. X. Zhou. 2011. Three-dimension surface characterization of grinding wheel using white light interferometer. The

International Journal of Advanced Manufacturing Technology **55**:133-141.doi: 10.1007/s00170-010-3054-z

Yodzis, P. 2001. Must top predators be culled for the sake of fisheries? Trends in Ecology & Evolution **16**:78-84.doi: 10.1016/S0169-5347(00)02062-0

Yonezaki, S., M. Kiyota, and N. Baba. 2008. Decadal changes in the diet of northern fur seal (*Callorhinus ursinus*) migrating off the Pacific coast of northeastern Japan. Fisheries Oceanography **17**:231-238.doi: 10.1111/j.1365-2419.2008.00475.x

Yonezaki, S., M. Kiyota, N. Baba, T. Koido, and A. Takemura. 2003. Size distribution of the hard remains of prey in the digestive tract of northern fur seal (*Callorhinus ursinus*) and related biases in diet estimation by scat analysis. Mammal Study **28**:97-102.doi: 10.3106/mammalstudy.28.97

Young, B. G., L. L. Loseto, and S. H. Ferguson. 2009. Diet differences among age classes of Arctic seals: evidence from stable isotope and mercury biomarkers. Polar Biology **33**:153-162.doi: 10.1007/s00300-009-0693-3

Zavala-Gonzalez, A., J. Urban-Ramirez, and C. Esquivel-Macias. 1994. A note on artisanal fisheries interactions with small Cetaceans in Mexico. Report of the International Whaling Commission **(Special issue 15)**:235-237,

Zeppelin, T. K., and R. R. Ream. 2006. Foraging habitats based on the diet of female northern fur seals (*Callorhinus ursinus*) on the Pribilof Islands, Alaska. Journal of Zoology **270**:565-576.doi: 10.1111/j.1469-7998.2006.00122.x